

Studies in Systems, Decision and Control 472

Kyandoghene Kyamakya  
Pitshou Ntambu Bokoro *Editors*

# Recent Advances in Energy Systems, Power and Related Smart Technologies

Concepts and Innovative  
Implementations for a Sustainable  
Economic Growth in Developing  
Countries

 Springer

# **Studies in Systems, Decision and Control**

Volume 472

## **Series Editor**

Janusz Kacprzyk, Systems Research Institute, Polish Academy of Sciences,  
Warsaw, Poland

The series “Studies in Systems, Decision and Control” (SSDC) covers both new developments and advances, as well as the state of the art, in the various areas of broadly perceived systems, decision making and control—quickly, up to date and with a high quality. The intent is to cover the theory, applications, and perspectives on the state of the art and future developments relevant to systems, decision making, control, complex processes and related areas, as embedded in the fields of engineering, computer science, physics, economics, social and life sciences, as well as the paradigms and methodologies behind them. The series contains monographs, textbooks, lecture notes and edited volumes in systems, decision making and control spanning the areas of Cyber-Physical Systems, Autonomous Systems, Sensor Networks, Control Systems, Energy Systems, Automotive Systems, Biological Systems, Vehicular Networking and Connected Vehicles, Aerospace Systems, Automation, Manufacturing, Smart Grids, Nonlinear Systems, Power Systems, Robotics, Social Systems, Economic Systems and other. Of particular value to both the contributors and the readership are the short publication timeframe and the worldwide distribution and exposure which enable both a wide and rapid dissemination of research output.

Indexed by SCOPUS, DBLP, WTI Frankfurt eG, zbMATH, SCImago.

All books published in the series are submitted for consideration in Web of Science.

Kyandoghere Kyamakya · Pitshou Ntambu Bokoro  
Editors


# Recent Advances in Energy Systems, Power and Related Smart Technologies

Concepts and Innovative Implementations for  
a Sustainable Economic Growth  
in Developing Countries

 Springer

*Editors*

Kyandoghere Kyamakya   
Institute of Smart Systems Technologies  
Alpen-Adria Universität Klagenfurt  
Klagenfurt, Austria  
Faculté Polytechnique  
Université de Kinshasa  
Kinshasa, Democratic Republic of Congo

Pitshou Ntambu Bokoro   
Department of Electrical Engineering  
Technology  
University of Johannesburg  
Johannesburg, South Africa

ISSN 2198-4182

ISSN 2198-4190 (electronic)

Studies in Systems, Decision and Control

ISBN 978-3-031-29585-0

ISBN 978-3-031-29586-7 (eBook)

<https://doi.org/10.1007/978-3-031-29586-7>

© The Editor(s) (if applicable) and The Author(s), under exclusive license to Springer Nature Switzerland AG 2024

This work is subject to copyright. All rights are solely and exclusively licensed by the Publisher, whether the whole or part of the material is concerned, specifically the rights of translation, reprinting, reuse of illustrations, recitation, broadcasting, reproduction on microfilms or in any other physical way, and transmission or information storage and retrieval, electronic adaptation, computer software, or by similar or dissimilar methodology now known or hereafter developed.

The use of general descriptive names, registered names, trademarks, service marks, etc. in this publication does not imply, even in the absence of a specific statement, that such names are exempt from the relevant protective laws and regulations and therefore free for general use.

The publisher, the authors, and the editors are safe to assume that the advice and information in this book are believed to be true and accurate at the date of publication. Neither the publisher nor the authors or the editors give a warranty, expressed or implied, with respect to the material contained herein or for any errors or omissions that may have been made. The publisher remains neutral with regard to jurisdictional claims in published maps and institutional affiliations.

This Springer imprint is published by the registered company Springer Nature Switzerland AG  
The registered company address is: Gewerbestrasse 11, 6330 Cham, Switzerland

# General Introduction

## Background and Motivation

Economic growth consists of legitimate aspiration and important objective for developing nations since it supports and enables increase in gross domestic products (GDP), which may consequently culminate into Job creation and to an improvement of human development index (HDI). However, growth in economy, such as observed in the various cases, is fundamentally energy intensive. In the current context of climate change and global warming, low-carbon energy or renewable energy sources (photovoltaic, wind, biomass, etc.) have become the ultimate substitutes for conventional approaches to energy production (fossil-fuel technologies) and consumption initiatives previously used to fuel industrialization and economic growth. Therefore, the idea of sustainable development, which compels the global community to pursue green economy among others, has been adopted by the United Nations as global standards and guidelines that should inform and assist both developed and developing nations in the formulation of their developmental policies. This notion of green economy has become the focus of global modern economy. Therefore, knowledge and skills, which are key attributes of modern economy, have now been tuned to the development of sustainable or green technologies. In other words, the prospect of sustainable economic development is consistently aligned with the pursuit of new technologies and/or innovative applications of existing technologies. Furthermore, in the context of the fourth industrial revolution, whereby knowledge expansion has led to the development of data-driven systems, models, and concepts with cognitive capability (artificial intelligence, machine learning, deep learning, Internet of Things (IoT), digital twin technology, virtual reality, pattern recognition, etc.). Therefore, these cutting-edge technologies have systematically disrupted perceptions and concepts of technology-driven economy and business models. Advancement of these technologies as well as their applications in the field of energy is of significant advantage to the global economy. Hence, advanced concepts as well as innovative applications of the fourth industrial technologies, discussed in this book, range from battery

and storage technologies, smart grids, and performance index of voltage security assessment to an IoT-based car parking system.

Therefore, this book consists of one important channel that seeks to effectively contribute to the dissemination of currently available conceptual approach and innovative applications of intelligent technologies in selected topics related to energy and power systems. It consists of a carefully constituted collection of 22 chapters, which are purposely grouped into 6 sections or key thematic areas under discussion:

- Batteries and Energy Storage Technologies;
- Distributed Generation, Smart Grids and Supply Reliability;
- Control of Static Converters, Power Quality, FACTS Devices and Hybrid Circuit Breaker Technology;
- Access to Clean Energy for Sustainable Development, Power System Infrastructure, and Policy Options;
- Concepts and Innovative Applications of Intelligent Systems and Technologies;
- Conclusions and Outlook.

## **Part: Batteries and Energy Storage Technologies**

Part deals with batteries and energy storage technologies in the context of renewable energy systems. This section consists of three fundamental chapters: Chap. “[Assessing Control of Battery-Supercapacitor Hybrid Storage System in Photovoltaic Based DC Microgrid](#)” investigates the power sharing control strategy between PV and load demand in a DC microgrid. It introduces the concept of hybrid energy storage (battery and supercapacitor) in the context of transient variation of the battery load demand and intermittent PV. It is argued that this control strategy provides the effective power sharing between PV and hybrid energy storage medium. Chapter “[Batteries, Energy Storage Technologies, Energy-Efficient Systems, Power Conversion Topologies, and Related Control Techniques](#)” reports on short longevity and limited range of battery system in electric transportation system, prior to stepping into the concept of battery energy storage system as one of the proposed approaches in order to improve the performance of electric vehicles and/or systems powered from renewable sources. Chapter “[Generation Expansion Planning Using Renewable Energy Sources with Storage](#)” discusses generation expansion planning (GEP) in the context of temporal and spatial variations of both supply and demand for energy. The integration of system elements with a complex mix of alternative candidate plants having different physical and production capabilities and characteristics is also analyzed in this work. This leads to the formulation of a realistic mathematical model whereby the deployment of GEP is the model solutions. The balance between the benefits of greater solar penetration with the cost of adapting conventional base load systems is also probed in this chapter.

## **Part: Distributed Generation, Smart Grids and Supply Reliability**

In Part, distributed generation concepts and applications of smart grids are discussed as well as supply reliability of such systems. Three chapters constitute this section: Chaps. “[A Smart Grid Ontology for Africa](#)”–“[Improving Electricity Supply Reliability: A Case Study of Remote Communities of Limpopo in South Africa](#)”. Therefore, in Chap. “[A Smart Grid Ontology for Africa](#)”, an ontological model for one of the smart grid (SG) domains is proposed in the context of non-flexible, non-extensive, and inadaptible market and access of traditional grids. This model will be built on the reuse of an already advanced European ontological model of SG. In addition, the identified gap in interoperability and technological integration between the IEC CIM and the IEC 61850 models is addressed in this chapter through an addition of ontology or semantic technology in SG. Chapter “[Smart Micro-Grid Energy Management with Renewable Energy Sources and Local SCADA](#)” introduces the concept of smart microgrid energy management, which comprises an in-built local grid operation through local SCADA while incorporating the best possible renewable energy resources and storage systems in a building apartment. The design approach is such that no additional operational cost is required from consumers rather an earning of additional revenue due to supply of excess power to the main grid. This will provide support to the main grid during peak hours. Chapter “[Improving Electricity Supply Reliability: A Case Study of Remote Communities of Limpopo in South Africa](#)” concludes this section by introducing a design and simulation of suitable architecture of a hybrid microgrid system for three isolated and rural communities or villages (Tjiane, Phosiri, and Malekapane) in the district of Ga-Mphahlele in Limpopo Province of South Africa. The unreliable national grid system is the main source of power in these communities while diesel generators are used as backup system during load shedding. The HOMER software is used for the design and simulation of hybrid microgrid power systems. Optimal microgrid system architecture was proposed based on lower net present cost (NPC), lower cost of energy (COE), a maximum renewable fraction (RF), loss of power supply probability (LPSP), and lower carbon emissions.

## **Part: Control of Static Converters, Power Quality, FACTS Devices and Hybrid Circuit Breaker Technology**

This part includes topics related to control aspects of static converters, power quality issues, and FACTS devices as well as hybrid circuit breaker technology. Four chapters are dedicated to this section: Chaps. “[Control of Grid-Connected Voltage Source Converters During Unsymmetrical Faults](#)”–“[Advances in Protection and Testing of Power Distribution Systems Within Emerging Markets](#)”.



Chapter “[Control of Grid-Connected Voltage Source Converters During Unsymmetrical Faults](#)” presents a current control scheme for grid-connected voltage source converters during unsymmetrical faults. The control scheme, such as proposed, is based on the modification of the direct power control with space vector modulation (DPC-SVM) for improving the converter control during unsymmetrical faults. In addition, it is able to maintain the magnitude of the current within its rated value, and keep the distortion in the current minimal, as well as minimizing the oscillations in the power caused by the negative-sequence components of voltage and current. In Chap. “[Power Quality Control of a PV-Assisted Realistic Microgrid Structure](#)”, a small size PV-assisted microgrid model is considered with the effect of line impedance for the replication of a realistic microgrid model. This model is extended to a large size realistic microgrid structure for the feasibility of control methodology. The variation in load profile, solar irradiance, and length of the line impedance is used to verify the realistic microgrid structure model. In Chap. “[Harmonics Reduction by Distributed Power Flow Control Using FACTS Devices in Power Supply](#)”, the modeling of several converters is evaluated for effective control strategy in the context of distributed power flow and reduced harmonics components. This section is concluded in Chap. “[Advances in Protection and Testing of Power Distribution Systems Within Emerging Markets](#)”, which presents an in-depth discussion on circuit breaker technologies as unfolded over the past few years. Therefore, the following Circuit Breaker technologies are presented: Moulded Case Circuit Breakers, Solid-State Circuit Breakers, Hybrid Circuit Breakers, and modern Power Monitoring Systems for application in Battery-Tripping Units. Additionally, a design of a low-cost circuit breaker testing system, as well as a mobile battery-tripping unit, is provided. The technologies are discussed in order to alleviate substation-tripping issues, which result in power distribution centers overloading and then burning or exploding.

## **Part: Access to Clean Energy for Sustainable Development, Power System Infrastructure, and Policy Options**

In Part, the question of access to clean energy for sustainable development is embraced alongside with central issues of power system infrastructure and policy options. Hence, a collection of four chapters is selected in this section. Chapter “[Green Energy for Sustainable Agriculture: Design and Testing of an Innovative Greenhouse with an Energy-Efficient Cooling System Powered by a Hybrid Energy System for Urban Agriculture](#)” presents the meteorological data analysis’ results, the proposed greenhouse design and operating system, the result of CFD simulations, and the field-based testing result of the validated cooling system. The result of CFD simulations has shown an even distribution of temperature and satisfactory air circulation in the proposed greenhouse structure. A strong emphasis has been put on the affordability, the simplicity of the technology, and the energy efficiency.

Chapter “[Comparative Study of Solar and Geothermal Renewable Energy Resources for Desalination of Seawater with Latest Case Studies](#)” provides a relative investigation of environmentally friendly power assets of solar and geothermal for desalination involving two contextual analyses for each and most recent advances and by thinking about the better with more efficiency, to prevent the upcoming scarcity of the world. In Chap. “[The Impact of Market-Based Policies on Access to Electricity and Sustainable Development in Sub-Saharan Africa](#)”, the six-step policy analysis technique is applied to probe the effectiveness of market-based policies (liberalization, privatization, unbundling, etc.) in enhancing access to electricity and agricultural development in rural communities of selected SSA countries. The effectiveness of market-based policies is evaluated against monopoly of state-owned electricity supply companies, known as vertically integrated or nationalization, on the basis of the attainment of sustainable development goals 7 and 2. Chapter “[Development of OTP Based Switch System for Power System Infrastructure Security and Personnel Safety](#)” concludes this section by introducing an identification of a comprehensive set of cybersecurity challenges and a need for security at multiple levels of the cyberphysical power system infrastructure security and personnel safety. The main challenge faced by electricity board is considered and solved using ICT.

## **Part: Concepts and Innovative Applications of Intelligent Systems and Technologies**

In this section, the concepts and innovative applications of intelligent systems and technologies are presented. Therefore, Chap. “[Artificial Neural Net Based Performance Index for Voltage Security Assessment](#)” introduces a novel, uncomplicated, and cursory process of transmission line outage analysis and evaluation for voltage security assessment is developed for real-time power system monitoring applications. The implied process uses the bus voltage magnitudes to develop artificial neural network models to monitor the bus voltages in the power network and provide outputs in binary form signifying the state of the power network. Chapter “[Multi-Class Classification of Power Network States Using Multi-Dimensional Neural Network](#)” proposes a simplified method for the classification of power network states which has been proposed based on the application of a multi-dimensional artificial neural network that has been employed for the prompt multi-class classification of power network states based on Fink and Carlsen’s approach. The whole setup for this study, including the power network and the artificial neural network models, was developed on the Simulink environment of MATLAB (R2021a). The system was simulated on the RT Lab OP-5600 simulator in real time. In Chap. “[Data Farming in a Smart Low Voltage Distribution System](#)”, the three fundamental elements of electricity data (current, voltage, and power factor) are discussed. These measurements can be obtained from a modified smart energy meter to develop data channels from all registers. To illustrate the concept of data farming using smart energy meters a

model in MATLAB that cultivates the data from existing electrical network. In Chap. “[Decision-Making Approach Using Fuzzy Logic and Rough Set Theory for Power Quality Monitoring Index of Microgrid](#)”, a design of an efficient decision-making approach based on the complex set of data and its analysis is presented. The main emphasis is on the complexity of data handling, data processing, and its dependent decision-making, the well-renowned and efficient fuzzy logic and Rough Set Theory (RST)-based methodology has been discussed in detail. Chapter “[Enabling Technologies in IoT: Energy, Sensors, Cloud Computing, Communication, Integration, Standards](#)” highlights several technologies of IoT, which includes energy sectors, sensors; cloud computing, communication, IoT integration and IoT protocol and standards. A wide-range of applications in the field of energy supply, transmission and distribution, and demand. The Internet of Things and cloud computing are related to each other. Due to the rapid growth of technology, there may be a need for storing, processing, and accessing large amounts of data. Chapter “[Secure Group Communication Among IoT Components in Smart Cities](#)” discusses the dynamic key management scheme for secure group communication among IoT components for constructing smart cities. The modern smart cities are developed with lot of IoT applications. The cost for constructing smart cities is mainly focusing on cost of the IoT applications. Chapter “[SCPS: An IoT Based Smart Car Parking System](#)” concludes this section by introducing the proposed SCPS (smart car parking system), which maps the parking slots into a dynamic real-time virtual map that updates the parking slot availability as the user parks their car, by sensing the existence of a vehicle in a parking area using IR sensors (infrared sensors). Therefore, this minimizes the unnecessary human interference that was required for the parking facility.

## **Part: Conclusions and Outlook**

This book concludes in Part wherein a comprehensive summary of the contributions and quintessence of this book is discussed in Chap. “[A Comprehensive Summary of the Contributions and the Quintessence of This Book](#)”.

# Contents

<b>Batteries and Energy Storage Technologies</b>	
<b>Assessing Control of Battery-Supercapacitor Hybrid Storage System in Photovoltaic Based DC Microgrid .....</b>	<b>3</b>
Mohd Alam, Kuldeep Kumar, and Viresh Dutta	
<b>Batteries, Energy Storage Technologies, Energy-Efficient Systems, Power Conversion Topologies, and Related Control Techniques .....</b>	<b>23</b>
Ngalula Sandrine Mubenga	
<b>Generation Expansion Planning Using Renewable Energy Sources with Storage .....</b>	<b>53</b>
K. Rajesh, A. Ramkumar, and S. Rajendran	
<b>Distributed Generation, Smart Grids and Supply Reliability</b>	
<b>A Smart Grid Ontology for Africa .....</b>	<b>105</b>
Isaac Kabuya Kamiba, Olasupo Ajayi, Antoine Bagula, and Kyandonghere Kyamakya	
<b>Smart Micro-Grid Energy Management with Renewable Energy Sources and Local SCADA .....</b>	<b>123</b>
J. Karra and K. Chandrasekhar	
<b>Improving Electricity Supply Reliability: A Case Study of Remote Communities of Limpopo in South Africa .....</b>	<b>135</b>
Vinny Motjoadi and Pitshou Ntambu Bokoro	
<b>Control of Static Converters, Power Quality, FACTS Devices and Hybrid Circuit Breaker Technology</b>	
<b>Control of Grid-Connected Voltage Source Converters During Unsymmetrical Faults .....</b>	<b>177</b>
Francis Mulolani	

<b>Power Quality Control of a PV-Assisted Realistic Microgrid Structure</b> .....	199
Jitender Kaushal and Prasenjit Basak	
<b>Harmonics Reduction by Distributed Power Flow Control Using FACTs Devices in Power Supply</b> .....	215
Rahul Kumar, Nitesh Tiwari, and Anurag Singh	
<b>Advances in Protection and Testing of Power Distribution Systems Within Emerging Markets</b> .....	257
Johan Venter	
<b>Access to Clean Energy for Sustainable Development, Power System Infrastructure, and Policy Options</b>	
<b>Green Energy for Sustainable Agriculture: Design and Testing of an Innovative Greenhouse with an Energy-Efficient Cooling System Powered by a Hybrid Energy System for Urban Agriculture</b> ....	301
Constant Kunambu Mbolikidolani, Venkatta Ramayya, B. Ngungu, and M. Yang'tshi	
<b>Comparative Study of Solar and Geothermal Renewable Energy Resources for Desalination of Seawater with Latest Case Studies</b> .....	331
Sujeeth Swami, B. P. Hemanth, Jaywant Kamal, M. Ravikumar, Krishna Pandit, and Harshal Kashyap	
<b>The Impact of Market-Based Policies on Access to Electricity and Sustainable Development in Sub-Saharan Africa</b> .....	343
Pitshou Ntambu Bokoro and Kyandoghere Kyamakya	
<b>Development of OTP Based Switch System for Power System Infrastructure Security and Personnel Safety</b> .....	377
D. Prasad, M. Gopila, G. Suresh, and M. Porkodi	
<b>Concepts and Innovative Applications of Intelligent Systems and Technologies</b>	
<b>Artificial Neural Net Based Performance Index for Voltage Security Assessment</b> .....	393
Shubhranshu Kumar Tiwary, Jagadish Pal, and Chandan Kumar Chanda	
<b>Multi-Class Classification of Power Network States Using Multi-Dimensional Neural Network</b> .....	413
Shubhranshu Kumar Tiwary, Jagadish Pal, and Chandan Kumar Chanda	
<b>Data Farming in a Smart Low Voltage Distribution System</b> .....	445
Noah Sindile Fakude and Kingsley A. Ogudo	

**Decision-Making Approach Using Fuzzy Logic and Rough Set Theory for Power Quality Monitoring Index of Microgrid** ..... 471  
Sahil Mehta, Jitender Kaushal, and Prasenjit Basak

**Enabling Technologies in IoT: Energy, Sensors, Cloud Computing, Communication, Integration, Standards** ..... 493  
S. N. Sangeethaa, P. Parthasarathi, and S. Jothimani

**Secure Group Communication Among IoT Components in Smart Cities** ..... 513  
P. Parthasarathi, S. N. Sangeethaa, and S. Nivedha

**SCPS: An IoT Based Smart Car Parking System** ..... 533  
Harikesh Singh, Animesh Pokhriyal, Anmol Sachan, and Meghna Saxena

**Conclusions and Outlook**

**A Comprehensive Summary of the Contributions and the Quintessence of This Book** ..... 545  
Kyandoghere Kyamakya and Pitshou Ntambu Bokoro

## About the Editors

**Kyandoghene Kyamakya, Dr.-Ing.** is currently Full Professor of Transportation Informatics and Deputy Director of the Institute of Smart Systems Technologies at the University of Klagenfurt in Austria. He is actively conducting research involving modeling, simulation, and test-bed evaluations for a series of concepts applied in various smart technical systems (e.g., intelligent transportation systems; smart logistics and supply chains; intelligent vehicles; active assisted living; robotics; smart grids; embedded systems; analog and mixed-signal circuits; etc.). His research does involve a series of fields such as nonlinear dynamics, systems science, data science, machine learning/deep learning, nonlinear image processing, neurocomputing, and telecommunications systems. He has co-edited more than 10 books, co-edited more than 10 special issues of SCOPUS-indexed journals, and has so far published more than 100 SCOPUS-indexed journal papers and some 100 conference papers. He also teaches and/or co-supervises some graduate students (Master's and Ph.D. levels) at the University of Kinshasa, (Polytechnic Faculty in DR-Congo), at ULPGL (Université Libre des Pays des Grand Lacs, Goma, DR-Congo), and at University of Johannesburg (South Africa). He is Editor and/or Editorial Board member of some renowned international journals, namely, *Sensors* (@ MDPI); *Mathematical Problems in Engineering* (@ Hindawi); *Frontiers in Robotics and AI* (@ Frontiers).

**Pitshou Ntambu Bokoro, Ph.D.** is Associate Professor with the Department of Electrical and Electronic Engineering Technology, University of Johannesburg, South Africa. He holds Senior Membership with the South African Institute of Electrical Engineers (SAIEE) as well as with the Institute of Electrical and Electronics Engineers (IEEE). He obtained a Bachelor's degree in Electrical Engineering from the Durban University of Technology, a Master's degree in Electrical Engineering from the University of Johannesburg, and a Ph.D. degree from the University of the Witwatersrand, Johannesburg. He has published over 133 research papers (which include over 63 journal articles and 70 conference papers) in high-quality journals and peer-reviewed conference proceedings. He authored a couple of book chapters in reputed books published by IGI-Global and IET. He serves as a Specialist Editor in Energy and Power Systems for the SAIEE Africa Research Journal (ARJ). He has also

performed several reviews for various prestigious journals, including IEEE Transactions on Power Delivery, IEEE Access, International Journal of Electrical Power and Energy systems (IJEPES/Elsevier), Advances in Electrical and Electronic Engineering (AEEE), International Transactions on Electrical Energy Systems (ITEES), Materials Today Proceedings (Elsevier), Journal of Engineering Design and Technology (JEDT), Engineering Failure Analysis (Elsevier), Power Engineering Letters, Measurement (Elsevier), Journal of Electrical Engineering and Technology (EETE), Journal of Energy in Southern Africa (JESA), Electric Power Systems Research Journal, Electronics MDPI, Energies MDPI, Microelectronics Reliability, Sustainability MDPI. He has supervised to completion over 18 postgraduate students (which include Master's and doctoral students). His major research interests include renewable energy systems, power systems, power system reliability, distributed generation, surge arresters, insulation and dielectrics, power quality, condition monitoring, microgrids, Internet of Things, and virtual sensing applications.



# **Batteries and Energy Storage Technologies**

# Assessing Control of Battery-Supercapacitor Hybrid Storage System in Photovoltaic Based DC Microgrid



Mohd Alam, Kuldeep Kumar, and Viresh Dutta

**Abstract** Photovoltaic (PV) energy in a DC microgrid enables variable power generation due to change in solar irradiation and ambient temperature. Hence, there is an essential requirement for an energy storage medium to tackle this issue. Battery is a primarily energy storage medium than can be used to overcome the intermittency involved with PV. However, battery alone is insufficient if there is a transient variation in the load demand. Thus, hybrid energy storage system i.e., battery and supercapacitor (SC) have strong application in a DC microgrid to balance the power flow between renewable energy source i.e., PV and load. In this chapter, a power sharing control strategy between PV and load demand in DC microgrid is investigated. This control strategy commands the MPPT DC-DC converter, and bidirectional DC-DC converters associated with battery and SC. By employing this control strategy, the reference currents for both the energy storage mediums are calculated such that the sudden variation in load demand can be met by SC whereas the average load demand met by the battery. The distribution of power between battery and SC is facilitated by utilizing a low pass filter such that the peak current is transferred to the SC whereas the average current is taken care by battery. The simulation results shows that this control strategy provides the effective power sharing between PV and hybrid energy storage medium i.e., battery and SC.

**Keywords** Photovoltaic · Battery · DC microgrid · Hybrid energy storage · Supercapacitor

---

M. Alam (✉) · K. Kumar · V. Dutta  
Photovoltaic Laboratory, Department of Energy Science and Engineering, Indian Institute of Technology Delhi, Delhi 110016, India  
e-mail: [gbpec.mohd.alam@gmail.com](mailto:gbpec.mohd.alam@gmail.com)

© The Author(s), under exclusive license to Springer Nature Switzerland AG 2024  
K. Kyamakya and P. N. Bokoro (eds.), *Recent Advances in Energy Systems, Power and Related Smart Technologies*, Studies in Systems, Decision and Control 472,  
[https://doi.org/10.1007/978-3-031-29586-7\\_1](https://doi.org/10.1007/978-3-031-29586-7_1)

## Abbreviations

### *Nomenclature*

A	Constant
$A_s$ (m <sup>2</sup> )	Total area of PV array
Ah <sub>res</sub>	Ampere hours restored in the battery cell
$a_{PV}$	Modified ideality factor
$a_{PVst}$	Modified ideality factor at standard conditions
$C_O$ (C <sub>O</sub> )	Constant capacitance
$C_{rat}$	Charge capacity of battery cell
$C_{real}$ (F)	Supercapacitor real capacitance
$C_{diff}$ (F)	Supercapacitor differential capacitance
$C_{10}$	C rating
$E_g$ (eV)	Energy band gap
$E_{gst}$ (eV)	Energy band gap in reference conditions
$I_{bc}$ (A)	Battery cell current
$I_{bc10}$ (A)	Battery cell current at C = 10
$I_{bat}$ (A)	Battery bank current
$i_c$ (A)	Current through the real capacitance
$i_{EPR}$ (A)	Current through effective parallel resistance
$I_r$ (A)	Diode reverse saturation current for module
$I_{rst}$ (A)	Diode reverse saturation current standard conditions for module
$I_L$ (A)	Photogenerated current
$I_{Lst}$ (A)	Photogenerated current in standard conditions for module
$I_{mst}$ (A)	Maximum current of the module
$i_{sc}$ (A)	Supercapacitor current
$I_{scst}$ (A)	Short circuit current in standard conditions for module
$I_{PV}$ (A)	Array current
$J$ (A/cm <sup>2</sup> )	Current density
$J_M$ (A/cm <sup>2</sup> )	Maximum current density
$k$ ( $= 1.3807 \times 10^{-23}$ J/K)	Boltzmann constant
$N_{cs}$	Number of battery cells in series
$N_{cp}$	Number of battery cells in parallel
$N_{bs}$	Number of batteries in series
$N_{bp}$	Number of batteries in parallel
$n_s$	Number of solar cells in series
$N_{PV}$	Number of photovoltaic modules
$P_{bat}$ (W)	Battery power
$P_{PV}$ (W)	PV power
$P_L$ (W)	Load demand
$q$ (C)	Electron charge

$R_{sh}(\Omega)$	Shunt resistance
$R_s(\Omega)$	Series resistance
$R_{ohm}(\Omega)$	Ohmic resistance
$R_M(\Omega)$	Membrane resistance
$R_{shst}(\Omega)$	Shunt resistance at standard test conditions
$R_{sst}(\Omega)$	Series resistance at standard test conditions
$SOC_{bc}$	State of charge of battery cell
$SOC_{bco}$	Battery state of charge at reference condition
$S_{Tst}(1KW/m^2)$	Solar irradiation in standard condition
$S_T(KW/m^2)$	Actual solar irradiation
t	Time
$T_c(K)$	PV module temperature
$T_{amp}(K)$	Ambient temperature
$T_{cst}(298K)$	PV cell temperature standard conditions
$\Delta T$	Temperature difference between the battery and reference condition ( $T = 298 K$ )
z(= 2)	Numbers of electrons transferred
$V_{bc}(V)$	Battery cell voltage
$V_c(V)$	Cell voltage
$V_{EC}(V)$	Final charge overvoltage
$V_{PV}(V)$	PV array voltage
$V_{mst}(V)$	Maximum voltage of module
$V_{ocst}(V)$	Open circuit voltage of module
$V_{bat}(V)$	Battery voltage
$V_{SC}(V)$	Supercapacitor voltage

### ***Greek Symbols***

$\alpha_i(A/K)$	Temperature coefficient of short circuit current
$\eta_b$	Charging efficiency of battery cell
$\eta_c(\%)$	Charging efficiency of battery
$\eta_d(\%)$	Discharging efficiency of battery
$\lambda$	Stoichiometric ratio
$\gamma$	Constant
$\tau$	Battery constant
$\mu$	Coefficient that is dependent on applied technology

### ***Abbreviations***

EPR	Effective parallel resistance
ESR	Effective series resistance

PV	Photovoltaic
MPPT	Maximum power point tracking
PMS	Power management strategy
SC	Supercapacitor

## 1 Introduction

The Paris Agreement 2016 sets out a global framework to avoid dangerous climate change by limiting global warming to well below 2 °C. It also aims to strengthen countries ability to deal with the impacts of climate change [1, 2]. Renewable energy sources (RES) can be deployed to lower down the greenhouse gas emissions [3, 4]. RES i.e. photovoltaic (PV), wind etc. are intermittent in nature thus the requirement of suitable energy storage medium arises [5, 6]. In recent years, microgrid comprising RES and energy storage mediums have shown strong application to cater the electricity demand [7–9]. Several energy storage mediums i.e. battery, hydrogen etc. have shown useful application in the microgrid [10, 11]. These energy storage technologies have different feature that can be characterized based on energy and power densities, charge–discharge cycle, response time, efficiency and lifetime as shown in Table 1 [12]. Single energy storage medium is not suitable for all the required applications. Therefore, hybridization of energy storage mediums provides an attractive solution [13, 14]. Battery has less power density whereas supercapacitor (SC) has higher power density. Therefore, combination of battery and SC provides an attractive solution for the microgrid application with improved battery life [15, 16].

In literature, several topologies of hybrid battery-SC have been proposed for various applications to exploit the advantages associated with each energy storage medium [17]. Battery-SC hybrid system can be configured in active, passive or hybrid mode [18]. In passive mode, storage mediums are directly connected to the DC bus whereas in active mode, storage mediums are connected to the DC bus via power electronics converters (bidirectional DC-DC converters). The drawbacks associated with passive mode are poor voltage regulation and less stability. These drawbacks can be mitigated by employing the active mode topology in which bidirectional DC/DC converters are used with battery and SC for effective charging and discharging. For the active mode configuration, there is a requirement of control strategy for proper power sharing between the different energy storage mediums [19]. In previous studies, different control strategies have been proposed. Jing et al. [20] provided a review of hybrid battery-SC energy storage system for standalone DC microgrid application. They have analyzed various topologies of battery-SC hybrid system such as passive, semi active and fully active. It was found that fully active strategy provides more flexibility and improved battery life. In another study, Jing et al. [21] proposed a multi-level hybrid storage topology and its power management strategy to lower down the charge/discharge stress on the battery energy storage medium. The

**Table 1** Comparison between different energy storage mediums

Technology	Energy density	Volumetric energy density (Wh/L)	Power density (W/kg)	Capital cost (€ kW)	Response time	Self-discharge (per day)	Life-time (years)	Overall efficiency	Advantages	Disadvantages
Lead-acid	30–50	80–90	75–300	50–150	2 h	0.1–0.3%	5–10	0.70–0.90	Capital cost in low	Efficiency is low
Lithium-ion	160–200	250–670	150–315	350–700	15 min to hours	0.1–0.3%	5–15	Up to 0.97	High efficiency, low maintenance	Ageing
Super-capacitor	0.1–5	1–10	800–23500	200–1000	ms-10 min	20–40%	5–8	0.85–0.98	High power quality, high durability, high efficiency, high power density	Low energy density

results shows that the proposed topology can mitigate the stress on the battery with minimum effect on its health. Song et al. [22] have done an economic evaluation of battery-SC hybrid system for electric vehicle application. They have found that total cost (capital, electricity and battery replacement costs) associated with hybrid storage system for 10 years operation is  $\approx 25.9\%$  less than the battery storage system. Hybrid energy storage system is a cost-effective solution in comparison to the battery storage system. Jing et al. [23] performed a study on hybrid storage system for standalone PV application. They considered different combinations of storage medium viz. battery only, passive hybrid storage system, semi active hybrid storage system, and three-level hybrid storage system. They have found that three level hybrid storage (lead-acid, li-ion and SC) provides an optimal solution for standalone PV system application. Wang et al. [24] performed a signal hardware-in-loop simulation to verify the hybrid storage medium control strategy. Chong et al. [25] proposed a particle swarm optimization-based learning control strategy for hybrid battery-SC hybrid system. The results shows that proposed strategy utilizes the SC optimally and power fluctuation, peak power demand of battery reduces which increases the battery life span. Zhang et al. [26] conducted an experimental study on semi active hybrid storage medium for electric vehicle application. Several other studies have been done on the hybrid storage medium for electric vehicle applications [27–29].

Ravada et al. [30] proposed a renewable sources-based grid connected system for hybrid energy storage mediums. The integration of hybrid storage with renewables have less complexity in the control circuit. Pinthurat et al. [31] proposed a decentralized communication-free control strategy for distributed energy storage devices for DC datacenter microgrid. In this decentralized control technique, they have used a virtual resistance-based control through which low frequency component of load current is transferred to battery whereas the high frequency component is transferred to the SC by employing a virtual capacitive droop control. An energy management strategy for PV-battery-SC has also been proposed in other studies [32, 33].

From the above discussion it is clear that hybrid storage system incorporating battery and SC have shown strong application in electric vehicles and renewable sources based microgrid. Present study is in line of previous studies, in which a power management strategy is investigated for DC microgrid to share the power among the PV power generator, and battery-SC hybrid storage medium. A mathematical modelling of the DC microgrid components such as PV, battery and SC has also been performed. The main objective of this study is that the sudden variation in the load demand can be met by SC whereas the average load demand is taken care by the battery energy storage. This objective can be achieved by employing a proper control strategy in which the load current is sensed and passed through a low-pass filter. The average component of the load current after passing through the low-pass filter becomes the reference current for battery whereas the transient component of load current becomes the reference for the SC. Therefore, proper power sharing among the PV, battery, and SC can be achieved by sensing the load current.

## **2 System Description and Modelling of Energy Source, and Storage Mediums**

This section describes the system topology and modelling of PV power generator, and battery-SC hybrid energy storage medium in detail.

### ***2.1 System Description***

The studied PV based DC microgrid with hybrid battery-SC energy storage medium is shown in Fig. 1. In this microgrid, PV acts as a main power generator and generates electricity. As the generated power from PV is intermittent in nature; therefore, in a standalone DC microgrid, energy storage medium is used to overcome this problem. Battery and SC energy storage medium are used in the microgrid to take care of the low and high frequency components of the load power, respectively. PV power is primarily used to meet the load demand. If there is a surplus electricity, then it is used to charge the battery bank and SC. If PV is in deficit, then battery and SC are discharged to cater the load demand. PV source is connected to the DC link capacitor via a maximum power point tracking (MPPT) enabled DC-DC converter whereas battery and SC are connected to the DC link capacitor via the bidirectional DC-DC converters. In order to ensure the proper power sharing among PV power generator and energy storage mediums, a proper power management strategy (PMS) is required. The PMS senses the PV, load, battery, and SC currents and generates the appropriate reference current signals for the battery and SC. These generated reference signals ensure the proper switching of energy storage converters.

### ***2.2 Modelling of PV Power Generator and Energy Storage Mediums***

A mathematical modelling of the PV power generator, battery, and SC energy storage medium has been performed using MATLAB simulation tool. A brief discussion of the mathematical modelling and working of various power sources is given as follows:

#### **Photovoltaic Generator**

Solar PV generator converts the sunlight directly into electricity. The generated electricity depends on the incident solar irradiation and temperature. The required PV power can be obtained by making the series and parallel combination of PV modules. PV power varies with the solar radiation therefore maximum power can be extracted by employing MPPT. The various equations involved in the modelling of PV generator are given below.



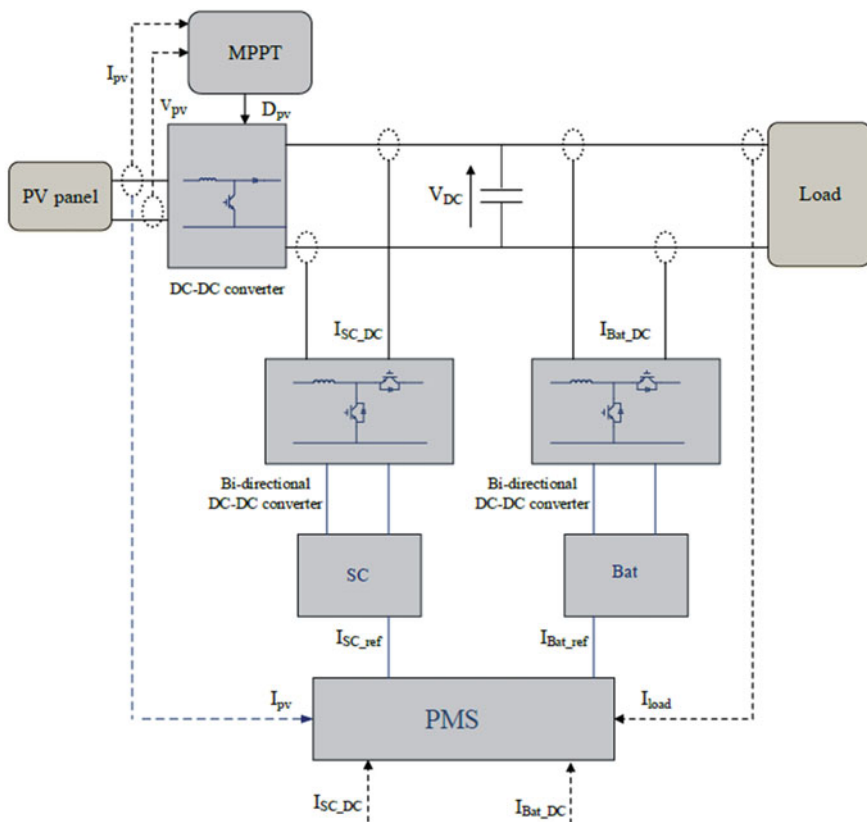


Fig. 1 PV generator-based DC microgrid with battery-SC hybrid energy storage

The relationship between PV voltage and current can be expressed as below [34, 35]:

$$I_{PV} = I_L - I_r \left[ \exp\left(\frac{V_{PV} + I_{PV}R_S}{a_{PV}}\right) - 1 \right] - \left[ \frac{V_{PV} + I_{PV}R_S}{R_{sh}} \right] \quad (1)$$

where  $I_L$  is photogenerated current and can be formulated as:

$$I_L = (I_{Lst} + \alpha_i(T_c - T_{cst})) \frac{S_T}{S_{Tst}} \quad (2)$$

$I_r$  is diode reverse saturation current and can be expressed as

$$I_r = I_{rst} \left(\frac{T_c}{T_{cst}}\right)^3 \exp\left[\frac{1}{k} \left(\frac{E_{gst}}{T_{cst}} - \frac{E_g}{T_c}\right)\right] \quad (3)$$

$\alpha_{PV}$  is modified ideality factor, given as:

$$\alpha_{PV} = \frac{\gamma K T_C}{q} \quad (4)$$

The value of constant

$$\alpha_{PV} = \alpha_{PVst} \frac{T_C}{T_{Cst}} \quad (5)$$

The shunt resistance can be calculated by following relationship:

$$R_{sh} = R_{shst} \frac{S_T}{S_{Tst}} \quad (6)$$

The PV power can be expressed as given below:

$$P_{PV} = N_{PV} V_{PV} I_{PV} \quad (7)$$

### Battery Energy Storage

Battery is an electrochemical storage system in which electrical energy is stored into chemical energy. In battery, there is a chemical reaction between the reactants which generates electricity in the form of voltage and current. The required voltage and current in the batteries can be achieved using the series-parallel connection of the cells. In lead-acid battery, lead-oxide (PbO<sub>2</sub>) and lead (Pb) are used in cathode and anode, respectively. Sulfuric acid (H<sub>2</sub>SO<sub>4</sub>) is used as an electrolyte in the lead-acid battery. Lead-acid battery has excellent energy density, charge retention capacity and fast response. The various equations involved in the modelling of battery storage medium are given as follows:

The equations involved during battery discharging are given as follows:

The battery cell voltage during discharging can be formulated as [36]:

$$V_{bc} = [2.085 - 0.12(1 - SOC_{bc})] - \frac{I_{bc}}{C_{10}} \left( \frac{4}{1 + I_{bc}^{1.3}} + \frac{0.27}{SOC_{bc}^{1.5}} + 0.02 \right) (1 - 0.007 \Delta T) \quad (8)$$

where,

$SOC_{bc}$  is battery state of charge during discharging and can be given as below:

$$SOC_{bc} = 1 - \frac{I_{bc}^t}{C_{rat}} \quad (9)$$

$V_{bc}$  is battery cell voltage during charging and can be given as:

$$V_{bc} = [2 - 0.16SOC_{bc}] + \frac{I_{bc}}{C_{10}} \left( \frac{6}{1 + I_{bc}^{0.86}} + \frac{0.48}{(1 - SOC_{bc})^{1.2}} + 0.036 \right) (1 - 0.025\Delta T) \quad (10)$$

Battery state of charge during charging can be given as:

$$SOC_{bc} = SOC_{bc0} + \frac{\eta_b I_{bc} t}{C_{rat}} \quad (11)$$

The charging efficiency of cell can be formulated as:

$$\eta_c = 1 - \exp\left[ \frac{20.73}{\frac{I_{bc}}{I_{bc10} + 0.55}} (SOC_{bc} - 1) \right] \quad (12)$$

The battery cell overvoltage can be given as:

$$V_{bc} = [2 - 0.16SOC_{bc}] + \frac{I_{bc}}{C_{10}} \left( \frac{6}{1 + I_{bc}^{0.86}} + \frac{0.48}{(1 - SOC_{bc})^{1.2}} + 0.036 \right) (1 - 0.025\Delta T) \quad (13)$$

The battery over voltage due to gassing effect is given as below:

$$V_G = \left[ 2.24 + 1.97 \ln \left( 1 + \frac{I_{bc}}{C_{10}} \right) \right] (1 - 0.002\Delta T) \quad (14)$$

The final overvoltage of the battery can be formulated as:

$$V_{EC} = \left[ 2.45 + 2.011 \ln \left( 1 + \frac{I_{bc}}{C_{10}} \right) \right] (1 - 0.002\Delta T) \quad (15)$$

The battery bank voltage and current can be given as below:

$$V_{bat} = N_{cs} N_{bs} V_{bc} \quad (16)$$

$$I_{bat} = N_{cp} N_{bp} I_{bc} \quad (17)$$

The battery bank power can be formulated as follows:

$$P_{bat} = V_{bat} I_{bat} \quad (18)$$

### Supercapacitor Energy Storage

A SC is a type of capacitor which have the capacitance value much higher than the other capacitors. The energy per unit volume of supercapacitor is 10 to 100 times more than the electrolytic capacitors. It consists of two carbon-based electrodes, an

electrolyte and a separator. The charge accumulates on the electrode surface when voltage is applied. Due to the attraction of unlike charges, ions in the electrolyte solution diffuse across the separator into the pores of the electrode of opposite charge. Thus, a double layer of charge is produced at each electrode. These double layers, coupled with an increase in surface area and a decrease in the distance between electrodes, allow SCs to achieve higher energy densities than conventional capacitors. The various equations involved in the modelling SC are given as follows [37]:

The real capacitance of supercapacitor can be given as:

$$C_{real} = C_0 + \mu.v_c \quad (19)$$

The current through the real capacitance can be formulated as:

$$i_c = \frac{dq}{dt} = \frac{d(C_{real}.v_c)}{dt} = \frac{d((C_0 + \mu.v_c).v_c)}{dt} = (C_0 + 2\mu.v_c)\frac{dv_c}{dt} \quad (20)$$

The differential capacitance of supercapacitor can be given as:

$$C_{diff} = C_0 + 2\mu.v_c \quad (21)$$

The real capacitor current is given as:

$$i_c = C_{diff}.\frac{dv_c}{dt} \quad (22)$$

The supercapacitor current and voltage can be formulated as:

$$i_{sc} = i_c + i_{EPR} = C_{diff}.\frac{dv_c}{dt} + \frac{v_c}{EPR} \quad (23)$$

$$v_{sc} = i_{sc}.ESR + v_c \quad (24)$$

The effective series resistance of supercapacitor can be given as:

$$ESR = \frac{\Delta v_{sc}}{\Delta i_{sc}} \quad (25)$$

The values of various parameters involved in the modelling of PV power generator, battery, and SC modelling are provided in Tables 2, 3, and Tables 4 (see Appendix).

### 3 PV-Battery-Supercapacitor Control Strategy

Control of the studied DC microgrid is required to ensure the maximum utilization of PV electricity and energy storage mediums. As the battery-SC hybrid energy storage is used in the microgrid, the control of both the energy storage mediums becomes essential for the proper working of isolated microgrid. PV electricity is primarily used to meet the load demand, and if there is a surplus electricity than it is used to charge the battery bank. If battery is fully charged than PV electricity is used to charge the supercapacitor. The control of hybrid battery-SC bidirectional DC-DC converters is shown in Fig. 2.

A PMS to ensure the proper power sharing between PV and hybrid energy storage mediums is developed using MATLAB Simulink tool. If there is a difference in PV generated current and load current, then there is a deviation in DC bus voltage from its nominal value. The difference in measured DC bus voltage and reference voltage is given to the proportional-integral (PI) controller. This PI controller generated a reference current signal equivalent to the load current. The developed PMS generates the reference current signals for battery and SC based on the received load current signal. Then, the reference current signals are compared with the actual value of the battery and SC current. The difference in the current signals after passing through a PI controller gives the optimum duty ratio to the battery and SC bidirectional DC-DC converters. In case that the PV power is equal to the load power than neither battery nor SC will be discharged and will not provide any power to the load. If the power generated from PV is less than the load power, and there is no transient in the load current then the deficit power is fed from the battery only. In this case, the SC will not provide any power to the load. However, if there is a transient variation in load demand, then the required amount of power is fed from the supercapacitor.

The detailed control strategy of battery-SC hybrid system is shown in Fig. 3. As discussed above, the reference load current is generated by comparing the actual DC bus voltage with the reference voltage. This reference current is passed through a low

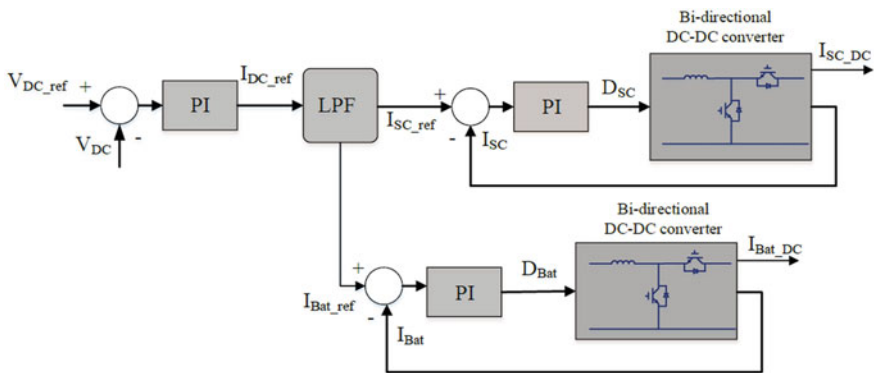
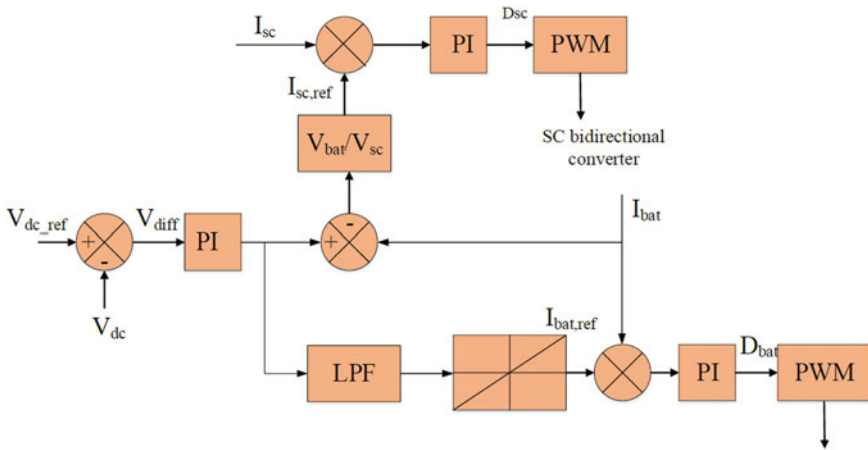


Fig. 2 Control algorithm of battery-SC bidirectional DC/DC converters



**Fig. 3** Control algorithm of hybrid battery-supercapacitor system

pass filter. The high frequency/or transient component of current is used to generate a reference current for SC whereas the low frequency/or average component of load current is used to generate a reference signal for battery current. These generated reference current signals are then compared with the actual value of current such that the duty ratios of battery-SC bidirectional DC-DC converters are modified to ensure the proper power sharing among the hybrid energy storage mediums.

### 4 Results and Discussion

This section describes the working of different operating modes of PV-battery-SC combination for the standalone DC microgrid application. The DC microgrid system has been implemented in the MATLAB/SIMULINK environment. The power sharing between the PV, battery, and SC to provide the changing load demand is shown in the Fig. 4. Initially, the PV and load power are almost same therefore, there is a perfect power balance in the system and no excess/deficit power is available. In this case, battery/SC are neither charged nor discharged. However, at time  $\approx 0.51$  s, the PV power and load demand suddenly increases, therefore this transient excess power is used to charge the SC. However, as per the control logic, the function of SC is only to absorb and/or provide the transient variation in power; therefore, after some time, battery is charged from the excess power. At  $t = 0.91$  s, the PV power is suddenly decreases therefore, SC discharges first to provide the transient power balance. However, after some time, battery takes over the SC and starts discharging to meet the deficit power demand.

The power sharing between the PV, battery and SC during constant load demand is shown in Fig. 5. Initially, the load power and PV power are almost same therefore,

**Fig. 4** Power sharing among the PV, battery, and SC with changing load

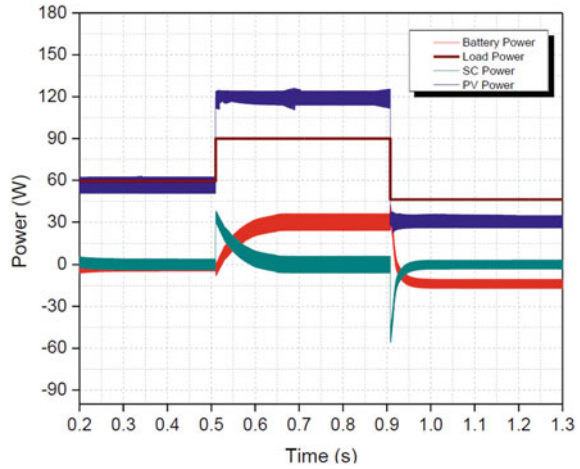
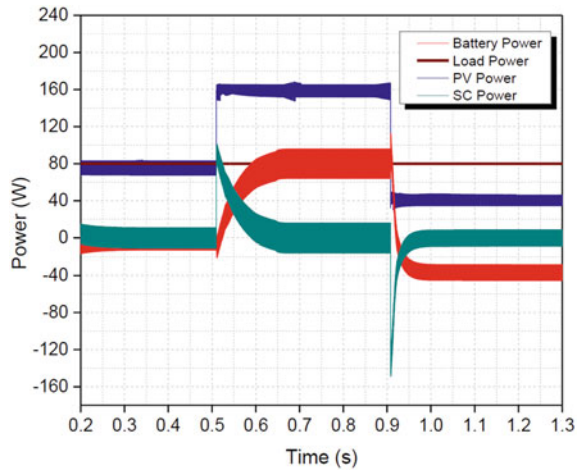


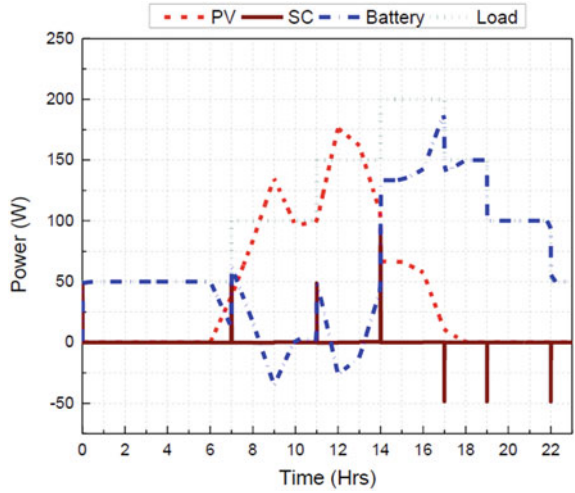
**Fig. 5** Power sharing among the PV, battery, and SC with changing load



SC and battery are inactive. However, at a time  $\approx 0.51$  s, PV power suddenly increases, therefore, to balance the demand and supply the SC starts charging. However, after some time, the battery takes over the SC and starts charging from surplus PV power. At time  $\approx 0.91$  s, the PV power suddenly decreases therefore, as per the control algorithm, the SC discharges first to provide the transient mismatch between supply and demand. Later on, battery starts discharging to provide the deficit load demand and SC stops discharging.

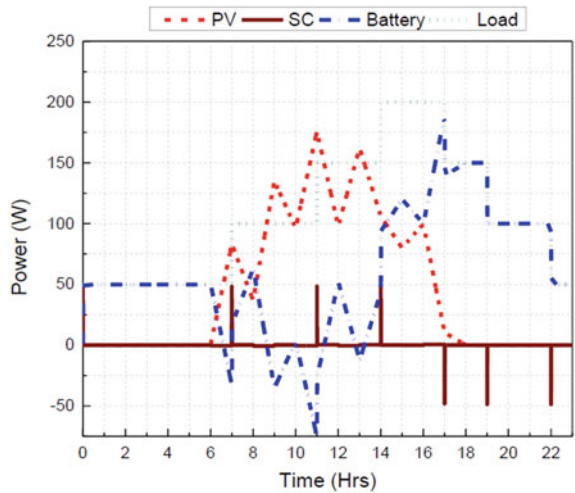
The power sharing between the PV, battery, and SC to meet the load demand during a sunny day is shown in Fig. 6. During the initial hours, PV power is not available, therefore, the load demand is met by the battery. When PV power is available at time  $t = 06:00$  h, then PV power is used to meet the load demand along with the battery. At  $t = 07:00$  h, there is a transient variation in the load demand therefore SC is

**Fig. 6** Power sharing among the PV, battery and SC during a sunny day



discharged to provide this sudden change in power. Further, PV power is higher than the load demand and the excess power is utilized to charge the battery. At  $t = 17:00$  h, the load is suddenly decreased, therefore, the battery is used to charge the SC along with meeting the required load demand. The power sharing between the PV, battery, and SC to meet the load demand during a partial cloudy day is shown in Fig. 7. The sudden increase and decrease in the load demand is facilitated by discharging and charging of the SC, respectively.

**Fig. 7** Power sharing among the PV, battery and SC during a partial cloudy day





## 5 Conclusion

In this study, the hybridization of battery-supercapacitor energy storage medium in a photovoltaic generator-based DC microgrid is provided to meet the required load demand. A control algorithm and power management strategy to ensure the proper power sharing among the photovoltaic generator and energy storage mediums is investigated. The power management strategy addresses the issues regarding transient power sharing among the hybrid energy storage mediums along with photovoltaic generator. The sudden or transient load demand is met by supercapacitor energy storage while the average load power is provided by the battery storage medium. The simulation results shows the effectiveness of the investigated power management strategy for DC microgrid application having hybrid energy storage mediums.

**Conflict of Interest** None.

## Appendix

See Tables 2, 3, 4.

**Table 2** Parameters used in the PV modelling

Parameters	Value
Module short circuit current (A)	7.6
Module open-circuit voltage (V)	21.6
Temperature in standard condition (K)	298
Voltage at maximum power point (V)	17.2
Current at maximum power point (A)	7.3
Temperature coefficient of short circuit current (A/K)( $\alpha_i$ )	0.05%
No. of modules in series	2
One module area (m <sup>2</sup> )	0.98
Nominal operating condition temperature (K)	313
Silicon band gap Egst (eV)	1.121
Eg	$E_g = E_{gst}[1 - 0.0002677(T_c - T_{ref})]$

**Table 3** Parameters used in the battery modelling

Parameters	Value
Number of batteries in series (Nbs)	1
Number of batteries in parallel (Nbp)	1
I (at C <sub>10</sub> )	15
Battery terminal voltage	12 V
Battery capacity	17 Ah

**Table 4** Parameters used in the SC modelling

Parameters	Value
Terminal voltage (V <sub>sc</sub> )	30 V
Capacitance	22 F

## References

- Zhang, Y., Qing-Chen C., Qiu-Hong Z., and Lei H.: The withdrawal of the U.S. from the Paris Agreement and its impact on global climate change governance. *Adv. Clim. Chang. Res.*, **8**(4): 213–219 (2017)
- Zhang, H., Han-Cheng D., Hua-Xia L., and Wen-Tao W.: U.S. withdrawal from the Paris Agreement: Reasons, impacts, and China’s response. *Adv. Clim. Chang. Res.*, **8**(4): 220–225 (2017)
- Ahiduzzaman, M., A.K.M. Sadrul I.: Greenhouse gas emission and renewable energy sources for sustainable development in Bangladesh. *Renew. Sustain. Energy Rev.* **15**(9), 4659–4666 (2011)
- Ma, T., Hongxing, Y., Lin, L.: Development of hybrid battery–supercapacitor energy storage for remote area renewable energy systems. *Appl. Energy* **153**, 56–62 (2015)
- Kamal, M.D., Imtiaz, A.: Modeling and assessment of economic viability of grid-connected photovoltaic system for rural electrification. *Energy Sources, Part A: Recovery, Utilization, and Environmental Effects*. (2021). <https://doi.org/10.1080/15567036.2021.1905108>
- Sharma, A., Kolhe, M.L.: Impacts of electricity pricing on techno-economic performance of photovoltaic-battery centered microgrid. *Energy Sources, Part A: Recovery, Utilization, and Environmental Effects* (2021). <https://doi.org/10.1080/15567036.2021.1905112>
- Razmjoo, A., Afshin, D.: Developing various hybrid energy systems for residential application as an appropriate and reliable way to achieve Energy sustainability. *Energy Sources, Part A: Recovery, Utilization, and Environmental Effects*. **41**(10), 1180–1193 (2019). <https://doi.org/10.1080/15567036.2018.1544996>
- Wang, Y., Fang, L., Haiyang, Y., Yudong, W., Chengyuan, Q., Jiale, Y., Fuhao, S.: Optimal operation of microgrid with multi-energy complementary based on moth flame optimization algorithm. *Energy Sources, Part A: Recovery, Utilization, and Environmental Effects* **42**(7), 785–806 (2020). <https://doi.org/10.1080/15567036.2019.1587067>
- Alam, M., Kuldeep, K., Viresh, D.: Design and Economic Evaluation of Low Voltage DC Microgrid based on Hydrogen Storage. *Int. J. Green Energy* **18**(1), 66–79 (2021). <https://doi.org/10.1080/15435075.2020.1831506>
- Alam, M., Kuldeep K., and Viresh D.: Design and analysis of fuel cell and photovoltaic based 110 V DC microgrid using hydrogen energy storage. *Energy Storage* (2019). <https://doi.org/10.1002/est2.60>
- Alam, M., Kuldeep, K., Saket, V., Viresh, D.: Renewable sources based DC microgrid using hydrogen energy storage: Modelling and experimental analysis. *Sustainable Energy Technol. Assess.* **42**, 100840 (2020)

12. Al-Shaqsi, A.Z., Sopian, K., Al-Hinai, A.: Review of energy storage services, applications, limitations, and benefits. *Energy Rep.* **6**, 288–306 (2020). <https://doi.org/10.1016/j.egy.2020.07.028>
13. Yang, B., Jingbo, W., Xiaoshun, Z., Junting, W., Hongchun, S., Shengnan, L., Tingyi, H., Chaofan, L., Tao, Y.: Applications of battery/supercapacitor hybrid energy storage systems for electric vehicles using perturbation observer based robust control. *J. Power Sources* **448**, 227444 (2020)
14. Lahyani, A., Riadh, A., Ahmed, C.A., Ali, S., Pascal, V.: Reinforcement learning based adaptive power sharing of battery/supercapacitors hybrid storage in electric vehicles. *Energy Sources, Part A: Recovery, Utilization, and Environmental Effects.* (2020). <https://doi.org/10.1080/15567036.2020.1849456>
15. Kotra, S., Mahesh, K.M.: Design and stability analysis of DC microgrid with hybrid energy storage system. *IEEE Transactions on Sustainable Energy* **10**(3), 1603–1612 (2019). <https://doi.org/10.1109/TSTE.2019.2891255>
16. Jia, H., Yunfei, M., Yan, Q.: A statistical model to determine the capacity of battery–supercapacitor hybrid energy storage system in autonomous microgrid. *Int. J. Electr. Power Energy Syst.* **54**, 516–524 (2014)
17. Zimmermann, T., Peter, K., Markus, H., Max, F.H., Simon, P., Andreas, J.: Review of system topologies for hybrid electrical energy storage systems. *Journal of Energy Storage* **8**, 78–90 (2016)
18. Kuperman, A., Ilan, A.: Battery–ultracapacitor hybrids for pulsed current loads: A review. *Renew. Sustain. Energy Rev.* **15**(2), 981–992 (2011)
19. Choi, M., Seong, K., Seung, S.: Energy management optimization in a battery/supercapacitor hybrid energy storage system. *IEEE Transactions on Smart Grid* **3**(1), 463–472 (2012). <https://doi.org/10.1109/TSG.2011.2164816>
20. Jing, W., Chean, H.L., Wallace, W., Wong, M.L.D.: Battery-supercapacitor hybrid energy storage system in standalone DC microgrids: a review. *IET Renew. Power Gener.* **11**, 461–469 (2017)
21. Jing, W., Chean, H.L., Wallace, S.H.W., M.L. Dennis W.: Dynamic power allocation of battery-supercapacitor hybrid energy storage for standalone PV microgrid applications. *Sustainable Energy Technol. Assess.* **22**, 55–64 (2017)
22. Song, Z., Jianqiu, L., Jun, H., Heath, H., Minggao, O., Jiuyu, D.: The battery-supercapacitor hybrid energy storage system in electric vehicle applications: A case study. *Energy* **154**, 433–441 (2018)
23. Jing, W., Chean, H.L., Wallace, S.H.W., M.L. Dennis W.: A comprehensive study of battery-supercapacitor hybrid energy storage system for standalone PV power system in rural electrification. *Appl. Energy* **224**, 340–356 (2018)
24. Wang, X., Dongmin, Y., Simon, L.B., Zhengming, Z., Peter, W.: A novel controller of a battery-supercapacitor hybrid energy storage system for domestic applications. *Energy Build.* **141**, 167–174 (2017)
25. Chong, L.W., Yee, W.W., Rajprasad, K.R., Dino, I.: An adaptive learning control strategy for standalone PV system with battery-supercapacitor hybrid energy storage system. *J. Power Sources* **394**, 35–49 (2018)
26. Zhang, Q., Gang, L.: Experimental study on a semi-active battery-supercapacitor hybrid energy storage system for electric vehicle application. *IEEE Trans. Power Electron.* **35**(1), 1014–1021 (2020)
27. Cabrane, Z., Mohammed, O., Mohamed, M.: Analysis and evaluation of battery-supercapacitor hybrid energy storage system for photovoltaic installation. *Int. J. Hydrogen Energy* **41**(45), 20897–20907 (2016)
28. Shen, J., Serkan, D., Alireza, K.: Optimization of sizing and battery cycle life in battery/ultracapacitor hybrid energy storage systems for electric vehicle applications. *IEEE Trans. Industr. Inf.* **10**(4), 2112–2121 (2014)
29. Mesbahi, T., Patrick, B., Nassim, R., Redha, S., Fouad, K., Philippe, L.M.: Advanced model of hybrid energy storage system integrating lithium-ion battery and supercapacitor for electric vehicle applications. *IEEE Trans. Industr. Electron.* **68**(5), 3962–3972 (2021)

30. Ravada, B.R., Narsa Reddy, T., Bala, N.L.: A grid-connected converter configuration for the synergy of battery-supercapacitor hybrid storage and renewable energy resources. *IEEE Journal of Emerging and Selected Topics in Industrial Electronics* **2**(3), 334–342 (2021). <https://doi.org/10.1109/JESTIE.2021.3051593>
31. Pinthurat, W., Branislav, H.: Fully decentralized control strategy for heterogeneous energy storage systems distributed in islanded DC datacentre microgrid. *Energy* **231**, 120914 (2021)
32. Cabrane, Z., Jonghoon, K., Kisoo, Y., Mohammed, O.: HESS-based photovoltaic/batteries/supercapacitors: Energy management strategy and DC bus voltage stabilization. *Sol. Energy* **216**, 551–563 (2021)
33. Naderi, E., Bibek, K.C., Meisam, A., Arash, A.: Experimental validation of a hybrid storage framework to cope with fluctuating power of hybrid renewable energy-based systems. *IEEE Trans. Energy Convers.* **36**(3), 1991–2001 (2021). <https://doi.org/10.1109/TEC.2021.3058550>
34. Valverde, L., Rosa, F., Real, A.J., Arce, A., Bordons, C.: Modeling, simulation and experimental set-up of a renewable hydrogen-based domestic microgrid. *Int. J. Hydrogen Energy* **38**, 11672–11684 (2013)
35. Carrero, C., Ramirez, D., Rodriguez, J., Platero, C.A.: Accurate and fast convergence method for parameter estimation of PV generators based on three main points of the I-V curve. *Renewable Energy* **36**, 2972–2977 (2011)
36. Achaibou, N., Haddadi, M., Malek, A.: Lead acid batteries simulation including experimental validation. *J. Power Sources* **185**, 1484–1491 (2008)
37. Zubieta, L., Bonert, R.: Characterization of double-layer capacitors for power electronics applications. *IEEE Trans. Ind. Appl.* **36**(1), 199–205 (2000)

# Batteries, Energy Storage Technologies, Energy-Efficient Systems, Power Conversion Topologies, and Related Control Techniques



Ngalula Sandrine Mubenga

**Abstract** Climate change has become one of the most important global challenges that both developing and developed nations face in the 21st Century. In the transportation sector, electric vehicles (xEV) have emerged as a viable solution to fight climate change. However, the short longevity of the battery system, and their limited range which depends on the battery performance, remains a drawback. In the electric power sector, renewable energy sources such as solar and wind have emerged as strong energy assets, but these sources are intermittent and cause fluctuations on the electrical power grid. To solve these issues, renewable energy systems are sometimes coupled with battery energy storage system (BESS). This chapter reviews batteries, energy storage technologies, energy-efficient systems, power conversion topologies, and related control techniques.

**Keywords** Batteries · Storage systems · Power conversion · Efficiency

## 1 Introduction

Batteries can also be used to make the grid more energy efficient. In order to operate the grid more efficiently, programs such as Demand Response have been put in place to provide energy from batteries during high peak periods, and to charge the batteries during off-peak periods. On a hot summer day, when air conditioning is using a lot of energy for cooling, the supply of electrical energy in the grid becomes tight, and hence the price of electricity increases. The grid operator can send a signal to customers to add capacity to the grid by reducing their electrical load or/and using energy from their batteries.

Historically, power generation has been implemented by turning on natural gas or diesel peaking generators. Clearly, this electricity produced from gas-fired plants heavily relies on natural gas and diesel fuel. That heavy reliance could pose a risk

---

N. S. Mubenga (✉)  
University of Toledo, Toledo, OH, USA  
e-mail: [ngalula.mubenga@utoledo.edu](mailto:ngalula.mubenga@utoledo.edu)

© The Author(s), under exclusive license to Springer Nature Switzerland AG 2024  
K. Kyamakya and P. N. Bokoro (eds.), *Recent Advances in Energy Systems, Power and Related Smart Technologies*, Studies in Systems, Decision and Control 472,  
[https://doi.org/10.1007/978-3-031-29586-7\\_2](https://doi.org/10.1007/978-3-031-29586-7_2)

for the grid if the fuel supply is altered [1]. In fact, recent events have shown that large battery energy storage systems would be a better alternative [2]. Indeed, during the week of August 18, 2016, utility companies in California asked the California Public Utilities Commission to approve contracts for 50 MW of lithium-ion battery energy storage for operation by December 2016 [3].

## 2 Li-Ion Battery Cell Imbalance and Weak Cell Issues

A battery pack consists of multiple cells connected in series. In terms of voltage, ideally, the cell voltage is equal to the pack voltage divided by the number of cells. The battery pack is balanced if all the cells have the same voltage level or State of Charge (SOC). The issue of cell imbalance arises when the cell voltages are not equal, also known as the weak (low storage capacity) cell issue. Li-ion battery cell imbalance is an important issue that needs to be resolved because [4]:

- **It increases safety risks:** A typical li-ion cell voltage is between 2.8 and 4.2 V. If the li-ion cell voltage exceeds 4.35 V, the cell can undergo a thermal runaway and catch fire.
- **It shortens the battery longevity:** Charging the cell above the maximum rated voltage even by a few millivolts will degrade the cell faster and shorten its life. Indeed, charging the cell to 4.25 V instead of the recommended 4.2 V increases the cell degradation rate by 30%. Since it charges faster than the other cells, the weak cell has a higher voltage and will degrade faster.
- **It causes incomplete charging of the battery pack:** Fig. 1 shows the battery pack with a weak cell during the charge cycle. If there is a weak cell in the pack during the charging cycle, the weak cell voltage will tend to increase faster than other cells. This one weak cell will cause the overvoltage protection circuit to prematurely stop the charge cycle in order to prevent thermal runaway. As a result, all the other cells in pack have lower voltages and are not fully charged.

**Fig. 1** Illustration of charge cycle

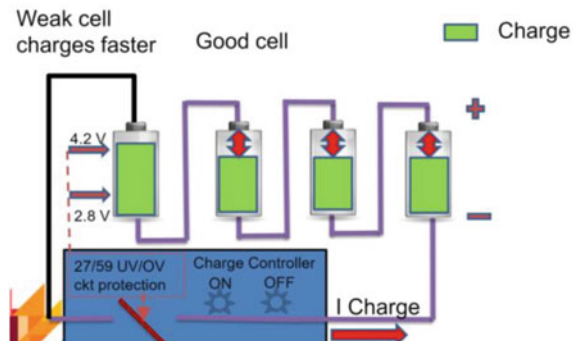
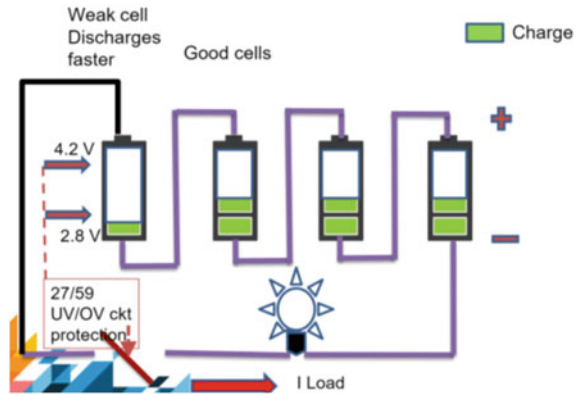


**Fig. 2** Illustration of discharge cycle



- **It reduces the battery pack discharge capacity:** Fig. 2 shows the battery pack with a weak cell during the charge cycle. During the discharge cycle, the weak cell will be depleted faster than the other cells, and it will have a voltage lower than the other cells. As a result, the under-voltage protection circuit will stop the discharge cycle if that one weak cell goes below 2.8 V. As a result, all the other cells still have voltages higher than the threshold voltage, and the battery pack still contains energy that is unused. Therefore, the pack discharge capacity is reduced because of the one weak cell.

When cells have different voltages, it means that the cells are at different SOCs. As the battery ages, the performance becomes limited by the weakest cell. For lithium-ion batteries, a battery management system (BMS) is needed to accomplish thermal management and cell voltage equalization functions.

The device that balances the cell voltages in the BMS is called an equalizer (EQU), and currently there are three types of EQUs: passive (PEQ), active (AEQ), and Bilevel Equalizer (BEQ). The passive equalizer connects each cell to a shunt resistor via a transistor as shown in Fig. 3a. It is also known as a resistive equalizer or dissipative equalizer. During the charging cycle, it monitors the cell voltages, and removes charge from all cells above the lowest voltage by dissipating their energy as heat through the shunt resistor until all cells voltages are equal [5]. The lowest voltage is the weakest when discharging, and it is the highest during charging because its cell capacity is lower and it charges faster.

The passive equalizer shown in Fig. 3a has an efficiency of 0%, and the discharge capacity of the battery pack is equal to that of the weakest cell. Hence, the PEQ leads to energy loss (heating), reduced capacity, and poor performance. Although the PEQ has a poor performance, the vast majority of users prefer to use passive equalizers because they are cheap [7].

The simplest active equalizer (AEQ) has each cell connected to an inductor and two transistors (FET) which operate at a high frequency, e.g. 5–20 kHz, as shown in Fig. 3b. It is also known as a non-dissipative equalizer or switching equalizer. The active equalizer transfers charge from one cell to another, from the highest voltage

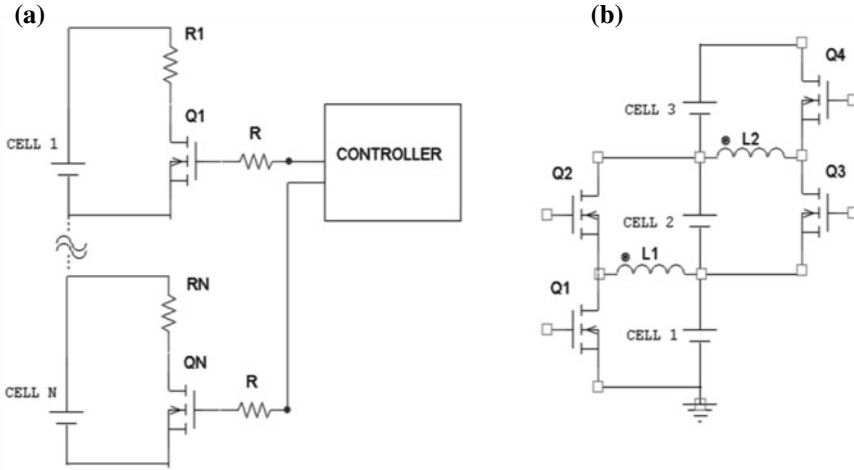


**Fig. 3** a Simplified passive equalizer [6] b simplest active equalizer [5]

cell to the lowest voltage cell. The efficiency of the AEQ can be quite high, close to 90%, but the efficiency is much lower when the transfer is between single cells. For the active equalizer, the discharge capacity of the battery pack is close to the average of all the cells [7]. This results in reduced energy loss, increased capacity, and high performance for the battery pack. Although active equalizers have a high performance, they remain expensive, costing up to 10 times the cost of a passive equalizer [8]. As a result, very few users use active equalizers.

To solve this problem, a combined passive-active (hybrid) equalizer known as the Bilevel Equalizer (BEQ) was developed in [9–16]. The BEQ has high performance close to an active equalizer, but at a low cost of only about 1.3 times the cost of a passive equalizer.

### 3 State of the Art for Li-Ion Battery Equalizers

The previous section introduced the weak cell issue and explained the need for cell equalization. In a stack of series connected cells, the weak cell limits the state of charge and the discharge capacity of the entire stack. To improve the battery performance, cells need to be balanced and charges need to be transferred to the weak cell during discharge or taken away from the weak cell during charge. Equalizers accomplish this balancing process. This section will review the current state of the art for Li-ion battery equalizers.

There are three types of equalizers, passive (resistive) equalizers (PEQ), active (switching) equalizers (AEQ), and combined active–passive (hybrid) Bilevel Equalizers (BEQ). This section reviews the advantages and disadvantages of different



varieties of each type. It also discusses the equalizer design tools. The section also reviews commercially available active equalizers and compares their performance against the Bilevel Equalizer. Applications that use Li-ion batteries are often critical and require batteries to perform reliably during their lifetime. Therefore, the last part provides a clear understanding of how lithium-ion cells work and how they age. It also provides an overview of the expected lifetime of Li-ion BESS based on their stationary and mobile applications.

### ***3.1 Passive Equalizers***

In the passive equalizer, each battery cell is connected to a shunt resistor and a field effect transistor (FET) as shown earlier in Fig. 3a, hence the name passive equalizer (PEQ). The transistor is also called a “switch”. A good summary of passive EQUs can be found in [6, 17–20].

There are two types of PEQs, parallel and multiplexed. A parallel PEQ has 1 resistor and 1 switch per cell whereas a multiplexed PEQ has multiple switches per cell. When charging the battery stack, the PEQ dissipates extra charge through heat until all cells are at the same voltage as the weakest (lowest charge capacity) cell. Hence, it is also known as a dissipative equalizer [6]. Consequently, PEQs have 0% efficiency, and they incur high heat loss and low performance, which translates into reduced battery capacity. As explained in Sect. 2, passive equalizers are the most common type currently used because they are cheap and simple. Passive equalizers only operate during battery charging cycle to keep the weakest cells from reaching full charge before the others. They are of no benefit during the discharge cycle since they cannot slow the discharge rate of the weak cells. Since the PEQ does not add charge to a cell, the discharge capacity of the battery stack is only equal to the weakest cell. The PEQ balances the state of charge of the cell; it does not balance charges inside the cell. Batteries also have a small internal resistance, which increases with age. As the internal resistance increases and the battery capacity decreases, the life of the battery is shortened. Section 3.7 will explain in depth how li-ion cells function, how they age and their expected life based on their application. To summarize, because they do not add charge to the cells, Passive Equalizers do not improve the discharge capacity of battery cells. Since passive equalizers do not improve the performance of the BES, our literature review will focus more on active equalizers.

### ***3.2 Active Equalizers***

Active equalizers transfer charge between cells and/or the stack. There are numerous types of active equalizers, which are reviewed in this section. Later on, Sect. 3.3 will focus on commercially available active equalizers. A few examples of current active equalizer technology can be found in [6, 17, 21–32]. Active equalizers can

be based on three main architectures: transformers-based, multiple dc-dc converters, and adjacent cell balancing.

**Transformer/Inductor based:** These AEQs use transformer windings or inductors for energy storage. The multi-winding architecture means a transformer with multiple windings. It uses only one transformer to equalize the entire battery stack, but that transformer is quite expensive. However, the main drawback is that it cannot balance all the cells accurately because the leakage inductances of the secondary transformer windings are hard to match [6, 21, 33–36]. Another difficulty is the fact that it is hard to implement because it requires numerous windings to be built into one transformer. This is not practical for EV or BESS applications that have hundreds of cells [6, 35, 36]. Other transformer-based architectures require at least one transformer for every cell, which also is not practical for large batteries. To solve these problems, Lee et al. [21] have proposed an active equalizer using a transformer as an energy carrier, as shown in Fig. 4.

The circuit has two parts: an energy transfer network and a cell access network. The circuit includes one (1) two-winding transformer regardless of the number of cells. The circuit has  $N + 3$  switches that select the target cell. The network selects the source cell and the destination cell. This circuit achieved a transfer efficiency of 80.4% [21], and losses are reduced through zero crossing switching.

**Multiple isolated DC-DC converters:** This architecture is based on multiple dc-dc isolated converters (MIC) as explained in [6, 17], and [28, 37–41]. MICs can be divided in three main types known as discharge, charge and bi-directional [6, 42]. The discharge MIC, transfers charge from the high voltage cells to the entire battery stack [6, 37]. Charge type MICs transfer charge from the entire battery stack to the low voltage cells [6]. The bi-directional type, also known as charge–discharge type, does both functions [42, 43].

The targeted charge/discharge (C/D) equalizer developed by Stuart and Zhu is a bidirectional equalizer that uses relays to either charge or discharge one cell at a time [43]. Figure 5 below illustrates the targeted C/D EQU.

Per Fig. 5, the targeted C/D EQU is a modularized BMS which consists of a central unit, local unit(s), a charger, and a network of relays. The microcontroller is the 8-bit SAB 80C515CA from Infineon, which communicates via a CAN serial data link to the local units. Each local module also contains a microcontroller that monitors cell voltage. The central unit compares the individual cell voltage versus the average cell voltage of the stack to determine the target cell, which is then equalized by turning on relays. The relays are single pole double throw (SPDT) that can carry up to 5A current. Note that the central unit controls the supply of operating power to the local units for safety reasons. If a local unit fails, it might not be able to turn off its EQU which could result in overcharging one of the Li-ion cell and cause thermal runaway; having the central unit control the operating power prevents that situation [43]. To test the targeted C/D EQU, Zhu built both a D type and the targeted C/D types of EQU. Then 6 series connected GAIA 3.6 V 60Ah Li-ion batteries were selected and tested under various cases. Results showed that the targeted C/D type equalizer

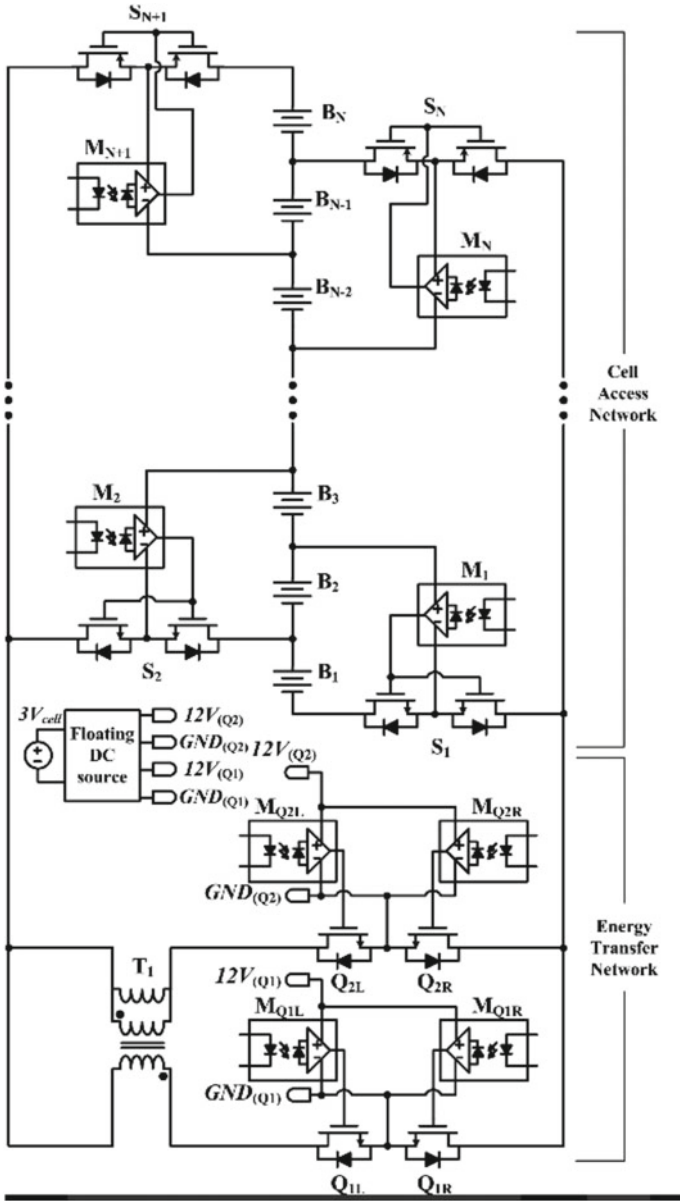


Fig. 4 AEQ circuit using a transformer as energy carrier [21]

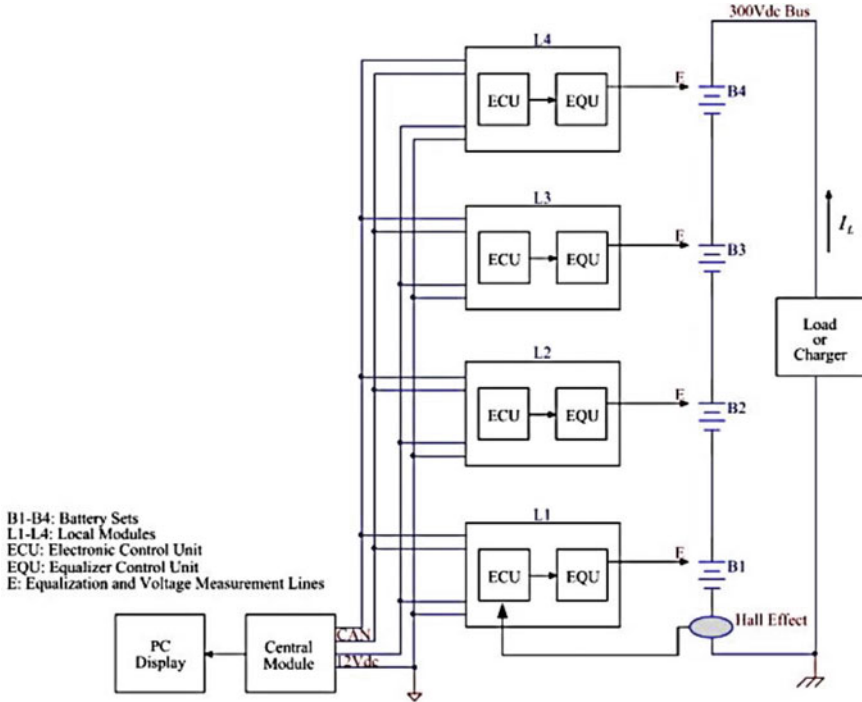


Fig. 5 Targeted charge/discharge equalizer [43]

improved the equalization time by a factor of 2X to 15X depending of the type of imbalance.

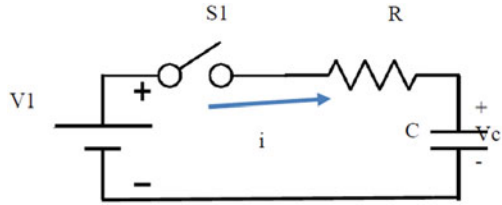
On the one hand, MICs equalize fast and have good efficiency. On the other hand, they are much more expensive and complex than PEQs [43].

**Balancing adjacent battery cells:** Two of the common subtypes within this group include the buck-boost converters [35, 36] and switched capacitor converters [6, 17, 24, 25, 44–47]. On the one hand, the main advantage for both technologies is that they have low voltage stress on the switches. On the other hand, the buck-boost equalizer requires complex circuitry to control it [48, 49]. The switched capacitor type requires a long time for equalization [28, 29, 36, 40, 50–55], and it has much higher losses than other AEQs. The switched capacitor type can be modelled as an RC circuit, so understanding how charge is transferred in an RC circuit will help us understand their high-power loss.

Figure 6 shows a simplified switched capacitor, which is a basic RC circuit.

Per Fig. 6, the circuit has one switch S1, a voltage source V1, a resistor R and a capacitor C. When the switch is closed, current  $i$  flows around the loop to charge the capacitor and is expressed as follows:

**Fig. 6** Simplified switched capacitor AEQ circuit



$$S1 \text{ ON} : i = \frac{V1}{R} e^{-\frac{t}{RC}} \tag{1}$$

After a long time, the capacitor C1 is charged to a voltage equal to the source. At  $t = \infty$ ,

$$Vc = V1 \tag{2}$$

And the energy stored in the capacitor is

$$Ec = \frac{1}{2} CV1^2 \tag{3}$$

As the current flows through the resistor, power is lost and can be expressed as follows

$$PR = R.i^2 \tag{4}$$

Substituting Eq. (1) into (4) yields

$$PR = R.\left(\frac{V1}{R} e^{-\frac{t}{RC}}\right)^2 \tag{5}$$

The energy loss in the resistor is found by integrating the power loss over a time interval, so

$$ER = \int_0^{\infty} PR dt \tag{6}$$

Equation (5) into (6) yields

$$ER = \frac{V1^2}{R} \int_0^{\infty} e^{-\frac{2t}{RC}} dt = \frac{V1^2}{R} \left[ \frac{-RC e^{-\frac{2t}{RC}}}{2} \right]_0^{\infty} = \frac{v1^2}{R} \left( \frac{RC}{2} \right)$$

Cancelling the resistance R yields

$$E_R = \frac{1}{2} = CV1^2 \quad (7)$$

The total power P from the source is

$$P = V1xi \quad (8)$$

Substituting Eq. (1) into (8) yields

$$P = \frac{V1^2}{R} e^{-\frac{t}{RC}}$$

The total energy E from the source V1 is found by integrating the total power over a time interval, so

$$E_{TOTAL} = \int_0^{\infty} P dt = \frac{V1^2}{R} \left[ -RC e^{-\frac{t}{RC}} \right]_0^{\infty}$$

$$E_{TOTAL} = CV1^2 \quad (9)$$

$$\text{Thus } E_R = \frac{1}{2} E_{TOTAL} \quad (10)$$

Equations (3) , (7) and (10) state that half the energy transferred from the source V1 to the capacitor C is lost in R. Then, the charge stored in C has to be further transferred to another cell, and thus the high loss in switched capacitor AEQs. This section reviewed the scholarly work on active and passive equalizes. It is also crucial to understand the commercial EQUs that are available on the market, focusing on AEQs because of their performance. So, the next section will review commercial AEQs.

### 3.3 Commercial Active Equalizers

This section reviews the latest multicell active equalizers that are commercially available; namely the LTC3300-1/2 from Linear Technology, the EMB1499Q and the TIDA-00817 both from Texas Instruments.

#### LTC3300 6 Cell AEQ

The LTC3300 is an active equalizer integrated circuit (IC) manufactured by Linear Technology [56]. It is similar to the Bilevel Equalizer, in that the LTC3300 stores equalization charge in the winding inductance whereas the BEQ stores charge in an inductor.

*Description*

The LTC3300 is a “bidirectional synchronous flyback balancing” IC [56]. It can equalize up to 6 cells at a high charge transfer efficiency that is reported to reach up to 92%. The LTC3300 equalization current can reach up to 10 A. It varies the switching frequency based on multiple factors such as peak current on the primary and secondary sides, turns ratio, transformer inductance, cell voltage, number of secondary cells, and whether it is the charge or discharge cycle [56]. The LTC3300 is intended for use with the LTC6803 12 cell voltage monitor. Figure 7 [56, p. 1] below shows a typical application.

Per Fig. 7, each LTC 3300 can equalize up to 6 series cells. Each cell requires one (1) transformer and two (2) FETs. Therefore, a stack of N cells requires N/6 LTC33000, N transformers and 2N FETs. As can be seen from the typical application, the LTC3300 is based on two-winding transformers. However, it can also be used with a multi-winding transformer where the custom transformer has one winding for the primary side for the stack up to 12 cells, and a secondary winding for each cell of the stack or up to 6 windings on the secondary side.

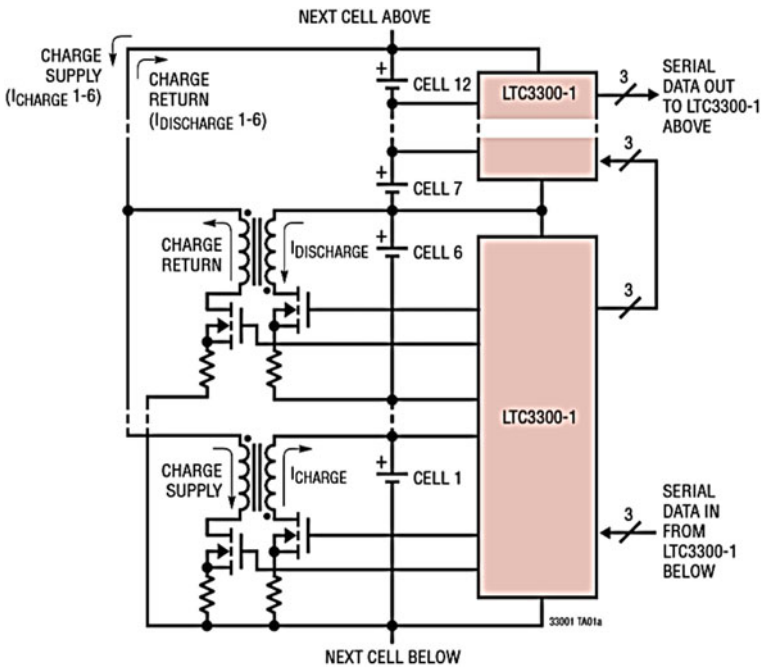
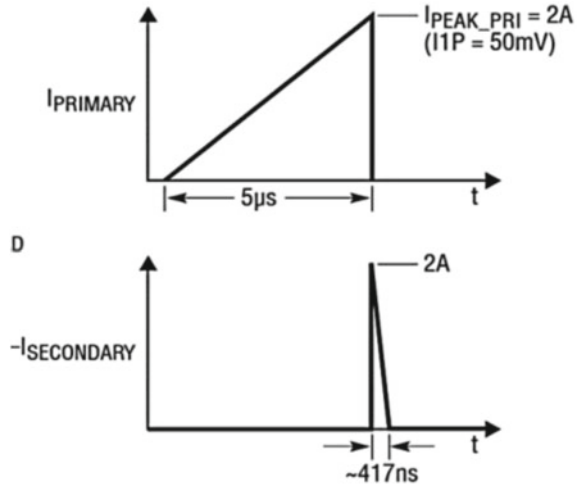


**Fig. 7** LTC3300 typical application

**Fig. 8** LTC3300 cell 1 discharge cycle



*Operation*

The discharge cycle is illustrated in the top transformer on Fig. 7. In addition, Fig. 8 [56, p. 16] shows the current in the primary and secondary winding during the discharge cycle.

To discharge a target cell, the primary (right) switch for that cell is closed and charge from the cell are stored in the transformer winding until it reaches the peak current as shown in Fig. 8. Then, the primary switch is opened, causing the charge stored in the transformers to flow in the secondary (left) winding. Next, the secondary (left) switch is synchronized to close during the charge transfer until the discharge current reaches 0. As soon as the current reaches 0 on the secondary side, the secondary switch is opened, and the primary switch is closed again to repeat the cycle. In summary, the LTC3300 transfers energy from the cell to up to 12 adjacent cells [56].

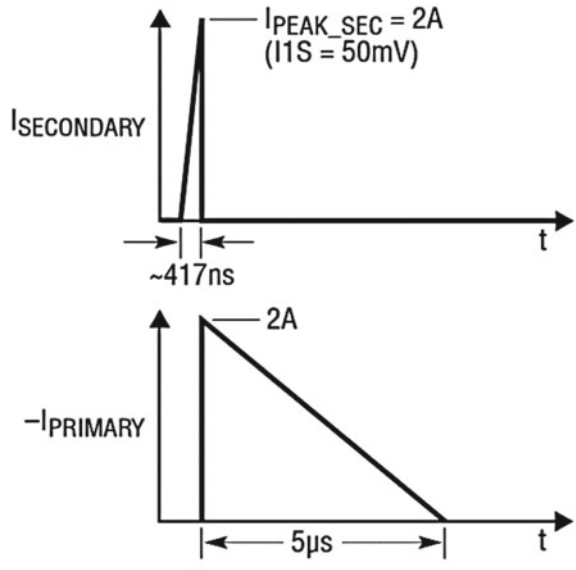
The charge cycle is illustrated in the bottom transformer in Fig. 7. In addition, Fig. 9 [56, p. 46] shows the current through the primary and secondary windings during the charge cycle.

The secondary (left) switch of the target cell closes and charge from the stack is stored in the transformer secondary winding until it reaches the peak current. Then, the secondary switch is opened, which causes a current to flow from the primary side winding to the target cell. The primary (right) switch is closed, thus causing charge current  $I_{charge}$  to flow counterclockwise and charge the target cell. When the primary current reaches 0, the primary switch is opened, and the secondary switch is closed to repeat the cycle.

In summary, to charge the target cell, the LTC3300 transfers energy from the stack to the cell [56].



**Fig. 9** LTC3300 cell 1 charge cycle



**EMB1499Q, 7 Cell AEQ**

The EMB1499Q is a 28 pin active equalizer IC manufactured by Texas Instruments [57]. It can balance up to 7 cells in series for a maximum voltage of 60 V. This section describes how the EMB1499Q operates in conjunction with the EMB1428.

*Description*

The EMB1499Q uses a “bidirectional forward converter” [57]. It generates PWM drive signals to control the current in the converter. It operates at a fixed switching frequency of 250 kHz.

This bidirectional dc–dc converter uses the EMB1428 switch matrix to route current to the cell that needs to be charged or discharged. Figure 10 shows the EMB1499Q in a typical application.

Per Fig. 10, the EMB1499Q requires two (2) 12 V supplies to function. The secondary side (left) of the transformer is connected to the switch matrix which will then connect to the target cell, while the primary (right) side is connected to the stack.

The EMB1499Q requires quite a few components to implement active balancing. Per Fig. 10, every 7 battery cells will require one EMB1499Q, one EMB1428Q, one transformer, one inductor and 24 MOSFETs. In other words, every N cells will require  $N/7$  EMB1499Qs, EMB1428s, inductors, transformers, and  $2N + 10$  FETs. The user can select the balancing current by setting VSET between 1.2 and 2 V.

*Operation*

The inductor on the secondary side stores energy. The EMB1499Q outputs (2) drive signals for the FETs on the secondary side and one (1) drive signal for the FET

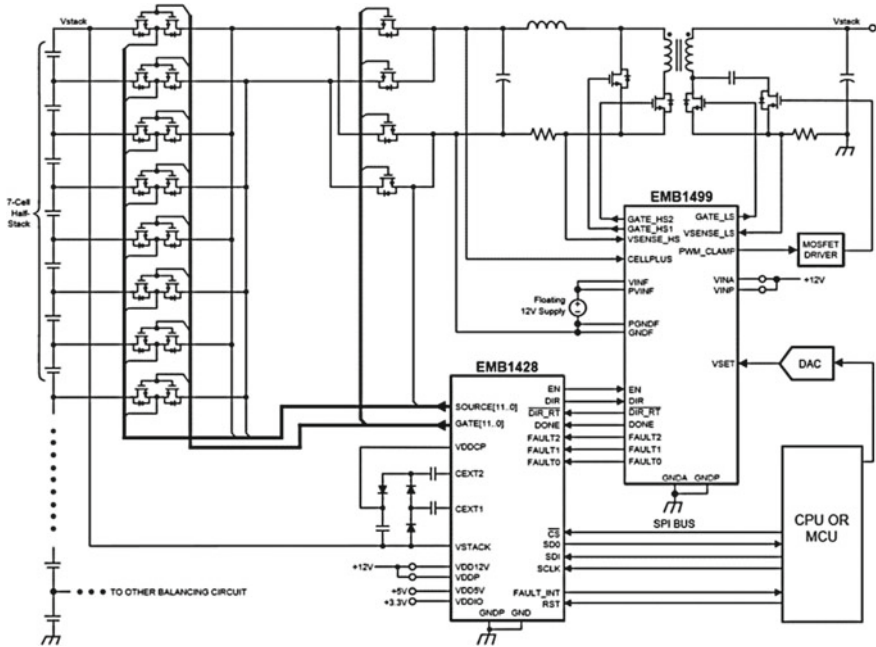


Fig. 10 EMB1499Q typical application [57, p. 2]

on the primary side. By driving these FETs, the EMB1499Q controls the inductor current that the EMB1428 routes to the target cell. The EMB1499Q transfers charge between the cell and the entire stack. Per Fig. 10, the microcontroller unit (MCU) communicates only one signal directly to the EMB1499Q: the VSET signal which is the equalization current set by the user. The rest of the communication between the MCU and the EMB1499Q is done via the EMB1428. To start the operating cycle, the EMB1428 sends two signals, EN and DIR, to the EMB1499Q per Fig. 10. The enable signal, EN, starts the equalization cycle. The direction signal, DIR, selects whether it is the charge or discharge cycle. If DIR is HIGH, it commands a charge cycle; when it is LOW it designates the discharge cycle. Upon receiving the EN input signal, the EMB1499Q goes through handshaking to start the normal operating cycle. Next, the EMB1499Q outputs the driver signal for the gates and the PWM\_clamp depending on the cycle. The following sections explain how the EMB1499Q and the EMB1428 operate during the charge and discharge cycles.

For the discharge cycle, the EMB1428 outputs a high EN and low DIR signals. Upon receiving these inputs, the EMB1499Q drives the GATE\_LS, and GATE\_HS2 high, and it sets the GATE\_HS1 and PWM\_CLAMP low. The dc-dc converter operates in the constant current mode and current flows counter clockwise in the primary loop. The inductor current ramps up until it reaches the peak set the by the user via VSET. During the second half cycle, the EMB1499Q flips all the FETs such that GATE\_LS and GATE\_HS2 are low, while PWM\_CLAMP and GATE\_HS1 are

high. The inductor current then flows from the inductor to the gate matrix to the target cell. And the equalization cycle repeats again. After less than 8 s of equalization, EMB1428 turns off the EN signal. When the EMB1499Q sees the falling edge of the EN, it starts ramping down the inductor current until it reaches 0. For the charge cycle, the sequence of operation is the same except that the EMB1428 outputs a low DIR signal to initiate the charge cycle.

### TIDA-0817, 16 Cell AEQ

In April 2016, Texas Instruments utilized the EMB1499Q along with other ICs to conceive a 16-cell active equalizer called TIDA-0817 and listed in the document of the same name. Figure 11 shows one 16 cell TIDA-0817AEQ module.

The TIDA-0817 operates at 250 kHz, and its equalization current can reach up to 5A. According to Texas Instrument Design Application (TIDA) #0817, this AEQ can transfer charge with an efficiency between 80 and 93%. Per Fig. 11, the 16-cell AEQ includes one EMB1499Q, one bq76PL455A-Q1 monitor and protector, and three EMB1428 gate matrices. Although the monitor and protector can provide passive balancing, the TIDA-0817 does not use the PEQ function, but instead it uses the EMB1499Q and the EMB1428 to actively balance any cell in the stack. Each module can equalize up to 16 cells and can be daisy chained to equalize up to 256 cells. The other features such as safety and communication are like the EMB1499Q previously listed in Sect. 3.3.

This design is complex to implement. Another major drawback for this design is the fact that each TIDA-0817 module requires many additional major components. In fact, the list of additional components for each module is listed on TIDA-0817

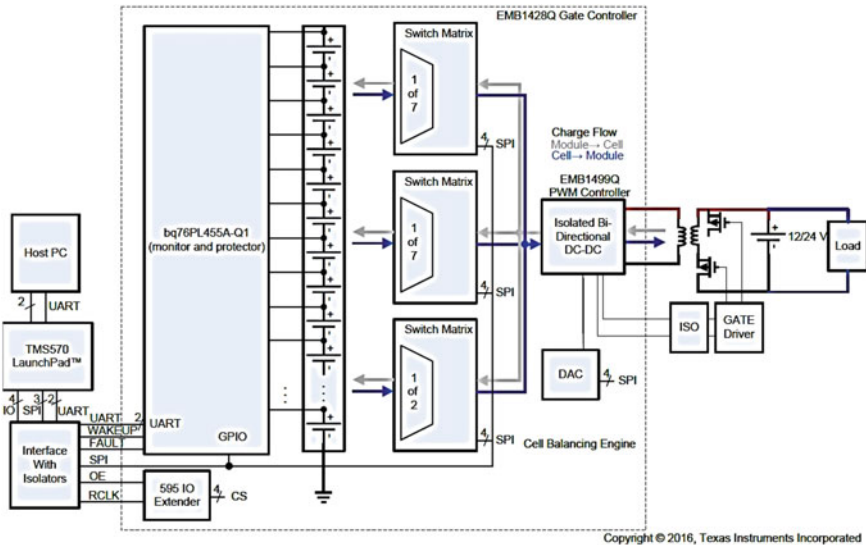


Fig. 11 TIDA-0817 16 cell AEQ module diagram

and includes (64) MOSFETs and (1) transformer along with other parts. The high number of components needed for the TIDA-0817 does not make it practical for large batteries because they would increase the cost and may offset other benefits.

### ***3.4 Combined Active Passive (Hybrid) Equalizer: The Bilevel Equalizer***

The literature review in Sects. 3.1–3.3 indicates that, on the one hand, passive equalizers dissipate energy through a resistor and do not transfer charge to the target cell. As a result, they have poor performance, but manufacturers use them because they are cheap. On the other hand, active equalizers transfer charge to the target cells and therefore help increase the discharge capacity and improve the performance of the battery. However, although they have high efficiency, active equalizers cost up to 10× the cost of passive equalizers; as a result, people do not utilize them. The review of commercial active equalizers in Sect. 3.3 revealed that the commercial equalizers are not practical for large Li-ion BESS because they are limited by the number of cells they service and by a low equalization current. There needed to be an EQU that can service a BESS with hundreds of cells and that is affordable. To solve these shortcomings, Stuart and Mubenga [9, 11–16, 58, 59] developed a new type of hybrid EQU called the Bilevel Equalizer (BEQ) that has high performance close to an active equalizer, but at a low cost of only about 1.3 times the cost of a passive equalizer.

#### **Description**

Figure 12 shows a block diagram of the Bilevel Equalizer (BEQ).

In this system, the series connected cells are divided into sections. Each section has its own passive equalizer, like Fig. 3a, called a passive equalizer unit (PEQ) to balance only the cell voltages within that section. A high efficiency active equalizer unit (AEQ) like Fig. 3b is then used to balance the section voltages [9]. Mubenga et al. developed a design procedure and software programs to formulate design criteria for the BEQ.

#### **BEQ Properties**

The BEQ is unique and original because It consists of both an active and a passive equalizer. It equalizes at two different voltage levels, hence the name “Bilevel Equalizer”. Current battery management systems use either a passive equalizer or an active equalizer, but they do not use both. In the BEQ, cells are currently grouped in sections of 4–14 cells, but a section can have any number of cells. Each cell is connected to a PEQ, and the sections are connected to AEQ units. Current AEQs use one AEQ per cell, which results in very high cost and lower efficiencies.

A weak cell in a section only drags down the other cells within that section (4–14), instead of all cells in the battery pack (96–192). During discharge, the AEQ transfers

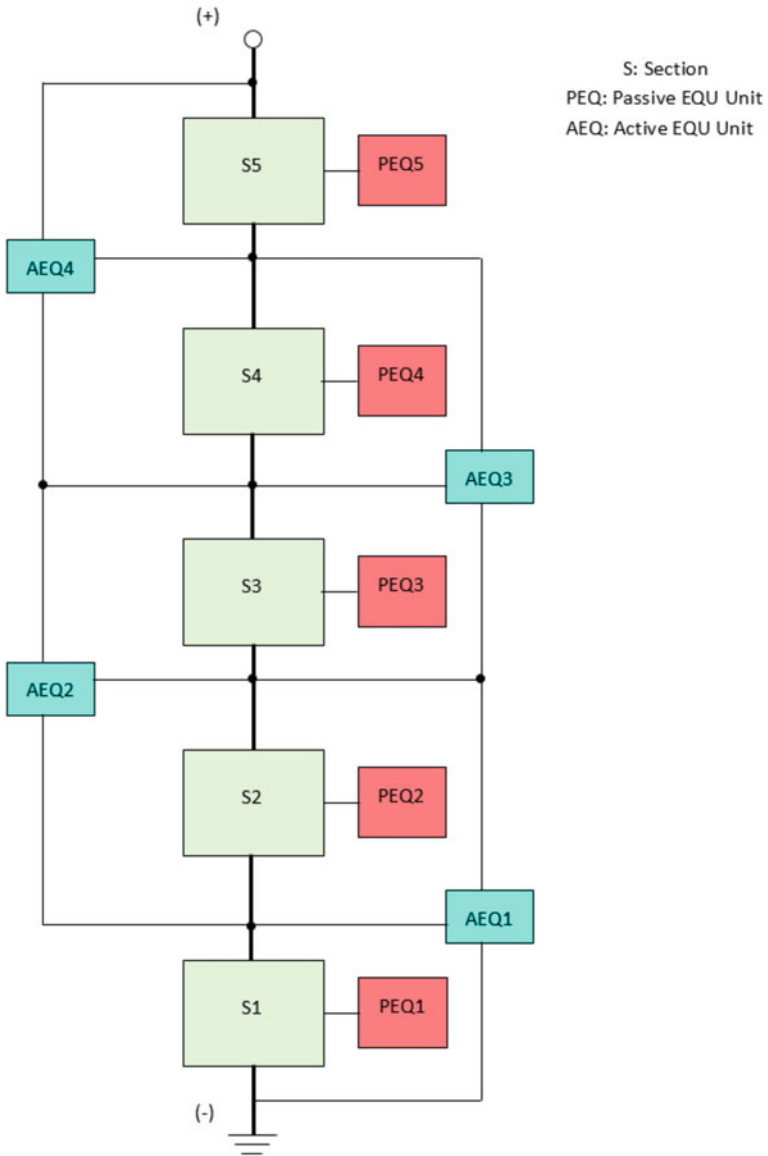


**Fig. 12** Bilevel equalizer (BEQ) with battery cells grouped in five sections

charge to the section with the weakest cell. During charge, the AEQ transfer charges from the weak cell section. As a result, the battery capacity is increased to a level close to a pure AEQ [9]. As stated earlier, the BEQ performs like the active equalizer, but it only costs about  $1.3\times$  the cost of a passive equalizer. However, the pure active equalizer costs about  $10\times$  the passive equalizer.

As shown in the Fig. 12, the BEQ sectionalizes the battery stack in groups, typically 4–14 cells. It then uses a separate PEQ to equalize the cells within each section. It then equalizes the section voltages through an AEQ. As a result, the BEQ yields low losses and increases the discharge capacity of large Li-ion batteries. Figure 13 summarizes the technical comparisons between various types of equalizers.

As shown in Fig. 13, the literature review revealed that the Bilevel Equalizer is the only one publicly known using both an active and a passive equalizer operating at two different voltage levels. This architecture allows an efficiency close to the AEQ.

### 3.5 Equalizer Design Tools

Lithium-ion batteries require an active equalizer (AEQ) or a Bilevel equalizer (BEQ) to transfer charges between the series connected cells or sections of cells. To design EQU, three tools were successfully developed by Mubenga et al. [9, 15, 16, 58] and protected under U.S. patent application 63/167,471 (pending) [58].

**The Active Equalizer (AEQ) Design Tool** was developed to design the inductor for the AEQ units that can be found in BEQs, and inductor based AEQs.

**The Efficiency Measuring Apparatus (EMA)** shown in Fig. 14a, b was developed to measure the efficiency of the charge transfer between series connected cells or sections of cells.

The research developed two sets of hardware: the 24 V EMA for sections with up to 6 cells, and the 48 V EMA for section with up to 12 cells.

To obtain experimental results, first the AEQ Inductor Design Tool was used to design the AEQs unit. Based on the outputs from the Inductor Design Tool, the inductor was built, and the switching components were selected as part of the AEQ units. Next, the EMA, was used to test the AEQ units that were previously designed with the Inductor Design Tool. The EMA measured the charge transfer efficiency of the AEQ units under various parameters such as operating voltage, frequency, and current and the results were recorded in Table 1. The efficiency computed by the AEQ Inductor Design Tool had an accuracy ranging from 96–99.99% compared to the measured efficiency by the EMA.

**The Equalizer (EQU) Design App** was developed to size the equalization currents and quantify the BEQ design specifications based on factors such as cell capacity, maximum discharge current, and level of imbalance amongst the cells. The EQU Design App simulates the performance of the battery stack under BEQ equalization and can be used for inductor based AEQ. As part of [9–14], the BEQ had been physically built with the AEQ unit that was designed using the AEQ Inductor Design Tool. A battery stack made up of 24 GAIA cells was assembled and placed in a thermal chamber for safety. The BESS was connected to the BEQ and submitted to various experimentation that can be found in [9–14]. These are the experimental results that were used to validate the design tools developed in this research. Experimental results showed that the MATLAB and Python EQU Design App had an

TYPE	ARCHITECTURE	SUBTYPE	ADVANTAGES	DISADVANTAGES	
PASSIVE	Parallel (1 resistor+1 switch per cell)		Simple	0% efficiency	
			Cheap	High heat loss	
	Multiplexed (1 resistor+network switch per cell)			Poor performance	
				Reduced stack capacity	
ACTIVE	Centralized Multi-transformer (1 transformer per stack)		1 transformer for entire stack	Inaccurate equalization	
				Difficult to implement multiple windings in 1 transformer	
	Multiple isolated DC-DC converter (MIC)		Simple	HV isolation	
			Good efficiency	switch network	
	Discharge (overcharged cells → stack) (1 transformer+1 switch + 1 diode per cell)		Fast equalization	High voltage stress on diode	
		Charge (stack → undercharged cells)			
	Two switch fly back (1 transformer+2 switches +3 diodes per cell)		Fast equalization		
			Simple	Low voltage stress on switches	
	Bi-directional (1 transformer+2 switches per cell)			Reduces the # of active switches	
Balancing adjacent cells			Low voltage stress on switches		
	Buck-boost (1 buck-boost converter per 2 adj. cells)		Medium efficiency	Bulky	
			Medium speed equalization	Complex control	
Switch capacitor (1 switch capacitor per 2 adj. cells)		High efficiency			
		Fast equalization			
HYBRID	BILEVEL EQU 4-32 Cells gouped in sections Passive EQU for each cell Active EQU for each section		Low cost		
			High performance		

Fig. 13 Summary of technical comparisons for Li-ion battery equalizers

accuracy ranging between 98.24% and 98.29% for predicting discharge time, Ah discharge and percent of rated Ah.

In conclusion, this experimental research showed that the AEQ Inductor De-sign Tool, the Efficiency Measuring Apparatus, and the EQU Design App are adequate tools for designing Bilevel Equalizers and inductor based active equalizers. Although these tools were first developed to design the BEQ, they proved to be adequate for designing inductor based AEQs as well. The novelty of that research resided mainly

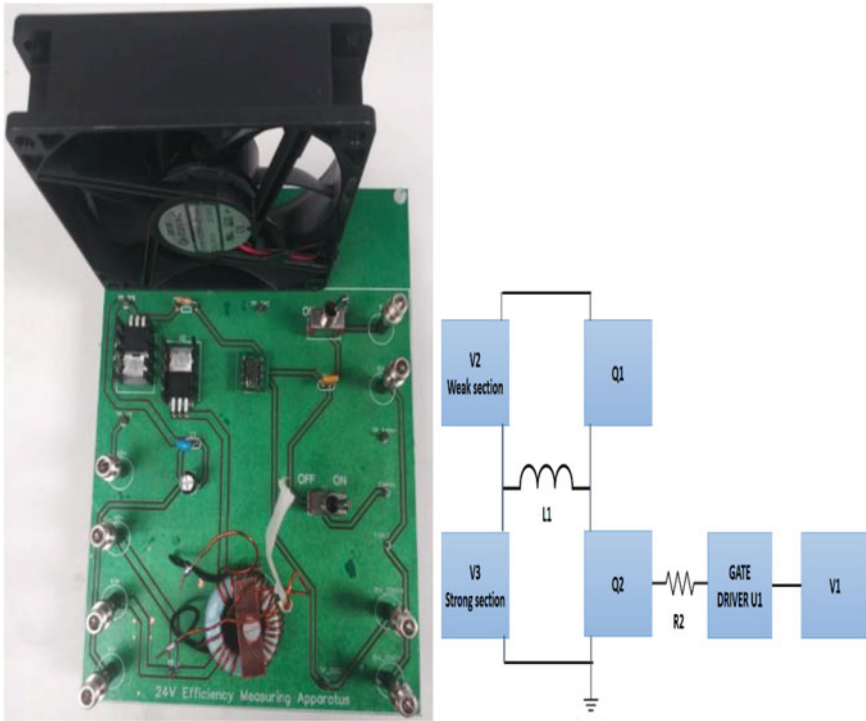


**Fig. 14** a 24 V Efficiency Measuring Apparatus (EMA) b 24 V EMA bloc diagram

**Table 1** Efficiency computed by the AEQ inductor design tool and measured by the EMA

	Inductor size (uH)	Inductor core#	Inductor winding size (AWG)	Freq. (Hz)	I peak (A)	Vin (V)	Measured efficiency (%)	Calculated efficiency (%)
48 V EMA	32.4	MP-106026-2	22	77,096	9	48	83.11	84.01
	31.1	MP-106026-2	20	76,760	9.2	48	84.35	84.75
	32.8	MP-106026-2	18	76,743	9	48	85.78	85.21
24 V EMA	54.4	MP-106026-2	22	24,456	10.9	24	82.94	82.93
	54	MP-106026-2	20	23,704	10.9	24	83.67	84.99
	54.5	MP-106026-2	18	23,704	10.9	24	84.4	86.29
	61.1	MP-106026-2	22	12,667	9.9	14.4	77.17	78.1
	62.2	MP-106026-2	20	12,531	9.9	14.4	79.6	81.62
	62.4	MP-106026-2	18	12,531	9.9	14.4	80.4	83.05



in presenting a suite of tools that can be used to design both AEQs and BEQs and predict the performance of the battery stack under different equalizations.

This leads us to the following question of how the Bilever Equalizer compares to the commercially available AEQs when designing a large BESS. The next section will compare the designs and their sustainability.

### 3.6 Sustainability Comparison Between the BEQ and Commercial AEQs

As stated earlier, large Li-ion batteries can include hundreds of cells. A design is said to be sustainable if it has high efficiency and has a reasonably low number of components. In addition, at the end of the life of the system, less waste needs to be managed. An xEV can have around 192 cells, while a stationary BESS can include around 384 cells. Let us compare what the design of a large BESS would include when implemented with the LTC3300, EMB1499, TIDA-0817 and the BEQ. We will use the part count of the main devices as a metric to evaluate the various designs. It is outside of the scope of this research to do a detailed cost analysis. We note that the part count does not provide system cost because additional circuitry is required for each design, and these circuits influence the cost. In addition, industrial manufacturers can get bulk pricing on these parts, which a university cannot access. However, comparing the part count for active balancing gives us a good benchmark. Table 2 shows a count for the main components of a design based on the AEQs of interest.

The parts count for these AEQs have been listed in Sects. 3.3 and 3.4. For this comparison, the Bilevel Equalizer divides the stack into sections of 12 cells: this is the main advantage over the other AEQs because it decreases the parts count. Per Table 2, for the 192 cell battery, the BEQ has 16 sections, while it has 32 sections for 384 cells. Indeed, a 192 cell stack will require only 30 FETs for the BEQ, while it requires 768 FETs for the TIDA and close to 400FETs for the LTC3300 and the EMB1499Q. The LTC3300 has no limitation to the number of cells N in the stack.

**Table 2** AEQ comparison 192 cell and 384 cell

	LTC3300	EMB1499Q	TIDA-0817	BEQ	Devices
192 cell	(32)LTC3300IC (16)6804 IC (192)Transf (768)FETs	(28) EMB1499QIC (28)EMB1428IC (28)Transf (788)FETs	(36) EMB1499QIC (12) bq76PL455A-Q1 (12)EMB1428IC (12)Transf (768)FETs	(16)6804IC (15)Ind (30)FETs	IC Transf/ Ind FETs
384 cell	(64)LTC3300IC (384)Transf (768)FETs	(56)EMB1499QIC (56)EMB148IC (56)Transf (788)FETs	N/A	(32)6804IC (30)Ind (60)FETs	IC Trans/ Ind FETs

The EMB1499Q can balance up to 7 cells in series and has an absolute maximum rating of 60 V. For illustration purposes, the design that is shown in Table 2 assumes that the battery is grouped into 7 cell sections, and the EMB1499Q does not transfer charges between the sections. It only equalizes cells within the same section so that multiple AEQs based on the EMB1499Q are needed.

The TIDA is limited to 256 cell stacks; therefore, it cannot provide equalization for a stack containing 384 cells. The number of devices is shown between parentheses (##).

In summary, the BEQ design requires only (30)FETs, (15)inductors, and (16)6804 ICs for 192 cells. Per Table 2 for 192 cells, other commercial AEQs require  $12\times$  to  $25\times$  more FETs than the BEQ,  $1\times$  to  $12\times$  more transformers/inductors, and about  $4\times$  more ICs. Indeed, the BEQ has far fewer components compared to other commercially available AEQs and appears to be an option that is much more sustainable and would cost less than the LTC3300, EMB1499Q, or TIDA-8017 designs.

In conclusion, the literature review has shown that, on one hand, Passive equalizers are simple to implement, but they have 0% efficiency, which leads to high heat loss. With a PEQ, the discharge capacity is still determined by the weakest cell in the pack. Although they perform poorly, most users prefer to use passive EQUs because they are cheap. On the other hand, active equalizers are more complex and expensive, but since they transfer charge between cells they have low losses, can provide fast equalization, and provide a battery capacity close to the average capacity of all the cells. However, commercial AEQs are not practical for large BESS because of their low equalization current and the limited number of cells they can service. Finally, the literature review and intellectual property search confirmed that the Bilevel EQU is indeed a new type of equalizer. The BEQ cost is close to a PEQ and has an efficiency close to an AEQ, and it increases the discharge capacity and longevity of the BESS. This leads us to the question of how the BEQ would improve the longevity of the BESS. To better understand how equalizers would improve the longevity of the BESS, it is important to understand Li-ion cell aging and the expected lifetime of BESS.

### ***3.7 Li-Ion Battery Aging***

This section explains the principle of operation of Li-ion battery cells, and then reviews the literature on Li-ion battery aging and symptoms.

#### **How Li-Ion Batteries Work**

Large Li-ion batteries are grouped into two main types: cylindrical and prismatic. The GAIA batteries used for this study are cylindrical batteries; therefore, the focus is on this type of battery. Li-ion battery consists of four main components: anode, cathode, separator and electrolyte as shown in Fig. 13 [60]. The battery contains two electrodes that are located in an ion rich electrolyte. A membrane called a “separator” holds the two electrodes apart.

The electrodes are wound into a cylindrical shape and immersed in the electrolyte. The negative electrode is called anode while the positive electrode is called cathode.

Figure 15 illustrates the operation of a Li-ion battery during charging and discharging. During the discharge cycle, the anode gives off electrons via the external wire, delivering power to the load. The Li is said to “deintercalated” the anode. In the electrolyte, the Li ion that just gave off electrons leaves behind positive ions (Li+) that migrate to the cathode via the electrolyte. The Li+ ion is said to “intercalate” the cathode. The current flows from the cathode to the anode (opposite to the direction of electron flow). During the charge cycle, current is injected into the cell, reversing the process.

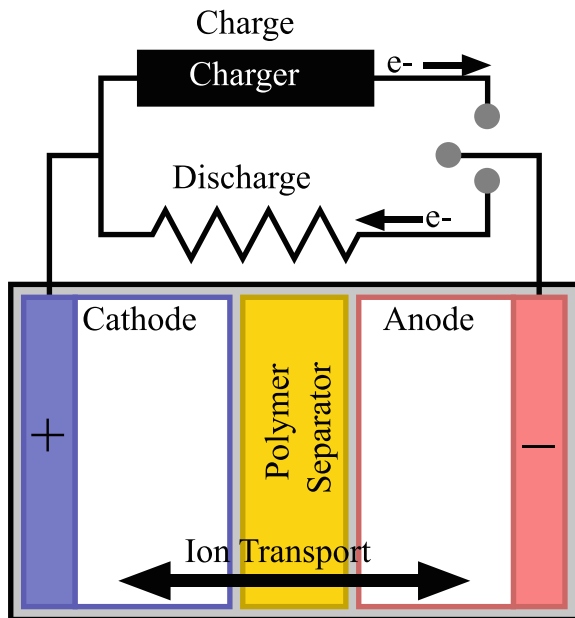
**Understanding Li-Ion Cell Aging**

Aging occurs either due to the passage of current in the battery (cycle life) or with the passage of time (calendar life) in both a uniform and non-uniform manner. Many factors affect aging such as temperature, depth of discharge, battery chemistry, cycling profile, etc. A review of [61–64] revealed the following main causes of Li-ion battery cell aging.

*Solid-electrolyte–interface (SEI) layer/lithium plating*

When the electrode is in contact with the electrolyte, a side reaction creates a film at the point of contact and increases the internal resistance. This film is called the solid-electrolyte–interface (SEI) layer [61, 62] and grows with each cycle. As explained earlier, the electrolyte is a solution composed of a lithium salt and a solvent. When the

**Fig. 15** Operation of Li-ion battery during charging and discharging [10]



battery operates under certain conditions, solid lithium forms from the electrolyte and the electrode. This phenomenon, also called Lithium plating, occurs at low temperatures and under high charging rates [64]. The SEI layer is made of Li particles that are coming from the electrode and are wasted because they do not migrate between the anode and the cathode to complete the battery cycling. As a result, this loss of usable Li ions decreases the capacity of the cell. In addition, the SEI prevents Li from accessing the electrode so fewer Li particles reach the electrode, and therefore the battery's internal resistance increases. The SEI grows mostly at the anode because the positive ions are attracted to the negatively charged electrode. Additives in the electrolyte can slow down the growth of SEI layer [64].

#### *Site Loss*

Cathodes consist of materials such as  $Mn_2O_4$  that sometimes dissolve in the electrolyte. When they dissolve, the volume of the electrode is reduced, which in turn decreases the availability of intercalation sites for Li. As the Li intercalation diminishes, the battery capacity decreases [62].

#### *Mechanical Stress*

Intercalation and deintercalation of the lithium into the electrode cause the electrode to expand and contract respectively. As a result, the mechanical stress can cause the binder that holds the electrode and the graphite together to break. High temperatures can also cause mechanical fracture.

In summary, the loss of cyclable lithium is the main cause of capacity fade, while the growth of the SEI layer and the increase in internal resistance are the main causes for power decrease [63, 64].

### ***3.8 Review of Expected Life of Large Li-Ion Batteries Per Applications***

This section considers the expected life of large Li-Ion batteries for stationary and mobile applications. As stated previously, the expected life can be specified in terms of total number of cycles or calendar years.

#### **Stationary applications: grid and renewable energy**

The Electric Power Research Institute (EPRI) has conducted a study to determine the benefits and life cycle costs of energy storage systems [65]. Table 3 shows a summary of the energy storage characteristics by applications for Li-ion batteries as they are used for stationary (grid) applications.

The expected life is listed in the column titled "Expected Life in Total Cycles". Note that the following costs were included in the calculations: cost of power electronics, all installation costs, step-up transformer, and grid interconnection to utility standards. Smart grid communication and controls are assumed to be included. The

**Table 3** Li-ion energy storage characteristics by stationary applications [65]

Li-ion energy storage stationary application	Capacity	Power	Duration (hrs.)	% Efficiency	Expected life in total cycles	Total cost (\$/kw)	Cost (\$/kw-hrs.)
ISO fast frequency regulation and renewable integration	0.25–25 MWh	1–100 MW	0.25–1	87–92	> 100,000	1085–1550	4340–6200
Utility T&D grid support applications	4.0–24 MWh	1–10 MW	2.0–4.0	90–94	4,500	1800–4100	900–1700
Commercial and industrial applications	0.1–0.8 MWh	0.05–0.2 MW	2.0–4.0	80–93	4,500	3000–4400	950–1700
Distributed Energy Storage System (DESS) applications	25–50 kWh	25–50 kW	1.0–4.0	80–93	5,000	2800–5600	950–3600
Residential energy management	7–40 kWh	1–10 kW	1.0–7.0	75–92	5,000	1250–11,000	800–2250

cost in \$/kW-h is found by dividing the total cost by the storage duration cost (\$/kW-h) = Total cost/hrs of storage. Rastler [65] concluded that for Transmission and Distribution support applications, the present value of benefit is less than \$500/ kW-h of energy storage. The biggest benefits are seen for grid regulation, transmission capacity, and transmission deferral where benefits can reach up to \$1,228 to \$2,755 per kilowatt-hour of energy storage.

**Mobile Applications: Electric Vehicles**

The United States Advanced Battery Consortium (USABC) is an organization of vehicle manufacturers and battery manufacturers whose mission is “to develop electrochemical energy storage to support the commercialization of fuel cell, electric and hybrid vehicles” [66]. The USABC was created in 1991 and it sets the standard and goals for new automotive battery technology, which are summarized in Table 4.

According to Table 4, a battery for automobile applications (xEV) is expected to last at least 15 years in calendar years [67–70]. The cycle time is also given for each application. An application that requires high power/energy would be more demanding than an application that only requires low power. Indeed, the BESS for a pure EV or battery vehicle is expected to operate for only 1,000 cycles. Whereas the BESS of PHEV which have an alternate source of power are expected to operate at least 300,000 cycles. These are important constraints for XEV manufacturers. Both PHEV, EV and power assisted HEV all operate at 420 V. The BESS for a 48 V HEV

**Table 4** Battery energy storage characteristics by mobile xEV applications

Li-ion energy storage stationary application	Cold cranking power/energy	Max voltage	Min voltage	Expected life in total cycles	Cal. life (yrs.)	Refs.
Power assisted hybrid electric vehicles	7 KW	420 V	300 V	300,000	15	[67]
Plug in Electrical Vehicle (PHEV)	7 KW	420 V	150 V	300,000	15	[67]
Electric Vehicle (EV)	45 KWh	420 V	220 V	1,000	15	[68]
48 V Hybrid Electric Vehicle (HEV)	6 KW 0.5 s 4 KW 4 s	52 V	38 V	75,000	15	[69]
12 V Start-Stop Vehicles	6KW 0.5 s 4KW 4 s	14.6 V	10.5 V	450,000 engine starts 150,000 miles	15	[70]

is expected to last 75,000 cycles and requires operating voltages between 32 and 52 V. Finally, the 12 V start-stop application requires a nominal 12 V voltage.

## References

1. Fairley, P.: The troubled link between gas and electricity grids. *IEEE Spectrum* **53**(6), 11–12 (2016). <http://ieeexplore.ieee.org/document/7473135/?ar-number=7473135&tag=1>
2. <https://globenewswire.com/news-release/2016/06/13/848095/0/en/Global-Battery-Man-agement-System-Market-2016-2022-Johnson-Matthey-Dominates-the-7-25-Market.html>
3. St. John, J.: California utilities are fast-tracking battery projects to manage Aliso Canyon Shortfall. *Greentech Med.* (2016). <https://www.greentechmedia.com/articles/read/california-utilities-are-fast-tracking-battery-projects-to-manage-aliso-can>
4. Barsukov, Y., Qian, J.: *Battery Power Management for Portable Devices*, pp. 111–138. ArtechHouse, Boston MA (2013)
5. Application Note “AN2013-02” V2.0, Infineon, (2013). [https://www.infineon.com/dgdl/Infineon-MOSFET\\_Small\\_Signal\\_selection\\_of\\_the\\_MOSFET\\_for\\_faster\\_balancing\\_of\\_Li-Ion\\_batteries-AN-v01\\_00-EN.pdf?fileId=db3a30433cfb5caa013cfbf079c10255](https://www.infineon.com/dgdl/Infineon-MOSFET_Small_Signal_selection_of_the_MOSFET_for_faster_balancing_of_Li-Ion_batteries-AN-v01_00-EN.pdf?fileId=db3a30433cfb5caa013cfbf079c10255)
6. Kim, H.-S., Park, K.-B., Park, S.-H., Moon, G.-W., Youn, M.-J.: A new two-switch flyback battery equalizer with low voltage stress on the switches. *IEEE Energy Conver Congress Expos* **2009**, 511–516 (2009)
7. Mubenga, N.S., Linkous, Z., Stuart, T.: A bilevel equalizer for large lithium-ion batteries. *Batteries*. Accepted for publication (2017) <https://www.mdpi.com/2313-0105/3/4/39>
8. Andreas, D.: White Paper-Dissipative vs. Non-Dissipative Balancing (a.k.a: Passive vs. Active Balancing) (2010). [http://liionbms.com/php/wp\\_passive\\_active\\_balancing.php](http://liionbms.com/php/wp_passive_active_balancing.php)
9. Mubenga, N.: A battery management system for large Li-ion batteries with Bi-level equalization. Dissertation, University of Toledo, Ohio (2017). [http://rave.ohiolink.edu/etdc/view?acc\\_num=toledo1513207337549147](http://rave.ohiolink.edu/etdc/view?acc_num=toledo1513207337549147)
10. Tkarcher: Battery with polymer separator. [https://upload.wikimedia.org/wikipedia/commons/c/c4/Battery\\_with\\_polymer\\_separator.svg](https://upload.wikimedia.org/wikipedia/commons/c/c4/Battery_with_polymer_separator.svg). Attribution: Tkarcher, CC BY-SA 3.0 <<https://creativecommons.org/licenses/by-sa/3.0/>>, via Wikimedia Commons
11. Mubenga, N.S., Stuart, T.: A low cost hybrid equalizer for Lithium Ion BESS. In: 2018 IEEE Clemson University Power Systems Conference (IEEE PSC18), Clemson, SC (2018)
12. Mubenga, N.S., Stuart, T.: A bilevel equalizer for lithium ion batteries. In: IEEE 2018 National Aerospace and Electronics Conference (NAECON 2018), Dayton, OH, USA (2018). <https://ieeexplore.ieee.org/document/8556725>
13. Mubenga, N.S., Sharma, K., Stuart, T.: A bilevel equalizer to boost the capacity of second life Li Ion batteries. *Batteries* (2019). <https://www.mdpi.com/2313-0105/5/3/55>
14. Mubenga, N.S., Salami, B., Stuart, T.: Bilevel vs. passive equalizers for second life EV batteries. *Electricity* **2**(1) (2021), 63–76. Retrieved online February 7, 2021 from <https://www.mdpi.com/2673-4826/2/1/4/htm>
15. Salami, B.: The efficiency measuring apparatus for li-ion battery equalizers. Master Thesis, University of Toledo, Ohio (2021). [http://rave.ohiolink.edu/etdc/view?acc\\_num=toledo1619460723390441](http://rave.ohiolink.edu/etdc/view?acc_num=toledo1619460723390441)
16. Mubenga, N.S.: The efficiency measuring apparatus for the design of li-ion batteries equalizers. In: NAECON 2021—IEEE National Aerospace and Electronics Conference, pp. 18–24 (2021). <https://doi.org/10.1109/NAECON49338.2021.9696391>
17. Andreas, D.: *Battery management systems for large lithium-ion battery packs*, pp. 35–87, ArtechHouse, Boston MA (2010)
18. Lindemark, B.: Individual cell voltage equalizers (ICE) for reliable battery performance. In: *Proceedings of 13th Annual International Telecommunication Energy Conference*, pp. 196–201

19. Williamson, S.S.: Design, testing, and validation of a simplified control scheme for a novel plug-in hybrid electric vehicle battery cell equalizer. *IEEE Trans. Ind. Electron.* **57**(12), 3956–3962 (2010)
20. Baronti, F., Fantechi, G., Leonardi, E., Roncella, R., Saletti, R.: Hierarchical platform for monitoring, managing and charge balancing of LiPo batteries. In: *Proceedings of Vehicle Power Propulsion Conference*, pp. 1–6 (2011)
21. Lee, K.M., Lee, S.W., Choi, Y.G., Kang, B.: Active balancing of Li-ion battery cells using transformer as energy carrier. *IEEE Trans. Ind. Electron.* **64**(2), 1251–1257 (2017)
22. Zhang, D.-A., Zhu, G-R, He, S.J, Qiu, S., Ma, Y., Wu, Q.-M., Chen, W.: Balancing control strategy for li-ion batteries string based on dynamic balanced point. *Energies* **8**, 1830–1847 (2015). <http://www.mdpi.com/1996-1073/8/3/1830>. Accessed July 2017
23. Lee, K.M., Chung, Y.C., Sung, C.H., Kang, B.: Active cell balancing of Li-ion batteries using LC series resonant circuit. *IEEE Trans. Ind. Electron.* **62**(9), 5491–5501 (2015)
24. Shang, Y., Xia, B., Lu, F., Zhang, C., Cui, N., Mi, C.C.: A switched-coupling-capacitor equalizer for series-connected battery strings. *IEEE Trans. Power Electron.* **32**(10), 7694–7706 (2017)
25. Baronti, F., Fantechi, G., Roncella, R., Saletti, R.: High-efficiency digitally controlled charge equalizer for series-connected cells based on switching converter and super-capacitor. *IEEE Trans. Ind. Inf.* **9**(2), 1139–1147 (2013)
26. Cadar, D., Petreus, D., Patarau, T., Palaghita, N.: Active balancing method for battery cell equalization. In: *ACTA Technica Napocensis Electronics and Telecommunications*, vol. 51, no. 2 (2010). [https://users.utcluj.ro/~ATN/papers/ATN\\_2\\_2010\\_1.pdf](https://users.utcluj.ro/~ATN/papers/ATN_2_2010_1.pdf). Accessed July 2017
27. Lee, Y., Jeon, S., Lee, H., Bae, S.: Comparison on cell balancing methods for energy storage applications. *Ind. J. Sci. Technol.* **9**(17) (2016)
28. Einhorn, M., Roessler, W., Fleig, J.: Improved performance of serially connected Li-ion batteries with active cell balancing in electric vehicles. *IEEE Trans. Veh. Technol.* **60**(6), 2448–2457 (2011)
29. Park, H.S., Kim, C.E., Kim, C.H., Moon, G.W., Lee, J.H.: A modularized charge equalizer for an HEV lithium-ion battery string. *IEEE Trans. Ind. Electron.* **56**(5), 1464–1476 (2009)
30. Kutkut, N.H., Divan, D.M.: Dynamic equalization techniques for series battery stacks. In: *Proceedings of 18th Annual International Telecommunication Energy Conference*, pp. 514–521
31. Moore, S.W., Schneider, P.J.: A review of cell equalization methods for lithium ion and lithium polymer battery systems. In: *Proceedings of SAE World Congress Doc. 2001-01-0959* (2001)
32. Lukic, S.M., Cao, J., Bansal, R.C., Rodriguez, R., Emadi, A.: Energy storage systems for automotive applications. *IEEE Trans. Ind. Electron.* **55**(6), 2258–2267 (2008)
33. Kutkut, N.H., Wiegman, H.L.N., Divan, D.M., Novotny, D.W.: Design considerations for charge equalization of an electric vehicle battery system. *IEEE Trans. Ind. Appl.* **35**(1), 28–35 (1999)
34. Sakamoto, H., Murata, K., Sakai, E., Nishijima, K.: Balanced charging of series connected battery cells. In: *Proceedings of 22nd Annual International Telecommunication Energy Conference*, pp. 311–315
35. Gottwald, T., Ye, Z., Stuart, T.: Equalization of EV and HEV batteries with a ramp converter. *IEEE Trans. Aerosp. Electron. Syst.* **33**(1), 307–312 (1997)
36. Tang, M., Stuart, T.: Selective buck-boost equalizer for series battery packs. *IEEE Trans. Aerosp. Electron. Syst.* **36**(1), 201–211 (2000)
37. Chen, T.C., Guey, Z.J.: Charge equalizer or series of connected battery strings. U.S. Patent 6 008 623 (1999)
38. Schmidt, H., Siedle, C.: The charge equalizer—a new system to extend battery life-time in photovoltaic systems, UPS and electric vehicles. In: *Proceedings of 15th Annual International Telecommunication Energy Conference*, pp. 146151
39. Einhorn, M., Guertlschmid, W., Blochberger, T., Kumpusch, R., Permann, R., Conte, F., Kral, C., Fleig, J.: A current equalization method for serially connected battery cells using a single power converter for each cell. *IEEE Trans. Veh. Technol.* **60**(12), 4227–4237 (2011)
40. Stuart, T.A., Zhu, W.: Modularized battery management for large lithium-ion-cells. *J. Power Sour.* **196**, 458–464 (2011)



41. Kim, M.-Y., Kim, J.-W., Kim, C.-H., Cho, S.-Y., Moon, G.-W.: Automatic charge equalization circuit based on regulated voltage source for series connected lithium-ion batteries. In: Proceedings of 8th International Conference on Power Electron. ECCE Asia, pp. 2248–2255 (2011)
42. Oriti, G., Julian, A.L., Norgaard, P.: Battery management system with cell equalizer for multi-cell battery packs. In: 2014 IEEE Energy Conversion Congress and Exposition (ECCE), pp. 900–905 (2014)
43. Zhu, W.: An improved targeted equalizer for battery management systems. Master Thesis, University of Toledo, Ohio, USA (2008)
44. Park, H.-S., Kim, C.-E., Kim, C.-H., Moon, G.-W., Lee, J.-H.: A modularized charge equalizer for an HEV lithium-ion battery string. *IEEE Trans. Ind. Electron.* **56**(5), 1464–1476 (2009)
45. Karnjanapiboon, C., Jirasereeamornkul, K., Monyakul, V.: High efficiency battery management system for serially connected battery string. In: Proceedings of IEEE International Symposium on Industrial Electronics, pp. 1504–1509 (2009)
46. Pascual, C., Krein, P.T.: Switched capacitor system for automatic series battery equalization. In: Proceedings 12th Annual IEEE Applied Power Electronics Conference Exposition, pp. 848–854
47. Baughman, A.C., Ferdowsi, M.: Double-tiered switched-capacitor battery charge equalization technique. *IEEE Trans. Ind. Electron.* **55**(6), 2277–2285 (2008)
48. Lee, Y.S., Cheng, G.T.: Quasi-resonant zero-current-switching bidirectional converter for battery equalization applications. *IEEE Trans. Power Electron.* **21**(5), 1213–1224 (2006)
49. Lee, Y.S., Cheng, M.W.: Intelligent control battery equalization for series connected lithium-ion battery strings. *IEEE Trans. Ind. Electron.* **52**(5), 1297–1307 (2005)
50. Manenti, A., Abba, A., Merati, A., Savaresi, S.M., Geraci, A.: A new BMS architecture based on cell redundancy. *IEEE Trans. Ind. Electron.* **58**(9), 4314–4322 (2011)
51. Kutkut, N., Divan, D.: Dynamic equalization techniques for series battery stacks. In: Proceedings of 18th International Telecommun Energy Conference, pp. 514–521 (1996)
52. Moore, S.W., Schneider, P.J.: A review of cell equalization methods for lithium ion and lithium polymer battery systems. In: Proceedings of SAE World Congress, Paper 2001-01-0959
53. Cao, J., Schofield, N., Emadi, A.: Battery balancing methods: a comprehensive review. In: Proceedings of IEEE Vehicle Power and Propulsion Conference, pp. 1–6 (2008)
54. Lindemark, B.: Individual cell voltage equalizers (ICE) for reliable battery performance. In: Proceedings of International Telecommunications Energy Conference, pp. 196–201 (1991)
55. Baronti, F., Fantechi, G., Roncella, R., Saletti, R.: Design of a module switch for battery pack reconfiguration in high-power applications. In: Proceedings of IEEE International Symposium on Industrial Electronics, pp. 1330–1335 (2012)
56. Datasheet “LTC3300–1 Datasheet”, document number 33001fb, Linear Technology accessed online at [www.linear.com/LTC3300-1](http://www.linear.com/LTC3300-1)
57. Datasheet “EMB1499Q”, Document# SNOSCV7B”, Rev 9/13 Texas Instrument, September 2013. Accessible online at <http://www.ti.com/product/EMB1499Q>
58. Mubenga, N.S.: Efficiency Measuring Apparatus, Active Equalizer Inductor Design Tool and Equalizer Design App. U.S. Provisional patent 63/167,471 (2021)
59. Stuart, T.A.: A Bilevel Equalizer for Battery Cell Charge Management, U.S. Provisional Patent Application # 62/287,575 (2016)
60. Voelker, T.: Fisher Scientific “Trace Degradation Analysis of Lithium Ion Battery” Sunnyvale, California, March 2014. <https://tools.thermofisher.com/content/sfs/brochures/AR-Lithium-Ion-Battery-Degradation-RandD-Mag-042214.pdf>
61. Smith, K., Wood, E., Santhanagopalan, S., Kim, G.H., Shi, Y., Pesaran, A.: Predictive Models of Li-Ion Battery Lifetime National Renewable Energy Laboratory, NREL/PR-5400-64622, Advanced Automotive Battery Conference and Large Li-Ion Battery Symposium, Detroit, Michigan, June 15–19 (2015)
62. Bartlett, A.: Electrochemical model-based state of charge and state of health estimation of Lithium Ion batteries. Dissertation, The Ohio State University, Ohio (2015)

63. Zhang, Y., Wang, C.Y., Tang, X.: Cycling degradation of an automotive LiFePO<sub>4</sub> lithium-ion batteries. *J. Power Sour.* **196**(2011), 1513–1520 (2010)
64. “BU808-b: What causes Li-ion to Die” Battery University [http://batteryuniversity.com/learn/article/bu\\_808b\\_what\\_causes\\_li\\_ion\\_to\\_die](http://batteryuniversity.com/learn/article/bu_808b_what_causes_li_ion_to_die)
65. Rastler, D.: Electricity Energy Storage Technology Options: A White paper Primer on Applications, Costs, and Benefits 1020676, EPRI (2010)
66. United States Advanced Batteries Consortium (USABC) Website. Online retrieved on 10/24/2017. <https://uscar.org/usabc/>
67. “PHEV Battery Goals” United States Advanced Batteries Consortium, USA. <https://uscar.org/usabc/#246-246-top>
68. “EV Battery Goals” United States Advanced Batteries Consortium, USA. <https://uscar.org/usabc/#246-246-top>
69. “48V HEV Battery Goals” United States Advanced Batteries Consortium, USA. <https://uscar.org/usabc/#246-246-top>
70. “12V Start Stop Vehicles Battery goals” United States Advanced Batteries Consortium , USA. <https://uscar.org/usabc/#246-246-top>

# Generation Expansion Planning Using Renewable Energy Sources with Storage



K. Rajesh, A. Ramkumar, and S. Rajendran

**Abstract** A vital component of maintaining economic growth is the development of the power infrastructure. Most power plants in India are powered by traditional energy sources such as coal, diesel, oil, gas, hydropower, and nuclear power. Numerous techniques for solving the models and resolving the efficiency issue have been put out in recent years. To create a realistic mathematical system and use GEP in the model solutions, the goal of this work is to analyze the GEP for the candidate system by integrating all important system components. The planning of the test system is done for two separate planning horizons, which are 6 and 14 years, respectively. For the same power system, GEP mathematical modeling studies are conducted to examine the effects of the addition of a solar power plant with a storage facility. Based on (a) the investment strategies of introducing solar plants as an alternative candidate plant or as a replacement for existing High Emission Plants (HEP), (b) whether the Solar Plant with Storage (SPWS) or Without Storage (SPWNS) capacity, and (c) inclusion of treatment/penalty costs on emissions from HEP, this is planned in a four-level hierarchy. For anticipated solar penetration levels of 5–10 and 10–20% for 6 and 14 years of planning horizons, respectively, the sensitivity of the system performance elements such as the capacity added, total cost, and Expected Energy Not Served (EENS) is also carried. The system's performance is very dependent on the FOR% that is expected. When SPWS is added to the system as an alternative investment candidate plant, the model studies present an upbeat prospect for power system planning. This study offers a four-level hierarchy to understand the full range of policy issues that may arise in GEP and enables planners to implement situation-specific solutions, while also attempting to illustrate the complexity of the decision-making process when introducing solar plants into an existing system.

---

K. Rajesh (✉) · A. Ramkumar · S. Rajendran

Kalasalingam Academy of Research and Education, Anand Nagar, Krishnankovil, Srivilliputhur, Tamil Nadu, India

e-mail: [k.rajesh@klu.ac.in](mailto:k.rajesh@klu.ac.in)

A. Ramkumar

e-mail: [a.ramkumar@klu.ac.in](mailto:a.ramkumar@klu.ac.in)

S. Rajendran

e-mail: [s.rajendran@klu.ac.in](mailto:s.rajendran@klu.ac.in)

**Keywords** Generation expansion planning · Emission forced outage rate · High emission · Low emission plants

## 1 Introduction

Due to the temporal and spatial fluctuations in both the supply and demand for energy, generation expansion planning (GEP) is a difficult task. Additionally, a complex mix of alternative candidate plants with various physical and production capabilities and features must be included in the system. The GEP is a large-scale, long-term, non-linear, mixed-variable mathematical modeling issue since all these components are integrated into a system framework. For the development of an effective and affordable power system, the precise solution of such realistic models is crucial. To maintain economic growth, the improvement of the power infrastructure is crucial. In India, most power plants rely on traditional energy sources such coal, diesel, oil, gas, hydropower, and nuclear power. Numerous techniques for solving the models and addressing the efficiency problem have been put forth in recent years.

The objective of this work is to analyze the GEP for the candidate system, integrating all important system components that will result in the development of a plausible mathematical system and the use of GEP in the model solutions. The planning of the test system is done for two separate planning horizons, which are 6 and 14 years, respectively. A special emphasis is placed on examining the effects of such an increase because it is anticipated that the system will contain an increasing number of solar and wind power facilities in the future.

It is examined how to strike a balance between the advantages of increasing solar penetration and the expense of modifying current base load systems. By applying a realistic set of Total Emission Reductions Constraints (TERC) and Emission Treatment Penalty Costs (ETPC) to the remaining amount of pollution, a balanced approach is taken to comprehend the long-term effects of solar additions. Additionally, it is examined how different solar power development and emissions reduction scenarios will affect the system generation mix and system reliability.

A power system faces expansion and operating issues when Renewable Energy Technologies (RET) like solar and wind power facilities are added. Due to the distinctive generation characteristics of these RET plants, earlier studies have shown the requirements for extra backup power facilities required for every installation of RET plants. Power system planners have recently become interested in alternate methods of building power storage facilities using energy from RETs and obtaining reliable supply from such storage facilities. Studies using GEP mathematical modeling are conducted for the same power system to determine how the addition of solar power plants with storage facilities will affect the system. Based on (a) the investment strategies of introducing solar plants as an alternative candidate plant or as a replacement for existing High Emission Plants, this is planned in a four-level hierarchy (HEP) (b) the capacity of either a solar power plant with storage (SPWS) or without storage (SPWNS), and (c) the inclusion of treatment and penalty charges for HEP emissions.

For assumed solar penetration levels of 5–10 and 10–20% for 6- and 14-year planning horizons, respectively, the sensitivity of the system performance factors such as the capacity added, overall cost, and Expected Energy Not Served (EENS) for variations in assumed Forced Outage Rate (FOR%) is also considered. The assumed FOR% has a significant impact on the system performance. When SPWS is added to the system as an alternative investment candidate plant, the model studies present a positive scenario for power system planning. This study offers a four-level hierarchy to understand the full range of policy issues that may arise in GEP and enables planners to adopt situation-specific solutions, while also attempting to illustrate the complexity of the decision-making process when introducing solar plants into an existing system.

## 2 Overview

Any power system's primary goal is to provide affordable, dependable electricity to all types of consumers, including residential, commercial, industrial, and agricultural ones. The power utilities' main duty is to anticipate future customer demands and carefully plan the installation of additional capacity to meet those demands. The growth of the nation's infrastructure as well as its technological, social, and economic advancements depend heavily on electric energy. The amount of power used per person in a nation indicates its level of development. It also serves as a gauge of a nation's citizens' standard of living. The demand for electricity rises because of economic growth and the related rise in economic activity. Human activities such as industrial production, domestic/residential life, agricultural endeavors, transportation, lighting, and heating all involve the use of electricity. Electric energy cannot be conveniently stored in huge quantities, therefore a constant and nearly immediate balance between production and consumption of power is required. To accommodate fluctuations in demand, some extra generation will be maintained on hand. Load shedding is inevitable if the supply system is unable to keep up with demand. The power shortage might be lessened by the improved installed capacity. The excessive investment and high operational costs could raise the cost of energy, which would then be reflected in the consumer's bill. On the other side, inadequate investment and low generation margins may result in poor customer reliability and a lack of access to power. The most crucial aspects of energy policy are the identification and analysis of energy development as well as the problems of use, distribution, and planning.

Power systems benefit from investments in generation systems. Researchers have proposed GEP to manage generation system planning that is optimal in this regard. Many research projects on GEP have been conducted in recent years. These issues have been researched using various viewpoints, approaches, restrictions, and goals.

The distribution, transmission, and generation sectors can all participate in the expansion of the electric power system. In comparison to TEP and the distribution portion of the power system, the investment in GEP is significantly greater. In terms of reliability, the power system engineers prioritize the increase of generation above

the other two sectors. The transmission and distribution networks might be regarded as one of the limits because GEP can be carried out without increasing them. Investors and consumers have long paid close attention to the GEP, which is associated with investments in energy generation. To ensure a profit in this industry and the happiness of the customers, the investment strategy should consider the various aspects of difficulties, such as sizing, timing, the technology of new generating units, investment reversibility, risks, and uncertainties. In GEP, the goal is to increase the current power system to meet future demand growth while maintaining reliability standards at the lowest possible cost. Over a planning horizon of typically 10–30 years, the GEP specifies the size, location, technology, and timing of installing new plants to serve the anticipated load within the specified dependability criteria.

All nations have become increasingly concerned about climate change and emissions since the United Nations Conference on Human Development in Stockholm in 1972, the creation of the Intergovernmental Panel on Climate Change (IPCC), and the adoption of the United Nations Framework Convention on Climate Change (UNFCCC) at the Rio Summit in 1992. As a result, the Kyoto Protocol and the Bali Action Plan were created (BAP). Today, there is a considerable global worry about the threat of climate change brought on by human emissions. The action plan for the growth of every nation on earth reflects it.

Policymakers have adopted policies to encourage investments in low-emissions renewable electricity generation to decarbonize the electric power networks. To balance the load and generation and ensure system reliability, different and more expensive procedures are needed as the use of Renewable Energy Technologies (RET) increases. Two significant problems have resulted because of this: (i) an increase in overall system costs as a result of the required renewable dispatches, and (ii) the offset of emission benefits as a result of the renewable by the ramping and cyclic operations of other plants in the system as suggested by the MIT Energy Initiative [1]. Planning for capacity growth presents a challenge because each technological generation has unique technical and economic characteristics. This makes it difficult to properly integrate these problems into a system architecture.

Due to their unreliability and widespread environmental concerns, many nations around the world are intending to employ wind and solar energy as major replacements for traditional energy produced from fossil fuels. The installed wind power capacity has increased by around 30% annually over the past 10 years. According to the European Wind Energy Association [2], Denmark, Germany, and Spain are the first few nations to produce 20% of their electricity from wind turbines. By the end of 2004, 200,000 off-grid wind turbine generators had been deployed, making industrialized nations like China the world's leaders [3].

There are numerous renewable energy sources available in India. From about 7.8% in 2008 to 12.3% in 2013, RET's share of power systems increased, and by 2017, it is anticipated to reach 17% of all installed capacity. The enormous environmental, social, and economic advantages of wind energy make it a particularly viable alternative for generating electricity. When compared to traditional sources, the behavior of electrical power generation from wind energy is very different. The use of wind energy in grid-connected and stand-alone systems will continue to be encouraged by

advancements in wind generation technologies. The reliability difficulties related to wind energy sources must therefore be properly considered by engineers and planners of power systems. One of the fastest-growing sources of energy for humans is the wind, which may also be used to generate fossil fuels and conventional electricity. Wind energy has no associated costs and requires little upkeep. As of the end of March 2017, India's installed wind generating capacity totaled 31.17 GW, a substantial growth over the previous few years.

Solar energy has expanded significantly during the past 10 years in addition to wind energy. The country receives the most amount of solar radiation in the globe due to its extensive landmass. India has enacted several legislative initiatives to encourage investments in low-emissions renewable electricity generation, keeping up with the worldwide trend. The expansion of solar energy potential has been encouraged by the Indian government. By 2013, the installed capacity of solar power plants has expanded to 1683 MW since the Jawaharlal Nehru National Solar Mission (JNNSM) was established in 2009. By 2022, it's anticipated that a combination of rising electricity demand, rising fossil fuel prices, difficulties in obtaining fossil fuels, and favorable environmental legislation will enable solar power capacity to reach more than 50 GW.

Research on assessing the solar and wind energy potential based on irradiation data, the effects of solar and wind energy technologies, and the market potential for investment has only been conducted in a small number of studies. Furthermore, no systematic investigation of the potential combinations of electricity-generating technologies under various future scenarios of solar and wind energy development has been done in India. This might be the case because the unique properties of solar and wind technologies call for specialized data and modeling capabilities. While conventional thermal generators can typically be dispatched within specified operational parameters, the output of solar and wind energy is influenced by the spatial and temporal heterogeneity of solar irradiation. While solar systems can produce electricity without any emissions, their limited capacity to forecast production, store electricity, and manage the supply of renewable energy is likely to have an impact on all levels of electric power system regulation. Between the dispatch point and the root nodes, where the capable generation of renewable energy takes place, there is now confusion and a stark divide. This makes capacity-expansion modeling more complex. No single model study can consider all the many problems involved in simulating solar and wind technology.

A GEP modeling analysis is conducted in this study for a test system to examine the effects of expanding the use of solar and wind power technologies. Long-term investments in conventional technology capacity-expansion modeling technique are used to conduct the analysis of the solar energy portfolio. In order to create an ideal system and aid in the analysis of the operational behaviors of the plants, the model uses a set of presumptive sun penetration levels. It is also done to determine how sensitive the system generation mix is to various solar power development and emissions reduction scenarios (as a replacement for various oil plants and also as a proportional addition to the current system capacity). The differences in reliability indices and other cost components as a result are also reported.

### 3 Literature Review

The levels of decarbonization targeted for energy in 2050 have been suggested by Ben Haley et al. [4]. Both substantially higher variable renewable penetrations and much stricter restrictions on the use of fossil power for system balancing are possible in low-carbon scenarios. Renewable energy sources, like wind and solar, have the potential to significantly reduce the reliance on fossil fuels and greenhouse gas emissions in the electric sector, according to Paul Denholm et al. [5].

High penetration RETs with affordable energy storage have been proposed by Pandzic et al. [6] in order to address the issues of uncertainty and unpredictability related to renewable energy sources, such as wind and solar power systems. In order to balance the imbalance between renewable energy generators and consumption and/or to store excess renewable energy for later use during low- or no-generation periods, energy storage devices will be required at various locations throughout the power system. Jewell and Hu have spoken about this in [7].

A few approaches that have recently been established to investigate the viability of coordinating electric energy storage (EES) with renewable technology plants have been put forth by Vasconcelos et al. [8]. Depending on the extent of the problems and the context of the applications, different modeling and optimization algorithms for GEP with RET with storage facilities are used.

India intends to significantly increase its use of renewable energy to 175 GW by 2022 to reduce emissions. Intended Nationally Determined Contributions provides details on this (INDCs). To handle the fluctuations in the generation from renewable (green) sources, additional conventional sources with some emissions, such as thermal, must also be present if renewables are to produce such a huge amount of power. Offering generation flexibility entails quick ramping, quick startup, and effective partial load operating in the absence of significant storage. These plants' operations, maintenance schedules, and anticipated operating lifetimes will all suffer if their capacity to ramp and the cycle is increased to various degrees.

The GEP problem, which has been studied by system designers for more than 40 years, has been presented by Francesco et al. [9]. The planners can choose the generation technology, the size of the generation units to be built, and the amount of energy that can be generated by both new and existing plants by solving the GEP problem while considering the limitations on construction times, life-cycle duration, and the total amount of investment.

Because fossil fuels are not sustainable and there are widespread environmental concerns, several nations throughout the world are aiming to employ wind and solar energy as significant replacements for conventional energy. The Global Wind Energy Council (GWEC) discusses how installed wind capacity has grown by around 30% annually over the past 10 years [10]. Future sustainable energy systems are projected to use a greater proportion of renewable energy. In 2007, 94 GW (2.5% of the installed electrical power capacity) came from wind energy [11]. George and Banerjee [12] examined the development of the wind's contribution in numerous grids, which is



large in several countries (22% in Denmark, 20% in Spain, 17% in Germany and Portugal, and 8% in the Netherlands).

Techniques for hydropower and fossil fuel plants are provided by conventional power planning. Depending on the site wind regime and machine parameters, the output of a wind power plant varies daily and over the course of the year. The challenges of capacity expansion planning and dispatch become more crucial as wind energy's proportion rises and becomes considerable. It has been investigated how wind energy affects the grid in terms of capacity credit. According to Milligan [13], the degree of a conventional generation that can be replaced by wind generation is known as the capacity credit of wind power.

According to Sharan et al. [14], a clean energy future will necessitate increasing investment in renewable energy sources, which can also offer appealing dividends including job creation, economic growth, energy security, and improved price stability in addition to environmental advantages. As a result, governments all around the world are increasingly focusing on renewable energy. Indian policymakers have supported renewables via tools including the Renewable Purchase Obligation (RPO), Renewable Energy Certificates (REC), Tax Credits, and Generation Based Incentives to decarbonize the electric power systems (GBI). Three major issues arise for generation and grid operations because of the integration of renewable energy sources into current conventional electrical power systems: non-controllable fluctuation, partial unpredictability, and location dependence. The basis for integrating large-capacity Renewable Energy (RE) power into the grid is an understanding of these distinctive characteristics and how they interact with other components of the power system, whereas conventional thermal generators can typically be dispatched within some operational parameters [15]. The external component of sun irradiation affects how much solar power is produced. This irradiance is heterogeneous geographically, temporally, and both.

Correct investment choices, a better regulatory environment, and beneficial government policies will be the results of knowledge regarding the performance of solar power plants [16]. With the aim of estimating the performance of solar power plants at various locations, they have looked at a variety of factors contributing to the performance of solar power plants, including radiation, temperature, and other climatic conditions, design, inverter efficiency, and degradation due to aging. They have also reviewed existing radiation data sources and design criteria for solar power plants.

Using the Google Earth TM application, which offers either satellite photos of building roofs or their number of floors via the Street View feature, Cellular et al. [17] have developed a good approach for the assessment of the photovoltaic potential in urban environments. The methodology's applicability has been examined in a particular urban area of the southern Italian city of Palermo. Understanding rooftop solar energy's potential is the first step in presenting it as a solution. Abhishek Pratap conducted and shared a thorough review of the prospects and hurdles for the efficient deployment of rooftop solar in Delhi city [18].

To consider how solar deployment interacts with the resource sufficiency and operating reliability of the power system, Sullivan et al. [19] have established efficient

capacity-expansion models. The system's operating-reliability load and expenses associated with the increased need for ancillary services are increased by the variability and uncertainty of the solar resource and operational characteristics. Some of them are still challenging to solve using current models, therefore they constitute a potential field for further study.

The crucial and unresolved subject of how the extra capacity will be built up and how it's ideal geographic distribution will be projected has been put up by Schroder and Bracke [20]. Particularly, the literature that is now available provides little or only hazy information about transmission networks, the availability of reserve capacity, and the geographic distribution of plants.

Many researchers use capacity expansion models to choose the best generation technologies that can be combined with solar or other renewable technologies. A overview of four main approaches—from straightforward screening-curve calculations to simultaneous capacity expansion modelling of dispatchable and non-dispatchable generators—for incorporating non-dispatchable technologies like solar into capacity-expansion modeling is described in [20]. Numerous researchers have also tested capacity expansion models using renewable energy [21–28].

According to Wang et al. [29], the GEP models split into three main categories: (1) Basic GEP models that determine what technology plants to integrate into the system, when, and how many. They do not offer full operational procedures as model decisions, (2) models deliver detailed operational procedures as a model solution while prioritizing the capacities of prospective plants, and (3) models provide both capacity and operational decisions simultaneously [30]. At various levels of approximation, these models have taken capacity and operational considerations into account. These estimates are either situation- or system-specific. When combining both capacity and operational constraints, there are significant variances in terms of the spatial and temporal resolutions. The placement, timing, and capacity considerations of the various technology plants outlined by Khokhar [30], have also been incorporated into models that aim for a finer resolution of spatial decisions. The geographical and temporal resolutions of models that included intricate operational difficulties also differ, each at the expense of the other.

Recent models that offer RETs as a choice have added operational problems like emissions, ramping, and cyclic problems on top of those relating to conventional plants. While system-specific concerns have driven the choice of a particular model for analysis, situation-specific concerns including data availability, processing power, and the goal of model analysis have also influenced the choice of model type and solution methodology.

According to Balkirtzis et al. [31], the modelling approaches can be divided into two categories: micro and macro. The micro approach uses analytical and sophisticated operational research and meta-heuristics to deal with complex non-linear transmission constraints and reliability criteria, whereas the macroeconomic approach minimizes modeling complexities by ignoring the complex features and constraints within the energy sector, typically with predictable results. Based on

model/approach, operation point of view (centralization or decentralization), transmission planning, uncertainties modeled, and implementation time step, they have developed an effective classification of models.

Using Long-range Energy Alternatives Planning (LEAP) software, Karapidakis et al. [24] examined the Crete Island power system under two long-term scenarios (with renewables penetrations of 20 and 50%) in order to calculate the costs and benefits related to the significant high electricity production from RETs in the years 2009–2020.

To discover the compromised solution, Promjiraprawat and Limmeechokcha [26] modeled CO<sub>2</sub> emissions and external cost as a multi-objective optimization problem. They have shown that, using carbon capture and storage technology, CO<sub>2</sub> emissions may be reduced by 74.7% from the least expensive option, which resulted in a 500 billion US dollar decrease in external costs over the planning horizon.

The creation of an Investment Model for Renewable Electricity Systems (IMRES) has been described by Sisternes [25], as an IMRES with unit commitment limitations, where decisions about investment, unit commitment, and energy dispatch are made simultaneously. The model is designed as a 0–1 MILP, taking capacity decisions at the level of each power plant while considering a variety of techno-economic factors, including ramp limits, startup costs, and the minimum steady outputs of thermal plants, among others.

An optimization model that considers several pertinent factors related to Photo Voltaic (PV) projects, such as location-specific solar radiation levels, a precise depiction of investment costs, and an approximation of the transmission system, has been provided by Muneer [27]. A thorough case study of the investment in large-scale solar PV projects in Ontario, Canada, is provided and analyzed to illustrate the value and practicality of the methodology and tools that are suggested.

To calculate the additional transmission capacity and reserve capacity necessary to meet customer demand and maintain grid reliability, the SunShot Vision Study examined the use of the Regional Energy Deployment System (ReEDS) to examine how the electric sector has evolved in meeting the SunShot targets. Based on a variety of variables, including regional solar resource quality, future technology, and fuel price projections, future electricity demand projections, the effects of variability in renewable generation, transmission requirements, and reserve requirements, ReEDS determines where PV, Concentrated Solar Power (CSP), and other generation technologies will be deployed.

An integrated power dispatch and load flow model with endogenous energy generation capacity augmentation has been described by Schroder and Bracke [20]. The goal is to estimate how much generation capacity would be needed in Central Europe by 2030 and where that capacity should be in relation to the planned grid structure. To assess the possibilities for replacing diesel, Rose et al. [21] utilized a system-level model for Kenya that included grid-connected solar PV and pre-existing reservoir hydropower.

With the help of High Voltage Direct Current (HVDC) transmission, Grossmann et al. [28] demonstrated that site selection optimization over sufficiently large geographic areas can address all three causes of intermittency and reduce costs

through later optimization of generation capacity and storage. They have provided techniques for converting daily insolation data from NASA's Solar Sizer to hourly scale, which can then be used to evaluate and compare large-scale networks and ultimately improve their generation and storage capabilities. Then, using solar data from 1986 to 2005, these techniques were applied to twelve potential large-scale solar networks in various locations of the world.

A regional action plan for the diffusion of renewable energy technology was evaluated by Beccali et al. [22] using the multicriteria decision-making technique. Sardinia's island has been the subject of a case study. Based on three hypothetical decision scenarios—each of which represents a cohesive set of actions—diffusion strategies have been created.

The quick expansion of solar PV generation has been fueled by factors such as the simplicity of installation, the falling cost of PV technology, and government policy that supports the development of solar energy. With less energy imports, many nations want to lower greenhouse gas emissions and increase energy security. The best way to accomplish these objectives is via renewable energy. By 2020, the European Union wants to use 20% renewable energy.

According to Zervos et al. [6], the renewable energy sector in Europe asserts that by the year 2050, 100% renewable energy will be technologically feasible. China and India are also aiming for a 15% reduction by 2020. 37 of the US's 50 states have guidelines or objectives with percentages ranging from 10 to 40% across various time frames [32].

According to Hand et al. [33] and NREL's primary findings, the US can attain 80% renewable energy by 2050. However, only thorough analyses that include 30% wind energy have supported this theoretical possibility, which is reviewed by Ackermann and Thomas [34].

Due to the erratic and unexpected nature of wind speed, high wind power generation will have a substantial influence on system security, stability, and reliability. The performance and dependability of the electricity grid may be impacted positively or negatively by the integration of numerous wind farms. System operation and system planning are typically the two angles from which the effects of wind power penetration on system security and dependability are examined. Bouffard et al. [35], Chan et al. [36], Lee et al. [37], Schlueter et al. [38], and Soder [39] have developed spinning reserve management with wind power generation for short-term system operation, which shows that spinning reserve from conventional units must be increased with the increased wind power generation to meet the specific reliability and security requirements.

According to Giebel [40], the power system needs for wind power are primarily determined by the configuration of the power system, the installed wind power capacity, and the variability of wind power production. Power systems are impacted by variations in wind resources on time spans ranging from seconds to years. The geographic region of interest will serve as the foundation for an investigation of this influence. In literature, capacity credit has typically been used to describe how wind energy affects the system. The amount of installed renewable capacity by which

conventional capacity can be decreased without compromising supply security is known as the capacity credit of wind power.

According to numerous studies [41–44] examining the consequences of grid integration of wind power in European nations, the main difficulties include effects on operational costs, power quality, imbalances, and transmission and schedule planning. According to the results, wind power impacts are minimal at low penetrations (5% or less), and they are still noticeable at penetrations of up to 20%.

The potential and popularity of wind energy as a source of electrical power has led to speculation that it could replace traditional fossil fuels. Ackermann [45] discussed how wind power is predicted to produce a sizeable share of all electrical energy in the years to come. Burke et al.'s [46] recommendation addresses the unfavorable effect of wind farms producing energy in the presence of transmission line constraints. Even if the wind farm must be cut, some of the works recommend that the remaining lines be operated as efficiently as possible.

One of the most frequently brought up issues in relation to operations research is the GEP problem. A forward dynamic programming method had been used to solve the GEP problem in the early 1970s. More focus has been placed on this subject because of the 1980s' improvements in computational techniques and power. Since 2000, more advanced computational methods have been created to address the GEP challenge.

The literature assessment conducted for this study supports the widely held belief that long-term use of non-renewable energy generation systems will result in a fervent demand for the discovery of resources necessary for their operation. A green energy generation plan based on solar and wind energy is an alternative energy generation method that is constantly improving and being warmly welcomed throughout the world. This research focuses on the prior and optimal use of solar and wind-based energy generation schemes alongside more conventional energy-producing facilities that are dependent on oil, LNG, coal, and nuclear resources. The proper analysis and effective application of renewable energy technology (RET), which offers us a proactive solution and functions as a replacement for the decreasing energy supplies that are dependent on energy-producing schemes, are the main foci of this research project.

## **4 Planning for Lowest Cost Generation Expansion with Solar Plant**

There are numerous renewable energy sources available in India. From about 7.8% in 2008 to 12.3% in 2013, RET's share of power systems increased, and by 2017, it is anticipated to reach 17% of all installed capacity. In addition to wind energy, solar energy has expanded significantly over the past 10 years. The country's extensive land area experiences some of the greatest sun radiation levels in the whole world.

India has taken policy measures to encourage investments in renewable electricity generation with low emissions, keeping up with the worldwide trend.

There is no specific reason for restricting the planning horizons to 6 and 14 years. We wanted to have small and medium range effective planning horizons for our studies. The same case studies, solution methods, analysis and techniques can be extended to long range planning horizons too.

In this chapter, a GEP is carried out by using DEA for a system for 6 and 14 years planning horizon with three different scenarios namely BCS, LSS and HSS. In this first scenario (BCS), the GEP is carried out without solar plants and in the second scenario called (LSS), in which solar plants are considered up to 5–10% penetration level.

In third scenario (HSS), penetrations of solar plants are increased to 10–20%.

## 4.1 GEP Problem Formulation

To meet the energy demand, GEP specifies WHAT, WHEN, and WHERE additional generation units are to be added across the planning timeframes under consideration [30, 47, 48]. Finding a collection of ideal decision vectors across a planning horizon that lowers investment and operating expenses while considering the necessary limitations is what the GEP problem entails. The GEP problem is corresponding to finding a set of optimum decision vectors over a planning horizon that reduces the investment and operating costs under relevant constraints.

## 4.2 Cost Objective

The cost objective is:

$$M \text{ in } C = \sum_{t=1}^T [I(U_t) + M(X_t) + O(X_t) - S(U_t)] \quad (1)$$

where,

$$X_t = X_{t-1} + U_t \quad (t = 1, 2, \dots, T) \quad (2)$$

$$I(U_t) = (1 + d)^{-2t} \sum_{i=1}^N (CI_i \times U_{t,i}) \quad (3)$$

$$S(U_t) = (1 + d)^{-T} \sum_{i=1}^N (CI_i \times \delta_i \times U_{t,i}) \quad (4)$$

$$M(X_t) = \sum_{s'=0}^1 ((1 + d)^{1.5+t'+s'}) (\sum (X_t \times FC) + MC) \tag{5}$$

$$O(X_t) = EENS \times OC \times \sum_{s'=0}^1 ((1 + d)^{1.5+t'+s'}) \tag{6}$$

The outage cost computation of (A.6), applied in (A.1), depends on EENS.

The equivalent energy function method [30] is applied to compute EENS and LOLP. Here, LOLP is used as a constraint.

$$t' = 2(t - 1) \text{ and } T' = 2 \times T - t' \tag{7}$$

Here,

- C overall cost, \$;
- CI<sub>i</sub> capital investment cost of unit i, \$;
- O(X<sub>t</sub>) outage cost of the existing and the introduced units, \$;
- FC fixed operation and maintenance cost of the units, \$/MW;
- I(U<sub>t</sub>) the investment cost of the introduced unit in stage t, \$;
- MC variable operation and maintenance cost of the units, \$; years);
- δ<sub>i</sub> salvage factor of unit i for calculating salvage value;
- λ% reduction in total emission;
- U<sub>t</sub> N-dimensional vector of newly introduced units in stage t (1 stage = 2.
- X<sub>t</sub> cumulative capacity vector of existing units at stage t, (MW);
- U<sub>(t,i)</sub> the number of introduced units of type i in stage t;
- D discount rate;
- N total quantity of dissimilar types of units;
- S(U<sub>t</sub>) salvage value of the introduced unit at interval t, \$;
- ec Emission coefficient;
- OC outage cost constant, \$/MWhrs;
- EENS expected energy not served, MWhrs;
- s' variable used to specify that maintenance cost is computed at the middle of each year;
- M(X<sub>t</sub>) overall operation and maintenance cost of existing and newly introduced units, \$;

### 4.3 Constraints

The following restrictions should be met by the minimum cost objective function.

### 4.3.1 Upper Construction Limit

Let  $U_t$  describe the units that should be included in the expansion plan at stage  $t$ .

$$0 \leq U_t \leq U_{\max,t} \quad (8)$$

where,

$U_{\max,t}$  maximum construction limit of the units at stage  $t$ .

### 4.3.2 Reserve Margin

The selected units should satisfy the minimum and maximum reserve margin.

$$(1 + R_{\min}) \times D_t \leq \sum_{i=1}^N X_{t,i} \leq (1 + R_{\max}) \times D_t \quad (9)$$

where,

$R_{\max}$  maximum reserve margin;  
 $X_{(t,i)}$  cumulative capacity of unit  $i$  at stage  $t$ ;  
 $D_t$  demand at stage  $t$  in megawatts (MW);  
 $R_{\min}$  minimum reserve margin.

### 4.3.3 Ratio of the Fuel Mix

The GEP has generating units that use a variety of fuels, including coal, LNG, oil, nuclear power, and solar power. The fuel mix proportion should be met by the chosen units and the existing units of each kind.

$$\leq / FM_{\max}^j \quad j = 1, 2, \dots, N \quad (10)$$

where,

$FM_{\min}^j$  minimum fuel mix proportion of type  $j$ ;  
 $FM_{\max}^j$  maximum fuel mix proportion of type  $j$ ;  
 $j$  type of the unit (e.g., oil, LNG, coal, nuclear, solar).

### 4.3.4 Reliability Standard

Along with the current units, the newly introduced units should meet the LOLP reliability standard.

$$\text{LOLP}(X_t) = \varepsilon \quad (11)$$



where,  $\varepsilon$  is the reliability criterion for permissible LOLP. Lowest reserve margin constraint avoids the need for a separate demand constraint.

### 4.3.5 Emission Constraints

The emission constraints are

$$\sum X_{t,j}ec_j < \lambda \tag{12}$$

where,

$ec_j$  is the emission coefficient of type  $j$ ,  $\lambda$  is the % reduction in total emissions.

The respective emission coefficients for oil, LNG and coal are 0.85, 0.5 and 1.05. The % reduction in total emissions is considered as 10, 20 and 30%.

Table 13 displays the anticipated peak demand for the test system for each step. Tables 14, 15, 16 and 17, respectively, provide the technical and economic information for potential plants, current plants, and solar power plants without and with storage [49–51]. Figure 1 shows the conceptual flow chart for the generation expansion model study.

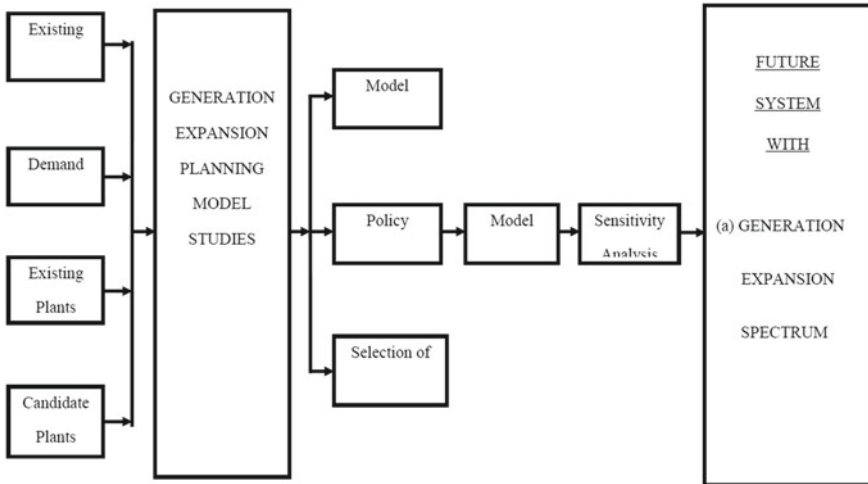


Fig. 1 Schematic flowcharts for the generation expansion model study

#### 4.4 Reliability Indices

The Equivalent Energy Function Method can be used to calculate the reliability indices Loss of Load Probability (LOLP) and Expected Energy Not Served (EENS), as advised in [52, 53].

#### 4.5 Assumptions Made

Reserve margin has defined lower and upper limitations of 20 and 60%, respectively.

- The salvage factor ( $\delta$ ) for oil, LNG, coal, PWR, PHWR and Solar plants are considered as 0.1, 0.1, 0.15, 0.2, 0.2 and 0.1, respectively 0–30.
- The fuel mix ratio for oil, LNG, coal, PWR and PHWR are considered as 0–30, 0–40, 20–60, 30–60 and 30–60% for the existing case.
- Cost of EENS is fixed at 0.05 \$/kWh.
- 8.5% is the set discount rate.
- Two years from the present day is assumed to be the date when the new generation will be accessible. It is assumed that the investment cost will be incurred at the outset of the project.
- The equivalent energy function approach is used to compute the maintenance cost, which is assumed to occur in the middle of the year [52].
- At the conclusion of the planning horizon, the salvage cost is appraised. The constraints are handled using the penalty function method.

#### 4.6 Discussion of the Results

Three possible scenarios of adding solar energy to the system were examined using the model. In the first instance, the BCS, only the existing technology types of plants were taken into consideration as potential candidates for expansion, with solar plants not being considered as a technological alternative. The second was the LSS, where solar power plants with an installed capacity of up to 5–10% were taken into consideration as alternate candidate plants. The third was the HSS, where solar power plants with an installed capacity of up to 10–20% were taken into consideration as alternative candidate plants. The effects of six policy options depending on the addition of TERC, ETPC, or both on the system plants' future generation mix were examined for each scenario. For planning horizons of 6 and 14 years, the analysis was conducted. Below is a breakdown of them, with a summary in Table 1.

**Table 1** Scenarios of analysis and policy alternatives for 6- and 14-year planning horizons

Scenario	Policy number	TERC (%)	ETPC*	Solar plants
BCS	1A	0	No	No
	1B	0	Yes	No
	1C	10	No	No
	1D	10	Yes	No
	1E	20	Yes	No
	1F	30	Yes	No
LSS (5–10%)	2A	0	No	Yes
	2B	10	Yes	Yes
	2C	10	No	Yes
	2E	20	Yes	Yes
	2F	30	Yes	Yes
HSS (10–20%)	2A	0	Yes	Yes
	2B	10	No	Yes
	2C	10	Yes	Yes
	2D	20	Yes	Yes
	2F	30	Yes	Yes

\* ETPC—Emissions Treatment Penalty Costs (considered equivalent to the total operating costs of the plants) + TERC—Total Emissions Reduction Constraints

#### 4.6.1 Alternatives to Current Policy for the 6- and 14-Year Planning Horizons

Future generation mix with no ETPC and no TERC is the goal of Policies 1A, 2A, and 3A.

Future generation mix with ETPC and no TERC under Policies 1B, 2B, and 2B.

Policies 1C, 2C, and 3C—Future generation mix with only TERC and no ETPC to cut policy 1A's emissions by 10%.

Policies 1D, 2D, and 3D—Future generation mix with ETPC and a cap on overall emissions to cut policy 1A's emissions by 10%. Policies 1E, 2E, and 3E—Future generation mix with ETPC and a cap on overall emissions to cut policy 1A's emissions by 20%.

Policies 1F, 2F, and 3F—Future generation mix with ETPC and a cap on overall emissions to cut policy 1A's emissions by 30%.

BCS policy 1A, in which neither an ETPC nor a TERC is considered in the analysis, is used as the reference example to compare the effects of other policies on the system. For simplicity, nuclear (PWR), nuclear (PHWR), and solar plants are classified as Low Emission Plants (LEP), while oil, LNG, and coal plants are categorized as High Emission Plants (HEP). However, in the respective examples in Tables 2 and 3, the division of individual plants into these two kinds is also provided.

**Table 2** For all policy options within the 6-year planning horizon, model solutions for BCS, LSS, and HSS are provided

Policy alternative	Scenario	Oil (MV)	LNG (CC)	Coal (Bitum.) (MW)	HEP (%)	Nuc (PWR) (MW)	Nuc (PWR) (MW)	Solar (MW)	LEP (%)	Added capacity (MW)	Cumulative capacity (MW)	Overall cost $\times$ 1010 (s)	EES $\times$ 104 (MWh)	
1A	BCS	2000	2250	1500	73.25	0	2100	0	26.75	7850	13,300	1.2009	2.7165	
1B		2000	2250	1500	73.25	0	2100	0	26.75	7850	13,300	1.2947	2.7165	
1C		1400	1800	1500	58.025	2000	1400	1400	0	41.975	8100	13,550	1.2773	3.0475
1D		1400	1800	1500	58.025	2000	1400	1400	0	41.975	8100	13,550	1.3187	3.0475
2E		800	1350	1500	44.785	1000	3500	3500	0	55.215	8150	13,600	1.3442	2.2878
2F		1000	450	3000	53.939	1000	2800	2800	0	46.061	8250	13,700	1.33709	4.0013
2A	LSS	800	2250	2500	62.011	1000	1400	1000	37.778	8950	14,400	1.4180	3.3317	
2B		400	2700	2500	62.222	1000	1400	1000	43.243	9000	14,450	1.6139	3.2326	
2C		600	3150	1500	56.757	3000	0	1000	51.087	9250	14,700	1.6253	3.0184	
2D		1200	1800	1500	48.913	3000	700	1000	54.839	9200	15,500	1.6647	2.9481	
2E		0	2700	1500	45.161	2000	2100	1000	54.839	9300	15,500	1.8948	2.3057	
2F		0	1350	1500	30.811	4000	1400	1000	69.189	9250	15,350	1.9339	3.8368	
3A	HSS	600	2250	2500	53.234	2000	700	2000	46.776	10,050	15,600	1.9934	3.2582	
3B		200	3150	2000	53.234	2000	700	2000	46.776	9900	15,600	1.9783	3.6022	
3C		600	1800	2000	44.444	0	3500	2000	55.556	10,150	14,850	2.0034	2.5630	
3D		200	2250	2000	43.842	3000	700	2000	56.158	10,150	15,600	1.9369	3.5039	
3E		0	1350	2000	33.005	2000	2800	2000	66.995	10,150	15,600	1.9783	2.7848	
3F		0	0	1000	10.638	5000	1400	2000	89.362	9400	14,850	2.0034	3.1381	

**Table 3** For all policy options within the 14-year planning horizon, model solutions for BCS, LSS, and HSS are provided

Policy alternative	Scenario	Oil	LNG	Coal (Bitum.)	HEP	Nuc (PWR)	Nuc (PHWR)	Solar	LEP	Added capacity	Cumulative capacity	Overall cost × 1010	LOLP	EES × 104
1A	BCS	2000	2250	5500	70.397	2000	2100	0	29.603	13,850	19,300	2.1811	0.0098	3.8012
1B		1200	1800	4500	53.571	3000	3500	0	46.429	14,000	19,450	2.2627	0.0088	3.6376
1C		1000	450	4000	37.201	5000	4200	0	62.799	14,650	20,100	2.1237	0.0038	1.5245
1D		1000	1350	2500	33.333	2000	7700	0	66.666	14,550	20,000	2.2035	0.0026	0.9825
1E		800	900	3500	36.879	4000	4900	0	63.121	14,100	19,550	2.2043	0.0085	3.5507
1F		1200	900	2500	31.724	5000	4900	0	68.276	14,500	20,500	2.2163	0.0046	1.9100
2A	LSS	1200	2250	2500	39.535	5000	2100	2000	60.465	15,050	21,350	2.6087	0.0091	3.8952
2B		1800	1800	3500	44.654	4000	2800	2000	55.346	15,900	22,250	2.6537	0.0096	3.9875
2C		600	0	3000	21.429	7000	4200	2000	78.571	16,800	21,900	2.7897	0.0023	0.9535
2D		400	450	3000	23.404	5000	5600	2000	76.596	16,450	22,500	2.7937	0.0046	1.9103
2E		0	450	2500	17.302	10,000	2100	2000	82.698	17,050	22,300	2.8237	0.0034	1.5490
2F		400	1350	2500	25.223	5000	5600	2000	74.777	16,800	22,450	2.8506	0.0023	0.9296
3A	HSS	3000	2700	2500	48.235	3000	2800	3000	51.765	17,000	22,500	2.9874	0.0056	2.1771
3B		4000	2250	2000	48.387	3000	2800	3000	51.613	17,050	22,250	3.0641	0.0045	1.6852
3C		600	1800	3500	35.119	3000	4900	3000	64.881	16,800	23,050	3.1480	0.0100	4.1695
3D		600	2700	3500	38.636	5000	2800	3000	61.364	17,600	15,600	3.1733	0.0035	1.4182
3E		1000	0	3500	24.064	6000	4200	4000	75.936	18,700	24,150	3.4128	0.0028	1.1460
3F		800	1350	2500	26.496	5000	4900	3000	73.504	17,550	23,000	3.3100	0.0035	1.4186
		MV	CC	MW	%	MW	MW	MW	%	MW	MW	s	Day/ year	MW/h

## 4.7 BCS—Model Solutions

Tables 2 and 3 provide the model solutions for each of the six above-proposed policy alternatives (from 1A to 1F), for both the 6- and 14-year planning periods, respectively.

### 4.7.1 Policy 1A Results

For the reference BCS policy 1A, the total cost of meeting the system's demand over a 6-year planning horizon was \$1.20091010; the proportions of HEP and LEP were 73.25 and 26.75%; the LOLP and EENS were 0.0086 days/year and 2.7165104 MWh; and the capacity added to the system was 7850 MW, bringing the total installed capacity of the system to 13,300 MW.

The Base Case Scenario (BCS) considered in all the cases of our thesis work is already available in the literature. Kannan et al. [54] applied and compared eight Meta-heuristic techniques with dynamic programming. The DP is one of the standards and popular conventional optimization techniques, which produces an optimal solution in each run. In other words, the success rate of DP in producing optimal solutions is 100%. For our BCS, the optimal solution for 6 years planning horizon is  $1.2009 \times 10^{10}$ . The DEA produces this result with a 100% success rate using the parameters assigned in this thesis work. Hence, we ensured that DEA produces the optimal solution for all the case studies considered.

Figure 2 denotes the convergence plot of the BCS. Our focus is to analyze the impact of various policies upon the GEP, rather than applying various algorithms to GEP. Hence, we have provided the convergence plot for the BCS only.

The total cost to meet the demand of the system for the reference BCS policy 1A over a 14-year planning horizon was \$2.18111010; the proportions of HEP and LEP were 70.397% and 29.603%; the LOLP and EENS were 0.0098 days/year and 3.8012104 MWh; and the capacity added to the system was 13,850 MW, bringing the total installed capacity to 19,300 M.

### 4.7.2 Results of Policy 1B

The total cost to meet the demand of the system for the BCS policy 1B over a 6-year planning horizon was \$1.29471010; the proportions of HEP and LEP were 73.25 and 26.75%; the LOLP and EENS were 0.0086 days/year and 2.7165104 MWh; and the capacity added to the system was 7850 MW, bringing the total installed capacity to 13,300 MW.

The total cost to meet the system's demand for the BCS policy 1B over a 14-year planning horizon was \$2.26271010; the proportions of HEP and LEP were 53.571 and 46.429%; the LOLP and EENS were 0.0088 days/year and 3.6376104 MWh;

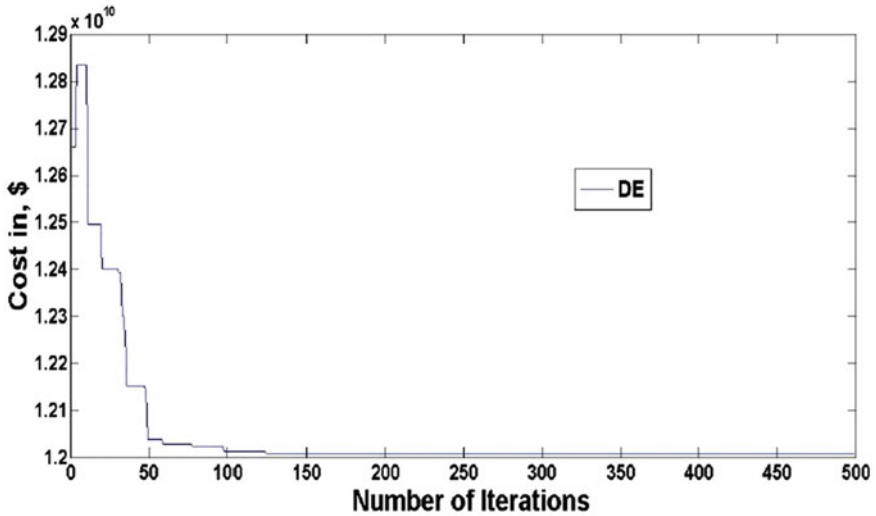


Fig. 2 Convergence plot of the DEA for 6-year planning horizon (BCS)

and the capacity added to the system was 14,000 MW, bringing the installed capacity to a total of 19,450 MW.

### 4.7.3 Results of Policy 1C

The total cost to meet the demand of the system for BCS policy 1C over a 6-year planning horizon was \$1.27731010; the proportions of HEP and LEP were 58.025 and 41.975%; the LOLP and EENS were 0.0088 days/year and 3.0475104 MWh; and the capacity added to the system was 8100 MW, bringing the total installed capacity to 13,550 MW.

The total cost to meet the demand of the system for BCS policy 1C over a 14-year planning horizon was \$2.12371010; the proportions of HEP and LEP were 37.201 and 62.799%; the LOLP and EENS were 0.0038 days/year and 1.5245104 MWh; and the capacity added to the system was 14,650 MW, bringing the total installed capacity to 20,100 MW.

### 4.7.4 Results of Policy 1D

The total cost to meet the demand of the system for BCS policy 1D over a 6-year planning horizon was \$1.31871010; the proportions of HEP and LEP were 58.025 and 41.975%; the LOLP and EENS were 0.0088 days/year and 3.0475104 MWh; and the capacity added to the system was 8100 MW, bringing the total installed capacity to 13,550 MW.

The total cost to meet the demand of the system for BCS policy 1D over a 14-year planning horizon was \$2.20351010; the proportions of HEP and LEP were 33.333 and 66.667%; the LOLP and EENS were 0.0026 days/year and 0.9825104 MWh; and the capacity added to the system was 14,550 MW, bringing the installed capacity to 20,000 MW overall.

#### **4.7.5 Results of Policy 1E**

The total cost to meet the demand of the system for BCS policy 1E over a 6-year planning horizon was \$1.34421010; the proportions of HEP and LEP were 44.785 and 55.215%; the LOLP and EENS were 0.0067 days/year and 2.2878104 MWh; and the capacity added to the system was 8150 MW, bringing the installed capacity to a total of 13,600 MW.

The total cost to meet the demand of the system for BCS policy 1E over a 14-year planning horizon was \$2.20431010; the proportions of HEP and LEP were 36.879 and 63.121%; the LOLP and EENS were 0.0085 days/year and 3.5507104 MWh; and the capacity added to the system was 14,100 MW, bringing the total installed capacity to 19,550 MW.

#### **4.7.6 Results of Policy 1F**

For the BCS policy 1F, the total cost of meeting the system's demand over a 6-year planning horizon was \$1.37091010; the proportions of HEP and LEP were 53.939 and 46.061%; the LOLP and EENS were 0.0107 days/year and 4.0013104 MWh; and the capacity added to the system was 8250 MW, bringing the total installed capacity of the system up to 13,700 MW.

The total cost to meet the demand of the system for BCS policy 1F over a 14-year planning horizon was \$2.21631010; the proportions of HEP and LEP were 31.724 and 68.276%; the LOLP and EENS were 0.0046 days/year and 1.9100104 MWh; and the capacity added to the system was 14,500 MW, bringing the total installed capacity to 19,950 MW.

### **4.8 LSS—Solutions of the Model**

Tables 2 and 3 provide the model solutions for each of the six policy possibilities (2A to 2F) put forward above, for both the 6- and 14-year planning periods, respectively.



### 4.8.1 Results of Policy 2A

The reference LSS policy 2A's overall cost to meet demand over a 6-year planning horizon was \$1.41801010; the proportions of HEP and LEP were 62.011 and 37.989%, respectively; the LOLP and EENS were 0.0096 and 3.3317 days/year, respectively.

### 4.8.2 The Highlights of Model Solutions Are

- The implementation of ETPC or TERC or both allowed for a balanced approach between the high emissions base load facilities and the low emissions peak load plants.
- For a variety of policy options, the effect of the addition of solar plants on the plant mix and system reliability was researched.
- The generating mix and the reliability factors were very responsive to the system's emission reduction policies. For all of the policy actions outlined, the influence on the system-generating mix led to lower overall costs and improved system reliability.
- With the addition of solar plants to the system, both the installed capacity and overall prices have increased. The system reliability has also increased.
- Why Higher additions in nuclear plants helped lower overall costs given the make-up of system technology choices at the time TERC was launched, However, because of LEP capacity restrictions, TERC values above 20% did not increase system variables.
- Compared to the scenario where they are not considered, the introduction of ETPC and/or TERC has increased the total system costs in all BCS, LSS, and HSS policy choices. The total costs were lower for the scenarios where just TERC was taken into consideration than for the scenario where we incorporated only ETPC.
- When solar plants were added to the system as a capacity alternative in LSS and HSS, the overall capacity added to the system increased more than the capacity of the solar plants added to the system, regardless of whether ETPC and TERC were considered or not. This was mostly caused by the discontinuous character of plant capacity.
- There were continuous increases in the incremental additions to the system greater than the capacity added by the solar plants when both ETPC and various levels of TERC were adopted for all policy alternatives, in both LSS and HSS, for both the 6- and 14-year planning periods. When we tightened the restrictions to lower the emission levels, the incremental additions outweighed the added solar capacity, requiring more baseload backup and costing more money.
- When we incorporated TERC, the reduction in the HEP was higher than when we only took ETPC into account for all policy choices, including BCS, LSS, and HSS. The LEP plants were unable to offset their hefty capital expenditures.
- The quantity of EENS, in general, decreased significantly for all policy alternatives across BCS, LSS, and HSS when the TERC with higher levels of emissions

reduction and in situations where incremental capacity additions were higher than the reference scenario, of course at a cost.

### 4.8.3 Scenario Based Analysis

For the BCS, the fraction of HEP ranges from 44.785 to 73.25% and the proportion of LEP plants ranges from 26.75 to 55.215% (Tables 42 and 43). HEP's share in the LSS ranges from 30.811 to 62.222%, and LEP plants' share is from 37.778 to 69.189%. The proportions of HEP and LEP plants in the HSS range from 10.638 to 53.234% and 46.776 to 89.362%, respectively. The range of HEP and LEP fluctuations is lowest for BCS and highest for HSS for the 6-year planning period, whereas the reverse is true for the 14-year planning horizon.

For the 6-year planning horizon, the total system costs for different policy measures varies from  $\$1.2009 \times 10^{10}$  to  $\$1.3709 \times 10^{10}$ , giving a range of  $\$0.17 \times 10^{10}$  for BCS; varies from  $\$1.4180 \times 10^{10}$  to  $\$1.6647 \times 10^{10}$ , giving a range of  $\$0.2467 \times 10^{10}$  for LSS; and varies from  $\$1.8948 \times 10^{10}$  to  $\$2.0034 \times 10^{10}$ , giving a range of  $\$0.1086 \times 10^{10}$  for HSS. For the 14-year planning horizon, the total system costs for different policy measures varies from  $\$2.1811 \times 10^{10}$  to  $\$2.2163 \times 10^{10}$ , giving a range of  $\$0.0352 \times 10^{10}$  for BCS; varies from  $\$2.6087 \times 10^{10}$  to  $\$2.8506 \times 10^{10}$ , giving a range of  $\$0.2419 \times 10^{10}$  for LSS; and varies from  $\$2.9874 \times 10^{10}$  to  $\$3.3100 \times 10^{10}$ , giving a range of  $\$0.3226 \times 10^{10}$  for HSS. For the LSS over a 6-year period and for the HSS over a 14-year period, the variances in overall expenses are greater. In the case of BCS, the total cost differences are minimal throughout the 6- and 14-year periods. This demonstrates how adding solar to the system makes it more susceptible to the policy actions.

For the 6-year planning horizon, the EENS for different policy measures varies from  $2.7165 \times 10^4$  to  $4.0013 \times 10^4$  MWh, giving a range of  $1.2848 \times 10^4$  MWh for BCS; varies from  $3.3317 \times 10^4$  MWh to  $3.8368 \times 10^4$  MWh, giving a range of  $0.5051 \times 10^4$  MWh for LSS; and varies from  $3.1381 \times 10^4$  MWh to  $3.2582 \times 10^4$  MWh, giving a range of  $0.1201 \times 10^4$  MWh for HSS. For the 14-year planning horizon, the total EENS for different policy measures varies from  $1.9100 \times 10^4$  to  $3.8012 \times 10^4$  MWh, giving a range of  $1.8912 \times 10^4$  MWh for BCS; varies from  $0.9296 \times 10^4$  to  $3.8952 \times 10^4$  MWh, giving a range of  $2.9656 \times 10^4$  MWh for LSS; and varies from  $1.4186 \times 10^4$  to  $2.1771 \times 10^4$  MWh, giving a range of  $0.7585 \times 10^4$  MWh for HSS. The variations in LOLP and EENS are also more sensitive to the policy variations when solar is included as an alternative. For the 6- and 14-year periods, respectively, the EENS variation range is considerable for the BCS.

### 4.8.4 A Mix of Generation and Overall System Costs

For the BCS, the total capacity additions to the system for all six policies range from 7850 to 8250 MW throughout the course of the planning horizon of 6 years. The combined capacity addition for policies 1A and 1B is 7850 MW. The generation mix

was the same in both circumstances. However, because we included the ETPC for the plants, the system's overall expenses have increased. The total system costs have increased from \$1.20091010 to \$1.29471010 since the implementation of ETPC. Policy 1C reduces the TERC by 10% compared to policy 1A while increasing total capacity from 7850 to 8100 MW. In policy 1D, where ETPC and TERC are both established, the generation mix was the same as it was in policy 1C. In this instance, there is an increase in the system's overall costs from \$1.2773 to \$1.3187 because of these rules. In addition to ETPC, TERC is introduced for policies 1E and 1F with the goals of 20 and 30% emissions reduction, resulting in policy 1A. The total additional capacity built into the system for these two scenarios is 8150 and 8250 MW, respectively. The sum of the additions' expenses is \$1.3442 1010 and \$1.3709 1010.

#### **4.8.5 System's Reliability**

The LOLP and EENS values for all the policy choices across BCS, LSS, and HSS are comparatively low for the 14-year Planning period than the LOLP and EENS values of identical policy alternatives of the 6-year planning period, according to research conducted for 6- and 14-year planning horizons.

The BCS's EENS has the lowest values for the policies (1E and 2E), where ETPC and TERC are targeted at 20%, for the 6- and 14-year planning periods.

For all three of the envisioned situations, the system's LOLP and EENS dependability factors are extremely sensitive to the system generation mix. The greatest value of EENS for LSS is higher than for the BCS and HSS in the scenario where neither ETPC nor TERC are considered. The EENS for HSS is highest when only the ETPC is considered in the model analysis when compared to the other two scenarios.

## **5 Generation Expansion Planning Based on Solar Plants with Storage**

As part of two investment methods for solar plant additions—either as a substitute for oil plants or as an alternative candidate plant for investment—an effort is made to analyze the long-term effects of increasing additions of solar plants into a system. Furthermore, a study on the adoption of solar technologies with built-in storage is elaborated.

The chapter also covers how the introduction of treatment/penalty charges may affect high-emission plant emissions. This chapter also attempts a variant by analyzing the effects of various FOR% combinations for SWPNS and SWPS on system performance. The GEP problem is solved using the DEA with various amounts of solar power penetration.

Two different types of solar plants are taken into consideration for integration into the GEP problem under research. They are Solar Power with Storage and Solar Plant

with No Storage (SPWNS) (SPWS). For SPWNS, the FOR% is predicated at 76%, and for SPWS, it is predicated at 6%. All the plants are divided into two categories: LEP (nuclear and solar) and HEP (oil, LNG, and coal).

### 5.1 Analysis of Model

Four levels of hierarchies are used to structure the GEP model analysis. Figure 3 provides a schematic diagram of the model analyses. The GEP of the system is considered at the first level without the inclusion of solar plants. In the second level, two distinct cases are taken into consideration based on the plan for the introduction of solar power plants, either as an alternative to oil plants or as a potential source of alternative investment. Based on whether the solar power plants had their own storage capacity or not, two different instances are further examined in the third level. In the fourth level, the GEP of the system is subjected to sensitivity analysis for various combinations of (a) solar penetration limits (5–10 or 10–20%), (b) treatment/penalty costs for emissions from HEP (with or without costs), and (c) FOR assumed for SPWNS and SPWS, for both 6- and 14-year planning horizons.

Table 4 provides an overview of the policy options that were taken into consideration for the 6- and 14-year planning periods.

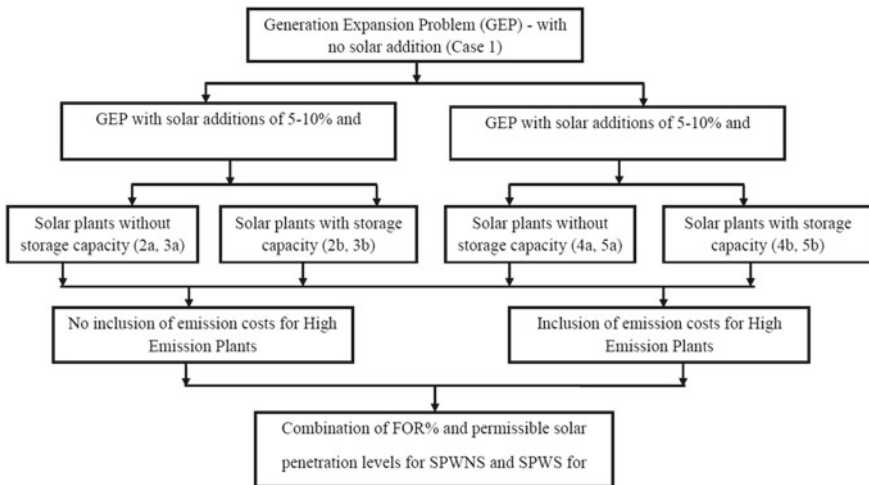


Fig. 3 Schematic diagram of the four levels GEP model analysis

**Table 4** Summary of policy cases for SPWNS and SPWS

S1. No.	Summary of policy cases	
1	Case 1	GEP without solar plants
2	Case 2a	5–10%—RES penetration/SPWNS replacing oil plants
3	Case 2b	5–10%—RES penetration/SPWS replacing oil plants
4	Case 3a	10–20%—RES penetration/SPWNS replacing oil plants
5	Case 3b	10–20%—RES penetration/SPWS replacing oil plants
6	Case 4a	5–10%—RES penetration/SPWNS as an alternative investment candidate
7	Case 4b	5–10%—RES penetration/SPWS as an alternative investment candidate
8	Case 5a	10–20%—RES penetration/SPWNS as an alternative investment candidate
9	Case 5b	10–20%—RES penetration/SPWS as an alternative investment candidate

## 5.2 Results and Discussion

Nine alternative policy case studies are conducted, as shown in Table 4, with the first instance being the case where no consideration of solar addition is made. The remaining eight examples concern studies that incorporate solar plants in the system; two cases deal with the investment plan to substitute solar plants for oil plants, and two cases look at solar plants as a potential alternative investment. The two categories above were divided into two subcategories based on whether the solar plants had storage capacity for the solar penetration levels of 5–10 and 15–20%, respectively. For the anticipated FOR% of 76% for SPWNS and 6% for SPWS, all policy scenarios are examined. Tables 5 and 6 provide the model solutions for the 6-year planning horizon, while Tables 7 and 8 provide the same information for the 14-year planning horizon.

### 5.3 Case 1: GEP Without Solar Plants

For the assumed demand pattern, capacities of candidate plants for investments, and other factors, when no treatment and penalty costs were imposed on emissions from HEP, the additional installed capacity for the system for the 6-year planning period was 7850 MW, with a breakup between HEP and LEP, respectively, of 5750 and 2100 MW. Oil, LNG, and coal plants each have an additional capacity of 2000, 2250, and 1500 MW for the HEP. Nuclear plants had an additional installed capacity of 2100 MW across the LEP sites. The overall capacity added to the system at the end of the planning horizon was 7850 MW, the total system costs were \$1.20091010, and the EENS was 2.7165104 MWh. The corresponding numbers were 13,850 MW, \$2.1811 10<sup>10</sup>, and 3.8012 10<sup>4</sup> MWh for the 14-year planning period.

The additional installed capacity for the system was the same as that of the policy with no treatment and penalty costs applied when treatment and penalty costs

**Table 5** Without emission costs: generation mix, Overall costs, LOLP and EENS for 6-year

Policy	Oil (MW)	LNG C/ C(MW)	Coal (Bi-tum) (MW)	Nuc. (PWR)	Nuc. (PHWR) (MW)	Solar (MW)	Added	Cumulative Cap (MW)	Overall cost × 10\$	LOLP (days/year)	EENS × 10 (MWh)
Case1	2000	2250	1500	0	2100	0	7850	13,300	1.2009	0.0086	2.7165
Case2a	0	3600	2000	1000	1400	200	8200	13,650	1.2627	0.0098	3.4470
Case2b	0	2250	3000	2000	700	200	8150	13,450	1.2812	0.0096	3.4435
Case3a	0	2250	3000	2000	700	1000	8950	13,600	1.4702	0.0093	3.3015
Case3b	0	1800	3000	1000	1400	800	8000	13,450	1.5131	0.0093	3.2424
Case4a	1600	2250	1500	2000	700	1000	9050	14,500	1.5208	0.0086	2.1755
Case4b	2000	1800	1500	1000	1400	1000	8700	14,150	1.7130	0.00093	3.1173
Case5a	1400	1350	2500	2000	700	2000	9950	15,400	1.8296	0.0098	3.4713
Case5b	2000	1350	1500	2000	700	2000	9950	15,000	2.2248	0.0100	3.4951

**Table 6** With emission costs: generation mix, overall costs, LOLP and EENS for 6-year period (FOR 76 and 6%)

Policy	Oil (MV)	LNG C/C (MW)	Coal (Bi-tum) (MW)	Nuc. (PWR)	Nuc. (PHWR) (MW)	Solar (MW)	Added	Cumulative Cap (MW)	Overall cost × 10\$	LOLP (days/year)	EENS × 10 (MWh)
Case1	2000	2250	1500	0	2100	0	7850	13,300	1.2947	0.0086	2.7165
Case2a	0	3150	3000	1000	1400	200	8750	14,200	1.2974	0.0083	2.9273
Case2b	0	2700	3000	0	2100	200	8000	13,450	1.3187	0.084	2.8275
Case3a	0	2700	3000	2000	700	1000	9400	14,850	1.5283	0.0093	3.4157
Case3b	0	1800	3000	1000	1400	800	8000	144,450	1.5370	0.0086	3.2424
Case4a	400	2700	2500	1000	1400	1000	9000	14,200	1.6139	0.0092	3.2323
Case4b	1600	2250	1500	1000	1400	1000	8750	15,500	1.7156	0.00089	2.7174
Case5a	200	3150	2000	2000	700	2000	10,050	22,200	1.9339	0.0099	3.6622
Case5b	1200	2700	2000	2000	700	2000	9700	15,150	2.2286	0.0086	2.9569

**Table 7** Without emission costs: generation mix, overall costs, LOLP and EENS for 14-year period (FOR 76 and 6%)

Policy	Oil (MV)	LNG C/C (MW)	Coal (Bi-tum) (MW)	Nuc. (PWR)	Nuc. (PHWR) (MW)	Solar (MW)	Added	Cumulative Cap (MW)	Overall cost $\times 10^6$	LOLP (days/year)	EENS $\times 10$ (MWh)
Case1	2000	2250	5000	2000	2100	0	13,850	19,300	2.1811	0.0098	3.8012
Case2a	0	1800	4000	7000	1400	600	14,800	20,250	2.3011	0.0094	0.4211
Case2b	0	1350	3500	6000	2800	600	14,250	19,700	2.3503	0.0073	3.1486
Case3a	0	2700	6000	3000	2100	1800	15,600	21,050	2.4580	0.0071	2.9172
Case3b	0	2250	3500	4000	3500	2000	15,250	20,700	2.4868	0.0009	0.3294
Case4a	2400	3150	3500	3000	2100	2000	16,150	21,600	2.6263	0.0052	2.0032
Case4b	1400	2250	4000	1000	4900	1000	14,550	20,000	2.7653	0.00097	3.7616
Case5a	2200	2250	4500	2000	2800	3000	16,750	22,200	2.9877	0.0085	3.7616
Case5b	1400	2700	3500	4000	2800	3000	17,400	22,850	3.2026	0.0016	0.5760



**Table 8** With emission costs: generation mix, overall costs, LOLP and EENS for 14-year period (FOR 76 and 6%)

Policy	Oil (MW)	LNG C/C (MW)	Coal (Bi-tum) (MW)	Nuc. (PWR) (MW)	Nuc. (PHWR) (MW)	HEP	Solar (MW)	LEP	Added	Cumulative Cap (MW)	Overall cost × 10\$	LOLP (Days/year)	EENS × 10 (MW/h)
Case1	1200	1800	4500	3000	3500	3500	0	14,000	19,450	2,2627	0.000888	0.0088	3.6376
Case2a	0	1800	5000	7000	700	700	600	15,100	20,550	2,3156	0.0059	0.0059	2.5915
Case2b	0	3150	4000	7000	0	0	600	14,750	20,200	2,3603	0.0047	0.0047	2.0383
Case3a	0	2700	4000	4000	3500	3500	1600	15,800	21,250	2,4613	0.0091	0.0091	3.9124
Case3b	0	2250	3500	2000	4900	4900	1400	14,050	19,500	2,5017	0.0065	0.0065	2.5246
Case4a	1800	1800	3500	4000	2800	2800	2000	15,900	21,350	2,6537	0.0096	0.0096	3.9875
Case4b	1800	2250	4500	0	4900	4900	1000	14,450	19,900	2,7654	0.0094	0.00094	3.5604
Case5a	4000	2250	2000	3000	2800	2800	3000	17,050	22,500	3,0641	0.0045	0.0045	1.6842
Case5b	1400	900	4000	3000	4900	4900	3000	17,200	22,650	3,2308	0.0015	0.0015	0.6598

were imposed on emissions from HEP, for the expected demand pattern, capacities of candidate plants for investments, and other criteria. At the conclusion of the planning horizon, the system's new capacity totaled 7850 MW, its expenses totaled  $\$1.2947 \times 10^{10}$ , and its EENS was  $2.7165 \times 10^{-4}$  MWh. The corresponding numbers were 14,000 MW,  $\$2.2627 \times 10^{10}$ , and  $3.6376 \times 10^4$  MWh for the 14-year planning period.

#### ***5.4 Case 2a: 5–10% RES Penetration/SPWNS Replacing Oil Plants***

The total capacity added to the system over the 6-year period was 8200 MW, with LNG, coal, nuclear (PWR), nuclear (PHWR), and solar plants adding, respectively, 3600, 2000, 1000, 1400, and 200 MW. During this time, no treatment or penalty fees were imposed on HEP emissions. The EENS was  $3.4470 \times 10^4$  MWh, while the total system expenses were  $\$1.2627 \times 10^{10}$  MWh.

The total capacity added to the system for the 14-year period was 14,800 MW, with LNG, coal, nuclear (PWR), nuclear (PHWR), and solar plants having respective added capacities of 1800, 4000, 7000, 1400, and 600 MW. During this time, no treatment or penalty costs were imposed on emissions from HEP. The total cost of the system was  $\$2.3011 \times 10^{10}$ ; the EENS was  $0.0094 \times 10^4$  MWh.

The total capacity added to the system for the 6-year period was 8750 MW, with increased capacities for LNG, coal, nuclear (PWR), nuclear (PHWR), and solar plants totaling 3150, 3000, 1000, 1400, and 200 MW, respectively. The total cost of the system was  $\$1.2974 \times 10^{10}$  dollars, and the EENS was  $2.9273 \times 10^4$  MWh.

The overall capacity added to the system for the 14-year period, when treatment/penalty fees were placed on emissions from HEP, was 15,100 MW, with increased capacities for LNG, coal, nuclear (PWR), nuclear (PHWR), and solar plants of respectively 1800, 5000, 7000, 700, and 600 MW. The EENS was  $2.5915104$  MWh, and the overall system expenses were  $\$2.31561010$ .

#### ***5.5 Case 2b: 5–10% RES Penetration/SPWS Replacing Oil Plants***

The total capacity added to the system for the 6-year period was 8150 MW, with LNG, coal, nuclear (PWR), nuclear (PHWR), and solar plants having respective added capacities of 2250, 3000, 2000, 700, and 200 MW. During this time, no treatment or penalty costs were imposed on emissions from HEP. The total cost of the system was  $\$1.2812 \times 10^{10}$  dollars, and the EENS was  $3.4435 \times 10^4$  MWh.

The total capacity added to the system for the 14-year period was 14,250 MW, with LNG, coal, nuclear (PWR), nuclear (PHWR), and solar plants having respective

added capacities of 1350, 3500, 6000, 2800, and 600 MW. During this time, no treatment or penalty costs were imposed on emissions from HEP. The system's total expenses came to  $\$2.3503 \cdot 10^{10}$  dollars, and the EENS was  $3.1486 \cdot 10^4$  MWh.

The overall capacity added to the system for the 6-year period, when treatment/penalty fees were imposed on HEP emissions, was 8000 MW. LNG, coal, nuclear (PWR), nuclear (PHWR), and solar plants had respective new capacities of 2700, 3000, 0, 2100, and 200 MW. The EENS was  $2.8275 \cdot 10^4$  MWh, while the entire system expenses were  $\$1.3187 \cdot 10^{10}$  in total.

The overall capacity added to the system for the 14-year period, when treatment/penalty fees were placed on emissions from HEP, was 14,750 MW, with increased capacities for LNG, coal, nuclear (PWR), nuclear (PHWR), and solar plants of 3150, 4000, 7000, 0, and 600 MW, respectively. The EENS was  $2.0383104$  MWh, and the total system cost was  $\$2.36031010$ .

### **5.6 Case 3a: 10–20% RES Penetration/SPWNS Replacing Oil Plants**

The total capacity added to the system for the 6-year period was 8950 MW, with LNG, coal, nuclear (PWR), nuclear (PHWR), and solar plants having respective added capacities of 2250, 3000, 2000, 700, and 1000 MW. During this time, no treatment or penalty costs were imposed on emissions from HEP. The EENS was  $3.3015104$  MWh, and the entire system expenses were  $\$1.47021010$ .

The total capacity added to the system for the 14-year period was 15,600 MW, with LNG, coal, nuclear (PWR), nuclear (PHWR), and solar plants having respective added capacities of 2700, 6000, 3000, 2100, and 1800 MW. During this time, no treatment or penalty costs were imposed on emissions from HEP. The system's entire expenses came to  $\$2.4580 \cdot 10^{10}$  dollars, and the EENS was  $2.9172 \cdot 10^4$  MWh.

The overall capacity added to the system for the 6-year period, during which treatment/penalty fees were levied on HEP emissions, was 9400 MW, with LNG, coal and nuclear (PWR), nuclear (PHWR), and solar plants having added capacities of 2700, 3000, 2000, 700, and 1000 MW, respectively. The EENS was  $3.4157104$  MWh, and the entire system expenses were  $\$1.52831010$ .

The overall capacity added to the system for the 14-year period, when treatment/penalty fees were levied on HEP emissions, was 15,800 MW, with LNG, coal, nuclear (PWR), nuclear (PHWR), and solar plants having respective new capacities of 2700, 4000, 3500, and 1600 MW. The EENS was  $3.9124104$  MWh, and the entire system expenses were  $\$2.46131010$ .

### **5.7 Case 3b: 10–20% RES Penetration/SPWS Replacing Oil Plants**

The total capacity added to the system for the 6-year period was 8000 MW, with LNG, coal, nuclear (PWR), nuclear (PHWR), and solar plants having respective increased capabilities of 1800, 3000, 1000, 1400, and 800 MW. The system's total expenses came to  $\$1.5131 \times 10^{10}$  dollars, and the EENS was  $3.2424 \times 10^4$  MWh.

The total capacity added to the system for the 14-year period was 15,250 MW, with LNG, coal, nuclear (PWR), nuclear (PHWR), and solar plants having respective added capacities of 2250, 3500, 4000, 3500, and 2000 MW. During this time, no treatment or penalty costs were imposed on emissions from HEP. The EENS was 0.3294104 MWh, and the entire system expenses were  $\$2.48681010$ .

When treatment/penalty charges were applied to HEP emissions during a 6-year period, a total of 8000 MW of new system capacity was added, with additions to LNG, coal, nuclear (PWR), nuclear (PHWR), and solar plants totaling 1800 MW, 3000 MW, 1000 MW, 1400 MW, and 800 MW, respectively. The EENS was  $3.2424104$  MWh, and the entire system expenses were  $\$1.53701010$ .

The total capacity added to the system for the 14-year period, during which treatment/penalty fees were imposed on HEP emissions, was 14,050 MW, with LNG, coal, nuclear (PWR), nuclear (PHWR), and solar plants adding, respectively, 2250 MW, 3500 MW, 2000 MW, 4900 MW, and 1400 MW. The EENS was  $2.5246104$  MWh, and the total system cost was  $\$2.50171010$ .

### **5.8 Case 4a: 5–10% RES Penetration/SPWNS as Alternative Investment Candidate**

The total capacity added to the system for the 6-year period was 9050 MW, with added capacities for solar, oil, LNG, coal, nuclear (PWR), and nuclear (PHWR) plants totaling 1600, 2250, 1500, 2000, 700, and 1000 MW, respectively. The total cost of the system was  $\$1.5208 \times 10^{10}$  dollars, and the EENS was  $2.1755 \times 10^4$  MWh.

The total capacity added to the system for the 14-year period was 16,150 MW, with added capacities for solar, oil, LNG, coal, nuclear (PWR), and nuclear (PHWR) plants of 2400, 3150, 3500, and 3000 MW, respectively. During this time, no treatment or penalty costs were imposed on HEP emissions. The total cost of the system was  $\$2.6263 \times 10^{10}$  and the EENS was  $2.0032 \times 10^4$  MWh.

The overall capacity added to the system for the 6-year period was 9000 MW, with increased capacities for solar, oil, LNG, coal, nuclear (PWR), and nuclear (PHWR) plants being, respectively, 400, 2700, 2500, 1000, 1400, and 1000 MW. The total cost of the system was  $\$1.6139 \times 10^{10}$ , and the EENS was  $3.2323 \times 10^4$  MWh.

The overall capacity added to the system for the 14-year period, when treatment/penalty fees were imposed on emissions from HEP, was 15,900 MW, with new capacities of 1800, 1800, 3500, 4000, 2800, and 2000 MW for solar, nuclear (PWR),

coal, LNG, and oil plants, respectively. The total cost of the system was \$2.6537 10, and the EENS was  $3.9875 \times 10^4$  MWh.

### ***5.9 Case 4b: 5–10% RES Penetration/SPWS as Alternative Investment Candidate***

The total capacity added to the system for the 6-year period was 8700 MW, with increased capacities for solar, oil, LNG, coal, nuclear (PWR), and nuclear (PHWR) plants of 2000, 1800, 1500, 1000, and 1400 MW, respectively. In total, the system cost \$1.7130 10<sup>10</sup> dollars, and the EENS was  $3.1173 \times 10^4$  megawatt hours.

The total capacity added to the system throughout the 14-year period was 14,550 MW, with increased capacities from oil, LNG, coal, nuclear (PWR), nuclear (PHWR), solar, and other plants totaling 1400, 2250, 4000, 1000, 4900, and 1000 MW, respectively. The total cost of the system was \$2.7653 10<sup>10</sup> and the EENS was  $3.7616 \times 10^4$  MWh.

The overall capacity added to the system for the 6-year period, when treatment/penalty fees were levied on HEP emissions, was 8750 MW, with increased capacities for solar, oil, LNG, coal, nuclear (PWR), and nuclear (PHWR) plants of 1600, 2250, 1500, and 1000 MW, respectively. The EENS was 2.7174104 MWh, and the entire system expenses were \$1.71561010.

The total capacity added to the system throughout a 14-year period when treatment/penalty fees were levied on HEP emissions was 14,450 MW, with capacities added by oil, LNG, coal, nuclear (PWR), nuclear (PHWR), and solar plants of 1800, 2250, 4500, 0, 4900, and 1000 MW, respectively. The system's total cost was \$2.7654 10<sup>10</sup>, and the EENS was  $3.5604 \times 10^4$  MWh.

### ***5.10 Case 5a: 10–20% RES Penetration/SPWNS as Alternative Investment Candidate***

The total capacity added to the system for the 6-year period was 9950 MW, with increased capacities for oil, LNG, coal, nuclear (PWR), nuclear (PHWR), and solar plants totaling 1400, 1350, 2500, 2000, 700, and 2000 MW, respectively. The EENS was  $3.4713 \cdot 10^4$  MWh, while the entire system expenses were \$1.8296 10<sup>10</sup> in total.

The total capacity added to the system throughout the 14-year period was 16,750 MW, with increased capacities from oil, LNG, coal, nuclear (PWR), nuclear (PHWR), and solar plants totaling 2,200, 2,250, 4,500, 2000, 2800, and 3000 MW, respectively. The total cost of the system was \$2.9877 10<sup>10</sup> and the EENS was  $3.3206 \times 10^4$  MWh.

The overall capacity added to the system for the 6-year period, when treatment/penalty fees were imposed on HEP emissions, was 10,050 MW, with increased

capacities for solar, oil, LNG, coal, nuclear (PWR), and nuclear (PHWR) plants of 200, 3150, 2000, and 700 and 2000 MW, respectively. The system's total expenses came to  $\$1.9339 \times 10^{10}$  dollars, and its EENS was  $3.6022 \times 10^4$  MWh.

The overall capacity added to the system for the 14-year period, when treatment/penalty fees were placed on emissions from HEP, was 17,050 MW, with increased capacities for solar, LNG, coal, nuclear (PWR), and nuclear (PHWR) plants of 4000, 2250, 2000, 3000, and 2800 MW, respectively. The whole system cost was  $\$3.0641$  per 10 square feet and the EENS was  $1.6852 \times 10^4$  MWh.

### ***5.11 Case 5b: 10–20% RES Penetration/SPWS as Alternative Investment Candidate***

The overall capacity added to the system for the 6-year period was 9950 MW, with added capacities of 2000, 1350, 1500, 2000, 2000, and 2000 MW for solar, oil, LNG, coal, nuclear (PWR), nuclear (PHWR), and nuclear plants, respectively. The system's entire expenses came to  $\$2.2248 \times 10^{10}$  dollars, and the EENS was  $3.4951 \times 10^4$  MWh.

During the 14-year period, when no costs for treatment or penalties were imposed on HEP emissions, a total of 17,400 MW of system capacity was added, with added capacities for solar, oil, LNG, coal, nuclear (PWR), and nuclear (PHWR) plants of 1400, 2700, 3500, 4000, and 2800 MW, respectively. Costs for the system were  $\$3.20261010$  and the EENS was  $0.5760 \times 10^4$  MWh.

The overall capacity added to the system for the 6-year period when treatment/penalty fees were levied on HEP emissions was 9700 MW, with increased capacities for solar, oil, LNG, coal, nuclear (PWR), and nuclear (PHWR) plants of 1200, 1800, 2000, 700, and 2000 MW, respectively. The EENS was  $2.9569104$  MWh, and the entire system expenses were  $\$2.22861010$ .

The overall capacity added to the system for the 14-year period, when treatment/penalty fees were placed on emissions from HEP, was 17,200 MW, with increased capacities for solar, oil, LNG, coal, nuclear (PWR), and nuclear (PHWR) plants of 1400, 900, 4000, 3000, and 4900 MW, respectively. Costs for the system were  $\$3.2308 \times 10^{10}$  and the EENS was  $0.6598 \times 10^4$  MWh.

In all scenarios where the solar plants had their own storage capacity, the capacity contributed to the system and EENS were, on average, lower than for cases where there was no storage capacity. However, when storage capacity for incoming solar plants was included, the overall prices increased in all situations. This held true for planning horizons of both 6 and 14 years.

### **5.12 Level 1 Study: GEP Without Solar Plants (Policy Case 1) (Tables 5, 6, 7 and 8)**

The overall electricity capacity increased during the 6-year period was 7850 MW, and for the 14-year planning period, it was 13,850 MW, when no treatment or penalty fees were imposed on emissions from the HEP. Like this, the overall expenses and EENS and horizons were \$1.20091010 and 2.7165104 MWh for a period of 6 years and \$2.18111010 and 3.8012104 MWh for a duration of 14 years.

The overall electricity capacity increased for the 6-year period was 7850 MW, and for the 14-year planning period, it was 14,000 MW, when treatment/penalty fees were placed on emissions from the HEP. The overall expenses for the 6-year and 14-year timeframes, respectively, were \$1.2947,10,10 and \$2.26,10,10, whereas the EENS were 2.7165,10,4 MWh and 3.6376,10,4 MWh.

### **5.13 Level 2 Study: GEP Based on the Introduction of Solar Plants as an Alternative Investment Candidate or as an Oil Plant Replacement (Table 5)**

In Table 4.2 for the 6-year planning horizon, the thorough analysis of GEP based on the introduction of solar plants as a replacement for oil plants or as an alternative investment option is offered.

### **5.14 Overall Costs and Capacity Additions**

When solar power plants, with or without storage, were evaluated as potential candidates for alternative investments, the system's capacity additions were consistently higher than when they were thought of as oil plant replacements. Whether or not the treatment/penalty charges were imposed on emissions from HEP plants, this qualification is still applicable to both scenarios. This means that the additional investment capacity for policy cases 2a and 3a were 8200 and 8950 MW, respectively, as opposed to policy cases 4a and 5a, which had additional investment capacities of 9050 and 9950 MW, respectively. Cases 2b and 3b as well as Cases 4b and 5b can be compared using the same criteria. When compared, the overall system costs also followed the pattern of capacity additions for the relevant situations.

## 5.15 EENS

However, as shown in Table 5, there were some mixed results in the EENS comparison between those patients.

### 5.15.1 When HEP Emissions Were not Subject to Any Costs

The EENS was lower when solar was added to the system as an alternative candidate plant rather than as a replacement for the oil plant, both for the scenarios of solar additions SPWNS and SPWS, for the estimated solar penetration level of 5–10%. To put it another way, it was less for policy cases 4a ( $2.1755 \times 10^4$  MWh) and 4b ( $3.1173 \times 10^4$  MWh) than for cases 2a ( $3.4770 \times 10^{10}$  MWh) and 2b ( $3.4435 \times 10^4$  MWh); for the assumed solar penetration level of 10–20%, both for the cases of solar addition SPWNS or SPWS, the EENS is higher for the case when solar was added to the system as an alternative candidate. This means that it was more for cases 5a (3.4713 MWh) and 5b (3.4951 MWh) than for cases 3a (3.3015 MWh) and 3b (3.2424 MWh).

### 5.15.2 When HEP Emission Costs for Treatment and Penalties Were Imposed (Table 6)

When incoming solar plants were considered as a replacement for existing oil plants, EENS values were higher than when they were considered as an alternative capacity option when the solar plant had its own storage capacity, and they were higher when they were considered as an alternative investment candidate than when they were considered as a replacement for existing oil plants when the incoming solar plants had no storage capacity of their own.

In other words, the EENS values for policy cases 4b (2.7174 MWh) and 5b (2.9569 MWh) were lower than those for cases 2b (2.8275 MWh) and 3b (3.2424 MWh), whereas the EENS values for cases 4a (3.2323 MWh) and 5a (3.6022 MWh) were higher than those for cases 2a (2.9273 MWh) and 3a (3.4157 MWh).

### 5.15.3 Level 3 Study: According to Whether Solar Plants Had the Storage Capacity

The analysis focuses on GEP with costs for emissions from HEP as shown in Tables 5 and 6 and GEP with no treatment/penalty costs imposed on emissions from HEP.

*GEP When No Costs Were Imposed for Treatment or Penalties for Emissions from HEP*

For cases 2a and 3a, with SPWNS and the strategy for replacing the oil plants with solar, the total capacity additions increased from 8200 to 8950 MW, the total costs



increased from  $\$1.2627 \cdot 10^{10}$  to  $\$1.4702 \cdot 10^{10}$ , and the EENS had decreased from  $3.4470 \cdot 10^4$  MWh to  $3.3015 \cdot 10^4$  MWh when the permitted solar additions to the system were increased from 5–10 to 10–20%.

When the permissible solar additions to the system were increased from 5–10 to 10–20% for cases 2b and 3b with SPWS and the strategy for SPWS replacing the oil plants, the additional capacity brought into the system for cases 2b and 3b was less than for cases 2a and 3a. The capacity added to the system between cases 2b and 3b fell from 8150 MW (for 2b) to 8000 MW (for 3b). Along with the overall capacity added, the EENS for examples 2a, 2b, 3a, and 3b followed the same pattern.

When the solar additions to the system had a storage capacity of their own, the overall system costs were higher than when the solar additions had no storage capacity. In other words, cases 2b ( $\$1.2812 \cdot 10^{10}$ ) and 3b ( $\$1.5131 \cdot 10^{10}$ ) had greater total system costs than cases 2a ( $\$1.2627 \cdot 10^{10}$ ) and 3a ( $\$1.4702 \cdot 10^{10}$ ).

#### *GEP with Costs for HEP Emissions (Tables 5 and 6)*

Solar plants were unable to store energy when penalty prices for HEP plant emissions were applied, but in identical situations where no such emission costs were considered, additional capacities were routinely added to the system. The situation was the exact opposite when solar power facilities had their own storing capability. In examples, 2a and 3a, the corresponding capabilities added to the system were 8200 and 8950 MW when no emission costs were considered, and 8750 and 9400 MW in cases when HEP emissions were subject to treatment or penalty fees.

But in cases, 2b and 3b, where the new solar power plants had storage capabilities, the system's capacity additions were 8150 and 8000 MW, respectively, when no treatment or penalty costs were imposed on HEP emissions, and the same amounts were 8000 and 8000 MW, respectively, when such costs were imposed. When treatment/penalty charges were levied on HEP emissions, the overall system costs were always greater. Regardless of the expenses associated with emissions, the EENS had a distinct pattern based on solar system additions. When penalty charges were imposed on emissions from HEP plants, the EENS had lower values when the solar penetration was expected to be between 5 and 10%. The situation changed when the assumed solar penetrations rose from 5–10 to 10–20%.

#### *Sensitivity Research on the Effects of FOR on GEP at Level 4 (Tables 10, 11, and 12)*

The literature assumed an outage ratio ranging from 6 to 76% for both a solar plant with storage and a solar plant without storage (SPWNS and SPWS). Researchers employed a mix of these values in their investigation. Sensitivity analysis was performed to examine the effects of various combinations of Forced Outage Rate (FOR) for SPWNS and SPWS, as shown in Table 9, to provide a realistic representation of the system performance.

Tables 10, 11, and 12 present the study's findings for various FOR% value combinations for both the 6- and 14-year planning horizons. For various combinations of policy instances, the variations in system capacity addition, overall costs, and EENS are also provided.

**Table 9** Details of FOR% for SPWNS and SPWS

Cases	For (%)		Reference (%)
	SPWNS	SPWS	
1	76	76	76/76
2	76	6	76/6
3	6	6	6/6

Given a policy case, the incremental investment capacity was consistently larger when the FOR% combination assumed was 76/76% for SPWNS/SPWS than for the FOR% combinations of 76/6 and 6/6% for SPWNS/SPWS. When we viewed solar as an alternative investment candidate plant rather than as a substitute for oil plants, the additions of solar to the system were consistently greater for all policy situations, for all combinations of FOR%. For the circumstances when solar storage was assumed, the total capacity of plants added to the system during planning was either equal to or lower than for the cases where no sun storage was assumed.

*Cases When HEP Emissions Were not Subject to Treatment or Penalty Costs*

The no treatment or penalty costs were imposed on emissions from HEP including overall costs, capacity additions and EENS.

- *Overall Costs*

Depending on the cap on solar installations, overall prices between FOR% combination of 76/6 and 6/6% for SPWNS/SPWS decreased from 2.63 to 18.94% for the various policy instances. Similar comparisons can be made between the situations of FOR% for SPWNS/SPWS of 76/76 and 6/6%.

- *Capacity Additions*

When the FOR% combination for SPWNS/SPWS was changed from 76/6 to 6/6% and when it was changed from 76/76% combo to 6/6% combination, capacity increases varied similarly. The system’s capacity was enhanced to accommodate combinations with higher FOR%.

- *EENS*

When solar additions were introduced as a capacity investment alternative, the comparison of EENS typically followed a similar pattern to that of overall costs and capacity additions.

**Table 10** Variations in capacity added based on FOR% pairings of 76/76, 76/6, and 6/6% for planning horizons of 6 and 14 years

Policy	6 Year planning period						14 Year planning period					
	Without emission costs			With emission costs			Without emission costs			With emission costs		
	Overall cost × 10\$						Overall cost × 10\$					
	FOR 76/ 76%	FOR 76/ 6%	FOR 6/ 6%	FOR 76/ 76%	FOR 76/ 6%	FOR 6/ 6%	FOR 76/ 76%	FOR 76/ 6%	FOR 6/ 6%	FOR 76/ 76%	FOR 76/ 6%	FOR 6/ 6%
Case 1	1.2009	1.2009	1.2009	1.2947	1.2947	1.2947	2.1811	2.1811	2.1811	2.2627	2.2627	2.2627
Case 2a	1.2725	1.2627	1.1960	1.2947	1.2947	1.2336	2.3212	2.3011	2.1847	2.3936	2.3156	2.2474
Case 2b	1.3156	1.2812	1.2391	1.3187	1.3187	1.2791	2.4276	2.3503	2.2704	2.4968	2.3603	2.3781
Case 3a	1.4854	1.4702	1.2956	1.5283	1.5283	1.3358	2.5603	2.458	2.2888	2.6606	2.4613	2.3679
Case 3b	1.6960	1.5131	1.4743	1.5370	1.5370	1.5204	2.1350	2.4868	2.4025	2.7879	2.5017	2.4899
Case 4a	1.4909	1.5208	1.3762	1.6139	1.6139	1.4179	2.5527	2.6263	2.3396	2.6814	2.6537	2.4283
Case 4b	1.7176	1.7130	1.6061	1.7156	1.7156	1.6462	2.7619	2.7653	2.5856	2.8835	2.7654	2.6521
Case 5a	1.7882	1.8296	1.5406	1.9339	1.9339	1.5851	2.8954	2.9877	2.4762	3.0031	3.0641	2.5543
Case 5b	2.2311	2.22248	1.8705	2.2286	2.2286	20,002	3.2259	3.2026	2.7580	3.3147	3.2308	2.8849

**Table 11** Variations in total costs depending on FOR% combinations of 76/76, 76/6, and 6/6 for planning horizons of 6 and 14 years

Policy	6 Years planning period						14 Year planning period					
	Without emission costs			With emission costs			Without emission costs			With emission costs		
	Overall cost × 10\$						Overall cost × 10\$					
	FOR 76/ 76%	FOR 76/ 6%	FOR 6/ 6%	FOR 76/ 76%	FOR 76/ 6%	FOR 6/ 6%	FOR 76/ 76%	FOR 76/ 6%	FOR 6/ 6%	FOR 76/ 76%	FOR 76/ 6%	FOR 6/ 6%
Case 1	1.2009	1.2009	1.2009	1.2947	1.2947	1.2947	2.1811	2.1811	2.1811	2.2627	2.2627	2.2627
Case 2a	1.2725	1.2627	1.1960	1.2947	1.2947	1.2336	2.3212	2.3011	2.1847	2.3936	2.3156	2.2474
Case 2b	1.3156	1.2812	1.2391	1.3187	1.3187	1.2791	2.4276	2.3503	2.2704	2.4968	2.3603	2.3781
Case 3a	1.4854	1.4702	1.2956	1.5283	1.5283	1.3358	2.5603	2.458	2.2888	2.660 6	2.4613	2.3679
Case 3b	1.6960	1.5131	1.4743	1.5370	1.5370	1.5204	2.1350	2.4868	2.4025	2.7879	2.5017	2.4899
Case 4a	1.4909	1.5208	1.3762	1.6139	1.6139	1.4179	2.5527	2.6263	2.3396	2.6814	2.6537	2.4283
Case 4b	1.7176	1.7130	1.6061	1.7156	1.7156	1.6462	2.7619	2.7653	2.5856	2.8835	2.7654	2.6521
Case 5a	1.7882	1.8296	1.5406	1.9339	1.9339	1.5851	2.8954	2.9877	2.4762	3.0031	3.0641	2.5543
Case 5b	2.2311	2.22248	1.8705	2.2286	2.2286	20,002	3.2259	3.2026	2.7580	3.3147	3.2308	2.8849

**Table 12** variations between the 76/76%, 76/6%, and 6/6% FOR% combinations using EENS for the 6-year and 14-year planning horizons

Policy	6 Years planning period						14 Year planning period					
	Without emission costs			Without emission costs			Without emission costs			Without emission costs		
	Overall cost × 10\$						Overall cost × 10\$					
	FOR 76/ 76%	FOR 76/ 6%	FOR 6/ 6%	FOR 76/ 76%	FOR 76/ 6%	FOR 6/ 6%	FOR 76/ 76%	FOR 76/ 6%	FOR 6/ 6%	FOR 76/ 76%	FOR 76/ 6%	FOR 6/ 6%
Case 1	2.7165	2.7165	2.7165	2.7165	2.7165	2.7165	3.8012	3.8012	3.8012	3.8012	3.8012	3.8012
Case 2a	3.7952	3.4770	2.7944	3.7952	2.9273	3.6464	2.8681	0.4211	4.0023	1.7224	2.5915	3.7182
Case 2b	2.9273	3.4435	2.7944	3.7952	2.8275	2.8607	2.7205	3.1486	3.1618	2.1669	2.0383	4.1675
Case 3a	3.4157	3.3015	2.1399	3.4157	3.4157	3.9519	1.0966	2.9172	3.4819	3.2904	3.9124	2.5003
Case 3b	3.4157	3.2424	3.2058	3.4157	3.2424	2.4079	2.1825	0.3294	2.5223	2.8326	2.5246	0.5172
Case 4a	3.2846	2.1755	3.217	0.6499	3.2326	3.1215	3.6649	2.0032	3.826	3.5226	3.9875	4.1608
Case 4b	3.2846	3.1173	4.5336	3.0745	2.7174	2.2339	2.7393	3.7616	3.6785	3.0922	3.5604	3.5879
Case 5a	2.7325	3.4713	2.9751	2.8284	3.6022	3.603	2.9424	3.3206	3.9512	2.8673	1.6852	3.4473
Case 5b	3.3586	3.4951	3.1631	2.8583	2.9569	2.1706	1.7414	0.576	2.4234	0.5238	0.6598	2.9476

*For Cases Where Treatment Costs or Penalty Costs Were Imposed on HEP Emissions*

Costs for capacity expansions, overall fees, and EENS were all included in the treatment or penalty costs imposed on HEP emissions.

- *Overall Costs*

Depending on the cap on solar additions and the capacity of solar plants for storage, the overall costs between FOR% combination of 76/6 and 6/6% for SPWNS/SPWS have decreased from 1.09 to 22%. Similar comparisons can be made for situations with FOR% of 76/76 and 6/6% for SPWNS/SPWS.

- *Capacity Additions*

When the FOR% combination for SPWNS/SPWS was adjusted from 76/6 to 6/6% and from 76/76% combo to 6/6% combination, capacity additions showed comparable variances. The system's capacity was expanded to accommodate combinations with higher FOR%.

- *EENS*

When the solar plants had storage capacity, the ENS was higher than when no storage was anticipated, ranging from FOR% combinations of 6/6 to 76/6%.

Depending on whether the Emission Costs for HEP were included or not, all the aforementioned policies were taken into account for two alternative scenarios.

## 6 Conclusions

The thesis focuses on applying single-objective optimization to solve a GEP problem. For planning horizons of 6 and 14 years, the effects of including solar and wind power plants are examined. The effects of switching from expensive conventional oil plants to renewable solar and wind energy facilities are attempted to be studied. Using a test case and the effect analysis of many essential aspects, the system identification, model formulation, and model solutions for the GEP problem with future solar and wind additions are standardized. This is done as policy choices in the system planning are carried out. To make the system more realistic in this study, several degrees of solar plants are added into the system as a capacity option. The system analysis also takes ETPC and TERC into account.

There is also a comparison of the scenarios with and without solar power plants. The range of policy concerns considered paints a clearer picture of how solar technologies added to the system may affect the generating mix, as subject to TERC or ETPC, or both. The appropriate depiction of the variables under discussion enables the planners to examine the influence of various policy actions. Additionally, they would be able to determine the effects of integrating any given technology type plant

and receive detailed information on the additional base load capabilities that will be needed when RET plants are added to the system.

Operation choices on shorter timescales must take dispatch characteristics into account to realize the true system scale benefits. Such a study would follow naturally from the one we conducted. Along with the choices on the planning of the generating mix, this would provide a deeper understanding of how the system functions. Professionals engaged in the system’s long-term generation growth planning might benefit from such a study.

The study’s evaluation of the effects of various FOR% combinations for SPWNS and SPWS plants on system performance and planning is another crucial component. The differential FOR% combinations employed for SPWNS and SPWS have a significant impact on the system performance and, consequently, the formulation of policy. This study, which aims to demonstrate the complexity of the decision-making process when adding solar power to an existing system, offers a four-level hierarchy to help planners grasp the full range of potential GEP policy concerns and take the appropriate course of action.

## Appendix

Data for generation expansion planning study (Tables 13, 14, 15, 16 and 17).

**Table 13** Forecasted peak demand [50]

Stage (year)	0 (2016)	1 (2018)	2 (2012)	3 (2022)	4 (2024)	5 (2026)	6 (2028)
Peak (MW)	5000	7000	9000	10,000	12,000	13,000	14,000
Stage (year)	0 (2016)	7 (2030)	8 (2032)	9 (2034)	10 (2036)	11 (2038)	12 (2040)
Peak (MW)	5000	15,000	17,000	18,000	20,000	22,000	24,000

**Table 14** Technical and economic data of candidate plants [50]

Candidate type	Construction upper limit	Capacity (MW)	FOR (%)	Operating cost (\$/kWh)	Fixed O&M cost (\$Kw-Mon)	Capital cost (\$/kW)	Life time (Years)
Oil	5	200	7.0	0.021	2.20	812.5	25
LNG C/C	4	450	10.0	0.035	0.90	500.0	20
Coal (Bitum.)	3	500	9.5	0.014	2.75	1062.5	25
Nuc. (PWR)	3	1.000	9.0	0.004	4.60	1625.0	25

(continued)

**Table 14** (continued)

Candidate type	Construction upper limit	Capacity (MW)	FOR (%)	Operating cost (\$/ kWh)	Fixed O&M cost (\$Kw-Mon)	Capital cost (\$/ kW)	Life time (Years)
Nuc. (PHWR)	3	700	7.0	0.003	5.50	1750.0	25
Solar	3	1000	0.76	0.001	2.08	3873	25
Wind	3	1000	0.754	0.001	1.46	1500	25

**Table 15** Technical and economic data of existing plants [50]

Name (fuel type)	No. of units	Unit capacity (MW)	FOR (%) (\$/kwh)	Operating cost (\$/ kW-Mon)	Fixed O&M cost (\$/ kW-Mon)
Oil#1 (heavy oil)	1	200	7.0	0.024	2.25
Oil#2 (heavy oil)	1	200	6.8	0.027	2.25
Oil#3 (heavy oil)	1	150	6.0	0.030	2.13
LNG G/T#1 (LNG)	3	50	3.0	0.043	4.52
LNG C/C#1 (LNG)	1	400	10.0	0.038	1.63
LNG C/C#2 (LNG)	1	400	10.0	0.040	1.63
LNG GC/C#3 (LNG)	2	450	11.0	0.035	2.00
Coal#1 (Anthracite)	1	250	15.0	0.023	6.65
Coal#2 (Bituminous)	1	500	9.0	0.019	2.81
Coal#3 (Bituminous)	1	500	8.5	0.015	2.81
Nuclear#1 (PWR)	1	1.000	9.0	0.005	4.94
Nuclear#2 (PHWR)	1	1.000	8.8	0.005	4.63



**Table 16** Technical and economic data of the solar and wind power plant without energy storage [51]

Plant type	FOR (%)	Operating cost (\$/kWh)	Fixed O&M cost (\$/Kw-Mon)	Capital cost (\$/kW)	Life time (Years)
Solar plant without energy storage	76	0.001	2.08	3873	25
Wind plant without energy storage	75.4	0.001	1.46	1500	20

**Table 17** Technical and economic data of the solar plant with energy storage [49]

Plant type	FOR (%)	Operating cost (\$/kWh)	Fixed O&M cost (\$/Kw-Mon)	Capital cost (\$/kW)	Life time (Years)	Storage/day time	Battery type
Solar plant with energy storage	6	0.0015	4.17	6530	15	6 h storage/day	Lead acid battery

## References

- MIT: Managing large-scale penetration of intermittent renewables. In: Proc. MIT Energy Initiative, Symposium, April 20 (2011)
- European Wind Energy Association, [Online]. <http://www.bwea.com/energy/europe.html>. Accessed on 6 July 2016
- Ecworld [Online]. <http://ecoworld.com/features/2006/07/15/wind-power-in-china/>. Accessed on 3 July 2016
- Haley, B., Hart, E., Williams, J.: Electricity system planning for long-duration energy imbalance CEF topical white paper, Energy Environmental Economics, pp. 1–6 (2013)
- Denholm, P., Ela, E., Kirby, B., Milligan, M.: The role of energy storage with renewable electricity generation. Technical Report NREL/TP-6A2–47187, pp. 1–61 (2010)
- Pandzic, H., Wang, Y., Qiu, T., y Dvor Kin, Y., Kirschen, D.S.: Near-optimal method for siting and sizing of distributed storage in a transmission network. IEEE Trans. Power Syst. **18**, 1–13 (2014)
- Hu, Z., Ward Jewell, T.: Optimal Generation Planning with Integration of Variable Renewables and Bulk Energy Storage Systems, this research was Funded by the Power Systems Engineering Research Center (pserc.org) Under Projects M24 and T48
- Vasconcelos, J., Ruester, S., He, X., Chong, E., Glachant, J.-M.: Electricity storage: how to facilitate its deployment and operation in the EU. Final report June 2012, [Online]. <http://think.eii.eu>. Accessed on 03.05.2015
- Careri, F., Gensi, C., Marannino, P., Montagna, M., Rossi, S., Siviero, I.: Generation expansion planning in the age of green economy. IEEE Trans. Power Syst. **26**(4) (2011)
- Global Wind Report, Global Wind Energy Council (GWEC), [Online]. <http://www.gwec.net/> (2005). Accessed on 05.07.2016
- GWEC 2008, Global Wind Energy Council, [Online]. <http://www.gwec.net/> (2008). Accessed on 5 July 2016
- George, M., Banerjee, R.: Analysis of impacts of wind integration in the Tamilnadu grid. Energy Policy **37**, 3693–3700 (2009)
- Milligan, M.: Modelling Utility Scale Wind Power Plants, Part 2: Capacity Credit, NREL/TP-500-27514, National Renewable Energy Laboratory, Colorado, USA (2002)

14. Vivian, S., Deisenrieder, A.: *Renewable Energy: Market and Policy Environment in India*, Observer research Foundation, ORF Occasional Paper #47 (2013)
15. IEC: *Grid integration of large-capacity renewable energy sources and use of large-capacity. Electrical Energy Storage*, White Paper (2012)
16. Central Electricity Regulatory Commission, Government of India, *Performance of Solar Power Plants in India* (2011)
17. Cellura, M., Di Gangi, A., Longo, S., Orioli, A.: Photovoltaic electricity scenario analysis in urban contexts: an Italian case study. *Renew. Sustain. Energy Rev.* **16**, 2041–2052 (2012)
18. Pratap, A.: *Rooftop Revolution: Unleashing Delhi's Solar Potential*, Greenpeace India (2013)
19. Sullivan, P., Eurek, K., Margolis, R.: *Advanced methods for incorporating solar energy technologies into electric sector capacity-expansion models: literature review and analysis*. Technical Report-NREL/TP-6A20-61185, National Renewable Energy Laboratory (NREL). [www.nrel.gov/publications](http://www.nrel.gov/publications) (2014)
20. Schroder, A., Bracke, M.: *Integrated Electricity Generation Expansion and Transmission Capacity Planning—An Application to the Central European Region*. <http://www.diw.de> (2012)
21. Rose, A., Stoner, R.J., Pérez-Arriaga, I.: *Prospects for grid-connected solar photovoltaic in Kenya—a systems approach*. WIDER Working Paper 2014/095, World Institute for Development Economics Research, wider.unu.edu (2014)
22. Beccali, M., Cellura, M., Mistretta, M.: *Decision-making in energy planning. Application of the Electre method at regional level for the diffusion of renewable energy technology*. *Renew Energy* **28**, 2063–2087 (2003)
23. DOE, USA, *SunShot Vision Study*, U.S. Department of Energy Report (2012)
24. Karapidakis et al.: *Generation expansion planning of Crete power system for high penetration of renewable energy sources*. *Mater. Sci. Forum* **670**, 407–414 (2011)
25. De Sisternes, F.J.: *Investment Model for Renewable Electricity Systems (IMRES), an Electricity Generation Capacity Expansion with Unit Commitment Constraints*, MICEEPR, CEEPR WP 2013–16 (2013)
26. Promjiraprawat, K., Limmeechokchai, B.: *Multi-objective and multi-criteria optimization for power generation expansion planning with CO2 mitigation in Thailand*. *Songklanakarinn J. Sci. Technol.* **35**(3), 349–359 (2013)
27. Muneer, W.: *Large-scale solar PV investment planning studies Waterloo*. *IEEE Trans. Power Syst. Ontario, Canada* **26**(4), 1–62 (2011)
28. Grossmann, W.D., Grossman, I., Steininger, K.W.: *Solar electricity generation across large geographic areas, part I: A method to optimize site selection, load distribution and storage*. Working Paper of the Wegener Center for Climate and Global Change and the Center for Climate and Energy Decision Making at Carnegie Mellon, Extended version submitted to *Renewable and Sustainable Energy Reviews*
29. Wang, X., McDonald, J.R.: *Modern Power System Planning*, pp. 208–229. McGraw Hill, London (1994)
30. Khokhar, J.S.: *Programming Models for the Electricity Industry*, pp. 21–84. New Delhi Commonwealth Publishers (1997)
31. Balkirtzis, G.A., Biskas, P.N., Chatziaathanasiou, V.: *Generation expansion planning by MILP considering mid-term scheduling decisions*. *Electr. Power Syst. Res.* **86**, 98–112 (2012)
32. European Commission: *Renewable Energy*, [Online]. [http://ec.europa.eu/energy/renewables/index\\_en.htm](http://ec.europa.eu/energy/renewables/index_en.htm). Accessed on 11 December 2013
33. Zervos, A., Lins, C., Muth, J.: *Re-thinking 2050: A 100% Renewable Energy Vision for the European Union*. European Renewable Energy Council, Brussels (2010)
34. DSIRE: *Renewable portfolio standard policies, Database of state incentives for renewables & Efficiency*, [Online]. [http://www.dsireusa.org/documents/summarymaps/RPS\\_MAP.pdf](http://www.dsireusa.org/documents/summarymaps/RPS_MAP.pdf). Accessed on 5th July 2016
35. Hand, M.M., Baldwin, S., DeMeo, E., Reily, J.M., Mai, T., Arent, D., Porro, G., Meshek, M., Sandor, D.: *National renewable energy laboratory, renewable electricity futures study*. In: Golden, C.O. (eds.): *National Renewable Energy Laboratory* (2012)
36. Ackermann, T. (eds.): *Wind Power in Power Systems*. Wiley, West Sussex (2012)

37. Bouffard, F., Galiana, F.D.: Stochastic security for operations planning with significant wind power generation. *IEEE Trans. Power Syst.* **23**(2), 306–316 (2008)
38. Chan, S.M., Powell, D.C., Yoshimura, M., Curtice, D.H.: Operations requirements for utilities wind power generation. *IEEE Trans. Power App. Syst.* PAS-102 (9), 2850–2860 (1983)
39. Galiana, F.D., Bouffard, F., Arryjo, J.M., Restrepo, J.F.: Scheduling and pricing of coupled energy and primary, secondary and tertiary reserves. *Proc. IEEE.* **93**(11), 1970–1983 (2005)
40. Lee, S.T., Yamayee, Z.A.: Load-following and spinning-reserve penalties for intermittent generation. *IEEE Trans. Power App. Syst.* PAS-100 (3), 1203–1211 (1981)
41. Schlueter, R.A., Park, G.L., Lotfalian, M., Shayanfar, H., Dorsey, J.: Modification of power system operation for significant wind generation penetration. *IEEE Trans. Power App. Syst.* PAS-102 **1**, 153–161 (1983)
42. Giebel, G.: Wind power has a capacity credit, a catalogue of 50+ supporting studies. *Windeng E J.* windwng.net (2006)
43. Akhmatov, V., Knudsen, H.: Large penetration of wind and dispersed generation into the Danish power grid. *Electr. Power Syst. Res.* **77**, 1228–1238 (2007)
44. Holttinen, H.: Estimating the impacts of wind power on power systems—summary of the IEA wind collaboration. *Environ. Res. Lett.* **3**, 1–6 (2008)
45. Holttinen, H., Meibom, P., Tusslin, C., Hoffman, L.: State of the Art of Design and Operation of Power Systems with Large Amounts of Wind Power, European Wind Energy Conference, Milan, Italy (2007)
46. IEA: Design and Operation of Power Systems with Large Amounts of Wind Power, State of the Art Report. Helsinki, Finland International Energy Agency (2007)
47. Ackermann, T.: *Wind Power in Power Systems*. Wiley, New York (2005)
48. Burke, D.J., O'Malley, M.J.: Optimal wind power location on transmission systems—a probabilistic load flow approach. In *Proc. IEEE PMAPS Conf.* Mayaguez, PR (2008)
49. Khokhar, J.S.: Programming Models for the Electricity Industry, New Delhi Commonw Cost Report “Cost and Performance data for power generation technologies” Prepare for the National Renewable Energy Laboratory [Online]. <http://bv.com/docs/reports-studies/nrel-cost-report.pdf> (2012). Accessed on 7 August 2015
50. Khokhar, J.S.: *Programming Models for the Electricity Industry*, pp. 21–84. New Delhi Commonwealth Publishers (1997)
51. Cost Report “Cost and Performance data for power generation technologies” Prepare for the National Renewable Energy Laboratory [Online]. <http://bv.com/docs/reports-studies/nrel-cost-report.pdf> (2012). Accessed on 7 Aug 2015
52. Park, J.B., Park, Y.M., Won, J.R., Lee, K.Y.: An improved genetic algorithm for generation expansion planning. *IEEE Trans. Power Syst.* **15**(3), 916–922 (2000)
53. U.S. Energy Information Administration: Updated capital cost estimates for utility scale electricity generating plants [Online]. [www.eia.gov/forecasts/capitalcosts/capacitors/pdf/updated\\_capcost.pdf](http://www.eia.gov/forecasts/capitalcosts/capacitors/pdf/updated_capcost.pdf) (2013). Accessed 3 Apr 2013
54. Kannan, S., Mary Raja Slochanal, S., Padhy, N.P.: Application and comparison of meta-heuristic techniques to generation expansion planning problem. *IEEE Trans. Power Syst.* **20**(1), 466–475 (2005)

# **Distributed Generation, Smart Grids and Supply Reliability**

# A Smart Grid Ontology for Africa



Isaac Kabuya Kamiba, Olasupo Ajayi, Antoine Bagula,  
and Kyandonghere Kyamakya

**Abstract** Sustainable development is a call that concerns both developing and developed countries and includes ensuring universal access to affordable, reliable, and modern energy services by 2030 (Goal 7). In the energy domain, there cannot be Smart City or Smart Village without a Smart Energy Management System (SEMS) managing a power grid aimed at providing electrical energy. Nowadays, access to electrical energy through optimal and cost-effective management in generation, transmission, distribution, and consumption, is a requirement that demonstrates the necessity and urgency of transforming traditional (or conventional) power grids into Smart Grids (SGs) in various parts of the world. This is pertinent for Africa where electricity supply is often intermittent even in countries with high hydropower potential. It is expected that if Africa is to develop, it should not fail to invest in an efficient electrical system in the next 20 to 30 years.

**Keywords** Smart grid · Ontology · Smart energy management systems · Sustainable development

---

I. K. Kamiba · O. Ajayi (✉) · A. Bagula  
University of the Western Cape, Cape Town, South Africa  
e-mail: [ooajayi@uwc.ac.za](mailto:ooajayi@uwc.ac.za)

I. K. Kamiba  
e-mail: [isaac.kamiba@esisalama.org](mailto:isaac.kamiba@esisalama.org)

A. Bagula  
e-mail: [abagula@uwc.ac.za](mailto:abagula@uwc.ac.za)

K. Kyamakya  
University of Klagenfurt, Klagenfurt, Austria

Université de Kinshasa, Kinshasa, Democratic Republic of the Congo

K. Kyamakya  
e-mail: [kyandonghere.kyamakya@aau.at](mailto:kyandonghere.kyamakya@aau.at); [kyandonghere.kyamakya@gmail.com](mailto:kyandonghere.kyamakya@gmail.com)

## 1 Introduction

In some parts of the world, research and development work has been done around the Smart Grid (SG) concept and related concepts, with notable achievements made in North America, Europe, and parts of Asia. However, Africa is still in the infancy stage when it comes to smart grids. Current electricity grids in most African countries consist of older generation conventional or traditional grids characterized by (i) a one-way flow of energy and data and (ii) mainly centralized generation. A decentralized power system intelligent enough to automate the grid network, capable of efficiently managing the flow of data and energy, while remaining generally reliable can be of great help in electrifying Africa. With decentralization, it is possible to build a federated smart grid, made up of a large interconnection of smaller renewable and non-renewable energy systems, which is backed up by computerization and automation to provide the intelligence required to handle the complexity of such interconnection of electricity grid networks.

As revealed in [1, 2], traditional grids are based on a closed system of production, transmission, distribution, and consumption that does not facilitate the exchange, visualization, monitoring, control, and security of information flows, and energy data between several operators. Furthermore, in such grids, market and access are not flexible, extensive, adaptable, and contextualized. Building around information and communication technologies (ICT) the Internet of Things (IoT) and Artificial Intelligence (AI), the European Union, North America, the USA, Japan, China, and other Asian countries have felt the need to create a smart grid system for an open, accessible, and optimal market. The birth of such SG has led to further research and development projects in these countries. For instance, the standardization and modeling work initiated by various international and national commissions, such as the International Electrotechnical Commission (IEC), European Network of Transmission System Operators for Electricity (ENTSO-E), National Institute of Standards and Technology (NSIT), and the Worldwide Consortium (W3C), etc., each focused at different layers of different frameworks. The UML-based CIM (Common Information Mode) by IEC [3] and the IEC 61,970/61968/61850 standards shaped the first-generation SG standardization. However, there was a gap in interoperability and technological integration between the IEC CIM model and the IEC 61,850 model. This gap was addressed through the addition of ontology or semantic technology in Smart Grid [4]. The power of ontologies consists of (i) integrating the knowledge required for interoperability, (ii) creating harmonization between these standards, and (iii) solving complex energy management problems. Ontologies have become what can be described as the functional and operational resources of SGs. Indeed, in the field of electrical energy, semantic technology has demonstrated its strength in managing more heterogeneous and interoperable SGs. Ontologies play a dual role in SG systems where subsystems and their components are interconnected through data integration and modeling [5]. As suggested in [2], this approach to the construction of current SGs is evolutionary.

Several research works have developed ontologies to support SGs. By considering SG as an application of the Internet of Things (IoT) in the energy sector, numerous ontology-based Home Energy Management Systems (HEMS) and Industrial Energy Management Systems have been developed. For instance, in Europe, ontologies such as the Smart Applications REFERENCE (SAREF) [2], Smart energy domain ontology SARGON [6], HomeThink, MIRABEL, SAREF4EE, SSG [7], etc. are in use. When applied to the SG, ontologies can bring high intelligence and efficiency to conventional grids, interconnected devices, appliances, and other machines. This is because the use of semantic technology in energy systems promotes the efficient use of energy, the interoperability, and sustainability of technologies, as well as efficient management of the resulting data volumes [8].

Rather than trying to reinvent the wheel, Africa should (i) leverage on the experiences of more advanced countries to build her own SGs and (ii) embrace a decentralized approach to power generation, transmission, and distribution, thus, transitioning from the traditional energy system to a dynamic and adaptable EMS (energy management system) [9]. To construct such SG, it can use and build on what is already being done elsewhere such as the European EMS in terms of intelligence, data, processes, and contextualization of the EMS. As a starting point, embracing the ontological approach of existing SGs is paramount. There are numerous robust and often complex ontologies available, both open and closed source. Suitable ontologies can then be adapted, modified, and reused. Finding suitable ontologies from the myriad of options can be a challenge, hence, the authors in [1] suggested using standardized ontologies recommended by W3C and ETSI as good targets for reuse.

Finding an ontological approach to be adopted by Africa to build its SGs from its current traditional grid is a key issue addressed in this book chapter. The main contribution of this chapter is to propose an ontological model for one of the SG domains. This model will be built on the reuse of an existing advanced European ontological model of SG. In a robust SG ontology, the management of data and energy flows requires elaborate representation of details, however, ontologies differ and do not all present the same data and/or with the same level of details. In some ontologies, consumption domain, distribution and performance might be omitted. In essence, when an ontology is to be reused, it could be reused as a whole, in parts, or have only some of its elements considered [10]. For this purpose, this study will focus on some sub-domains of ontology applications in SGs, specifically those suited for Home Energy Management Systems, and Urban or District Energy Management Systems. From these two categories, recommended and related ontologies will first be considered and analyzed. The focus will be given to the adaptation of such ontologies to the African SG context. Lastly, this African SG ontological approach will be mapped into a system model. The SAREF ontology proposed in the framework of HEMS has been selected as the target model for this chapter. As suggested in [1], it is an open ontology recommended by ETSI and W3C.

## 2 The Evolution of Smart Grid

Monitoring, controlling, managing, and using energy resources in a flexible, automated, and optimized way is a key requirement upon which the operation of energy systems depends. On one hand, this implies the interoperability of infrastructures, sharing of data and information, and energy flows between end-users, energy operators, and service providers. On the other hand, the development of the web of things for semantic-based automation of energy and operation flow data is a key feature that may support such interoperability and sharing. It is widely recognized that in the field of energy and electricity networks, flexibility in energy supply, as well as the use and exploitation of resources and infrastructure are current open challenges of smart grid deployment in the context of a smart city or smart village.

With sustainability in the generation and use of electrical energy becoming global, electricity operators are now seeking flexible approaches including cooperative federation, which involves “joining forces” to link their infrastructures and rationalize their energy resources for end-consumers [11]. This raised the need for semantic interoperability in a web of energy using an electrical network that builds around the IoT to enable semantic technology. Such a network implements an electrical network model where machines reason and communicate with humans [11, 12] to provide the instantaneous and temporal supply and consumption of energy based on Human-to-Machine (H2M), Machine-to-Machine (M2M), oneM2M, and smartM2M communication models. Authors such as Laure Daniele [11, 12] have addressed the migration from the traditional grid to the current modern grid as perceived by the European Union.

In a period of growth of Renewable Energy Resources (RES), or “Green Energy” as it is commonly termed, it is necessary to rely on the semantic integration of ICTs in electrical energy systems to build a model of energy flow and information flow in real-time for a large digital electrical energy market. Semantic integration is a key enabler for building the electrical networks of smart cities and smart villages using H2M and M2M communications in conjunction with the provision of energy. Semantic integration can be implemented through the application of standardized ontologies. Several ontologies are being standardized by the European Union for application in electrical energy. However, before reusing them in Africa, it is important to understand the environment in which they were applied, how they evolved, and what can be done with them in the immediate and the future.

The smart grid is one of the IoT applications in the energy domains and can only be achieved if there is a smart energy management link between the end-user(s) and the operator(s). In Europe, for example, the development of standards for SG applications first began with the development of oneM2M and smartM2M. It then graduates with the development of SAREF ontologies and their extensions for different application domains. The SAREF project has been applied in diverse domains, but one of concern to this work is the SAREF4ENER or SAREF FOR ENERGY extension. SAFER4ENER, one of the 11 domains or extensions of SAREF, was created with



the collaboration of two non-profit industrial associations - Energy@Home in Italy [26] and EEBUS in Germany [13].

The electrical energy generated, transmitted, distributed, and consumed, constitutes both an exchange market on the one hand and an energy, data, information, and automation control system on the other hand. A bi-directional flow is important between these two sides. A bi-directional flow of automation data, energy, information, and market data promotes the flexibility of each stakeholder in the system. At a time when renewable energies can come from different sources, and when customers can have become prosumers capable of also injecting energy into the grid, any smart grid project that supports these features and the bi-direction flow can be considered sustainable. In developing countries including those in Africa, and in sharp contrast to the developed world, energy insufficiency is still a present-day problem. Energy generation is still mostly still centralized, and the exchange of market, data, and energy flow is mono-directional. There is little or no automation in the distribution stations and consumption facilities of the services. There are no networks of sensors that collect and transmit information or servers that store information, neither is there any means of communicating, analyzing, and making decisions in a common language and in a decentralized manner. The conventional network is centralized and therefore does not offer openings for optimization and flexibility on the demand side as well as on the utility side. For Africa, smart management at the end-user level seems to be a valid starting point, as it is a safe space to experiment with building frameworks whose foundations allow smart energy management at the home level. This implies efficient energy management and economic gain for the user's end.

As we have already shown that SG is a concept introduced in the 2000s. It allows the inclusion of a bi-directional communication infrastructure to the conventional or traditional network based on ICT at the 4 levels of an electrical network: generation, transmission, distribution, and consumption sections of the services [14]. For instance, power generation in the grid is moving from centralized to distributed generation (DG) [14]. The distributed grid facilitates the integration of decentralized sources of energy. Energy generation and supply to consumers is no longer solely the responsibility of the operator, but customers themselves can also generate energy and feed excess into the grid. Thus, there is a need to simultaneously manage the supply of energy (both from the operator and the prosumer. This is called Demand-Side Management and Response-Side Management. SG leverage three ICT pillars, which are:

- (i) the sensor network, which is the lowest interface level and measures different parameters such as energy characteristics, control, detection, etc.
- (ii) the communication systems, which can be wired, wireless or heterogeneous [14].
- (iii) smart grid applications, implemented in the different logical and structural components of the grid (generation, transmission, distribution, and consumption).

Though the contributions of ICT in electrical systems might seem mostly physical, there are indeed other intangible yet highly important benefits, which are efficient,

low-cost, and sustainable use of energy. These parameters cut across every household, institution, industry, district, city, and country. However, for this work, we would concentrate on the tangible. The emergence of the ICT-powered smart grid concept has resulted in better management and optimization of the 4 levels of the electrical service network (i.e., generation, transmission, distribution, and consumption). By introducing cyber communication networks, improved communication, and control of elements within the power grid are achievable. Kabalci [15] highlighted this by stating that, the contribution of the smart grid can be summarised as the promotion of energy flow and communication in the grid. This can be considered the first step in building a smart grid, which would then be followed by the incorporation of simple automation.

The importance of a reliable communication network becomes relevant when developing an Internet of Energy system [16], wherein the underlying communication network interconnects various highly interdependent components of a smart grid energy network. These components include the RES or green energy sources, the ESS (Energy Storage Systems), which ensure a sustainable and economical energy supply, the operators, regulators, administrators, and the final consumers (or prosumers). We would term this composite interdependent network as “smart grid 2.0” or SG2.0. Most often the components of SG2.0 are manufactured by different manufacturers and hence speak different “languages”. The communication network should therefore be heterogeneous and support interoperable technologies and protocols.

Smart grids were considered one of the 5 pillars of the 3rd industrial revolution (characterized by new information and communication technologies), as Jeremy Rifkin pointed out in his thesis [17]. Though the fundamentals SG discussed in [17] remain relevant, they have been improved upon to comply with the core requirements of the current 4th industrial revolution. Now smart grids need to manage diverse sources of electrical energy efficiently, reliably, and cheaply. This is driving the development of web or semantic technology as applied to electrical services. While the historical grid had a top-down architecture, with the producer providing the necessary energy to the grid through transmission and distribution without worrying about each customer, the grids of today’s SG2.0 have a bi-directional architecture consisting of both the top-down and bottom-up architectures. Though it maintains the basic works of the classic grids, it is also concerned with each consumer, power losses during transmission, and other custom needs. For instance, to reduce line losses to a customer, SG2.0 tries to draw energy from the RES or ESS closest to the customer. SG2.0 emphasizes decentralized energies, proximity to the user, and an integrated energy distribution network. The principal actors in this bi-directional architecture are the producers, distributors, and consumers, which can either be small or large scale. Figures 1 and 2 show the integration of electricity and intelligence in SG2.0.

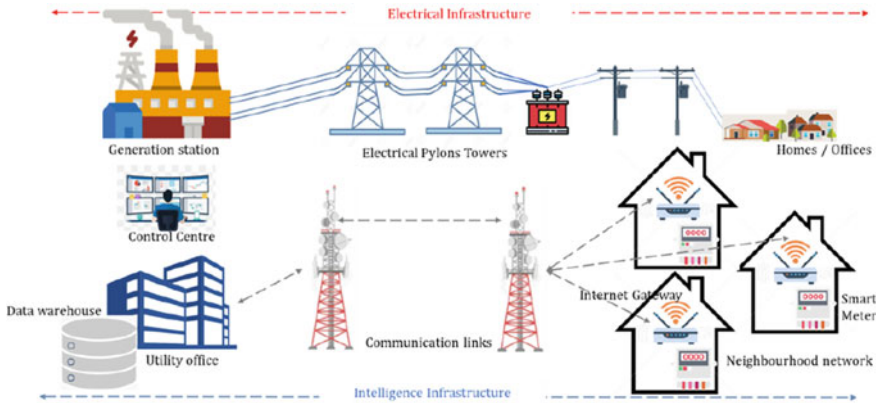


Fig. 1 Smart grid: integration of electricity infrastructure with intelligence infrastructure

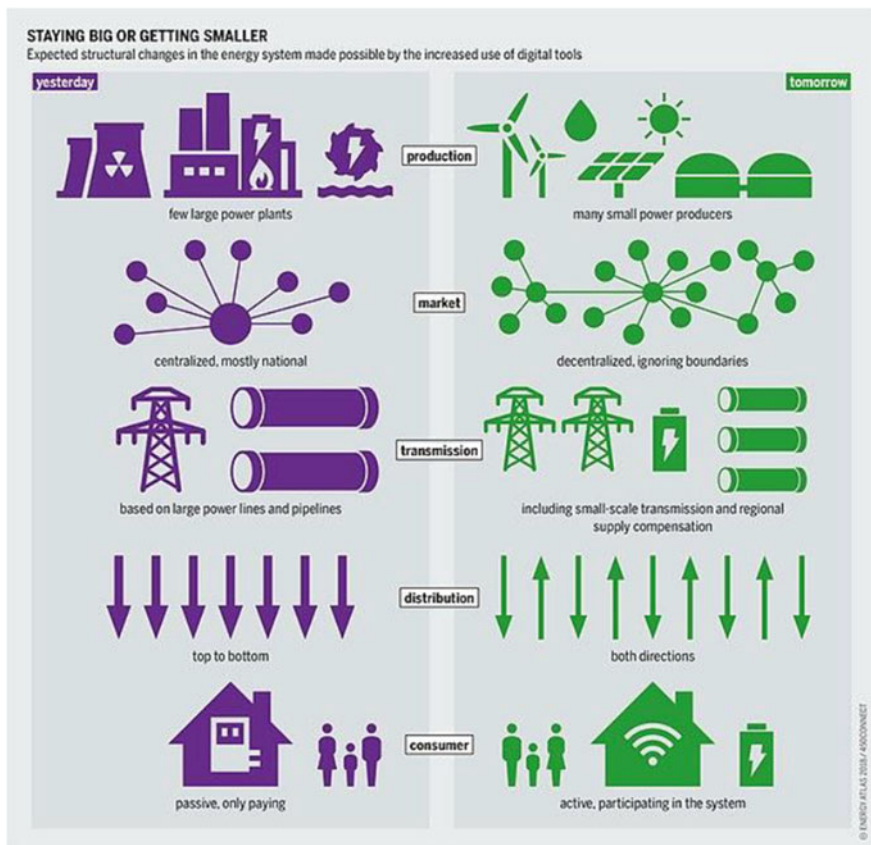


Fig. 2 Top-down and bottom-up approach to the smart grid (image source) [https://fr.wikipedia.org/wiki/R%C3%A9seau\\_%C3%A9lectrique\\_intelligent](https://fr.wikipedia.org/wiki/R%C3%A9seau_%C3%A9lectrique_intelligent)

### 3 Conceptual Models for a Contextualized Smart Grid

Experimenting with research, demonstrating at different scales, following the feedback from the demonstrators, and implementing is the innovation path that different smart grid projects have followed. The grid is not “born” smart, it becomes smart, hence a series of demonstrations are required to make this transition happen. The feedback from these demonstrations serves to prepare this energy transition from the traditional grid to the contextualized smart grid. This contextualized grid can be user-oriented, tertiary, or collective.

A conceptual model is often the first step in developing a smart grid. One of the first conceptual smart grid models was developed by the NIST, an agency of the US Department of Commerce, in 2010 [18].

The model was made up of 7 core domains namely Generation, Transmission, Distribution, Marketing, Operations, Service Providers, and Customers; and is illustrated in Fig. 3.

The model has since been adopted by the ETSI [19] and IEEE [20] respectively. ETSI extended the model to 8 domains and 32 subdomains, while the IEEE extension had 9 domains as shown in Fig. 4. In Europe, the smart grid project is discussed around different conceptual models such as NIST, IEC, ETSI, and IEEE depending on the context. In a bid to develop a standardized model for smart grids in Europe, models such as the Smart Grid Architecture Model SGAM [19] reference architecture and the SG reference architecture from the CEN-CENELEC-ETSI group were developed.

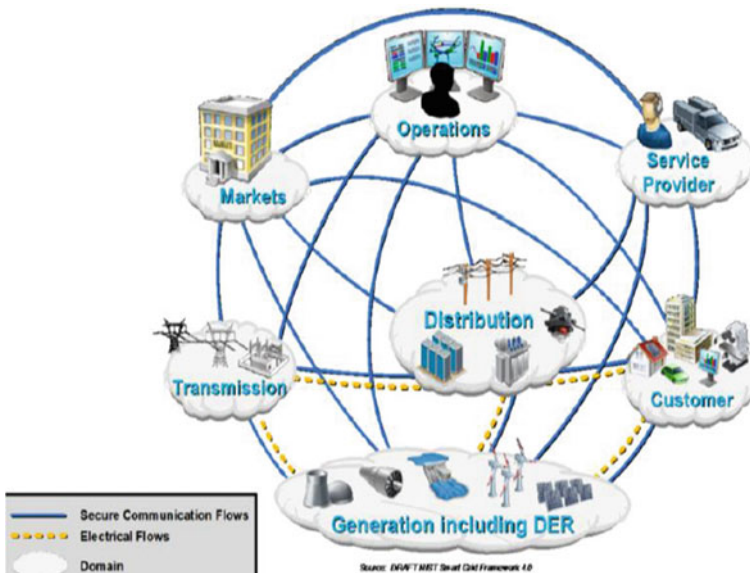
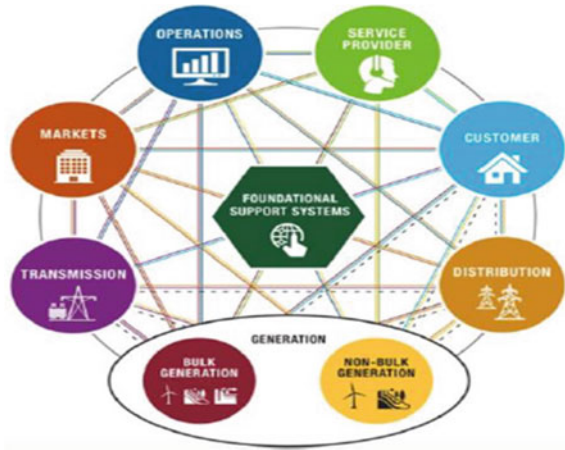


Fig. 3 NIST conceptual SG model [21]

Fig. 4 IEEE SG model [19]



These standardization processes were meant to be completed as part of the European 20/20/20 objectives [21].

When analyzing the different concept models, two key features that can be easily noticed are the non-bulk generation of electricity and the Distributed Energy Resources (DER). These show a movement from a centralized system to a decentralized energy system and finally to a smart grid vision of distributed energy. The analysis of these conceptual models also reveals three assumptions, which are interoperability, interconnection, and communication in the grid. Interoperability cuts across the other two, while sensors serve as the interface for interconnection and interoperability.

The systems approach used by IEEE Standards Coordinating Committee (IEEE SCC21) is shown in Fig. 5 as reported by the National Renewable Energy Laboratory (NREL) [23]. It shows how the smart grid is a system of systems with a dynamic electricity infrastructure and interconnections between the DERs and the bulk power generators. The IEEE Std 2030–2011 also develops a model for the evolution of smart grid interoperability based on three groups of standards that are indispensable in today’s bottom-up approach. These are the smart grid applications, the IEEE2030 Smart Grid Interoperability Guidance, and the Smart Grid Conceptual Reference Model [23], this can be seen in Fig. 6.

Irrespective of the source (standard frameworks or conceptual models), certain elements are constant for all SG, which are the domains and their sub-domains, secure communication for the flow of data and information, and the flow of energy from bulk generations or DER. These are most evident in the NIST framework and its numerous adaptations. It can therefore be concluded that contextual analysis and understanding of each standard, the corresponding application area(s), and the interoperability strategy are remarkably important.

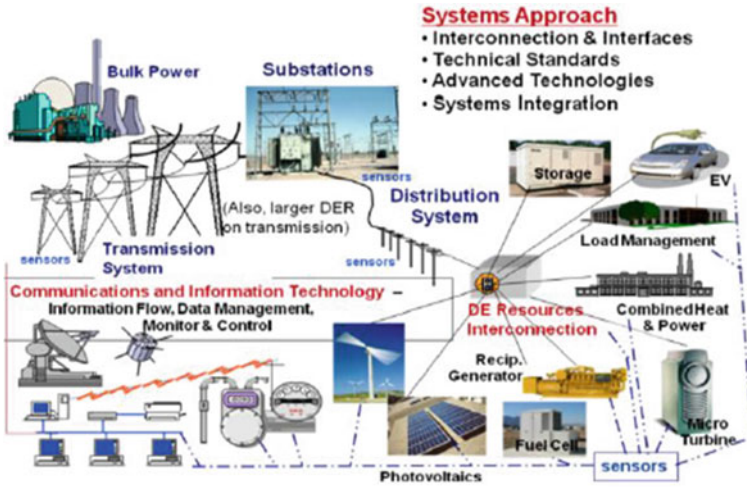
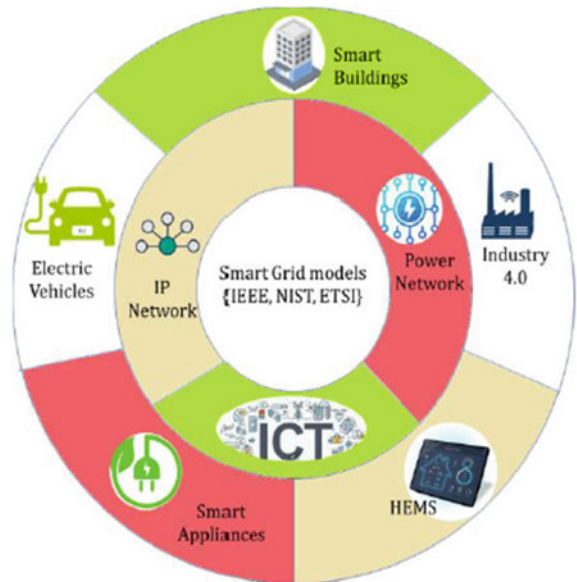


Fig. 5 Interoperability smart grid concepts (“system of systems” approach) [23]

Fig. 6 Smart grid infrastructural components



## 4 Moving from a Syntactic to a Semantic Level of Interoperability

Automation and home automation have made the power grid evolve while keeping it at a syntactic level of interoperability in both the energy supply and consumption sectors. However, the implementation of artificial intelligence at the level of the Internet of Things layer applied to the power grid moves the grid from an operational syntax level to a semantic level. The latter focuses on the support of data and communication structures of systems composed of energy sources on the one hand and those composed of appliances in industry and at home on the other. Since the semantic level of interoperability allows for a high degree of flexibility on both sides, there is a lot of work to be done by experts and standardization organizations in the field of standardization of protocols, interfaces, and infrastructures. On the household energy management side, for a given energy and power profile, it is important that intelligence is implemented at the appliance and device level as well as at the network equipment level. Thus, IoT allows for complete management of the production and consumption ecosystem as highlighted in [24]. Ultimately, there are three data models to be expected: the energy data model, the appliance model, and the network device model.

The European industry associations E@H (Energy at Home) [25] and EEBUS [13], put together two data models which served as enablers for ETSI to produce a standard energy ontology known as SAREF4ENER [24]. In a decentralized and distributed approach to electrical energy, this ontology had the role of enabling E@H and EEBUS customers to achieve efficient and economical energy management at the end-user level. This has resulted in a highly sought-after CEM (customer experience management) optimization in both developed and developing countries.

## 5 Exploring SAREF4ENER Ontology for African Smart Grids

SAREF4ENER is a smart grid standard accepted and published by ETSI in the Energy domain. It is one of the Energy Domain Framework Extensions of SAREF Ontology. From the joint work of E@H and EEBUS [13], respectively the German and Italian industry associations, a vision for the development of renewable energies on the one hand and IoT on the other in the electricity network [24] is derived. In fact, already in the case of households, artificial intelligence applied to the home use of electrical energy begins with the semantic character of this use in the context of IoT and Ontologies. Two two-way communication systems are then put into practice between Demand-Side Management (DSM), and Distribution Management. The latter includes Bulk Generation and Distributed Generation (Non-Bulk Generation) which basically includes the use of RES or DERs. This requires secure data transmission in both communication paths.

Europe's experience with the SAREF4ENER ontology, following SAFEF4EE, has shown that semantic energy management is centered around the decentralized character of energy generation and distribution at commercial, industrial, and residential levels, bringing more flexibility to the management, generation, use, and sale of energy. The interconnection and interoperability of grids and microgrids achieved by the intelligence that ontologies bring to the power grid mean that the Internet of Energy is an unavoidable necessity in the SG of today. The use of DERs consisting of renewable energy sources offers multiple advantages, including higher supply reliability for consumers, resiliency, better power quality (lower line losses), lower costs, and lower environmental emissions [26]. Managing consumption and access to reliable, efficient, and resilient energy is a major challenge on the demand side. It is this side that has interested in the work on extending the SAFEF Ontology energy or its standardization into SAFEF4ENER to support European initiatives on energy use and production. Becoming an ETSI standard, SAREF formalizes in OWL (Web Ontology Language) the "Energy Profile" concept. This was developed by the Zigbee alliance to represent the energy consumption of devices over time [12].

Indeed, as stated earlier, the SAREF4ENER ontology was born from the development of the SAFER4EE ontology, the first ontology allowing the communication and exchange of the two data models coming respectively from the EEBUS and E@H products and extension of SAREF ontology which is the heart of it. With the E@H data model [11, 25] being represented in UML diagrams and the EEBUS data model depicted in XML Schema Definition (XSD) specification, it was necessary to find an intermediary data model that could allow an IoT network to communicate between the E@H DER entities on the one hand and the EEBUS devices on the other hand. Thus, their common EEBUS & E@H model (UML + XSDs) became OWL. There is a transformation from UML to OWL and XSD to OWL. The transformation of the UML data model of E@H and XSD of EEBUS into OWL resulted in two separate ontologies intermediate to SAREF4ENER, a single ontology for a common OWL model. This SAREF4ENER development is followed by SAREF4EE ontology and SAREF itself which is at its core. SAFEF4ENER became an ontology of E@H and EEBUS in the energy domain and an extension of the SAREF ontology at its core. A bottom-up and top-down approach used to create the SAREF4ENER ontology is described and schematized in the technical specification ETSI TS 103 410-1 V1.1.2 (2020-05) [27] and presented in Fig. 7. The image depicts a transformation from a syntactic to a semantic model. It should be noted that SAREF4ENER focuses on offering the CEM for energy optimization in consumption as well as in production [27, 28].

When addressing the semantic domain of the smart grid, the management of both the intelligent data model and the intelligent architecture model must be considered. The data model is based on ontologies, while the architecture model is based on M2M logic (as documented in ETSI [27, 29]). The SAREF4ENER ontology is an OWL-DL ontology that extends SAREF with 63 classes, 17 object properties, and 40 datatype properties, these are illustrated in the overview presented in Figure, adopted from ETSI TS 103 410-1 V1.1.1 (2017-01) []. The SAFER4ENER



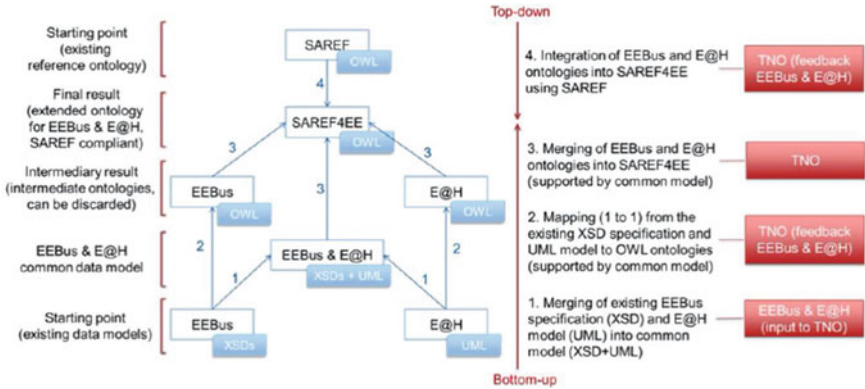


Fig. 7 Transforming SAREF ontology into SAREF4ENER [27]

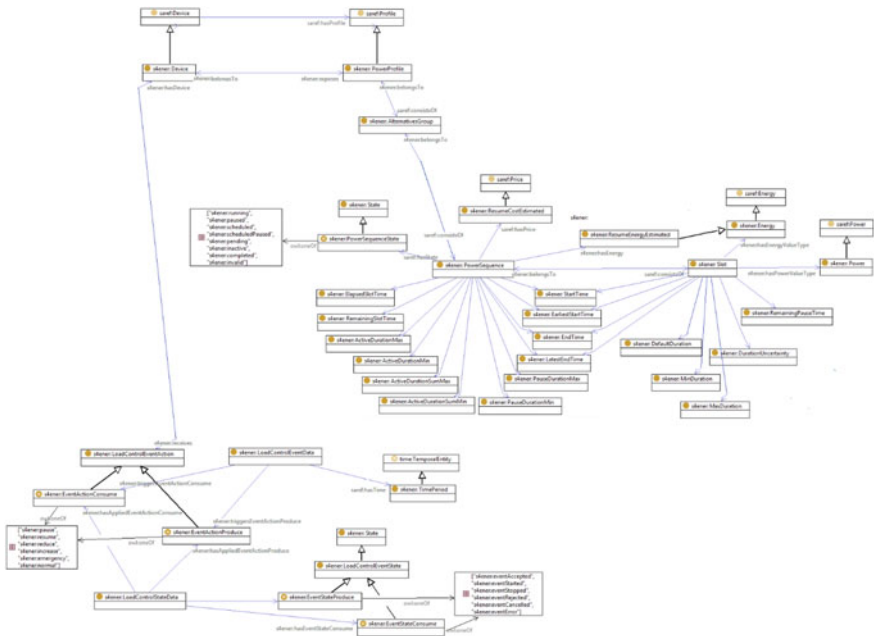


Fig. 8 An overview of the SAREF4ENER Ontology [27]

ontology not only allows for interoperability of energy sources or load management of devices and machines but also acts as a gateway allowing smart appliances or machines to communicate with each other and with energy sources. The gateway allows appliances from different manufacturers can exchange messages, by interpreting or mapping between specific protocols of choice [27].

Concepts such as the power profile of the device or energy source, the time and sequence of operation, the cost of energy, etc. have been formally exploited. By reusing these concepts and their relationships, their inherent advantages can also be leveraged. The SAREF4ENER ontology has the following home-use energy sub-domains: device, source alternatives, the power demanded or supplied, power sequences, and power or operating time. It takes into account that devices or machines are intelligent and can all be connected in a computer network in a private area network at the home or (Home Area Network (HAN) or the Home Network (HN) in IoT terms). The semantic model of the data is constituted by the energy management ontology being housed in the local network or in the Cloud [27].

## 6 Suitable Models and Ontologies for African Smart Grids

The biggest energy challenge in developing countries, especially in Africa, is the inadequacy of electricity supply resulting in incessant load shedding. Many of the conventional electricity-generating utilities in developing countries produce and supply little energy to industrial, commercial, and residential users. This implies that it is difficult to envisage today an inter-grid electricity market between countries as is the case in Europe or in other continents where the smart grid is already operational. Figure 9 is a depiction of what the ideal SG electricity network envisaged for developing countries should look like. Unfortunately, this is not the case, as each element remains in isolation with little or no communication between them.

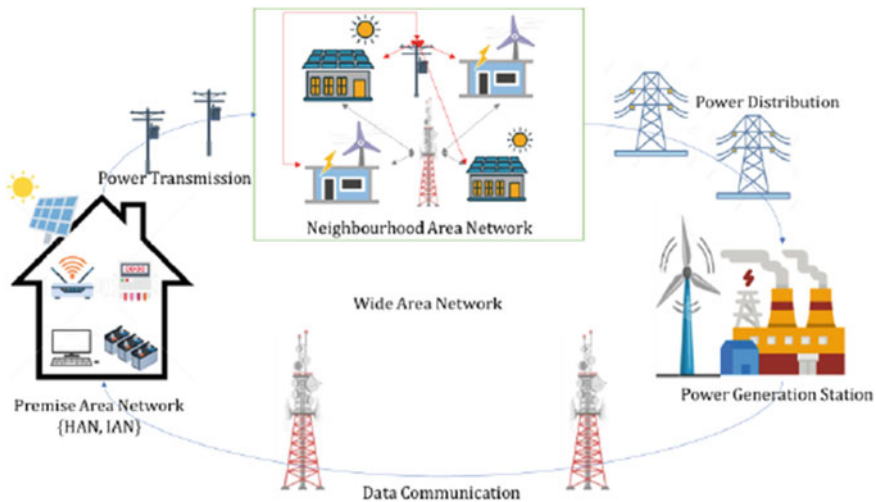


Fig. 9 Interconnected elements in an ideal SG electricity network

Based on our survey and experience in villages in DR Congo (DRC), it is difficult to envisage in the next ten years a smart grid demonstration in which energy and telecommunication networks between neighboring countries are interconnected and interoperable for the sale of energy. It is difficult to envisage this because, in these remote locations, DERs and ESS are barely in existence. Numerous households still live below the poverty line and the digital divide is extremely wide. Concepts such as the Internet of Things, smart appliances, and interoperability in the IoT world as outlined in [24] are still foreign to most of the populace. In the current electricity network infrastructure in many parts of DRC or other developing countries, bi-directional (top-down and bottom-up) energy does not exist, rather only the top-down model is in play.

The reverse is the case in urban areas and cities of DRC. Industrialization and Internet penetration is higher in these cities, as such, there is potential for the bottom-up approach. However, to actualize this bottom-up approach, three layers of development must be achieved. At the lowest layer, the development of DERs must be prioritized. This involves a decentralized energy supply structure, coupled with bulk power distribution and energy storage resources. With the abundance and accessibility of solar energy in countries such as DRC, this can be achieved. DERs can easily be developed from photovoltaic and battery energy storage.

The second layer involves installing smarter and energy-conserving appliances. These would lay the foundation for the establishment of IoT-based communication and interoperability protocols. At the third layer, the development of data models for home energy networks and connected appliances takes place. It is only at this stage that ontologies can be considered. Figure 10 gives a visual depiction of our proposed framework of progression towards the smart grid. Being a framework proposed for launching smart grids in development contexts, it would be transitional and might take a few years to achieve.

Once the framework is in place, parts of the E@H and EEBUS data model, SAREF4ENER, can be copied and reused in Africa. The SAREF4ENER is ideal because it is already standardized and has been shown to work in parts of Europe. However, full implementation of an African SG model might not be feasible until the entire 7–9 domains (from the NIST, ETSI or IEEE contextualized models) are implemented.

In conclusion, addressing the electricity challenge in developing nations is a vital step in moving them to the era of the 4th industrial revolution. Smart grids, coupled with intelligent management of electrical energy from renewable sources [30] can be a vital steppingstone to actualizing this, while simultaneously building an eco-friendly environment.

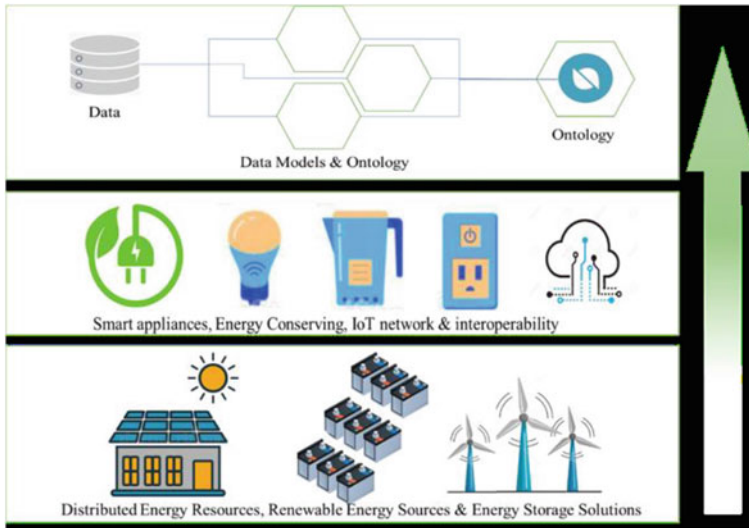


**Fig. 10** Framework for building SGs in an African context

## References

1. Ayele Eshete, G.: Semantic description of IoT security for smart grid, Thesis master, University of Agder/Faculty of Engineering and Science Department of Information and Communication Technology (2017)
2. A. Tang Yee Chong, A., et LIM, F.-C.: Description for smart grid: towards the ontological approach. 2020 8th Intl. Conf. on Information Techn. and Multimedia (ICIMU), pp. 218–222 (2020)
3. Uslar, M., Specht, M., Rohjans, S., Trefke, J. Vasquez Gonzalez, J.M.: The common information model CIM. IEC 61968/61970 and 62325 – A Practical Introduction to the CIM. Verlag Berlin Heidelberg: Springer (2012)
4. Schumilin, A., Duepmeier, C., Stucky, K.-U., Hagenmeyer, V. et al.: A consistent view of the smart grid: bridging the gap between IEC CIM and IEC 61850. 44th Euromicro Conf. on Software Engineering and Advanced Applications, pp. 321–325 (2018)
5. Dogdu, E., Ozbayoglu, A.M., Benli, O., Akinç, H.E., Erol, E.: Ontology-centric data modelling and decision support in smart grid applications a distribution service operator perspective. 2014 Intl. Conf. on Intelligent Energy and Power Systems (IEPS), pp. 198–204 (2014)
6. Haghgoo, M., Sychev, I., Monti, A., Fitzek, F.H.P.: Sargon – smart energy domain ontology. IET Smart Cities, vol. 2, no 4, pp. 191–198 (2020) [Online]. Available from: [www.ietdl.org](http://www.ietdl.org)
7. Salameh, K., Chbeir, R., Camblong, H.: SSG: an ontology-based information model for smart grids. Germany, pp. 94–124 (2019)
8. Laura, D., den Hartog, F., Roes, J.: Created in close interaction with the industry: the smart appliances reference (SAREF) ontology. Springer International Publishing, Switzerland, pp. 100–112 (2015)
9. Santodomingo, R., Rohjans, S., Uslar, M., Rodriguez-Mondejar, J.A., Sanz-Bobi, M.A.: Ontology matching system for future energy smart grids. Engineering Applications of Artificial Intelligence, pp. 242–254 (2014)
10. Cuenca, J., Larrinaga, F., Curry, E.: A unified semantic ontology for energy management applications. Conference: 2nd International Workshop on Ontology Modularity, Contextuality, and Evolution

11. Laura, D.: Energy, smart homes & smart grids: towards interoperability for demand side flexibility using Saref and Saref4ener. Semantics/Amsterdam (2017) Available from: <https://2021-eu.semantics.cc/energy-smart-homes-smart-grids-towards-interoperability-demand-side-flexibility-using-saref-and>
12. Laura, D.: SAREF and SAREF4EE: Towards interoperability for smart appliances in the IoT world (2016). Accessed on: 25 October 2021. [Online]. Available from: <https://2021-eu.semantics.cc/users/laura-daniele>
13. EEBUS, What is EEBUS. [Online]. Available from: <https://www.eebus.org/what-is-eebus/>
14. Kabalci, E., Kabalci, Y.: Introduction to smart grid architecture, in Smart Grids and Their Communication Systems, Springer (2019)
15. Kabalci, Y.: A survey on smart metering and smart grid communication, pp. 302–318 (2016)
16. J. RIFKIN, « Créer un Internet de l'énergie ». Liberation. Accessed on: 13 January 2022. [Online]. Available from: [https://www.liberation.fr/futurs/2013/02/24/jeremy-rifkin-creer-un-internet-de-l-energie\\_884213/](https://www.liberation.fr/futurs/2013/02/24/jeremy-rifkin-creer-un-internet-de-l-energie_884213/)
17. Rifkin, J.: The third industrial revolution: how lateral power is transforming energy, the economy, and the world. Palgrave Macmillan (2013)
18. NIST, NIST Framework and Roadmap for Smart Grid Interoperability Standards, Release 1.0. (2010)
19. CEN-CENELEC-ETSI, CEN-CENELEC-ETSI Smart Grid Coordination Group Smart Grid Reference Architecture. 2012. Consulté le: 20 février (2022). Accessed: 20 February 2022. [Online]. Available from: [https://www.cencenelec.eu/media/CEN-CENELEC/AreasOfWork/CEN-CENELEC\\_Topics/Smart%20Grids%20and%20Meters/Smart%20Grids/reference\\_architecture\\_smartgrids.pdf](https://www.cencenelec.eu/media/CEN-CENELEC/AreasOfWork/CEN-CENELEC_Topics/Smart%20Grids%20and%20Meters/Smart%20Grids/reference_architecture_smartgrids.pdf)
20. IEEE Smartgrid: IEEE Smart Grid Domains & Sub-domains
21. Commission Européenne, M/490. Mandat pour un réseau intelligent (2011)
22. Gosptein, A., Nguyen, C., O'Fallon, C., Wollman, D.: NIST Framework and Roadmap for Smart Grid Interoperability Standards, Release 4.0 (2020)
23. Bosso, T., Deblasio, R.: IEEE Smart Grid Series of Standards IEEE 2030 (Interoperability) and IEEE 1547 (Interconnection) Status », NREL (2011)
24. Laura, D., Solanki, M., Den Hartog, F., Roes, J.: Interoperability for smart appliances in the IoT world, Springer International Publishing, pp. 21–29 (2016)
25. Energy@home: Energy@home Data Model. (2015)
26. Parhizi, S., Lotfi, H., Khodaei, A., Bahramirad, S.: State of the art in research on microgrids: a review. IEEE (2015). [Online]. Available from: <https://ieeexplore.ieee.org/document/7120901>
27. ETSI TS 103 410–1 V1.1.2 (2020–05). SmartM2M; Extension to SAREF; Part 1: Energy Domain (2020)
28. TNO: Ontology <https://w3id.org/saref4ener>. [Online]. Available from: Ontology <https://w3id.org/saref4ener>
29. ETSI TS 103 410–1 V1.1.1 (2017–01): [Online]. Available from: [https://www.etsi.org/deliver/etsi\\_ts/103400\\_103499/10341001/01.01.01\\_60/ts\\_10341001v010101.pdf](https://www.etsi.org/deliver/etsi_ts/103400_103499/10341001/01.01.01_60/ts_10341001v010101.pdf)
30. Yang, Q. et al.: Energy management system for renewable distributed generation and energy storage. in Smart Grids and Their Communication Systems, Springer (2019)

# Smart Micro-Grid Energy Management with Renewable Energy Sources and Local SCADA



J. Karra and K. Chandrasekhar

**Abstract** Smart self-sufficient microgrids in apartments are grabbing the researcher's interest. Smart microgrid key design components are distributed energy generation, storage, and intelligent communication. This paper presents smart microgrid energy management with inbuilt local grid operations through local SCADA by incorporating the best possible renewable energy resources as well as storage systems in an apartment building. This system is designed without any additional operational cost to the individual consumer. It helps consumers in earning revenue with the supply of excess power to the main grid and supports the main grid in peak-hour load distribution. This smart microgrid protects the local system from grid disturbances as well as poor voltage regulation and radial HT feeder breakdowns, interruptions, and stabilizing the island grids/Remote army grids or grid outages with available resources & modern storage systems (i.e. EVs).

**Keywords** Smart grid · Microgrid · PV Solar · EV battery storage · Local SCADA

## 1 Introduction

Day by day the existing fossil fuels in particular coal gas etc. are exhausting and at the same time, energy demand is increasing. The penetration of renewable energy sources like PV solar, wind, and biomass are remarkably increasing in the grid garbing its share from fossil fuels. The traditional grids became inefficient, congested in terms of load balancing, and incapable of meeting future demand. The Smart grid concept was introduced for better grid operations incorporating the available renewable energy sources generation at load centers, to minimize the transmission line losses, for better voltage regulation at the consumer end [1]. The Indian government is encouraging renewable energy sources to minimize carbon emissions by providing a 40% subsidy

---

J. Karra · K. Chandrasekhar (✉)

Electrical & Electronics Engineering Department, Acharya Nagarjuna University, R.V.R. & J.C. College of Engineering, Chowdavaram, India  
e-mail: [cskoritala@gmail.com](mailto:cskoritala@gmail.com)

on PV solar panels along with total equipment hence hybrid renewable energy sources contribution is increased up to 20% of the total energy during the year 2019–20. The smart grid implementation is at the infant stage in India due to insufficient budget allocation to the PSUs and the use of ICT is not significant. However, the major obstacles in the smart grid implementation can be overcome through local SCADA in balancing the state grid every day in 24 h cycle with hybrid energy sources.

The generated power from renewable or non-renewable sources is to be delivered to the consumer efficiently. Here comes the role of smart grids that are basically used for the transmission of electricity. The traditional grids provide one-way communication, that is from the plants to the consumers, and which leads to the loss of energy. But a smart grid provides two-way communication, from plants to consumers and from consumers to plants, making sure of reducing the losses. The Smart Grid is a system of networked utility and consumer devices, through technologies that ensure secure, reliable, and efficient production, delivery, and consumption of energy [2]. To implement this smart grid effectively a microgrid concept was developed to meet the small individual demands at the local level with their contribution in terms of equipment and area to reduce the burden on the grid and make the microgrid owners' stakeholders in the power business market so as to accelerate the mission.

This smart microgrid is an intelligent power distribution network, operating at or below 11 kV, in order to provide uninterrupted supply to an isolated area of the community. For effective utilization, advanced sensing, communication, and control technologies are to be used to generate, manage, and distribute power. The power generated by renewable generation sources such as PV solar, micro hydel power generation units, windmills, biomass, and small conventional diesel generator sets, in combination with each other form hybrid microgrids. Basically, this hybrid microgrid concept is designed for providing power supply to the localized loads through the conventional utility grid or into the isolated islands only. The microgrid concept was successfully implemented in many countries other than India particularly on the radial network at tail-end villages, mini-army remote training bases/camps. In India, rural electrification corporation is providing switching capacitor banks in 33 and 11 kV networks for tail-end voltage regulation. In urban cities/towns of India, microgrids are rapidly growing with rooftop PV solar arrangements with government incentives/subsidies especially in apartment buildings and in gated communities. Nowadays this arrangement is made mandatory in urban areas during the construction of the apartment building (group housing) and all common auxiliary loads are to be kept on it. In this paper, we propose a smart microgrid energy management system and analyze its economics using HOMER Grid software.

Section 2 describes the literature on useful concepts used in the design of our system. Section 3 describes our proposed smart microgrid energy management system in an apartment building with details on its economical operative cost savings. In Sect. 4 the working of the Intelligent Charging Inverter Controlling Metering System used in our system in intelligent grid controlling is explained and briefs our smart microgrid system simulation results in Homer Grid software.

## 2 Literature Review

Some of the related works done related to the design of microgrids used for design, cost analysis, and efficient communication in establishing local SCADA in our proposed system is presented here. Akhil Nigam et al. used advanced metering infrastructure [AMI] comprising of collection, storing, and energy usage data as part of a smart grid. AMI transfers data from the smart meter to the utility consumer [3]. Puja et al. used the Availability Based Tariff (ABT) concept in the conventional power grid to support the locally generated power from RES to be utilized for consumer loads or even excess power can be fed back to the grid to earn financial benefits [4]. Gehlot et al. [2] applied digital processing and communications to the power grid, making data and power flow bidirectional. They proposed the upgradation of a Smart Grid using three key components Distribution Automation (DA), Personal Energy Management (PEM), and Advanced Metering Infrastructure (AMI) to bring revolutionary changes in electrical networks. Jangaiah et al. [5] dealt with the design and performance analysis of a simple Microgrid in the apartments with HOMER GRID software. They proposed an Energy Management System based on finding the optimal operating strategies to minimize energy costs and carbon emissions with renewable energy resources. Habib et al. proposed smart grid management with wireless communication simulated using MATLAB Simulink in two cases of operation On and OFF-Grid Systems and showed its indispensability in the energy control and management in the Smart Grid [6].

## 3 Proposed Smart Microgrid

### 3.1 *Smart Micro Grid Energy Management System of an Apartment*

The proposed smart microgrid energy management system in an Apartment building with a conceptual block diagram is shown in Fig. 1.

Various components of smart micro grid with PV Solar and EV battery storage systems in an apartment building shown in Fig. 1 are explained as follows.

- a. PV Solar panels on the rooftop of an apartment block are connected to Automatic Integrated Control System (AICS) through a solar energy meter (SEM). All the residential flats are connected to AICS through bi-directional energy meters with smart home loads.
- b. All the common auxiliary loads (i.e., lifts, groundwater pumping, common corridor and cellar lighting, solar security system, and fire and safety systems, etc.) in the apartment are connected through an energy meter to the AICS.
- c. All Electric Vehicles (EVs) considering 4 wheelers charging through Intelligent Charging Inverter Controlling Metering (ICICM) are connected to a microgrid



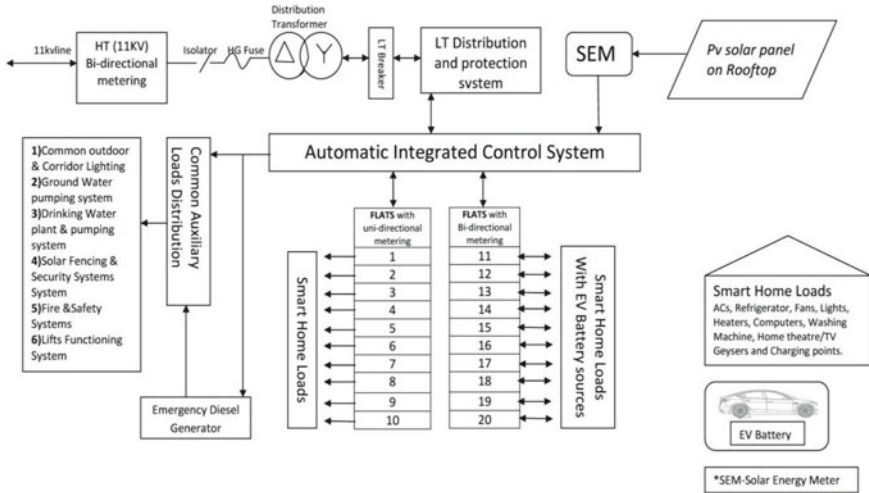


**Fig. 1** Block diagram of smart micro grid energy management system in an apartment building

at parking places. The ICICM Consists of an Inverter and Converter circuit, an Energy Import and Export Meter, and a Battery Management System.

- d. Basic input supply is an 11 kV line, connected to HT bi-directional energy metering cubicle/equipment.
- e. The Distribution Transformer (DTR) is having Isolator & HG Fuse on the 11 kV side and an LT Breaker, LT distribution, and protection system on the LT side. Emergency diesel Generator is provided in case of grid blackout or AICS failure.
- f. Electric vehicle’s battery is taken as a storage source for the system through ICICM connected to a Bi-directional Energy meter.

The sales statistics of electric vehicles (cars) in India are as shown in Table 1. Their battery capacity varies based on the Model/Cost/Brand of the vehicles. In this paper, the design of the microgrid considered is optimized by assuming unequal capacities of battery sources and different charging and discharging timings. The Indian government is gradually insisting that all vehicle manufacturers in India switch over to electric vehicles from fossil fuel vehicles by 2025. Hence many manufacturers are on the racetrack to produce economically feasible vehicles getting a subsidy of 2 lakhs per vehicle.

**Table 1** Electric vehicle sales in India by some branded companies

Rank	Brand/model	April–October 2019 sales	Monthly average sales	Battery capacity/max life (Kwh/8 Years)
1	Mahindra Verito EV	434	62	21.2
2	Tata Tigor	389	56	21.5
3	Hyundai Kona (June' 19 onwards)	227	45	39.2
4	Mahindra E20	21	3	16

### 3.2 Proposed Micro-Grid Schematic Diagram with Its SCADA Functions

The proposed Smart Micro Grid arrangement with PV Solar & EV’s battery storage system schematic diagram is shown in the Fig. 2 and its working is explained as follows.

The generated solar energy from PV Solar panels erected on apartment roofs during the daytime meets the demand of all the residential flats and common auxiliaries’ loads. The excess energy available is sent out through AICS to the main grid. The utilized energy of the individual flats during daytime including home loads and EV charging is metered through a bi-directional/unidirectional meter as shown in Fig. 2. The unutilized energy is sent out through AICS as excess power to the grid. If

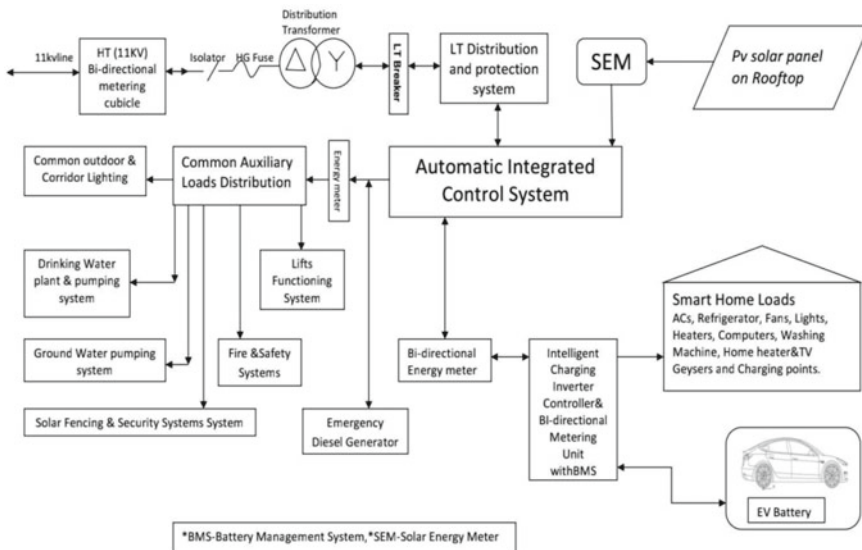


**Fig. 2** Schematic diagram of Smart Micro Grid energy management system in an apartment building with PV Solar and EV battery storage systems

the PV Solar power generation reduces due to clouds, the AICS will take overloads of flats through the grid as per their demand. This separate control logic programme (loading and unloading) is incorporated in AICS for each consumer to get the most benefit.

In India as per the power demand in 24 h cycle, an energy peak hour distribution is classified as (i) Night Peak Hours (18.00–22.00 h) during which all the commercial, and domestic loads get added to the grid in addition to industry & office loads. (ii) Night Off Peak Hours (22.00–06.00 h) during which the 3rd shift of some industries continues as load and all the commercial and major domestic loads get detached from the grid. During these hours excess power from base load plants is transferred to hydel stations for the water reverse pumping system. (iii) Day Peak Hours (06.00–10.00 h) during which all the drinking water pumping schemes and industries (iv) Day off Peak Hours (10.00–18.00 h) with only Industries and offices loads).

In India, we don't have frequency/hourly-based tariffs to the domestic LT consumer level but Availability Based Tariffs in terms of 96-time blocks are applied to the state grids or distribution companies. Table 2 describes various home loads and operating loads during different peak hours. Consider loads of apartments implementing the smart microgrid concept located/situated at the tail end of the 11 kV radial feeder. During peak hours increase in load causes voltage drop and fluctuation in frequency and hence regulation becomes difficult with respect to the state grid. To overcome this technically switching capacitor banks should be provided which is a costly affair for the organization and domestic consumers. In the proposed system the controller (AICS) takes over this functionality of regulating voltage and frequency and it virtually acts as a grid controller i.e., Importing the power/Exporting the power, to the grid from existing available ELECTRIC VEHICLES batteries (considering each car has minimum 20 kWh battery contribution goes to  $20 \text{ kWh} \times 10 \text{ flats} = 200 \text{ kWh}$ ) acts as a source during this peak hour. Generally, each flat/house consists of operating loads from 2 to 5kW load maximum during a particular session. It can be easily fed by the Electric Vehicle battery, even though the solar energy reduces slowly in the evening when peak hour starts to the grid. During off-peak hours i.e., 22.00–06.00 h, the Electric vehicle battery/s connected to the system (our smart microgrid) will be charged from the grid supply. After morning Peak hours, the generation of PV Solar energy increases gradually and can meet the needs of the total apartment block. Hence renewable energy and storage systems are utilized properly in 24 h cycles with the grid support in operating our microgrid technically. Thus, the ICICM concept enhances the quality of the system and is economically beneficial.

Considering one flat/villa consumption having an electric vehicle (Storage) and PV Solar panel (RES) the economical savings calculations are shown in Table 3.

ICICM is a 1st stage of supervision and mini controller between AICS and electric power-driven vehicles along with smart home loads. It manages the 1st step of the application of smart home loads, taken into the consideration with respect to the battery status as well as 24 h. cycle the basic functions will be initiated with the coordination of the AMICS. It deals with economically intelligent charging and discharging strategies of the connected batteries treated as storage systems, to bring the title into reality. The basic function of ICICM is explained with the help of

**Table 2** General and operative home loads during different peak hours

Acs 1000 w/ each	Gyea 1500 W/each	Heaters 1000 W/ each	Home theater	TV 100 W/each	Washing machine 600 W/each	Mixer/ grinder 500 W/ each	Refrigerator 250 W/each	Fans 40 W/each	Lights 10 W/each	E-Fans 20 W/ each	CPU/laptops 50 W/each	Plug points 10 W/each
<i>General home loads in one flat</i>												
4 Nos	3 Nos	3 Nos	1 No	2 Nos	1 No	1 No	1 No	10 Nos	30 Nos	4 Nos	2 Nos	10 Nos
4000	4500	3000	150	200	600	500	250	400	300	80	100	100
Total installed loads 14,180 W												
<i>Operating home loads</i>												
Night peak hour loads												
(18.00–22.00 Hrs)												
ACs	Lights	Fans	Refrigerator	Home theater	Operating loads	ACs	Lights	Fans	Refrigerator	Operating loads		
1 No	10 Nos	2 Nos	1 No	1 No		2 Nos	5 Nos	2 Nos	1 No			
1000	200	80	250	150	1680 W	2000	50	80	250	2380 W		
Day peak hours loads												
Day off peak hours loads												
06–10 Hrs.												
Lights	Fans	Refrigerator	TV	Mixer/ grinder	Operating loads	ACs	Lights	Fans	Refrigerator	Home theater	Washing machine	Operating loads
3 Nos	1 No	1 No	1 No	1 No		1 No	2 Nos	2 Nos	1 No	1 No	1 No	
30	40	40	100	500	920 W	1000	20	80	600	150	2100 W	

**Table 3** Power consumption and savings in billing with and without PV Solar and EV battery storage systems

SI. No	Period	Flat load in watts	With grid only supply consumption/day	PV solar panel consumption/day	With EVs (car) battery storage consumption/day	With EVs (car) battery storage consumption/day (holiday)
1	Day peak Hrs. (4)	920	$920 \times 4 \text{ h} = 3680$	$920 \times 4 \text{ h} = 1840$	$920 \times 4 \text{ h} = 18 \times 1840$	$920 \times 4 \text{ h} = 1840$
2	Day off peak Hrs. (8)	2100	$2100 \times 8 \text{ h} = 16,800$	$2100 \times 8 \text{ h} = 16,800$	–	–
3	Night off peak Hrs. (4)	1680	$1680 \times 4 \text{ h} = 6720$	–	$1680 \times 4 \text{ h} = 6720$	$1680 \times 4 \text{ h} = 6720$
4	Night off peak Hrs. (8)	2380	$2380 \times 8 \text{ h} = 19,040$	–	$2380 \times 6 \text{ h} = 14,280$	$2380 \times 6 \text{ h} = 14,280$
5	Total units		42.240	18.640	22.840	22.840
6	Monthly consumption/flat		1387.2 units (30 days)	484.64 units (26 days)	593.84 units (26 days)	91.36 units (4 holidays)
7	HT Billing Rs 8.00/unit		Rs.11097.60	Rs.3877.12	Rs. 4750.72	Rs. 730.88
			Rs.10667.56	Sub-total Rs	8996.05 Net payment	Rs. 1738.88
8	LT Billing Rs7.69/unit			Rs. 3726.88	Rs. 4566.62	Rs. 702.55
				Sub-total Rs	8996.05 Net payment	Rs. 1671.51

a flowchart. It operates by balancing the priority of the application of the source (Battery of a power-driven vehicle) and load simultaneously. Intelligent Charging Inverter Controller & Bi-directional Metering Unit (ICICM) is a unique charging kit, that consists of an Inverter/Converter with a protection system, Bi-directional metering equipment, Battery management system, and Charging socket AC 3 phase 433 V (Boost/Trickle).

- (a) **Inverter/Converter with protection system:** The basic function of inverter/converter is to convert DC to AC and AC to DC, which enables the function during peak hours with an existing Electric Vehicle Battery as source i.e., minimum of 20 kWh capacity of each flat. Considering 10 flats it can be built as a big source of the capacity of 200 kWh that can operate for a period of 4 h during Night Peak Hours and can cater as per the demand. During Night Off Peak hours, it performs the function of a converter which acts as a battery charging circuit depending on the rapid/slow charging of the EV as per the manufacturer's design. The protection system is designed as follows. Protection in inverter and converter control circuit for catering to home loads and regulating charging and discharging the battery. It allows maximum charging up to 90–100% as per manufacturer design and discharging is limited to 40%. It protects the system by tripping and thereby isolating from any faults (within

ICICM and from the home loads charging circuit of the car) or overloading or short circuits of the system.

- (b) **Bi-directional metering equipment:** In 24 h cycle, the function of this meter is to record the import (consumed) and export (generated) units, i.e., during Night Off Peak hours starts the charging of the battery in the Electric Vehicle till it gets fully charged (90–100% depending upon manufacturer’s specifications). The total units consumed during charging; the total units supplied to the microgrid are being recorded. This is also useful in the calculation of battery economics in its lifetime (5–8 years) by calculating battery life cycles in terms number of units consumed for charging and the number of units discharged to the grid.
- (c) **Battery management system:** When connected to the charging point at the car parking, it checks the healthiness of the battery as well as no faulty circuits in the system, then it switches to the state of charge % i.e., prediction of the available charge in Electric Vehicle’s (EV) battery in its capacity in the control time-step for the Vehicle to Grid (V2G) service. The assessment is made by the software available in ICICM in terms of the number of kilometers that can run further with available charge, balance charge available in battery, ready for V2G service, or badly need the charging. The status will be intimated through the registered cell of the owner. Consumer choice gets executed as shown in Table 4 as per the requirement given by him. This methodology benefits in the reduction of charge/discharge cycles, ultimately increasing the battery life (Fig. 3).

In this circuit the existing intelligent charger ensures the electric vehicle battery voltage, temperature, and time under charge to determine the optimum charge current and charging termination by adopting a suitable charging mode i.e., boost/trickle charging depending upon requirement with respect 24 h cycle when it is connected to ICICM the status would be communicated to the registered cell of the owner.

Homer Grid software is used to simulate micro grid-connected solar, wind, and storage systems, with or without the ability to operate independently from the grid [7]. The operational loads of an apartment flat explained in Table 2 are used in the simulation From Fig. 4, it can be observed that during the day times energy source from PV solar plates is producing maximum power and is consumed by the loads. It can also be observed that very less or no energy is consumed from the external main grid connected. The plots in green color show the charging status of the battery storage device and it is clear that around 70% of the daytime is fully charged.

## 4 Conclusion

Previous microgrid research work published the organization and controlling was complex with regard to the EVs battery charging and discharging like controlled, uncontrolled, multistage depending upon the capacity of the battery [8]. In this chapter, the simple and intelligent energy management system was proposed, and it

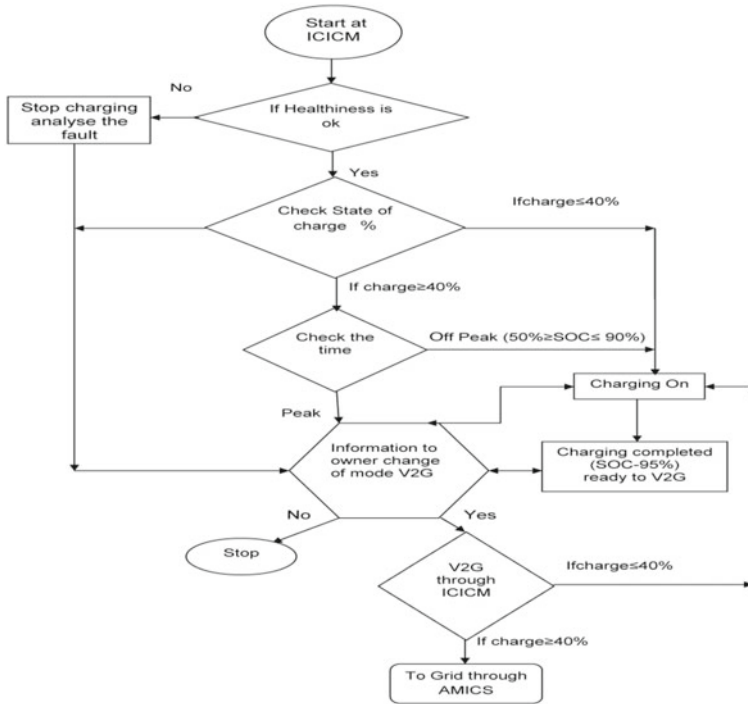


**Fig. 3** Flowchart communicating the EV’s Owner with ICICM and AMICS

**Table 4** Operational states of ICICM

Parameters	Initial status	Command	Final status
Healthiness check	Ok	Check	Ok
State of charge%	%	On/off	% Completed (at 95% auto cut off
No. of km can run	km	km	km
Trickle (w.r.t.SOC)	Minutes	On/off	Completed/not completed
Boost charging time (w.r.t.SOC)	Minutes	On/off	Completed/not completed
Vehicle to grid (Restricted to 40%)	Available	On/off	Completed/not completed

is shown that adopting local SCADA in Micro Grid makes the system smart and efficient. It helps in operating the microgrid in V2G, G2V, Solar to Vehicle, and protects the microgrid from the failure of the radial feeder from the main grid or incoming supply breakdown due to natural disasters. In addition to this local SCADA, the proposed system monitors the gas metering, water metering, final billing calculation per individual, etc. Thus, we emphasize that the smart microgrids are more reliable

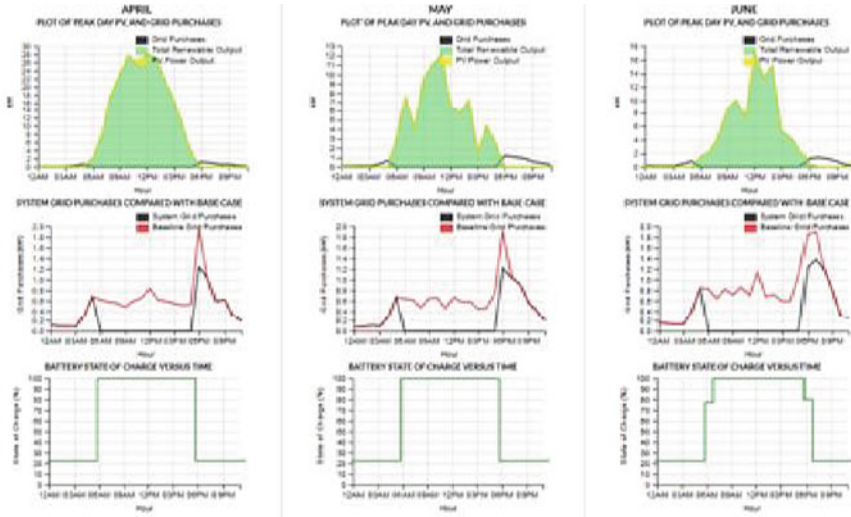


**Fig. 4** Peak Day PV (green), consumption from PV sources (red) and main grid (black), and Storage levels of ESS

in all aspects i.e., voltage and frequency control, in addition, to increase in the grid stability.

## References

1. Jha, S., Kumar, S.R.: Smart grid development in India—a case study. In: 2014 Eighteenth National Power Systems Conference (NPSC), Guwahati, 1–6 (2014)
2. Gehlot, V., Parihar, R.: Smart Grid: the future Grid of India. *Int. J. Eng. Res. Technol.* **4**(12) (2016)
3. Nigam, A., Kaur, I., Sharma, K.K.: Smart grid technology: a review. *Int. J. Recent Technol. Eng. (IJRTE)* **7**(6S4), 243–247 (2019)
4. Mahajan, P.P., Parate, P.: Active and reactive power using renewable energy sources. *IOSR J. Eng.* 31–34 (2019)
5. Jangaiah, K., Chandrasekhar, K.: Performance analysis of microgrid using homer grid for net metering. *J. Adv. Res. Dyn. Control Syst.* **12**(2), 2216–2222 (2019)
6. Elkhorchani, H., Grayaa, K.: Smart micro Grid power with wireless communication architecture. In: International Conference on Electrical Sciences and Technologies in Maghreb (CISTEM), Tunis, pp. 1–10 (2014)
7. Mehta, S., Basak, P.: A case study on PV assisted microgrid using HOMER Pro for variation of solar irradiance affecting cost of energy. In: 2020 IEEE 9th Power India International Conference (PIICON) SONEPAT, India, pp. 1–6 (2020)
8. Agarwal, Y., Weng, T., Gupta, R.K.: Understanding the role of buildings in a smart microgrid. In: Design, Automation & Test in Europe, Grenoble, pp. 1–6 (2011)



# Improving Electricity Supply Reliability: A Case Study of Remote Communities of Limpopo in South Africa



Vinny Motjoadi and Pitshou Ntambu Bokoro 

**Abstract** Energy is playing a more fundamental function in human growth and advancement. Many rural households in developing nations, like South Africa, are still lacking access to basic electricity due to being located far away from the national grid and grid expansion to these areas is quite expensive. Fewer rural communities are electrified through the use of diesel and grid systems of which are having a high operating and maintenance cost and are the biggest carbon emissions producers. The deployment of renewable energy sources (RES) based microgrid systems are considered as a more viable approach to supply power to rural communities in the world. RE-based microgrid systems have the greatest potential to meet load demand, improve quality of life and create job opportunities, and provide electricity access for rural communities of SA. In this study, a case study is utilized to design and simulate a suitable grid-tied hybrid microgrid system architecture for rural communities' conditions. The study selected three isolated rural communities (Tjiane, Phosiri, and Malekapane villages) of Ga-Mphahlele in Limpopo province (SA) as case studies, and these communities have similar weather conditions because they are located in close proximity. The unreliable national grid system is the main source of power in these communities while diesel generators (DG) are used as backup system during load shedding. In this study, HOMER software was used to design a grid-tied hybrid microgrid power system of which will help with eradicating system power failure and load shedding from the national grid. Based on the simulation, optimization, and sensitivity analyses results show that the optimal grid-tied microgrid system architecture was proposed based on lower net present cost (NPC), lower cost of energy (COE), a maximum renewable fraction (RF), loss of power supply probability (LPSP), and the optimal system should produce fewer carbon emissions. The achieved results for all examined rural communities show that the optimum microgrid system architecture consists of a grid, solar PV, wind turbine (WT), DG, battery, and power converter is more capable of satisfying customer electricity demand in a dependable approach and provide good power quality. The

---

V. Motjoadi · P. N. Bokoro (✉)

Department of Electrical Engineering Technology, Doornfontein Campus, University of Johannesburg, Johannesburg, South Africa

e-mail: [pitshoub@uj.ac.za](mailto:pitshoub@uj.ac.za); [80203757@student.uj.ac.za](mailto:80203757@student.uj.ac.za)

© The Author(s), under exclusive license to Springer Nature Switzerland AG 2024  
K. Kyamakya and P. N. Bokoro (eds.), *Recent Advances in Energy Systems, Power and Related Smart Technologies*, Studies in Systems, Decision and Control 472,  
[https://doi.org/10.1007/978-3-031-29586-7\\_6](https://doi.org/10.1007/978-3-031-29586-7_6)

135

results showed that Grid/PV/WT/DG/Battery/Converter is a winning hybrid micro-grid system architecture that is more cost-effective and environmentally friendly with NPC of R2.973793; COE of R0.02842 and an RF of 97.8% with total emissions of 58.626 kg/yr for Tjiane, NPC of R1.836202; COE of R0.03092 and an RF of 97.9% with a total emission of 32,888 kg/yr for Phosiri, and NPC of R1.209773; COE of R0.02370 and an RF of 97.9% with total emissions of 28.002 kg/yr for Malekapanane. The proposed Grid/PV/WT/DG/Battery/Converter microgrid is considered the most favorable grid-connected hybrid microgrid system architecture which is a more suitable and reliable electricity supply solution for rural communities. The results showed that sensitivity variables, financial parameters, wind speed, solar irradiations, and diesel price differences have a substantial influence on the optimal design of grid-connected hybrid power systems for rural electrification.

**Keywords** Energy · Renewable energy sources · Microgrid · Homer · Rural communities

## 1 Introduction

Electricity poverty in Africa is still a fundamental issue that is currently dominating and the majority of the people still have no access to basic electricity [1, 2]. The distributed renewable energy systems are electrifying developing countries in a less costly and most rapid approach. In Sub-Saharan African (SSA) nations like Kenya, South Africa (SA), Tanzania, Nigeria, and a few others have already started investing in these renewable-based systems as to achieve and support this remarkable electricity access development [3]. Globally, there are 1.4 billion people who still live disadvantaged of having access to electricity [4, 5], and about 640 million individuals in SSA still have no access to basic electricity [5, 6]. Roughly 80% of them are African rural households where there is no utility grid power [7, 8], and grid expansion is extremely logistically and economically not viable. However, this lack of access to electricity threatens socio-economic activities and growth, energy security, and lastly, it incapacitates the development of these rural communities [6, 9, 10]. Thus far, several governments and utilities are continuing to be unsuccessful in meeting the electricity demand of remote rural homes, as more emphasis is been on achieving the demand of different businesses or extremely occupied urban areas. However, hybrid mini-grids systems are having the potential of providing rural electricity access at a low price. In SA, about 31% of residents are located in the rural remote regions whereby 60% of the households still lack access to basic electricity [11, 12]. However, the South African government (SAG) is sharpening the access to electricity curve to accomplish rural electrification and exterminate the poverty of electricity. South Africa is well-positioned in terms of renewable energy resources (solar, wind, hydrogen, geothermal, etc.) [13, 14]. The country has substantial natural resources and sunny areas, which make it viable for clean energy systems and they could contribute to remedying the electricity crisis. Electricity is a fundamental need for sustainable

development of any country [1, 2, 15], which could be used for poverty eradication, for quality of life improvement, and also for stimulating economic growth and development [16, 17]. The lack of access to clean, cost-effective, and reliable electricity in remote rural communities is a massive challenge of which cannot be ignored [17–19]. As a result of this, conventional systems have become unsustainable and unable to meet electricity demand [20]. It is economically unsustainable for power utilities to extend their grid to these communities given the high level of unemployment, lack of prospect of economic activity, and no ROI. Microgrids could be an alternative solution to electricity supply and be a vector of development for such communities [21, 22]. In this context, renewable energy source-based decentralized energy systems (DES) provide great prospects of improving access to electricity in such rural communities [23]. There is substantial potential for renewables-based systems across African countries with their rich natural resources. Renewables are the current fastest growing electrical energy segment whereby they are distributing safe, clean, and cheap electricity to all communities. Renewables are playing a fundamental role in eradicating electricity poverty in African rural communities. Remote rural communities of poor countries in particular African countries are frequently at a disadvantage position of receiving access to electricity and these communities have a low population, low electricity consumption, and low wage earner [24, 25]. Electricity affordability is still a major issue in these rural communities because most of them are jobless and low-income earners and lack of access to RES are still leading in these areas [26–28]. The poorer rural families are most probably to lack access to electricity because most of them are unskilled and unemployed. However, the level of electricity access in the majority of African remote rural areas is still in an infant stage because of the difficulty of utility grid expansion which comes along with higher costs. In SA and other countries, some remote areas are powered by diesel systems and failing grid networks, hence diesel price varies and is increasing at high speed [29, 30]. Any alternative power system going to replace the utility grid system needs to be able to supply reliable and sustainable electricity to these rural communities, and also be more efficient. Most of the developed countries are having a consistent, dependable, and exceptional quality of power distribution. However, in developing countries like South Africa, most of the urban and rural communities are experiencing load shedding, power failures, frequency disturbances, and insufficient supply capacity for utilities [31, 32]. These are mutual challenges encountered by these communities which stimulates a shift from conventional to renewable energy technologies (RET). The renewable energy-based microgrid applications are considered as emerging sustainable alternatives which are electricity benefactors and more capable of resolving lack of access to electricity [33–35]. Microgrids provide diverse benefits which are more effective, reliable, and sustainable electrical power systems, and also offer zero emissions of carbon dioxide, and lastly improve the lives of the people in communities [36, 37]. The deployment of microgrids is considerably expanding at exponential proportion, and is also gaining a global energy competitive advantage [38, 39]. Microgrids are hypothetically extending electricity access to rural areas. The optimal design analysis is considered as a significant requirement for the best capacity sharing of system parameters which can make sure

that effective operation of a micropower system is achieved [40, 41]. A Micropower system is expressed as a hybrid network that is involved in power production to assist meet the load demand. Micropower systems consist of solar PV, wind, diesel generators, biomass, electrical loads, and energy storage devices [42–45]. The hybrid power network incorporates two or more power conversion systems and includes power storage systems [46]. Whenever these systems are effectively and efficiently integrated could increase the overall system performances or result in overcoming inherent limitations. However, hybrid systems are possibly economical solutions to overcome the handicap of a short possibility of RES [47, 48]. In these rural communities of South Africa lack of access to electricity is still a major challenge. There is no prospect of return on investment (ROI) that justifies the lack of grid electricity in these communities. However, the main objective of this study is to design a suitable grid-connected microgrid system architecture for the electricity supply of remote communities of Limpopo in South Africa. HOMER software was used to design and model suitable microgrid system architecture and also to fundamentally explore related costs involved, the cost of energy (COE), net present cost (NPC), initial capital cost (ICC), and the operating cost (OC), and lastly to accomplish minimal greenhouse gas (GHG) emissions. This kind of architecture needs to produce high-quality performance and must be more reliable in order to meet the electricity demand of these communities. The effective application of renewable energy technologies for power generation specifically SHS, off-grid, or mini-grid systems are essentially expanding and increases electricity access in rural regions. Hence, the anticipated power system will be determined by the related parameters, cost factors, and current limitations. Data related to solar irradiation levels in these areas of the Limpopo province of South Africa, indicated that the resources could be reliable for electricity production [49–51]. This study proposes a suitable architecture of a hybrid microgrid system to provide reliable electricity to remote rural communities of South Africa. Therefore, HOMER was used to simulate the proposed optimal grid-connected microgrid system architecture that is capable of powering the load demand of these rural communities. The results showed that a Grid/PV/Wind/DG/Battery/Converter-powered microgrid system architecture is considered to be techno-economically feasible, maintainable and environmental friendly when compared to the other feasible architectures. This study evaluated different parameters and renewable energy sources to determine a more suitable microgrid system architecture that can satisfy a preferred load demand, provide improved financial flexibility, improve system reliability, decreases the cost of energy and reduce carbon dioxide emissions, increase a friendly environment, and diminish the possibility of climate change and global warming. In this study, HOMER software evaluated different power sources like RES, diesel generator, national grid, converter, and battery system for the remote communities of sub-Saharan Africa countries, particularly in South Africa. This paper is structured in the following manner: Sect. 1 represents the introduction whereas Sect. 2 covers the literature review, Sect. 3 covers methodology. Section 4 expresses system modeling and Sect. 4.7 system reliability. Section 4.8 is about economic viability and Sect. 5.5 discusses emission factors. Section 5 presents a discussion of results, and finally, Sect. 6 demonstrates the conclusion.

## 2 Review of Microgrid Architecture

Numerous associated studies were performed to plan, design, and simulated hybrid renewable energy structures for different remote rural environments, as discussed underneath. Iqbal et al. [40] focused on implementing and optimizing a maintainable campus microgrid configuration whereby various related cost exploration, greenhouse effects gases (carbon emission), and user-friendliness of energy resources are conferred. Muslih et al. [41] utilized HOMER software to design and optimize hybrid micropower energy stations whereby economic effect and design trade-offs were fundamentally considered in improving the cost and performance of the power network. Benalcazar et al. [31] reviewed the impacts of economic inducements and appropriation policies of the optimum design and the application of microgrids for rural electrification whereby networks are separated from the central. Micangeli et al. [42] discussed the analysis of the production of energy and the improvement of the mini-grid system in remote rural regions, hence the Habaswein community in Kenya was considered as a case study because of the shortage of access to electrical energy. Yong et al. [43] described the design and plan methods of a Hybrid PV/Wind system utilizing a progressive control structure aimed at the rural regions. However, Sandakan in Malaysia was utilized through a case study. Restrepo et al. [44] presented a case study whereby the HOMER Pro was employed for planning, evaluating, and exploring the performance of a microgrid system while focusing on the analysis of microgrid. Hafez et al. [45] concentrated on the ideal design, scheduling, evaluating, and functioning of a hybrid renewable energy system (HRES) which is an established microgrid while considering achievable environmental friendliness and reduction of development cost. Sureshkumar et al. [46] discussed the operative analysis of economic costs involved in designing a hybrid renewable energy system (HRES) by utilizing HOMER software. In this work, HRES optimum cost consideration was significantly completed, established on the solar radiation, wind speed, and load profile which were accumulated as of Tamil in India. Huang et al. [47] examined how to decrease the costs of electricity by the allocation of energy in sustainable microgrid configurations. Okundamiya et al. [29] focused on the utilization of HOMER to plan, simulate, and evaluate the performance of the micropower systems intended for off-grid areas. In this work, cost-effective, practical, and environmental effects of hybrid power systems at a rural place in Nigeria were evaluated. Kansara et al. [48] utilized HOMER software to model and simulate the distributed generation system which is a hybrid renewable energy system. Adetunji et al. [34] presented a microgrid for rural electrification which is to accomplish paramount optimization outcomes employing HOMER software. Ahn et al. [33] focused on the planning and configuring of a standalone or interconnected renewable micropower system aimed at an isolated settlement in Mongolia that meets load demand and reduces the creation of emission and system operating cost. The designed configuration was stimulated by the application and utilization of HOMER software. Stiel et al. [49] utilized HOMER to assess the possibility of energy-storing devices that are applied in the utilization of diesel or wind systems, hence the considered energy-storing device was vana-

dium redox battery due to its long lifecycle, high efficiency, flexible power output, and capacity. Fernando et al. [50] reviewed the optimum design of a hybrid power structure, maintainable energy solutions, and energy demand aimed at Abertay University's library operational in Dundee Scotland of which utilized diverse forms of renewable power source configurations. Akindeji et al. [51] explored the utilization and application of different renewable energy sources in a university campus microgrid. Mejbil Ali et al. [52] designed an optimum configuration of a hybrid hydro wind micro-power network for remote rural communities by utilizing HOMER software. Ghenai et al. [53] explored the existing renewable energy sources in Sharjah and determined an optimum structure to meet the preferred electrical loads of the city. Masrur et al. [54] analyzed the techno-economic environmental sustainability of an inaccessible microgrid network positioned in an isolated site of Bangladesh. Belu et al. [55] presented in what way the usages of the HOMER platform could be a treasured instrument that could assist with designing, modeling, and analyzing renewable energy education configurations. Ghenai et al. [56] discussed the plan, improvement, and control of the off-grid solar PV/hydrogen fuel cell power network used for green buildings. Qolipour et al. [57] presented the case study which was implemented targeting the technical-economic possibility of instituting the hybrid photovoltaic-wind energy site to produce electrical energy and hydrogen by application of the Homer model for the Hendijan region located in South West of Iran. Zhang et al. [58] designed a financial model comprehending the investment and operative price of respective components while power creation and the heat salvage were also measured in a financial model. They articulated the life-cycle of the capital improvement problem in finding the optimum hybrid renewable energy network structure, by using limits to balance the specified load profile. Ghorbani et al. [59] applied and utilized the hybrid genetic algorithm with particle swarm optimization (GA-PSO) which is aimed at achieving the greatest size of the off-grid house system incorporated with energy-storing devices, wind turbines, and photovoltaic panels. Jung et al. [60] presented a method intended for the optimum planning and design of hybrid renewable power configuration aimed at microgrid applications.

Current economic studies are showing that hybrid energy systems for example renewables-based hybrid mini-grids may perhaps help African countries form a low carbon economy, be climate-resilient in a post-pandemic world, and support financial recovery with climate and sustainable improvement objectives. Literature advocate that renewables-based hybrid energy systems might assist with bridging the gap between supply and demand whereas providing the African rural populations' with energy access. The use of microgrids aimed at off-grid electrification for emerging nations is disadvantaged by an important limitation which is considered to be high upfront capital costs [61, 62]. Therefore, governments have commonly developed different incentive methods to support microgrids advancement. Political, economic, institutional, and social barriers are restraining the effective addition of microgrid systems in the rural communities, however, these barriers might be mitigated by an improved and more robust policy framework, and extra investment in the projects [63, 64]. The main motivation of this study is the rural areas of which they have limited income, less ability to be able to pay, the lower rate of electricity access, lack of human

and economic growth, high discharges of GHG which negatively influences the environment and human health, shortage of investment, poor infrastructure, and from studies observations, they have frequent grid failure (blackouts and load shedding), the high turnaround time for repairing faults. This study aims to find and design the optimal system architecture that incorporates the use of RES available in the selected rural locations, which may fulfill the electricity demand in a viable and consistent way, and also to evaluate if such a hybrid energy system is cost-effective or not. To attain this aim, three rural communities were used as a sample, assessing the prospective load demand, and recognizing the existing resources, using HOMER software to design a power supply system that is dependent on various fusion of RE systems, and choose the more suitable system architecture based on lowest net present cost (NPC), lowest Levelized cost of energy (LCOE), and maximum renewable energy fraction (RF), and less carbon emissions. It is important to purposefully design appropriate and feasible architecture of microgrid networks that is effectively functioning in both remote and grid-tied modes. The architectures of a microgrid are classified as AC, DC, and hybrid (ac-dc) of which are pursuing the highest dependability and effectiveness of the system. The related shortcomings of microgrid architectures are protection, control (frequency and voltage regulation), power quality and management, power-sharing and balancing, planning and grid connection, high initial cost, and lack of operative policies.

### 3 Methodology

In this study, we used HOMER software established by the U.S. National Renewable Energy Laboratory (NREL) for the design of the optimal architecture of microgrid systems [65]. The primary objective of this model is to find and design the best sizes of decentralized energy systems, to determine the financial viability, and to assess and analyze different energy performances such as scenario and sensitivity analysis. The full assessment of the three community loads and accessible renewable energy resources were conducted and fed as input data to HOMER before starting with simulations. In this study, the input data fed to HOMER software include available energy resources (solar profiles, fuel prices. etc.), variety of component sizes considered, system components related costs comprise of capital cost, maintenance, and operating (O&M) cost, replacement cost, lifespan, system efficiency, hourly load demand, losses in grid parameters and supply, sensitivity values, and economic data such as inflation and discount rate, and also project lifetime was added and assumed. This data was collected from various sources and was added to the software. The output of HOMER software is optimal architectures of microgrid systems, their finances, and energy performances. In this study, less NPC, less LCOE, maximum RF, and fewer carbon emissions are used as core selective parameters for choosing optimum microgrid system architecture for these communities. HOMER output is utilized as input data into MATLAB for system reliability analysis. After completing a series of sensitivity cases with different vital parameters, the results are exported to an

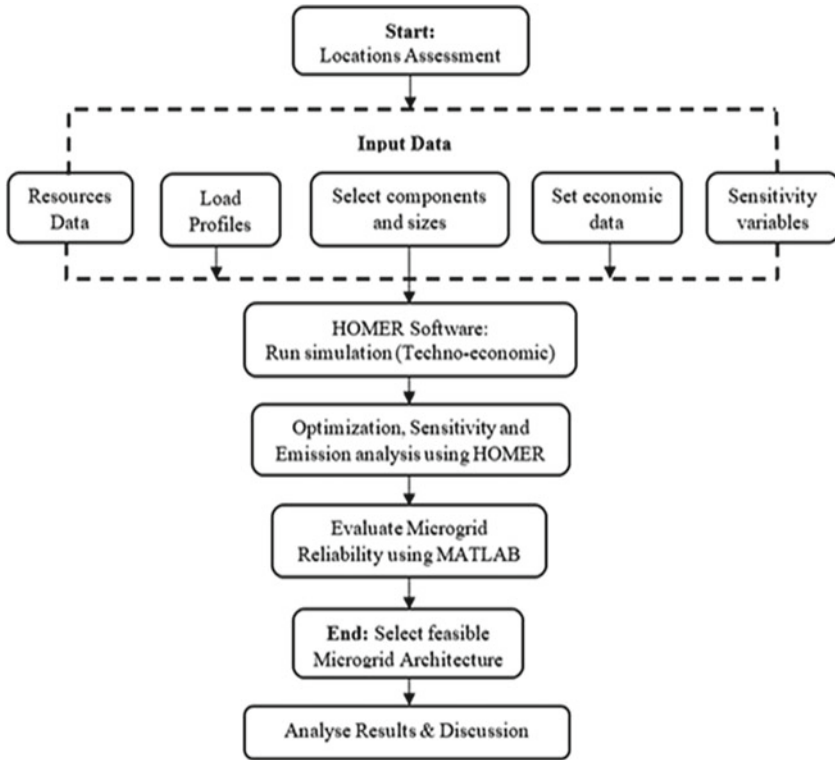


**Fig. 1** Method framework

excel file of which is added to MATLAB for processing. MATLAB is capable of performing various tasks like assessing voltage, PQ instabilities, and also evaluating current profiles through unstable conditions. Additionally, MATLAB will be used for validating the results of this study. The microgrid system architectures are simulated and followed by a techno-economic analysis which is carried out through determining whether the optimal system architecture can fulfill electricity demand and also assessing the installation, initial capital, and operation cost of the system over project lifespan. As a result, HOMER shows various feasible microgrid system architectures organized via life cycle cost that can be used to achieve the suitable microgrid architecture. The methodological framework of the study is indicated in Fig. 1.



**Table 1** Data of the communities

Communities	Latitude	Longitude	Population	Households
Tjiane	24°41'59"S	29°60'64"E	1400	380
Phosiri	24°36'38"S	29°69'92"E	1060	290
Malekapane	24°39'41"S	29°57'60"E	560	165

### 3.1 Description of the Study Areas

In this study, three rural remote communities were considered as case studies for the design of the optimal architecture of a microgrid system, including Tjiane (T), Phosiri (P), and Malekapane (M). All of these rural communities are encircled by mountains, physically accessible, and sparsely populated of which they are under Lepelle Nkumpi Local Municipality in Limpopo province, South Africa (SA). Tjiane and Malekapane villages are in close vicinity to one another whereas Phosiri village is partially isolated, and as observed from the aerial view shown in Fig. 2. The author visited all these three communities to gather data and explore existing power systems. These rural communities are partially developed and face issues like lack of job opportunities, bad road structures, high level of poverty, shortage of water and electricity services, lack good housing, poor service delivery from the municipality, and most residents are low-income earners. Even though the national grid electricity is present in these three rural communities, and persistent system failure, blackouts, load shedding, and poor reliability are normal difficulties. When grid system is experiencing load shedding some households use diesel generators as backup system to provide electricity. Table 1 reviews the basic data acquired from the communities.

Tjiane village is regarded as a rural region that has a population of about 1400 people, Phosiri village is a rural region that has a population of almost 1060 people while Malekapane village is also considered as a rural region that has a population of approximately 560 people. In this study, 100 households of each community with an average of five family members per house were considered and used. Currently, some households in these communities are electrically powered through the use of the national grid of which is unstable and failing to meet the demand due to experiencing overloading, blackouts, or load shedding more often. Even though is quite expensive to extend the national grid to other households and communities due to not having any prospect of economic activities or no return on investment (ROI). Most of the households in these communities have no access to grid electricity that provides an opportunity for off-grid or grid-connected electrification of the communities. The fundamental financial activities of these communities consist of agricultural activities mainly, for example, poultry farming, vegetable plantation, and cattle, sheep, and goats raising, this is only for survival. Figure 2 below, indicates the locations of these rural remote communities in Limpopo province, South Africa.



Fig. 2 Map of study areas (source Google Maps)

### 3.2 Assessment of Resources

In this study, the assessment of the energy creation coming from the solar PV and wind, global horizontal irradiance (GHI), wind and temperature resources data is essential to the designing of optimal microgrid system architecture. All this renewable energy sources data is downloaded from NASA's surface meteorology and solar energy [66, 67]. It is important to collect correct weather-related information about the selected locations. This data is collected from NASA is the initial and input data to HOMER of which is needed for examining the accessibility of RES potential in these rural locations.

**Solar Resources** In this study, the solar radiation profiles of these rural communities are considered. GHI is considered as a total quantity of irradiance coming from the sun through a horizontal surface to the ground [68, 69]. The accurate solar radiation data of these rural communities were acquired and downloaded from the database of NASA's surface meteorology and solar energy. From this data, it is observed that solar resources have the greatest potential in South Africa while wind resources are more dominating in the coastal areas of the country. These rural areas are extremely exposed to higher solar irradiation levels. The data utilized was the clearness index and the solar irradiation of the selected areas. However, these were collected from the National Renewable Energy Laboratory (NREL) [70]. The monthly average solar irradiation and clearness index at investigated locations are presented in Fig. 3.

The results show that these communities have similar weather conditions and are located in the same climatic zones because their monthly average solar irradiation fluctuates from 4.054 to 6.964 kWh/m<sup>2</sup>/day. They have annual average solar irradiations and a clearness index of 5.66 kWh/m<sup>2</sup>/day and 0.619 for each site. It

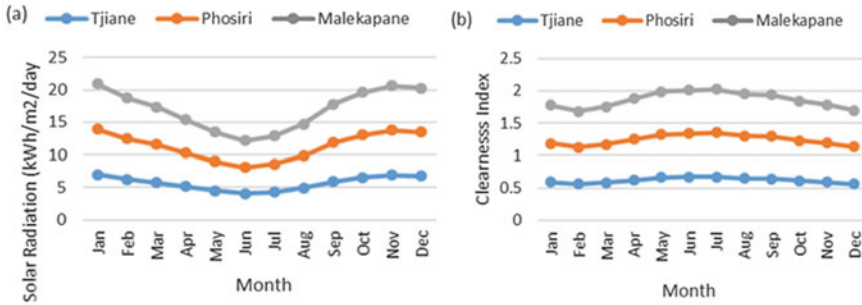


Fig. 3 Left: monthly average solar irradiation and right: clearness index for each location

is observed that the solar irradiation values are high in the summer season when the power demand is significantly higher and lower in the winter season. Furthermore, this indicates that solar energy potential and availability are quite great and this energy system is capable of electrifying many rural communities in the country, and also proficient in decreasing carbon dioxide emissions.

**Wind Resources** The monthly average information of wind speed has been acquired from NASA’s surface meteorology and solar energy for each location. The scaled annual average wind speed is 4.13 m/s with an anemometer height of 10m, peak wind speed is 15 h, wind changeability factor is 0.85 while diurnal pattern strength is 0.25 for each location. The wind speed of inner areas of the country is very low when compared to the coastline area’s wind speed. It can be seen that the wind speeds are high in the month of August to February as related to the other months. Additionally, this means that the wind systems are more capable of generating more energy during these months when compared to the other months. The results also show that there is a minimal variation of monthly average wind speed from one month to another (Fig. 4).

**Temperature Resources** The essential temperature data was collected or downloaded from surface meteorology and solar energy at NASA, this data helps with factors for evaluating, formulating, and planning renewable energy systems. These temperature data also help with computing the solar PV derating factor and assessing the system performance under difficult meteorological or climate settings. In this work, nominal operative cell temperature and the temperature effects on power yield were essentially considered. The scaled annual average temperature is 19.29 °C for each location. It can be seen that the temperatures are high in the summer season (September to April) as associated with the lower winter (May to August) temperatures. The readings of temperatures for each site are illustrated in Fig. 5.

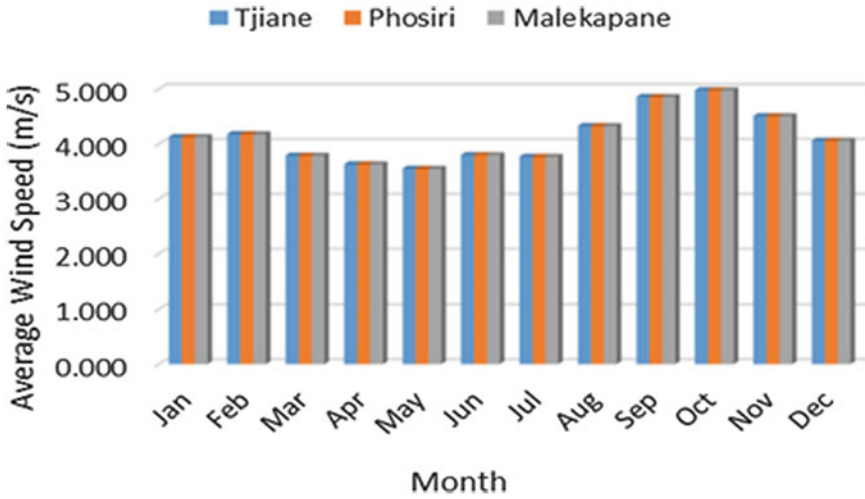


Fig. 4 Monthly average wind Speed for each location

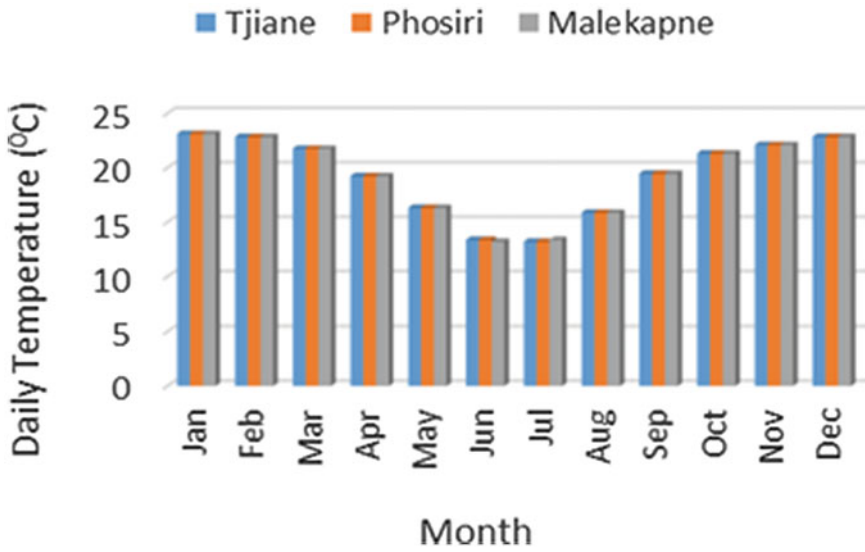


Fig. 5 Average daily temperature readings per month

### 3.3 Assessment of Electricity Demand

In this study, extensive load demand data is significant data required for designing renewable energy systems such as hybrid power systems (HPS), grid-tied, and off-grid microgrid systems. This kind of load data often does not exist in remote rural communities. A survey method was not utilized and applied in this particular study because the researcher acquired an extensive hourly load demand and load profile for a couple of weeks during the site visits. The load power rating and operating hours data of commonly used loads in these remote communities were collected. All loads were randomly selected from households in these three remote rural communities and we also considered loads with a lower wattage because they are more affordable. The commonly used loads are TV sets, lights, radios, kettles, fans, refrigerators, electric irons, and cell phone chargers. Some of the appliances that are not commonly used are laptops, printers, washing machines, microwaves, heaters, pressure, and slow cookers were considered as others in the model. Other loads also include appliances that are utilized in the health care centres, shops, and schools. Furthermore, related additional data of these communities was obtained from the Lepelle Nkumpi Local Municipality to generate other months' demand profiles. The electricity consumption of these communities assists with calculating the total load, average daily load, peak load, and load factor of which were generated and simulated by HOMER. The electricity consumption has a minimal change during the course of the year while load consumption season was considered. The electrical load calculation is considered as the initial stage in the design of HPS to determine the size of system modules. The necessary calculations were considered in computing the total energy consumed by households in these communities. It is observed that the electrical load of these communities is influenced by the lifestyle of the individuals and also the demographic, cultural, religious, socioeconomic, technological, and geographical conditions they are living in. Tables 2, 3 and 4 show a list of commonly used loads, their quantity, daily operating hours, load power rating, and electricity consumption in these remote rural communities.

The total energy used up (ET) by homes in these communities is expressed as:

$$E_T = \sum_{i=1}^m n \times P_i \times T_i = E_1 + E_2 + E_3 + \dots + E_m \quad (1)$$

where  $E_T$  is the total energy used up by homes,  $n$  is the number of appliances or loads  $i$  in usage,  $P_i$  is regarded as power rating of appliances or loads  $i$ , and  $T_i$  refers to the time of appliances or load usage. The total energy consumed of listed appliances below was added up to get the required load to be provided by the optimal microgrid architecture.

HOMER applies the hourly analyses to produce daily load profiles for each community. Figure 6 depicts the daily and seasonal load profile for each location. In this study, the random variability to the electric load was considered to make it more accurate, and the used variability values of day to day and timestep are 10% and 20%

**Table 2** Daily load estimation for Tjiane

Loads	Quantity per household ( <i>n</i> )	Power rating	Operating time	Energy
TV	3	0.04	6.00	0.72
Lights	6	0.02	12.0	1.44
Kettle	2	0.90	3.0	5.40
Iron	2	1.00	2.50	5.00
Stove	2	1.50	4.00	12.0
Cellphone charger	5	0.01	2.00	0.10
Fan	3	0.08	2.50	0.60
Refrigerator	2	0.40	24.0	19.2
Radio	3	0.15	5.00	2.25
Others	5	0.35	5.50	9.63
Total	–	–	–	56.34
Units	–	kW	hrs	kWh/day

**Table 3** Daily load estimation for Phosiri

Loads	Quantity per household ( <i>n</i> )	Power rating	Operating time	Energy
TV	2	0.04	5.00	0.40
Lights	5	0.02	11.0	1.10
Kettle	1	0.90	2.50	2.25
Iron	1	1.00	2.00	2.00
Stove	1	1.50	3.50	5.25
Cellphone charger	2	0.01	2.50	0.10
Fan	2	0.08	2.00	0.32
Refrigerator	1	0.40	24.0	9.60
Radio	2	0.15	4.50	1.35
Others	4	0.35	6.00	8.40
Total	–	–	–	30.77
Units	–	kW	hrs	kWh/day

for each location respectively. The scaled annual average load for Tjiane, Phosiri, and Malekapane is 600 kWh/day, 330 kWh/day, and 250 kWh/day respectively. The peak load in the produced profile for the communities is determined to be 74.34 kW with 0.34 load factor, 40.68 kW with 0.34 load factor, and 31.55 kW with 0.33 load factor respectively. The same daily load profile is applied to produce for a year

**Table 4** Daily load estimation for malekapane

Loads	Quantity per household ( <i>n</i> )	Power rating	Operating time	Energy
TV	1	0.04	4.00	0.16
Lights	3	0.02	10.0	0.60
Kettle	1	0.90	2.0	1.80
Iron	1	1.00	1.30	1.30
Stove	1	1.50	3.00	4.50
Cellphone charger	2	0.01	2.30	0.05
Fan	1	0.08	1.50	0.12
Refrigerator	1	0.40	24.0	9.60
Radio	1	0.15	4.00	0.60
Others	3	0.35	3.50	3.68
Total	–	–	–	22.41
Units	–	kW	hrs	kWh/day

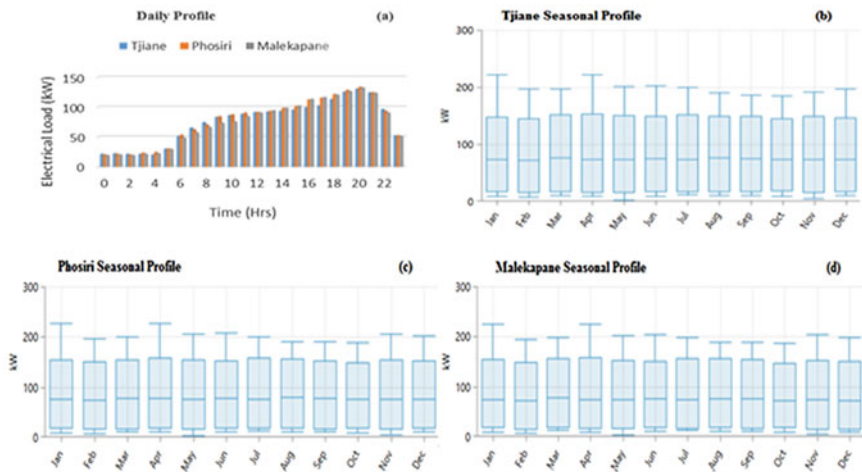


**Fig. 6** Daily and seasonal load profile for each Location

through a usual variation. There is a vast variation in load profile throughout holiday seasons, however, in peak summer and winter days, the load energy demand swiftly rises.

**Table 5** Techno-economic parameters of DER technologies

Components	Size	Lifetime	Capital Cost	Replacement cost	O&M	Fuel Price
PV	1	25	3000	3000	200	–
Wind Turbine	3	20	14700	14700	500	–
Diesel Gen.	1	1.71	2500	2500	1300	15
Batteries	1	10	5500	5500	100	–
Converter	1	15	4000	4000	100	–
Grid Capacity (10 km)	999999	–	50000	–	160	–
Units	km	Year	R/km	–	R/year/km	–

### 3.4 Techno-Economic Parameters of der Technologies

In choosing PV module, wind turbine (WT), grid, converter, diesel generator (DG), and energy storage technology, some significant factors were regarded for example safety, lifespan, cost-effectiveness, growth of technology, efficiency and size ranges, and environmental friendliness. These technical parameters were considered for the successful performance of the simulation process. These parameters data were collected from several producer specification datasheets and also from published materials. PV, WT, DG are supplementary power sources considered in this study, while the grid electricity is available in these communities. The supplementary power sources are more effective when are used with power storage technologies and the integration of RES into the currently power system improves system reliability. The lead-acid battery was chosen in this study due to the benefits they offer when compared to other batteries. All these considered technologies in the microgrid networks have detailed economic data consisting of capital, replacement, and operating and maintenance costs which are expressed in R/kW and R/kW/yr and also lifespan is vital. The economic data of these systems is gathered from different manufacturers and published information. This data is an important input data to the homer software which assists with designing optimal system architecture for rural electrification purposes. The techno-economic parameters of all these DER technologies are summarized in Table 5.

### 3.5 Economic Parameters and Assumptions

HOMER is built-in with financial input functions which assist with deriving the NPC and other imperative system indicators. In this study, the discount and inflation rate



**Table 6** Sensitivity parameters and values

Power price	Sellback Price	Power rating	Grid repair mean time
1.10	0.55	4	10
1.30	0.75	8	15
1.50	1.15	12	20
1.70	1.35	16	25
R	R	—	hrs

are considered as one of the most important constraints in any financial analysis. They are various factors that influence the selection of discount rates of which are ROI, interest rate, project lifetime [71]. The project's lifespan is selected to be 25 years with an inflation rate of 3% and also annual discount rate of 3% was utilized in this study to assess the RE investment. In this project lifetime, the optimal system architecture can meet the load demand of these rural communities that might stay constant.

### 3.6 Sensitivity Variable Inputs

In this study, various sensitivity input parameters or variables were considered. HOMER software performed a sensitivity analysis to explore the effect of variations in power price (tariff), sell-back price (SBP), grid mean repair time (GMRT), and grid failure frequency (GFF) from lowest to maximum values for these parameters, and diesel price, discount, and inflation rate and also project lifespan were kept constant and lastly, electric load, solar radiation, and grid distance and extension cost varies according to the position of these locations. These selected sensitivity parameters have an essential influence on the design and cost analysis of the optimal system architecture, and the effectiveness and efficiency of the RET is greatly relied on the substantial use of these parameters. These sensitivity parameters and values were considered as input data into HOMER software to determine the best possible system architecture and adequate techno-economic analysis for those systems. These sensitivities and economic parameters have a great influence on the formulation of energy policy frameworks. The sensitivity factors and their distinct values are shown in Table 6.

## 4 Modelling of Hybrid Energy System Components

In this study, solar PV, grid, wind turbine (WT), diesel generator (DG), energy storage system, and power converter are utilized as important system components for the analysis. The objective is to design and simulate a more appropriate power dis-

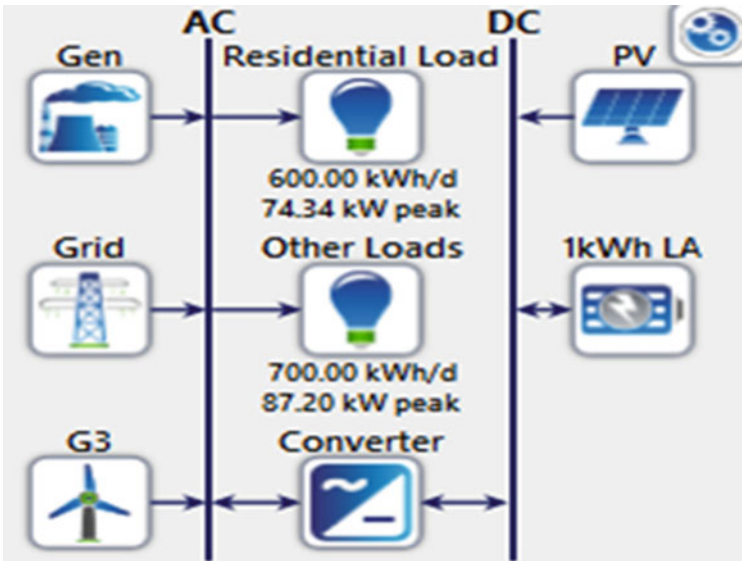


Fig. 7 Schematic diagram of microgrid architecture in HOMER

tribution system that can efficiently and effectively satisfy the load demand of these communities with a reliable supply of power. The PV, WT, DG, and energy storage system are added to the system as backup systems because the main aim is to design and model a reliable grid-connected hybrid microgrid system architecture. Figure 7, is a schematic diagram that displays a microgrid system architecture used in these three communities of Limpopo, South Africa. In this hybrid power system, the load demand of these communities, the grid, WT, and DG are coupled to the AC side of the system. While solar PV and energy storage systems are coupled to the DC side. The energy storage systems are applied to store electrical power, supply uninterrupted power, and can also be utilized to improve the power quality (PQ) of RES due to their unstable nature. The power converter is utilized to convert AC to DC or vice versa. The hybrid microgrid system needs to be reliable, maintainable, clean, and environmentally friendly while supplying high-quality electricity to the rural communities.

#### 4.1 Utility Grid Modelling

The extension of the grid to non-electrified communities is frequently very expensive and economically not feasible due to the high scattering of the remote rural households [72]. The first impediment is the cost associated with the grid expansion to rural regions. The utility grid association is similarly measured in the HOMER design

method [73]. The utility grid is reflected as an immeasurable bus that is competent to provide any quantity of electricity. Whenever microgrid remains in a grid-tied approach, the power provided from the utility grid to the microgrid involves various costs which are very important, and are expressed as follows [74, 75]:

$$C_{grid} = P_{grid} \times \alpha \quad (2)$$

where  $C_{grid}$  is the grid cost supply,  $P_{grid}$  is the power provided from the grid,  $\alpha$  is the electric unit cost provided by the grid in ZAR/kWh.

Consequently, the cost of energy sold towards the utility grid is illustrated below [74, 75]:

$$C_{mgrid} = P_{grid} \times \beta \quad (3)$$

where  $C_{mgrid}$  is the cost of power retailed towards the utility grid,  $P_{grid}$  is negative due to harmonizing the cost equation and also producing profits for the microgrid systems, and  $\beta$  is the selling rate of power in ZAR/kWh. Either way the excess energy is to be wholesaled to the utility grid or the price configuration is different from one region to the other.

## 4.2 Solar PV Modelling

The data utilized was the everyday clearness index and solar irradiation of the designated sites of the hybrid microgrid architecture, as illustrated in Fig. 3. Solar irradiation and clearness index were generated from the national renewable energy laboratory (NREL) [44, 55, 58]. Solar PV systems are more capable of converting solar energy which is directly from the sun into electrical energy [76]. Solar PV power is currently one of the best promptly emerging categories of RES which is integrated into central grids in the previous period [77]. The solar PV panels' output power is completely reliant on environmental circumstances such as temperature and irradiance, hence is consequently disrupted and fluctuates in nature [78]. The level of solar PV penetration is quite enormous currently which affects the dependability and safety of the central grid could degrade. The unpredictability of solar PV power may perhaps have a remarkable impact on the development and application of the central grid setup [79]. However, the immediate unpredictability of solar PV power might result in triggering degradation of voltage quality and overvoltage complications. The power yield of the solar PV array is determined by the ambient temperature and irradiance data of the location used [80], and is formulated by the utilization of the below equation [29, 40, 55, 58, 75]:

$$P_{pv} = f_{pv} \times Y_{pv} \times \frac{I_T}{I_S} \quad (4)$$

where  $f_{PV}$  is the PV derating factor,  $Y_{pv}$  is the peak capacity of the PV array in kW,  $I_T$  is the total solar radiation occurrence on the surface of the solar PV array in  $\text{kW/m}^2$ , and  $I_S$  is the standard quantity of the radiation utilized for assessing the size of the solar PV array. The derating factor is responsible for the effects of increased temperature, wire losses along with the effects of filth on the PV array illustration.

### 4.3 Diesel Generator (DG) Modelling

Diesel generators are necessary as the standby energy system in achieving the energy demand of vital loads. The intervention of diesel systems application makes the hybrid system to be more reliable and consistent [81]. HOMER has general data for diesel systems incorporated [82]. In HOMER, the generator has a fixed cost of energy and is expressed by the following equation [74, 75]:

$$C_{(gen, fixed)} = C_{(om, gen)} + \frac{C_{(rep, gen)}}{R_{gen}} + F_0 \times Y_{gen} \times C_{(fuel, eff)} \quad (5)$$

where  $C_{gen, fixed}$  is the generator operation and maintenance cost per hour,  $C_{rep, gen}$  is replacement cost,  $R_{gen}$  is the generator lifespan in hours,  $F_0$  is the fuel curve intercept coefficient in fuel/hr/kW,  $Y_{gen}$  is the generator capacity in kW, and  $C_{fuel, eff}$  is the effective fuel price.

The current diesel price in South Africa is presently at ZAR 15.00 of which is continuously changing. The diesel price has an enormous influence on COE [83–85]. Poor weather conditions negatively disturb the performance of WT and solar PV systems of which are extremely intermittent [86]. Therefore diesel and RE systems used with the battery banks could be used as standby systems for power supply.

### 4.4 Energy Storage Modelling

Energy storage is an essential component of microgrids [87]. Battery energy storages are critical in the application of a hybrid power system whereby they stored up produced electricity, whenever there is low demand, and during high demand, electricity is released [88]. They are more capable of handling the disturbances and unpredictable nature of renewable energy sources. They are also an operative and cost-effective technique that improves electricity supply, stabilizes power output variations, and diminishes their impact thereof [89]. In this study, the lead-acid battery was considered as a suitable electricity-storing technology due to its high powered efficiency, safe and reliable-performance. It has been extensively applied in battery energy storage systems (BESS) [90, 91]. The equation of battery state of charge (SOC) is articulated below [92–95]:

$$SOC(t) = SOC(t-1) + \frac{I(t)}{Q_n} \cdot \Delta t \quad (6)$$

where  $SOC(t)$  and  $SOC(t-1)$  are the states of charge at the time  $(t)$  and  $(t-1)$ ,  $Q_n$  is the nominal capacity of the battery, and  $I(t)$  is the current capacity.

The effective application and operation of the power storage system relies on the charge and discharge boundaries, depth of discharge (DOD), and accessibility of confined solar resources [89, 90]. This specifies that the storage system should function within acceptable SOC boundaries stipulated by each producer as indicated in the equation below:

$$SOC^{min}(t) \leq SOC(t) \leq SOC^{max}(t) \quad (7)$$

The optimum operation of the power storage system through considering the DOD is stated as:

$$SOC^{min}(t) = (1 - DOD) \times SOC^{max}(t) \quad (8)$$

#### 4.5 Power Converter Modelling

A converter plays an important role in changing and transforming dc power acquired from the Solar PV panels and also from the hybrid energy system to ac power with needed frequency. Generally, a converter is established on the power of solar PV system considered and the converter has efficacy of 85%, which is exceptionally good. The technical and financial specifications of the converter are summarised in Table 5.

#### 4.6 Wind Turbine (WT) Modelling

The wind system was also considered in this study even though the inland areas have low wind speed and high installation cost and the wind speed is very high along the coastlines of the country. The average wind speed is 4.13 m/s for each location. The power produced through the utilization of wind turbines is entirely dependent on wind speed availability and variances. The HOMER software enables the estimation of the power production of a wind turbine using the below equation [91–93]:

$$P_{wt} = \frac{\rho}{\rho_o} \times P_{wt,STP} \quad (9)$$

where  $P_{wt}$  is the wind turbine power output in kW,  $P_{wt,STP}$  is the wind turbine power production at standard temperature and pressure in kW,  $\rho$  refers to real air density in  $\text{kg/m}^3$ , and  $\rho_o$  is the air density at standard temperature and pressure ( $1.225 \text{ kg/m}^3$ ).

## 4.7 System Reliability

As a result of the intermittent nature of power produced through the use of renewables like solar PV and wind generators, there is a need for reliability analysis to take place of which has an imperative role to play in the designing of hybrid renewable energy systems. The intermittent nature of renewables and changing power demand will disturb the power stability of the microgrid system. Therefore, it is important to evaluate the reliability of the microgrid system. The studies show that the loss of power supply probability (LPSP), loss of load probability (LOLP), and unmet load are commonly applied methods in the reliability assessment of RE-microgrid systems [24, 89, 94]. These reliability methods are used in the performance of selecting a more feasible system architecture. LPSP is considered as the possibility that an inadequate power supply system will result when the microgrid system fails to satisfy or is incapable of meeting customer's load demand. The equation of the loss of power supply probability (LPSP) is expressed below in the below equation [24, 95–98]:

$$LPSP = \frac{\sum(P_{load} - P_{pv} - P_{wind} + P_{SOC_{min}} + P_{diesel} + P_{grid})}{\sum P_{load}} \quad (10)$$

This study aims to design a suitable grid-tied microgrid system architecture that is more reliable and cost-effective for rural electrification. It is very important to design an optimal system architecture that provides reliable power and satisfies customers' load demands. Therefore, reliability analysis of this microgrid system is essential. For example, if a microgrid system in the electrical field has inadequate power to satisfy the load, it means that the system has a lesser LPSP and is considered a more consistent and reliable system. Furthermore, if the system has zero LPSP means that the load demand is met and also if the system has one LPSP means that the power produced cannot satisfy the load demand.

## 4.8 Economic Assessment

Economic assessment can be used as an evaluation metric that assists with selecting the optimal architecture of microgrid systems. The metrics can be environmental, financial, or reliability metrics. The metric utilized in this study was the lowest net present cost (NPC) and Levelized cost of energy (LCOE), less carbon emissions, and maximum renewable energy fraction (RF). The analysis of variable costs assumes a pivotal role both in the HOMER model and minimization of NPC whereby the software examines for the best possible system architecture through the lowest NPC [74]. Therefore, the greatest realistic alternative is the one with the lowest possible NPC and LCOE. HOMER expresses collective optimization processes of NPC and LCOE, and are indicated in the following equations [96–99]:

$$C_{NPC} = \frac{C_{TANN}}{CRF_{(i,N)}} \quad (11)$$

$$CRF_{(i,N)} = \frac{i(1+i)^N}{(1+i)^N - 1} \quad (12)$$

$$COE = \frac{C_{TANN}}{E_{iS} + E_{grid}} \quad (13)$$

where  $C_{NPC}$  is the net present cost and  $COE$  is the Levelized cost of energy.  $C_{TANN}$  is the total annual cost,  $CRF$  is capital recovery factor, whereby  $i$  is interest rate, and  $N$  is the number of years.  $CRF$  can be expressed as per the above equation.  $E_{iS}$  is the energy provided from a recommended microgrid, whereas  $E_{grid}$  is the quantity of power sold back towards the utility grid. Also, our simulation considered selling back prices to the utility grid as important. The initial capital costs of the apparatuses are utilized to determine the total connected cost of those apparatuses at the start of the hybrid system, which is illustrated in equation (14) below [99]:

$$C_{acap} = C_{cap} \times CRF \quad (14)$$

whereby  $C_{acap}$  is the annualized capital cost and  $C_{cap}$  is the initial capital cost. The other vital costs considered in this study include fuel, operating and maintenance costs, capital cost (CC), replacement costs, and also emission fines. The above costs are compared and analyzed in order to accomplish an optimum hybrid system architecture that will be more applicable for rural environments and also meet rural communities' electricity demand.

## 4.9 Emission Factor

Emission factor (EF) is considered as a demonstrative value that tries to describe the number of toxins produced in the air with progress linked with the production of such impurities. The emissions of these pollutants are generated from different energy generators. The pollutants are carbon dioxide, carbon monoxide, unburned hydrocarbons, nitrogen oxides, sulfur dioxide, and particulate matter [95, 96]. These emissions negatively contribute to climate change and global warming of which needs to be reduced, monitored, and controlled by the governments of undeveloped and developing countries. This study is looking at proposing optimum microgrid system architecture that produces less carbon emissions and is environmentally friendly. The basic emission equation is expressed as:

$$E = E_f \times A \times \frac{1 - E_R}{100} \quad (15)$$

where  $E$  is emission,  $E_f$  is emission factor,  $E_R$  is the total emission reduction efficiency in (%), and  $A$  is the activity rate.

The study proposed that the optimal architecture of microgrid systems based on RES is environmentally friendly with minimal carbon emissions.

## 5 Results and Discussion

### 5.1 Optimization and Simulation

The results presented in this study for all three rural communities consist of best sizing, cost summary, and system performance. In the design of a hybrid power system, load demand and weather-related data, techno-economic data, and sensitivity variables are considered and used as input data to HOMER software. In this study, HOMER was utilized to perform multiple simulations on the designing of optimal microgrid system architecture that satisfies the load demand for each considered community. These simulation processes took hours to be completed, and the majority of simulated solutions were feasible, and some were infeasible due to the capacity shortage constraint and also due to the minimum battery life. The viable solutions of the microgrid system architectures were selected and listed in ascending order of the net present cost (NPC). In this study, the optimal microgrid system architecture for these rural communities is chosen based on the least of NPC and Levelized cost of energy (LCOE), fewer carbon emissions, and a maximum renewable fraction (RF). The system that has all these parameters stand out as optimal system architecture. The results show that Grid/PV/Wind/DG/Battery/Converter power system is proposed to be the most economical alternative and suitable microgrid system architecture for rural electrification in South African rural communities. This optimal grid-tied hybrid microgrid system architecture is found to be the best power generation system in all three rural communities considered in this study.

### 5.2 Optimal Sizing and Cost Summary of Proposed MG System Architecture

The optimal sizing of the microgrid components are chosen from the HOMER optimization results. The optimization results of the optimal sizing supplied the best sizes of DER technologies in microgrids especially Solar PV, WT, DG, grid, battery, and converter. The optimal sizing of the proposed microgrid components are shown in Table 7. As shown in Table 7, the optimization results of the optimal system show that the system consists of 837 kW solar PV, 3900 kW WT, 180 kW DG, 999 999 kW grid, 6 kWh with 6 strings battery, and 392 kW converter for Tjjane, and 484 kW solar PV, 2196 kW WT, 100 kW DG, 999 999 kW grid, 6 kWh with 6 strings battery,



**Table 7** Optimal sizing of the proposed microgrid components

Optimal MG components	Tjiane capacity	Phosiri capacity	Malekapane capacity
Solar PV	837	484	470
Wind Turbine	3900	2196	1809
Diesel Gen.	180	100	87
Grid	999999	999999	999999
Battery	6 with 6 strings	6 with 6 strings	1 with 1 string
Converter	392	228	312
Units	kW	kW	kW

**Table 8** Cost summary for optimal MG system architecture

Cost	Base case DG only	Lowest cost system
<b>Tjiane</b>		
NPC	123.000000	2.97000000
Initial capital	450,000	24.2000000
O & M	4.88000000/year	-847.909/year
LCOE	10.33/kWh	0.028/kWh
	Rands	Rands
<b>Phosiri</b>		
NPC	71.000000	1.84000000
Initial capital	250,000	13.9000000
O & M	2.85000000/year	-482.791/year
LCOE	10.73/kWh	0.031/kWh
	Rands	Rands
<b>Malekapane</b>		
NPC	62.2000000	1.21000000
Initial capital	217,000	11.9000000
O & M	2.48000000/year	-425.611/year
LCOE	11.35/kWh	0.024/kWh
	Rands	Rands

and 228 kW converter for Phosiri, and 470 kW solar PV, 1809 kW WT, 87 kW DG, 999 999 kW grid, 1 kWh with 1 strings battery, and 213 kW converter lastly for Malekapane. The cost summary for the optimum grid-connected microgrid system architecture for each considered community is displayed in Table 8.

The cost summary presented results such as NPC, initial capital, M&O, and COE as shown in the table below. The MG system architecture that has low NPC, low COE, and maximum RF is recommended as the most favorable system and is compared to the base case which is the DG system. The results show that optimum grid-tied

microgrid system architecture and DG system are using the cycle charging dispatch strategy. The battery banks are exclusively charged by the RES particularly solar PV and wind systems.

### ***5.3 Optimized Designs for Tjiane, Phosiri, and Malekapane***

The optimized results and the associated costs of cases for Tjiane, Phosiri, and Malekapane are explored. The optimization results of the best cases are presented in Tables 9, 10, 11.

In this study, the five best MG system architectures were selected and compared to a diesel-only system for each community. These MG base cases were simulated using different operating strategies like load following (LF) and cycle charging (CC). The optimized results show that case 1 (Grid/PV/WT/DG/Battery/Converter) is considered the optimal MG system architecture for each community and is also simulated through the use of CC of which is a frequently used dispatch strategy in standalone or grid-tied microgrid applications. The other MG base cases are simulated using LF operating strategies. This MG case 1 for each community is the ideal system for a microgrid that has the lesser NPC and COE. In these rural communities, the RF of the more suitable MG system architecture is higher than 95%. Additionally, this shows that there is a higher penetration of RES of which they have a high initial capital cost and improves system reliability when used with battery systems. As indicated in Tables 9, 10, 11, in all three communities, Malekapane has the smallest NPC and COE followed by Phosiri and Tjiane. This shows that load demand and community size have an impact on the COE. The overall results indicate that the deployment of an optimal MG system architecture (Grid/PV/WT/DG/Battery/Converter) in all these three rural communities is the most cost-effective, reliable, sustainable, and environmentally-friendly system architecture that has less NPC, less COE, and produce fewer carbon emissions.

### ***5.4 Electricity Production and Consumption***

In all three communities, the electricity production of the proposed microgrid system architecture for case 1 consists of Solar PV, WT, DG, and grid power sources. Figure 8 illustrates the monthly electricity production from PV, WT, DG, and grid power sources for each community. It is observed that during winter (May, June, and July) season solar PV irradiation levels and wind speed are very low and, the grid is used as the main power source while a diesel generator is used as a backup system. In the summer season, solar PV and wind production establish a key part in the overall power generation. The results show that the optimum microgrid system components (Grid, PV, WT, and DG) are capable of producing adequate electricity to meet the load demand of the communities. In these communities, the optimal system

**Table 9** Optimized results for the proposed MG system architecture in Tjiane

Cases	Optimum architecture	NPC	COE	OC	ICC	RF	Energy purchased
1	Grid/PV/WT/DG/Battery/Converter	$1.97 \times 10^6$	0.028	152.141	$24.2 \times 10^6$	97.8	89,204
2	Grid/PV/WT/DG/Battery/Converter	$2.73 \times 10^6$	0.036	180.786	$24.2 \times 10^6$	97.9	89,159
3	Grid/PV/DG/Converter	$4.63 \times 10^6$	0.164	1.022541	$5.07 \times 10^6$	83.90	217,237
4	Grid/PV/DG/Converter	$4.69 \times 10^6$	0.168	1.027892	$4.99 \times 10^6$	83.6	217,878
5	Grid/WT/DG	$8.40 \times 10^6$	0.121	572.578	$20.1 \times 10^6$	95.0	151,294
6	DG only	$122 \times 10^6$	10.33	5.88	450.00	0	0
Units		Rands	R/kWh	R/year	R	%	kWh

**Table 10** Optimized results for the proposed MG system architecture in Phosiri

Cases	Optimum architecture	NPC	COE	OC	ICC	RF	Energy purchased
1	Grid/PV/WT/DG/Battery/Converter	840.675	0.031	517.299	$13.9 \times 10^6$	97.9	49.887
2	Grid/PV/WT/DG/Battery/Converter	$3.42 \times 10^6$	0.091	683.024	$12.3 \times 10^6$	97.2	53.432
3	Grid/PV/DG/Converter	$2.31 \times 10^6$	0.167	1.006.890	$3.14 \times 10^6$	84.3	122.048
4	Grid/PV/DG/Converter	$2.32 \times 10^6$	0.168	1.007.239	$3.14 \times 10^6$	84.3	122.036
5	Grid/WT/DG	$4.52 \times 10^6$	0.126	700.407	$11.5 \times 10^6$	95.1	84.585
6	DG only	$70.4 \times 10^6$	10.73	$3.85 \times 10^6$	250.00	0	0
Units		Rands	R/kWh	R/year	R	%	kWh

**Table 11** Optimized results for the proposed MG system architecture in Malekapane

Cases	Optimum architecture	NPC	COE	OC	ICC	RF	Energy purchased
1	Grid/PV/WT/DG/Battery/Converter	257.910	0.024	574.479	$11.9 \times 10^6$	97.9	42.477
2	Grid/PV/WT/DG/Battery/Converter	354.910	0.027	593.943	$11.5 \times 10^6$	97.9	42.781
3	Grid/PV/DG/Converter	$1.51 \times 10^6$	0.136	980.856	$2.99 \times 10^6$	85.7	102.905
4	Grid/PV/DG/Converter	$1.55 \times 10^6$	0.142	986.151	$2.90 \times 10^6$	85.3	103.397
5	Grid/WT/DG	$3.65 \times 10^6$	0.129	802.656	$9.58 \times 10^6$	95.0	103.290
6	DG only	$61.2 \times 10^6$	11.35	$3.48 \times 10^6$	217.500	0	0
Units		Rands	R/kWh	R/year	R	%	kWh

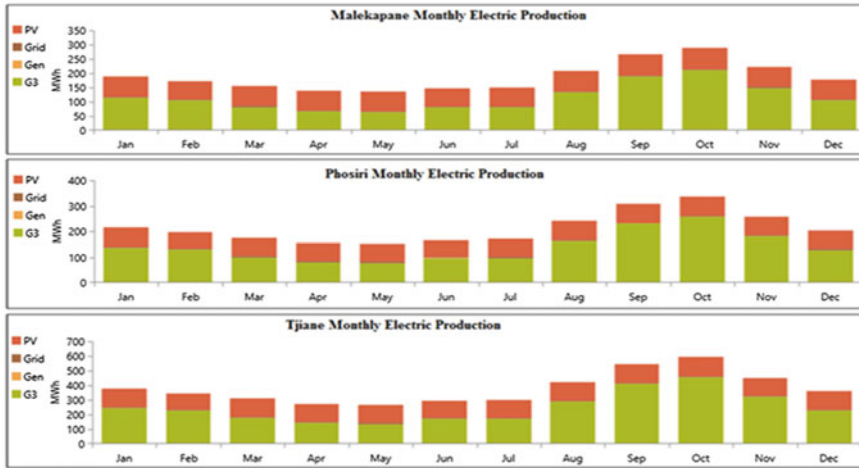


Fig. 8 Average monthly electricity production for each location

architectures produce total electricity of 4,544,353 kWh/yr, 2,579,954 kWh/yr, and 2,254,70 kWh/yr for Tjiane, Phosiri, and Malekapane respectively. The total electricity consumption by the load is 4,185,065 kWh/yr, 2,375,050 kWh/yr, and 2,041,508 kWh/yr for Tjiane, Phosiri, and Malekapane respectively. The results show that the proposed grid-tied hybrid microgrid system architecture is reliable and capable of expanding electricity access and also able to generate enough electricity to satisfy the customer’s load demands. The annual electricity production from PV, Grid, WT, and DG systems, as well as electricity consumption by the loads, are indicated in Table 12.

### 5.5 Emission

The emission results show that the presence of solar PV and wind systems decreases and reduces the number of emissions of different system components. Table 13 shows the pollutant emissions from the optimized MG system architectures as assessed by HOMER software. In this study, DG is used as a backup system of which is a non-renewable module. When comparing the DG system with the proposed optimal MG system architecture, the results show that the optimum system is more environmentally friendly and generates the lowest greenhouse gas emissions through all the other feasible system architectures. It is observed from previous studies that solar PV and wind systems cannot be the only power sources in attaining a steady baseload because they depend on the weather. Hence, these systems have the substantial potential of reducing the use of traditional power sources. From the simulation results, it is quite clear that a mixture of Grid/PV/WT/DG/ Battery/Converter appears to be

**Table 12** Electricity production and consumption for each power source

Components	Production	Percent	Components	Consumption	Percent
<b>Tjiane</b>					
Gen. PV	1.485709	32.7	AC Prim. Load	474.053	11.3
Autosize genset	2.060	0.0453	DC Prim. Load	0	0
Gen. Wind 3 kW	2.967380	65.3	deferrable load	0	0
Grid purchases	89.204	1.96	Grid sales	3.714013	88.7
Total	4.844353	100	Total	4.185066	100
Units	kWh/year	%		kWh/year	%
<b>Phosiri</b>					
Gen. PV	858.062	33.3	AC Prim. Load	264.499	11.1
Autosize genset	1.142	0.0443	DC Prim. Load	0	0
Gen. Wind 3 kW	1.670863	64.8	deferrable load	0	0
Grid purchases	49.887	1.93	Grid sales	2.110551	88.9
Total	2.579964	100	Total	2.375050	100
Units	kWh/year	%		kWh/year	100
<b>Malekapane</b>					
Gen. PV	834.878	37.0	AC Prim. Load	217.289	10.0
Autosize genset	941	0.0417	DC Prim Load	0	0
Gen. Wind 3 kW	1.376408	61.0	deferrable loads	0	0
Grid purchases	42.479	42.479	1.88	1.82433	89.4
Total	2.254706	100	Total	2.041508	100
Units	kWh/year	%		kWh/year	100

a more suitable MG system with a less negative impact on environmental and economic features. The other feasible system architectures are the worst cases because they are having high values of NPC, COE, and also have high carbon emissions with the lowest renewable fraction. These architectures pose economic and environmental concerns of which are not desirable to use in meeting the electricity demand of these three communities.

**Table 13** Comparison of emissions for optimal MG systems

Pollutant	Grid/PV/WT/DG/Batt./Conv.	DG only
<b>Tjiane</b>		
Carbon dioxide	58.234	451.908
Carbon monoxide	11.7	2.849
Hydrocarbons	0.511	124
Particulate matter	0.071	17.3
Sulphur dioxide	249	1.107
Nitrogen oxides	131	2.676
Total	58.626	458.681
Unit	kg/year	kg/year
<b>Phosiri</b>		
Carbon dioxide	32.668	274.526
Carbon monoxide	7.18	1.730
Hydrocarbons	0.313	75.5
Particulate matter	0.044	10.5
Sulphur dioxide	139	672
Nitrogen oxides	73.6	1.626
Total	32.888	278.640
Unit	kg/year	kg/year
<b>Malekapane</b>		
Carbon dioxide	27.814	238.876
Carbon monoxide	6.10	1.506
Hydrocarbons	0.266	65.7
Particulate matter	0.037	9.13
Sulphur dioxide	119	585
Nitrogen oxides	62.7	1.414
Total	28.002	242.456
Unit	kg/year	kg/year

## 5.6 Reliability

Sensitivity analysis was carried out in order to determine the reliability of the system using LPSP calculation (as explained in Sect. 5.1) and other parameters of different architectures. Figure 9 depicts the trend between the LPSP values and the PV output given different number of days of autonomy for Tjiane community. The graph is plotted given a constant battery size of 1204 kWh and a converter of 98 kW. It can be observed that the LPSP is proportional PV power output but does not connote a linear relationship. An interesting point to note is the 2-day autonomy trend which looks better than the 3-day autonomy, thus also showing a non-linear relationship between LPSP and the days of autonomy. Figure 10 depicts the relationship between



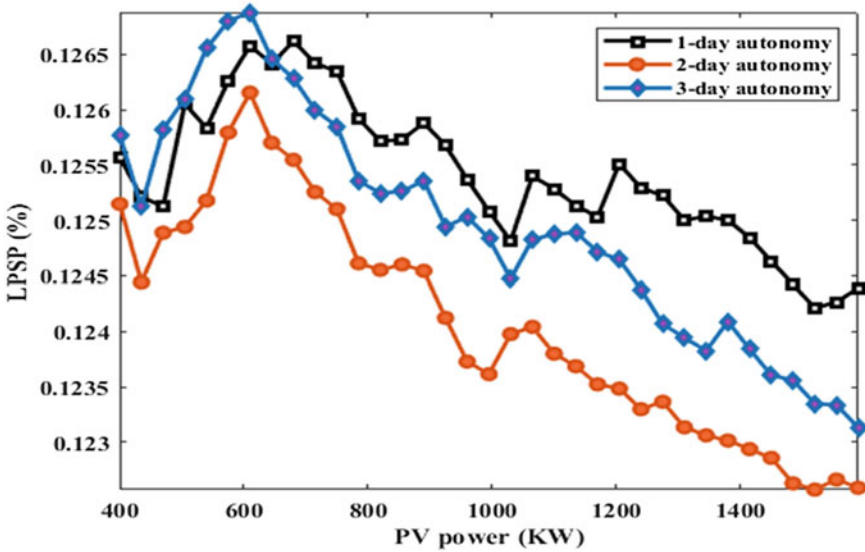


Fig. 9 LPSP versus PV power plot for Tijane community under different number of autonomy days

the LPSP and the NPC of the three communities. The proportionality is observed, showing that a costlier NPC of the project will yield a better LPSP value of the architecture. The same is said for Fig. 11, where a higher ICC is minimized according to a high renewable fraction. An important discussion for developing microgrids is the proper implementation of RES-based generators. There should be a suitable trade-off of implementing RES while maintaining a high system reliability. Figure 12 illustrates the relationship between the renewable fraction of the architecture and its reliability. It is observed that a high renewable fraction tends to adversely affect the reliability of the system. It is also seen that a 3-day autonomy has the best spread of value that improves the reliability but at the expense of a low renewable fraction.

## 6 Conclusion

Subsequent to load profile formulation and assessment of energy resources, a techno-economic analysis consists of the next logical and important stage for optimum design of a hybrid microgrid system. This latter stage of microgrid design incorporates reliability assessment, which evaluates factors such as: LPSP and Output Power; LPSP and NPC; % RF and ICC as well as LPSP and % RF. Based on the assessment of energy resources available in the communities under study as well as on the environmental impacts obtained, the following microgrid architecture is recommended: solar PV, WT, main grid, DG, Battery, and converters. In addition, the less NPC, less

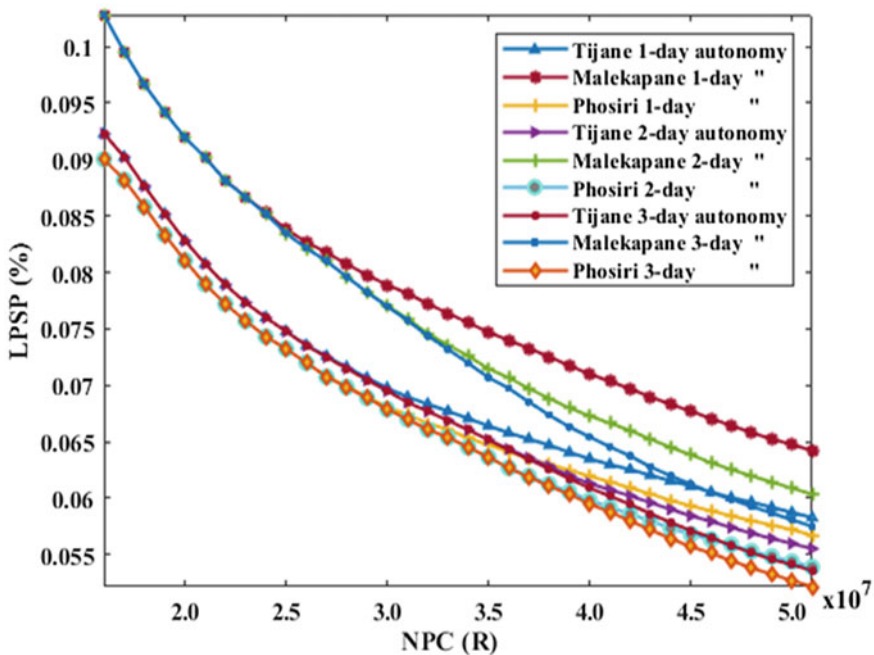


Fig. 10 LPSP vs NPC plot for three communities under different number of autonomy days

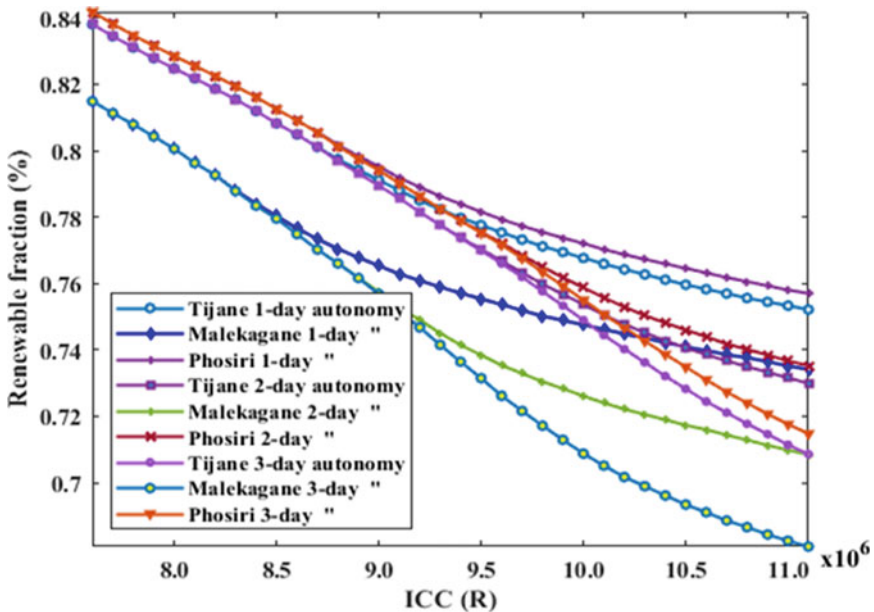
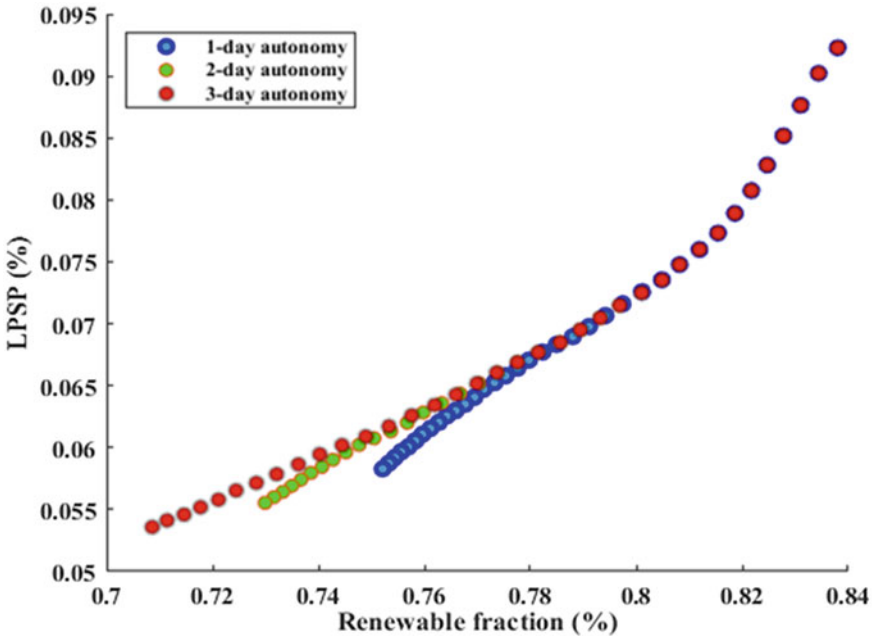


Fig. 11 Renewable fraction and ICC plot for three communities under different number of autonomy days



**Fig. 12** Relationship between the LPSP and renewable fraction values under different number of autonomy days

COE, and a high renewable fraction observed in the three case studies indicates that the proposed hybrid microgrid system could provide reliable electricity supply to these remote communities despite a few disturbances resulting from power prices, power grid mean repair time and power grid frequency failure.

## References

- Williams, N.J., Jaramillo, P., Taneja, J., Ustun, T.S.: Enabling private sector investment in microgrid-based rural electrification in developing countries: a review. *Renew. Sustain. Energy Rev.* **3**, 1268–1281 (2015)
- Chetty, R.: Smart microgrids for rural electrification. In: 23rd Southern African Universities Power Conference (SAUPEC) 2015, pp. 129–133. Johannesburg, South Africa (2015)
- Peerapong, P., Limmeechokchai, B.: Optimal electricity development by increasing solar resources in diesel-based micro grid of island society in Thailand. *Energy Rep.* **3**, 1–13 (2017)
- Walwyn, D.R., Brent, A.C.: Renewable energy gathers steam in South Africa. *Renew. Sustain. Energy Rev.* **41**, 390–401 (2015)
- Ali, A., Li, W., Hussain, R., He, X., Williams, B.W., Memon, A.H.: Overview of current microgrid policies, incentives and barriers in the European Union. *United States China. Sustain.* **9**(7), 1146 (2017). <https://doi.org/10.3390/su9071146>

6. Danisha, M.S.S., Senjyua, T., Funabashiaa, T., Ahmadia, M., Ibrahimia, A.M., Ohtaa, R., Howladera, H., Saboryb, N.R., Sediqia, M.M.: A sustainable microgrid: A sustainability and management-oriented approach. *Energy Procedia*. **159**, 160–167 (2019)
7. Arunkumar, G., Elangovan, D., Sanjeevikumar, P., Nielsen, J.B.H., Leonowicz, Z., Joseph, P.K.: DC grid for domestic electrification. *Energies* **12**(11), 2157 (2019). <https://doi.org/10.3390/en12112157>
8. Zhou, X., Guo, T., Ma, Y.: An overview on microgrid technology. In: *IEEE International Conference on Mechatronics and Automation (ICMA) 2015*, pp. 76–81. Beijing, China (2015)
9. Sarma, S., Jayalakshmi, S.: Hybrid micro grid architectures and challenges. *Int. J. Modern Trends Sci. Technol.* **2**, 109–116 (2016)
10. Nasir, M., Khan, H.A., Zaffar, N.A., Vasquez, J.C., Guerrero, J.M.: Scalable solar dc micrigrids: on the path to revolutionizing the electrification architecture of developing communities. *IEEE Electrification Mag.* **6**, 63–72 (2018)
11. Motjoadi, V., Bokoro, P.N., Onibonoje, M. O.: Review of switching and control techniques of solar microgrids. In: *IEEE PES/IAS Power Africa 2020*, pp. 1–5. Nairobi, Kenya (2020)
12. Torero, M.: The impact of rural electrification: challenges and ways forward. *Rev. Econ. Dev.* **23**, 49–75 (2016)
13. Ellabban, O., Abu-Rub, H., Blaabjerg, F.: Renewable energy resources: current status, future prospects and their enabling technology. *Renew. Sustain. Energy Rev.* **39**, 748–764 (2014)
14. Islam, M.A., Hasanuzzaman, M., Rahim, N.A., Nahar, A., Hosenuzzaman, M.: Global renewable energy-based electricity generation and smart grid system for energy security. *Sci. World J. Hindawi Publishing Corporation*. **2014**, 1–14 (2014)
15. Olorunfemi, T.R., Nwulu, N.I.: Multi-agent based optimal operation of hybrid energy sources coupled with demand response programs. *Sustainability* **13**(14), 7756 (2021). <https://doi.org/10.3390/su13147756>
16. Panwar, N.L., Kaushik, S.C., Kothari, S.: Role of renewable energy sources in environmental protection: a review. *Renew. Sustain. Energy Rev.* **15**, 1513–1524 (2011)
17. Eras-Almeida, A.A., Egado-Aguilera, M.A.: What is still necessary for supporting the SDG7 in the most vulnerable contexts? *Sustainability* **12**(17), 7184 (2020). <https://doi.org/10.3390/su12177184>
18. Chandra, S., Agrawal, S., Chauhan, D.S.: Soft computing based approach to evaluate the performance of solar PV module considering wind effect in laboratory condition. *Energy Rep.* **4**, 252–259 (2018)
19. Hansen, J.M., Xydis, G.A.: Rural electrification in Kenya: a useful case for remote areas in sub-Saharan Africa. *Energy Effic.* **13**, 257–272 (2020)
20. Zhong, H., Tan, Z., He, Y., Xie, L., Kang, C.: Implications of COVID-19 for the electricity industry: a comprehensive review. *CSEE J. Power Energy Syst.* **6**, 489–495 (2020)
21. Blaabjerg, F., Ma, K., Yang, Y.: Power electronics for renewable energy Systems-status and trends. In: *8th International Conference on Integrated Power Electronics Systems (CIPS) 2014*, pp. 1–11. Nuremberg, Germany (2014)
22. Hafeez, M., Hariri, M., Khairunaz, M., Desa, M., Masri, S.: Grid-connected PV generation system-components and challenges: a review. *Energies* **13**(17), 4779 (2020). <https://doi.org/10.3390/en13174279>
23. Canelas, E., Pinto-Varela, T., Sawik, B.: Electricity portfolio optimization for large consumers: Iberian electricity market case study. *Energies* **13**(9), 2249 (2020). <https://doi.org/10.3390/en13092249>
24. Husein, M., Kim, H.J., Chung, I.Y.: The Impact of Policy and Technology Parameters on the Economics of Microgrids for Rural Electrification. *Energies*. **13**(4), 877 (2020). <https://doi.org/10.3390/en13040877>
25. Bhattacharyya, S.C., Palit, D.: Mini-grid based off-grid electrification to enhance electricity access in developing countries: what policies may be required? *Energy Policy* **94**, 166–178 (2016)
26. Wang, T., Gong, Y., Jiang, C.: A review on promoting share of renewable energy by green-trading mechanisms in power system. *Renew. Sustain. Energy Rev.* **40**, 923–929 (2014)

27. Commission, European: Concerning common rules for the internal market in electricity. Off. J. Eur. Union. **211**, 55–93 (2009)
28. Motjoadi, V., Kilimi, M., Bokoro, P. N., Roro, K.: On the review of microgrid systems: benefits, control techniques, and risk analysis. In: IEEE AFRICON, 2021, pp. 1–7. Arusha, Tanzania (2021)
29. Okundamiya, M.S., Ojjeabu, C.E.: Optimum design, simulation and performance analysis of a micro-power system for electricity supply to remote sites. J. Commun. Technol. Electron. Comput. Sci. **12**, 6–12 (2017)
30. Han, Y., Chen, W., Li, Q.: Energy management strategy based on multiple operating states for a photovoltaic/fuel cell/energy storage DC microgrid. Energies **10**(1), 136 (2017). <https://doi.org/10.3390/en10010136>
31. Benalcazar, P., Suski, A., Kaminski, J.: The effects of capital and energy subsidies on the optimal design of microgrid systems. Energies **13**(4), 955 (2020). <https://doi.org/10.3390/en13040955>
32. Kumar, N.M., Chopra, S.S., Chand, A.A., Elavarasan, R.M., Shafullah, G.M.: Hybrid renewable energy microgrid for a residential community: a techno-economic and environmental perspective in the context of the SDG7. Sustainability **12**(10), 3944 (2020). <https://doi.org/10.3390/su12103944>
33. Ahn, J., Oh, Y., Kim, C., Park, C.: Configuration of a renewable micro-power system for a remote village in Mongolia. In: International Smart Grid Conference and Exhibition 2013, pp. 1–6. Cheju, South Korea (2013)
34. Adetunji, K.E., Hofsjajer, I.W., Abu-Mahfouz, A.M., Cheng, L.: A review of metaheuristic techniques for optimal integration of electrical units in distribution networks. IEEE Access **9**, 5046–5068 (2021)
35. Vuc, G., Borlea, I., Barbulescu, C., Prosteian, O., Jigoria-Oprea, D., Neaga, L.: Optimal energy mix for a grid connected hybrid wind – Photovoltaic generation system. In: 2011 IEEE 3rd International Symposium on Exploitation of Renewable Energy Sources (EXPRES), pp. 129–132. Subotica, Serbia (2011)
36. Chel, A., Kaushik, G.: Renewable energy technologies for sustainable development of energy efficient building. Alexandria Eng. J. **57**(2), 655–669 (2018)
37. Azimoh, C.L., Klintonberg, P., Wallin, F., Karlsson, B., Mbohwa, C.: Electricity for development: mini-grid solution for rural electrification in South Africa. Energy Convers. Manage. **110**(15), 268–277 (2016)
38. Jamal, N.: Options for the supply of electricity to rural homes in South Africa. J. Energy Southern Africa **26**(3), 58–65 (2015)
39. Madziga, M., Rahil, A., Mansoor, R.: Comparison between three off-grid hybrid systems (solar photovoltaic, diesel generator and battery storage system) for electrification for Gwakwani Village, South Africa. Environments **5**(5), 57 (2018). <https://doi.org/10.3390/environments5050057>
40. Iqbal, F., Siddiqui, A.S.: Optimal configuration analysis for a campus microgrid: a case study. Protect. Control Modern Power Syst. **2**(23), 1–12 (2017)
41. Muslih, I.M., Abdellatif, Y.N.: Hybrid micro-power station: output power analysis, cost analysis, and environmental impact by using homer modeling software. In: Proceedings of the International Conference on Modelling, Simulation, Identification (IASTED/MSI), pp. 156–162. Innsbruck, Austria (2011)
42. Micangeli, A., Del Citto, R., Kiva, I.N., Santori, S.G., Gambino, V., Kiplagat, J., Vigano, D., Fioriti, D., Poli, D.: Energy production analysis and optimization of mini-grid in remote areas: the case study of Habaswein, Kenya. Energies **10**(12), 2041 (2017)
43. Yong, P.S., Ramasamy, A., Kean, Y.W., Ramachandaramurthy, V.K.: Design of PV/wind hybrid system with improved control strategy for rural area: case study of Sandakan, Malaysia. Indian J. Sci. Technol. **9**(48), 1–5 (2016)
44. Restrepo, D., Restrepo-Cuestas, B., Trejos, A.: Microgrid analysis using HOMER: a case study. DYNA rev.fac.nac.minas. **85**(207), 129–134 (2018)
45. Hafez, O., Bhattacharya, K.: Optimal planning and design of a renewable energy based supply system for microgrids. Renew. Energies **45**, 7–15 (2012)

46. Sureshkumar, U., Manoharan, P. S. and Ramalakshmi, A.P.S.: Economic cost analysis of hybrid renewable energy system using HOMER. In: IEEE-Advances In Engineering, Science And Management (ICAESM), pp. 94–99. Nagapattinam, India (2012)
47. Huang, Z., Zhu, T., Gu, Y., Irwin, D., Mishra, A., Shenoy, P.: Minimizing electricity costs by sharing energy in sustainable microgrids. In: BuildSys'14: Proceedings of the 1st ACM Conference on Embedded Systems for Energy-Efficient Buildings, pp. 120–129. Memphis, Tennessee, USA (2014)
48. Kansara, B.U., Parekh, B.R.: Modelling and simulation of distributed generation system using HOMER software. In: International Conference on Recent Advancements in Electrical, Electronics and Control Engineering (IConRAEeCE'11), pp. 328–332. Tamilnadu, India (2011)
49. Stiel, A., Skyllas-Kazacos, M.: Feasibility study of energy storage systems in wind/diesel applications using the HOMER model. *Appl. Sci.* **2**(4), 726–737 (2012)
50. Fernando, W., Gupta, N., Linn, H.H., Ozveren, C.S.: Design of optimum configuration of a hybrid power system for Abertay University campus. In: IEEE Conference of Russian Young Researchers in Electrical and Electronic Engineering (EIConRus), pp. 1795–1800 (2018)
51. Akindeji, K.T., Tiako, R., Davidson, I.E.: Use of renewable energy sources in university campus microgrid: a review. In: International Conference on the Domestic Use of Energy (DUE), pp. 76–83 (2019)
52. Mejbel Ali, A., Saadoon Algburi, S., Abdelmajed Aljaradin, R.M.: Design Optimization of a Hybrid Hydro-Wind Micropower System for Rural Communities. *J. Eng. Sustain. Dev.* **22**(02), 1–10 (2018)
53. Ghenai, C., Janajreh, I.: Design of solar-biomass hybrid microgrid system in Sharjah. *Energy Procedia* **103**, 357–362 (2016)
54. Masrur, H., Howlader, H.O.R., Lotfy, M.E., Khan, K.R., Guerrero, J.M., Senjyu, T.: Analysis of techno-economic-environmental suitability of an isolated microgrid system located in a remote island of Bangladesh. *Sustainability* **12**(7) (2020)
55. Belu, R.G., Chiou, R., Tseng, T.L.B., Cioca, L.I.: Teaching renewable energy system design and analysis with HOMER. In: ASEE Annual Conference & Exposition, Indianapolis, Indiana (2014)
56. Ghenai, C., Bettayeb, M.: Optimized design and control of an off grid solar PV/hydrogen fuel cell power system for green buildings. In: IOP Conference Series: Earth and Environmental Science (2017)
57. Qolipour, M., Mostafaeipour, A., Tousi, O.: Techno-economic feasibility of a photovoltaic-wind power plant construction for electric and hydrogen production: a case study. *Renew. Sustain. Energy Rev.* **78**, 113–123 (2017)
58. Zhang, Y., Hua, Q.S., Sun, L., Liu, Q.: Life cycle optimization of renewable energy systems configuration with hybrid battery/hydrogen storage: a comparative study. *J. Energy Storage* **30**, 101470 (2020)
59. Ghorbani, N., Kasaeian, A., Toopshekan, A., Bahrami, L., Maghami, A.: Optimizing a hybrid wind-PV-battery system using GA-PSO and MOPSO for reducing cost and increasing reliability. *Energy* **154**, 581–591 (2018)
60. Jung, J., Villaran, M.: Optimal planning and design of hybrid renewable energy systems for microgrids. *Renew. Sustain. Energy Rev.* **75**, 180–191 (2017)
61. Mazzola, S., Vergara, C., Astolfi, M., Li, V., Perez-Arriaga, I., Macchi, E.: Assessing the value of forecast-based dispatch in the operation of off-grid rural microgrids. *Renew. Energy* **108**, 116–125 (2017)
62. Motjoadi, V., Bokoro, P.N., Onibonjoje, M.O.: A review of microgrid-based approach to rural electrification in South Africa: architecture and policy framework. *Energies* **13**(9), 2193–2215 (2020)
63. Samoita, D., Remmen, A., Nzila, C., Østergaard, P.A.: Renewable electrification in Kenya: potentials and barriers. In: Innovation and Renewable Electrification in Kenya (IREK) (2019)
64. Bahramara, S., Moghaddam, M.P., Haghifam, M.R.: Optimal planning of hybrid renewable energy systems using HOMER: a review. *Renew. Sustain. Energy Rev.* **62**, 609–620 (2016)

65. Mohammad, S.T., Al-Kayiem, H.H., Aurybi, M.A., Khlif, A.K.: Measurement of global and direct normal solar energy radiation in Seri Iskandar and comparison with other cities of Malaysia. *Case Stud. Therm. Eng.* **18**, 100591 (2020)
66. Enriquez-Velasquez, E., Obukhov, S., Lozoya-Santos, J., Benitez Baltazar, V.H., Felix-Herran, L.C.: Estimation of solar resource based on meteorological and geographical data: Sonora state in Northwestern territory of Mexico as Case Study. *Energies* **13**, 1–42 (2020)
67. Mabasa, M.B., Botal, J. Ntsangwane, M.L.: Update on the re-establishment of the South African Weather Services (SAWS) Radiometric Network in all six Climatological Regions and the Quality of the Data. In: Proceedings of the South African Solar Energy Conference (SASEC), pp. 25–27. Blue Waters Hotel, KwaZulu-Natal, South Africa (2018)
68. Mabasa, B., Tazvinga, H., Zwane, N., Botal, J., Ntsangwane, L.: Assessment of Global Horizontal Irradiance in South Africa. In: Proceedings of the South African Solar Energy Conference (SASEC), pp. 25–27. Mpekweni Beach Resort, Eastern Cape Province, South Africa (2019)
69. Guaita-Pradas, I., Blasco-Ruiz, A.: Analyzing profitability and discount rates for solar PV Plants. A Spanish case. *Sustainability* **12**(8) (2020)
70. Korkovelos, A., Zerriffi, H., Howells, M., Bazilian, M., Rogner, H.H., Fuso Nerini, F.: A retrospective analysis of energy access with a focus on the role of mini-grids. *Sustainability* **12**(5), 1793 (2020)
71. Mari, C.: Power system portfolio selection under uncertainty. *Energy Syst.* **10**(2), 321–353 (2019)
72. Farret, F.A., Godoy Simões, M.: Micropower system modeling with homer. In: Integration of Alternative Sources of Energy, pp. 379–418. IEEE (2006). <https://doi.org/10.1002/0471755621.ch15>.
73. Akram, U., Khalid, M., Shafiq, S.: Optimal sizing of a wind/solar/battery hybrid grid-connected microgrid system”. *IET Renew. Power Gener.* **12**(1), 72–80 (2018)
74. Katiraei, F., Aguero J. R.: Solar PV integration challenges. *IEEE Power Energy Mag.* **9**, 62–71 (2011)
75. Zhou, J., Zhang, J., Cai, X., Shi, G., Wang, J., Zang, J.: Design and analysis of flexible multi-microgrid interconnection scheme for mitigating power fluctuation and optimizing storage capacity. *Energies* **12**, 11 (2019)
76. Aghamohamadi, M., Mahmoudi, A., Haque, M.H.: Robust allocation of residential solar photovoltaic systems paired with battery units in South Australia. In: IEEE Energy Conversion Congress and Exposition (ECCE), pp. 6673–6679 (2019)
77. Memon, M.A., Bhattu, G.M.: Effect of optimum sized solar PV inverter on energy injected to AC grid and energy loss in Pakistan. *Indian J. Sci. Technol.* **13**(8), 954–965 (2020)
78. Ramli, M.A.M., Hiendro, A., Twaha, S.: Economic analysis of PV/diesel hybrid system with flywheel energy storage. *Renew. Energy* **78**, 398–405 (2015)
79. Peng, Q., Sangwongwanich, A., Yang, Y., Blaabjerg, F.: Grid-friendly power control for smart photovoltaic systems. *Solar Energy* **210**, 115–127 (2020)
80. Sinha, S., Chandel, S.S.: Review of recent trends in optimization techniques for solar photovoltaic-wind based hybrid energy systems. *Renew. Sustain. Energy Rev.* **50**, 755–769 (2015)
81. Ma, C., Dong, S., Lian, J., Pang, X.: Multi-objective sizing of hybrid energy storage system for large-scale photovoltaic power generation system. *Sustainability* **11**(19), 5441 (2019)
82. Lei, C., Meng, J., Stroe, D., Peng, J., Luo, G., Teodorescu, R.: Multi-objective optimization of data-driven model for lithium-ion battery soh estimation with short-term feature. *IEEE Trans. Power Electron.* **35**(11), 11855–11864 (2020)
83. Hannan, M.A., Hoque, M. M., Hussain, A., Yusof, Y., Ker, P.J.: State-of-the-art and energy management system of lithium-ion batteries in electric vehicle applications: issues and recommendations. *IEEE Access* **6**, 19362–19378 (2018)
84. Sawle, Y., Gupta, S.C., Bohre, A.K.: PV-wind hybrid system: a review with case study. *Cogent Eng.* **3**(1) (2016)
85. Chang, W.Y.: The state of charge estimating methods for battery: a review. *ISRN Appl. Math.* **2013** (2013)

86. Adefarati, T., Bansal, R.C.: Reliability, economic and environmental analysis of a microgrid system in the presence of renewable energy resources. *Appl. Energy* **236**, 1089–1114 (2019)
87. Adefarati, T., Bansal, R.C., Justo, J.J.: Reliability and economic evaluation of a microgrid power system. *Energy Procedia* **142**, 43–48 (2017)
88. Elnozahy, A., Abdel-Salam, M.: Financial feasibility of grid-connected PV/wind renewable power generation systems in Egypt. In: *IEEE Conference on Power Electronics and Renewable Energy (CPERE)*, pp. 206–211. Aswan, Egypt (2019)
89. Rahimi, A., Jahangiri, M., Haghgo, Simulation of biogas utilization effect on the economic efficiency and greenhouse gas emission: a case study. *Int. J. Renew. Energy Develop. (IJRED)* **8**(2), 149–160 (2019)
90. Osama Abed Elraouf, M., Mossad, M.I., Alahmar, M., Bendary, F.: Techno-economic analysis of hybrid renewable energy power network for new community in Egypt, case study new El-Farafra oasis. *Int. J. Eng. Res. Adv. Technol.* **4**, 40–55 (2018)
91. Esan, A.B., Agbetuyi, A.F., Oghorada, O., Ogbeide, K., Awelewa, A.A., Afolabi, A.E.: Reliability assessments of an islanded hybrid PV-diesel-battery system for a typical rural community in Nigeria. *Heliyon* **5**(5), 1–13 (2019)
92. Jahanbani, F., Riahy, G., Abedi, M.: Optimal sizing of a stand-alone hybrid wind/PV/battery system considering reliability indices accompanied by error propagation assessment. *Int. Rev. Electr. Eng.* **5**, 748–757 (2010)
93. Dong, W., Li, Y., Xiang, J.: Optimal Sizing of a Stand-Alone Hybrid Power System Based on Battery/Hydrogen with an Improved Ant Colony Optimization. *Energies* **9**(10), 785 (2016)
94. Hosseini, S.J.A.D., Moazzami, M., Shahinzadeh, H.: Optimal sizing of an isolated hybrid wind/PV/battery system with considering loss of power supply probability. *Majlesi J. Electr. Eng.* **11**, 63–69 (2017)
95. Borhanazad, H., Mekhilef, S., Gounder Ganapathy, V., Modiri-Delshad, M., Mirtaheri, A.: Optimization of micro-grid system using MOPSO. *Renew. Energy* **71**, 295–306 (2014)
96. Naderi, M., Bahramara, S., Khayat, Y., Bevrani, H.: Optimal planning in a developing industrial microgrid with sensitive loads. *Energy Rep.* **3**, 124–134 (2017)
97. Miao, C., Teng, K., Wang, Y., Jiang, L.: Technoeconomic analysis on a hybrid power system for the UK household using renewable energy: a case study. *Energies* **13**(12), 3231 (2020)
98. Boke, E., Okutan, H., Aydin, N.: Effect of coal volatile matter on emissions of boiler combustion. In: *27th Annual International Pittsburgh Coal Conference*, Istanbul, Turkey (2010)
99. Cokorilo, O., Ivkovic, I., Kaplanovic, S.: Prediction of exhaust emission costs in air and road transportation. *Sustainability* **11**, 17 (2019)



# **Control of Static Converters, Power Quality, FACTS Devices and Hybrid Circuit Breaker Technology**

# Control of Grid-Connected Voltage Source Converters During Unsymmetrical Faults



Francis Mulolani

**Abstract** In this chapter, a current control scheme for grid-connected voltage source converters during unsymmetrical faults is presented. The method that is being given is based on a modification of direct power control with space vector modulation (DPC-SVM), which makes it ideal for controlling the converter during asymmetrical failures. The presented results show that the control scheme can maintain the magnitude of the current within its rated value and keep the distortion in the current minimal; as well as minimize the oscillations in the power caused by the negative-sequence components of voltage and current.

## 1 Introduction

Grid-connected voltage source converters are widely used in modern power systems. They provide a bridge between the grid and renewable energy sources that are not grid-compatible, such as solar and wind photovoltaic systems. They are also utilized for harmonic filtering and reactive power correction. The current control strategy of grid-connected voltage source converters affects how well they operate. To obtain good dynamic performance during normal operation, conventional current control techniques like voltage-oriented control (VOC) and direct power control with space vector modulation (DPC-SVM) are used. However, during their operation, grid-connected converters get exposed to grid disturbances which can adversely affect their control and performance. The most common grid disturbances are unsymmetrical faults which lead to the flow of high unsymmetrical currents and unsymmetrical voltage dips at the point of connection of the converter to the grid. During unsymmetrical voltage dips there, is, a loss of symmetry in the voltage and current waveforms, and the presence of negative-sequence voltage and current components leads to distortion in the current and oscillations at twice the grid frequency in the power waveforms from the converter.

---

F. Mulolani (✉)

School of Engineering, Copperbelt University, PO Box 21692, Kitwe, Zambia  
e-mail: [fmulolani@cbu.ac.zm](mailto:fmulolani@cbu.ac.zm)

In this chapter, a control strategy based on employing the grid virtual flux's positive-sequence component for grid synchronization and power estimates in a DPC-SVM control strategy is put into practice. By restricting the power references proportionately to the voltage dip, the current is kept to its rated value during faults. Controlling the converter during unsymmetrical failures has the advantage of allowing it to maintain grid connectivity and assist with grid voltage support, which is necessary under current grid standards for renewable energy sources.

## 2 Mathematical Model of a Grid-Connected VSC

The circuit of a three-phase grid-connected voltage source converter is shown in Fig. 1. It consists of a two-level IGBT converter connected to the grid through an LCL filter. The design procedure of the LCL filter is comprehensively described in [1–4].

For modeling purposes, the IGBTs are assumed to be ideal switches. The output of each phase leg is then determined by the switching state of that leg. The switching state is given by  $S_k$ , where  $k = a, b, c$ . A switching state equal to 1 means the upper switch is on while the lower switch is off, and a switching state equal to 0 means the upper switch is off while the lower switch is on. The two switches in a phase leg cannot be on at the same time.

The single-phase equivalent model of the system is shown in Fig. 2. In the figure,  $R_1, R_2, L_1$  and  $L_2$  are the resistances and inductances of the inverter-side and grid-side filter inductors, respectively.

In space vector notation, the inverter voltage is given by:

$$v_{inv} = \frac{2}{3} \left( S_a + S_b e^{j\frac{2\pi}{3}} + S_c e^{-j\frac{2\pi}{3}} \right) \quad (1)$$

**Fig. 1** Grid-connected voltage source converter

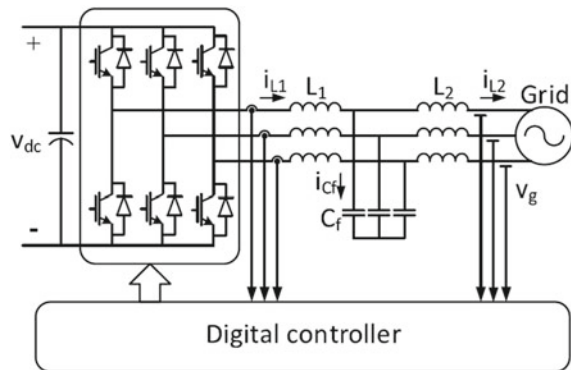
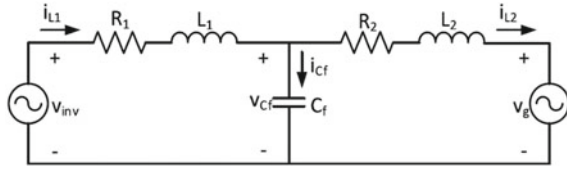


Fig. 2 Single-phase model



The inverter voltage is related to the grid voltage by the equation below:

$$v_{inv} = L \frac{di_L}{dt} + Ri_L + v_g \tag{2}$$

where  $L = L_1 + L_2$ ;  $R = R_1 + R_2$ ;  $v_{inv} = \begin{bmatrix} v_{inva} \\ v_{invb} \\ v_{invc} \end{bmatrix}$  is the inverter voltage.

Space vector;  $v_g = \begin{bmatrix} v_{ga} \\ v_{gb} \\ v_{gc} \end{bmatrix}$  is the grid voltage space vector;  $i_L = \begin{bmatrix} i_{La} \\ i_{Lb} \\ i_{Lc} \end{bmatrix}$  is the

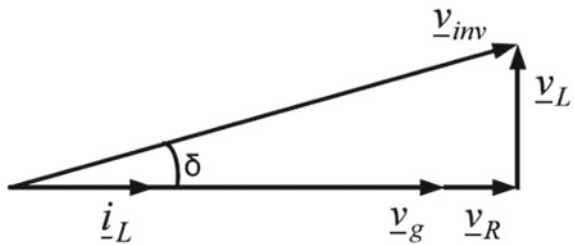
line current space vector.

The effect of the filter capacitor is neglected in the above equations because at frequencies less than half the resonance frequency of the LCL filter, its characteristics are like the L filter.

The phasor diagram of the phase voltage and current is shown in Fig. 3, for a power factor of one. The voltage across the filter resistance is depicted as R and the voltage across the filter inductance is depicted as L.

Since the grid voltage vector is essentially constant, the line current can be controlled by controlling the inverter voltage magnitude and phase angle between the inverter voltage and the grid voltage,  $\phi$ . By regulating both the magnitude and phase angle of the inverter voltage relative to the current demand, the inverter behaves like a controlled current source. The current controller and the modulator set the correct switching sequence of the inverter devices to give the required current.

Fig. 3 Phase diagram of the grid-connected converter



The current can be controlled directly as in the common voltage-oriented current control, or the less common virtual-flux-oriented current control; or it can be controlled by controlling the active power and reactive power, as is the case in direct power control.

### 3 Virtual-Flux-Based Control

The concept of using virtual flux in the control of grid-connected converters makes use of the analogy between inverter-fed AC machine drives and grid-connected converters [5]. In this analogy, the grid is viewed as a virtual AC machine and the grid voltage is visualized as being induced by the time variation of a virtual flux. This makes the grid voltage analogous to the back emf in an AC machine and is given by:

$$v_g = \frac{d\psi_g}{dt} \quad (3)$$

The flux is called the virtual flux and its vector is represented by  $\psi_g$  in Eq. (3). In virtual-flux-based control schemes, the virtual-flux is used in place of the voltage for synchronization and power estimation in direct power control schemes.

The virtual flux cannot be measured directly and is estimated from the grid voltage using:

$$\psi_g = \psi_{g0} + \int v_g dt \quad (4)$$

where  $\psi_{g0}$  is the initial value of the virtual flux.

In practice, direct integration of the grid voltage to obtain the virtual flux is not used because of possible integrator drift and saturation if there is an offset in the measured voltage [6]. The virtual-flux estimation methods in the literature are based on filters that give a phase shift of  $90^\circ$  at the fundamental frequency [6–9]. Due to the use of filters, the distortion in the grid voltage is damped and the virtual-flux vector rotates more smoothly than the grid voltage vector. Thus, the virtual-flux angle can be tracked more easily than the voltage angle even without using a phase-locked loop (PLL) [10]. Virtual flux-based control schemes tend to perform better than voltage-based control schemes in distorted grids [11].

The basic implementation of virtual-flux based DPC-SVM is shown in Fig. 4.

#### 3.1 Coordinate Transformation

The measured voltage and current are transformed from three-phase to the stationary reference frame using the equation below:

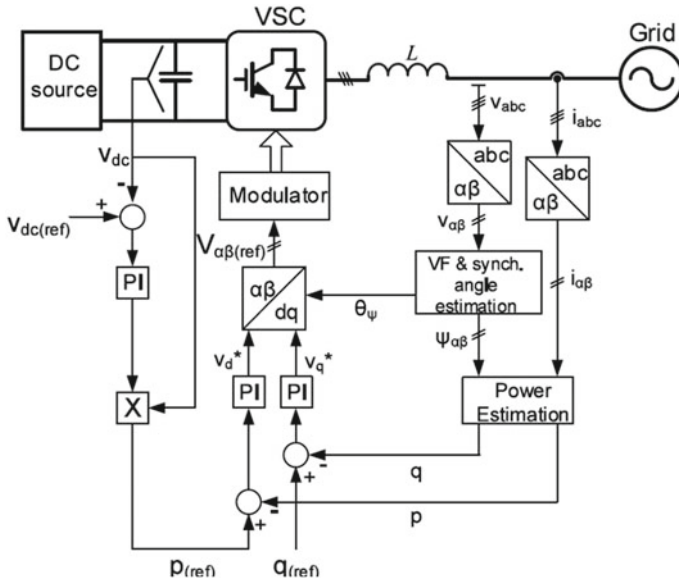


Fig. 4 Virtual-flux-based DPC-SVM

$$v_\alpha + jv_\beta = \frac{2}{3} [v_a + a^2v_b + av_c] \tag{5}$$

where  $v_\alpha$  and  $v_\beta$  are the orthogonal components of the voltage in the stationary reference frame;  $v_a$ ,  $v_b$  and  $v_c$  are the phase voltages and

$$a = 1e^{\frac{j2\pi}{3}}$$

### 3.2 Virtual-Flux Estimation

The virtual flux is estimated from the measured or estimated grid voltage using cascaded first-order low-pass filters. This is a more practically viable method than using pure integrators though it has the drawback of magnitude and phase errors due to frequency variations away from the nominal grid frequency. However, with an expected grid frequency variation of  $\pm 1\%$  of the nominal grid frequency using cascaded low-pass filters gives a maximum magnitude error of  $\pm 1\%$  and a maximum phase error is  $\pm 0.5^\circ$  [12].

The transfer function of the cascaded low-pass filters is given by:

$$G(s) = \frac{\psi_{g\alpha\beta}}{v_{g\alpha\beta}} = \left( \frac{2\omega_o}{s + \omega_o} \right) \left( \frac{\omega_o}{s + \omega_o} \right) \tag{6}$$

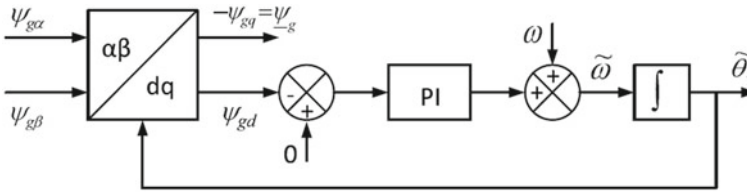


**Fig. 5** Virtual-flux-based PLL

where  $\omega_o$  is the nominal grid frequency.

The multiplication factor of 2 is needed to make the magnitude of the estimated virtual-flux equal to the magnitude of the voltage. The output of the filter is therefore not equal to the virtual flux in Wb, but it is equal to the virtual flux multiplied by the angular frequency, and its unit is Wb rad/s (same as voltage).

### 3.3 Synchronization

Grid synchronization is one of the most important control functions in a grid-connected converter. It involves obtaining information about the grid voltage magnitude, phase angle, and frequency. The phase angle of the grid voltage is useful in synchronizing the switching on and off the semiconductor devices, reference frame transformation of the feedback variables and in the determination and control of the active and reactive power flow [13]. The quality of the synchronization affects the quality of the control. The main synchronization techniques found in the literature are the zero-crossing detector (ZCD) [14, 15] and the phase-locked loop (PLL) [16, 17].

When a virtual flux-based control technique is implemented, the virtual flux can be used for synchronization [5]. The performance of virtual flux-based synchronization can be enhanced for improved operation with distorted and unbalanced grid voltages by using a virtual-flux-based PLL [18]. The block diagram of a virtual-flux-based PLL is shown in Fig. 5.

### 3.4 Power Estimation

In direct power control schemes, the inner control loop controls the active power and the reactive power, which are estimated using the current and the voltage or the virtual flux [19]. The power estimation is based on the instantaneous power theory or p-q theory. The generally agreed definition of instantaneous power is that it consists of at least two components, which are the active power and the reactive power. The active power is the real component, while the reactive power is the imaginary component of the instantaneous power, respectively, as given by the equations below.

$$p = \frac{3}{2} \operatorname{Re}[v \cdot i^*] \quad (7)$$

$$q = \frac{3}{2} \operatorname{Im}[v \cdot i^*] \quad (8)$$

where  $i^*$  is the complex conjugate of the current.

Using the stationary reference frame components of the voltage and the current, Eqs. (7) and (8) can be written as:

$$p = \frac{3}{2} (v_\alpha i_\alpha + v_\beta i_\beta) \quad (9)$$

$$q = \frac{3}{2} (v_\beta i_\alpha - v_\alpha i_\beta) \quad (10)$$

Using the virtual flux for power estimation has been shown to improve the quality of the converter current even in the presence of distorted grid voltage [20]. The active and reactive power estimation using virtual flux is given by the equations below:

$$p = \frac{3}{2} (\psi_\alpha i_\beta - \psi_\beta i_\alpha) \quad (11)$$

$$q = \frac{3}{2} (\psi_\alpha i_\alpha + \psi_\beta i_\beta) \quad (12)$$

### 3.5 Power Control

The power controller consists of a pair of PI controllers which control the active power and the reactive power, respectively. The active power reference is obtained from the outer loop DC voltage controller to maintain an active power balance. The reactive power reference is set to zero to give a power factor of 1, or it can be obtained from an outer control loop for voltage or power factor in reactive power compensation mode.



## 4 Analysis with Unbalanced Grid Voltage

### 4.1 Symmetrical Components

The method of symmetrical components, first proposed by Fortescue, is used to analyze unbalanced three-phase systems. In a set of unbalanced three-phase voltages or currents, each phase voltage or current can be decomposed into three components which are referred to as the positive-sequence component, the negative-sequence component, and the zero-sequence component. The positive-sequence components are a balanced three-phase system, with the phase voltages mutually displaced by  $120^\circ$ , rotating at the fundamental angular frequency with phase-sequence a-b-c. The negative-sequence components are also a balanced three-phase system rotating at the fundamental angular frequency in the opposite direction to the positive-sequence components with phase sequence a-c-b. The zero-sequence components are a set of three in-phase voltages with equal magnitude and no phase shift. The symmetrical components are shown in Fig. 6.

In an unbalanced three-phase system the phase voltages are given by:

$$v_a = v_a^p + v_a^n + v_a^0 \quad (13)$$

$$v_b = v_b^p + v_b^n + v_b^0 \quad (14)$$

$$v_c = v_c^p + v_c^n + v_c^0 \quad (15)$$

where the superscript ' $p$ ' denotes the positive-sequence components, superscript ' $n$ ' denotes the negative-sequence components, and superscript ' $0$ ' denotes the zero-sequence components.

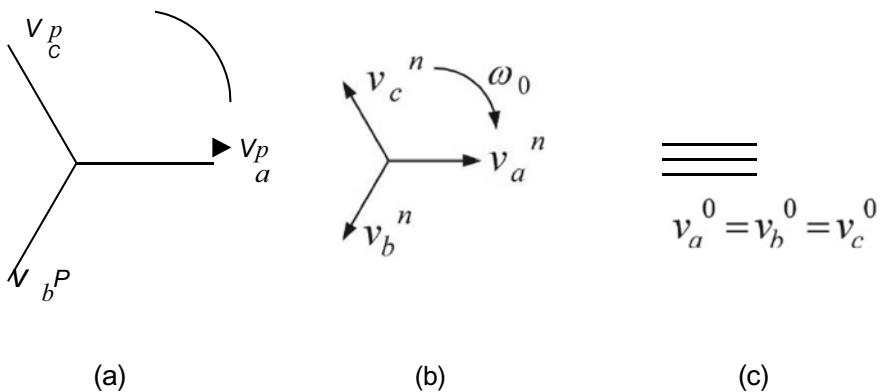


**Fig. 6** Symmetrical components **a** Positive-sequence **b** Negative-sequence **c** Zero-sequence

In a three-phase three-wire system without a neutral connection, the zero-sequence components are not present, and thus will be omitted from the following analysis.

In the stationary reference frame, the unbalanced voltages are given by

$$v_\alpha = v_\alpha^p + v_\alpha^n \quad (16)$$

$$v_\beta = v_\beta^p + v_\beta^n \quad (17)$$

Using space vector notation, the unbalanced voltage vector is given by

$$\underline{v} = \underline{v}^p + \underline{v}^n = |\underline{v}^p| e^{j(\omega t + \theta_p)} + |\underline{v}^n| e^{-j(\omega t + \theta_n)} \quad (18)$$

where  $\underline{v}^p$  is the positive-sequence vector;  $\underline{v}^n$  is the negative-sequence vector;  $\theta_p$  is the angle of the positive-sequence vector, and  $\theta_n$  is the angle of the negative-sequence vector.

The symmetrical components in the stationary reference frame are given by:

$$\begin{bmatrix} v_\alpha^p \\ v_\alpha^n \end{bmatrix} = \frac{1}{2} \begin{bmatrix} 1 & j \\ 1 & -j \end{bmatrix} \begin{bmatrix} v_\alpha \\ v_\beta \end{bmatrix} \quad (19)$$

$$\begin{bmatrix} v_\beta^p \\ v_\beta^n \end{bmatrix} = \frac{1}{2} \begin{bmatrix} -j & 1 \\ j & 1 \end{bmatrix} \begin{bmatrix} v_\alpha \\ v_\beta \end{bmatrix} \quad (20)$$

where the  $j$  operator denotes rotation through  $90^\circ$ .

In the time domain, the space vectors of the symmetrical components are given by:

$$\underline{v}^p(t) = \frac{1}{2} \left[ \underline{v}(t) + j \underline{v}\left(t - \frac{T}{4}\right) \right] \quad (21)$$

$$\underline{v}^n(t) = \frac{1}{2} \left[ \underline{v}(t) + j \underline{v}\left(t - \frac{T}{4}\right) \right] \quad (22)$$

where  $T$  is the periodic time of the grid voltage.

Equations (21) and (22) form the basis of symmetrical component separation methods. The signal is decomposed into its symmetrical components and needs to be delayed in time by a quarter of the fundamental cycle. This is equivalent to a phase shift of  $-90^\circ$ . Any method that can achieve this delay or phase shift would be suitable for symmetrical component separation depending on their suitability in the system under consideration.

## 4.2 *Unsymmetrical Voltage Instantaneous Power*

The unsymmetrical grid voltage during an unsymmetrical voltage dip is given by

$$v_g = v_g^p + v_g^n \quad (23)$$

where  $v_g^p$  is the positive sequence grid voltage vector and  $v_g^n$  is the negative-sequence grid voltage vector.

If the current is imbalanced but does not have harmonic distortion, a comparable expression can be written for it. This is given by

$$i_{L2} = i_{L2}^p + i_{L2}^n \quad (24)$$

where  $i_{L2}$  is the grid current vector;  $i_{L2}^p$  and  $i_{L2}^n$  are its positive and negative-sequence component vectors respectively.

The instantaneous active power and reactive power are demonstrated to be made of constant and oscillating components as illustrated below by using the instantaneous power theory [21] and describing the voltages and currents in terms of their orthogonal stationary reference frame components.

$$p = P_O + P_c \cos(2mt) + P_s \sin(2mt) \quad (25)$$

$$q = Q_O + Q_c \cos(2mt) + Q_s \sin(2mt) \quad (26)$$

where  $P_O$  and  $Q_O$  are the average values of the powers,  $P_c$ ,  $P_s$ ,  $Q_c$  and  $Q_s$  are the amplitudes of the oscillating components of the powers.

The voltage and current components can be used to express each power component, as shown below.

$$P_o = \frac{3}{2} [v_{g\alpha^p} i_{L2\alpha^p} + v_{g\beta^p} i_{L2\beta^p} + v_{g\alpha^n} i_{L2\alpha^n} + v_{g\beta^n} i_{L2\beta^n}] \quad (27)$$

$$Q_o = \frac{3}{2} [v_{g\alpha^p} i_{L2\beta^p} - v_{g\beta^p} i_{L2\alpha^p} + v_{g\alpha^n} i_{L2\beta^n} - v_{g\beta^n} i_{L2\alpha^n}] \quad (28)$$

$$P_c = \frac{3}{2} [v_{g\alpha^n} i_{L2\alpha^p} + v_{g\beta^n} i_{L2\beta^p} + v_{g\alpha^p} i_{L2\alpha^n} + v_{g\beta^p} i_{L2\beta^n}] \quad (29)$$

$$Q_c = \frac{3}{2} [v_{g\alpha^n} i_{L2\beta^p} - v_{g\beta^n} i_{L2\alpha^p} + v_{g\alpha^p} i_{L2\beta^n} - v_{g\beta^p} i_{L2\alpha^n}] \quad (30)$$

$$P_s = \frac{3}{2} [v_{g\alpha^n} i_{L2\alpha^p} - v_{g\beta^n} i_{L2\beta^p} - v_{g\alpha^p} i_{L2\alpha^n} + v_{g\beta^p} i_{L2\beta^n}] \quad (31)$$

$$Q_s = \frac{3}{2}[-v_{g\alpha^n} i_{L2\beta^p} - v_{g\beta^n} i_{L2\alpha^p} + v_{g\alpha^p} i_{L2\beta^n} + v_{g\beta^p} i_{L2\alpha^n}] \quad (32)$$

Grid virtual flux and inverter current are used in the controller to estimate power. The virtual flux estimated from the unsymmetrical grid voltage will be unsymmetrical, while the inverter current will have a similar waveform to the grid current. Thus, the estimated powers will have constant and oscillating components as given in Eqs. (25) and (26). However, the power controllers are unable to control the oscillating powers effectively and the resulting current is unbalanced and distorted and with no current limitation its magnitude could exceed the rated current of the VSC.

To improve the power estimation and synchronization, the positive-sequence grid voltage [22, 23] or virtual flux is used [24]. The positive-sequence virtual flux-based power estimation is described in more detail below.

### 4.3 Instantaneous Power Based on Positive Sequence Virtual Flux

The estimated instantaneous powers made accessible to the power controllers by simply considering the positive-sequence virtual flux is given by:

$$p = \frac{3}{2}(\psi_{g\alpha^p} i_{L1\beta} - \psi_{g\beta^p} i_{L1\alpha}) \quad (33)$$

$$q = \frac{3}{2}(\psi_{g\alpha^p} i_{L1\alpha} + \psi_{g\beta^p} i_{L1\beta}) \quad (34)$$

The grid current will be balanced and devoid of a negative-sequence component since the inverter current is balanced. However, there are negative-sequence components and an imbalance in the grid voltage. Therefore, because of the interplay between the balanced current and the unbalanced voltage, the real power at the grid side will oscillate. The sources of the oscillating power components are:

$$P_c = \frac{3}{2}[v_{g\alpha^n} i_{L2\alpha^p} + v_{g\beta^n} i_{L2\beta^p}] \quad (35)$$

$$Q_c = \frac{3}{2}[v_{g\alpha^n} i_{L2\beta^p} - v_{g\beta^n} i_{L2\alpha^p}] \quad (36)$$

$$P_s = \frac{3}{2}[v_{g\alpha^p} i_{L2\alpha^n} - v_{g\beta^p} i_{L2\beta^n}] \quad (37)$$

$$Q_s = \frac{3}{2}[-v_{g\alpha^p} i_{L2\beta^n} - v_{g\beta^p} i_{L2\alpha^n}] \quad (38)$$

Positive-sequence control reduces power oscillations, as evidenced by a comparison of the magnitudes of the oscillating power components in Eqs. (29) to (32) and those in Eqs. (35) to (38).

### 4.4 Positive-Sequence Virtual Flux Estimation

It is necessary to separate the positive-sequence component of the virtual flux from the unbalanced virtual flux estimated from the unbalanced grid voltage to use it for power estimation and synchronization.

The virtual flux’s positive-sequence components are given by:

$$\psi_{g\alpha^p} = \frac{1}{2}(\psi_{g\alpha} + j\psi_{g\beta}) \tag{39}$$

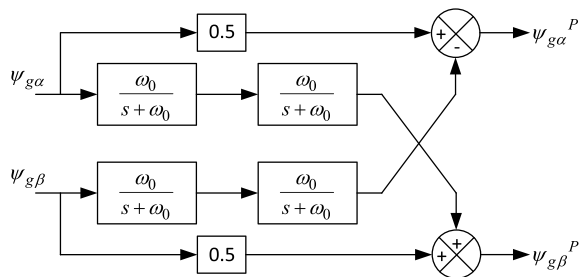
$$\psi_{g\beta^p} = \frac{1}{2}(-j\psi_{g\alpha} + \psi_{g\beta}) \tag{40}$$

where  $j$  represents a 90° counterclockwise rotation of the vector

There are numerous ways described in the literature that can be used to obtain the 90° phase shift. The delayed signal-canceling method is one of them [25, 26]. Using this technique, a signal is delayed by one-fourth of the fundamental time to produce a phase shift. For sequence decomposition and virtual flux calculation, cascaded low-pass filters were first described in [6]. This method is based on these filters. This technique makes use of the 90° phase shift and 0.5 attenuations at the fundamental grid frequency of the cascaded filters. The second method, which is also used to estimate the grid virtual flux, is adopted, and its implementation is illustrated in Fig. 7.

For power estimates, synchronization, and current restriction, the positive-sequence virtual flux is employed.

**Fig. 7** Positive-sequence VF estimation



## 5 Proposed Control Method

The current-carrying capacity of a voltage source converter's IGBTs regulates the maximum permitted current. This in turn establishes the converter's maximum power capacity at nominal voltage. Because the grid voltage typically falls within 10% of its nominal value, the converter may operate regularly without using more current than it can handle. A voltage dip occurs when the grid voltage drops below 90% of its nominal value. For the converter to produce the rated power, its current must increase, which could harm the IGBTs. Unbalance in the voltages, which results in unbalance and distortion in the current exacerbates the issue during unsymmetrical voltage dips. A current limitation method is suggested and put into practice in [12] to safeguard the VSC and restrict the current to safe levels during voltage dips. The steps below describe how the algorithm was derived. A factor  $k$  is used to quantify the voltage's per-unit magnitude during voltage dips.

$$k_1 = \frac{|v_g|}{|v_{gref}|} = \frac{|\psi_g|}{|\psi_{gref}|} \quad (41)$$

where  $|v_g|$  and  $|\psi_g|$  are the magnitudes of the voltage and the virtual flux respectively;  $|v_{gref}|$  and  $|\psi_{gref}|$  are the nominal magnitudes of the voltage and the virtual flux respectively. During a voltage dip, the value of  $k_1$  is less than 0.9 while during normal operation  $k_1 \geq 0.9$ .

The per-unit loading of the VSC is given by a factor  $k_2$  defined as:

$$k_2 = \frac{p}{S} \quad (42)$$

where  $S$  is the nominal apparent power rating of the VSC.

To calculate the converter's active power capacity, the  $k_2$  factor must be employed. The capacity of the system remains unchanged if  $k_2$  is smaller than one. If necessary, a converter can be employed to support reactive power. To prevent overloading the converter, the reactive power is restricted to its capability. The reactive power cap is based on the concept described in [27], according to which the amount of reactive power that a grid connected VSC can offer is only limited by the capacity that isn't being used for active power.

The active power reference is decreased according to the voltage dip if  $k_2 = 1$  and  $k_1 = 0.9$ , and the new active power reference is given by:

$$p'_{ref} = k_1 p_{ref} \quad (43)$$

where  $p'_{ref}$  is the limited active power reference.

The reactive power reference is set to zero since the converter is being used to its full potential for active power.

If  $k_2 < 1$  and  $k_1 \geq 0.9$ , Since the grid voltage, is within the permitted range, the active power reference limitation is not in effect. However, the converter is not entirely filled, and if reactive power is required, the remaining capacitance can be used. The capacity of the converter used inactively is determined by:

$$q_a = \sqrt{S^2 - p_{ref}^2} \quad (44)$$

where  $q_a$  is the capacity of the converter available for reactive power.

The active power reference is decreased as indicated in if  $k_2 < 1$  and  $k_1 < 0.9$ .

Equation (29). The converter's capacity that is not being used to generate active electricity is provided by:

$$q_a = \sqrt{\left((k_1 S)^2 - (k_2 p'_{ref})^2\right)} \quad (45)$$

Equations (41) outline the current limiting algorithm's use to (45) makes sure that, both during regular operation and, more crucially, during voltage dips, the converter is operated safely without going over its current rating. Figure 4 depicts the current limiting algorithm's flowchart. Every sampling cycle involves one implementation of the algorithm.

Figure 8 depicts the block diagram of the control strategy with positive-sequence virtual flux control and current restriction. With the settings listed in Table 1, the grid-connected converter and its controller are simulated in Matlab/Simulink. The per-unit system, which uses the peak values of the phase voltage and the line current as base voltage and base current, respectively, enables comparison of systems with various power and voltage levels.

## 6 Simulation Results

The dynamic performance of the control system is shown in Fig. 9. In Fig. 9a, the active power reference is increased from 0.5 to 1 p.u., and in Fig. 9b the reactive power reference is increased from 0.5 to 1 pu. In both cases, the controller showed a fast-dynamic response, which makes it suitable for use during grid disturbances.

When the single-phase voltage dips by 50% in phase-a during an unsymmetrical failure, the system's performance is examined for various active power and reactive power levels. Comparing and contrasting the outcomes of the proposed positive-sequence virtual flux control with current limiting and the results of the traditional direct power control with space vector modulation (DPC-SVM).

The converter is supplying the grid with its rated active power and no reactive power as the first example under investigation. Figure 10a for the traditional DPC-SVM control and Fig. 10b for the positive-sequence VF control with current limiting both displays the results obtained during the voltage dip. The current is twisted in

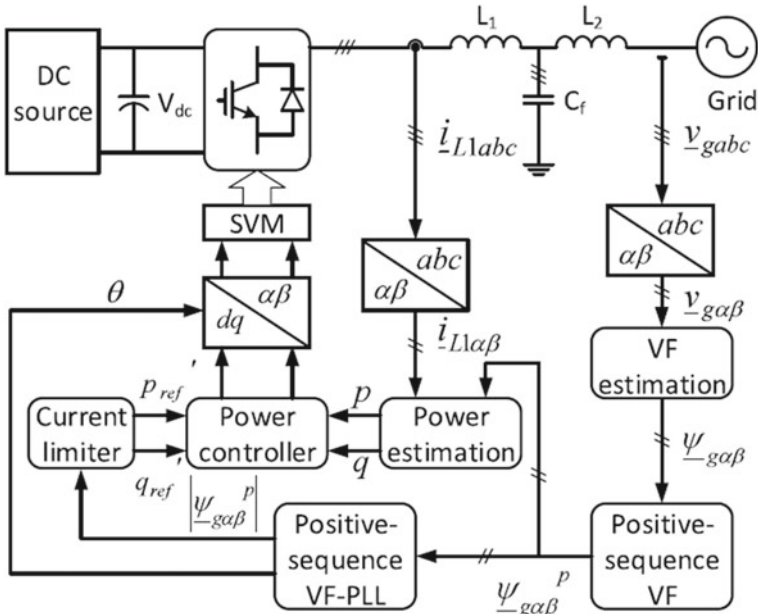


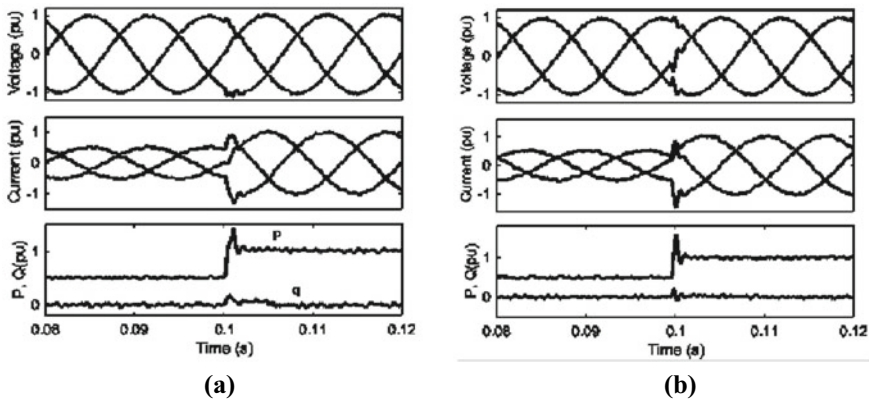
Fig. 8 Block diagram of the proposed control scheme

Table 1 Parameters of simulation model

Parameter	Value
Rated power, Pn	100 kW
Grid voltage, VL	415 V
Grid frequency, f	50 Hz
DC voltage, Vctc	800 V
Inverter side inductance, L1	0.35 mH
Grid side inductance, L2	0.1 mH
Filter capacitor, Cr	90 μF
Sampling frequency, fs	10 kHz
Switching frequency, fsw	10 kHz
Base power, Sb	100 kVA
Base voltage, Vb	339 V
Base current, lb	197 A

Fig. 10a, and the peak values of the currents in phases b and c exceed 1 pu. For all phases, the current average total harmonic distortion (THD) is 19.8%. The double grid frequency oscillations in both the active and reactive power have a peak-to-peak value of 0.8 pu. Figure 10 shows a balanced, sinusoidal current with a peak value of just 1 pu and an average THD of 2.58%. The active power and reactive power still





**Fig. 9** Dynamic performance to a step change in **a** active power **b** reactive power

exhibit double grid frequency fluctuations, but their peak-to-peak values have been decreased to 0.35 and 0.65 pu, respectively.

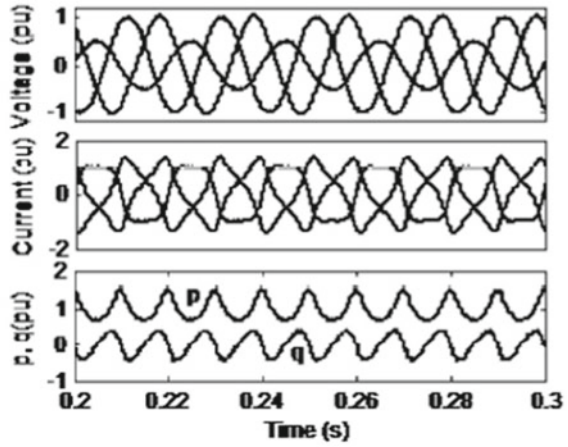
The converter delivering its rated reactive power but zero active power is the second scenario examined. Figure 1a for the traditional DPC-SVM and Fig. 1b for the positive-sequence VF with current limiting both displays the results. Although the peak value of the current in all phases is approximately 1 pu, Fig. 1a shows that the current is imbalanced and distorted with an average THD of 19%. The oscillations in active power and reactive power have peak-to-peak values of 0.77 and 0.43 pu, respectively. The current in Fig. 1b is balanced, sinusoidal, and has a maximum peak value of 1 pu and an average THD of 2.22%. Peak-to-peak values for the oscillations in active power and reactive power are 0.4 and 0.2 pu, respectively.

The converter is delivering 0.8 pu of active power and 0.6 pu of reactive power in the third case under investigation. The outcomes are displayed in Fig. 11.

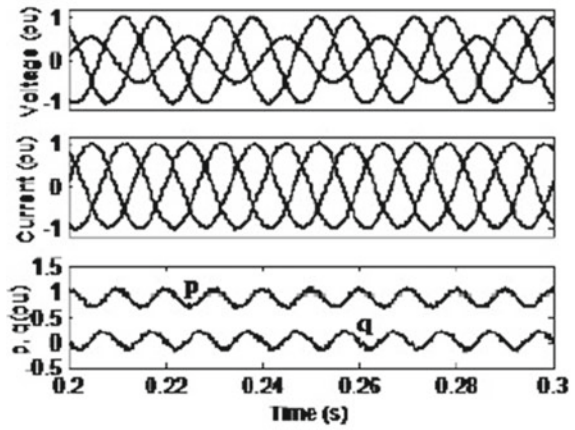
Figure 12a, b show the traditional DPC-SVM and the positive sequence VF with current limiting, respectively. The currents in Fig. 12a are imbalanced and distorted, with the current in phase-c having the maximum peak value exceeding 1 pu and an average THD of 18.6%. The oscillations in the active power and the reactive power have a peak-to-peak value of 0.75 pu. In Fig. 12b, the current is balanced, sinusoidal, and has a maximum value of 1 pu and an average THD of 2.41%. Peak-to-peak oscillations in both active and reactive power have been reduced to 0.35 pu.

Positive-sequence virtual-flux control has been successful in all of the aforementioned circumstances in reducing the current's distortion and imbalance significantly. Additionally, there is a notable reduction in the magnitude of the oscillations in both the active and reactive power. This is so that the current's magnitude is kept to its rated value in each phase and the current's negative-sequence component is eliminated. This demonstrates unequivocally that the proposed positive-sequence virtual-flux control is appropriate for controlling a grid-connected converter during unsymmetrical voltage dips at various active and reactive power levels.

**Fig. 10** Simulation results with active power output  
**a** conventional DPC-SVM  
**b** positive-sequence VF with current limiting



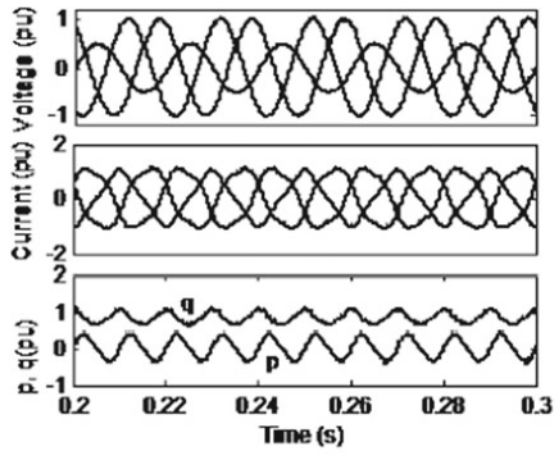
(a)



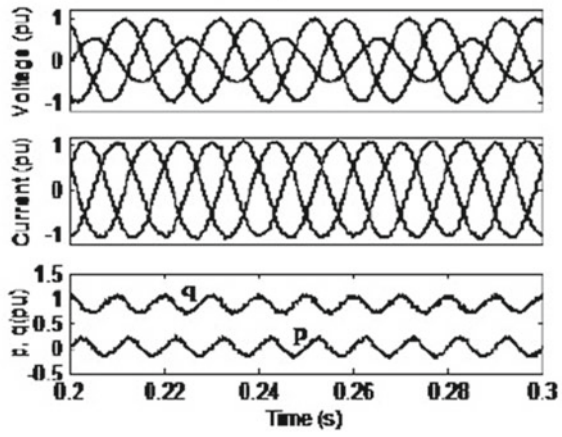
(b)

A comparison of the average distortion in the line currents, the peak magnitude of the line currents, and the average value of the peak-to-peak power oscillations achieved with the two control schemes is summarized in Table 2.

**Fig. 11** Simulation results with reactive power output  
**a** conventional DPC-SVM  
**b** positive-sequence VF with current limiting

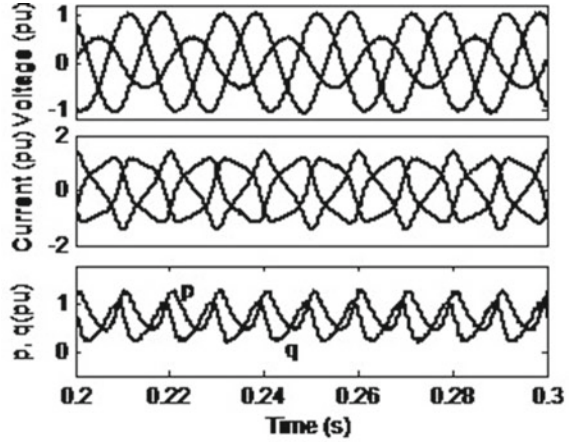


(a)

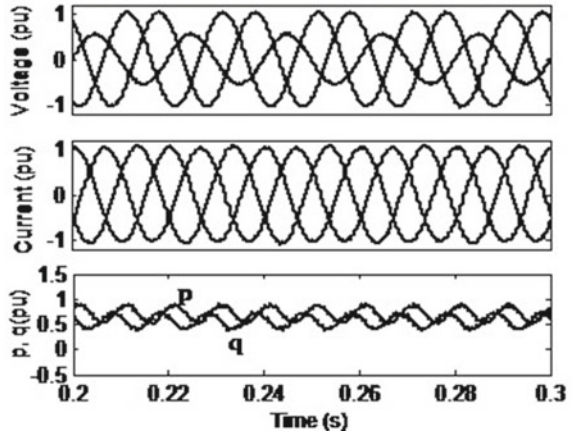


(b)

**Fig. 12** Simulation results with active and reactive power output **a** conventional DPC-SVM **b** positive-sequence VF with current limiting



(a)



(b)

**Table 2** Comparison of results for DPC-SVM and positive-sequence VF with current limiting

Control scheme	Converter output	Current THD (%)	Peak current (pu)	Ave power oscillations (pu)
DPC-SVM	P only	31	>1	0.7
	P and Q	30	>1	1.0
	Q only	29	>1	0.6
Positive sequence VF	P only	3	1	0.375
	P and Q	3.8	1	0.4
	Q only	3.3	1	0.375

## 7 Conclusion

This chapter describes how to control a grid-connected voltage source converter when there are unsymmetrical voltage dips. When the voltage dips are asymmetrical, the control concentrates on restricting the current and injecting balanced, sinusoidal currents. The suggested control synchronizes the grid and estimates power using the positive-sequence virtual flux. A current limitation algorithm has been suggested and put into practice in simulations and experiments to limit the current. The current limiting algorithm has been proven for the unsymmetrical voltage drop, which is the more frequent and worst case scenario. It can operate for both symmetrical and unsymmetrical voltage dips. The results of the simulation demonstrate that the control goals are met, and the VSC can withstand grid voltage fluctuations without risking damage to the semiconductor devices because the current is restricted to the converter's rated capacity.

## References

1. Liserre, M., Blaabjerg, F., Hansen, S.: Design and control of an LCL-filter-based three-phase active rectifier. *IEEE Trans. Ind. Appl.* **41**, 1281–1291 (2005)
2. Liserre, M., Blaabjerg, F., Dell' Aquila, A.: Step-by-step design procedure for a grid-connected three-phase PWM voltage source converter. *Int. J. Electron.* **91**, 445–460 (2004)
3. Rockhill, A.A., Liserre, M., Teodorescu, R., Rodriguez, P.: Grid-filter design for a multi-megawatt medium-voltage voltage-source inverter. *IEEE Trans. Industr. Electron.* **58**, 1205–1217 (2011)
4. Ahmed, K.H., Finney, S.J., Williams, B.W.: Passive filter design for three-phase inverter interfacing in distributed generation. In: *Compatibility in Power Electronics, 2007. CPE '07*, pp. 1–9 (2007)
5. Duarte, J.L., Van Zwam, A., Wijnands, C., Vandenput, A.: Reference frames fit for controlling PWM rectifiers. *IEEE Trans. Industr. Electron.* **46**, 628–630 (1999)
6. Kulka, A.: *Sensorless Digital Control of Grid Connected Three-Phase Converters for Renewable Sources*. Ph.D., Department of Electric Power Engineering, Norwegian University of Science and Technology, Trondheim (2009)
7. Bhattacharya, S., Veltman, A., Divan, D.M., Lorenz, R.D.: Flux-based active filter controller. *IEEE Trans. Ind. Appl.* **32**, 491–502 (1996)
8. Hao, L., Guojun, T., Jinghuan, F., Xuanqin, W.: Study of multi-level rectifier in high power system based on a novel virtual flux observer. In: *Power Electronics and Motion Control Conference, 2009. IPEMC '09. IEEE 6th International*, pp. 1618–1621 (2009)
9. Guojun, T., Hao, L., Jinghuan, F., Meng, L.: Study of Multi-level Active Power Filter Control without phase-locked-loop. In: *Power and Energy Engineering Conference (APPEEC), 2010 Asia-Pacific*, pp. 1–4 (2010)
10. Suul, J.A., Undeland, T.: Flexible reference frame orientation of virtual flux-based dual frame current controllers for operation in weak grids. In: *PowerTech, 2011 IEEE Trondheim*, pp. 1–8 (2011)
11. Malinowski, M., Marques, G., Cichowlas, M., Kazmierkowski, M.P.: New direct power control of three-phase PWM boost rectifiers under distorted and imbalanced line voltage conditions. In: *IEEE International Symposium on Industrial Electronics, 2003. ISIE '03*, vol. I, pp. 438–443 (2003)

12. Mulolani, F.: Performance of Direct Power Controlled Grid-connected Voltage Source Converters. PhD Thesis, School of Electrical and Electronic Engineering, Newcastle University, Newcastle Upon Tyne (2017)
13. Kaura, V., Blasko, V.: Operation of a phase locked loop system under distorted utility conditions. In: Applied Power Electronics Conference and Exposition, 1996. APEC '96. Conference Proceedings 1996, Eleventh Annual, vol. 2, pp. 703–708 (1996)
14. Mur, F., Cardenas, V., Vaquero, J., Martinez, S.: Phase synchronization and measurement digital systems of AC mains for power converters. In: Power Electronics Congress, 1998. CIEP 98. VI IEEE International, pp. 188–194 (1998)
15. Choi, J.W., Kim, Y.K., Kim, H.G.: Digital PLL control for single-phase photovoltaic system. *IEE Proc.-Electric Power Appl.* **153**, 40–46 (2006)
16. Chung, S.K.: Phase-locked loop for grid-connected three-phase power conversion systems. *IEE Proc.-Electric Power Appl.* **147**, 213–219 (2000)
17. Arruda, L.N., Silva, S.M., Filho, B.J.C.: PLL structures for utility connected systems. In: Industry Applications Conference, 2001. Thirty-Sixth IAS Annual Meeting. Conference Record of the 2001 IEEE, vol. 4, pp. 2655–2660 (2001)
18. Serpa, L.A., Ponnaluri, S., Barbosa, P.M., Kolar, J.W.: A modified direct power control strategy allowing the connection of three-phase inverters to the grid through LCL filters. *IEEE Trans. Ind. Appl.* **43**, 1388–1400 (2007)
19. Malinowski, M., Jasinski, M., Kazmierkowski, M.P.: Simple direct power control of three-phase PWM rectifier using space-vector modulation (DPC-SVM). *IEEE Trans. Industr. Electron.* **51**, 447–454 (2004)
20. Malinowski, M., Kazmierkowski, M.P., Hansen, S., Blaabjerg, F., Marques, G.D.: Virtual-flux-based direct power control of three-phase PWM rectifiers. *IEEE Trans. Ind. Appl.* **37**, 1019–1027 (2001)
21. Akagi, H., Watanabe, E.H., Aredes, M.: *Instantaneous Power Theory and Applications to Power Conditioning*. Wiley (2007)
22. Kabiri, R., Holmes, D.G., McGrath, B.P.: Control of active and reactive power ripple to mitigate unbalanced grid voltages. *IEEE Trans. Ind. Appl.* **52**, 1660–1668 (2016)
23. Rodriguez, P., Timbus, A.V., Teodorescu, R., Liserre, M., Blaabjerg, F.: Flexible active power control of distributed power generation systems during grid faults. *IEEE Trans. Industr. Electron.* **54**, 2583–2592 (2007)
24. Suul, J.A., Luna, A., Rodriguez, P., Undeland, T.: Voltage-sensor-less synchronization to unbalanced grids by frequency-adaptive virtual flux estimation. *IEEE Trans. Industr. Electron.* **59**, 2910–2923 (2012)
25. Svensson, J., Bongiorno, M., Sannino, A.: Practical implementation of delayed signal cancellation method for phase-sequence separation. *IEEE Trans. Power Deliv.* **22**, 18–26 (2007)
26. Cardenas, R., Diaz, M., Rojas, F., Clare, J.: Fast convergence delayed signal cancellation method for sequence component separation. *IEEE Trans. Power Deliv.* **30**, 2055–2057 (2015)
27. Mulolani, F., Armstrong, M., Zahawi, B.: Modeling and simulation of a grid-connected photovoltaic converter with reactive power compensation. In: 9th International Symposium on, Communication Systems, Networks & Digital Signal Processing (CSNDSP), pp. 888–893 (2014)

# Power Quality Control of a PV-Assisted Realistic Microgrid Structure



Jitender Kaushal and Prasenjit Basak

**Abstract** The power quality-related challenges in microgrid operation and control are influenced by the voltage sag/swell, frequency, THD, and power factor as per the nature of local loads and the geographical location of distributed energy resources (DERs). The relationship between power quality and the set of these variables is non-linear in nature. To maintain a proper balance among the power quality parameters, conventional and static solutions are available in the power engineering market such as voltage regulators, battery backup, protection devices, uninterruptible power supply (UPS), etc. The biological-inspired techniques are also used to enhance the power quality of the microgrid like artificial neural network (ANN) based control keeping the boundaries of IEEE/IEC standards. The realistic PV-assisted microgrid model is considered in this chapter with the effect of line impedance on the power quality parameters. This model is extended to a large-size realistic microgrid structure for the feasibility of control methodology. The realistic microgrid structure is verified under the variation of load profile, solar irradiance, line impedance, and communication delay in breaker operation. The importance of power quality with protection and reliability is also discussed in this chapter for the motivation of the readers.

**Keywords** Realistic microgrid structure · Power quality · Photovoltaic · Line impedance communication delay

---

J. Kaushal (✉)

Apex Institute of Technology, Chandigarh University, Mohali, Punjab, India

e-mail: [jitender.e14621@cumail.in](mailto:jitender.e14621@cumail.in)

P. Basak

Electrical and Instrumentation Engineering Department, Thapar Institute of Engineering and Technology, Patiala, India

e-mail: [prasenjit@thapar.edu](mailto:prasenjit@thapar.edu)

## 1 Introduction

Power quality plays a very important role in low voltage (LV) grids due to the close connection of the commercial, industrial, and domestic loads. Since the microgrid is built up in the form of an LV grid comprising a combination of the DERs. Due to the different generating and load profile constraints, it becomes very important to maintain the power quality within its allowable range as per the IEEE/IEC standards [1]. The power quality for both power suppliers and consumers is maintained using custom power devices. These devices are installed to investigate the status of voltage sag/swell, THD, power factor, frequency, and unbalanced system [2, 3]. In the case of an LV grid/microgrid, the acceptable range of the voltage deviation must lie within 10% of its nominal value as per IEEE Std. 1250-2011. The allowable change in frequency should be  $\pm 0.1$  Hz as framed in IEEE Std. 1159-2009. The voltage or current THD level should not be more than 5% as listed in IEEE Std. 519-2014 and the power factor of the LV power system must be equal to or greater than 0.9 as appended in IEC 60831-1/2 standard [4]. The above problems show an effective and reliable requirement of the controller which needs to be installed at the load centers. The protection and control of a real-time system could be predicted for voltage and frequency using ANN [5]. The main aim and objectives of this chapter are listed below to explore the operating condition of microgrid systems and loads.

- Why is the term ‘power quality’ important in the smooth operation of a microgrid system?
- Definition of power quality in reference to the microgrid operation and control.
- Problems associated with power quality while integrating the DERs of different natures and capacities.
- Power quality issues and mitigation for the healthy operation and control of the microgrid system.

## 2 System Description and Methodology

The power quality is associated mainly with three terminologies such as problems, issues, and mitigations due to the integration of DERs. The realistic microgrid structure is implemented to assess the status of power quality parameters such as voltage variation (sag/swell), frequency, total harmonic distortion (THD), and power factor.

### 2.1 System Description

The realistic microgrid structure comprises three clusters of microgrids that are MG1, MG2, and MG3. The realistic microgrid structure comprises photovoltaic (PV) generators, a utility grid, and local loads. The PV modules are connected to the utility grid



through a 3-level voltage source converter (VSC) without having the battery energy storage (BES) systems. Hence, the entire microgrid structure is supplying the loads in two zones. In the first zone, the load demand is fulfilled by PV during day hours when solar irradiance is available. During night hours, the load demand is supplied from the utility grid because the PV generation is not charged while satisfying the second zone.

The variations in PV generators have been initiated under grid-connected and islanded modes of operation. Depending upon the availability of the solar irradiance level, accordingly, the loads are curtailed or adjusted. The continuous supply to the critical loads is maintained by the utility grid in case of any failures or non-availability of PV generation. Different cases have been created through which the performance of the microgrid can be assessed especially for the power quality-related parameters. The effect of line impedance on microgrid operation and control is also considered in this study. Figure 1 shows the three-phase realistic microgrid structure which includes three small clusters of microgrids MG1, MG2, and MG3. These clusters have a total generation capacity of 20 kW as a break-up of each 5 kW in MG1, MG2, and 10 kW in MG3. All three buses of the MGs have the same line distance of 600 m from the point-of-common coupling (PCC) on the utility grid side bus as shown in Fig. 1. The utility grid is connected to PCC through a three-phase step-down transformer 40 kVA, 11 kV/440 V.

The maximum irradiance level of the PV module is  $1000 \text{ W/m}^2$  and the minimum is set to  $500 \text{ W/m}^2$  as shown in Fig. 2a. The atmospheric temperature varies from 25 to 45 °C in reference to the different irradiance levels as presented in Fig. 2b. It is assumed that the irradiance level is lowered from 1000 to  $500 \text{ W/m}^2$  in the interval of 0.5 to 1.0 s. From 1.0 to 1.5 s, the irradiance level is kept constant at  $500 \text{ W/m}^2$ . The islanded condition is initiated at 1.5 s and the irradiance level is increased immediately to  $1000 \text{ W/m}^2$  up to 2.5 s.

## 2.2 Schematic and Methodology

The PV generator connected to the utility grid is shown in Fig. 3 which represents one set of the DER within the cluster of microgrids such as MG1, MG2, and MG3. The PV array generates output as per the variation in two input signals which are irradiance and temperature levels. The variations in irradiance and temperature levels are already presented in Fig. 2a, b respectively. It is assumed that the proposed system is running under grid-connected mode from 0 to 1.5 s and 2 to 2.5 s while the islanded operation is initiated from 1.5 to 2 s. The output of the PV array is fed to the buck-boost converter to make the constant DC voltage. Now, this voltage is supplied to the 3-level voltage source converter (VSC) which converts DC into controlled three-phase AC voltage. Each power electronic switch is protected by parallel connected series RC snubber circuits. The output terminals of the VSC are connected to the circuit breaker or PCC to perform on-grid and off-grid operations.

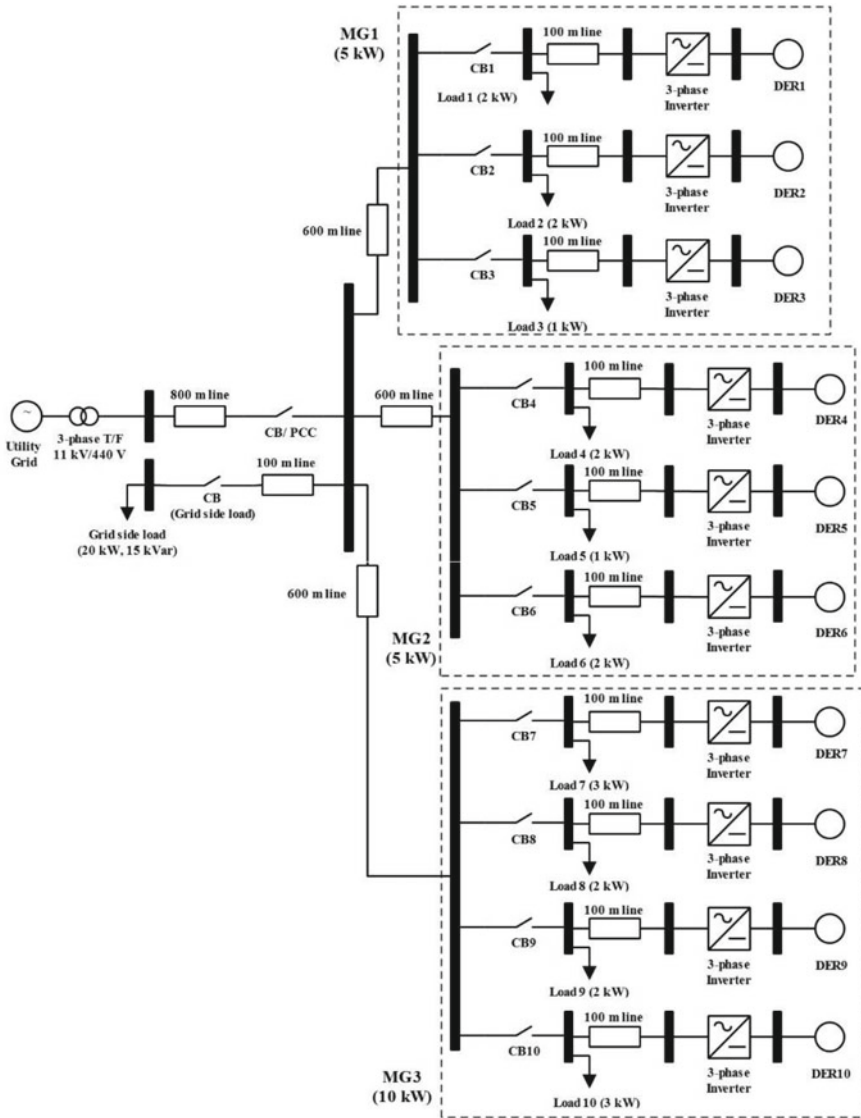


Fig. 1 Realistic three-phase microgrid structure with the consideration of line impedances

The maximum power point tracking (MPPT) is initiated by the use of the incremental conductance method which is a basic approach of the MPPT controller. The PWM switching of the boost control is considered as 5 kHz with an initial value of duty cycle as 0.5. Maximum power point is obtained when  $dP/dV = 0$  where  $P = VI$ .

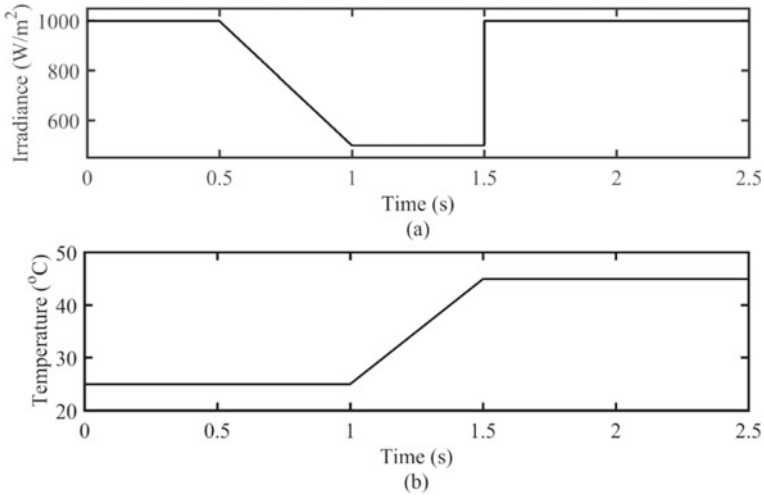


Fig. 2 PV module profile variation of a irradiance level and b temperature

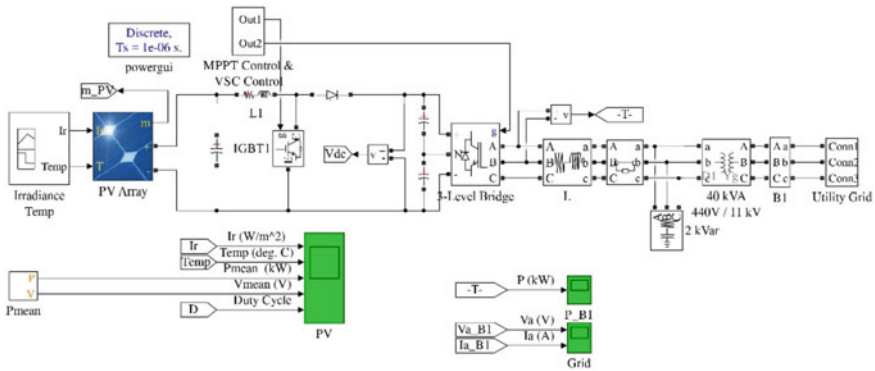


Fig. 3 Simulation diagram of one DER connected to the utility grid

$$d(VI)/dV = I + VdI/dV = 0$$

$$dI/dV = -I/V$$

Also,  $dI$  and  $dV$  are the fundamental components of  $I$  and  $V$  ripples measured respectively.  $I$  and  $V$  are the mean measured values of current and voltage respectively. The error  $(dI/dV + I/V)$  is reduced by the integral regulator and the regulator output is equivalent to the duty cycle correction.

The VSC controller generates the 3-level PWM pulses with the help of a DC voltage regulator and current regulator. Both regulators are further supported by the PI controllers which renovate the measured values of voltage and current into the reference signal for the generation of controlled PWM pulses. The calculations of

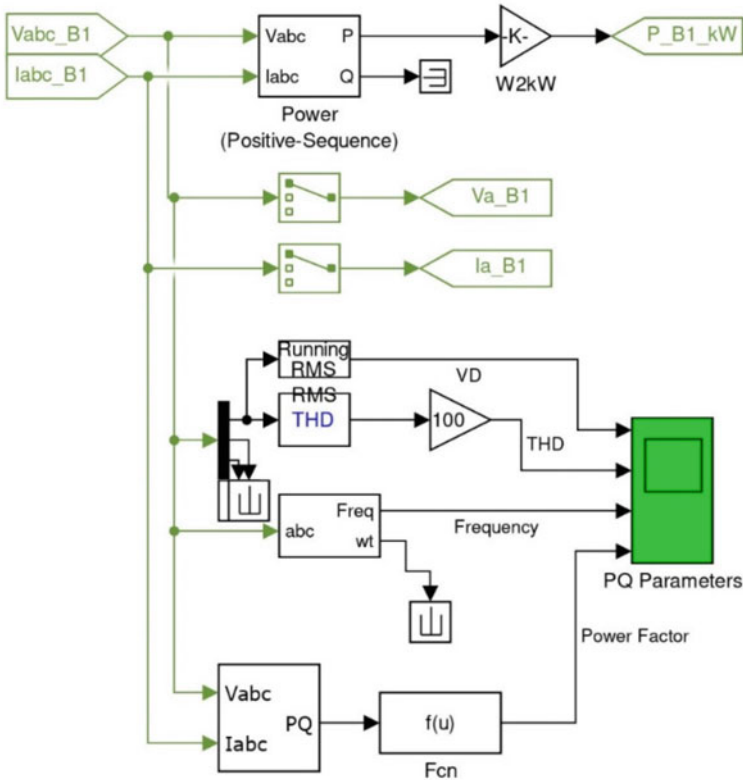
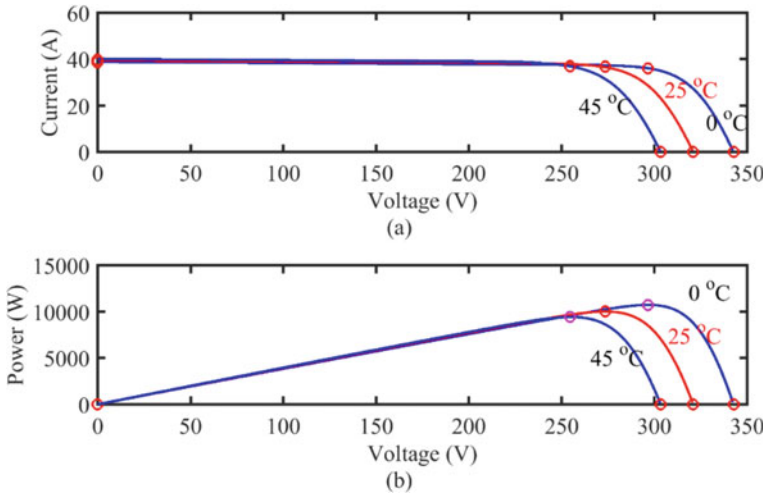


Fig. 4 Subsystem for the calculation of power quality parameters

power quality related parameters such as voltage variation, frequency, THD, and power factor are shown in Fig. 4.

The PV array is implemented with the parallel connected string modules. The I–V and P–V characteristics of the PV array are shown in Fig. 5a, b respectively in reference to Fig. 2. The maximum power is tracked at two operating temperatures that are 25 and 45 °C to perform on-grid and off-grid conditions.

The proposed model is simulated for 2.5 s out of which islanding or off-grid operation is initiated at 1.5 s. So, during the transition period the transients have been observed in the voltage, active power and duty cycle waveforms as shown in Fig. 6a–c. In Fig. 6b, the active power generation waveform is following the irradiance profile as presented in Fig. 2a where irradiance level 1000 W/m<sup>2</sup> is lowered to 500 W/m<sup>2</sup> from 0.5 to 1.0 s and kept constant up to 1.5 s. The PV module generates 20 and 10 kW when the irradiance level is 1000 and 500 W/m<sup>2</sup> respectively. Due to the sudden switching of off-grid mode, the irradiance level is immediately increased



**Fig. 5** PV module profile of **a** I-V characteristics and **b** P-V characteristics

to  $1000 \text{ W/m}^2$  at 1.5 s with the assumption that solar energy is fully available. So, once the irradiance level reaches  $1000 \text{ W/m}^2$  after 1.5 s the system will start again to generate 20 kW as shown in Fig. 6b.

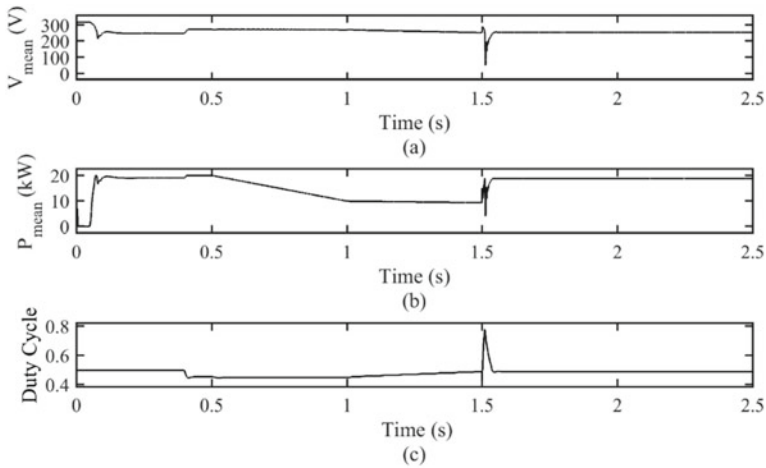


**Fig. 6** PV module system parameters **a** mean voltage, **b** mean active power generation and **c** duty cycle

### 3 Results and Discussion

In this section, the performance of the realistic microgrid structure is assessed and analyzed under on-grid and off-grid conditions. This structure is tested with the effect of line impedance on power quality parameters. The power-sharing profile and losses of all three clusters have been monitored and utilized in automated demand-side management (ADSM). During the variation in solar irradiance level, the effect of communication delay is also analyzed for the assessment of power quality parameters. The load variations have also been incorporated due to the intermittent behavior of the individual consumer.

A three-phase AC microgrid is tested for the assessment of the power quality parameters under on-grid and off-grid conditions. The microgrid with generating capacity of 20 kW is connected to an 11 kV grid for satisfying the consumers' load demand. The microgrid comprises a DC-DC boost converter and a three-phase three-level voltage source converter (VSC). A 20 kW PV array is proposed to cater to the load under on-grid and off-grid conditions.

The results have been presented by considering the following cases.

Case 1. Power quality enhancement using VD, THD, F, and PF.

Case 2. Power quality assessment using voltage sag and swell.

Case 3. Localized power backup for critical load.

Case 4. Effect of line impedance on power quality parameters.

Case 5. Power sharing and losses in utility grid and DERs.

Case 6. Effect of communication delay on power quality parameters.

#### ***3.1 Power Quality Enhancement Using VD, THD, F, and PF (Case-1)***

In case 1, the realistic microgrid structure of 20 kW is tested for the assessment of power quality parameters such as voltage variation, frequency, power factor, and THD without considering the effect of line impedance and communication delay. The on-grid operation is initiated from 0 to 1.5 s when the total impedance of the line is maximum from the location of DER to the utility grid. Due to this, the voltage variation is high about 9% as that of off-grid operation. Now, the off-grid operation is implemented at 1.5 s and during this period the utility grid is disconnected. So, the overall line impedance will be reduced, and the voltage variation is also going down to about 6.5% as shown in Fig. 7a. Hence, it is understood that the percentage variation is depending on the line voltage drop due to the presence of line impedance or length. During the total simulation run time, the frequency and power factor profiles are not violated reasonably to affect the performance of the microgrid structure as shown in Figs. 7b, c. The power converters are well known to introduce the non-linearity in the system so it is quite possible during the off-grid condition that the THD may

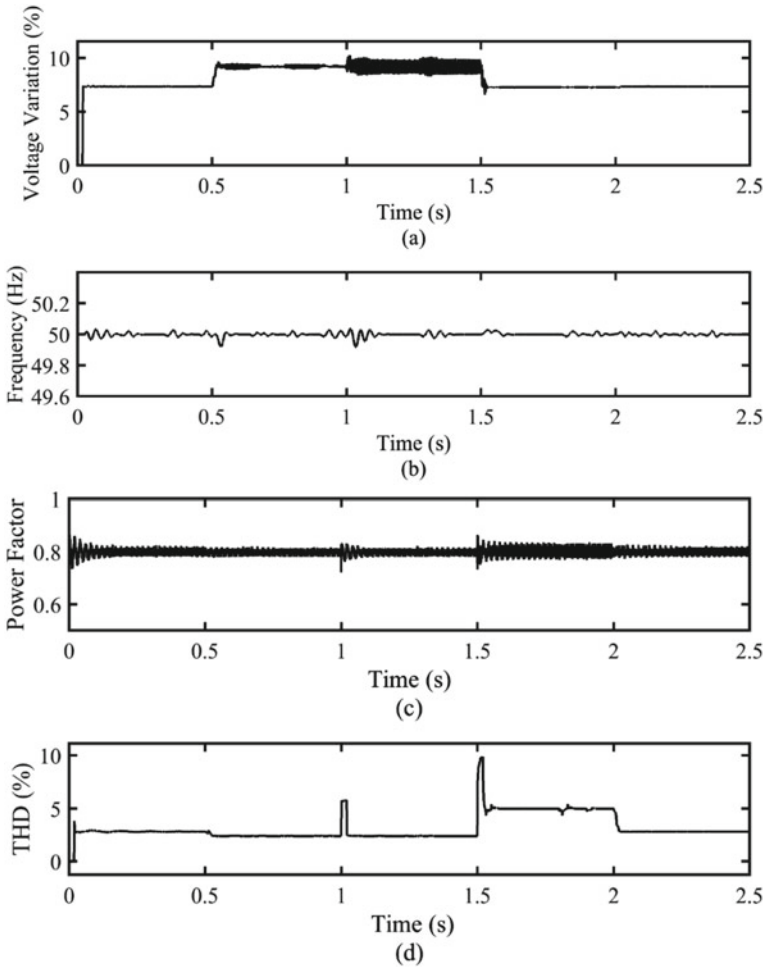


**Fig. 7** Assessment of power quality parameters **a** voltage variation, **b** frequency, **c** power factor, and **d** THD

go high beyond its permissible range of 5%. Hence, the THD is found slightly more than 5% under off-grid conditions (from 1.5 to 2.0 s) as shown in Fig. 7d.

### 3.2 Power Quality Assessment Using Voltage Sag and Swell (Case-2)

The performance of the microgrid structure is investigated for the overloading and underloading conditions to highlight the effects of voltage sag and swell. It is assumed

that there is an overloading situation from 0.1 to 0.2 s. During this period, there is a dipping (sag) in the per-phase load voltage and an increase in the load current as shown in Fig. 8a, b. In Fig. 9a, b, the effect of the light loading condition is assessed again for the same period of 0.1–0.2 s. During light loading or underloading condition, the system is drawing less current so the voltage may go high which can be observed easily in the voltage waveform as shown in Fig. 9a. This shows the existence of voltage swell under light loading conditions. Although, the amount of decrease in current is not a major concern it has created a reasonable voltage swell from 0.1 to 0.2 s as shown in Fig. 9a, b.

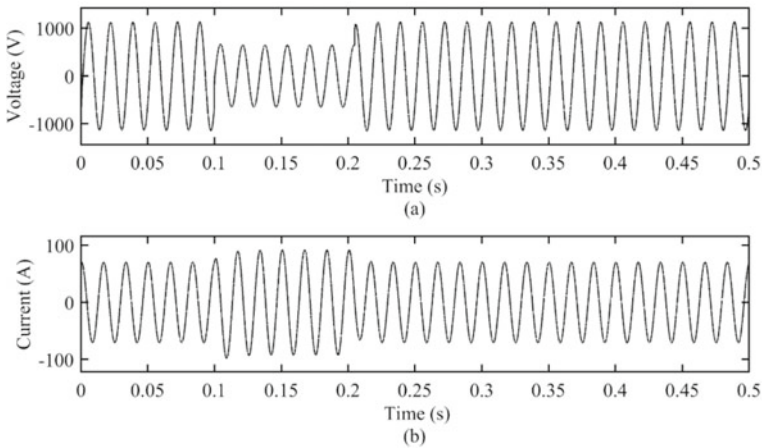


**Fig. 8** Overloading condition **a** voltage sag and **b** load current profile

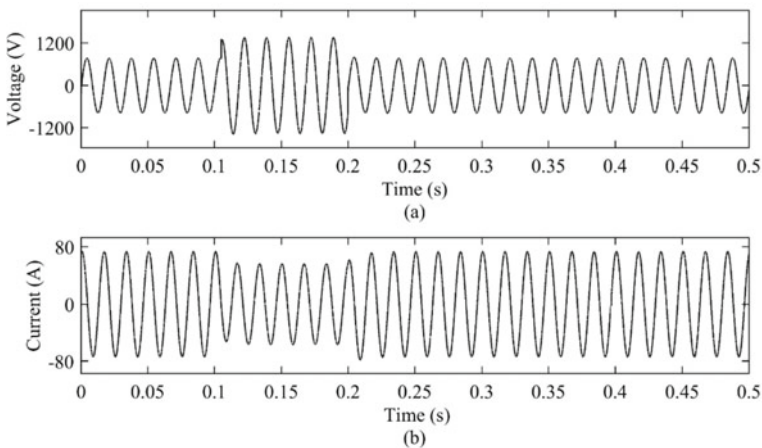


**Fig. 9** Light loading condition **a** voltage swell and **b** load current profile



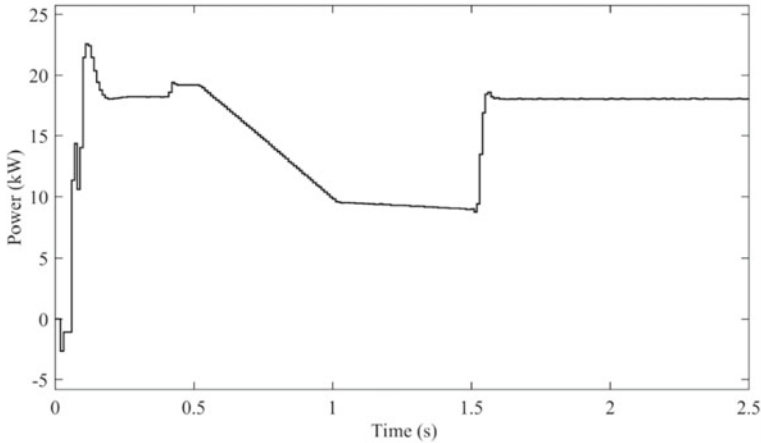


**Fig. 10** Active power generation profile of microgrid structure

### ***3.3 Localized Power Backup for the Critical Load (Case-3)***

In reference to Fig. 1, the local load can be powered by its directly connected DER or by the nearest DERs. All three clusters have local loads and a common supply to the utility grid through PCC. The MG3 has two emergency loads of 3 and 2 kW connected with DER7 and DER8 respectively. So, it is mandatory to maintain a continuous supply to these critical loads not only by the local DERs but also through other DERs of the MG1 and MG2. The variation in power is shown in Fig. 10 which is presenting the generating active power flow under on-grid and off-grid conditions. The maximum and minimum generations are about 20 and 10 kW respectively as per the availability of solar irradiance (from 1000 to 500 W/m<sup>2</sup>).

### ***3.4 Effect of Line Impedance on Power Quality Parameters (Case-4)***

The effect of additional line impedance is imposed in the realistic microgrid structure to assess the power quality-related parameters. The value of line impedance is calculated in such a way as to keep a high R/X ratio in the case of the LV distribution system [6]. Table 1 shows the line impedances as per their lengths which are formulated in simulation work to introduce the effect on the performance of microgrid structure under on-grid and off-grid operations. Due to the presence of additional line impedance, it has created more voltage drop across the line as compared to the normal impedance of the line. From Fig. 11a, the percentage voltage is more in the case of additional line impedance than that of no line impedance. It is known that a higher value of impedance leads to more potential or voltage drop in the electrical

**Table 1** Calculation of line impedance as per line length

Line length (m)	Line impedance ( $\Omega$ )
100	$0.0642 + j0.0083$
600	$0.3852 + j0.0498$
800 (UG side)	$0.5136 + j0.0664$

circuits. In reference to frequency and THD waveforms shown in Fig. 11b, d, these are not affected so much by the presence of additional line impedances. However, there is a slight improvement in the power factor due to the additional line impedance which further leads to a high R/X ratio as shown in Fig. 11c.

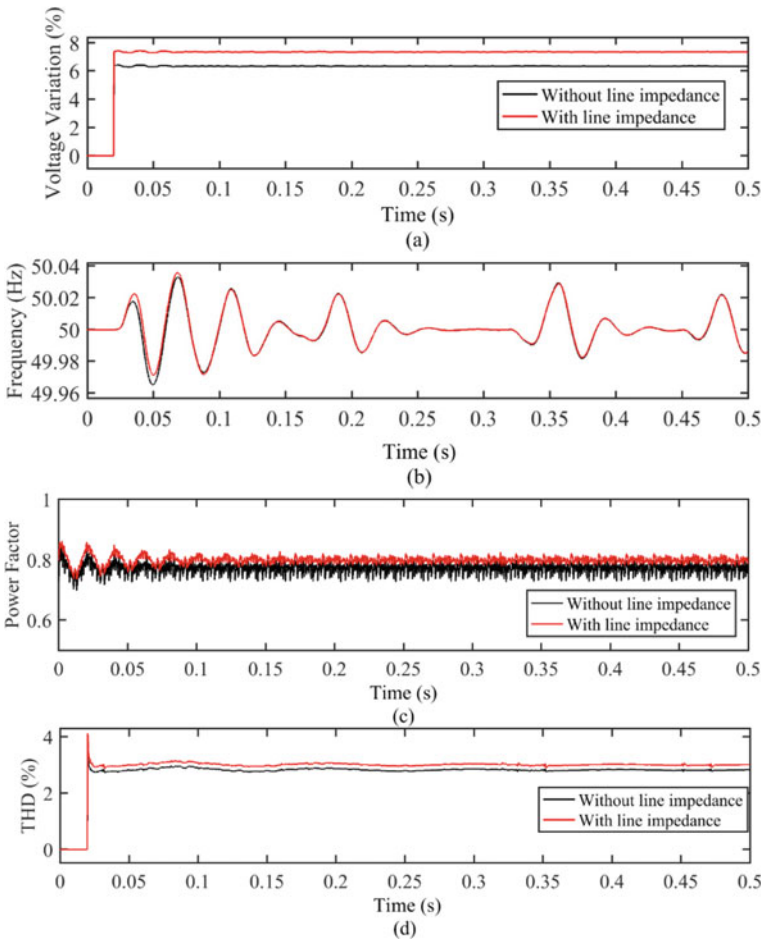


**Fig. 11** Assessment of power quality parameters with/without the effect of line impedance on **a** voltage variation, **b** frequency, **c** power factor, and **d** THD

### 3.5 Power Sharing and Losses in Utility Grid and DERs (Case-5)

The amount of power-sharing and loss depends upon the distance between the source and load feeders. It is revealed that all three clusters of microgrid structure and utility grid have a non-uniform distribution of power and losses. Since MG1 and MG2 are rated on the same capacity and load demands so they are contributing an equal amount of power sharing and losses as can be seen in Tables 2 and 3. In the case of on-grid operation, both MGs are generating 8 kW and fulfilling the demand of 7.5 kW with a line loss of 0.5 kW (6.25%) as per the total line distance of 700 m from the PCC. MG3 generates 12 kW to cater to the load demand of 11.1 kW with a loss of 0.9 kW (7.5%) in reference to the 700 m line from the PCC supported by four DERs (DER7-DER10). On the utility grid side, it is contributing 20 kW generation, 19 kW load demand, and 1 kW power loss (5%) with a total line distance of 1400 m from the buses of all three microgrid clusters (MG1–MG3). Similarly, the power-sharing and losses can be calculated during off-grid conditions while the utility grid is disconnected. Since the 800 m line of the utility grid is disconnected then the overall power loss will be reduced as compared to the on-grid operation. Table 3 shows the same distribution of generation, demand, and power loss (5%) in case of the MG1 and MG2 while MG3 contributes 12 kW generation, 11.3 kW demand, and 0.7 kW power loss (5.83%). Hence, it is concluded that the realistic microgrid structure experiences less power loss in the case of off-grid operation due to the removal of grid-side line impedance.

**Table 2** On-grid power sharing and losses among MG1, MG2, MG3 and utility grid

Operating area	Generation ( $P_g$ , kW)	Demand ( $P_d$ , kW)	Power loss ( $P_{loss}$ , kW)	Power loss (%)
MG1	8.0	7.50	0.50	6.25
MG2	8.0	7.50	0.50	6.25
MG3	12.0	11.10	0.90	7.5
Utility grid	20.0	19.0	1.0	5.0

**Table 3** Off-grid power sharing and losses among MG1, MG2 and MG3

Operating area	Generation ( $P_g$ , kW)	Demand ( $P_d$ , kW)	Power loss ( $P_{loss}$ , kW)	Power loss (%)
MG1	8.0	7.60	0.4	5.0
MG2	8.0	7.60	0.4	5.0
MG3	12.0	11.3	0.7	5.83

### **3.6 *Effect of Communication Delay on Power Quality Parameters (Case-6)***

In addition to the normal operation, it is proposed to validate the performance of the microgrid with the inception of delay in breaker operation while the transition takes place from grid to isolated condition. The three-phase realistic microgrid structure presented in Fig. 1 is simulated for 2.5 s by providing a communication delay in the breaker (PCC) operation during the transition from grid-connected to islanded mode. The breaker operation is delayed by 0.1 s just at the time of 2 s when the islanding condition is initiated as shown in Fig. 12a–d. It is assumed that the relay circuit has given a tripping command to the breaker with a time delay of 1 s which seems like a communication delay for the required operation. The limits of four power quality-related parameters are violated during the transition subjected to the delay in breaker operation at PCC.

## **4 Conclusion**

This chapter describes power quality control based on voltage sag/swell, frequency, THD and power factor in PV integrated three-phase AC realistic microgrid system. A simple microgrid model could be extended to a realistic structure/architecture of a microgrid considering the effect of line impedance as a part of the distribution network. The effect of line impedance on power quality parameters has been analyzed during the on-grid and off-grid operation of microgrids. The power-sharing, load demand, and power losses have been assessed considering the variations in solar irradiance, temperature, and load profile. The power losses in sources and distribution wires are measured to maintain a possible balance between demand and supply. The effect of communication delay in breaker operation during the transition of islanding condition is also investigated to assess the performance of the microgrid system in terms of power quality parameters. In future propositions, the existing work would be extended by synchronizing the wind generator and PV generator with the utility grid. This proposed model would be assessed for power quality-related parameters considering the variations in PV and wind variables, the effect of line impedance, and communication delays.

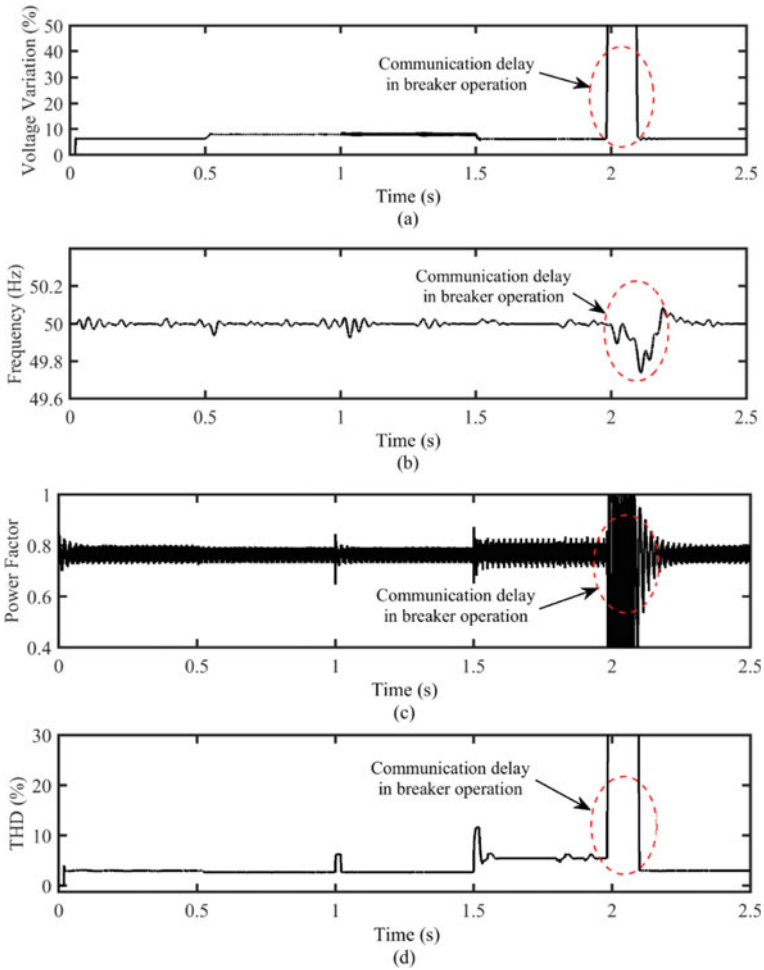


**Fig. 12** Effect of communication delay in breaker operation on power quality-related parameters **a** voltage variation, **b** frequency, **c** power factor, and **d** THD

**Authors’ Contributions** All the authors have worked hard for completing this chapter work. The authors collectively discussed the design of the work, whereas Dr. Jitender Kaushal was responsible for both simulation and analysis work. With the guidance of Dr. Prasenjit Basak, drafting and correction of the content have been done. The final approval of the version was given by both authors to be published.

**Funding** The authors clearly state that no funding was taken for carrying out the present work.

**Ethics Approval** The work is not submitted in any other journal, and it is not published in any previous work.

**Competing Interests** The authors declare no competing interests.

## References

1. Chakraborty, R., Samanta, A., Agrawal, K.M., Dutta, A.: Towards smarter grid: policy and its impact assessment through a case study. *Sustain. Energy Grids Netw.* **26** (2021)
2. Golla, M., Chandrasekaran, K., Simon, S.P.: PV integrated universal active power filter for power quality enhancement and effective power management. *Energy Sustain. Dev.* **61**, 104–117 (2021)
3. Shunmugham Vanaja, D., Albert, J.R., Stonier, A.A.: An Experimental Investigation on solar PV fed modular STATCOM in WECS using Intelligent controller. *Int. Trans. Electr. Energ Syst.* **31**, e12845 (2021)
4. Kaushal, J., Basak, P.: Power quality control based on voltage sag/swell, unbalancing, frequency, THD and power factor using artificial neural network in PV integrated AC microgrid. *Sustain. Energy Grids Netw.* **23** (2020)
5. Chettibi, N., Massi Pavan, A., Mellit, A., Forsyth, A.J., Todd, R.: Real-time prediction of grid voltage and frequency using artificial neural networks: an experimental validation. *Sustain. Energy Grids Netw.* **27** (2021)
6. Kaushal, J., Basak, P.: A novel approach for determination of power quality monitoring index of an AC microgrid using fuzzy inference system. *Iran. J. Sci. Technol. Trans. Electr. Eng.* Springer **42**(4), 429–450 (2018)

# Harmonics Reduction by Distributed Power Flow Control Using FACTS Devices in Power Supply



Rahul Kumar, Nitesh Tiwari, and Anurag Singh

**Abstract** Nowadays, inside the group of FACTS, an additional device has been introduced named a distributed power flow controller. Unified power flow controller and DPFC has the same controller capacity DPFC is derived form of UPFC. The DPFC came into action between the shunt and series converter through the transmission line at the third harmonic frequency. DPFC uses the distributed faults ideas it's about to use multiple small sizes single-phase converters in place of one large size three-phase as in UPFC. The performances of DPFC are based on the symmetrical three-phase fault near the load area. The Mat lab/Simulink results got to show a further developed exhibition in voltage sag mitigation and exceptional reduction in load voltage harmonics.

**Background:** Various series and shunt FACTS devices are used to control the distributed power flow and reduced the harmonics component.

**Objective:** DPFC technology/control strategy is discussed to control the power flow.

**Control:** Modeling of different converters and converters is discussed for DPFC control.

**Result:** DPFC is controlled within the permissible total harmonic distortion.

**Conclusion:** Depending on the situation various FACTS devices need to be used for distributed power flow.

**Keywords** Static Var Compensator (SVC) · Static Synchronous Compensator (STATCOM) · Thyristor Switched Series Capacitor (TSSC) · Thyristor Controlled Series Capacitor (TCSC) · Static Synchronous Series Compensator (SSSC) · Distributed Static Series Compensator (DSSC) · Unified Power Flow Controller (UPFC) · Interline Power Flow Controller (IPFC)

---

R. Kumar

Department of Electrical Engineering, National Institute of Technology Patna, Patna, Bihar, India  
e-mail: [rahulk.ph21.ee@nitp.ac.in](mailto:rahulk.ph21.ee@nitp.ac.in)

N. Tiwari (✉) · A. Singh

Department of Electrical Engineering, Madan Mohan Malaviya University of Technology  
Gorakhpur, Gorakhpur, Uttar Pradesh, India  
e-mail: [niteshwr1994@gmail.com](mailto:niteshwr1994@gmail.com)

# 1 Introduction

Now, electricity has become the most important part of our life. The power system consists of three most important components first one is a production system, the second one is a transmission system where power has been transmitted and the third one is a distribution system where power has been distributed to consumer's homes [1]. Within the typical production of power, production of electricity at the generating power plants and providing the power for the clients through the transmission networks and distribution networks. Amid the latest twenty years, the task of the power system has transformed because of creating usage, the progression of new development, the performance of the electricity market, and the change of non-conventional energy sources [2]. Despite surviving variations, later on, new apparatuses, for example, smart grid systems, based on the electric vehicles etc. [3, 4]. These systems make the whole power system complicated. Within Fig. 1, as demonstrated by the timetable, these progressions are going ahead in the progression from base to upper of Fig. 1.

Previously said progressions and advancement must extraordinarily influence the networks of power, particularly the flow of the power [5]. Routinely, the flow of power, from transmission station to the distribution station. Within the power network, the flow of the power is settled way [6]. Inside the networks, deviations within the flow of power are arranged considering hours, not more consistently [7]. In any case, as a result of the examples recorded above, more present systems with more significant limits are currently becoming placed to utilise; the flow of power in both directions and also fluctuations happen in less time. It is shown in Fig. 2 in the way [8].

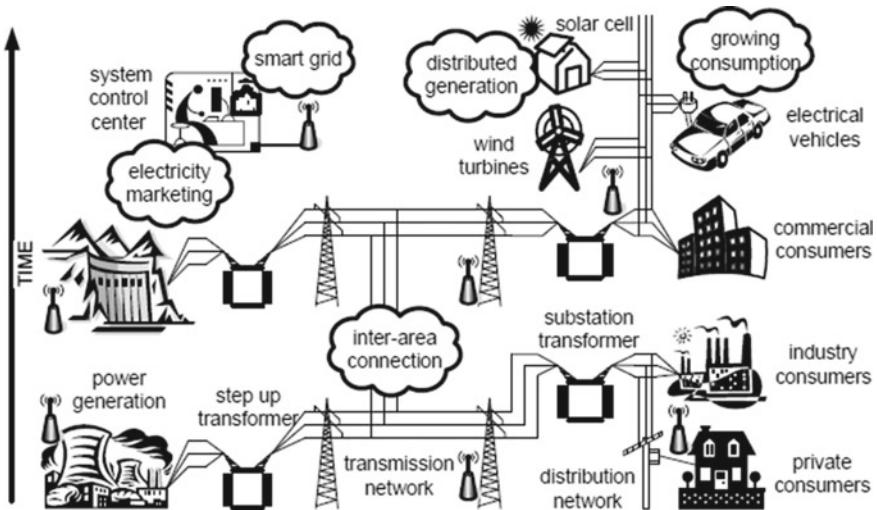
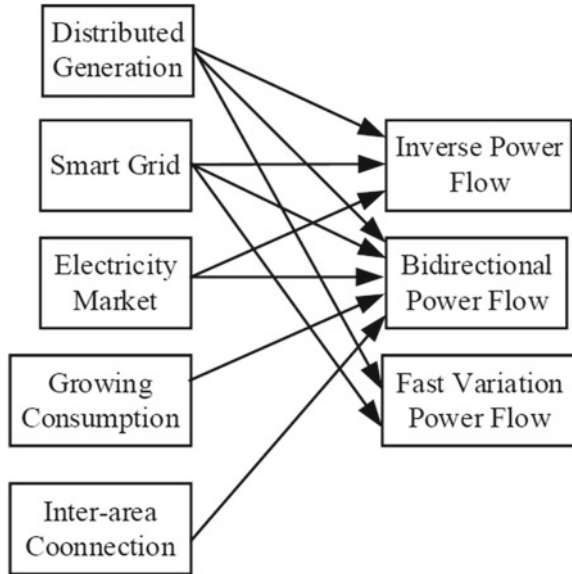


Fig. 1 Basic diagram of power system and its developments



**Fig. 2** Relationship between the diagrams of the developments and its effect on the power flow



In power networks, there are various distributed generations units used for the distribution of power which is linked with distribution networks [9]. These types of units rely upon non-conventional resources, for instance, sun situated and winds [10]. Driven by government techniques went for reducing ozone hurting substance releases and proportioning oil subsidiaries, it is decided by international agreement like Kyoto rules, various distributed generator units are growing which are link with the networks of grid [1, 11]. The flow of power is dissimilar from the outdated course.

In this system, initial generation units in one region maintain power in various zones, then power can be flow in opposite direction and it is flowing first from the distribution network then after flowing to the transmission network [12]. Another, the production of a power of non-conventional resources relies on atmosphere situations [13]. The production level of power is growing in a large quantity from the non-conventional resources [14]. But when the non-conventional energy resources are not enough and do not supply the power [15]. In this way, it is necessary to control the flow of power procedures. So, to continue this growth, taking the power from generating station and also transmission station. Regardless, growth of as far as possible can't take after the extended demand because of the huge price, atmospheric issues etc. [16–18]. so, need to improve these issues with probable result. The whole network of power in many places are linked, allowing the power interchange amid many locations [19]. In midst of a crisis time, to continue the flow of power with loads, the interconnection has been redirected. In this way extending the stability of the system [20]. Due to the inter zones links, it makes the loop flow among the clients and power generating sites [21]. For improving the loop flow and also maintaining the power level, there is used the flow of power in both directions amid the areas [22]. In the market of electricity, which is a scheme to influence the buying and trade of energy,

to set the price, using supply and demand [23]. When rising the movement within the market of electricity, the flowing of power from the source along with lesser price towards the most important cost [24]. For monitoring power, diminishing price and saving power and augmentation trustworthiness, straightforwardness, now smart grid system is used [2, 25]. It provides detailed information about the power level to the main controlling station and all components like transmission station and distribution station appropriately is well-ordered by it [26]. As a result of the already said changes, the power network should become a meshed system in the upcoming and the flowing of power within the system, will be well-ordered [27]. For maintaining the process of structure stable, for the duration of the fault otherwise, climate changes, the reaction period for controlling the flow of power will become fast [28]. Lacking appropriate regulates, the power may not flow as essential, since the flow of power is unwavering with parameters of the power system [3, 29]. Thus, for fulfilling the flow of power necessities in the future system, the devices are required to regulate the flow of power.

### 1.1 Power Flow Control Theory

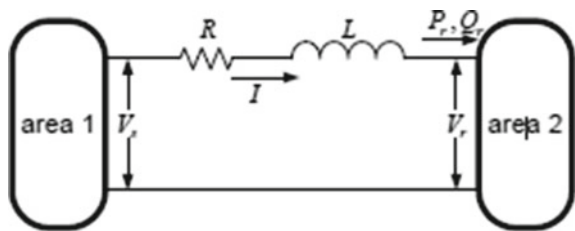
For studying the flow of power which are flowing in the transmission line, there is necessary for a mathematical presentation of the transmission system [23, 30]. In transmission, there are four parameters: inductor, capacitor, resistance and conductance [24]. For small and medium distances in the transmission system, capacitance and conductance are ignored with less loss. Figure 3, depicts the basic line of the power networks. Where  $V_s$  depicts sending end voltage which is phase voltage of line to ground.  $V_r$  depicts receiving end voltage which is phase voltage of line to ground.  $I$  depict phase current in the line.  $R$  depicts series resistance.  $L$  depicts the inductance of the line [25].

Here,  $S_r$  depicts the real power at receiving end. This power is obtained from the basic diagram of the transmission system shown in Eq. (1).

$$S_r = V_r \cdot I^* = V_r \cdot \left( \frac{V_r - V_s}{R + j\omega L} \right) = P_r + jQ_r^* \tag{1}$$

where  $*$  depicts conjugation of the complex number,  $Z$  depicts line impedance, and it is equivalent to  $R + j\omega L$ .  $P_r$  shows the active power of the line.  $P_r$  is the real part.

**Fig. 3** Basic diagram of the single line of the transmission system



$Q_r$  shows reactive power of line, it is the imaginary part.  $S_r$  shows real power which is the real part [26].

$$P_r = \frac{|V_r|^2}{|Z|} \cos \delta + \frac{|V_r||V_s|}{|Z|} \cos(\theta - \delta) \quad (2)$$

$$Q_r = \frac{|V_r|^2}{|Z|} \sin \delta - \frac{|V_r||V_s|}{|Z|} \sin(\theta - \delta)$$

In Eq. (2),  $\theta$  depicts transmission angle. This angle is in between sending end voltage and receiving end voltage.  $\delta$  is known as  $\tan^{-1}(wL/R)$ . In the medium distance of transmission network, reactance should be large and also in long-distance transmission network, reactance should be large. In both transmission networks, resistance is ignored. Because of less loss in resistance. In Eq. (3),  $P_r$  depicts active power,  $Q_r$  depicts reactive power in a lossless transmission network [27].

$$P_r = \frac{|V_r||V_s|}{|X|} \sin \theta \quad (3)$$

$$Q_r = \frac{|V_r||V_s|}{|X|} \cos \theta - \frac{|V_r|^2}{X}$$

Within Eq. (3),  $\theta$  depicts transmission angle.  $X$  shows the impedance of the transmission network,  $X = wL$  shows the inductive impedance of the transmission network. With the three parameters, power can be controlled according to Eq. (3). The first is transmission angle [28]. The second is inductive impedance. The third is magnitudes of voltage which are  $|V_s|$  and  $|V_r|$ . Where  $|V_s|$  is the magnitude of sending end voltage. For controlling the flow of power on a small scale, voltage magnitude is changed. But, for adjusting the flow of power on a large scale, this process is not suitable [29]. When the magnitude of the voltage at the sending end is equivalent to the magnitude of the voltage at the receiving end voltage, then the equation is shown by Eq. (4).

$$P_r = \frac{|V|^2}{X} \sin \theta \quad (4)$$

$$Q_r = \frac{|V|^2}{X} (\cos \theta - 1)$$

As appeared in the equation both powers will change consequently which are active ( $P_r$ ) and reactive power ( $Q_r$ ). Both powers are joined to each other. From (1.4), the locus of ( $P_r$ ,  $Q_r$ ), with Impedance, transmission angle like the control parameter is obtained and shown in Eq. (4).

For adjusting the flow of active power, the transmission angle can be varied. Within the process, Active power's magnitude and its direction can be controlled.

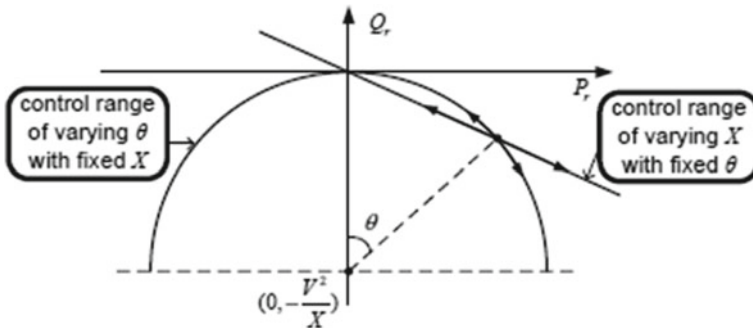


**Fig. 4** Control scale of the flow of active power ( $P_r$ ) and reactive power ( $Q_r$ ) varies impedance and transmission angle

For adjusting the flow of reactive power, the transmission angle is varied. Within the process, reactive power's magnitude can be controlled only. Figure 4 shows this process.  $(-90^\circ, 90^\circ)$  is deviation scale of  $\theta$ .

For the connection of grid and ground, shunt devices are used. At the point of the joining, for delivering or absorbing reactive power, the shunt devices are used [4]. Thus, regulating the system parameter like voltage magnitude. Inside particular restrictions, the voltage magnitude of the bus fluctuate. Thus, the Regulation of power flow is incomplete. For another task, shunt devices are used. It is used for enhancement of the power and dropping the losses in the line.

For improving the power system networks, shunt devices are used which delivered the reactive power in line and reduced the losses in line Furthermore, Shunt devices are improved the power quality when power demands vary from the consumer side [5]. Some devices are used to connect the transmission line in series. Because of this, it is called Series devices. The transmission network is affected by impedance. After embedding the capacitor, the impedance of the transmission line is altered. And also, the reactor is used for the task. A capacitor is used for reducing the voltage drop of the inductive circuit. The series device is used in various operations, it is utilised for adjusting the impedance of the line for stopping the extra heating. Shunt and series devices are called joint devices. For interchanging the active power between series and shunt device, it is used. This device is linked with the grid. It also manages the power network due to the function of trigonometric are periodic. Appropriately, the direction and magnitude of both powers ( $P_r$ ) and ( $Q_r$ ) can be controlled by the impedance of the line. Hypothetically, by varying impedance of the line, both powers ( $P_r$ ,  $Q_r$ ) can be balanced from zero to infinity. Active power is selected first [31].

### 1.2 Power Flow Controlling Devices

With the help of power system parameters, we control the power like voltage magnitude, the impedance of the line. And also regulate the power with the help of transmission angle parameter. Power flow controlling devices are the most important devices which regulate the parameters of the networks. Therefore, Power is controlled by it appropriately. They are delineated as power flow control devices.

PFC is divided into the series, shunt and combined devices both are used in power systems according to their task. As appeared in Fig. 5.

For the connection of grid and ground, shunt devices are used. At the point of the joining, for delivering or absorbing reactive power, the shunt devices are used [4]. Thus, regulating the system parameter like voltage magnitude. Inside particular restrictions, the voltage magnitude of the bus fluctuate. Thus, the Regulation of power flow is incomplete. For another task, shunt devices are used. It is used for enhancement of the power and dropping the losses in the line.

For improving the power system networks, shunt devices are used which delivered the reactive power in line and also reduced the losses in line Furthermore, Shunt devices are improved the power quality when power demands vary from the consumer side [5]. Some devices are used to connect the transmission line in series. Because of this, it is called Series devices. The transmission network is affected by impedance. After embedding the capacitor, the impedance of the transmission line is altered. And also, the reactor is used for the task. A capacitor is used for reducing the voltage drop of the inductive circuit. The series device is used in various operations, it is utilised for adjusting the impedance of the line for stopping the extra heating. Shunt and series devices are called joint devices. For interchanging the active power between series and shunt device, it is used. This device is linked with the grid. It also manages the power network parameters, for example, bus voltage, line impedance etc. According to the innovative development in tools, Power Flow Controlling Devices can be separated into power electronics devices and mechanical devices. Mechanical PFCs contain settled otherwise they are mechanical substitutable components, these components are passive for instance capacitors, inductors etc. Conventionally, mechanical Power Flow Controlling Devices have a comparatively small price and high stable quality. Due to the comparatively less speed and step by step modification, these types of devices have less regulation limit [6, 7]. And it cannot be used

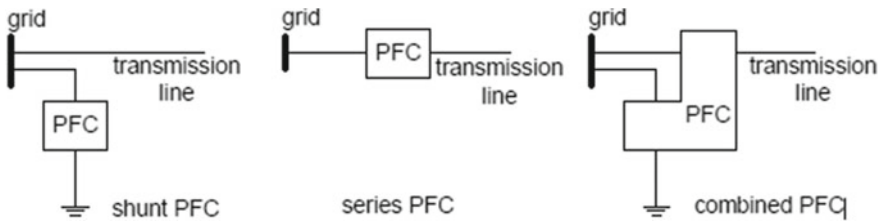
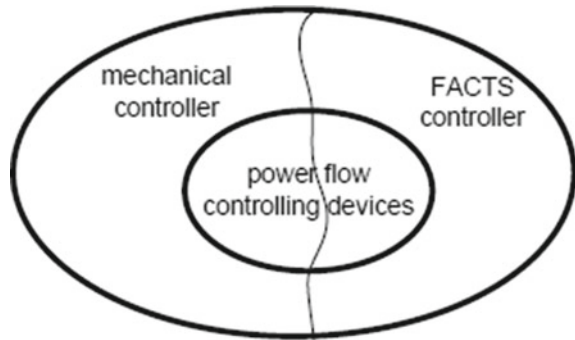


Fig. 5 A diagram of power flow controlling devices (Shunt PFC, Series PFC, Combined PFC)

**Fig. 6** A diagram of connection between the power flow controlling devices, flexible AC transmission system controllers and mechanical based controller



for composite systems in the upcoming. Power Electronics Power Flow Controlling Devices similarly contain passive components, however join additional switches in power electronics-based devices for achieving lesser advances, speedier variations.

Power electronics devices are used in FACTS. In the distribution system, power electronics devices are used and also High Voltage DC transmission is useful for instance, DVR, are furthermore considered as Flexible AC Transmission System controllers [8]. For controlling the power flow, we used the advanced technology FACTS Devices in a large quantity. Figure 6 depicts the A diagram of Connection between the Power Flow Controlling Devices, Flexible AC Transmission System controllers and mechanical based controller.

There are two types of Power Electronics, Power Flow Controlling Devices: Voltage Source converters and thyristor-based devices. Thyristor Power Flow Controlling Devices use a thyristor which is an inverse and parallel thyristor. It is connected in series and otherwise parallel. They are connected with the passive components. A Thyristors can handle the impedance of PEs. It has a specific quality, for adjusting the turn on the switch, it is used. For turning off the switch, they are not utilised. When the current goes in the negative direction, it becomes turn off spontaneously. Therefore, it must be turned on one time inside one cycle only. For getting low switching losses, Power Flow Controlling Devices limited the frequency of the system. Thyristor's power rating is larger so, it will be managing the voltages and currents. It is simpler than the Voltage Source Converters. It is allowing them greater dependability. In any case, after creating the waveforms of currents and waveforms of voltages by thyristor-based Power Flow Controlling Devices contain harmonics in large quantity. In this way needing big filters circuits. Voltage Source Converter Power Controlling Devices use moved switch tools, for instance, IGBT, MOSFET etc. for developing the converters-based devices. Along these lines, it is likely to turn switches on and switch off inside the Voltage Source Converters frequently in one cycle. A couple of sorts of Voltage Source Converters have been created, for instance, multi-pulse and multi-level converters, etcetera. Voltage Source Converters Power Flow Controlling Devices make immediate control likely. Its switching frequency is high and allow Power Flow Controlling Devices to maintain disrupting impacts from system networks. In this way, Voltage Source Converters Power Flow Controlling

Devices are used for regulating the power upcoming. Additional side many problems have in these controlling devices immediately, for allowing the power, a big number of switches are used. And this power flow with the Voltage Source Converters Power Flow Controlling Devices. Immediately, the Voltage Source Converters are expensive because of using a big switching device that is linked in parallel and series in the networks to enable the currents, voltages. Besides, on account of their greater switching frequency and higher on-state voltage in relationship with thyristors devices, Voltage Source Converters Power Flow Controlling Devices losses are higher as well, Voltage Source Converter look at swing to be more feasible and fiscally insightful later.

As showed by the above considerations of different sorts of Power Flow Controlling Devices, it can be assumed that Power Electronics merged Power Flow Controlling Devices (moreover suggested as joined FACTS) have the best control capacity among all Power Flow Controlling Devices. There are some most power full controllers like UPFC, and IPFC are used; they can control and vary the impedance of the line, transmission line angle, and voltage of bus.

### 1.3 Classification of the Power Flow Controlling Devices

Within the classification of the Power Flow Controlling Devices, there are two important groups. (1) Mechanical based Power Flow Controlling Devices. (2) Power Electronics based Power Flow Controlling Devices. In Fig. 7 provide detailed information, types and importance of PFCDs.

#### Shunt Devices

Figure 8 shows the working standard of the shunt device. For getting the reactive power, shunt devices are used. Reactive power is necessary for the loads. The infused reactive current of the shunt device which is shown as  $I_{sh}$  in Fig. 8 is regulated by changing the impedance. Thus, line current  $I$  am controlled ultimately. In a transmission line, based on Ohm's law,  $V_s - V_r$  is a voltage drop through the line. It is associated with the current of line  $I$ .  $V_s$  shows sending end voltage. It is supposed as constant.  $|V_r|$  shows the magnitude of receiving end voltage. The shunt device regulates the  $|V_r|$ .

There is a connection between current  $I_{sh}$  and  $V_r$  indirectly.  $I_{sh}$  is infused current of shunt device.

$$V_r = V_s - IZ \tag{5}$$

$$V_r = (I_s - I_{sh})Z$$

where impedance  $Z$  is equal to the  $R + jwL$ . In Eq. (5), for the maintaining load current  $I_r$ , shunt current  $I_{sh}$  can be compensated, thus by adjusting the impedance

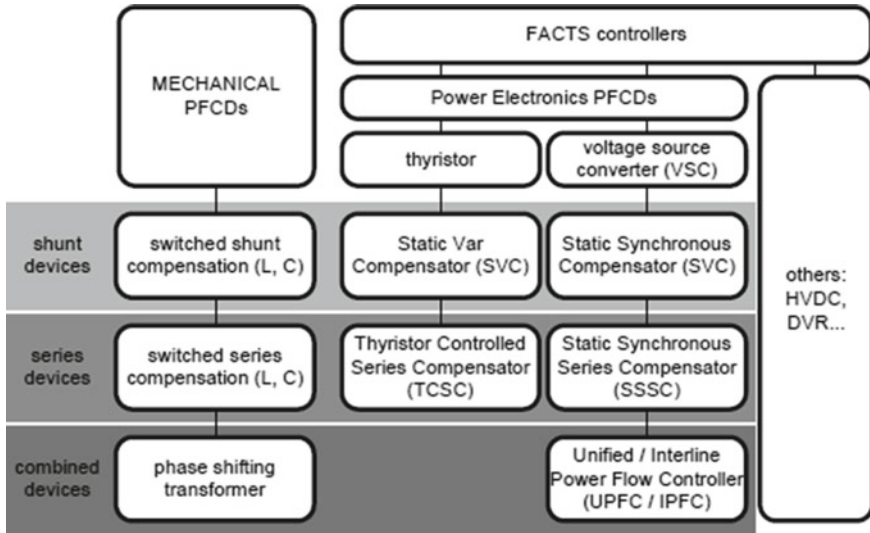
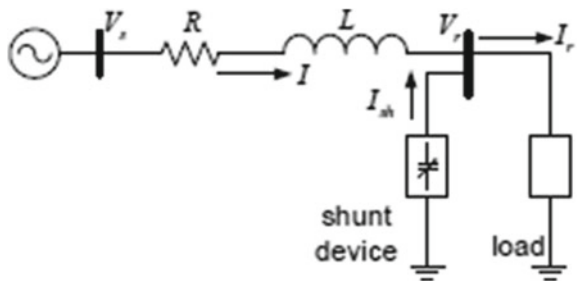


Fig. 7 Classification of the power flow controlling devices

Fig. 8 Shunt device operating principle



of the shunt device, the magnitude of voltage is regulated. Here, will be discussed about Static Var Compensator and Static Synchronous Compensator.

*Static Var Compensator (SVC)*

As shown in Fig. 9 within Static Var Compensator (SVC) device, it has been infused the current in the line and also it is used to adjust the special types of parameters like voltage of bus. SVC also control the parameters like bus voltage of the networks [32].

In 1972, SVC has come into the picture. From that point forward, it is utilized in many applications for power flow control [9]. Within Static Var Compensator, it is used, for regulating the power. Thyristor Switched Capacitor devices and Thyristor Controlled Reactor devices are used in Static Var Compensator. There is also used a harmonic filter circuit in SVC as shown in Fig. 10.



**Fig. 9** **a** Basic structure of the switched shunt inductor, **b** basic structure of the switched shunt capacitor

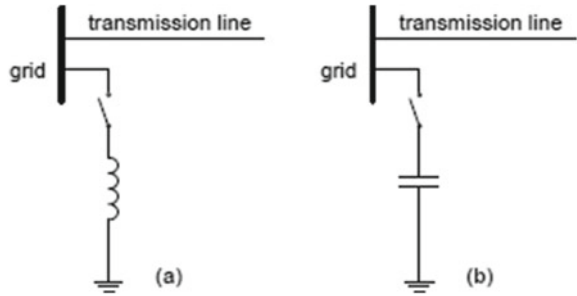
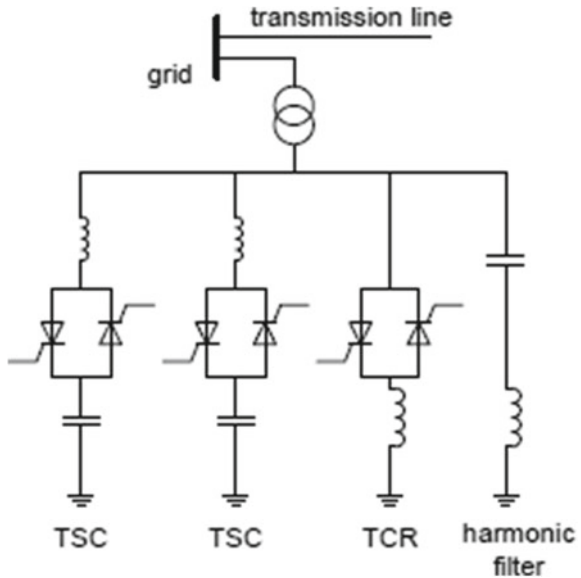


**Fig. 10** Basic structure of static Var compensator



Inside Thyristor Switched Capacitor and Thyristor Controlled Reactor, there are used a thyristor which is inverse parallel and they are connected with reactor otherwise capacitor in series. For controlling the inrush currents, the inductor is used. It is connected with circuits in series when happening the transient process [33]. To regulate the reactance of the shunt of the thyristor-controlled reactor, the firing angle of the thyristors is controlled. There are two conditions for the conduction of the thyristor-controlled reactor. In continuous conduction of TCR, the firing angle changes from the 90-degree interval. For lesser conduction, interval to 180°. When Thyristor Controlled Reactor and Thyristor Switched Capacitor are joined together, they can give continuously variable Var infusion or absorption which is appeared in Fig. 11.

The reactive power of the Static Var Compensator depends on the voltage of the bus. So, it provided the reactive power is proportional to the square of the voltage of the bus. Therefore, this device has not been so effective. SVC does not provide

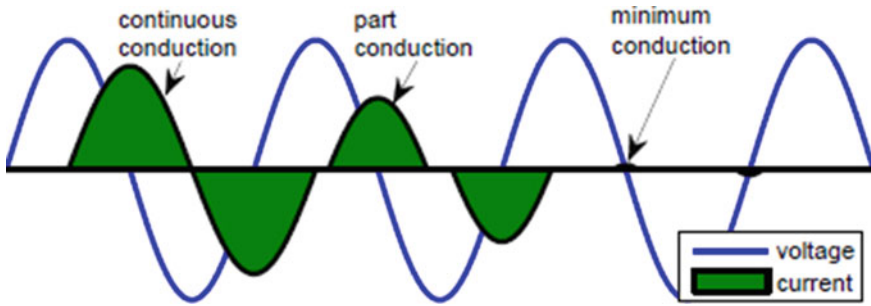


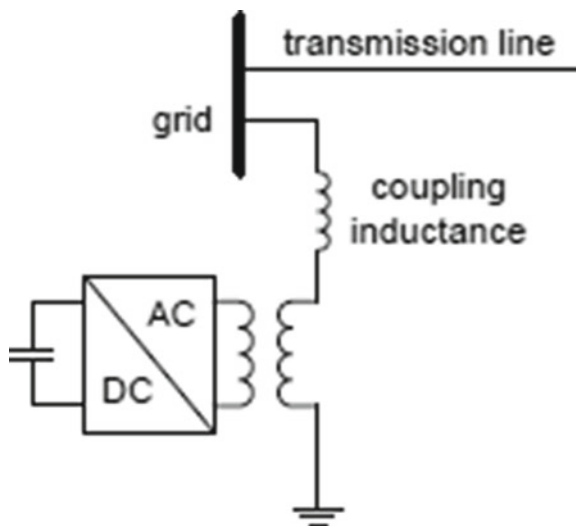
**Fig. 11** A waveforms of voltage and current of the thyristor controlled reactor at the many firings' angles

enough reactive power if the bus voltage is low. In Fig. 11, there can be used the filter to reduce the harmonics in the waveform.

*Static Synchronous Compensator (STATCOM)*

For regulating the power inline, a Static Synchronous Compensator is used. It is recognized as a synchronous condenser. It is known as STATCOM. It is Voltage Source-based Power Electronic Device [10]. In STATCOM, there are used force commutating devices like GTO, IGBT. For controlling the power inline, these devices are used. For designing the STATCOM, there are important parts: (a) Voltage Source converters (b) Harmonic Filter (c) Inductive Reactance (d) DC Capacitor. In Fig. 12, there is STATCOM which is joined between the grid system and the grounding [34, 35].

**Fig. 12** Basic structure of static synchronous compensator



It acts as a source. And it is the same as a synchronous condenser. For infusing the current within the quadrature, STATCOM is utilised [36]. STATCOM works as an inductive load when it produces voltage lower than the voltage of the grid system. Then, it takes the reactive power from the grid. STATCOM performs as a capacitive load when it produces a voltage higher than the voltage of the grid system. Thus, it gives reactive power to the system [37].

STATCOM has a faster device because it is a power electronics-based device. And it has no inertia. STATCOM performs as a DC source [11]. There is used of PWM converter which is a multi-phase, multi-level. From this converter within STATCOM, there is no requirement of an additional filter to reduce the harmonics in the output waveforms of current [38].

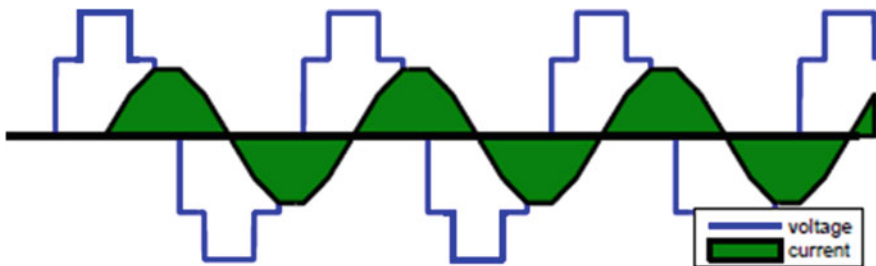
For example, shown in Fig. 13 appeared, a static synchronous compensator has preferable characteristics over the Static Var Compensator because the output comprises lesser harmonic components. A static synchronous compensator is more composite than the static var compensator due to the use of the Voltage Source Converter. As needs are, a Static Synchronous Compensator is more costly than the Static Var Compensator, particularly for the high-voltage transmission lines networks.

**Series Devices**

For improving the stability of the line, series devices are utilised. Series devices are connected to the line in series which is shown in Fig. 14.

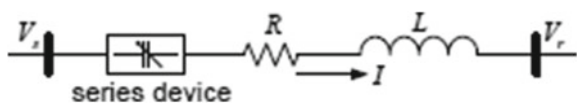
For regulating the flow of power, series devices are utilised. These devices are capacitive or inductive as indicated by this Eq. (6).

$$P_r = \frac{|V_r||V_s|}{|X|} \sin\theta \tag{6}$$



**Fig. 13** Generating a voltage waveform and current waveform using five-level static synchronous compensator

**Fig. 14** Working principle of series device



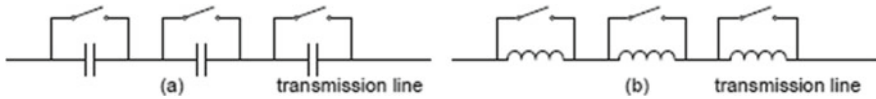


**Fig. 15** A structure of mechanical switched series devices connected to the inductor and capacitor

$$Q_r = \frac{|V_r||V_s|}{|X|} \cos\theta - \frac{|V_r|^2}{X}$$

For controlling the flow of power, the reactance of the device is improved. And at this condition, the series device performs like an inductor. For increasing the voltage and angular stability, series devices are utilised [7–12]. Further, series devices are improved. Many FACTS Devices are joined with the series devices. For example, Thyristor Controlled Series compensator (TCSC), Thyristor Switched Series Capacitor (TSSC) etc. In Fig. 15, there are shown mechanical switched series devices.

*Thyristor Switched Series Capacitor (TSSC)*

Within Fig. 16, TSSC is connected to the line. Inside the structure of the TSSC, there are used a thyristor. And these thyristors are inverse parallel in connection. There are used a part of the capacitor bank which is joined in series. This capacitor is known as a series capacitor bank. Series capacitor bank is used for inserting or removing quickly a part of the capacitor bank with the discrete periods [39]. TSSC device has a faster response in comparison to the mechanical based switched compensators. TSSC is not widely used because it does not work fast [40].

*Thyristor Controlled Series Capacitor (TCSC)*

For providing variable series capacitive reactance, Thyristor Controlled Series Capacitor is utilised. Inside the structure of Thyristor Controlled Series Capacitor, there is a used capacitor bank which is shunted by TCR [41]. It is also called like capacitive reactance compensator. Inside Fig. 17, there is a structure of Thyristor Controlled Series Capacitor [42].

Inside the structure of the Thyristor Controlled Series Capacitor, there is utilised a thyristor which is opposite parallel. These thyristors are used for adjusting the reactance within the thyristor-controlled reactor branch. For controlling the total impedance, Thyristor Controlled Series Capacitor is utilised [13]. For controlling

**Fig. 16** Structure of thyristor switched series capacitor

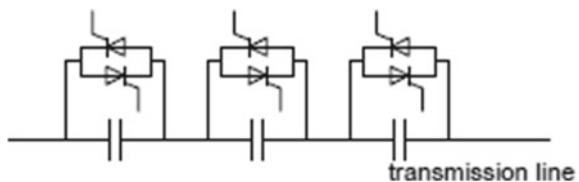


**Fig. 17** Structure of thyristor-controlled series capacitor

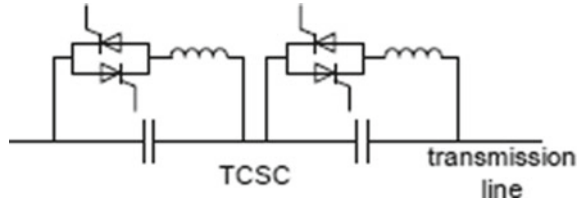
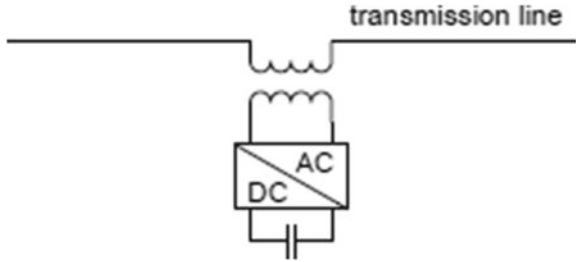


**Fig. 18** Structure of the Static synchronous series compensator



the impedance of the line, it is utilised. The controlling process of the impedance of the line is done in a single cycle [14]. Thus, TCSC is a faster response in comparison to mechanical based devices [43].

*Static Synchronous Series Compensator (SSSC)*

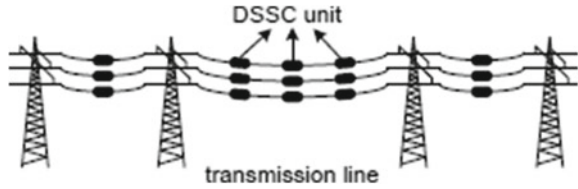
In Fig. 18, the structure of the Static Synchronous Series Compensator device is shown. It regulates the power. It contains a converter [44]. This is no need for an external energy source for this device. It is connected to the line and its output voltage is quadratic. It regulates the current of the line independently [45]. For regulating the reactive power in the line, it is used [9]. For compensating for the losses in the converter.

Inside the Static Synchronous Series Compensator, there is used a Voltage Source Converter. Voltage Source Converter injects the voltage, and its voltage is associated with line current [36, 46]. In this way, it controls independently. In comparison to the thyristor-controlled reactor, there are fewer harmonic components in the Static Synchronous Series Compensator [47]. But a Static Synchronous Series Compensator is more complicated than the STATCOM in structure. Inside the SSSC, there is used bypass protection to reduce the failures in line [48].

*Distributed Static Series Compensator (DSSC)*

Inside the Distributed Static Series Compensator, there is used low rated unit in large numbers. And these units have fewer power ratings [49]. Distributed Static Series Compensator is associated with the SSSC. But in SSSC, there are used high rated units with fewer numbers [50]. Thus, in DSSC, the reliability is increased and can be reduced. There is shown a connection of the distributed static series compensator units with the transmission line system in Fig. 19.

**Fig. 19** Connection of distributed static series compensator with transmission line



Within the DSSC, there are used voltage source converters in a large number. These converters have less rated. These converters are joined with the transmission network by single turn transformers. The secondary winding of the single-turn transformer injects manageable voltage within the transmission line. For emulating capacitive impedance or inductive impedance, the DSSC unit injects the voltage in quadrature with the line current. For controlling the DSSC, there is used PLC or wireless communication systems [15]. There is shown a structure of the distributed static series compensator in Fig. 20. It is less costly and increases reliability. There is no need for phase ground isolation. It provides the continuous power flow in line because many numbers of DSSC are used.

**Combined Devices**

In this segment, there are three combined devices which are explained here. (a) Phase Shifting Transformer (b) Unified Power Flow Controller (c) Interline Power Flow Controller.

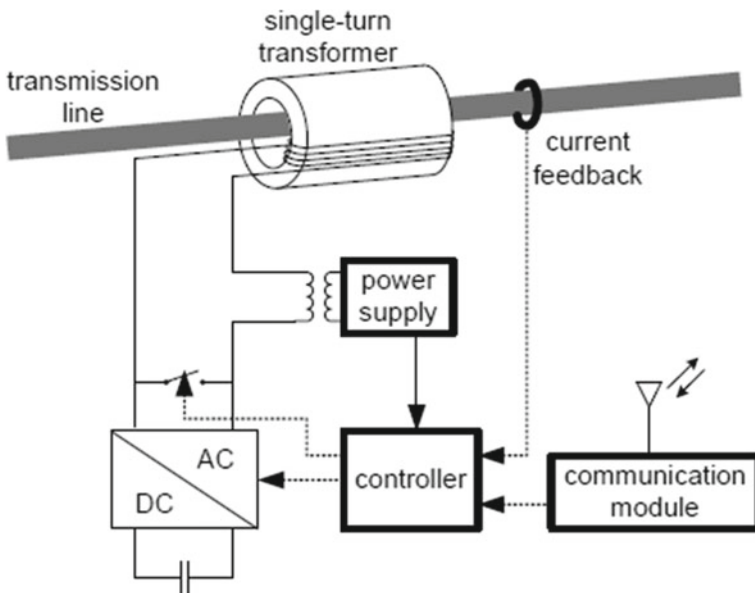


**Fig. 20** A structure of distributed static series compensator unit

*Phase Shifting Transformer*

For regulating the active power within the transmission line, the phase-shifting transformer is used. It is a special type of transformer. It contains different devices like a series transformer, shunt transformer with a tap changer etc. Inside the Phase Shifting Transformer, a voltage is inserted by the series transformer and this voltage is gained by the shunt transformer [16].

To change the transmission angle, there is injected voltage which is in quadrature with the phase voltage  $V_{ph}$  and reasons shifting of a phase angle across the transformer. For regulating quadrature voltage, the taps of the shunt transformer are varied. In this way, across the Phase-shifting transformer, the voltage is removed. There is the basic structure of the phase-shifting transformer is shown in Fig. 21. And there are some demerits in PST. Its response is not so fast because of using a mechanical tap changer. This device is not used appropriately because there is a required short circuit current protection. Its maintenance is high.

*Unified Power Flow Controller (UPFC)*

Unified Power Flow Controller is the most powerful Power Flow Controlling Device. It contains SSSC and STATCOM with a common dc link. Inside the UPFC, bidirectional flow of active power between STATCOM and SSSC [51]. These devices generate reactive power or absorb reactive power on their individual AC terminal. There is used a dc link in between converters. There is shown a structure of the UPFC in Fig. 22.

For injecting the voltage in the transmission line, the series converter is used within the UPFC [52]. It is connected to the line in series. To compensate for the active power

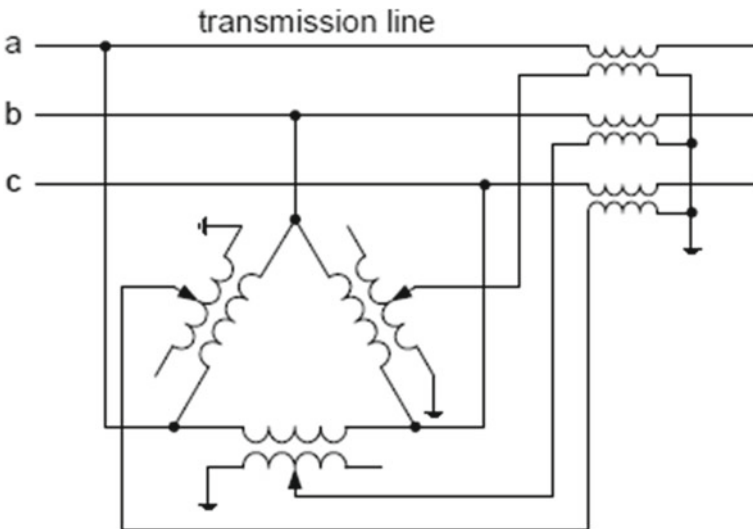
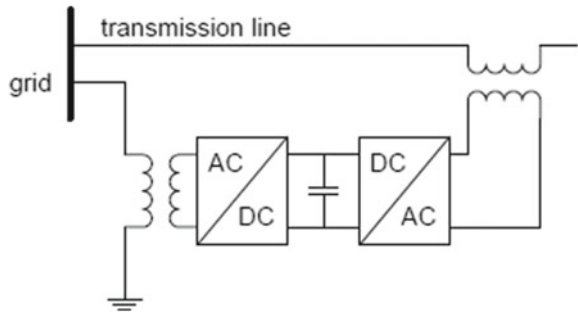


**Fig. 21** A basic structure of the phase shifting transformer

**Fig. 22** A structure of the UPFC



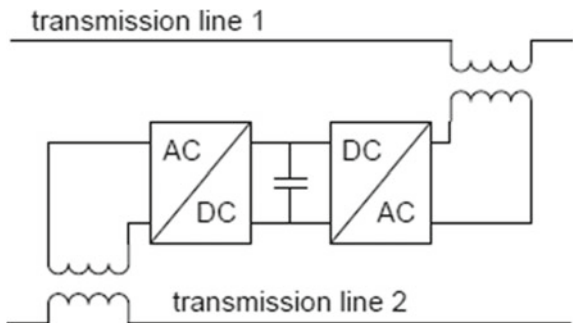
and reactive power in line, it is also utilised. The external source is not required for the series converter. Active power and reactive power are interchanged between line and series converter. The series converter generates the reactive power [53]. The shunt converter is generated the active power. And this power is interchanged by the common DC link. For the regulating of the DC voltage, active power is generated or absorbed by the shunt converter from the bus. UPFC is used for the series compensation, voltage regulation etc. But there are some demerits in UPFC. UPFC is more costly. Because High rated voltage source converters are used in UPFC. For these converters, protection is necessary [54].

*Interline Power Flow Controller (IPFC)*

There is used another powerful controller named Interline Power Flow Controller. Within the IPFC, there are using two or more series converters for different transmission lines. And series converters are joined with the common DC link. The structure of the Interline Power Flow Controller is shown in Fig. 23. It is used for the controlling of the power flow in two or more transmission networks.

For reactive power compensation, every converter gives the reactive power of its transmission line. For interchanging the active power among the converters, a DC link is used. And this DC link is joined between converters. For providing the active power, IPFC is also used. Within the IPFC, a shunt converter can be used for active power compensation. IPFC is more complicated than the UPFC.

**Fig. 23** A structure of the interline power flow controller





### ***1.4 Problem Definition***

There are two most powerful controllers: Unified Power Flow Controller, Interline Power Flow Controller. These have the solid capability to regulate the power inline. In this section, to concern the price related and its dependability. Price related problems are primary apprehension. In the FACTS, there is used joint Flexible AC Transmission System. For transmitting the power from one place to another place with less power loss, a big number of switches are used. And switches are costly. For controlling the powers and faults, transformers are used which are joint with series in line. To make the isolation of voltages, also transformers are used. These transformers have high voltage ratings. Thus, this system makes costly. Secondary apprehension is dependability. Within this system, joint devices are linked with each other to interchange the power. Capacitors are used between the joint devices. Thus, these joint devices rise the cost and make the system composite. In this system, devices' maintenance is high. And also, when the disturbances occur line, these devices do not work appropriately. Because of these two remarkable disadvantages, the IPFC and UPFC are not generally connected practically speaking. Notwithstanding when there is an expansive request for power control inside the power system, the IPFC and UPFC are not as of now the business' first decision. Phase Shifting transformer can be used because it has less capacity of the control appropriately, small price, dependable joined Flexible AC Transmission device has awesome market prospective.

### ***1.5 Objective of This Book Chapter***

For regulating the power, there are utilised a combined device. These devices are used widely in the power network. But combined devices have some demerits such as dependability and price-related problems. Based on the fact, the summary of the book chapter objective is shortened as:

- To remove the sag of the voltage at the fault condition utilising a most powerful power flow controlling device distributed power flow controller. DPFC is a new combined device. Within this device, there are new two approaches. The first approach is the removal of the DC link in between the converters of the combined device DPFC, and the second approach is the DSSC concept for the series converters. Inside the DSSC concept, there is distributed a low rating series converter in line.
- To reduce the harmonics in power supply using distributed power flow controller.
- To certify the concept of the distributed power flow controller using the simulation.
- To examine the DPFC rating and its control capability.
- To design the systems of the control of the DPFC.

## 1.6 Literature Survey

With the help of power system parameters, we control the power like voltage magnitude, the impedance of the line. And also regulate the power with the help of transmission angle parameter. Power Flow Controlling Devices are the most important devices which regulate the parameters of the networks [5]. PFCD is divided into the series, shunt and combined devices both are used in power systems according to their task. To reduce the cost and increase the dependability of the combined devices. There is used a new combined device named DPFC. It is a most powerful Power Flow Controlling Device. It contains SSSC and STATCOM. It is derived from the Unified Power Flow Controller [18]. It regulates the power appropriately and improves the reliability of the system. It is less costly than other FACTS devices [19]. It is obtained from UPFC. It regulates the parameters of the power system like impedance of the line, the voltage of bus, transmission angle [20] the Comparable as the UPFC, the DPFC comprises of shunt and series linked converters. Within DPFC, the shunt converter is comparative as a STATCOM, while the series converter utilizes the DSSC idea, which is to utilize various single-phase low rating converters rather than one high rating three-phase converter. Within this device, there are new two approaches. The first approach is the removal of the DC link in between the converters of the combined device DPFC and the second approach is the DSSC concept for the series converters. Inside the DSSC concept, there is distributed a low rating series converter in line. Inside the DPFC, every converter is autonomous and has its own particular DC capacitor to give the required DC voltage. In Distributed Power Flow Controller device, the transmission line system is utilized as a connection between the direct current terminal of shunt converter and the alternating current terminal of series converters, rather than coordinate association utilizing direct current connection for power interchange between converters.

Because of the unique structures of third harmonic frequency parts in a three-phase system, the third harmonic is chosen for active power interchange in the DPFC. In DPFC, there are three types of controllers for controlling the converters: central control, series control and shunt control [21]. Unified Power Flow Controller is the most powerful power flow controlling device. It contains SSSC and STATCOM with a common dc link. Inside the UPFC, bidirectional flow of active power between STATCOM and SSSC [22]. This device is linked with the grid. It also manages the power network parameters during the fault conditions, for example, bus voltage, line impedance etc.

In this section, Power Flow Controlling Devices are explained. And also review the regulation of the power flow. There is a used DSSC device. This device has a comparatively low price and high dependability. It has limited control competency. Since DSSC merely injects the reactive power. There is used a combined device. These devices have more power control capacity. It can regulate the power appropriately. But it is complicated relatively. In any case, their high cost and multifaceted turn into the bottleneck for their application by and by.

## 2 Distributed Power Flow Controller

Within the past section, there is explained about power electronics-based Power Flow Controlling Devices and mechanical based Power Flow Controlling Devices. These devices have high control ability, particularly Unified Power Flow Controller and Interline Power Flow Controller are appropriate for the future power system. Be that as it may, the UPFC and IPFC are not generally connected practically speaking, because of their high cost and the powerlessness to failures. For the most part, the dependability can be enhanced by diminishing the number of modules; be that as it may, this isn't conceivable because of the composite topology of the powerful controllers which are Interline Power Flow Controller and Unified Power Flow Controller. To decrease the failure rate of the components by choosing modules with higher ratings than should be expected or utilizing excess at the components or power system levels are likewise alternatives. To reduce the cost and increase the dependability of the combined devices. There is used a new combined device named DPFC. Within this device, there are new two approaches. The first approach is the removal of the DC link in between the converters of the combined device DPFC and the second approach is the DSSC concept for the series converters. Inside the DSSC concept, there is distributed a low rating series converter in line [18]. Figure 24 shows the structure Distributed Power Flow Controller. Within this part, there is introduced the DPFC topology and its working rule.

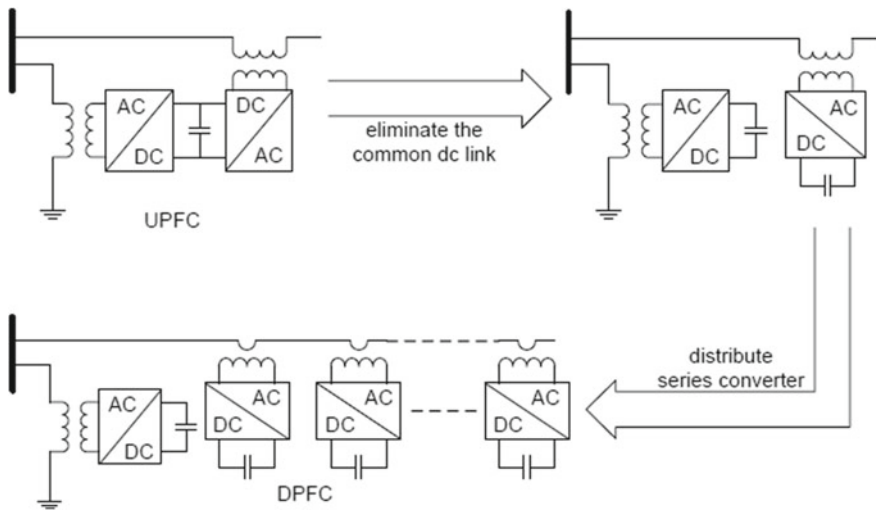


Fig. 24 Flowchart from unified power flow controller to distributed power flow controller

### 2.1 DPFC Topology

By presenting the two methodologies delineated within the past area (removal of the common DC connection and appropriation of the series converter) within the UPFC, the DPFC is accomplished. Comparable to the UPFC, the DPFC comprises shunt and series linked converters. Within DPFC, the shunt converter is comparative as a STATCOM, while the series converter utilizes the DSSC idea, which is to utilize various single-phase low rating converters rather than one high rating three-phase converter [19]. Inside the DPFC, every converter is autonomous and has its own particular DC capacitor to give the required DC voltage. The configuration of the DPFC has appeared in Fig. 25.

As appeared, other than the key parts—shunt and series converters, a DPFC likewise requires a high pass filter that is shunt attached with the further side of the transmission line and a Y-Δ transformer on each side of the line. There is identical control quality of the Unified Power Flow Controller. Inside the UPFC, the series converter and shunt converter are interconnected with dc link. This type of interconnection allows the active power interchange easily. The further new controller is DPFC. This controller is the same as UPFC. But inside the DPFC, the dc-link between the converters is removed. So, active power is interchanged between the converters of the DPFC.

#### Exchanging of Active Power with the Removal of Common DC Connection

In Distributed Power Flow Controller device, the transmission line system is utilized as a connection between the direct current terminal of shunt converter and the alternating current terminal of series converters, rather than coordinate association utilizing direct current connection for power interchange between converters. This type of method of power interchange between the converters is based on an important theory called power theory which is included non-sinusoidal components. In light of the Fourier concept, a non-sinusoidal voltage or current can be displayed as the sum of sinusoidal parts at various frequencies. The result of voltage and current segments gives the active power [20]. Since the necessity of a few terms with various frequencies are zero, so the active power condition is:

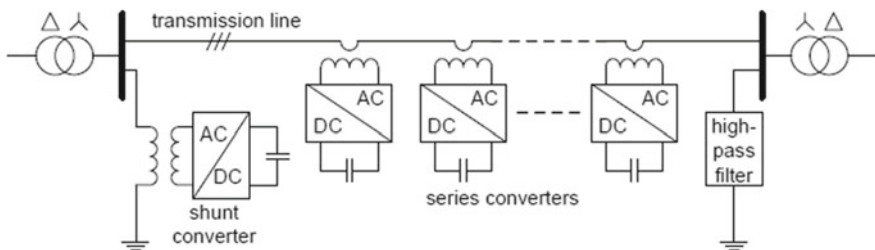


Fig. 25 DPFC configuration

$$P = \sum_{i=1}^{\infty} V_i I_i \cos\theta_i \tag{7}$$

where  $V_i$  and  $I_i$  are the voltage and current at the  $i$ th harmonic, individually, and  $\theta_i$  is the angle between the voltage and current at a similar frequency component. Equation (7) communicates the active power at various frequencies free. Because of this reality, a shunt converter in DPFC can retain the active power in one frequency and creates output power in another frequency. In Fig. 26, there is a two-bus network in the transmission line system. While the power supply produces the active power, there is the capability of a shunt converter for absorbing the power at the fundamental of the current.

**Utilizing Third Harmonic Components**

Because of the unique structures of third harmonic frequency parts in a three-phase system, the third harmonic is chosen for active power interchange in the DPFC [20]. Within the three-phase Transmission system which is the part of the power system, the third-harmonic component in each phase is matchless, which implies they are ‘zero-sequence components. Since the zero-sequence harmonic component can be normally obstructed by Y-Δ trans-formers and these are generally integrated into power system networks (as a means of varying voltage), there is no additional filter required to avoid harmonic leakage. As presented above, for harmonic current, a high-pass filter is necessary to make the close loop of the system and the cut-off frequency of this filter is around the fundamental frequency. Since the voltage isolation is high and the harmonic frequency is near the cut off frequency, the filter will be expensive. By utilizing the zero-sequence harmonic, the expensive filter can be displaced by a cable that associates the neutral point of the Y-Δ transformer on the right side in Fig. 26 with the ground. In Fig. 27, for filtering the zero-sequence harmonic component, a star-delta winding transformer is used. In this process, all the harmonic current components will pass through the star winding transformer and concentrate on the ground cable.

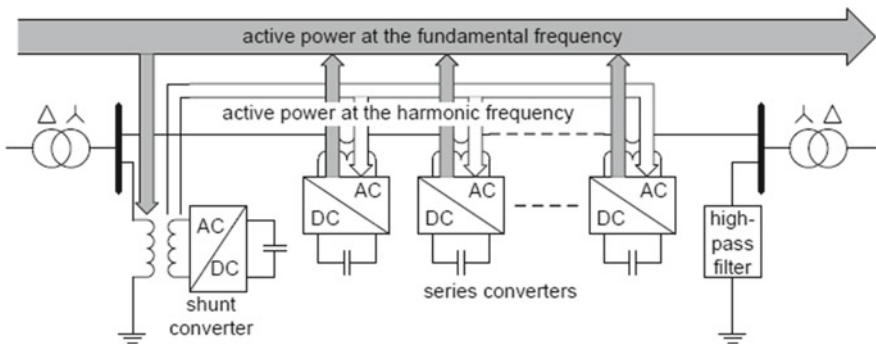
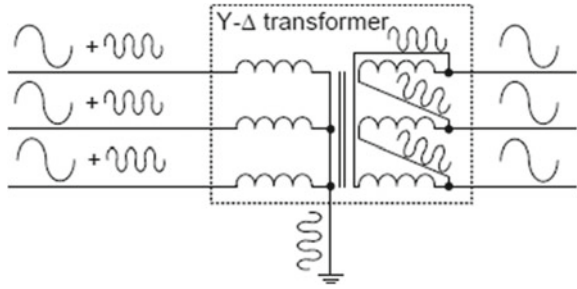


**Fig. 26** Active power exchange between DPFC converters

**Fig. 27** Utilize grounded Y-Δ transformer to filter zero-sequence harmonic



Another favourable position of utilizing the third harmonic component for interchanging active power is that the grounding of the star-delta transformers is utilized to route the harmonic current within the meshed system. On the off chance that the system requires the harmonic current to flow through a particular branch, the neutral point of the star-delta transformer in that branch, other on the side reverse to the shunt converter, which can be grounded and inversely. Within Fig. 28, has been shown the route of the harmonic current by using the grounded star-delta transformer.

Third, sixth, ninth... harmonics are each of the zero-sequence and it can be utilized to interchange active power in distributed power flow controller. Be that as it may, the third harmonics is chosen, since it is the most minimal frequency among each of the zero-sequence harmonics. The connection between the interchanged active power at the  $i$ th harmonic frequency  $P_i$  and the voltages produced by the converters is communicated by the notable power flow condition and given by Eq. (8).

$$P_i = \frac{|V_{sh, i}| |V_{se, i}|}{X_i} (\sin\theta_{sh, i} - \sin\theta_{se, i}) \tag{8}$$

where  $X_i$  indicates line impedance at  $i$ th is the frequency,  $|V_{sh, i}|$  depicts voltage magnitude at the  $i$ th harmonic frequency of shunt converter and  $|V_{se, i}|$  depicts the

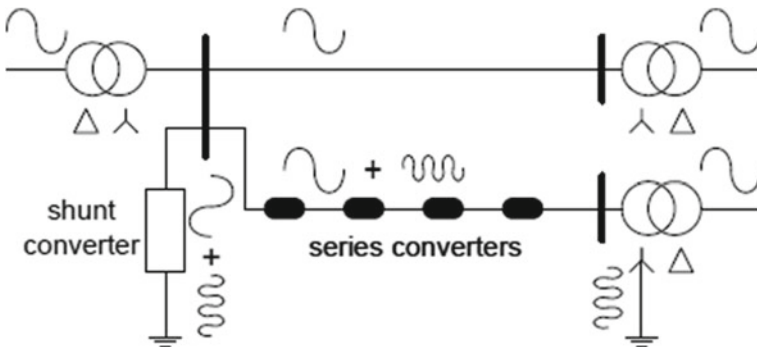


**Fig. 28** Utilizing the grounding of the star-delta transformer to route the harmonic current

voltage magnitude an  $i$ th harmonic frequency of the series converter and  $\theta_{sh,i} - \theta_{se,i}$  indicates the angle difference between the two voltages of the shunt and series converters.

### 2.2 DPFC Control

In DPFC, there are three types of controllers for controlling the converters: central control, series control and shunt control which are depicted in Fig. 29. The central control deals with the DPFC task at the power system level [21, 22]. The task of every controller is recorded.

#### Central Control

In the central control, it creates the reference signals for shunt and series converters. It can be worked for DPFC to maintain power level especially. It can be used for the balancing of the asymmetrical components, for power controlling and for low-frequency power oscillation damping. Central control provides the voltage reference signal for the shunt converters and series converters, according to the requirement of the system. It generates all the references at the fundamental frequency.

#### Shunt Control

In shunt control, it provides active power to the series converters. For the series converters, it infuses the 3rd harmonic current in the transmission line at the fundamental frequency; the 3rd harmonic current is locked with the voltage of the bus. For capturing the voltage of the bus, a Phase Lock Loop is used. And, for the 3rd harmonic component, the output phase signal of Phase Lock Loop is multiplied by three for generating the virtual rotation reference frame. It works specially to inject the current into the line for maintaining the dc voltage of the capacitor. There are two cascaded controllers of the fundamental frequency components. For modulating the shunt current at the fundamental frequency, current control is used which is the inner control loop system. In the system, the d-component is created by the dc control

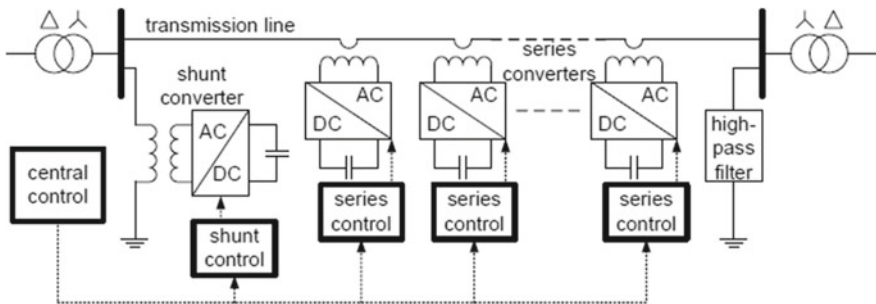
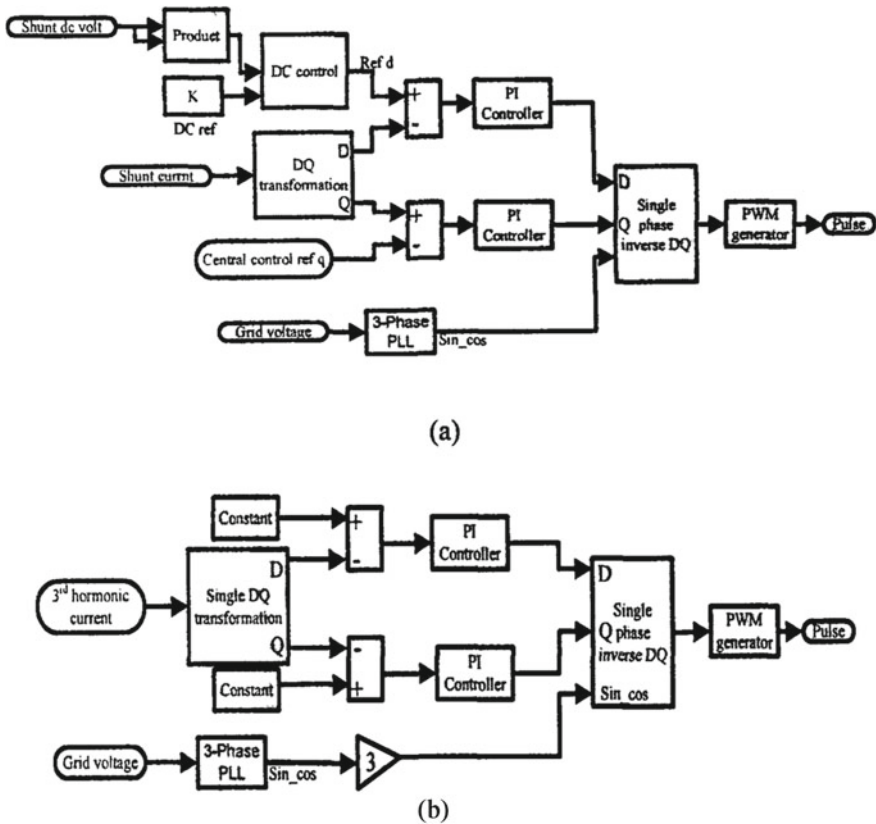


Fig. 29 DPFC control block diagram

system and central control provided the q-component of the reference signal of the shunt converter. Figure 30 depicts the two cascaded controllers which are the current control and d.c. voltage control system.

**Series Control**

Each series converter has its particular series control. The controllers used to keep up the capacitor DC voltage of its converter, by utilizing third harmonic frequency components, central control approved the series voltage at the fundamental frequency. Within the series control system diagram, the third harmonic frequency controller is depicted which is the principal controller loop in Fig. 31. For the controlling of capacitors' voltages, the vector control principle is utilised. In series converters' capacitor d.c voltages, there are high voltage ripples because of using single-phase series converters are used. There is a technique to reduce voltage ripples, first is, to reduce the converters' currents magnitudes which are obtained by taking a bigger turns ratio of the transmission line equipped single-phase transformers. And second



**Fig. 30** a Block diagram of fundamental frequency control system. b Block diagram of harmonic frequency control system



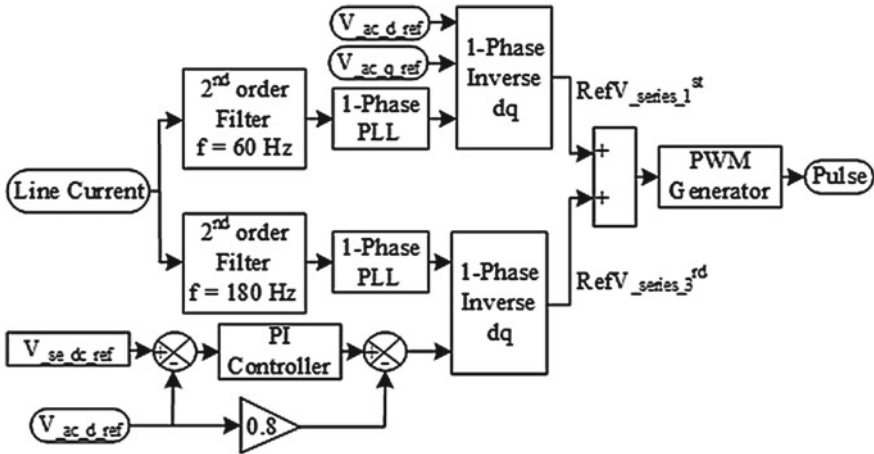


Fig. 31 Block diagram of Controller of series converters

is to maintain the larger values of the capacitance of the capacitors of the series converters.

### 2.3 Advantages of Distributed Power Flow Controller

In DPFC, D-FACTS concept has been applied for exchanging the active power. Along these lines, the DPFC acquires every one of their important points:

- **High controllability:** The DPFC can instantaneously regulate every one of the line parameters like impedance of the line, voltage of buses and transmission angle.
- **High dependability quality:** Within the DPFC, there is the repetition of the series converter gives high dependability without expanding cost. Converters are independent of each other and failure of one won't impact alternate converters.
- **Low price:** there is utilised a few powers rating converter. Due to the using a huge number of series converters, these converters are fabricated in a series generation. In any case, there is a disadvantage to utilizing the DPFC.

### 2.4 Disadvantages of Distributed Power Flow Controller

**Excessive currents:** Since the interchanging of the power amid the series converters and shunt converters happens with a similar transmission line as the primary power, additional currents are presented which are at the third harmonic components. And

these currents diminish the limit of the transmission network and result in additional losses inside the line and the two-star delta transformers.

There is utilised a new FACTS device Distributed Power Flow controller. DPFC is a combined device. Within this device, there are new two approaches. The first approach is the removal of the DC link in between the converters of the combined device DPFC and the second approach is the DSSC concept for the series converters. Inside the DSSC concept, there is distributed a low rating series converter in line. Within the DPFC, there is the repetition of the series converter gives high dependability without expanding cost than Unified Power Flow Controller. Converters are independent of each other and failure of one won't impact alternate converters.

### 3 Control Scheme for the Distributed Power Flow Controller

Within the DPFC, there are three controllers: central control, series control and shunt control. In the central control, it creates the reference signals for shunt and series converters. It can be worked for DPFC to maintain power level especially. In shunt control, it provides active power to the series converters. For the series converters, it infuses the 3rd harmonic current in the transmission line at the fundamental frequency; the 3rd harmonic current is locked with the voltage of the bus. Each series converter has its particular series control. The controllers used to keep up the capacitor DC voltage of its converter, by utilizing third harmonic frequency components, central control approved the series voltage at the fundamental frequency. For modelling of the Distributed Power Flow Controller, Park's transformation is utilised. This transformation converts the AC components into the DC components. And also, there are used a PI controller. PI controllers regulate the DC components of the DPFC.

Within this segment, The Distributed Power Flow Controller is modelled for creating the DPFC control system. This model has explained the nature of the DPFC at the level of the scheme, which is at the third harmonic frequency and fundamental. For modelling of the converters, its switching nature model is not necessary for this system.

#### 3.1 Summary of DPFC Model

In the DPFC modelling, there is network modelling and converter modelling. Here single-phase converters are used so they are also modelled. For confirming the model of the single-phase series converter is well-matched with the model of the three-phase system. The modelling of the network is modelled like three single-phase systems with 120-degree phase shifting. Within Fig. 32, there is a flow chart of the Distributed Power Flow Controller model method.

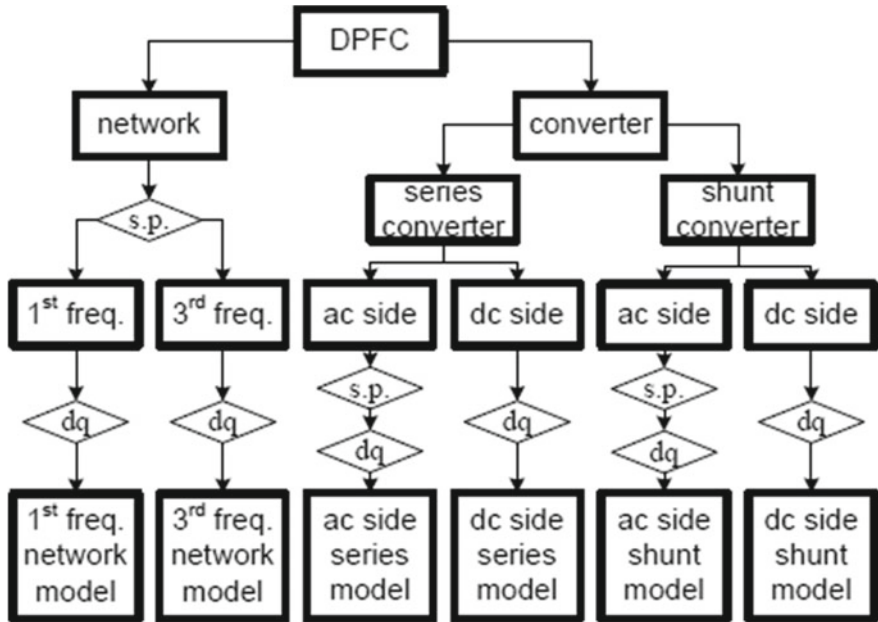


Fig. 32 The flow chart of the DPFC modelling

There are two theorems are applied for the modelling of the Distributed Power Flow Controller: (a) Superposition theorem (b) Park’s transformation [17]. Since the transmission line system is linear so superposition theorem is applied. In this flow chart of DPFC, s.p in diamond shape indicates the procedure of the superposition theorem. And in also dq in diamond shape indicates the procedure of the Park’s transformation. For the study of the signal, the park’s transformation is used which is at a single frequency. The superposition theorem divides the frequency. And when the components are at dissimilar frequencies, for analysing, the park’s transformation is utilised. Also used for analysing the electrical machinery, for changing the a.c. to d.c. components. The principle of Park’s transformation is to scheme a.c. signal in vector demonstration on to the structure of the rotating reference mentioned to as the “dq-frame”. In this method, rotation frequency is chosen similar to the a.c. signal frequency. So, in dq frame, currents and voltages are constant in a steady-state condition.

At the dissimilar frequencies, the components are changed into the two rotating references frames which are independent at dissimilar frequencies. Park’s transformation is applied because at the fundamental frequency, the components are three-phase components. The Park’s transformation is applied in the three-phase power system. For this, the reason is that the three-phase system’s third harmonic component is measured as a single-phase component, and also that one component is in phase. The Modelling of the network, in this segment, is presented. Firstly, separated models are introduced.

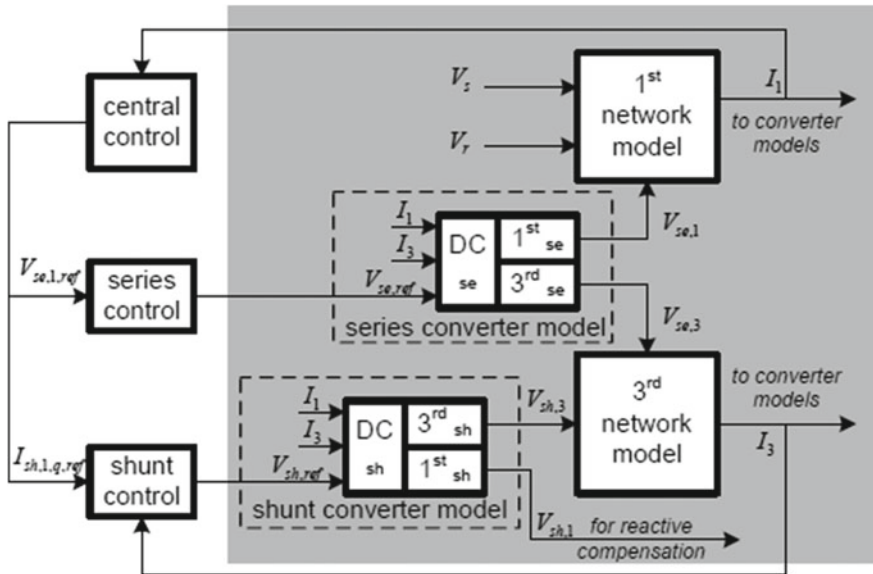


Fig. 33 A construction of the separated models within Distributed Power Flow Controller

### 3.2 Connection of Separated Model

In Fig. 33, the separated model is represented in the DPFC model. In the DPFC model, there are four models, model of the series converter, and model of shunt converter, fundamental frequency network model and the model of third harmonic frequency network. Within the model of the fundamental frequency network, there are calculated the current through line I1 which is based on the voltages of sending end, receiving end also series converters. For the calculation of the d.c voltage, this current feeds back to the model of the series converter and shunt converter. From the voltage is injected through the series converters and shunt converters, current I3 is calculated within the model of the third harmonic frequency network. For the calculation of the dc voltage of the converter, the third harmonic current is utilised.

### 3.3 Modelling of Network

In this segment, there is a mathematical representation of the fundamental frequency and third harmonic frequency. The two frequencies have been separated by the superposition theorem.

### The Modelling of the Fundamental Frequency Network

Amid the procedure of the network modelling, there is used a converter of the Distributed Power Flow Controller. These converters are identified as a manageable voltage source. Within a Practical transmission network, idealize regulation among the phases are frequently expected because the impact of the asymmetry is normally little. Inside the overhead transmission system, there are used an overhead conductor, which is known as a ground wire. And it is grounded with uniform intervals along the length of the transmission system. So, grounding is called an ideal conductor. And this ideal conductor has zero impedance. Its mutual impedance between phases is ignored. In Fig. 34, there is an equivalent circuit configuration of the fundamental frequency network. From the equivalent circuit,  $V_{se,1}$ , depicts the voltages injected by the series converters which are at the fundamental frequency.  $Z_1$  depicts the impedance of the transmission line. And also,  $V_r$  depicts the sending end voltage and  $V_s$  depicts the receiving end voltage. Column vectors voltages are  $V_{se,1}$ ,  $V_r$ ,  $V_s$  and also  $I_1$  is a column vector, which consists of info for the three phases. For the modelling of the network which at the fundamental frequency, there is modelled like three single-phase systems. These three single phases are moved by  $120^\circ$ .

From the equivalent circuit configuration of the fundamental frequency network, the association between the line current  $I_1$  and series voltage is shown in Eq. (9).

$$\begin{bmatrix} V_{s,a} \\ V_{s,b} \\ V_{s,c} \end{bmatrix} - \begin{bmatrix} V_{r,a} \\ V_{r,b} \\ V_{r,c} \end{bmatrix} - \begin{bmatrix} V_{se,1,a} \\ V_{se,1,b} \\ V_{se,1,c} \end{bmatrix} = \begin{bmatrix} Z_1 & 0 & 0 \\ 0 & Z_1 & 0 \\ 0 & 0 & Z_1 \end{bmatrix} \cdot \begin{bmatrix} I_{1,a} \\ I_{1,b} \\ I_{1,c} \end{bmatrix} \tag{9}$$

Inside the network model, there is explained about series converters of the DPFC. And how it affects the current in the line, is shown. After changing the injected voltage of the series converter, the current can be affected in the transmission line. Appropriately,  $V_{se,1}$  depicts the input injected voltage of the model and  $I_1$  depicts the output line current of the model. In two-port networks, there are sending end voltage and receiving end voltage. Both voltages are assumed constant. Although as shown

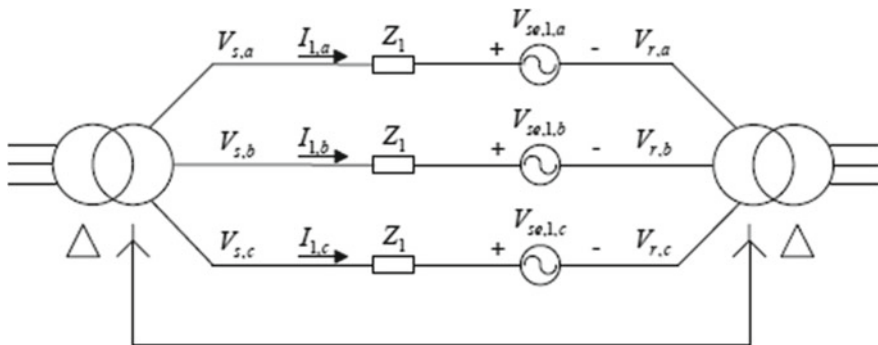
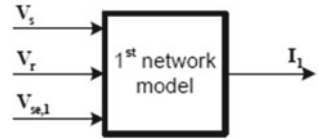


Fig. 34 The equivalent circuit configuration of the fundamental frequency network

**Fig. 35** Model of the input and output of the fundamental frequency network



in Fig. 35, these voltages are considered as input for the modelling of the meshed network.

**The Modelling of the Third Harmonic Frequency Network**

In Fig. 36, the shunt converter is used for infusing the third harmonic current which is at the star delta transformer’s neutral point. The third harmonic current circulates over three-phase and creates a close loop system through the neutral point of the other star-delta transformer. Figure 36 shows the use of a grounded star-delta transformer for filtering the zero-sequence harmonic.

As shown in Fig. 37, inside the equivalent circuit, there are line impedance and zero sequence reactance of the two transformers. Both are joined.  $Z_3$  depicts the total impedance at the third harmonic frequency. As depicted previously, supposing when the neutral impedance is zero. Thus, the association between currents and voltages are shown in Eq. (10).

$$\begin{bmatrix} V_{sh,3} - V_{se,3,a} \\ V_{sh,3} - V_{se,3,b} \\ V_{sh,3} - V_{se,3,c} \end{bmatrix} = \begin{bmatrix} Z_1 & 0 & 0 \\ 0 & Z_1 & 0 \\ 0 & 0 & Z_1 \end{bmatrix} \cdot \begin{bmatrix} I_{3,a} \\ I_{3,b} \\ I_{3,c} \end{bmatrix} \tag{10}$$

Within the model of the third harmonic frequency network,  $V_{sh,3}$  depicts the input voltage which comes from the model of the converter.  $V_{se,3}$  depicts the also input voltage which comes from the model of the converter. And  $I_3$  depicts the third

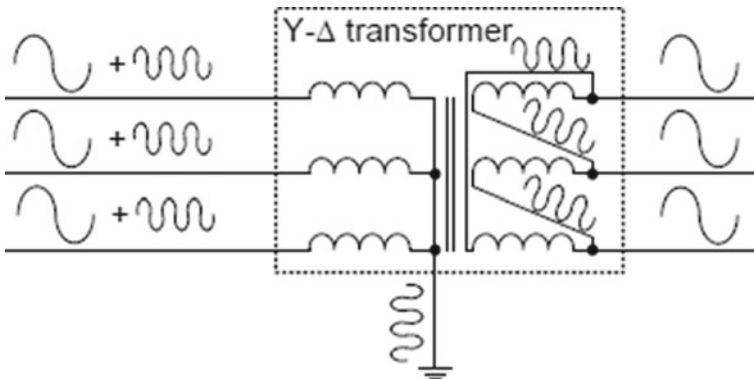


**Fig. 36** Use of grounded Y-Δ transformer for filtering the zero-sequence harmonic

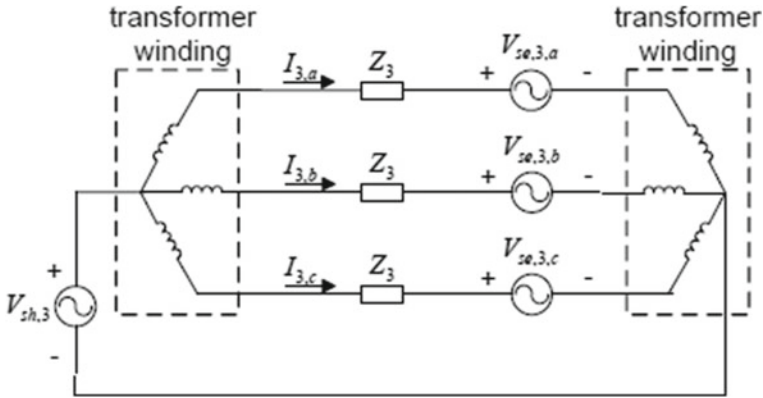
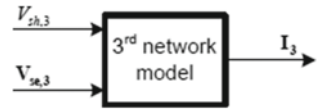


Fig. 37 Equivalent circuit diagram of the third harmonic network

Fig. 38 The model of the input and output of the third harmonic frequency network



harmonic current of every phase as shown in Fig. 38. This third harmonic current is the output of the model.

### 3.4 Series Converter Model

In DPFC, there is a series converter that is identical and single-phase and its series converter is based on the PWM control system. For simplification purposes, the loss of the converter is not considered which is shown in Fig. 39.

Fig. 39 Basic model of the series converter

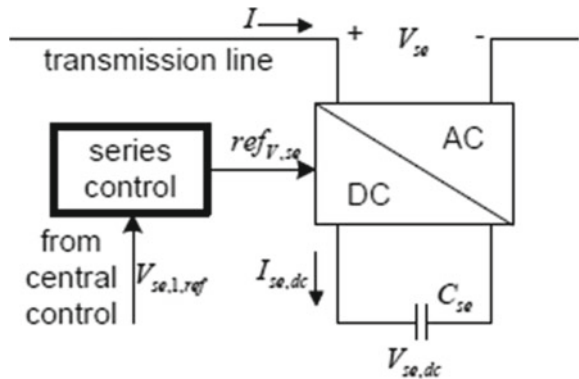
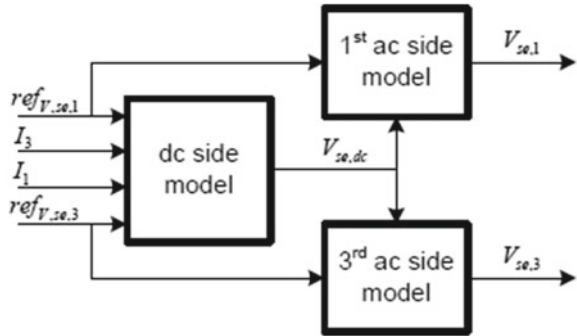


**Fig. 40** A simplified model of the series converter



In the model of the series converter, there is a  $V_{se,dc}$  which depicts the dc voltage of the series converter,  $refv_{se}$  depicts the reference a.c signal amplitudes. series control generates this reference signal.  $V_{se,1}$  is the voltage component that is at the fundamental frequency and  $V_{se,3}$  is also the voltage component that is at the third harmonic frequency. The relationship between two voltages is shown in Eq. (11).

$$V_{se} = V_{se,1} + V_{se,3} \tag{11}$$

Inside Fig. 40, there is a simplified model of the series converter. Within the model, the AC side and DC side are joined to each other.

The reference voltage is the input signal for the series current. The series converter generates the A.C voltage and this voltage is the output signal of the model.

### 3.5 Modelling of the Shunt Converter

Inside the shunt converter, there is used a three-phase converter. These three-phase converters are joined with a single-phase converter. It's like a Static synchronous compensator. For absorbing the active power from the line, the three-phase converter is joined with the star delta transformer. Within the figure of the shunt converter, a single-phase converter is used which is linked amid the neutral point of the Y-Δ transformer and ground. This is shown in Fig. 41 of the shunt converter diagram.

Within the shunt converter, the third harmonic component is not present at the delta side of the transformer. And the left side converter consists of only components. These components are at the fundamental frequency. These are:  $V_{sh,1}$  depicts voltage and  $I_{sh,1}$  depicts current,  $V_{sh,3}$  depicts voltage which at the third harmonic frequency and  $I_{sh,3}$  depicts current which at the third harmonic frequency. These components are single phases.

For modelling of the Distributed Power Flow Controller, Park's transformation is utilised. This transformation converts the AC components into the DC components. And also, there are used a PI controller. PI controllers regulate the DC components of



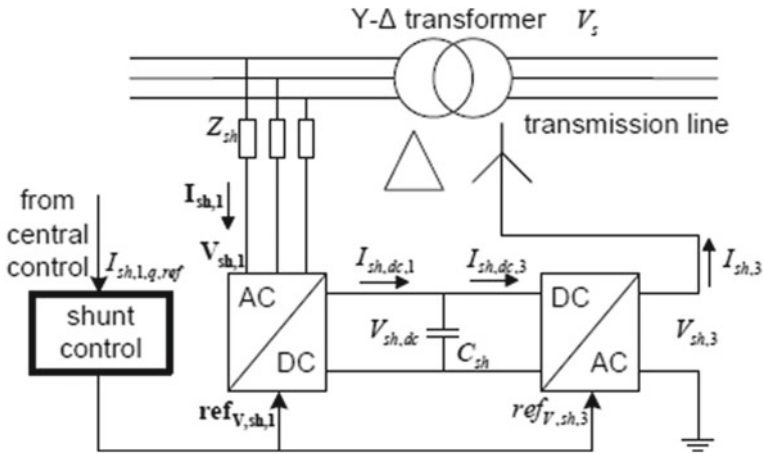


Fig. 41 A basic shunt converter configuration

the DPFC. There is designed a parameter of the Distributed Power Flow Controller. Shunt and series controllers are improved proper.

## 4 Results

There is a description of the Distributed Power Flow Controller Model. Three-phase sources have been connected with nonlinear RLC load through the transmission line in the DPFC model. There are two lines and their length is 100 km each. For simulating the dynamic task, a three-phase fault has occurred near the RLC load. Without the DPFC, the fault duration is 0.5 to 0.7 min. And voltage sag of the load is approximately 0.5 per unit. After using the DPFC, the voltage sag of the load is alleviated [22].

### 4.1 Simulation Results of the Distributed Power Flow Controller

See Figs. 42 and 43.

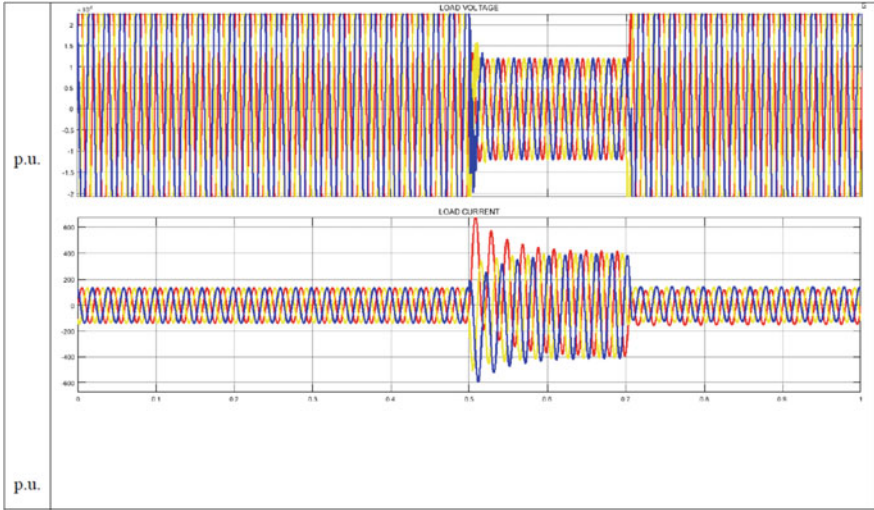


**Fig. 42** Voltage sag and current swell of the three-phase load without distributed power flow controller

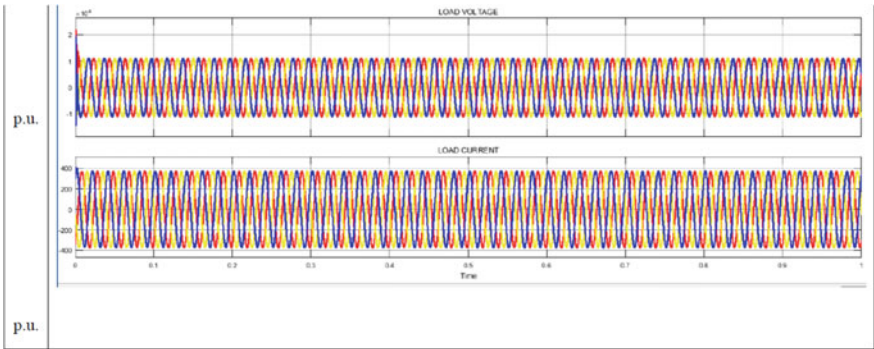


**Fig. 43** Mitigation of the voltage and current of the three-phase load with distributed power flow controller

### 4.2 *FFT Analysis of the Three-Phase Load Voltage of the Distributed Power Flow Controller*

See Figs. 44 and 45, Tables 1 and 2.

The three-phase source has been connected with nonlinear RLC load through the transmission line in the DPFC model. With DPFC, voltage sag of the load is alleviated and also THD of the load is reduced.

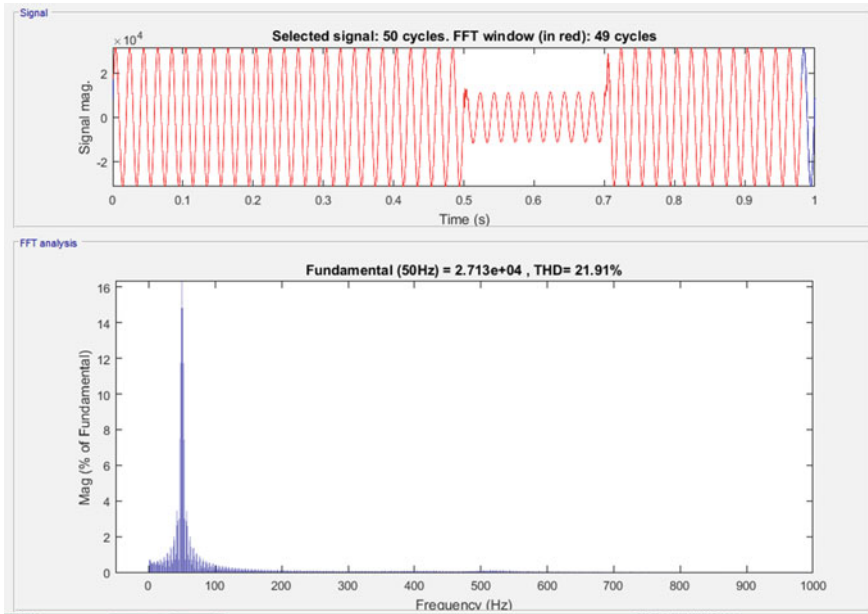


**Fig. 44** Total harmonic distortion of the three-phase load voltage without distributed power flow controller

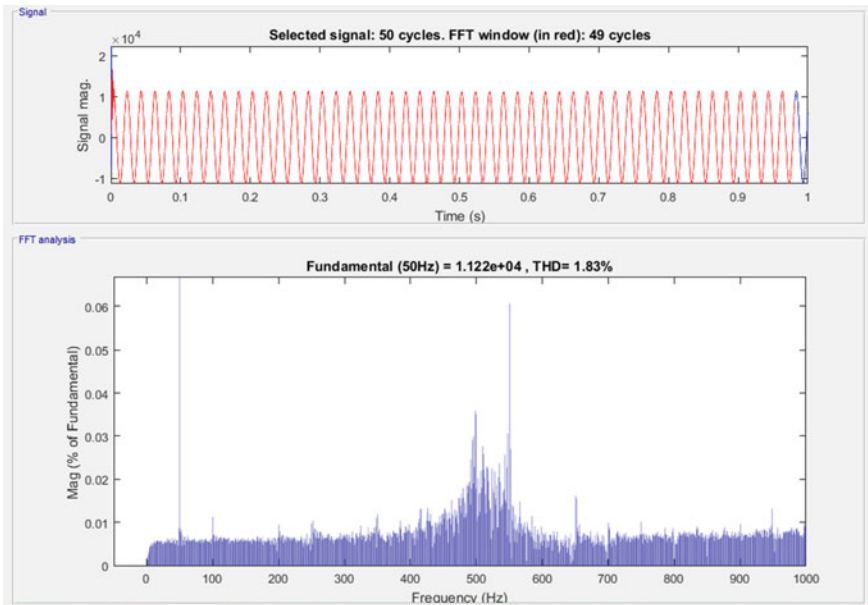


**Fig. 45** Total harmonic distortion of the three-phase load voltage with distributed power flow controller

**Table 1** FFT Analysis of DPFC

Description	Percentage of the Total Harmonic Distortion
Without DPFC	21.91
With DPFC	1.83

**Table 2** The simulated system parameters of the Distributed Power Flow Controller

Description of the parameters	Value of the parameters
Voltage of the three-phase source	11 kV
Rated frequency of the system	50 Hz
The ratio of X/R	3
<i>Transmission system</i>	
Resistance	0.012 pu/km
Inductance reactance	$0.933 e^{-3}$ pu/km
Capacitance reactance	$12.74 e^{-9}$ pu/km
Length of the transmission line	100 km
<i>Three-phase shunt converters</i>	
Capacitor of the DC link	2000 $\mu$ F
<i>Coupling transformer of the shunt converter</i>	
Nominal power	250 MVA
<i>Transformer (series converter)</i>	
Nominal power	250 MVA
Type of the three-phase fault	ABC-G
Ground resistance	0.01 $\Omega$

## 5 Conclusion

Inside the new device DPFC, there are new two methodologies. The first methodology is the removal of the DC link in between the converters of the combined device DPFC and the second methodology is the DSSC concept for the series converters. In the DSSC concept, there is distributed a low rating series converter in line. Within the DPFC, there is the repetition of the series converter gives high dependability without expanding cost than Unified Power Flow Controller. Converters are independent of each other and failure of one won't impact alternate converters.

## 6 Future Work

This project describes the Distributed Power Flow Controller. This controller has a more dependable and lower cost than the Unified Power Flow Controller. Nevertheless, Inside the DPFC, the third harmonic component is fixed at the constant value.

This problem can be addressed in designing the controllers to vary the magnitude of the third harmonic current in a way that it is adjusted according to the necessity for active power. Thus, the loss has been decreased in the DPFC. For reducing disturbance effects, series converters have functioned outdoors.

**Acknowledgements** Declared none.

**Consent for Publication**

Not applicable.

**Funding** Declared none.

**Conflict of Interest** The authors declare no conflict of interest, financial or otherwise.

## References

1. Puttgen, H.B., MacGregor, P.R., Lambert, F.C.: Distributed generation: semantic hype or the dawn of a new era? *IEEE Power Energ. Mag.* **1**(1), 22–29 (2003)
2. Farhangi, H.: The path of the smart grid. *IEEE Power Energ. Mag.* **8**(1), 18–28 (2010)
3. Van Hertem, D., Verboomen, J., Belmans, R., Kling, W. L.: Power flow controlling devices: an overview of their working principles and their application range. In: 2005 International Conference on Future Power Systems, pp. 1–6 (2005)
4. Mohanty, A.K., Barik, A.K.: Power system stability improvement using FACTS devices. *Int. J. Modern Eng. Res. (IJMER)* **1**(2), 666–672 (2011)
5. Peng, F.Z.: Flexible AC transmission systems (FACTS) and resilient AC distribution systems (RACDS) in smart grid. *Proc. IEEE* **105**(11), 2099–2115 (2017)
6. Baum, W.U., Frederick, W.A.: A method of applying switched and fixed capacitors for voltage control. *IEEE Trans. Power Appar. Syst.* **84**(1), 42–48 (1965)
7. Pillai, G.N., Ghosh, A., Joshi, A.: Torsional interaction studies on a power system compensated by SSSC and fixed capacitor. *IEEE Trans. Power Delivery* **18**(3), 988–993 (2003)
8. Moore, P., Ashmole, P.: Flexible AC transmission systems. *Power Eng. J.* **9**(6), 282–286 (1995)
9. Edris, A.A.: Proposed terms and definitions for flexible AC transmission system (FACTS). *IEEE Trans. Power Delivery* **12**(4), 1848–1853 (1997)
10. Gyugyi, L.: Dynamic compensation of AC transmission lines by solid-state synchronous voltage sources. *IEEE Trans. Power Delivery* **9**(2), 904–911 (1994)
11. Yu, Q., Li, P., Liu, W., Xie, X.: Overview of STATCOM technologies. In: 2004 IEEE International Conference on Electric Utility Deregulation, Restructuring and Power Technologies, vol. 2, pp. 647–652 (2004)
12. Huang, G.M., Li, Y.: Impact of thyristor controlled series capacitor on bulk power system reliability. *IEEE Power Eng. Soc. Summer Meeting Chicago* **2**, 975–980 (2002)
13. McDonald, D.J., Urbanek, J., Damsky, B.L.: Modeling and testing of a thyristor for thyristor controlled series compensation (TCSC). *IEEE Trans. Power Delivery* **9**(1), 352–359 (1994)
14. Mahajan, V.: Thyristor controlled series compensator. In: 2006 IEEE International Conference on Industrial Technology, pp. 182–187 (2006)
15. Ferreira, H.C., Grove, H.M., Hooijen, O., Han Vinck, A.J.: Power line communications: an overview. In: *IEEE AFRICON 4th, Stellenbosch*, vol. 2, pp. 558–563 (1996)
16. Verboomen, J., Van Hertem, D., Schavemaker, P.H., Kling, W.L., Belmans, R.: Phase shifting transformers: principles and applications. In: 2005 International Conference on Future Power Systems, pp. 1–6 (2005)

17. Han, S.-B., Cho, G.-H., Jung, B.-M., Choi, S.-H.: Vector-transformed circuit theory and application to converter modeling/analysis. In: PESC 98 Record. 29th Annual IEEE Power Electronics Specialists Conference, vol. 1, pp. 538–544 (1998)
18. Yuan, Z., de Haan, S.W.H., Ferreira, B.: A new FACTS component—Distributed Power Flow Controller (DPFC). In: 2007 European Conference on Power Electronics and Applications, pp. 1–4 (2007)
19. Yuan, Z., de Haan, S.W.H., Ferreira, J.A.: Construction and first result of a scaled transmission system with the Distributed Power Flow Controller (DPFC). In: 2009 13th European Conference on Power Electronics and Applications, pp. 1–10 (2009)
20. Yuan, Z., de Haan, S.W.H., Ferreira, J.B., Cvoric, D.: A FACTS device: Distributed Power-Flow Controller (DPFC). *IEEE Trans. Power Electron.* **25**(10), 2564–2572 (2010)
21. Pushpanadham, C., Rao, T.S.: A novel power quality improvement technique using multi-connected Distributed Power Flow Controller (MC-DPFC). *Int. J. Adv. Res. Electr. Electron. Instrum. Eng.* **2**, 106–117 (2013)
22. Jamshidi, A., Masoud Barakati, S., Ghahderijani, M.M.: Power quality improvement and mitigation case study using distributed power flow controller. In: 2012 IEEE International Symposium on Industrial Electronics, pp. 464–468 (2012)
23. D'Ovidio, G., Ometto, A., Valentini, O.: A novel predictive power flow control strategy for hydrogen city rail train. *Int. J. Hydrogen Energy* **45**(7), 4922–4931 (2020)
24. Chorghade, A., Deodhar, V.A.K.: FACTS devices for reactive power compensation and power flow control—recent trends. In: 2020 International conference on industry 4.0 technology (I4Tech), pp. 217–221 (2020)
25. Khalil, U., Khan, M.Y.A., Khan, U.A., Atiq, S.: Power flow control by unified power flow controller. *Mehran University Res. J. Eng. Technol.* **39**(2), 257–266 (2020)
26. Shimpi, R.J., Desale, R.P., Patil, K.S., Rajput, J.L., Chavan, S.B.: Flexible AC transmission systems. *Int. J. Comput. Appl.* **1**(15), 54–57 (2010)
27. Mohamed, S.E.G.: Power flow control capability of the power transistor-assisted Sen transformer and the unified power flow controller: a close comparison. *IET Gener. Transm. Distrib.* **14**(15), 3033–3041 (2020)
28. Kechroud, A., Myrzik, J.M.A., Kling, W.: Taking the experience from flexible AC transmission systems to flexible AC distribution systems. In: 2007 42nd International Universities Power Engineering Conference, pp. 687–692 (2007)
29. Agelidis, V.G., Demetriades, G.D., Flourentzou, N.: Recent advances in high-voltage direct-current power transmission systems. In: 2006 IEEE International Conference on Industrial Technology, pp. 206–213 (2006)
30. Wang, C., Feng, C., Zeng, Y., Zhang, F.: Improved correction strategy for power flow control based on multi-machine sensitivity analysis. *IEEE Access* **8**, 82391–82403 (2020)
31. Naidu, R.P.K., Meikandasivam, S.: Power quality enhancement in a grid-connected hybrid system with coordinated PQ theory & fractional order PID controller in DPFC. *Sustain. Energy, Grids Netw.* **21**, 1–12 (2020)
32. Wan, Y.: Extended SVC modeling for frequency regulation. *IEEE Trans. Power Delivery* **36**(1), 484–487 (2020)
33. Meng, J., Lu, H., Liu, J.: Joint quality selection and caching for SVC video services in heterogeneous networks. In: 2020 IEEE Wireless Communications and Networking Conference (WCNC), pp. 1–6 (2020)
34. Maurya, D.S., Jadhav, P.D., Joshi, R.S., BendkhaLe, R.R., Thakre, M.P.: A detailed comparative analysis of different multipulse and multilevel topologies for STATCOM. In: 2020 International Conference on Electronics and Sustainable Communication Systems (ICESC), pp. 1112–1117 (2020)
35. Selvaraj, J., Mohammed, A.S.: Mutation-based PSO techniques for optimal location and parameter settings of STATCOM under generator contingency. *Int. J. Intell. Sustain. Comput.* **1**(1), 53–68 (2020)
36. Gotham, D.J., Heydt, G.T.: Power flow control and power flow studies for systems with FACTS devices. *IEEE Trans. Power Syst.* **13**(1), 60–65 (1998)

37. Xiao, Q., Chen, L., Jin, Y., Mu, Y., Cupertino, A.F., Jia, H., Teodorescu, R.: An improved fault-tolerant control scheme for cascaded H-bridge STATCOM with higher attainable balanced line-to-line voltages. *IEEE Trans. Indus. Electron.* **68**(4), 2784–2797 (2020)
38. Orcajo, G.A.A., Diez, J.R., Cano, J.M., Normiella, J.G., González, J.F.P., Rojas, C.H., Cifrián, D.: Enhancement of power quality in an actual hot rolling mill plant through a STATCOM. *IEEE Trans. Ind. Appl.* **56**(3), 3238–3249 (2020)
39. Saxena, A., Singh, B., Rai, J.N.: Comparative study of static VAR compensation techniques—thyristor switched reactor and thyristor switched capacitor. In: 2020 5th International Conference on Communication and Electronics Systems (ICCES), pp. 1–5 (2020)
40. Moftah, A.A.M., Rajab, Z., Ighneiwa, I.: Investigation in thyristor-controlled reactor (TCR). In: Proceedings of the 6th International Conference on Engineering & MIS 2020, pp. 1–7 (2020)
41. Singh, P., Tiwari, R., Sangwan, V., Gupta, A.K.: Optimal allocation of thyristor-controlled series capacitor (TCSC) and thyristor-controlled phase-shifting transformer (TCPST). In: 2020 International Conference on Power Electronics & IoT Applications in Renewable Energy and its Control (PARC), pp. 491–496 (2020)
42. Emarloo, A.A., Changizian, M., Shoulaie, A.: Application of gate-controlled series capacitor to mitigate subsynchronous resonance in a thermal generation plant connected to a series-compensated transmission network. *Int. Trans. Electr. Energy Syst.* **30**(12), 1–20 (2020)
43. Rahmani, S., Hamadi, A., Al-Haddad, K., Dessaint, L.A.: A combination of shunt hybrid power filter and thyristor-controlled reactor for power quality. *IEEE Trans. Indus. Electron.* **61**(5), 2152–2164 (2013)
44. Juneja, K.: A fuzzy-controlled differential evolution integrated static synchronous series compensator to enhance power system stability. *IETE J. Res.* 1–16 (2020)
45. Smolovik, S.V., Chudny, V.S., Denisenko, A.I., Liamov, A.S., Tupitsina, A.L.: Control characteristics of static synchronous series compensator. In: 2020 IEEE Conference of Russian Young Researchers in Electrical and Electronic Engineering (EIConRus), pp. 1329–1332 (2020)
46. Salim, N.A., Zain, N.D.S.M., Mohamad, H., Yasin, Z.M., Ab Aziz, N.F.: Multi-machine transient stability by using static synchronous series compensator. *Int. J. Power Electron. Drive Syst.* **11**(3), 1249–1258 (2020)
47. Sarathkumar, D., Venkateswaran, K., Santhosh, P., Gaayathry, K., Yadav, K.T.: Simulation of static synchronous series compensator (SSSC) by using doubly fed induction generator (DFIG) for stability enhancement. *Int. J. Adv. Sci. Technol.* **29**(5), 345–354 (2020)
48. Song, S.H., Lim, J.U., Moon, S.I.: Installation and operation of FACTS devices for enhancing steady-state security. *Electr. Power Syst. Res.* **70**(1), 7–15 (2004)
49. Aneke, N.E., Ngang, N.B.: Improving the efficacy of the Nigerian electric power transmission network using static synchronous compensator (STACOM). *J. Inform. Eng. Appl. (JIEA)* **11**(2), 7–17 (2021)
50. Dash, S.K., Ray, P.K.: A new PV-open-UPQC configuration for voltage sensitive loads utilizing novel adaptive controllers. *IEEE Trans. Industr. Inf.* **17**(1), 421–429 (2020)
51. Mosaad, M.I., Alenany, A., Abu-Siada, A.: Enhancing the performance of wind energy conversion systems using unified power flow controller. *IET Gener. Transm. Distrib.* **14**(10), 1922–1929 (2020)
52. Biswas, S., Nayak, P.K.: A fault detection and classification scheme for unified power flow controller compensated transmission lines connecting wind farms. *IEEE Syst. J.* **15**(1), 297–306 (2020)
53. Abasi, M., Saffarian, A., Joorabian, M., Seifossadat, S.G.: Fault location in double-circuit transmission lines compensated by generalized unified power flow controller (GUPFC) based on synchronous current and voltage phasors. *IEEE Syst. J.* **15**(2), 2190–2200 (2020)
54. Thumu, R., Harinadha Reddy, K., Rami Reddy, C.: Unified power flow controller in grid-connected hybrid renewable energy system for power flow control using an elitist control strategy. *Trans. Inst. Meas. Control* **43**(1), 228–247 (2021)

# Advances in Protection and Testing of Power Distribution Systems Within Emerging Markets



Johan Venter

**Abstract** In this chapter, a thorough discussion regarding technology as it advanced in the past few years of Moulded Case Circuit Breakers, Solid-State Circuit Breakers, Hybrid Circuit Breakers and modern Power Monitoring Systems for application in Battery Tripping Units is presented. Additionally, a design of a low-cost circuit breaker testing system, as well as a mobile battery tripping unit, is provided. A large part of the discussion centres around how the available technology would assist emerging markets with the inclusion of availability of testing equipment, as well as the technical expertise required to use this equipment. Technicians will be able to use this as a background in developing new testing techniques especially for emerging markets to ensure that circuit breakers are relatively reliable. This discussion can be used by newly trained technicians to gain valuable knowledge in the protection and testing of power distribution centres. Technicians will be able to develop techniques and systems to test circuit breakers where funding is low. Additionally, techniques are discussed to try and alleviate substation tripping issues, which result in power distribution centres overloading and then burning. Once this happens, power outages occur, which take time to repair. With the implementation of remote monitoring functionality, efficiency levels for maintenance, aspects will increase tremendously, keeping the areas functional and costs relatively low. By keeping these costs low, funding that was typically used for maintenance can be used elsewhere and downtime is reduced significantly. Thus, the advantages of these implementations are staggering. In order to ensure that power distribution systems long-viability in emerging markets, it is essential to ensure that functionality is correct. Two essential aspects that are of great importance is the functionality of the circuit breakers and the ability to properly disconnect a power distribution system when too much energy is drawn. Unfortunately, limited work has been done in the development of testing techniques for circuit breakers, post-manufacturing. Additionally, power stations need to trip effectively when an overload condition is experienced; however, this is not possible if substandard circuit breakers are used. Providentially, recent battery-tripping unit technology has advanced to the point where a mobile system can be designed that

---

J. Venter (✉)  
University of Johannesburg, Johannesburg, South Africa  
e-mail: [johanv@uj.ac.za](mailto:johanv@uj.ac.za)



also allows for enough power injection to trip a substation effectively. In emerging markets, several problems exist such as the technical ability of staff, funding, the time it takes to determine a fault as well as the availability of components and devices. Additionally, the availability of testing equipment can also be severely limited. For instance, in remote areas, technicians travel long distances to arrive at a site where there is potential problem is at a power distribution centre.

**Keywords** Moulded case circuit breaker · Distribution systems · Protection · Condition-based maintenance · Solid-state · Hybrid

## 1 Chapter Overview

### 1.1 *Advancement in Moulded Case Circuit Breakers Technology*

In this section, the advancement of moulded case circuit breaker (MCCB) technology is discussed to enable the reader to gain a comprehensive insight into available technology. The function of a circuit breaker is to provide overcurrent and isolating functions by means of switches [1, 2]. For DC CBs, three categories of CBs exist which are: mechanical, solid-state and hybrid [3]. A discussion of all three of these categories are given in this section.

MCCBs uses a mechanical spring type actuator that needs manual closing which cannot be controlled remotely [4]. To overcome this problem, a Lorentz force actuator was designed and implemented in MCCB to enable remote controlling (able to reset the CB). It uses a rotating disk driven by links in a permanent magnet structure to open and close the contacts of the circuit breaker. The usage of this type of actuator is a step ahead into remote motoring and remote resetting of the breaker, which makes it perfectly suitable for emerging markets especially where funding and skills are in short supply.

Very specific standards exist to which a circuit breaker must comply, in order for it to be deemed safe and functional of which the UL489 standard (for circuit breakers for ratings of less than 600 V) is a widely adopted standard which states the following:

- Circuit breaker must not trip at 100% of the rated current
- Circuit breaker must trip within 1 h at 135% of the rated current
- If the circuit breaker does not trip within 1 h at 135% of the rated current, the current is increased to 200% of the rated current where it should trip within 2, 4 or 6 min depending on the rating.

Usually if a circuit breaker fails the second test (must trip within 1 h at 135% of the rated current), the circuit breaker is deemed to be a safety risk and thus not useable and should be discarded. Different brands of circuit breakers deteriorate at

different rates when new circuit breakers are compared to used circuit breakers for conformance to the UL489 standard [5]. This justifies the need to develop testing techniques for emerging markets where access to quality testing is limited for a variety of reasons. The IEC Standard 60,947.2 [6] standard of circuit breaker testing for ratings up to 1000 V ac or 1500 V dc applies for mining applications. This could be used for circuit breakers rating lower than 600 V in mining applications. Where a circuit breaker needs to be replaced, there are several reasons to justify replacing the whole unit, as opposed to replacing parts which range from parts not manufactured to specifications to removal of lubricants and abrasive processes that can cause corrosion and weaken components [7]. This degrades the quality of circuit breakers. Remote operation improves safety for operators [7]. Thus, it is imperative to ensure correct circuit breaker functionality.

An increase of linkages from a 4-bar linkage system to a 5-bar linkage system in the MCCB resulted in a 1 ms reduction in opening time of the mechanism as well as an increase of 1228.3 deg/s operating velocity seen in simulations [8]. This improved the functionality of MCCBs without changing the prospective short circuit current rating.

Series resistance of MCCB greatly vary with different ratings [9]. To be able to design a testing method for MCCBs, the series resistance needs to be accommodated for. Two methods of testing can arise from this:

- Design a MCCB tester for each rating
- Design one multi-rating MCCB tester

The second method does require more design time, but it will greatly reduce the operation cost and time required for testing MCCBs making it more suitable for emerging markets. Power utilities are increasingly looking for new ways of reducing cost whilst maintaining quality of supplies where predictive or condition-based maintenance of High Voltage Circuit Breakers (HVCBs) looks promising [10]. With some modifications, the predictive or condition-based maintenance techniques for HVCBs can work for Low Voltage Circuit breakers. Little to not effort has been put into this transition according to the authors knowledge. Four methods of parameter measurement were introduced in [10]:

- Closing/trip coil current
- Minimum operating voltage
- Closing resistance
- Contact travel and velocity

Most of these methods are still being used today, albeit in different forms of monitoring techniques. Every type of circuit breaker exhibits different characteristics which needs to be considered when a testing system is designed. For this system, the test circuit setup is given in Fig. 1.

To generate high voltages, a charge pump circuit is required for High Voltage Circuit breakers. As seen in Fig. 1 when the capacitor is fully charged, it is fed through an inductor to the test product. Since inductors are short circuits at low frequency, this makes this setup perfectly suitable for high voltage DC circuit breaker testing.

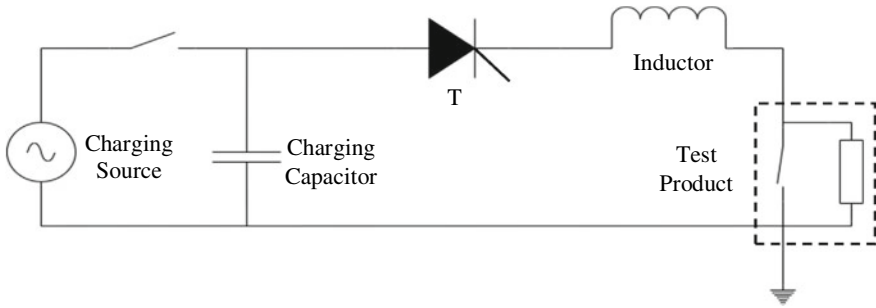


**Fig. 1** A test circuit setup for high voltage circuit breakers [11]

Several methods have been employed to model HVCBs using testing methods such as machine learning, coil current data with Bayesian approach, timing parameters of the coil current data and prediction of mechanical curves [12].

Ramming and Aristizabal [13] reported a cold characteristic development test of a high voltage circuit breaker which made use of an impulse generators trigger circuit equipped with a position measurement circuit that releases the firing signal for the impulse voltage at a precise predefined contact position. The operating sequence of this system is as follows [13]:

1. Breaker placed in a closed position and the impulse generator charged.
2. The triggering generator is programmed for desired contact position.
3. When the breaker receives trip signal during contact movement, transducer sends an impulse to trigger generator.
4. At predefined position, triggering generator releases trigger impulse and fires impulse generator.
5. Breakdown/withstand voltage across breaker contacts is recorded. By repeating this sequence, a pass/fail envelope of the breaker's dielectric recovery performance can be created. A test bench simulating all the components can be developed which could aid emerging markets in understanding these circuit breakers and enable them to thoroughly test them on their own.

Another type of testing circuit called a synthetic testing circuit is given in Fig. 2.

This synthetic testing circuit contains two main switches, a boost conversion inductor, TRV shaping circuit and a current as well as a voltage source. A similar configuration was reported in [15]. The advantages of a synthetic testing are as follows [14]:

- The breaker can be tested for desired TRV and RRRV.
- The short-circuit generator has to supply current at a relatively smaller voltage (as compared to direct testing).
- Both test current and test voltage can be independently varied. This gives flexibility to testing.

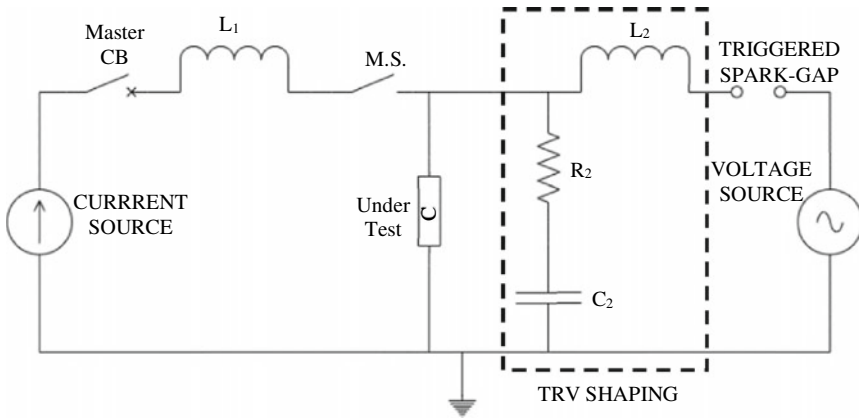


Fig. 2 Synthetic testing circuit using TRV shaping [14]

A synthesis test circuit for HVDC circuit breakers where the control system is based on a Digital Signal Processor in Fig. 3.

In the work of [17], short-circuit current interruption performance of HVDC CBs using a complete test setup is presented. The circuit for this test setup is given in Fig. 4.

Where MB is the Master Breaker, MS is the Making Switch, Ladj is the adjustable reactor, PT is the power transformers, AB is the auxiliary AC breaker, Lsynth is the Inductance in the synthetic circuit, DS is the disconnector switch, TSG is the triggered spark gap, limit is the initial current limiting reactor, C is the capacitor bank and TO is the test object. As with almost all testing equipment of this nature, voltage and current measuring equipment is included. TO is the place where the circuit breaker is inserted. It must be noted that this system is designed for HVDC circuit breaker

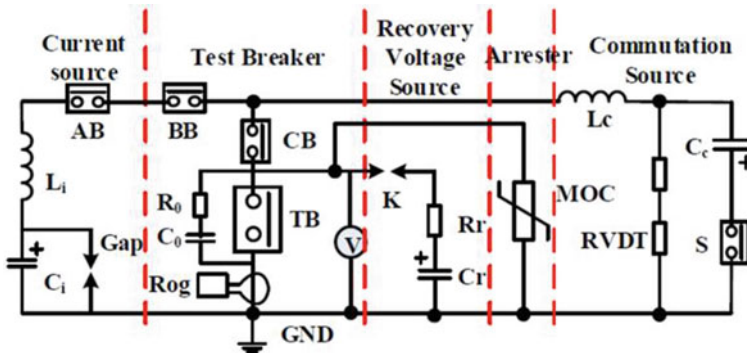


Fig. 3 Synthetic HVDC CB circuit using digital signal processors [16]

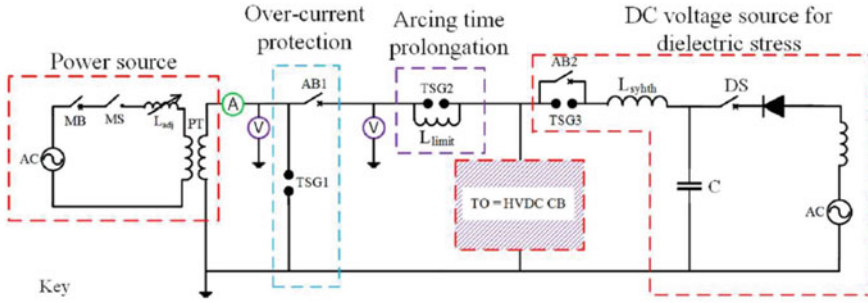


Fig. 4 Short circuit interrupt performance test circuit for HVDC CB [17]

only. Similarly [15] confirmed the type of tests that needs to be conducted on HVDC circuit breakers which is given below:

- Dielectric Tests
- Measurement of power losses of the main current branch
- Short time withstand (STW) current test
- Current making and breaking tests
- Auto-reclosing test

It is worth noting the importance of closing resistance which could be modelled using the testing program given in Fig. 5.

In Fig. 5, R1 is the closing resistance, K1 is the main contact of the HVCBs, K2 is the auxiliary contact and C1 is the capacitor in parallel. R1 can be calculated using Eq. 1.

$$R_1 = R_2 \frac{U_A}{9 - U_A} \tag{1}$$

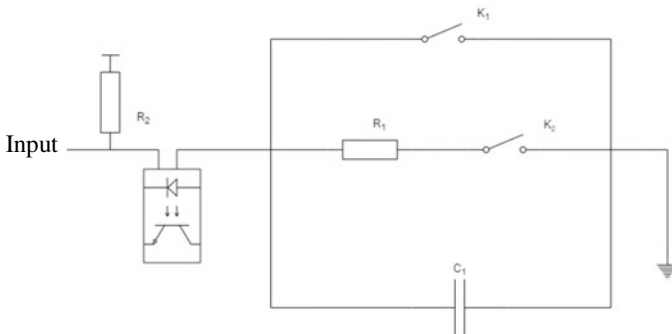
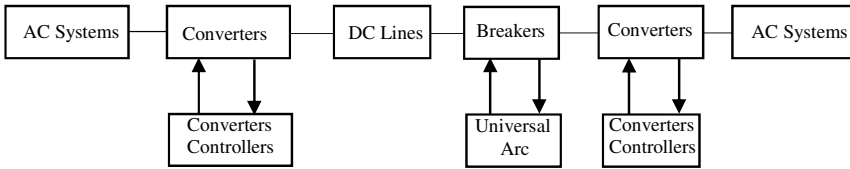


Fig. 5 Circuit model used for calculating of closed resistance [10]



**Fig. 6** Transient recovery using EMPT including TACS [19]

where UA is the voltage signal at the input. It was reported that the entire testing system was accurate meeting required demands.

In the work of [18], thermoset and chopped fiberglass filled PA46 chutes were compared in a 100 A single pole MCCB without changing the design. It was found that chopped fiberglass-filled PA46 performed the best during short-circuit tests. The arc time was reduced and peak arc voltage increased when compared to thermoset chutes, which is beneficial in many ways such as reduced soot formation.

In the work of [19], a transient voltage recovery (TRV) study using electromagnetic transient program (EMTP) is performed. A TRV signal could either be overdamped or underdamped (much the same as PID control loops). The same principles of overshoot and derivate kick is applicable here and appropriate modifications using traditional PID theories could improve operation.

TACS comprises of converter controllers and universal arc representation as seen in Fig. 6. The improvement came about through focusing more on breaker switching as opposed to the combined action of converter control and isolators.

### 1.2 *Advancement in Solid-State and Hybrid Circuit Breakers Technology*

In this section, an evolution of solid-state and hybrid circuit breakers in the form of digital or smart circuit breakers are discussed. Solid-state and hybrid circuit breakers might exhibit more cost due to development, but in the long run the use of these breakers will make it suitable for emerging markets, due to the reduced number of replacement circuit breakers that need to be ordered. In addition to this, testing will be much easier since the models are based on electrical components as opposed to trying to model mechanical springs at different angles (as mentioned earlier in this section, the change from 4-bar linkage system to a 5-bar linkage system produced different results). It is important to understand the differences between these circuit breakers and the traditional mechanical circuit breakers to know how to effectively test them. The discussion provided is on a high-level to enable the reader to understand the characteristics of Digital and Smart Circuit Breakers to develop novel circuit breaker testing techniques, as limited work for testing post-manufacturing has been done.

In the work of [20], the authors developed a SiC MOSFET based, digitally controlled Solid State Circuit Breaker. This system includes a current-limiting soft

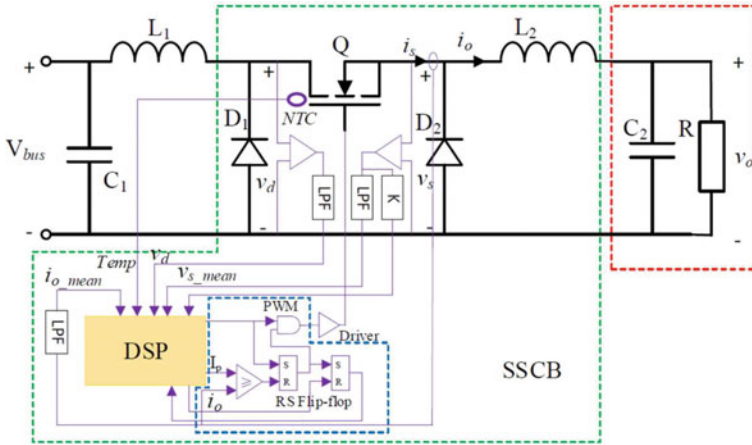


Fig. 7 Specialised solid-state circuit breaker [20]

start function as well. This system contains three separate states: ON, OFF and PWM Current Limiting (PWM-CL). The normal ON and OFF states have been covered extensively in literature whereas the PWM-CL mode is relatively new. The PWM-CL mode gradually charges the input capacitors of loads at a current limiting level during start-up using a variable frequency PWM control technique. This technique operates a buck converter for optimal soft start and short fault detection. The schematic for this circuit breaker is given in Fig. 7.

This SSCB comprises of a buck converter, current/voltage/temperature sensors, a Digital Signal Processor and an overcurrent detection circuit. The important part is to understand the functionality of the Variable Frequency PWM algorithm which is explained below. The PWM frequency for successful start-up is given in Eq. 2.

$$f_{pwm} > \frac{2v_0^2(V_{bus} - v_0)}{V_{bus}L_2I_p^2R} \tag{2}$$

where:

- VBUS is the DC bus voltage,
- vO is the output voltage of the buck converter,
- L2 is the last inductor before the output,
- IP is the overcurrent threshold and.
- R is the load impedance.

The PWM off time will set the upper limit of the PWM frequency. This can be used to determine the maximum TOFF to successfully charge the load capacitor to all reasonably possible output voltages for any practical load resistors. This value can be determined using the Eq. 3:

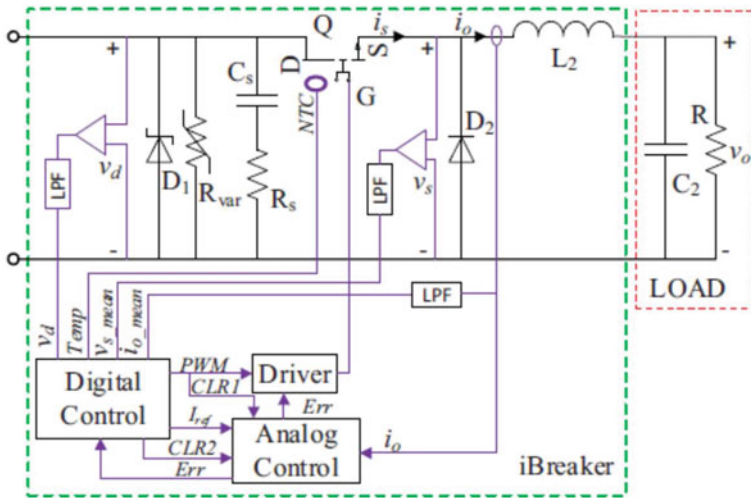


Fig. 8 iBreaker solid-state circuit breaker [21]

$$T_{off} = \frac{L_2 I_p^2 R_{rated}}{2V_{bus}^2} \tag{3}$$

In the work of [21], an extension of the Tri-State intelligent circuit breaker using SiC.

MOSFETs and GaN HEMTs is presented comprising of four key elements:

- Wide Bandgap Semiconductor switches
- Tri-mode operation
- Digital and analog control
- Universal hardware/software architectures.

The configuration of this intelligent circuit breaker is given in Fig. 8.

Where the green box is the intelligent circuit breaker, and the red box is the load. A similar type of circuit breaker using JFETs was developed in [22]. In that work the junction temperatures for different over-currents as well as tripping times versus multiples of the rated currents was measured. It is worth noting the latter where the tripping time decreases exponentially with a rise in current flow. Thus, it is possible to use the UL489 tripping standard in a modified form to determine correct functionality. This modified form is the UL489I standard covering 1000 VAC and 1500 VDC Solid State Circuit breakers.

Traditional mechanical circuit breakers typically operate on unidirectional current flow only. In some applications, bidirectional current flow circuit breakers are required. This is another evolution of the Solid-State Circuit breakers developed recently, using a SiC Super Cascode power switch and a multi-layered absorption network [23]. The circuit diagram of this circuit breaker is given in Fig. 9.



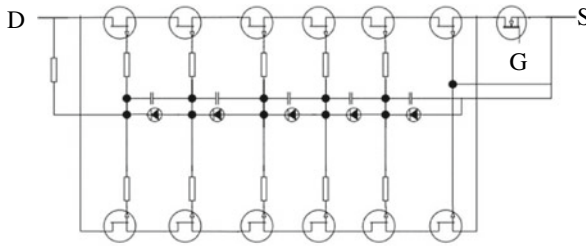


**Fig. 9** SiC supercascode solid-state circuit breaker [23]

In the work of [24], a hybrid solid-state based DC circuit breaker is proposed which includes a mechanical circuit relay, two bilateral power switching devices, a buffer circuit, a surge absorber, current limiting resistor and a microcontroller. The circuit diagram of this circuit breaker is given in Fig. 10.

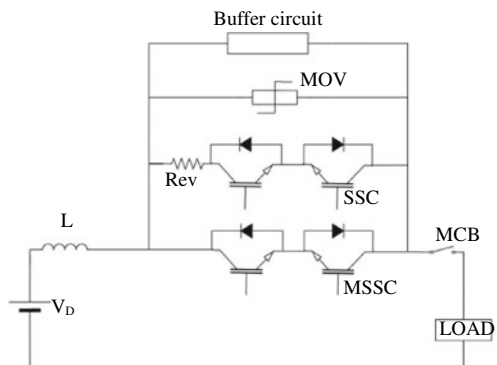
In this circuit breaker, there are 5 modes of timing operation governing all aspects of a fault and enables safe cutting of the rush current.

A bidirectional, GaN based intelligent solid-state circuit breaker is presented in [25] based on a back-to-back buck converter with variable PWM frequency technique. This SSCB also has three states as with [20]. The SSCB circuit breaker diagram and test circuit setup is given in Fig. 11.

In Fig. 11a version of the SSCB dubbed the Tri-state iBreaker is introduced. Functionality is much the same as with other SSCBs except this one can operate in both directions with three different states (ON, OFF and PWM Current Limiting Mode). This is done by analysing the current through buck converter output inductor L2 ( $i_{L2}$ ). Assuming the positive current flow through L2 is from left to right, the following applies:

- If  $i_{L2} > 0$ , then the current flows from left to right.
- If  $i_{L2} < 0$ , then the current flows from right to left.

**Fig. 10** Hybrid solid-state DC circuit breaker [24]



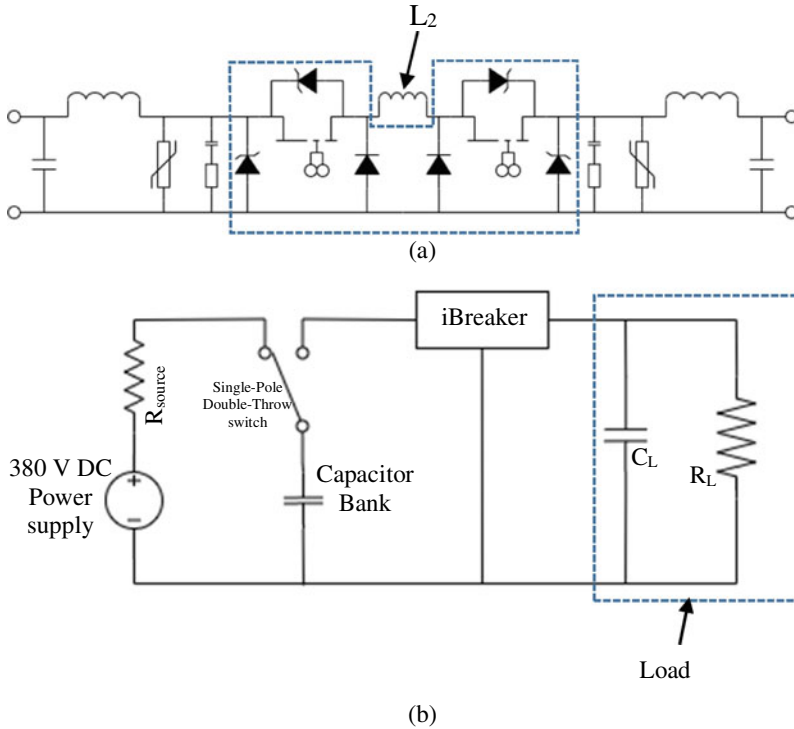


**Fig. 11** GaN based iBreaker solid-state circuit breaker **a** Circuit breaker and **b** test circuit setup [25]

The finite state-machine model and discussion of the SSCB given in Fig. 11 can be found in [20]. Another type of technology for SSCB implemented in 2020 used mass-produced SiC JFETs [46]. This technology makes use of gate-biased switch-mode supercascode. This supercascode diagram is given in Fig. 12.

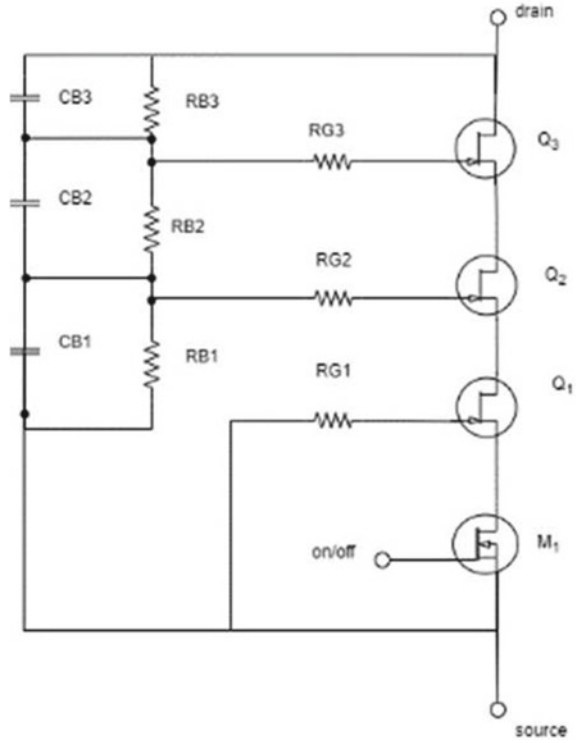
As it can be seen in Fig. 12, this basic supercascode configuration uses semiconductors utilizing fewer components compared to the iBreaker. Two methods to operate power semiconductors at medium voltage are given below:

- High voltage rated power semiconductors and
- Series connecting multiple devices with lower current ratings.

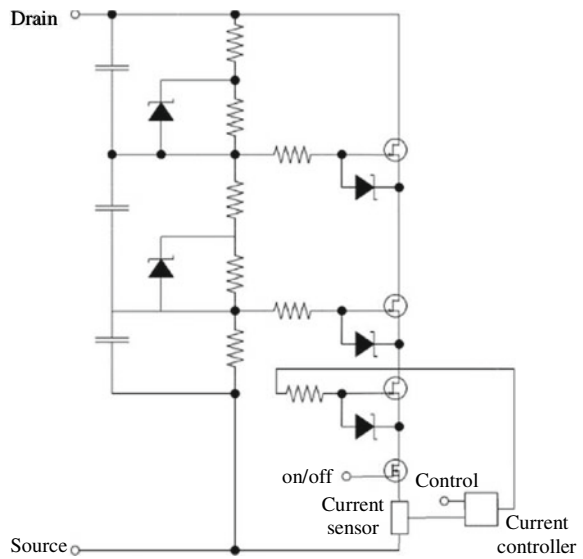
The latter has been used extensively since it is a more economical approach due to lower per unit costs. In the work of [26], they combined current limiting technology using a modified dual mode supercascode configuration with analog control given in Fig. 13.

Figure 13 can only function with DC currents. To enable functionality for AC currents, this configuration should be mirrored where the same current sensor and current controller should be used.

**Fig. 12** SiC based JFET solid-state circuit breaker [26]



**Fig. 13** Dual mode supercascode solid-state circuit breaker [26]



The ability to process medium voltages with lower rated JFETs and in parallel due to the back-to-back connection, several advantages are presented such as lower power dissipation, lower cost of components, simplified network, lower total on-resistance compared to a single high-voltage FET. The need for isolated power supplies to drive the gate at higher potential is also eliminated with this configuration.

The earliest hybrid circuit breaker was proposed in [27] in 2012. Since then many variations and upgrades have been published in literature. An improved configuration of such variation of a hybrid circuit breaker is given in Fig. 14.

As seen in Fig. 14 a hybrid circuit breaker circuit which makes use of an ultra-fast disconnecter (UFD), load commutation switch (comprising of IGBTs, shunt diodes and a pre-charged capacitor), main circuit breaker (MB), parasitic inductor (LP) to obtain realistic commutation time and a varistor.

A twin contact mechanical switch is another type of hybrid circuit breaker technology for use in DC microgrids is presented in [28]. This Twin Contact Hybrid Circuit Breakers offers significantly smaller Current Limiting Reactance (CLR) making it a great alternative to Solid State CBs with considerably high conduction loss and pre-requisite of a cooling system. To better understand the impact of the twin contact mechanical switch hybrid circuit breaker, several parameters of this breaker are compared to that of a single contact mechanical switch hybrid circuit breaker which is given in Table 1.

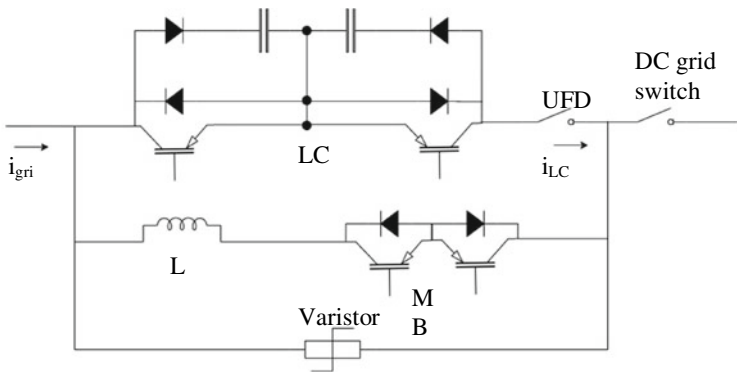


Fig. 14 Hybrid circuit breaker [3]

Table 1 Comparison between twin contact and single contact Hybrid CBs with mechanical switches [28]

Type of breaker	HCB with twin contact MS	HCB with single contact MS
Power efficiency	High	High
Dynamics	Fast	Slow
Snubber	Small	Large
Energy dissipation	Fast	Slow
Speed	Medium	Slow

As it can be seen in Table 1, the twin contact HCB is superior in many aspects to the single contact HCB. Thus the testing system can be somewhat more difficult to implement but it will reduce costs at the end. Hybrid CBs contain 4 individual units listed below:

- Mechanical switch
- High voltage solid-state switch as main breaker
- MOV
- Series Current Limiting Reactor (CLR).

Residual Current Circuit Breaker with Overcurrent Protection (RCBO) is a device that combines the functionalities of Residual Current Device (RCB) and Miniature Circuit Breakers (MCBs) [29].

A Bridge Type Solid State Fault Current Limiter (BFCL) for DC fault current suppression and a novel DC circuit breaker was reported in [30]. The interesting fact of this CB is that it is designed to interrupt DC fault currents below 10 kA within 1.9 ms. When this is connected in series with the Solid-State Bridge, an interruption time of 7.1 ms is seen for currents higher than 10 kA. The circuit diagram for this BFCL is given in Fig. 15.

It can be clearly seen in Fig. 15 that the BFCL consists of three resistors, one inductor, one Insulated Gate Bipolar Transistor (IGBT) and one gate turn-off thyristor (GTO). These are relatively cheap components compared to a MCCB making it more suitable for emerging markets.

A Novel DC circuit breaker diagram and circuit diagram for testing is given in Fig. 16.

The use of Smart Circuit Breaker presents the following functions [31]:

- Thermal overload protection
- Electromagnetic protection against overcurrent and short-circuits

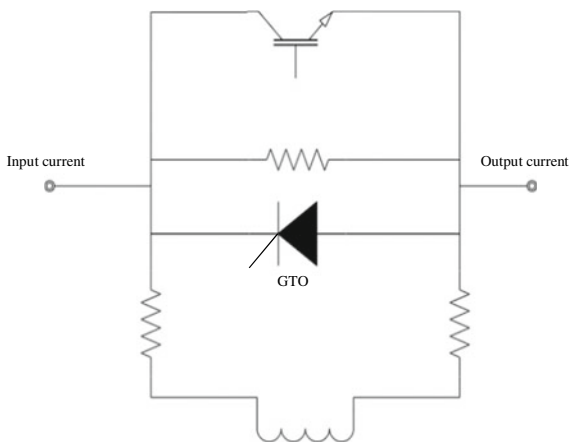


**Fig. 15** Bridge type solid state fault current limiter [30]

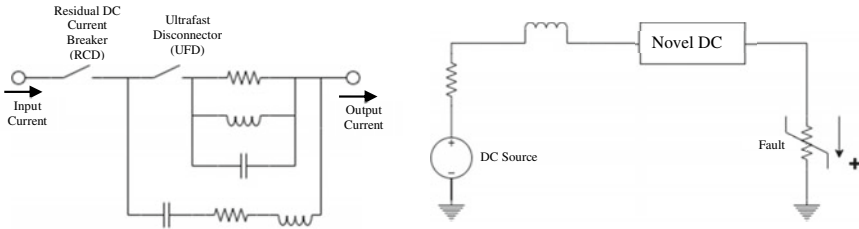


Fig. 16 Novel DC circuit breaker diagram and test circuit [25]

- Current leakage protection (triggered if the phase current differs from neutral current)
- Line arc prevention (triggered if a longer-than-0.15 s arc occurs)
- On-demand disabling (triggered by the user via RS-485 or WiFi interfaces)
- Load specific current and power metering
- Voltage, fundamental-frequency and frequency spectrum measurement
- Circuit-breaker causation data storage and reporting to external devices via RS-485 or WiFi interfaces.

This can be seen as a dramatic improvement over MCCBs thus showing how circuit breaker technology has evolved over the past few years. Mass-scale implementation is yet to be done in emerging markets which served as motivation for the compiling of this chapter. This section can be used as a basis to understand how circuit breaker technology has evolved and will enable technicians and engineers to develop low-cost circuit breaker testing equipment, making it perfectly suitable for emerging markets. One aspect that needs to be investigated by a technician deciding to pursue a career in developing smart circuit breakers, is to thoroughly understand what an IGBT is. Since this chapter is to present advancements in circuit breaker testing technology, the basics of IGBT is left for the reader to research in his or her own time.

### 1.3 Advancement in Monitoring and Protection Technology of Power Distribution Systems

In this section, the evolution of the monitoring and protection technology is presented to illustrate improvements that have been made. Several aspects are discussed on how researchers solved problems or improved the monitoring and protection technologies over the last few years.

Power distribution systems can consist of many components, one of which is usually a transformer. There are 21 different tests that can be performed to determine

if a transformer operates to specification [32]. These 21 tests can be divided into 3 groups:

- Electrical Testing
- Insulating Oil Testing
- Visual Inspection

Many factors forming part of these tests can, when neglected, lead to substation tripping. It is therefore critical if a substation needs to trip, that it must trip effectively. In this section, the efforts of researchers are discussed comprehensively to show how technology for emerging markets has improved over the last few years.

In the work of [33], they identified that the DC link capacitor presents a bottleneck due to its size in the AC-DC converter stage of the charger. They argued that if ripple current could be supplied to the battery without significant degradation, the DC link capacitor could be removed. They implemented a configuration using and AC-DC converter feeding a DC-DC stage with success. The circuit diagram of this implementation is given in Fig. 17.

The four types of relays commonly used in substations are.

- Auxiliary relays
- Tripping relays
- Interposing relays
- Opto-Isolated relays

However, software is a problem to monitor the State of Charge (SOC) and State of Health (SOH). One way to overcome this problem is to make use of the Shepherd Battery Equivalent Model together with an extended Kalman filter given in Fig. 18.

The equation describing the terminal voltage  $U_T$  is:

$$U_T = \alpha \times e^{\beta \times DOD} + \sum_{i=0}^3 \theta_i \times DOD^i \tag{4}$$

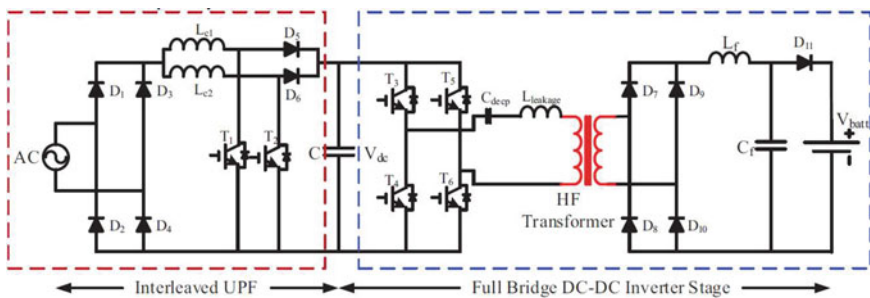


Fig. 17 AC-DC and DC-DC circuit breaker topology [33]

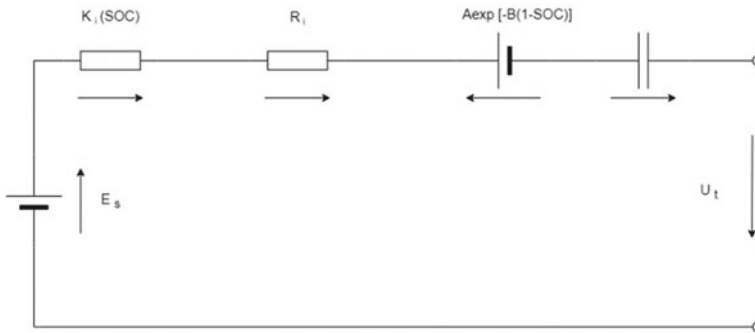


Fig. 18 Shepherd Battery Equivalent Model using extended Kalman filter [34]

where DOD is the discharged capacity (Depth of Discharge), and  $\alpha$ ,  $\beta$  and  $\theta_i$  parameters were experimentally obtained. This Incremental Method for Updating (IUM) can be used to obtain the SOH which is valuable and significant for substation’s power systems with a great degree of accuracy (5%).

Battery Energy Storage Systems (BESS) is instrumental in Renewable Energy Applications, which consists of batteries, a DC-DC converter and a PWM converter which feeds a grid [35].

Battery selection in BESS is important. Four types of batteries are briefly discussed below:

- Lead-Acid batteries are low cost, low self-discharge batteries capable of operating effectively in a wide range of temperatures. The disadvantage is that they exhibit slow charge time and have a relatively short lifespan. A major disadvantage is the low energy density.
- Sodium Sulfur Batteries are molten-salt type batteries with a relatively larger energy density and longer life span. The production costs of these batteries are high which makes them unsuitable for these types of applications.
- Li-ion batteries are lithium-ion based batteries. These batteries are popular in many applications especially in BESS applications. The disadvantage is that these batteries are expensive which makes them unsuitable for emerging markets.
- Flow batteries are batteries designed for bulky BESS. This type of battery is relatively new and thus further work needs to be done to evaluate the suitability of these batteries in BESS applications. Three disadvantages are complexity, low energy density and high costs.

One method to produce better systems is to make use of multiple battery types forming a Hybrid BESS. In Table 2, different batteries are compared in relative terms for price per kWh, energy density and lifespan.

Based on the discussion and the provided Table 2, one can gather the expected behaviour of these types of batteries for BESS. Essentially a BTU performs more or less the same functions. Therefore, the knowledge gained in this work could be used to improve BTUs.



**Table 2** Comparison of Battery Types [35]

Battery type	Price per (kWh)	Energy density	Life-span
Lead-Acid	Relatively low	Low	Short
Sodium Sulphur	Moderate	High	Moderate-Long
Lithium-Iron	Moderate-high	High	Long
Flow battery	Moderate-high	Low	Long

In the work of [36], some functionalities of Power Management Systems that have been published are discussed. At a certain point in time, DC power status monitoring and evaluation systems were able to monitor a limited number of variables due to capacity constraints. This resulted in more problems as site supervisors and technicians were not able to monitor equipment records effectively.

It was proposed to veer away from traditional monitoring methods due to this capacity constraint and use new modern technology such as intelligent monitoring systems comprising of neural networks and fuzzy logic. One can safely include the usage of extended Kalman filters mentioned earlier. Multifunctional monitoring systems came about in literature to further improve the monitoring which is widely used today. In Sect. 1.5, detail of multiple functions included in one system is discussed. In the work of [4], the importance of monitoring is highlighted. Storage conditions are also considered to be very important.

In the work of [37], the fluctuations of power generation levels in renewable energy applications is listed as a major problem. Many studies use Unified Power Flow Converter to overcome these power and frequency fluctuations. This is established through the use of intelligent Power Conditioning Systems (PCS) containing control selection, reactive-power control functions and Fault Ride Through (FRT) functionality.

In the work of [38], the 800 kW energy storage system was implemented using a PCS, Energy Management System (EMS) and batteries. Three different wind power control techniques were used in this application for different requirements which are set out in Table 3 using a smoothing algorithm.

An expansion and implementation of the smoothing mode was implemented in the work of [38] named Wind Power Smoothing Algorithm. The block diagram for this algorithm is given in Fig. 19.

Where

- G(s) is the Wind Power Output,
- H(s) is the Battery Output Power,
- C(s) is the Smoothing Reference,
- REL(s) is Remained Energy Level,
- E is the Capacity of the Battery,
- $\alpha$  is the REL feedback coefficient,
- T is the smoothing coefficient,
- CWF is the Capacity of Wind Turbine, and.
- A is the inverse of the smoothing coefficient (= 1/T).

**Table 3** Comparison of different smoothing techniques

Mode	Output		Characteristics
Smoothing mode	Day	Smoothing	Only the output power smoothing control is implemented
	Night	Smoothing	Relatively small energy storage devices are available
Constant power mode	Day	Constant power	Constant power output during the constant hour the day before pre-consulted with power company
	Night	Charging	Medium energy storage devices are available
Energy shift mode	Day	Discharging (Peak Time)	The energy saved at night is released during peak time of the day
	Night	Charging	Large energy storage devices are needed

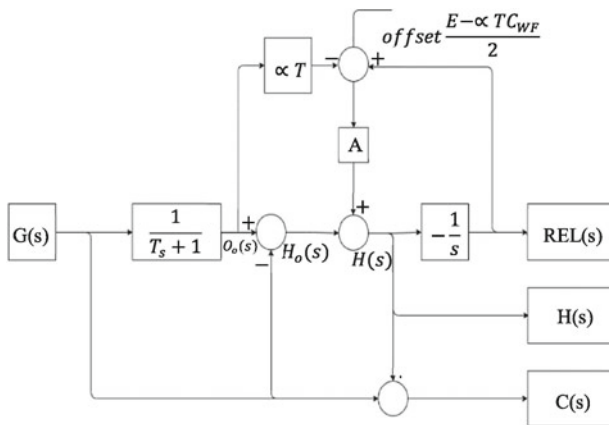


**Fig. 19** Wind power smoothing algorithm [38]

This algorithm could be expanded for implementation in BTUs with some modifications which is left for future work.

In the work of [39] the importance of PCS is highlighted. Disturbances due to instability and output fluctuations are still a problem. To overcome these problems, BESS is shown to be effective. In this work, a 500 kVA and 100 kVA utility scaled PCS system is presented overcoming the mentioned problems. Efficiency, reliability in operating conditions and extensibility to accommodate more batteries are focused upon. It was argued that the removal of the fans and the implementation of a fan-less cooling system reduced noise resulting in improved reliability and decreased

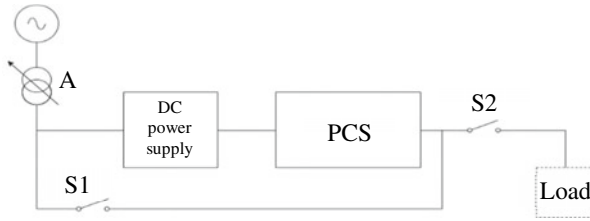


**Fig. 20** Test setup for efficiency determination of high wattage PCSs [39]

maintenance cost. Finally, it also reduced power consumption. In addition, a number of features were introduced with this implementation which are:

- Active/reactive power control
- Soft-start functions
- Grid interaction features
- Stand-alone operating capability

The efficiency of both 500 kVA PCS and 100 kVA PCS was found to be over 98% and 95% for 0 to 100% output power which are excellent efficiency levels. The test setup to determine the efficiency levels is given in Fig. 20.

In the work of [40], it again highlights the importance of monitoring and evaluation of DC power system state. Internal resistance analysis is another method to effectively monitor the SOC and SOH of batteries which is focused on in this work.

On-line monitoring of battery internal resistance and remote discharge technology seems to be a reliable method for monitoring and predicting battery performance. Double battery dual charging method was introduced resulting in improved monitoring capabilities.

At substations, the battery is operated in a constant charge mode (supporting charge) [41]. This is to enable compensation of small current losses as a result of self-discharge. In Sect. 1.5 where the design considerations for BTUs are presented, this mode is discussed and implemented.

Periodic charges and discharges of the battery have a detrimental effect on their characteristics, which leads to premature outages. Deep discharges are most damaging to the battery, as this leads to the sulphation of lead plates which is difficult to restore.

Temperature plays a very important role in the lifetime of a battery. However, it should be noted that one cannot simply cool the battery too much, as crystallization of the liquid can take place as well as carrier freezeout can occur. Both of these effects will result in reduced electrical flow. The influence of temperature on the life of a battery can be determined using Eq. 5 [42]

$$L = k \exp(\alpha T) \quad (5)$$

where

- L is the battery life in number of cycles,
- T is the ambient temperature in degrees Celcius,
- k and  $\alpha$  are material specific parameters.

For lead-acid batteries, the k and  $\alpha$  values are 3198.8 and  $-0.063$  respectively. To illustrate the effect of the temperature on the number of cycles, Eq. 5 is simulated with the use of the known k and  $\alpha$  values.

As it can be seen in Fig. 21 the life cycle of lead acid batteries drop exponentially with a rise in temperature. The physical explanation for this is that with a rise in temperature, the speed of internal physical and chemical processes increases resulting in much faster degradation of poles for instance. This is for a full charge and discharge.

Konstantinov and Zelenyuk [41] proposed an impulse charger which aids in the reduction of temperature increase with the use of semiconductor devices. The control diagram of this pulsed charger is given in Fig. 22.

where

- VR is the voltage regulator,

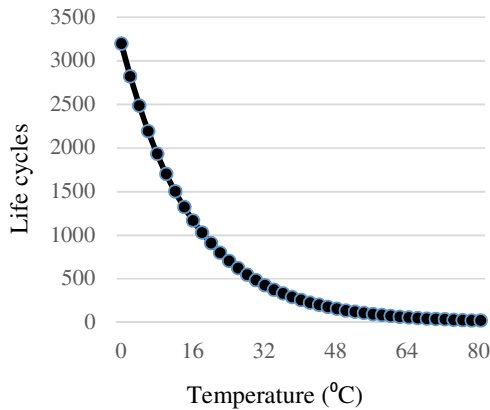


Fig. 21 Life cycle versus temperature curve for lead acid batteries

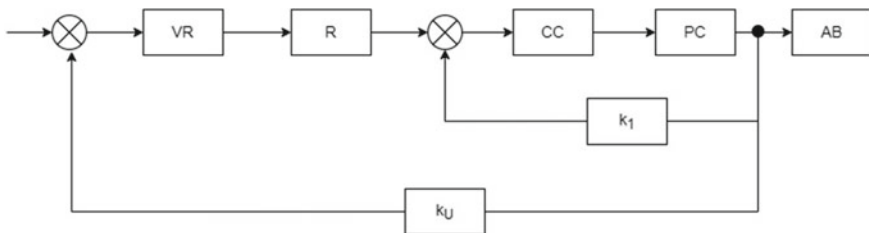


Fig. 22 Flow diagram of constant charge mode using a two-circuit automatic control system [41]

R	is the rectifier,
PC	is the pulse converter,
AB	is the accumulator battery,
kI and kU	are the feedback coefficients, and.
CC	is the current controller.

Backup batteries are very important to secure substations in an electrical network [6]. Multiple string battery arrays have been implemented as well as a battery management system for monitoring to reduce costs and improve performance. Innovations pertaining to monitoring and maintenance include [6]:

- Automatic management—Can be implemented using PLCs and accompanying electronic systems
- Capacity tests by complete discharge—The most accepted testing method to determining battery capacity. Not commonly done due to many reasons such as non-existent maintenance budget and that capacity testing kills hurt batteries
- Floating state optimization—To eliminate self-discharge by performing float charging
- Monitoring and Remote control—With the use of alarm cards in conjunction with control systems, BTUs can be monitored remotely and valuable data could be obtained to improve BTUs.

Fast-Scalable-Adaptable (FSA) fault protection algorithm to improve the MG's reliability and adaptability operation [43]. This FSA algorithm makes use of voltage, current and phase angle parameter optimization. The features of this algorithm is fast fault clearing time, scalability operation of the protection algorithm and adaptability operation of the protection algorithm.

Requirements of a PCS for substation scale BESS [44]:

- High efficiency
- Large capacity
- Low harmonics
- DC voltage variation capability
- Fast response time

Improvements in PCS was made through the use of parallel connections of PCSs. An optimal real time SOC algorithm making use of a Kalman filter to overcome initial SOC deviation is given by Eq. 6 [45]:

$$X_{soc} = \alpha U + \beta R + \gamma \sqrt{U} + \delta \sqrt{R} + \lambda \quad (6)$$

A three-stage charging method can be used in power monitoring which is constant current threshold voltage to constant current limiting to float charging [44].

A DC system must be continuously on-line monitored [46]. Grounding resistance measurement is a good method to monitor the state of a substation DC system. These measuring systems can be subdivided into 2 (two) groups namely Measurement of Bus Grounding Resistance and Measurement of Branch Grounding Resistance. The

latter can be further subdivided into two groups which are Method Based on Balanced Bridge and Method Based on Unbalanced Bridge. Two causes for wrong or missed selections could be the influence of DC leakage current sensor drift as well as magnetic remanence. This needs to be thoroughly analysed and appropriate modifications need to be made which is left for future work.

#### ***1.4 Design Considerations for Low Voltage Circuit Breaker Tester***

In this section, design considerations for Low Voltage Circuit Breaker Testing is discussed. To the best of the authors knowledge, testing of circuit breakers for low voltage systems are only done at the manufacturer level. As soon as the circuit breaker is dispatched, very little work has been done to ensure that these circuit breakers still function according to specifications, such as the UL489 standard (mostly used world wide). Some countries may have their own standards to which circuit breakers should comply, which might not be stated directly, but be stated as part of another standard. One such standard is the South African National Standard for Low-Voltage Installation (SANS 10,142-1:2020). Other standards that could be of use are the Circuit breakers for overcurrent protection for household and similar installations Circuit breakers for AC operation (BS EN 60,898) and Low-voltage Circuit-Breakers for use in Industrial and Similar Installations (BN EN 60,947). The applicable standards of each country should be consulted, and work should proceed from there.

The focus of this section is in respect of all necessary aspects that need to be taken into consideration to design a system to test circuit breakers to ensure that the circuit breakers. Thereafter an example implementation of these considerations is presented focussing on.

Moulded Case Circuit Breakers. Finally, some aspects that could be considered for future work, based on these design considerations is presented. Firstly, the Cable Criteria should be considered as it directly influences the characteristics of a circuit breaker.

The following criteria is applicable to the load that a cable should carry:

- The load type: Motor or Feeder.
  - This is important since different characteristics exist for cable needs for a motor versus feeder such as continuous load current versus spike currents. Temperature plays a large role in this.
- Single phase, three phase or DC loads.
  - Since DC loads do not have alternating currents where the cables can recover somewhat, larger cross-sectional area cables are required for DC loads versus AC loads.

- System or Source Voltage and Full Load Current
  - The combined effect of these two aspects determine the power that needs to be transferred. The temperature coefficient of the conductor affects the cooling which directly affects the cross-sectional area required for a specific cable. Copper (most widely used material for conductors) for instance has a temperature coefficient of  $0.00386 \Omega/\Omega/^\circ\text{C}$ . The well-known resistance temperature equation could be used:

$$R_T = R_o(1 + \alpha \Delta T) \quad (7)$$

where  $\alpha$  is the temperature coefficient of the specific material per unit length.

- Imperatively, then one would want to keep the installation as cold as possible since it decreases resistance due to the atoms moving closer to each other. However, there are limits as to how cold an installation should be kept, as at a certain point a phenomena called Carrier Freeze-Out occurs. Carrier Freeze-Out is when the atoms are so close to each other that vibrations cannot occur any longer, resulting in electrons not being able to move freely, therefore increasing the resistance of the material. To the best of the authors knowledge, work to determine the Carrier Freeze-Out point of copper is yet to be done. Much work in this area for Silicon, has been done previously.
- Distance/length of the cable which runs from the source to the load. This is to account for possible voltage drops which might influence the intended operation of the circuit breaker.
- Cross-sectional area.
  - Since modern low voltage circuit breakers are less than 80 A, a cable capable of carrying 100 A or more would suffice. The corresponding cross-sectional area required for this cable is  $25 \text{ mm}^2$  or more.

Installation conditions criteria of the cable that would affect the design considerations.

- Whether the cable runs above ground or underground:
  - For underground cables, these are directly buried or buried in a conduit. For above ground cables, it is installed on a cable tray or against a wall, in the air etc. There are different limits set as to where a cable is located which can be found in the applicable standards document for installation mentioned above.
- Ambient or soil temperature of the installation site.
- Cable bunching and spacing of multiple cables.

The key to testing for overload is to have a variable high current source with a load that is rated to the specified current. The first solution is with the use of a variable power resistor in the line of the circuit breaker given in Fig. 23.

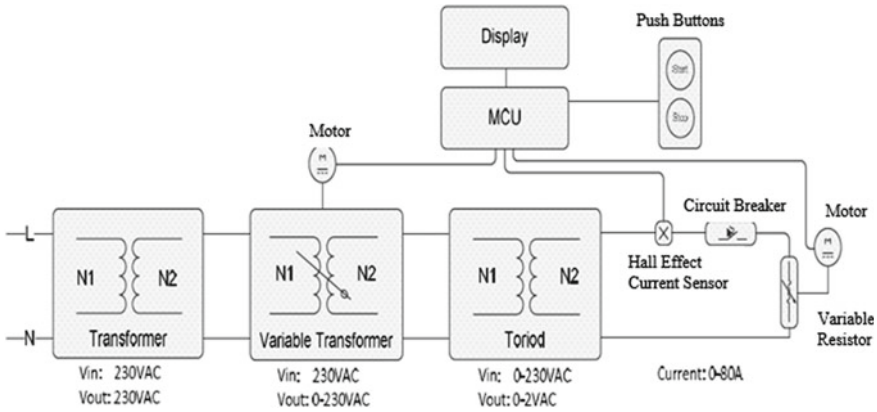


Fig. 23 Variable power resistor method for overload testing

The second method is to use a set fixed value power resistor in the line of the circuit breaker given in Fig. 24.

The third method is to short circuit the cable as a load which is the preferred method as no compensation is needed for a resistor or variable resistor, since inclusion of an extra resistor requires more power and can complicate operations due to temperature changes as a result of high current flow.

As seen in Fig. 25, there are two variable transformers, a toroid transformer, Hall Effect Sensor, Microcontroller Unit, Push buttons and a display. Some of these require careful design considerations which are discussed below.

The variable transformers are included to create a variable high current source. The justification of including 2 variable transformers as opposed to 1 variable transformer is for stability and fine-tuning. To use 1 variable transformer, a stepper motor with

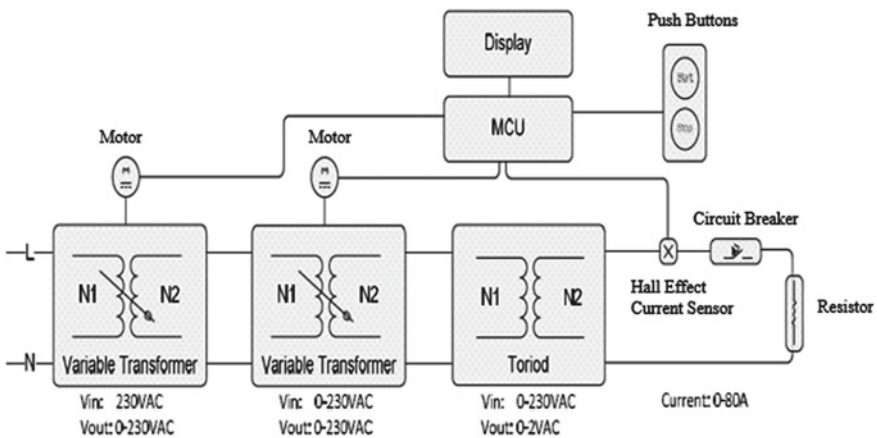


Fig. 24 Fixed power resistor method for overload testing



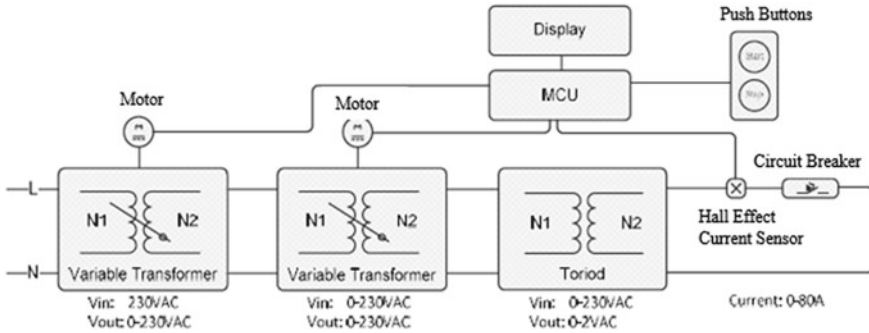


Fig. 25 Short circuit cable as a load method for overload testing [47]

an extremely small resolution is required which usually powers smaller loads. This will not be an effective way to implement. With the use of 2 variable transformers, the combined effect of two stepper motors will result in finer control where larger stepper motors can be used.

The last toroidal transformer is where the current is increased by implementing a smaller ratio of turns. The well-known equations confirming this theory is given below for quick reference.

$$\frac{N_p}{N_s} = \frac{V_p}{V_s} = \frac{I_p}{I_s} = \text{turns ratio} \tag{8}$$

Standard variable transformers for 230 V AC power can be used.

For the toroidal transformer, the required turns ratio might be a challenge to obtain when it is bought off-the-shelf. Thus it is advised to modify a toroidal transformer to adhere to specifications. It is advised that the ampere rating of the cable used to channel current through the circuit breaker be 25% higher than the rating of the circuit breaker to have some extra current available. This same cable should be manually wound as the secondary coil of the toroidal transformer. Justification for the use of a toroidal transformer is that it is easier to manually wind windings compared to shell type transformers. It must be noted that for the first two variable transformers, it must be possible to vary the transmitting power. Typically, toroidal transformers would be used, since one can implement a stepper motor to control transmissibility which is much more complicated to implement when using a shell-type transformer.

For the manually wound toroidal transformer, one cannot use the supplied ratings as the secondary windings would be modified to suit desired specifications. Thus the following steps should be performed for this part of the design:

- Remove the complete secondary winding of the transformer.
- Determine the required cable thickness as discussed above.
- Wind 2 windings around the toroidal transformer.
- Determine the output voltage by measuring it with a multimeter using the AC voltage scale.

- Calculate the output current using Eq. 7.
- Analyse if the largest possible current is 25% higher than the required rated current.
- If the output voltage is less than half of the possible output voltage, the resolution will be quite big resulting in larger current steps. Depending on the requirements, this could be seen as inadequate. Therefore, one should then increase the number of windings in increments of 1 until the desired output voltage is reached. In the example provided later in this section, the effect of the number of windings on the resolution and output current can easily be seen.
- Lastly the VA rating of the transformer should be at least twice that of the intended VA requirements. For example, if 250 VA is intended to be channelled through, the manufacturer rating should be at least 500 VA as a safety precaution so that the transformer would not overheat etc.

### 1.4.1 RMS Current Calculations

To measure the RMS current successfully, a current sensing component needs to be used. There are several available, of which one is mentioned in the example. Since the AC current needs to be measured, one needs to determine the frequency of the input signal (50 Hz or 60 Hz). Adapt the following method to suit the applicable frequency. Follow the steps below:

- Choose a sampling rate of a multiple of the signal frequency (m). This is also the number of samples per period.
- Determine the ADC bit resolution or choose one and set it accordingly (RESBIT)
- Determine the ADC resolution with the use of the following formula  $ADCRES = 2RESBIT$ .
- Determine the number of bits per volt (BperV) using the supply voltage of the MCU ( $BperV = ADCRES/SupplyMCU$ )
- With the use of the maximum output current (HCURMAX) obtainable from the Hall Effect sensor datasheet, determine the Hall Effect Conversion Factor (Hall Effect Conversion Factor =  $BperV \times HCURMAX$ ).
- Analyse the output wave and plot the Amplitude Bits versus Sampling time. From here quite simply read the bit offset and note it (BOFFSET). A program could be written to obtain this offset of which the flow diagram is given below for a MCU (Fig. 26).
- Using known ADC acquisition methods applicable to each specific MCU, determine the required parameters such as the sample and hold capacitor value.

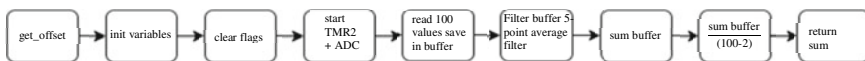


Fig. 26 Flow diagram for bit offset determination

- Next subtract the number of bits measured with the offset for the actual amplifier bit level with no DC ( $ActAmpB = \text{Amplitude Bits} - \text{BOFFSET}$ )
- Determine the RMS hall sensor value for a full cycle

$$RMS\ hall\ sensor = \sqrt{\frac{(ACT_{AmpB1})^2 + (ACT_{AmpB2})^2 + (ACT_{AmpB3})^2 + \dots + (ACT_{AmpBm})^2}{m}} \quad (9)$$

- Using the Eq. 8, the actual RMS current could be calculated using the MCU:

$$RMS\ Current = \frac{RMS\ hall\ sensor}{Hall\ effect\ conversion\ factor} \quad (10)$$

- It is this value that is documented until the circuit breaker trips
- The RMS Current Calculation Algorithm (RMSCCA) flow diagram is given in Fig. 27.

#### 1.4.2 Possible Error and Proposed Correction in the ADC Sampling Process

When the ADC samples low current (below 8 A), the program might detect zero crossings where there should not be any. The following figure illustrates this (Fig. 28).

There could be many reasons for this such as noise while sampling, induced voltage from the DC or AC circuit or drift of the sensor. Fortunately, an easy method can be employed in software to solve this problem for a low number of errors. The method is to employ a moving average filter (general equation for a 5-point moving average filter is given below):

$$fil(n) = \frac{1}{5}[unf(n+2) + unf(n+1) + unf(n) + unf(n-1) + unf(n-2)] \quad (11)$$

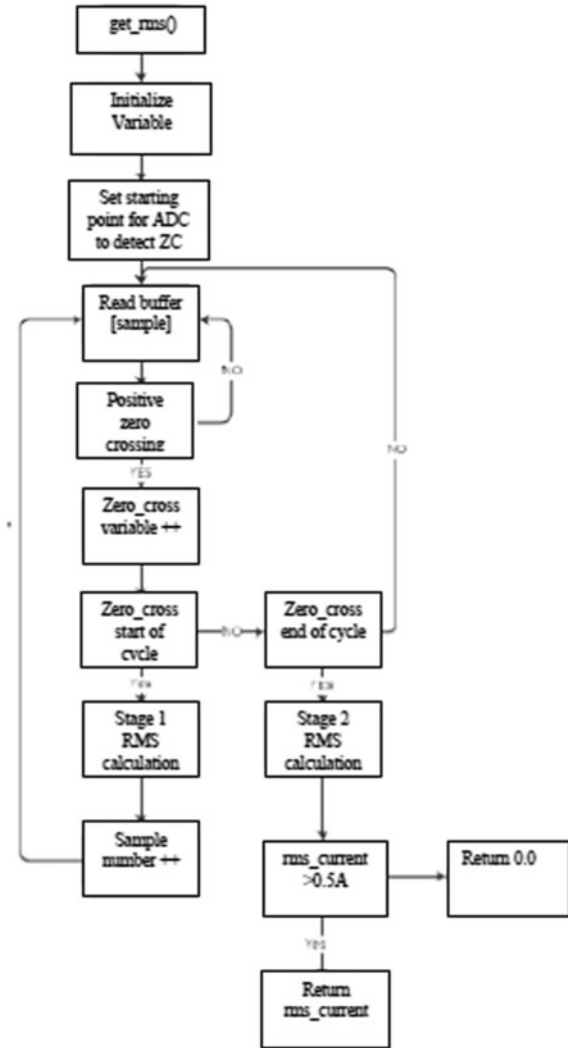
where  $unf(n)$  is the specific unfiltered sample and  $fil(n)$  is the specific filtered sample.

Intuitively it can be seen that the larger this moving average filter is, the smoother the signal would be. However, one should be careful not to implement a too large point filter to result in a significant error which might jeopardize the results obtained. Also one should not implement a too small point filter, since incorrect samples could then be processed. It is suggested that the moving point filter number be equal to one 20th of the samples per period ( $m$ ) i.e.:

$$\text{moving point filter number} = \frac{m}{20} \quad (12)$$

The designer should analyse the actuals samples and determine the appropriate number based on the Eq. 11 and adjust accordingly.

Fig. 27 RMS current calculation algorithm



### 1.4.3 Different Circuit Breaker Resistance

During testing, different circuit breakers displayed vastly different current values and the same voltage settings. This is due to circuit breakers having different contact resistance and the voltage of the toroidal being very low, means it had a significant impact on the current values. This meant that known voltage and current values for one circuit breaker would not be the same for the other. A simple but effective algorithm was developed to circumvent this issue. A separate program was written and implemented in the MCU to automatically increase or decrease the current based on a set point. A flow diagram illustrating this algorithm is provided in Fig. 29.

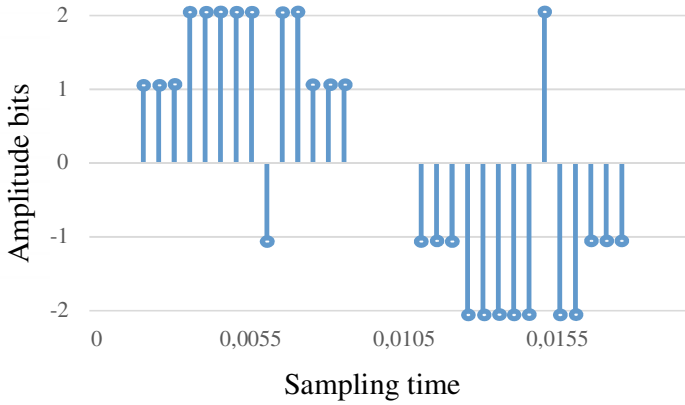


Fig. 28 Illustration of errors in ADC sampling process

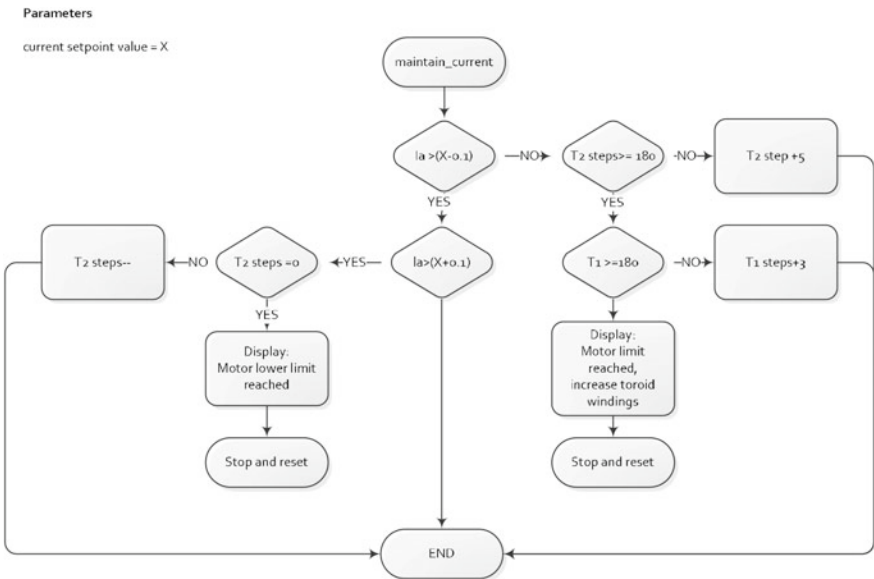


Fig. 29 Automatic circuit breaker resistance determination algorithm flow diagram

The basic principle of this part of the programme is to determine the lower or higher end of the current required to trip the circuit breaker based on the previous sample. Intuitively the lower end is when the motor of the toroid is at absolute minimum. The higher end of the limit is reached when the motor on the toroid is at maximum. The current output should be 25% higher than the rated current of the

circuit breaker. If this value is lower, then the toroid windings must be increased in increments of 1 until this point is reached.

A number of other algorithms are critical to ensure correct functionality of which the common ones are:

- Interrupt Service Routine (ISR),
- Implementation of an emergency stop (ESTOP),
- Resting algorithm to return to 0 A current flow (RA),
- Capture Cycle Algorithm (CCA), and
- Current reading algorithm making use of CCA and RMSCCA in series.

It is assumed that the reader is somewhat experienced with these basic flow diagrams and will be able to develop such programs with ease and therefore these flow diagrams are not included here. Using the common algorithms and the new ones introduced here, a controller can be programmed to perform the required functions. It is possible to use different types of controllers such as MCUs and PLCs etc. A successful implementation of these algorithms can be done using a PIC microcontroller.

## ***1.5 Design Considerations for Battery Tripping Units***

In this section, design considerations for Battery Tripping Units are discussed which is based on an implementation of a mobile Battery Tripping Unit. Due consideration is given to weight as the goal is to develop mobile Battery Tripping Units that could be easily transported to remote locations such as urban areas in Middle Africa where an electricity grid is very unstable.

### **1.5.1 Transformer Choice**

Firstly, the transformer size should be decided upon. It is advised to make use of the general supply voltage for single phase (230 V or 115 V) on the input side. It is not required to make use of a three phase transformer as only one battery charger should be implemented owing to the weight consideration. It is entirely possible to design a Battery Tripping Unit using a three phase transformer, but that is beyond the scope of this chapter. It is advised to make use of a centre tap transformer (0-115 VAC/0-115 VAC) configuration. Using this configuration, one would not need to purchase separate transformers when one wants to convert from 230 to 115 V. One can simply modify the wiring accordingly and change the appropriate settings to effect this conversion.

### 1.5.2 Battery Choice

The battery choice is very important since parameters such as temperature, size, cost and reliability needs to be taken into account. Battery cell failure is generally defined and the point where it fails to yield 80% of its rated capacity. A number of ways exist to increase battery life and reliability which are summarised below for the purposes of BTU implementations [41]:

- Automated support for temperature and electrolyte level,
- Asymmetric current,
- Charging with pulse current,
- Use of new charge stabilization circuits,
- Installation of additional capacitive modules,
- Use of larger amplitudes impulse or asymmetrical currents with natural commutation reduces gas evolution and electrolyte heating, and
- Use of MOSFETs to create pulsed supplies much easier.

These ways or methods can increase reliability but that would mean nothing if it is implemented on the wrong battery types due to different characteristics. It is therefore critical to understand the characteristics of different battery types. Three commonly available battery types are discussed below in context of Battery Tripping Units.

- Lead Acid Batteries
  - This is a battery where the lead and iron plates are submerged in a Hydrochloric Acid solution. For the purposes of this discussion, a cell that produces 2 volts is discussed.
  - This battery voltage needs to be charged to about 2.23 V per cell called the Float Charge to release the acid from the plates back into the water solution. The battery should be Boost charged at a rate of 2.4 V per cell to assist in the circulation and mixing of heavy acid and lighter water.
  - If this battery type is not charged or left for a long period of time, the battery will have sulphate on the negative plate. Unwanted impurities would be produced making the battery unsuitable for service.
  - This battery is suitable for substation applications. However, it may require regular swapping out.
  - It costs less when comparing to other types such as Nickel Cadmium batteries
- Nickel Cadmium Batteries
  - Steel is used on the side of the cell. “Pockets” are made to encapsulate the cadmium. The pockets are slotted between the steel sides the same as palisade wall segments.
  - The plates are typically not welded as in Lead Acid Batteries, but bolted to make a strong bond and to make a better electrical connection.
  - Materials are costlier than that of the Lead Acid Battery and the cells have high self-discharge rates.

- Overcharging and undercharging should be prevented to eliminate possible damage to the battery.
- The Charging Rate (CR) is recommended to be the following:

$$CR < \frac{\text{Capacity (AH)}}{5} \quad (13)$$

- The proposed charging rate is set to account for temperature effects that may be detrimental to the performance of the battery.
- The variables that need to be considered when estimating actual cell capacity required for a certain application are:
  - Discharge rate and time
  - Depth of discharge
  - Cell temperature during charge, at rest and during discharge
  - Charge rate and, where applicable, overcharge rate
  - Charge time and rest time after charge
  - Previous cycling history
- Can be kept on trickle charging once the battery is fully charged.
- This battery is suitable for substation applications since the charging rate is controlled and trickle charge is implemented when it is fully charged to ensure that the battery does not deplete through leakage currents
- Lithium Batteries
  - Lithium Cell requires a specialised method of charging. At the start the charging is constant current charging and at nominal voltages the charging method should be changed to a constant voltage charging until the rated charging voltage is reached. Charging should then stop.
  - Overcharging could result in damage to the cells and therefore could ignite.
  - Each cell has its own Battery Monitoring System that monitors the voltage of each cell on charge.
  - Due to the requirement that lithium cells must not be overcharged and also not undercharged (which could also cause the cell to ignite), makes lithium cells not suitable for substation tripping applications.
- Proposed charging voltages for Lead Acid Batteries as well as Nickel Cadmium Batteries for 12 V, 24 V, 30 V, 36 V and 48 V systems. For Lead Acid Batteries, 2 V per cell is a good value and for Nickel Cadmium Batteries 1.2 V per cell. These two voltage types are commonly available. This serves only as a guideline to choose the right number of batteries and type (Tables 4, 5).
  - These two tables indicate the charging voltage for different configurations. The unique aspect is that the same charging system could be used where quite simply the settings must be adjusted to conform to the type of battery used. To illustrate this aspect, attention is drawn to the shaded block. Using Lead Acid



**Table 4** Lead acid battery voltages

	Volts per cell	12 V	24 V	30 V	36 V	48 V
		6 cells	12 cells	15 cells	18 cells	24 cells
	1.5	9.0	18.0	22.5	<b>27.0</b>	36.0
	1.6	9.6	19.2	24.0	28.8	38.4
	1.8	10.8	21.6	27.0	32.4	43.2
Rest voltage	2.0	12.0	24.0	30.0	36.0	48.0
Float (Antimony)	2.2	13.4	26.8	33.5	40.1	53.5
Float (VRLA)	2.3	13.5	27.0	33.8	40.5	54.0
Boost (VRLA)	2.3	13.8	27.6	34.5	41.4	55.2
Boost (Flooded)	2.4	14.4	28.8	36.0	43.2	57.6
	2.6	15.6	31.2	39.0	46.8	62.4
Gassing stage	2.8	16.8	33.6	42.0	50.4	67.2
	3.0	18.0	36.0	45.0	54.0	72.0

**Table 5** Nickel cadmium battery voltages

	Volts per Cell	12 V	24 V	30 V	36 V	48 V
		18 Cells	24 Cells	24 Cells	30 Cells	40 Cells
	1.00	18.0	20.0	24.0	30.0	40.0
	1.10	19.8	22.0	26.4	33.0	44.0
	1.15	20.7	23.0	27.6	34.5	46.0
Rest voltage	1.20	21.6	24.0	28.8	36.0	48.0
	1.30	23.4	26.0	31.2	39.0	52.0
Float	1.40	25.2	28.0	33.6	42.0	56.0
Boost (VRPP)	1.45	26.1	29.0	34.8	43.5	58.0
	1.50	<b>27.0</b>	30.0	36.0	45.0	60.0
Boost (Flooded)	1.60	28.8	32.0	38.4	48.0	64.0
	1.65	29.7	33.0	39.6	49.5	66.0
	1.70	30.6	34.0	40.8	51.0	68.0

Batteries, for a 36 V system at 1.5 volts per cell, 27 V charging is needed which is the same as a 12 V system using 18 cells for Nickel Cadmium Batteries.

- This could be used to determine the appropriate Float Voltages for a particular system as well as the number of cells needed for a specific system.
- Using this, a detailed cost analysis could be developed.
- The configuration chosen is then highly dependent on the funds available for this system allowing emerging markets to choose battery types and the number of batteries required. It is merely required to change some settings in software to effect the physical change.

- Since there is a considerable physical size difference from one battery type to another, this table is valuable to enable the designer to choose the correct configuration.

The following general comments are applicable to NCP, VLA and VLRA batteries:

- VLRA Batteries are maintenance free [34],
- Rapid deterioration of battery capacity occurs until the capacity is about 80% [48]. For VLA and VRLA batteries after the capacity reaches 90%, it is recommended by [49] to reduce capacity tests to once per year.
- These increased testing intervals for VRLA batteries are necessary to detect accelerated ageing to determine replacement intervals which can result in a cost saving and reduced maintenance [48].
- High output current capability of VLA and VLRA are dependent on SOH and SOC [48].
- Ambient environment of battery is an important design selection parameter. Temperature and non-temperature-controlled installations exhibit different characteristics which affect sizing and service life span [48].

### 1.5.3 Charger Sizing

- The charger output current is of great concern.
  - This is needed in order to determine the correct configuration. The following Eq. 13 can be used:

$$\text{Charger size} = (\text{Arh} \times R) + \text{constant load amps} \quad (14)$$

where R is a factor linked to a specific battery type given in the Table 6.

And Ahr is the total ampere-hours required to charge the battery. The constant load amps are the constant amperes that needs to be channelled to the battery to enable safe trickle charging.

- The charger size is therefore the ampere-hour value charger needed to charge the batteries where all the surrounding effects like battery type has been taken into account.

**Table 6** R Factor and Expected Lifetime for different battery types

Type	R factor	Expected lifetime [48]
VLA	1.1	10–15 years
VRLA	1.15	3–8 years
NCP	1.3	20–25 years
VRPP	1.4	–
RNCP	–	20–25 years

### 1.5.4 Rectifiers

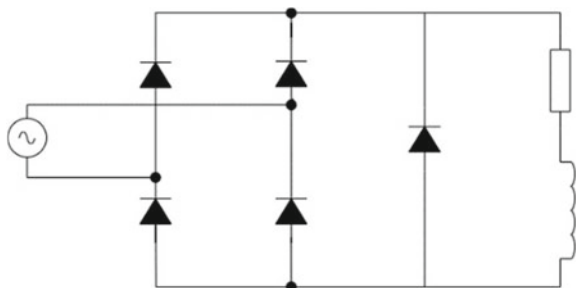
A rectifier is a circuit converting AC signals to a DC equivalent. The two most common types of rectifiers which are well known are discussed in context and evaluated.

- Half-wave bridge rectifier
  - This circuit contains a dead band every half cycle making use of only one diode. Since it is desired to charge at an appropriate rate, twice the charging time is required with this circuit. Therefore, it can be used but it is not advisable due to the longer charging time.
- Full-wave bridge rectifier
  - This circuit makes use of 4 diodes in a Wheat-Stone bridge configuration resulting in two positive waves per cycle. This is the most widely used base configurations for rectification as it is stable and robust. Several variations have been developed using this basis for different applications due to varying requirements of which one is provided in Fig. 30.

This circuit makes use of Thyristors to effectively control the current flow to the battery. The firing angle is directly equal to the current flow and should be controlled accordingly.

- Operational Amplifier based rectifiers
  - The last type of rectifiers is operational amplifier based rectifiers making use of OPAMPs. Since OPAMPs are predominately light current based, it is possible to convert them to heavy current based rectifiers by replacing the OPAMP with the equivalent differential amplifier configuration. The disadvantage of this configuration is that it is a lot more complicated to design and requires more components compared to discrete level full-wave rectifiers explained above. Although it is not widely known if such configurations are actually used, it is possible to use.

**Fig. 30** Thyristor type full-wave bridge rectifier



- Usage of Schottky diodes
  - Since Schottky diodes have a faster recovery time than other diodes as one of the doped regions are replaced with a metal plate, it is ill advised to use as much more rigorous filters are required (with higher ampere and capacity requirements).

### 1.5.5 Filters

There is one filter required after rectification. A smoothing filter is necessary to remove ripple that may harm the batteries. Logically it can be argued that with full-wave rectification, twice the number of positive waves appear in the same time period. Thus for a 50 Hz input signal to the charger, a filter at 100 Hz is required. There are many configurations for such a filter which is well known and therefore it will not be discussed here. As seen in Fig. 30, there is an inductor included. This, together with the capacitance of the batteries, forms an LC filter which is used to smooth the rectified signal.

### 1.5.6 Alarms

It is advised to implement 4 different alarms which can be done using 1 single implementation of a circuit board [50].

- Battery load test alarm
  - Since the Battery Tripping Unit is required to produce a constant voltage, it is periodically required to test the system. If this falls below acceptable levels (preset), this alarm condition will be present where the load is disconnected and connected to a high wattage resistor where a separate test will be conducted.
- Under voltage alarm
  - Will trigger when the battery voltage per cell drops below the preset voltage for the specified cell type.
- Charge failure alarm
  - Triggered if the under voltage alarm is triggered and when the maximum demand equals maximum output. Then the charger will switch off automatically.
- Mains Failure Delay alarm
  - Triggered when the main supply fails. This is not triggered immediately but after a preset time to eliminate false alarms occurring from unplanned impulses or dips that occur in a short period of time.

**Fig. 31** Portable implemented BTU closed cabinet



### 1.5.7 Example Implementation

Several design considerations have been provided in this section. There are many more factors that need to be taken into account when designing a Battery Tripping Unit. However, the other factors are typical factors that are applicable to many other applications and therefore are not discussed here. In 2018, a final year student in engineering at the University of Johannesburg completed such a Battery Tripping Unit for his project with great success which at the time cost R14 700 (estimated 1000 USD) to complete. Below are pictures of this implementation to highlight the fact that it is compact enough to easily move but contains enough power to effectively trip a substation. The dimensions of the unit are only 750 mm × 570 mm × 280 mm weighing between 65 and 100 kg depending on the type of batteries used. This specific implementation made use of Nickel Cadmium Batteries.

In Fig. 31, the closed cabinet is shown. On the right is the operation panel in which the unit can be setup accordingly and active data can be read. On that same panel are the controls where an operator can effectively control all aspects of the alarm card and control system.

## 1.6 Summary

In this chapter, a useful and detailed summary of work published in Circuit Breaker Technology and Battery Tripping Units was presented. This will enable the reader to understand the characteristics of circuit breakers and battery tripping units. Then, in two sections design considerations are presented, to enable the reader to develop own circuit breaker test benches as well as mobile battery tripping units which will be suitable for emerging markets where funding is an issue as well as technological skills. Not only will it assist customers and governments but it will also assist aspiring

technical staff to be trained to the necessary standards in order to understand these aspects.

The design considerations are based on two implemented applications. The low voltage circuit breaker test bench was developed by a student for his final year project and is yet to be implemented on a larger more professional scale. A similar implementation has been done for medium volt circuit breakers; however the demand is much lower as operation, testing and “repair work” on these circuit breakers require highly qualified staff. Therefore, the implementation on low voltage circuit breakers solved the much-needed requirement for testing of these circuit breakers post-manufacturing which was not readily found in literature.

Secondly the design considerations for battery tripping units presented an easy but novel way to develop battery tripping units capable of delivering enough power to a substation to enable effective tripping. It is also mobile for easy transported in emerging markets especially in rural areas where access to effective maintenance is difficult due to distance required to travel, funding and qualified technicians. This will enable technicians to understand the necessary to be able to develop, test and maintain these units effectively. In some cases, techniques used in other applications are discussed, which has the potential to be implemented in these two applications. This is left for future work as an extension to this chapter.

## References

1. Valentine, R.D.: A perspective of low-voltage circuit breaker interrupting rating. *IEEE Trans. Ind. Appl.* **36**(3), 916–919 (2000)
2. Choi, Y.K., Jee, S.W.: The effect of the magnetic grids and arc runner on the arc plasma column in the contract system of a molded case circuit breaker. *IEEE Trans. Plasma Sci.* **46**(3), 1–5 (2018)
3. Lin, Y., Wickramasinghe, H.R., Konstatinou, G.: Hardware-in-the-loop implementation of a hybrid circuit breaker controller for MMC-based HVDC systems. In: 2018 IEEE PES Asia-Pacific Power and Energy Engineering Conference (APPEEC), Kota Kinabalu, pp. 19–24 (2018)
4. Rui, B.: The research of substation battery on-line inspection and repair system. In: 2016 China International Conference on Electricity Distribution (CICED), X’an, pp. 1–4 (2016)
5. Aronstein, J., Carrier, D.W.: Molded case circuit breakers—some holes in the electrical safety net. *IEEE Access* **6**(1), 10062–10068 (2018)
6. Desanti, J., Schweitz, G.: Decreasing owning costs of MV/LV substations backup batteries. In: 2010 7th International Conference on Service Systems and Service Management, Rhode Island, pp. 1–6 (2006)
7. Durocher, D.B., Walls, L., Becker, S.: Understanding circuit breaker design and operation to improve safety and reliability in underground mining. *IEEE Trans. Ind. Appl.* **49**(1), 3–9 (2013)
8. Ji, L., Chen, D., Liu, Y., Li, X.: Analysis and improvement of linkage transfer position for the operating mechanism of MCCB. *IEEE Trans Power Deliv.* **26**(1), 222–227 (2010)
9. Hall, W.M., Gregory, G.D.: Short-circuit ratings and application guidelines for molded-case circuit breakers. In: IAS ‘96. Conference Record of the 1996 IEEE Industry Applications Conference Thirty-First IAS Annual Meeting, Diego, vol. 35, no. 1, pp. 135–143 (1999)
10. Xiaoguang, H., Chao, L.: Research on the condition parameter tester of high voltage circuit breakers. In: 2008 3rd IEEE Conference on Industrial Electronics and Applications, Singapore, pp. 2389–2398 (2008)

11. Shu-Zhen, Z., Jin-Xiang, Z., Zhen-Dong, L., Wen-Bo, Y., Yu-Qiang, W., Xue-Fei, N., Shi-Yang, K.: Research on short-circuit test of 500kV Hybrid HVDC circuit breaker. In: 2017 International Conference on Smart Grid and Electrical Automation (ICSGEA), Changsha, pp. 126–130 (2017)
12. Li, G., Wang, X., Rong, M., Zhong, J.: Health status centered mechanical feature extraction for high voltage circuit breakers. In: 2017 4th International Conference on Electric Power Equipment—Switching Technology (ICEPE-ST), X'an, pp. 911–915 (2017)
13. Ramming, L., Aristizabal, M.: Cold characteristic development test of a new SF6 high voltage circuit breaker. In: 2006 IEEE/PES Transmission and Distribution Conference and Exposition: Latin America, Caracas, pp. 1–4 (2006)
14. Jamnani, J.G., Kanitkar, S.A.: Computer aided optimized design and simulation of synthetic test circuit for testing 800kV rating circuit breakers. In: 2009 IEEE Region 10 Conference (TENCON 2009), Osaka, pp. 1–6 (2020)
15. Jia, S., Tang, Q., Shi, Z.: Review on HVDC circuit breaker tests. In: 2020 4<sup>th</sup> International Conference on HVDC, Xi'an, pp. 808–814 (2020)
16. Wang, S., Wang, Y., Dong, E., Zou, J., Sun, C., Jiang, L.: Synthesis test control of HVDC circuit breaker. In: 5th International Conference on Electric Power Equipment—Switching Technology (ICEPE-ST), Kitakyushu, pp. 263–267 (2019)
17. Belda, N.A., Plet, C.A., Smeets, R.P.P.: Full-power test of HVDC circuit-breakers with AC short-circuit generators operated at low power frequency. *IEEE Trans. Power Deliv.* **34**(5), 1843–1852 (2019)
18. Thangarajan, R.B., Chetwani, S., Shrinet, V., Oak, M., Jain, S.: A comparison of thermoset and thermoplastic arc chutes in molded-case circuit breakers under fault clearing. *IEEE Elect. Insul. Mag.* **31**(2), 30–35 (2015)
19. Darwish, H.A., Izzularab, M.A., Elkalashy, N.I.: Real-time testing of HvdC circuit breakers part I: bench test development. *Int. Conf. Electr. Electron. Comput. Eng. ICEEC '04*, Cairo 765–769 (2004)
20. Zhou, Y., Feng, Y., Liu, T., Shen, Z.J. (2018) A digital-controlled SiC-based solid state circuit breaker with soft-start function for DC microgrids. In: 2018 9th IEEE International Symposium on Power Electronics for Distributed Generation Systems (PEDG), Charlotte, pp. 1–7 (2018)
21. Zhou, Y., Feng, Y., Liu, T., Shen, Z.J.: iBreaker: intelligent tri-mode solid state circuit breaker technology. In: 2018 IEEE International Power Electronics and Application Conference and Exposition (PEAC), Shenzhen, pp 1–7 (2018)
22. He, D., Shuai, Z., Lei, Z., Wang, W., Yang, X., Shen, Z.J.: A SiC JFET-based solid state circuit breaker with digitally controlled current-time profiles. *IEEE J. Emerg Select Topics Power Electron* **7**(3), 1156–1565 (2019)
23. Mehrota, U., Ballard, B., Hopkin, D.C.: Bidirectional solid-state circuit breaker using super cascode for MV SST and energy storage systems. *IEEE J. Emerg Select Topics Power Electron.* <https://doi.org/10.1109/JESTPE.2021.3081684>
24. Tsai, M.-T., Chu, C.-L., Huang, B.W., Lien, C.-H., Chao, K.-H.: Design a DC solid-state circuit breaker for smart grid applications. In: 2019 IEEE 15th International Conference on Automation Science and Engineering (CASE), Vancouver, pp. 1–5 (2019)
25. Zhou, Y., Feng, Y., Shen, Z.J.: Design considerations of tri-mode intelligent solid state circuit breaker using GaN transistors. In: 2019 IEEE Applied Power Electronics Conference and Exposition (APEC), Anaheim, pp. 2439–2444 (2019)
26. Dodge, J.: Dual mode medium voltage solid-state circuit breaker based on mass-produced SiC JFETs. In: PCIM Europe digital days 2020; International Exhibition and Conference for Power Electronics, Intelligent Motion, Renewable Energy and Energy Management, Nuremberg, pp. 1788–1974 (2020)
27. Häfner, J., Jacobson, B.: Proactive hybrid HVDC breakers—a key innovation for reliable HVDC grids. In: The Electric Power System of the Future—Integrating Symposium, Bologna, pp. 1–9 (2011)
28. Banihashemi, F., Beheshtaein, S., Cuzner, R.: Novel hybrid circuit breaker topology using a twin contact mechanical switch. In: 2021 9th International Conference on Smart Grid (icSmartGrid), Setubal, pp. 132–136 (2021)

29. Mafi, H., Yared, R., Bentabet, L.: Smart residual current circuit breaker with overcurrent protection. In: 2019 IEEE 2nd International Conference on Renewable Energy and Power Engineering, Toronto, pp. 6–9 (2019)
30. Rehman, H.: Solid state bridge type FCL and novel DC circuit breaker for HBMMC. IEEE EUROCON-2021, Lviv, pp. 460–464 (2021)
31. Vlasov, A.I., Filin, S.S., Krivoshein, A.I.: Universal smart circuit breaker concept. In: 2019 International Conference on Industrial Engineering, Applications and Manufacturing (ICIEAM), Sochi, pp. 1–4 (2019)
32. Haema, J., Phadungthin, R.: Development of condition evaluation for power transformer maintenance. In: 4th International Conference on Power Engineering, Energy and Electrical Drives, Istanbul, pp. 620–623 (2013)
33. Choudhury, A.: A 2.2 kW SiC based high frequency battery charger for substation backup power supply. In: 2016 IEEE region 10 conference (TENCON), Singapore, pp. 77–80 (2016)
34. Liu, Y., Meng, Y., Lu, Z., Gao, X.Z.: An incremental updating method for online monitoring state-of-health of VRLA batteries. In: 2017 12th International Conference on Intelligent Systems and Knowledge Engineering (ISKE), Nanjing, pp. 1–7 (2017)
35. Chatrung, N.: Battery energy storage system (BESS) and development of grid scale BESS in EGAT. In: 2019 IEEE PES GTD Grand International Conference and Exposition Asia (GTD Asia), Bangkok, pp. 589–591 (2019)
36. Yiding, G.: Design and application of DC power management system of substation. In: 2018 International Conference on Advanced Mechatronic Systems (ICAMEchS), Zhengzhou, pp. 238–241 (2018)
37. Tamaki, M., Takagi, K., Shimada, K., Kawakami, N., Iijima, Y.: Development of PCS for battery system installed in megawatt photovoltaic system. In: 2012 15th International Power Electronics and Motion Control Conference (EPE/PEMC), Novi Sad, pp. 1–4 (2012)
38. Kim, Y., Choi, J., Son, U., Lee, J., Min Lee, J., Sun, I.Y., Kim, E.: Development of 800 kW energy storage system for smart renewable. In: 8th International Conference on Power Electronics—ECCE Asia, Jeju, pp. 2947–2954 (2011)
39. Li, H., Iijima, Y., Kawakami, N.: Development of power conditioning system (PCS) for battery energy storage systems. In: 2013 IEEE ECCE Asia Down-Under, Melbourne, pp. 1295–1299 (2013)
40. Du, X., Li, B., Jia, Z., Wang, H., Rao, Q.: Development of state monitoring and evaluation platform in substation DC power. In: 2017 EPTC Power Transmission and Transformation Technology Conference, Chongqing, pp. 1–5 (2017)
41. Konstantinov, A.M., Zelenyuk, D.A.: Impulse charger for lead-acid batteries electrical substations. In: 2018 International Multi-Conference on Industrial Engineering and Modern Technologies (FarEastCon), Vladivostok, pp. 1–5 (2018)
42. Qian, K., Zhou, C., Yuan, Y., Allan, M.: Temperature effect on electric vehicle battery cycle life in vehicle-to-grid application. In: 2010 China International Conference on Electricity Distribution, pp. 1–6, Nanjing (2010)
43. Bui, D.M., Lien, K., Chen, S.: Investigate dynamic and transient characteristics for islanded/grid-connected operation modes of microgrid and develop a fast scalable-adaptable fault protection algorithm. In: 12th IET International Conference on Developments in Power System Protection (DPSP 2014), pp. 1–6 (2014)
44. Yamabe, K., Komatsu, H., Iijima, Y.: Requirement analysis and development of MW-range PCS for substation-scale battery energy storage systems. In: 2016 19th International Conference on Electrical Machines and Systems (ICEMS), Chiba, pp. 1–5 (2016)
45. Huang, S., Wang, R., Yang, Z.: Substation DC system intelligent monitor and maintenance system. In: 2017 IEEE 2nd Advanced Information Technology, Electronic and Automation Control Conference (IAEAC), Chongqing, pp 2068–2072 (2017)
46. Xing, L., Nan, X., Wei, S., Chunyi, D., Zhaode, X.: Improvement of on-line monitoring method for insulation of substation DC systems. In: 2015 IEEE international conference on cyber technology in automation, control, and intelligent systems (CYBER), Shenyang, pp. 1350–1355 (2015)



47. Venter, J., Van Niekerk, D.R.: A cost-effective low-voltage moulded-case circuit breaker test jig. In: 2019 11th International Conference of Electrical and Electronic Engineering, pp. 121–125, Bursa (2019)
48. Thompson, M.J., Wilson, D.: Auxiliary DC control power system design for substations. In: 2007 60th Annual Conference for Protective Relay Engineers, Texas, pp. 522–533 (2007)
49. IEEE Std. 450 (2002) Recommended Practice for maintenance, testing, and replacement of vented lead-acid batteries for stationary applications
50. Venter, J., van Niekerk, D.R.: Battery tripping unit for space constrained substation container applications. In: 2021 Southern African Universities Power Engineering Conference/Robotics and Mechatronics/Pattern Recognition Association of South Africa (SAUPEC/RobMech/PRASA), Potchefstroom, pp. 1–6 (2021)

**Access to Clean Energy for Sustainable  
Development, Power System  
Infrastructure, and Policy Options**

# Green Energy for Sustainable Agriculture: Design and Testing of an Innovative Greenhouse with an Energy-Efficient Cooling System Powered by a Hybrid Energy System for Urban Agriculture



Constant Kunambu Mbolikidolani, Venkatta Ramayya, B. Ngungu, and M. Yang'tshi

**Abstract** This research is geared towards developing a new greenhouse for urban and peri urban agriculture, adequate to tropical savanna weather conditions with an energy-efficient cooling system powered by a small hybrid energy system. A design and CFD-based simulations were carried out and the prototype was built and tested in Kinshasa. This chapter aims at presenting the proposed greenhouse shape, the result of CFD simulations, the energy demand, the greenhouse operating system and the field-based testing result. Based on the meteorological Data analysis, a specific greenhouse structure of  $32 \times 13.5$  m was designed with an opening in the West. The proposed cooling technology uses an evaporative cooling approach harnessing natural ventilation associated with 6 exhaust fans, a misting system, and a shading system used in intermittent way to enhance energy efficiency. The CFD simulations has shown an even distribution of temperature and satisfactory air circulation in the proposed greenhouse. The field-based testing has shown  $1-7$  °C of indoor air cooling compared to the outside temperature and  $1-24\%$  in relative humidity increasing including a slight influence of the shading system on solar irradiation penetration. The greenhouse costs 3.9 USD/m<sup>2</sup> with 6.3 kWh/day energy-consumption in summer and 1.7 kWh/day in winter.

---

C. Kunambu Mbolikidolani (✉)

Energy and Environmental Engineering, Université de Kinshasa and Pan African University, Kinshasa, Democratic Republic of Congo  
e-mail: [constant.kunambu@unikin.ac.cd](mailto:constant.kunambu@unikin.ac.cd)

V. Ramayya

Mechanical Engineering, Jimma Institute of Technology, Oromia, Ethiopia

B. Ngungu · M. Yang'tshi

Energy and Environmental Engineering, Université de Kinshasa, Kinshasa, Democratic Republic of Congo

**Keywords** Greenhouse · Food production · Cooling system · Energy system · Energy efficiency

## 1 Introduction

The world's population is expected to reach 9.7 billion by 2050 [1]. Most of the growth and economic development is expected to occur in emerging and developing countries, where basic infrastructure remains a daunting challenge [2]. While population growth in the rest of the world will clearly slow down, the number of populations in sub-Saharan Africa will double, reaching 2.2 billion [3]. Approximately one in four people will live in sub-Saharan Africa especially in urban cities where from 2010, more than 50% of the global population are urban dwellers [4].

The Democratic Republic of Congo (DRC) is the second largest African country with 2,345,000 km<sup>2</sup> of surface area [5] and 80 million of arable land. The urban population of the country was 42% in 2015 as the third-largest urban population in Sub-Saharan Africa, after South Africa and Nigeria. The country's average urban growth rate in the last decade was 4.1%, equaling an increase of 1 million urban dwellers every year [3]. Based on this trend, the urban population will double in only 15 years. The capital city, Kinshasa, is one of the megacities of the continent with 12 million populations in 2016 with the highest country population growth rate [3]. This growth in population put high pression on basic infrastructure of the city including food production and supply. As in many sub-Saharan African cities, the food production in Kinshasa faces numerous constraints including technology limitation, poor energy access, dependence on rain-fed agriculture, low use of irrigation, limited public investment and institutional support, climate change effects and gender gap in resources access [6].

To tackle this challenge, new adequate technologies for the improvement of the urban and peri-urban agriculture have to be developed. And one of the appropriate technologies for sustainable food production is the greenhouse technology. The greenhouse technology provides an optimal microclimate condition for crops [7, 8]. Despite the well-known benefits of greenhouse in terms of high food production yield, this technology faces many challenges in Kinshasa including the local weather condition, the poor access to electricity utility and the high-cost of greenhouse components for small as well as large scale farmers.

Kinshasa has a specific and complex climate. According to the Köppen-Geiger climate classification, the capital city of the Democratic Republic of Congo has a tropical savanna climate (tropical wet and dry climate) with a dry winter [9, 10]. The temperature variation within a year ranges between 20 and 35 °C with a high average relative humidity 82.5%, expanded in 11 months of a year. The rainfall is abundant in 10 months of a year with a low average wind speed of 3 m/s.

The greenhouse technology deployment in Kinshasa requires suitable cooling technology and sustainable as well as affordable energy system. Current cooling

technologies demand large investments as energy is one of the largest overhead costs in the greenhouse industry especially in the weather condition of Kinshasa [11, 12].

The objective of this research was of designing, simulating, prototyping and testing a new greenhouse configuration with an energy efficient cooling system adequate to the savannah tropical climate of Kinshasa/DRC. The design and optimization of the energy system was carried out in different scenarios, taking into consideration the energy demand as well the equipment used [13]. The greenhouse was powered by a hybrid energy system made of a solar photovoltaic system and a small Horizontal Axial Wind Turbine (HAWT) with battery storage system. The choice of solar energy as the many energies resource was based on the resource availability and the low cost of solar PV panels.

An emphasis was put more on the energy efficiency, affordability and the use of locally available materials.

The experimentation was conducted in the agricultural zone of Kinshasa (Plateau de Bateke) from March to September 2020.

## 2 Definition of Concepts and Existing Technologies

### 2.1 Greenhouse Technology

Most greenhouses are built in mild climate areas, and more than 90% of them are plastic film greenhouses [14]. The greenhouse technology increases crop yield and quality, and therefore have the potential to contribute in addressing the growing concerns of food security due to climate change, population growth and urbanization [15].

The cultivation in large scale under greenhouses has been successfully carried out in temperate climates whereas in warm climate regions especially those with tropics and subtropics climates, the greenhouse technology faces challenges due to the high temperatures and humidity that can occur in the hottest months requiring a suitable air-cooling system.

The air cooling in greenhouse technology is energy intensive [16]. For optimizing the cooling system in a given geographical area, some key parameters like temperature, relative humidity, solar radiation and wind speed among others have to be grasped and an appropriate greenhouse structure has to be designed.

#### 2.1.1 Temperature

The temperature is one of the most key parameters to take into consideration in greenhouse farming [17]. The indoor greenhouse air temperature is a crucial parameter of the greenhouse microclimate [18]. Regardless the local climate, the indoor

greenhouse air temperatures are generally higher during the day and drops at night. The yield of many common vegetable crops decreases at temperatures above 26 °C.

### **2.1.2 Relative Humidity**

The recommended range of the indoor greenhouse relative humidity is between 40 and 70%. However, it can vary depending on air temperature, crop type and age of the crop [19].

### **2.1.3 Solar Radiation**

The crop uses light for photosynthesis [20]. The rate of this process is highly dependent on the amount of light. The rate of photosynthesis is higher with the increasing levels of Photosynthetic Active Radiation (PAR) [21]. Each crop has its starting point of photosynthesis [22].

## ***2.2 Greenhouse Energy Balance***

The energy transfer into and out of the greenhouse impacts the indoor microclimate and determines the required cooling or heating system [23]. Many energy balance models have been proposed to predict the performance of many types of greenhouse under various climatic conditions and for different crops [24, 25].

In the region with poor relative solar radiation, the energy required for greenhouse lighting accounts for approximately 30% of operating costs [7]. The greenhouse technology is energy intensive and requires high investment. In order to reduce the costs and save energy, researches have to be conducted on greenhouse design and construction based on specific local weather condition [7]. Regardless the geographic climate condition, the greenhouse energy demand depends on the greenhouse size and shape, and the inherent energy management system.

## ***2.3 Greenhouse Cooling Technologies***

The evaporative cooling system is the foremost broadly utilized greenhouse cooling system. It uses fans, pads, misting and fogging system to stabilize the greenhouse indoor air temperature. The evaporative cooling system is indispensably used in regions with high ambient temperature and significant solar radiation rate [26]. Many studies explored and evaluated the evaporative cooling systems in hot regions, and most of them has shown that the evaporative cooling systems create negative pressure inside the greenhouse due to continuous suction of the exhaust fans. Thus, there is

always a problem of outside hot air mixing with the inside cool air through infiltration, which reduces the efficiency of the system [27].

### 2.3.1 Natural Ventilation Cooling System

The natural ventilation is the well-known technique of providing cooling in the greenhouses using wind and buoyancy driven flows [28]. This simple technique requires little or almost no external energy consumption to cool down the greenhouse. This technique can be under some specific conditions effective for the greenhouse cooling system. The air speed and distribution are the key factor for the efficiency of the natural ventilation cooling system [14]. It is driven by the difference in pressure between the greenhouse indoor and outdoor environmental conditions [29]. This cooling technique is achieved by careful positioning of sidewall openings and roof openings. Researches have been carried out to investigate the influence of the natural ventilation on the greenhouse microclimate in hot regions.

### 2.3.2 Evaporative Greenhouse Cooling System

The evaporative cooling is one of the foremost proficient technologies for giving appropriate greenhouse climatic conditions in hot and dry regions [23]. It changes over sensible heat into latent heat through water evaporation provided straightforwardly into the greenhouse by means of fog or mist system, sprinklers or evaporative cooling pads [30]. This procedure can essentially decrease the air temperature below the surrounding temperature and increment the humidity to the essential levels [27]. This cooling system can be separated into 3 distinctive cooling technologies utilizing the same principle. We have:

#### a. Fan-pad system

This system is comprised of fans on one greenhouse sidewalls and pads on the converse sidewall, Franco et al. [31]. The evaporative cooling is fulfilled by sprinkling water over the pads and extract and convey the pads' water droplets inside the greenhouse using fans [23]. The main challenge is the uneven indoor temperature created by the cooling system [17, 26].

#### b. Fog and mist system

This technology provides cooling by pressurizing and spraying water through minor nozzles in the form of micro-fine fog [32]. The terminal velocity of the water droplets is low and the greenhouse air streams can easily transport water droplets. This results in high evaporation rate of water whereas keeping the crops dry [32]. Several studies were carried out to explore mist and fog cooling systems for greenhouses. For instance, the research conducted by Katsoulas amid summer with a mist system

working under 75% indoor relative humidity, showed that the fog system contributed up to 20%, [33].

### c. Natural Ventilation Augmented Cooling

The Natural Ventilation Augmented Cooling (NVAC) greenhouse is naturally ventilated and improved by augmenting the thermal buoyancy with a strategically placed misting system [14]. The testing was carried out in Trents, Barbados, where an empty NVAC greenhouse showed a cooling ranging from 1.3 to 3.6 °C relative to outside temperatures, while increasing relative humidity by 5.7–17.7% [14].

To overcome the limitations showed by Fan-Pad and NVAC greenhouse cooling system in Kinshasa weather condition (high relative humidity, low wind speed and average temperature of 25 °C), an energy efficient cooling system has been investigated based on the aforementioned local weather condition. The greenhouse shape [34] and the covering as well as the shading system properties were also investigated for optimizing the cooling system and reducing energy consumption [13, 35]. The proposed cooling system was made of natural ventilation, exhausted fans, misting system and shading system. The misting system intermittently intervenes when it is needed so to balance the greenhouse indoor relative humidity and temperature while saving water.

## 3 Methodology

In general, the methodology of conducting this research and building the prototype was:

- Description of case study area;
- Data collection and analysis;
- Greenhouse design, CFD simulation and validation of the model;
- Design of the cooling configuration and sized components;
- Design of the energy system and operating system;
- Greenhouse construction and IoT based testing;
- Results and discussion;
- Conclusion and recommendations.

## 4 Results and Discussion

### 4.1 Data Collection and Analysis

Data used in this research came from METTELSAT (Agence Nationale de Météorologie et de Télédétection par Satellite) in the Democratic Republic of Congo. The METTELSAT was created by Decree No. 12/040 of October 2, 2012 with the



missions of observation, meteorological and climatological monitoring as well as the study and evaluation of natural resources.

The used data in this research extend from 1975 to 2005 and mainly include:

- Relative humidity data of Kinshasa;
- The rainfall data of Kinshasa;
- Temperature data of Kinshasa;
- Solar radiation resource in Kinshasa;
- Wind speed in Kinshasa and wind speed on field (data collected during the field research);
- The effect of climate change on food production in Kinshasa.

The summary of data analysis is presented on the below figures for understanding of local weather conditions in Kinshasa.

The Fig. 1 shows that the muggier period of the year lasts for 10.6 months, from the end of September to the end of July. The muggiest months of the year are May, December and January, with muggy conditions which can reach 98%. The least muggy months of the year are, August and early September.

It is shown on Fig. 2 that the wetter season lasts 7.9 months, from September to May and the drier season lasts 4.1 months, from May to September.

The length of the day in Kinshasa does not vary substantially along the year. The average solar irradiation is 4.62 kWh/m<sup>2</sup>/day as shown on Fig. 3.

From the Fig. 4, the hottest day has an average high temperature of 32 °C and the lowest day has an average low temperature of 22 °C. The cool season lasts for 1.8 months, from June to August, with an average daily high temperature below 28 °C. The coldest day of the year is around July, with an average low of 18 °C and high of 26 °C.

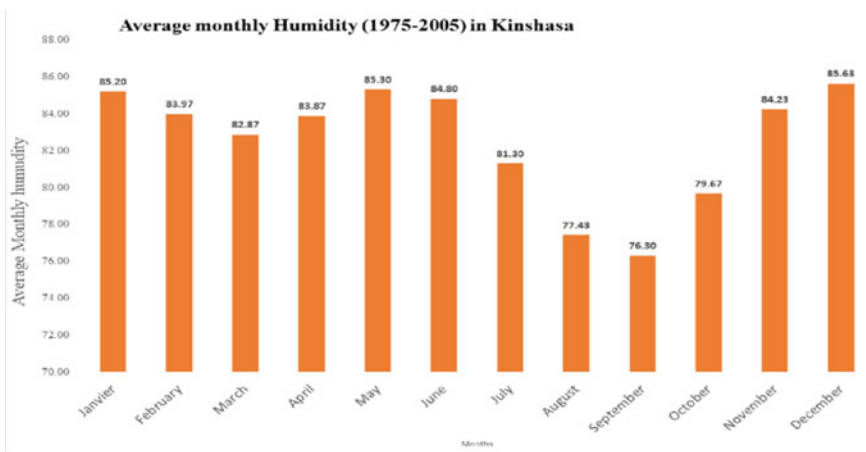


**Fig. 1** The monthly relative humidity in Kinshasa (1975–2005)

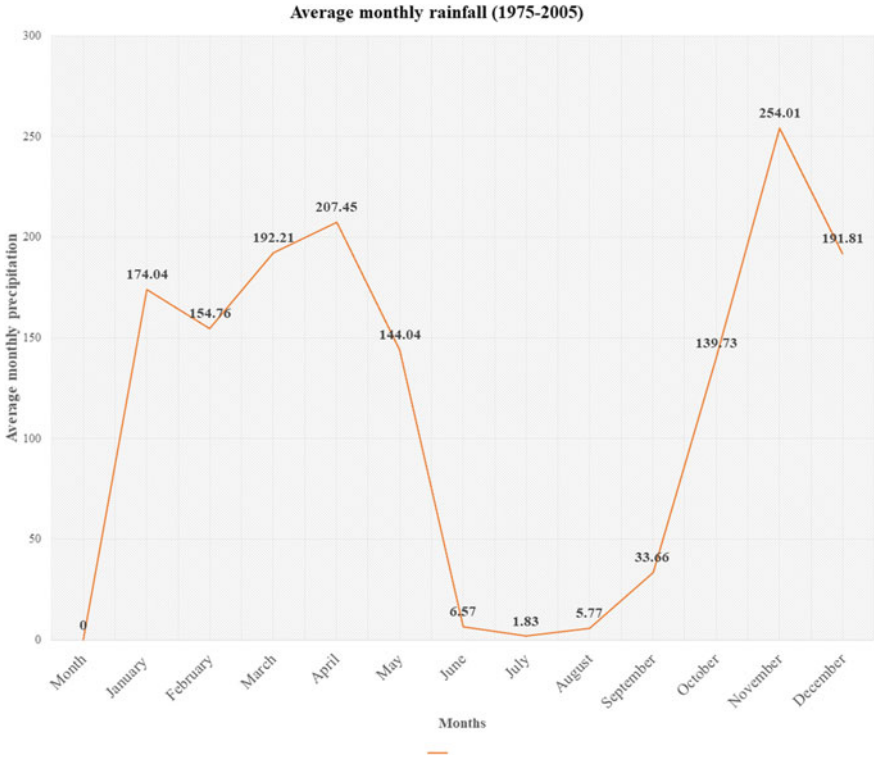


Fig. 2 Average monthly rainfall in Kinshasa (1975–2005)

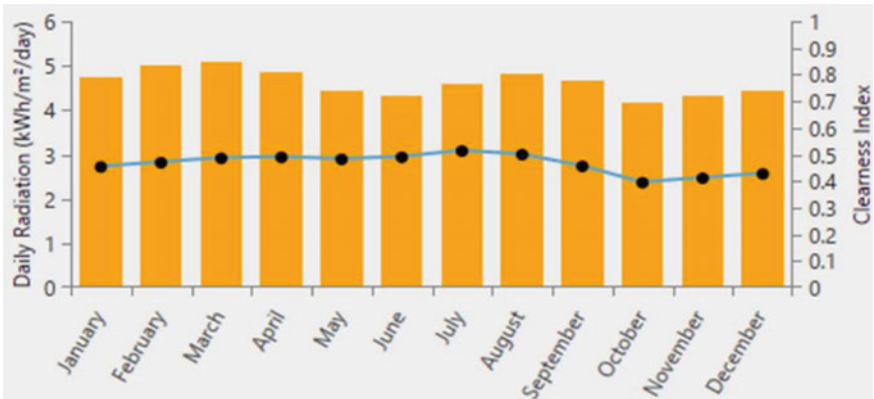


Fig. 3 Average monthly radiation in Kinshasa (Source HOMER PRO)

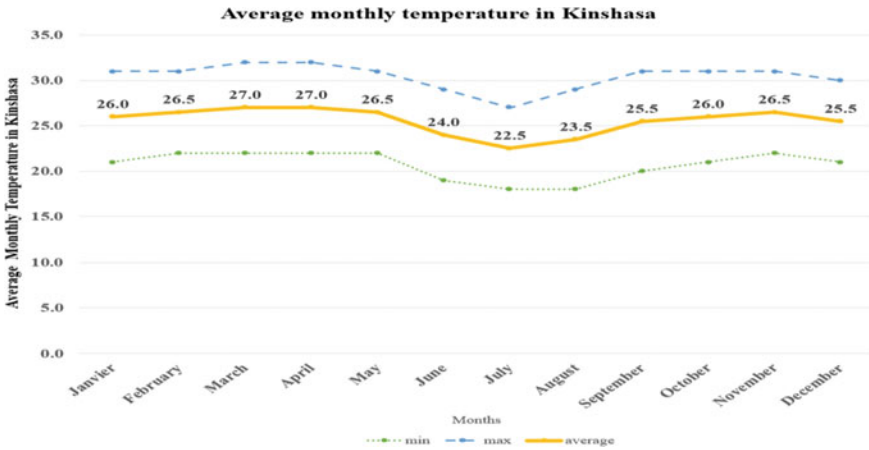


Fig. 4 Average monthly temperature in Kinshasa (1975–2005)

From Fig. 5, the wind direction is most often from the East for 1 month, from April to May, with a peak percentage of 36%. It is most often from the South for 1 month, from May to June, with a peak percentage of 41% on June. The wind is most often from the West for 10 months, from June to April, with a peak percentage of 84% in August.

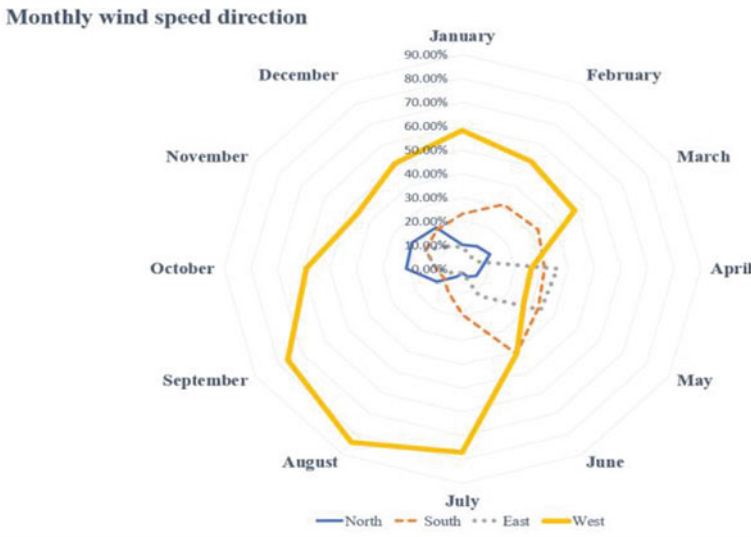


Fig. 5 Average monthly wind direction in Kinshasa (1975–2005)

### 4.2 Greenhouse Design

Previous researches have clearly revealed that up to 80% energy saving can be achieved through appropriate configuration of conventional greenhouses with a payback period of 4–8 years depending on climatic conditions and crop type [36]. Those researches provided clear guidelines for the construction of more water efficient evaporatively cooled greenhouses [37].

The greenhouse proposed has a specific shape as shown on Fig. 6 with a cooling technology adequate to savannah tropical climate.

The proposed greenhouse as shown on the Figs. 6 and 7 is aimed at overcoming the challenges faced by both large scale and small-scale farmers in Kinshasa as well as in other tropical savannah climate regions. The proposed cooling technology is an evaporative cooling system harnessing natural ventilation cooling system associated to 6 exhaust fans, misting system with 16 nozzles and a shading system used in intermittent way.

This proposed cooling technology optimizes the natural ventilation. For implementing all these, a specific shape was design with a “modified shed roof” opened in the major direction of wind direction as shown on the Figs. 6 and 7. The misting system is strategically placed on the top of the second roof longitudinal to the length of greenhouse structure using a well sized solar pump for providing the misting system with pressured water. Along the lateral sidewall, 6 exhaust fans are placed (3 per

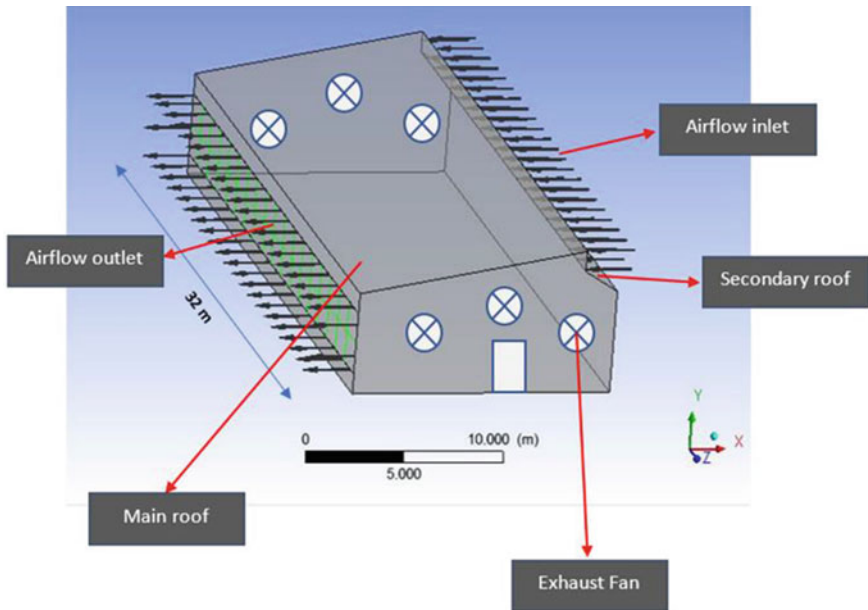


Fig. 6 Validated greenhouse shape

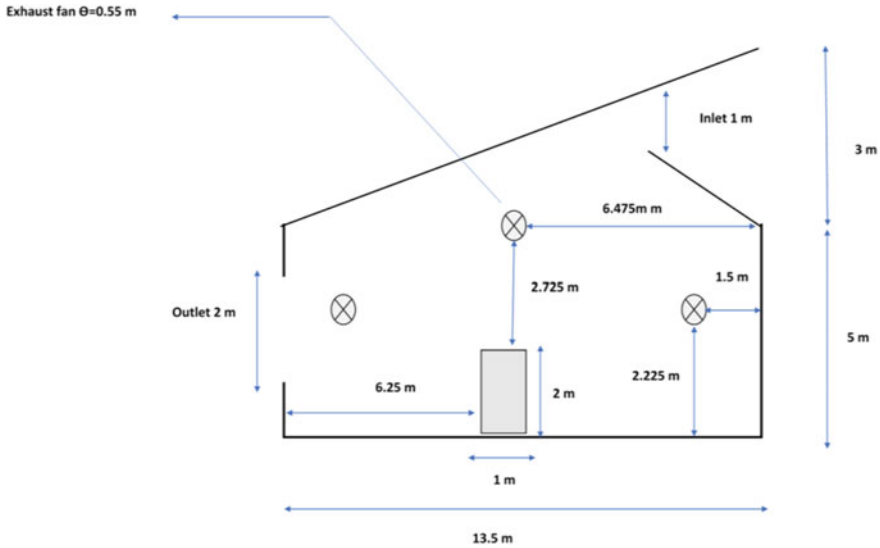


Fig. 7 Proposed greenhouse sizing

face). The entire greenhouse is powered by a standalone solar PV-Small Horizontal Wind Turbine hybrid energy system.

### 4.3 Physical Model of the Proposed System

To study the phenomena seen in a greenhouse under different conditions, physical models are often used which consist of the numerical solution. These models allow the characterization of the greenhouse indoor climate with a fine field grasping of parameters, such as: temperature, humidity, pressure and air circulation etc.

The numerical modeling of fluid flows, which is in fact a mathematical representation of the studied phenomenon, consists in determining at any point and at any time the state variables representative of the flow (velocity, pressure, temperature), by solving a system of partial differential equations, with a set of boundary and initial conditions drawn from the problem.

In this part of our work, we have exposed the complete physical model which simulates the movements of air in our greenhouse and which is based on the basic equations called the Navier Stokes equations.

In order to characterize the turbulent transfers in the greenhouse, we presented the different turbulence models, in particular the standard k-ε model used during this study. Solving a convection problem means determining at any point in the field of study and at any time the characteristic quantities of the fluid studied (air for our study), namely: pressure, temperature, and wind speed field.

### 4.3.1 The Boundaries Condition

See Tables 1, 2, 3, 4, 5 and 6.

**Table 1** Greenhouse inlet conditions

<i>Condition in the entrance</i>		
Relative humidity	80%	80%
Temperature (°C)	25–31	25–31
Air velocity (m/s)	1.5	3
Mass flow rate (kg/s)	56.832	113.664
Air change rate (h <sup>-1</sup> )	79.74511	159.498

**Table 2** Properties of sidewall plastic

<i>Properties–sidewall (Plastic polyethylene)</i>	
Density (kg/m <sup>3</sup> )	1400
Specific heat (J/kg · K)	1046
Thermal conductivity (W/m · K)	0.17
Thickness (in micron meter)	200
Heat transfer coefficient W/m <sup>2</sup> · K	0.33

**Table 3** Roof properties

<i>Properties–roof</i>	
Materials	Transparent FRP roof fiberglass
Light transmittance	55%
UV protection	UV protection
Heat transfer coefficient W/m <sup>2</sup> K	0.55
Density (kg/m <sup>3</sup> )	1550
Thermal conductivity (W/m °C)	0.57
Thermal expansion (10 <sup>-6</sup> m/m °C)	20
Thickness	1 mm

\***FRP**: Fiber-reinforced plastic is a composite material made of a polymer matrix reinforced with fibers

**Table 4** Netting system

<i>Netting system</i>	
Material	100% HDPE + UV
Mesh hole size	2 × 2 mm
Type of mesh	10 Mesh
Open area (outlet)	60.8%
Ventilation reduction	25.088 m <sup>2</sup>

**Table 5** Air properties

<i>Fluid properties</i>	
Dynamic viscosity	1.7894. 10 <sup>-5</sup> kg/m · s
Specific heat	1006.43 J/kg · K
Thermal conductivity	0.0242 W/m · K
Density	Incompressible-ideal-gas

**Table 6** Exhausted fans’ properties

Blades diameter (mm)	Blades rotational speed (rpm)	Motor rotational speed	Blades diameter (mm)	Blades rotational speed (rpm)
200	1400	1400	2000	120

### 4.4 Interpretation of CFD Simulation Results

The following physical and thermodynamic parameters were identified and determined: Velocity field, indoor air circulation, temperature field, the distribution of relative humidity and pressure inside the proposed greenhouse:

- For velocity field: the wind speed (in inlet) of 1.5 and 3 m/s, were used
- For temperature and pressure profile were presented both in YZ and XZ planes.

The simulation has shown an even distribution of temperature and a satisfactory air circulation in the validated greenhouse structure. The temperature and pressure were found slightly high around the inlet and out let regions, especially for the wind speed of 3 m/s. The air velocity in inlet region was also observed to be slightly high. This slight increasing of air velocity around the inlet region was attributed to the specific roof structure and air inlet emplacement chosen and validated for the proposed greenhouse.

#### 4.4.1 Wind Speed Field

The circulation of air inside the proposed greenhouse is shown on the Figs. 8, 9 and 10. On Fig. 8, the proposed greenhouse uses only natural ventilation and the wind speed from the inlet is 3 m/s.

On Fig. 10 the proposed greenhouse uses both natural ventilation and exhaust fans (6 fans) with the wind speed of 1.5 m/s. The increase in velocity generates an increase in air circulation in the proposed greenhouse and the homogeneity of the flow over the entire greenhouse is mainly due to the proposed shape of the greenhouse. Recirculation regions can also be seen in the middle part of the greenhouse.

From Figs. 8, 9, 10 and 11, we observed the velocity near the air entry because of the slope of the main roof. And the same observation is on the exit opening where the wind speed is high, and decreases slightly in the middle of the proposed greenhouse structure. On the other hand, it is much weaker in the inlet downstream side. We can see the air recirculation phenomenon from those profiles. This airflow pattern has a significant influence on the indoor air temperature cooling.

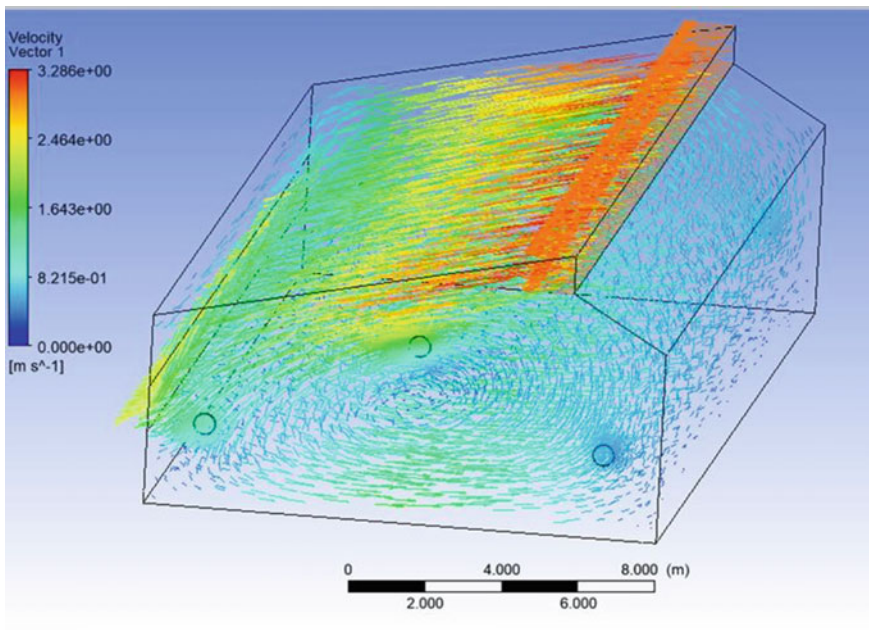


**Fig. 8** Airflow profile with  $v = 3\ m/s$  (no exhaust fan)



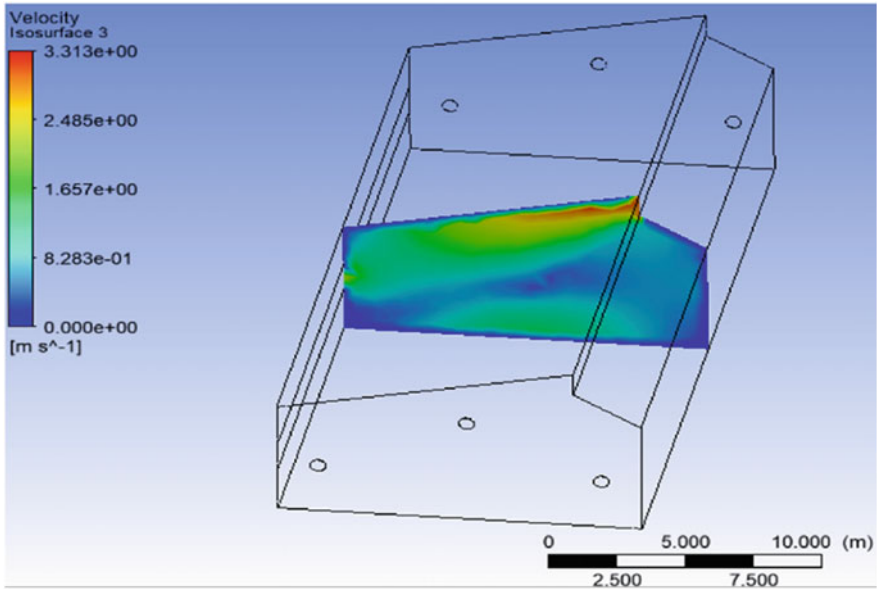


Fig. 9 Airflow profile in the XZ plane with Y = 16 m with v = 3 m/s (no exhaust fan)

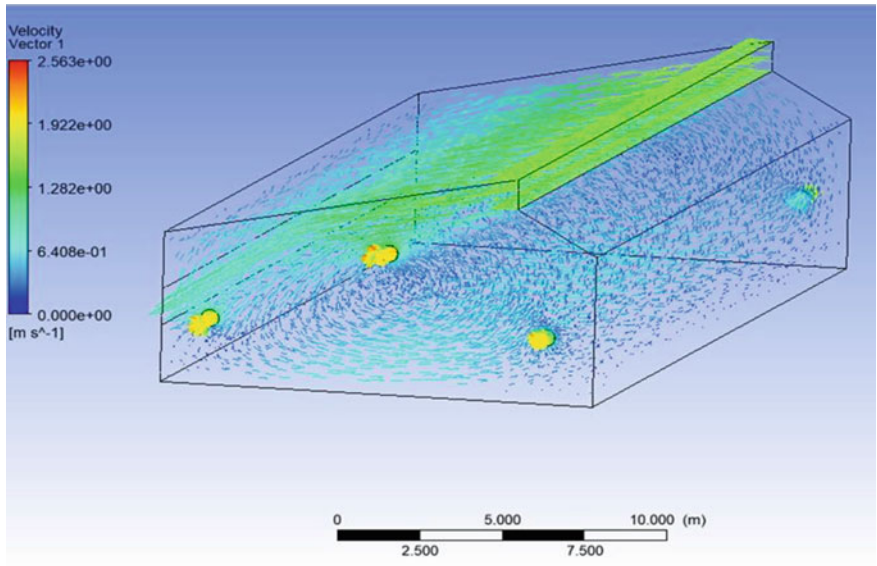


Fig. 10 Airflow profile with v = 1.5 m/s (with six exhaust fans working)

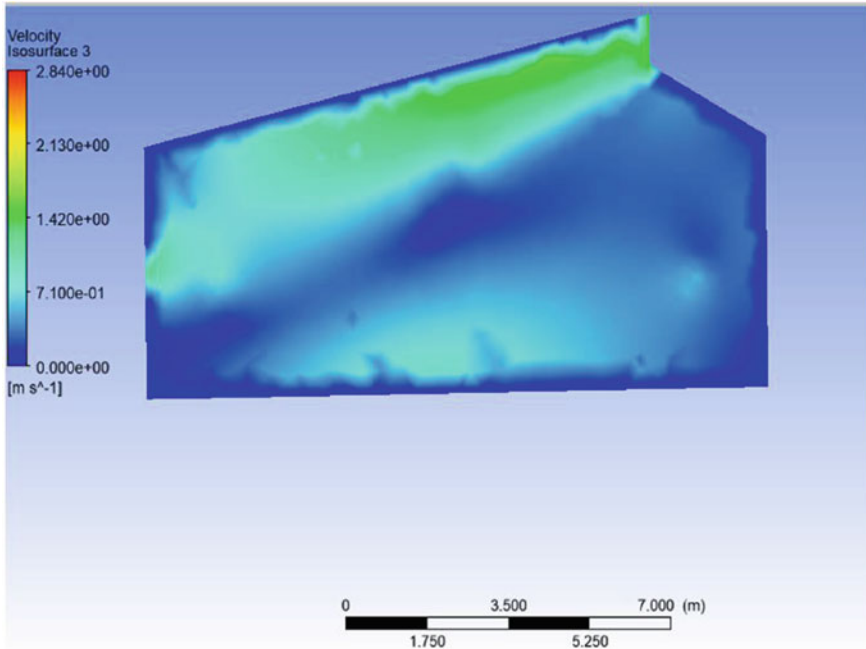


Fig. 11 Airflow profile with  $v = 1.5$  m/s (with exhaust fan)

#### 4.4.2 Temperature Field

The Figs. 12 and 13 show the temperature field. The increasing in wind speed leads to the increasing temperature inside the greenhouse around the outlet. This increase would be mainly due to the stagnation of the flow in that part of the greenhouse. The Fig. 13 shows how the temperature is constant and well distributed when  $v = 1.5$  m/s.

#### 4.4.3 Pressure Field

The Figs. 14 and 15 show the increase of pressure with the velocity, even though the comparison is at two different elevations resulting in the same pattern. The increase in pressure around the inlet and outlet regions of the proposed greenhouse is mainly due to the shape of the proposed greenhouse.

### 4.5 Design of Hybrid Energy System

For powering the proposed greenhouse, a small hybrid energy system of Solar PV-HAWT (Horizontal Axis Wind Turbine) has been designed and sized to meet the

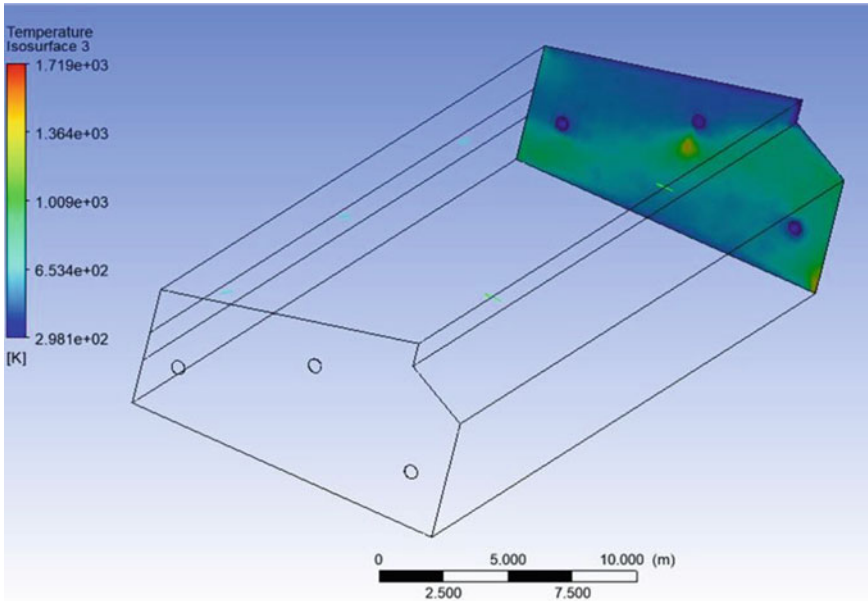


**Fig. 12** Temperature profile in the XZ plane with  $Y = 32$  m with  $v = 1.5$  m/s

greenhouse energy demand of 6.3 kWh/day in summer months with 2.08 kW peak and 1.7 kWh/day in winter. The hybrid energy systems represent a very promising sustainable solution for power generation in stand-alone applications, especially in remote regions far from the grid. However, in this research we have followed the below steps the design and sizing of our greenhouse:

- The definition of the available energy resources;
- The load energy determination;
- The Solar PV system and Wind turbine sizing;
- The sizing of the battery capacity;
- The planification of energy usage per day (in summer and winter);
- The estimation of the cost of the system (Fig. 16).

The planification is mainly based on the daily solar energy distribution. The proposed greenhouse cooling system combines a misting system, a shading system and exhausted fans, used intermittently. For optimizing the greenhouse energy consumption, the proposed cooling system will be used from 11:00 AM to 3:00 PM in each summer season. From 11:00 AM to 1 PM, the shading system will be used to regulate the temperature and relative humidity inside the greenhouse. From

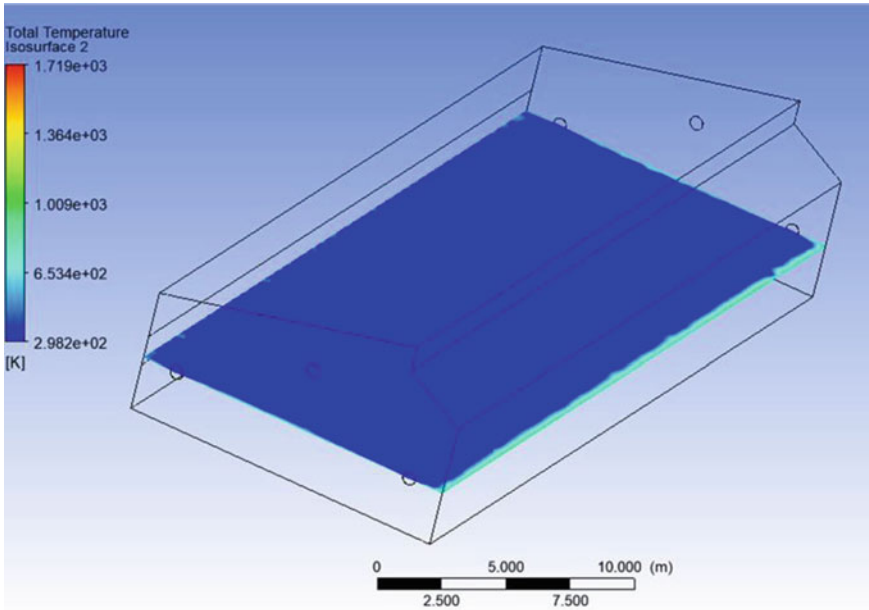


Fig. 13 Temperature profile in the XY plane with  $Z = 2.5$  m for  $v = 1.5$  m/s

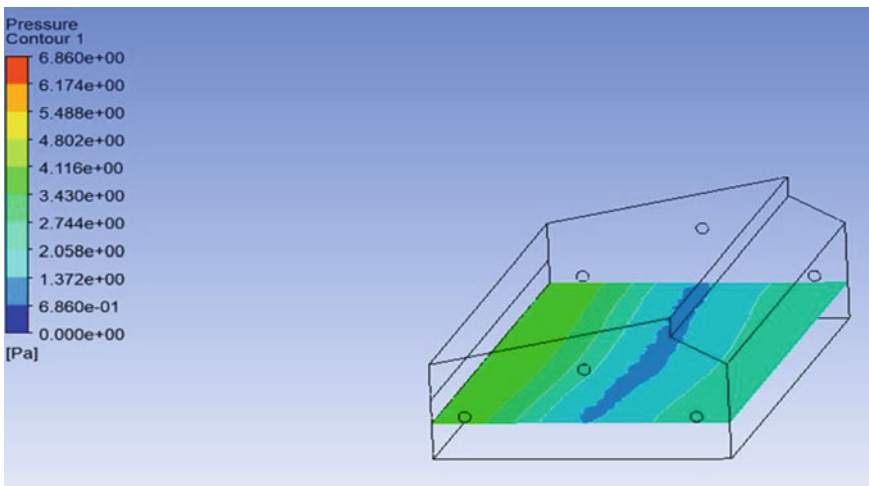
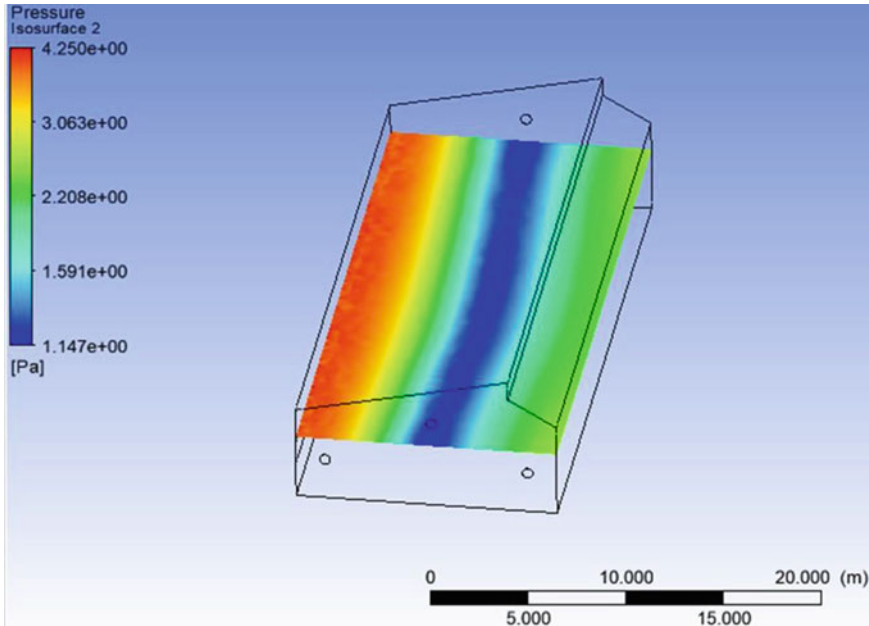
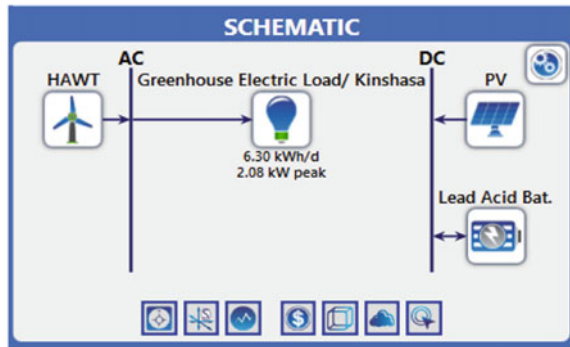


Fig. 14 Pressure in the XY plane with  $Z = 2.5$  m for  $v = 1.5$  m/s



**Fig. 15** Pressure profile in the XY plane with  $Z = 4.5$  m for  $v = 3$  m/s

**Fig. 16** Hybrid energy system



1 to 3 PM the misting system will be used with exhaust fans to cool down the air temperature and balance the inside relative humidity (Table 7 and Fig. 17).

### 4.6 Greenhouse Configuration and Sized Components

The proposed greenhouse has a “modified shed roof” and its surface area is of  $13.5 \text{ m} \times 32 \text{ m}$  and the volume of  $2166.798 \text{ m}^3$ . The structure has a side height of 8 m to

**Table 7** Planification of the greenhouse energy usage and load demand per day

Greenhouse electric load/day	Power (W)	Qt	Load (kW)	Working time (h)/day	Period	Energy (kWh/d)
Lighting (to fill the light transmittance deficit due to the use of the shading system from 11:00 AM to 1 PM and providing light in the greenhouse from 6:00PM to 4:00 AM)	40	2	0.08	12	11 am–1 pm; 6 pm–4 am	0.96
Solar submersible Water Pump (misting system)	750	1	0.18	0.33 (20 min)	1 pm–3 pm	0.2475
Exhaust fans	150	6	0.9	3	1 pm–3 pm	2.7
Electronic components (monitoring and control)	200	1	0.2	12	6 am–6 pm	2.4
Electric linear actuator	55	4	0.22	0.05 (3 min)	11–11: 1 min 30s am; 6–6:1 min 30s pm	0.011
Rotary electric actuator	150	8	1.2	0.06 (2 min)	10:58 am–11 am; 12:58 min–1:00 pm	0.08

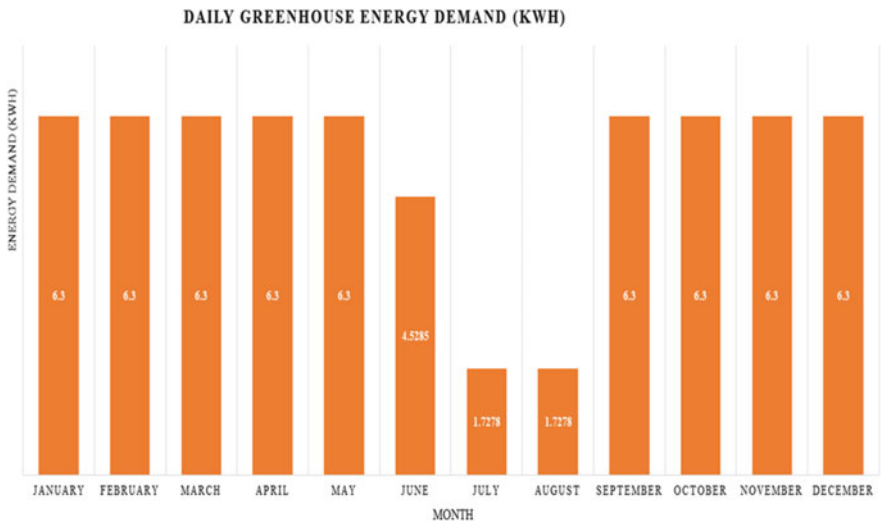


**Fig. 17** Daily greenhouse energy demand (kWh)

the top of main roof. The greenhouse has an air inlet opening area of  $32 \text{ m}^2$  ( $1 \text{ m} \times 32 \text{ m}$ ) oriented perpendicular towards the main direction of wind flow (west for the Kinshasa region).

A window (for air inlet) with a well sized electric actuators is designed to open or close the air inlet opening as needed. For an average window's mass of  $m = 80 \text{ kg}$  the electric actuators were oversized with a maximum load of  $3600\text{N}$  as the pushing force (4 actuators) with a respectively stroke length of  $600 \text{ mm}$  moving at  $15 \text{ mm/s}$ .

The greenhouse also has a secondary roof separated from the main roof by the air inlet opening. The misting system is located above the level of the secondary roof of the greenhouse and sprays water in a direction parallel to the slope of the main roof. The misting system of 16 nozzles of  $0.9 \text{ mm}$  bore diameter each was selected based on the power of the sized pump ( $P = 750 \text{ kW}$ , Pressure =  $30 \text{ bar}$ , flow rate of  $25 \text{ L/min}$ ) connected to the filtered water tank. The pump was slightly oversized to prevent prospective nozzle clogging.

The cold air entering through the air inlet opening is led to the interior space of the greenhouse and exits to the opposite side area of  $64\text{m}^2$  ( $2 \text{ m} \times 32 \text{ m}$ ) covered by a netting system of  $60.8\%$  of holes. The air change rate  $n_1 = 79.74511 \text{ h}^{-1}$  and  $n_2 = 159.498 \text{ h}^{-1}$  (calculated at an average temperature of  $25 \text{ }^\circ\text{C}$ ) are respectively related to the air-inlet velocity  $v_1 = 1.5 \text{ m/s}$  and  $v_2 = 3 \text{ m/s}$ . In the event of a low wind speed and a high relative humidity rate which would have the additional consequence of increasing the temperature, a forced evacuation system using 6 exhaust fans is started.

The shading system mounted on 8 electric rotary actuators of  $12\text{V}55\text{W}-1600 \text{ rpm}$  each is temporarily rolled up or unrolled below the main roof, stabilizing the air temperature and the relative humidity, by the way, reducing the energy consumption of exhaust fans. Moreover, a lighting system is used to compensate light deficits due to the shading system. An effective and efficient coordination of the proposed cooling configuration is presented on Table 7 for economical use of water and especially energy. This configuration based on the proposed energy usage planning saves the entire greenhouse energy consumption,  $6.3 \text{ kWh/day}$  in summer months and  $1.7 \text{ kWh/day}$  in winter months (for  $24 \text{ h}$ ). To optimize the energy consumption of the greenhouse, a specific timing is set for different cooling components (natural ventilation, misting system, shading system and exhaust fans).

#### ***4.7 The IoT-Based Testing Phase***

The proposed greenhouse in its miniaturized form ( $1/24$  scale) was built in Kinshasa Menkao ( $4.2099771 \text{ S}$ ;  $15.7011222 \text{ E}$ ). The testing phase was carried out between  $12:00$  noon to  $1:00 \text{ PM}$  in five days (time when the solar irradiation high (September 2020). The DHT11 sensor, LDR embedded on Arduino features, and PC data recording station were placed in the outlet region as shown on Fig. 19. The smoke source for air circulation visualization test was placed in the middle of the miniaturized greenhouse (region with low pressure and where the air recirculation has been observed clearly on CDF simulation profiles) as shown on Fig. 18.

**Fig. 18** Airflow visualization test

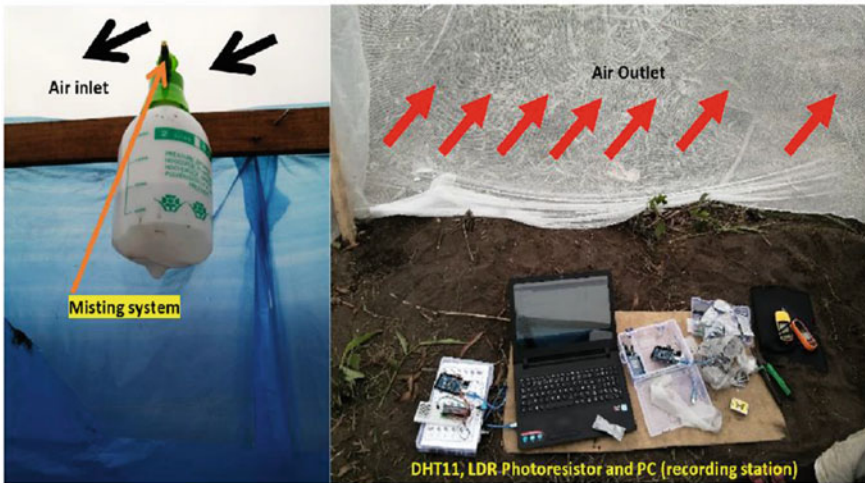


**Fig. 19** Misting system used in the testing phase and sensors location

The result of the shading testing has shown a little impact on light transmittance on Fig. 20. The shading system did not quite affect light transmittance in the greenhouse, whereas it had a high contribution in the stabilization of the relative humidity at 64%. A slight temperature drop was observed from 30 to 29.2 °C in 1 min and 18 s due to the use of shading system.

The result of the cooling test has shown a rapid and sharp drop in inside greenhouse temperature and a corresponding increase in inside relative humidity. The temperature change occurred quickly, within 48 s (from 12:58:48 to 12:59:30 as shown Fig. 21), upon the use of configured cooling system compared to the average outside temperature of 30.4 °C observed during the testing phase.



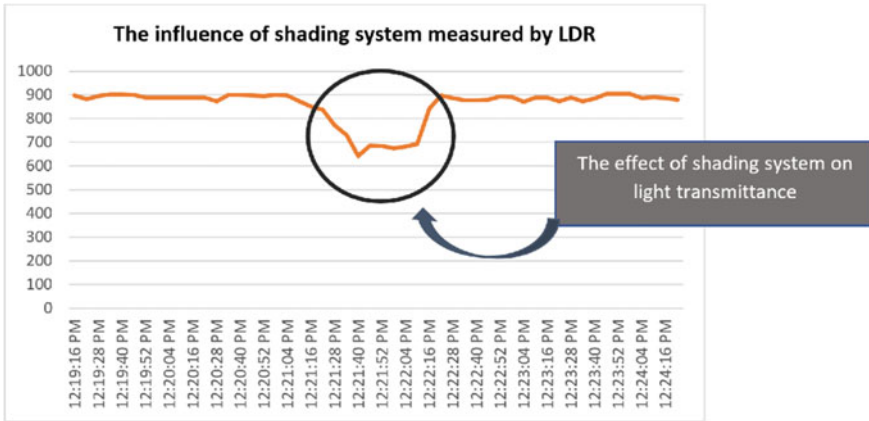


Fig. 20 The influence of shading system measured by LDR

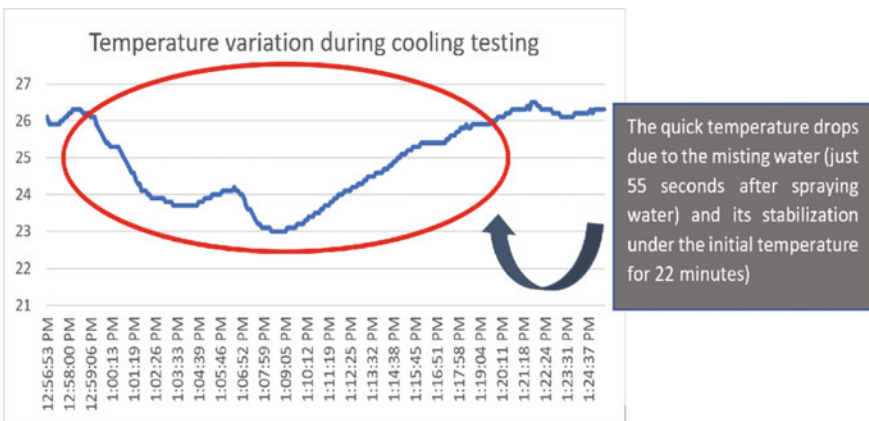


Fig. 21 Temperature variation during cooling testing

The proposed greenhouse under Kinshasa outdoor conditions, provided 1–7 °C of cooling compared to the outside temperature as shown on Fig. 21. The cooling system has shown a high reactivens. The temperature drop due to the misted water has been observed 48 s after spraying water from the misting system for the spraying duration of 1 min 11 s (12:58:48 PM to 12:59:59 PM). The temperature reached its lowest level 23 °C after 10 min 11 s and started increasing slowly. The temperature was stabilized under the initial temperature for 22 min.

The management of relative humidity has been identified to be the big challenge for greenhouse used in Kinshasa with a tropical savannah climate as relative humidity remains very high along the year. The cooling system proposed in this research has shown on Fig. 22. an increasing in relative humidity of 1–24% during the testing phase (from 63 to 87%). The repercussion, in terms of the effect on interior relative

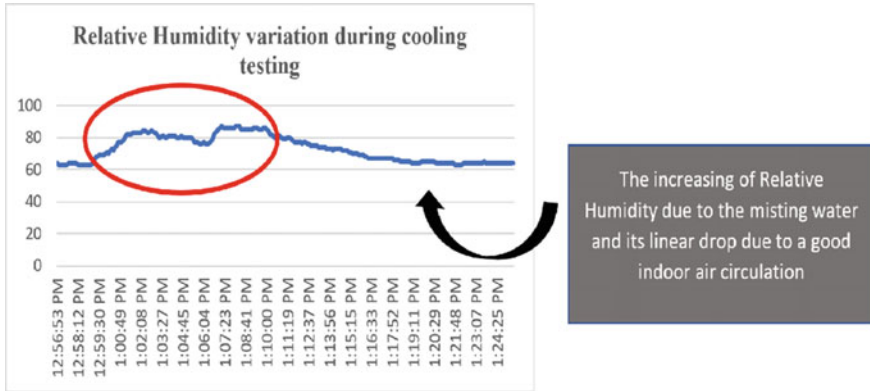


Fig. 22 Relative Humidity variation during the testing phase

humidity were rapid, after the activation of the cooling system. In 3 min, 31 s (from 12:58:48 PM to 1:02:13 PM) after activating the misting system, the relative humidity increased by 21% followed by a short stagnation period and slight drop due to the air circulation and 4 min 57 s later, the relative humidity reached its highest level of 87%. We have observed a drastic increasing in relative humidity of 24% in a short time (8 min 28 s) and a linear drop towards the initial value. The quick stabilization of relative humidity while the temperature remained at lower than its initial value was realized thanks to the designed roof shape and the air inlet emplacement which have favored a good greenhouse indoor air circulation playing the role of dehumidifier.

On Fig. 23, some remarkable heterogeneity has been observed during a same phase nobly during the increasing phase of relative humidity and decreasing phase of temperature. Ideally, after the activation of misting system, the relative humidity is supposed to increase while the temperature decreases. A remarkable heterogeneity was seen on the Fig. 23, where instead of observing respectively the increasing and decreasing of relative humidity and air temperature, we observed a reverse situation where the relative humidity slightly decreases while the air temperature slightly increases. This would likely be the mere consequence of an abrupt change in air velocity and the position of DHT11 sensor placed in the outlet region, where the temperature is inclined to be high as demonstrated in the result of CFD temperature simulation.

### 4.8 Greenhouse Cost Estimation

The cost estimation is summarized on Fig. 24 (the cost is in US dollar, with an exchange rate of 1900 CDF = 1\$, as in 2020). The related tax charge is not taken into consideration and for international purchase, shipping cost is not considered. The platforms consulted for international prices were Alibaba and amazon, August

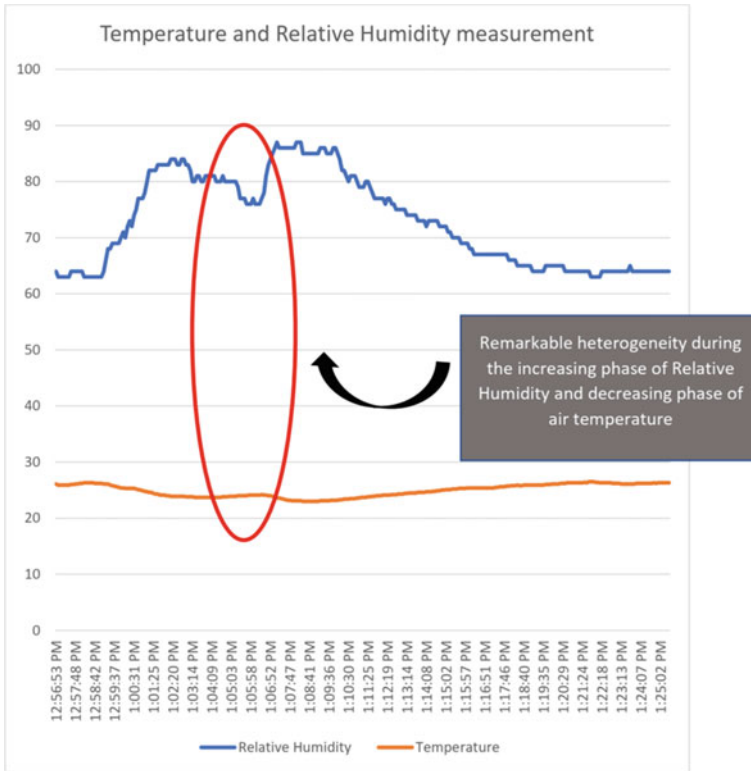


Fig. 23 Temperature and relative humidity (superposition)

2020). The area of the proposed greenhouse being expressed in square meter (432 m<sup>2</sup>), the cost has been also estimated per square meter (m<sup>2</sup>).

### 4.9 Limitations and Prospective Researches

Based on the objective and the aim of the research, the above compiled results were satisfactory. However, our study had several limitations notably, the lack of carrying out the experimentation of electric actuators for window and shading system. This limitation restricted our research from a full demonstration of the concept. The main reason of not overcoming those limitations was the Covid-19 pandemic coerced us to slightly change our research topic (by removing the smart and automation section) and pushed us to change the location of the prototype construction. In addition, the covid-19 pandemic effect rendered the equipment shipping quasi-impossible in the needed time.

<b>Item</b>	<b>Total Cost</b>	<b>Cost/m<sup>2</sup> of greenhouse</b>
Solar Panel (W)	380.8	0.881481
Small Horizontal Wind Turbine	150	0.347222
Solar Battery	48	0.111111
Solar charge controller	45	0.104167
Wind turbine controller	51	0.118056
Inverters	180	0.416667
PV cable (m)	2.5	0.005787
Covering system for roof (m <sup>2</sup> )	151.8	0.351389
Covering system sidewall (m <sup>2</sup> )	68.25	0.157986
Shading system (m <sup>2</sup> )	21.6	0.05
Netting system (m <sup>2</sup> )	12.8	0.02963
Windows	44	0.101852
Misting system	30	0.069444
Exhaust fans	132	0.305556
Solar submersible pump	142	0.328704
Erecting system and concrete	50	0.115741
Water tank	60	0.138889
Filters for misting system water	8	0.018519
Electric linear actuators	56	0.12963
Electric rotary actuators	80	0.185185
Wire (m)	4	0.009259
Lighting	10	0.023148
<b>Total greenhouse cost</b>		<b>3.999421</b>

**Fig. 24** Cost estimation US dollar per square meter

We recommend further full-scale testing for the proposed greenhouse for providing a full demonstration of the concept and we strongly suggest future studies may be oriented towards a design of a smart monitoring and control as well as the automated system that should optimize the use of energy and water in the proposed greenhouse.

## 5 Conclusion

The proposed greenhouse (13.5 m × 32 m) uses a new energy efficient cooling method designed and tested for savanna tropical climates in emphasizing more on the simplicity of technology, use of local materials, affordability and energy efficiency. A specific cooling configuration was proposed based on energy efficiency and the running cost. The proposed greenhouse cooling system is mainly based on natural ventilation sustained by a misting system, a shading system and 6 exhaust fans. An effective and efficient coordination of the proposed cooling configuration was developed for an economical use of water and especially energy in the entire greenhouse. This configuration based on the designed energy usage planning saves significantly the entire greenhouse energy consumption; 6.3 kWh/day in summer and 1.7 kWh/day in winter.

The testing phase of the proposed greenhouse provided 1–7° C of cooling compared to the outside temperature. And showed an increase in relative humidity of 1–24%. A design and sizing of a small hybrid energy system with the battery storage system was carried out for the full-scale greenhouse. Finally, the cost of the proposed full-scale greenhouse was estimated to be 3.9 USA dollar per square meter, cost which made the proposed greenhouse affordable.

The result of this research has provided a new tropical greenhouse structure with an adequate energy efficient cooling configuration meeting the meteorological constraints of savannah tropical climate. This offers a new perspective for modern and urban agriculture and can boost significantly food production (especially vegetables and fruits) in Kinshasa as well as in other countries with similar weather conditions.

**Acknowledgements** At the end of this research, we would like to warmly thank all those who have contributed from near or far. I would like to express my gratitude to Professor Dr. Venkatta Ramayya, who has given me assistance to complete this research project accounting for my Master thesis in Energy engineering at Pan African University, Institute of Water and Energy sciences including Climate Change (The African Union program). I would like to thank the DAIPN center and TAMANO FOOD Company for providing me with research visit despite the COVID 19 pandemic effect and providing me with helpful information on the greenhouse challenges in Kinshasa. I would not forget the helping hand of HALIME Abdoulaye in the equipment purchase and the one of Christian BAYI AYIKO during the testing phase, Thank you. I would like also to thank the department of mechanical engineering of the University of Kinshasa, for giving me access to the laboratory where I have used CFD for the simulation of the proposed greenhouse. Particularly Mr. Derick Badibanga and Engineer Seba.

## References

1. United-Nations: World population prospects (2019)
2. Jean-Jacques Dethier, A.M.: Infrastructure in developing countries: an overview of some economic issues. ZEF-Discussion Papers on Development Policy No. 165 (2012)
3. Bank, T.W.: Democratic Republic of Congo urbanization review. In: Internet (ed) 2018 International Bank for Reconstruction and Development (2018a)

4. Xuemei Bai, T.B., Dhakal, S., Fisk, D.J. (Imperial College London, UK) Ichinose, T., Keirstead, J.E., Sammer, G., Satterthwaite, D., Schulz, N.B., Shah, N., Steinberger, J., Weisz, H.: Urban energy systems. *Glob. Energy Assess.* **2**, 1307–1400 (2012)
5. Bank, W.: Democratic Republic of Congo systematic country diagnostic: policy priorities for poverty reduction and shared prosperity in a post-conflict country and Fragile State (2018b)
6. Gashu, D., Demment, M.W., Stoecker, B.J.: Challenges and opportunities to the African agriculture and food system. *Afr. J. Food Agric. Nutr. Dev.* **19**, 14190–14217 (2019)
7. Baudoin, W.O., Zabeltitz, C.V.: Greenhouse constructions for small scale farmers in tropical regions. FAO Rome, Horticultural Crops Group Institute for Horticultural Engineering Via delle Terme di Caracalla (2002)
8. Zabeltitz, C.V.: Integrated greenhouse systems for mild climates climate conditions, design, construction, maintenance, climate control (2011)
9. Gadhalaria, G., Desai, C., Bhatt, R., Salah, B.: Thermal analysis and experimental validation of environmental condition inside greenhouse in tropical wet and dry climate. *Sustainability* **12** (2020)
10. Munzimi, Y.A., Hansen, M.C., Adusei, B., Senay, G.B.: Characterizing Congo basin rainfall and climate using tropical rainfall measuring mission (TRMM) satellite data and limited rain gauge ground observations. *J. Appl. Meteorol. Climatol.* **54**, 541–555 (2015)
11. Acosta-Silva, Y.J., Torres-Pacheco, I., Matsumoto, Y., Toledano-Ayala, M., Soto-Zarazua, G.M., Zelaya-Angel, O., Mendez-Lopez, A.: Applications of solar and wind renewable energy in agriculture: a review. *Sci. Prog.* **102**, 127–140 (2019)
12. Kumar, K.S., Tiwari, K.N., Jha, M.K.: Design and technology for greenhouse cooling in tropical and subtropical regions: a review. *Energy Build* **41**, 1269–1275 (2009)
13. Belkadi, A., Mezghani, D., Mami, A.: Energy design and optimization of a greenhouse: a heating, cooling and lighting study. *Eng. Technol. Appl. Sci. Res.* **9**(3), 4235–4242 (2019)
14. McCartney, L., Lefsrud, M.G.: Field trials of the natural ventilation augmented cooling (NVAC) greenhouse. *Biosys. Eng.* **174**, 159–172 (2018)
15. Watson, R.T., Boudreau, M.-C., Van Iersel, M.W.: Simulation of greenhouse energy use: an application of energy informatics. *Energy Inform.* **1** (2018)
16. Choab, N., Allouhi, A., El Maakoul, A., Kouskou, T., Saadeddine, S., Jamil, A.: Review on greenhouse microclimate and application: design parameters, thermal modeling and simulation, climate controlling technologies. *Sol. Energy* **191**, 109–137 (2019)
17. Hasan, Ö., Atilgan, A., Buyuktas, K., Alagoz, T.: The efficiency of fan-pad cooling system in greenhouse and building up of internal greenhouse temperature map. *Afric. J. Biotechnol.* **8**(20), 5436–5444 (2009). <https://doi.org/10.4314/ajb.v8i20.65986>
18. Shamshiri, R.R., Jones, J.W., Thorp, K.R., Ahmad, D., Man, H.C., Taheri, S.: Review of optimum temperature, humidity, and vapour pressure deficit for microclimate evaluation and control in greenhouse cultivation of tomato: a review. *Int. Agrophys.* **32**, 287–302 (2018)
19. Campiotti, C.A., Morosinotto, G., Puglisi, G., Schettini, E., Vox, G.: Performance evaluation of a solar cooling plant applied for greenhouse thermal control. *Agricult. Agricult. Sci. Procedia* **8**, 664–669 (2016)
20. Subin, M.C., Karthikeyan, R., Periasamy, C., Sozharajan, B.: Verification of the greenhouse roof-covering-material selection using the finite element method. *Mater. Today: Proc.* **21**, 357–366 (2020)
21. Silke Hoffmann, D.W.: Tropical and subtropical greenhouses—a challenge for new plastic films. Institute of Environmental and Agricultural Engineering IMAG, Acta Hort. 578, ISHS 2002 (2002)
22. Tang, Y., Ma, X., Li, M., Wang, Y.: The effect of temperature and light on strawberry production in a solar greenhouse. *Sol. Energy* **195**, 318–328 (2020)
23. Ghoulem, M., El Moueddeb, K., Nehdi, E., Boukhanouf, R., Kaiser Calautit, J.: Greenhouse design and cooling technologies for sustainable food cultivation in hot climates: review of current practice and future status. *Biosyst. Eng.* **183**, 121–150 (2019)
24. Al-Mahdouri, A., Baneshi, M., Gonome, H., Okajima, J., Maruyama, S.: Evaluation of optical properties and thermal performances of different greenhouse covering materials. *Sol. Energy* **96**, 21–32 (2013)

25. Viloría, A., Altahona, T.A.R., Lezama, O.B.P.: Retraction: energy balance in a greenhouse: temperature and humidity monitoring. In: IOP Conference Series: Materials Science and Engineering, Science Engineering, vol. 872, p. 012196 (2020)
26. Youssef, G.D.M., Yakout, T.R., Mostafa, D.M.: Improving performance of the evaporative cooling system inside the greenhouses and its effect on tomato productivity. *Alexandria Sci Exchange J.* **36**(1) (2015)
27. Cuce, P.M., Riffat, S.: A state of the art review of evaporative cooling systems for building applications. *Renew. Sustain. Energy Rev.* **54**, 1240–1249 (2016)
28. Lee, S.-Y., Lee, I.-B., Kim, R.-W.: Evaluation of wind-driven natural ventilation of single-span greenhouses built on reclaimed coastal land. *Biosys. Eng.* **171**, 120–142 (2018)
29. Chiesa, G., Grosso, M.: Cooling potential of natural ventilation in representative climates of central and southern Europe. *Int. J. Vent.* **16**, 84–98 (2016)
30. Watson JA, Gómez C, Bucklin RA, Leary JD, McConnell DB (2016) Fan and pad greenhouse evaporative cooling systems. His document is CIR1135, one of a series of the Department of Agricultural and Biological Engineering, UF/IFAS Extension
31. Franco, A., Valera, D., Peña, A.: Energy efficiency in greenhouse evaporative cooling techniques: cooling boxes versus cellulose pads. *Energies* **7**, 1427–1447 (2014)
32. Arbel, A., Yekutieli, O., Barak, M.: Performance of a fog system for cooling greenhouses. *J. Agric. Eng. Res.* **72**, 129–136 (1996)
33. Katsoulas, N., Baille, A., Kittas, C.: Effect of misting on transpiration and conductances of a greenhouse rose canopy. *Agricult. Forest Meteorol.* **106**, 233–247 (2000)
34. Ahmed, H.A., Tong, Y.-X., Yang, Q.-C., Al-Faraj, A.A., Abdel-Ghany, A.M.: Spatial distribution of air temperature and relative humidity in the greenhouse as affected by external shading in arid climates. *J. Integr. Agric.* **18**, 2869–2882 (2019)
35. Cascone, S., Ingrao, C., Valenti, F., Porto, S.M.C.: Energy and environmental assessment of plastic granule production from recycled greenhouse covering films in a circular economy perspective. *J. Environ. Manag.* **254**, 109796 (2020)
36. Cuce, E., Harjunowibowo, D., Cuce, P.M.: Renewable and sustainable energy saving strategies for greenhouse systems: a comprehensive review. *Renew. Sustain. Energy Rev.* **64**, 34–59 (2016)
37. Tsafaras, I., Campen, J.B., Stanghellini, C., De Zwart, H.F., Voogt, W., Scheffers, K., Harbi, A.A., Assaf, K.A.: Intelligent greenhouse design decreases water use for evaporative cooling in arid regions. *Agricult. Water Manag.* **250** (2021)

# Comparative Study of Solar and Geothermal Renewable Energy Resources for Desalination of Seawater with Latest Case Studies



Sujeeth Swami, B. P. Hemanth, Jaywant Kamal, M. Ravikumar, Krishna Pandit, and Harshal Kashyap

**Abstract** While 71% of the earth is covered by water, just 1% of surface water is reasonable for homegrown and modern purposes, and undeniably less can be utilized economically. As of now, more than a fourth of the total populace needs admittance to adequate decontamination offices, which might be exacerbated with populace development, environmental change, and expanded farming requirements. The interest for new water surpasses the stock. It is assessed that by 2025, around 2.1 billion individuals won't approach water; this number will increment to close to half of the total populace. In addition, by 2025, the world might experience the ill effects of water pressure as 80% of sicknesses are because of water abuse and around 20% of the total populace doesn't have new water that meets least sterilization necessities. This paper fundamentally centers around giving a relative investigation of environmentally friendly power assets of solar and geothermal for desalination involving two contextual analyses for each and most recent advances and by thinking about the better with more efficient, to prevent the upcoming scarcity of the world.

**Keywords** Desalination · TDS · Solar · geothermal latest case studies with current all information's in contrast

## 1 Introduction

Water shortage is a seething worldwide issue that is relied upon to deteriorate before very long. Today, north of two billion individuals need admittance to safe and clean water [1]. Populace development and ensuing interest for horticulture have multiplied human water utilization during the most recent couple of many years [2]. Quick metropolitan development has likewise added to water pressure through expanding interest for water in metropolitan regions [3], and weakening of water quality because

---

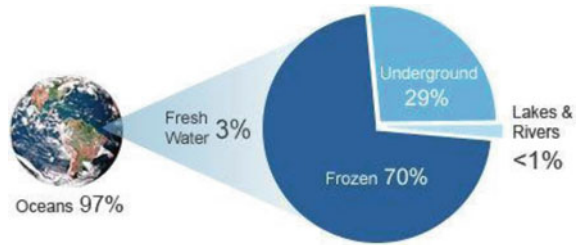
S. Swami (✉) · B. P. Hemanth · J. Kamal · M. Ravikumar · K. Pandit · H. Kashyap  
Department of Mechanical Engineering, New Horizon College of Engineering, Bengaluru, India  
e-mail: [sujeeth89@gmail.com](mailto:sujeeth89@gmail.com)

© The Author(s), under exclusive license to Springer Nature Switzerland AG 2024  
K. Kyamakya and P. N. Bokoro (eds.), *Recent Advances in Energy Systems, Power and Related Smart Technologies*, Studies in Systems, Decision and Control 472,  
[https://doi.org/10.1007/978-3-031-29586-7\\_12](https://doi.org/10.1007/978-3-031-29586-7_12)

331



**Fig. 1** Availability of water in different forms (Freshwater 3%, Oceans 97%)



of release of modern squanders [4]. Human prompted environmental change is likewise connected to changes in water accessibility and expanded danger of dry season [5]. These elements have brought about developing weight on the world’s water saves, which thus influences worldwide admittance to well-being and disinfection as issues identified with sterilization simultaneously rise [6] (Fig. 1).

Total Dissolved Solids (TDS) in water are some natural and inorganic materials, which incorporate minerals and particles that are broken up in a specific amount in water. At the point when water goes through stones, pipes or various surfaces, the particles are assimilated into the water. TDS in water can emerge out of various sources, for example, minerals in synthetic compounds utilized for treating water, overflow from the street salts and synthetic compounds or composts from the home-steads. The water that you get surpasses the greatest degree of TDS that should be available in water. Water that has a TDS level of more than 1000 mg/L is ill suited for utilization. An undeniable degree of TDS in water can prompt various medical issues. The presence of potassium, sodium, chlorides increment the TDS level in the water (Table 1).

Notwithstanding, the presence of poisonous particles like lead, nitrate, cadmium, and arsenic present in water can prompt various genuine medical conditions. This is particularly significant for kids since they are considerably touchier to impurities in light of the fact that their protection frameworks have not completely evolved. The cleaner the water, one can be guaranteed of good well-being. KENT gives one of the most outstanding water purifiers in India that accompany a TDS regulator to guarantee that the water you drink is ok for utilization [8].

**Table 1** TDS level range given in ppm [8]

TDS level in parts per ppm	potability quotient
150–250	Excellent for drinking
250–300	Good
300–500	Fair
Above 1200	Unacceptable

## ***1.1 Solar and Geothermal Energy***

Solar energy is the radiation from the Sun equipped for creating heat, causing synthetic responses, or producing power. The aggregate sum of sun powered energy got on Earth is tremendously more than the world's current and expected energy prerequisites. Assuming that appropriately bridled, sun powered energy can possibly fulfil all future energy needs [9].

Heat is a type of energy and geothermal energy is the hotness held inside the Earth that creates topographical peculiarities on a planetary scale. Geothermal angle (GG) communicates the expansion in temperature with profundity in the Earth's outside layer. Down to north of 10,000 m (profundities open by penetrating), the normal GG is around 2.5–3 °C/100 m. E.g., if the temp. inside the initial not many meters subterranean—level, is 15 °C, then, at that point, it very well may be accepted that the temp. will be around 65–75 °C at 2000 m profundity, 90–105 °C at 3000 m, etc. for a further scarcely any thousand meters. In locales in which the significant stone tornado shelter has gone through fast sinking, and the bowl is stacked up with geographically 'uncommonly energetic' build-up, the GG may be lower than 1 °C [10].

## **2 Case Study: Jordan**

### ***2.1 Large SMADES Flat Plate Solar Collector SPMD System***

The framework is implemented on a “large SMADES” SPMD on coast Red Sea in Jordan. Data from same plant are being used. The system had a capacity of 1000 L per day and having a pair of loops where PV panels generate electricity for operation. The first loop is called “Solar loop” where tap water is used for heat transfer medium, and the second loop is called “desalination loop” where the sea water is fed for desalination, as shown in Fig. 2 [11].

### ***2.2 Results and Discussions***

The after effects of the LCA concentrate on centre around the acknowledgment of a maintainable MD framework corresponding to the 22 effect classifications, as displayed in the accompanying charts. It tends to be seen that CMD has the most noteworthy natural effect among any remaining situations, while Single-Si rules among the SPMD-PV board situations. This paper alluded to the a-Si and Single-Si wafers because of their low and high natural effects, individually, contrasted with the other board types. The effect of a-Si, which gives a base level of 3.23% in freshwater ecotoxicity and a greatest level of 88% in an Earth-wide temperature boost was

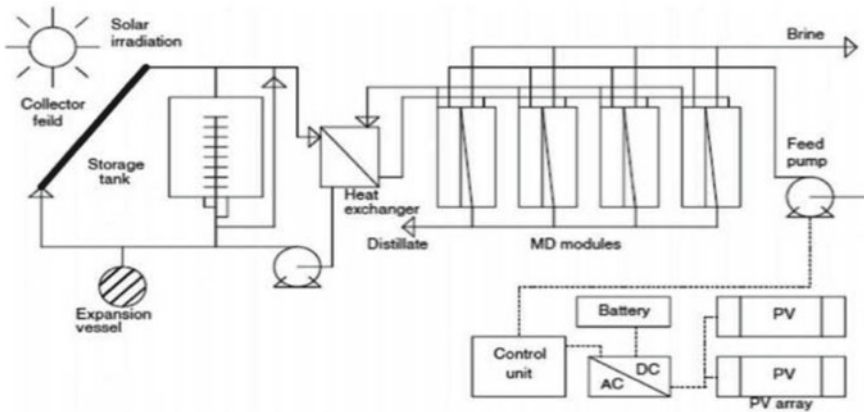


**Fig. 2** Solar desalination process in Jordan using large flat plate [12]

discussed. In addition, the effect of a solitary Si wafer with a worth of 100% in a dangerous atmospheric deviation and 3.32% in freshwater ecotoxicity; concerning CMD, the worth lessens to 89.7% in an Earth- wide temperature boost was also discussed. The after effects of the ecological classifications of the SPMD and CMD were also analysed. The Fora-Si, values of 23.8, 21.9 and 58.3 were attained for the same above orders, independently, as shown in Fig. 5. In the case of Ribbon-Si, values of 24.3, 22.5 and 64 are obtained and appeared to be close enough to CIS and a-Si PV panels. For multi-Si, it explosively told the results where it also reached 24.4, 22.6 and 67.4. In Fig. 4, Single Si shows analogous test to multi-Si, where it achieved 24.5, 22.8, and 70.9, independently. The overall test of CIS, a-Si and Ribbon-Si are veritably analogous, and they were the PV types in this study that have the least environmental impact, with a-Si being the type that contributes the least to the environmental foot mark among them (Fig. 3) (Table 2).

The conduct of multi-Si and single-Si is additionally basically the same, with single-Si ruling as it for the most part has the most noteworthy ecological effect, contrasted with multi-Si, yet in addition to CIS, a-Si and lace Si. As a rule, all the above PV board types add to asset utilization with rates going from 58 to 71%; this is because of the way that PV boards are produced using materials that are not accessible wherever on the planet and ought to be reused at removal to preserve assets and material utilization. From one perspective, the CMD framework scored 100% in all classes for CIS, a-Si and Ribbon PV boards (Figs. 4 and 5).

Then again, it scored 100% in all classes with the exception of a dangerous atmospheric deviation for Multi-Si and Single-Si, where it scored 96.4 and 89.7%, separately, and it additionally scored 100% in the classes of human well-being, environments and asset consumption. This can be closed by the utilization of petroleum products and non-sustainable power strategies as an energy source on the off chance that it is a power lattice blend during the activity time frame, and furthermore by the development of the power conveyance lines as the outflows increment with the

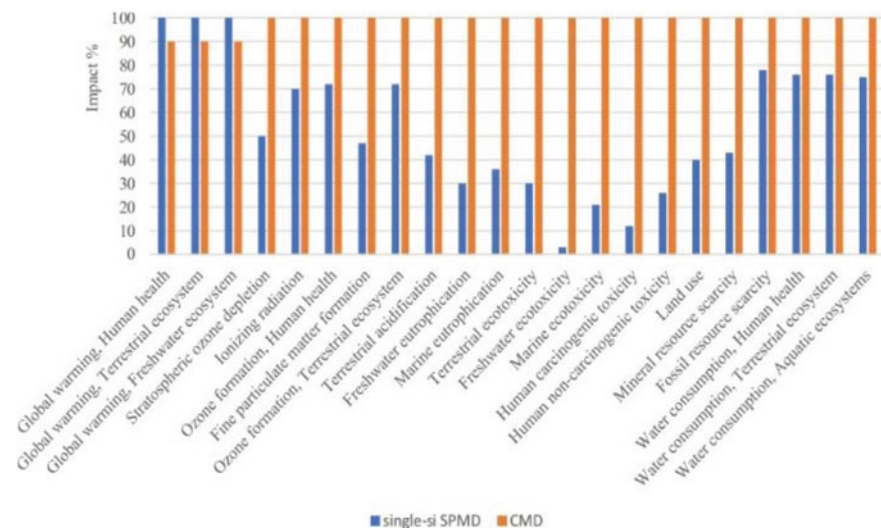


**Fig. 3** LCA findings for both SPMD single-Si and CMD and corresponding impact orders as recaptured from the software

**Table 2** Characteristics of the large SPMD system in Aqaba, Jordan [12]

System	Parameter	Value
SPMD		
Aqaba	(m <sup>2</sup> ) PV	14.00
	(kWp)	1.44
Jordan	Collector area with Cu absorber (m <sup>2</sup> )	72.00
		Flat
	Collector type feed flow rate (L.d <sup>-1</sup> ) distillate amount	Flat
	Distillate amount	Plate
		1000.00
		468.00
		10.00
	Average (L)	PTF
	Membrane area	E
	(m <sup>2</sup> ) Membrane	4.00
	Material number of membrane modules	3.00
	Solar heat storage capacity (m <sup>3</sup> )	

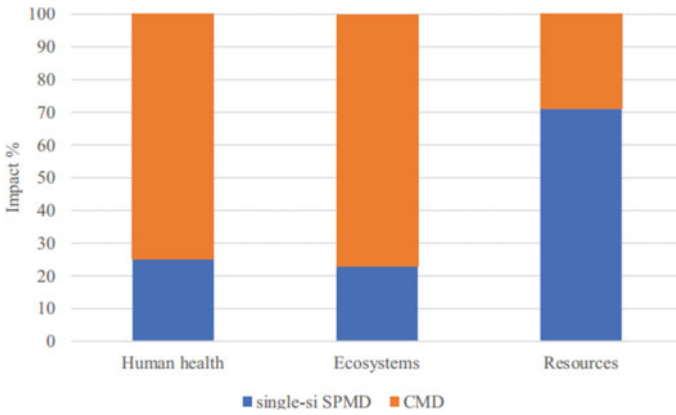


**Fig. 4** LCA discoveries for both SPMD single-Si and CMD and comparing human well-being, biological systems and asset consumption endpoint sway classifications as recovered from the product

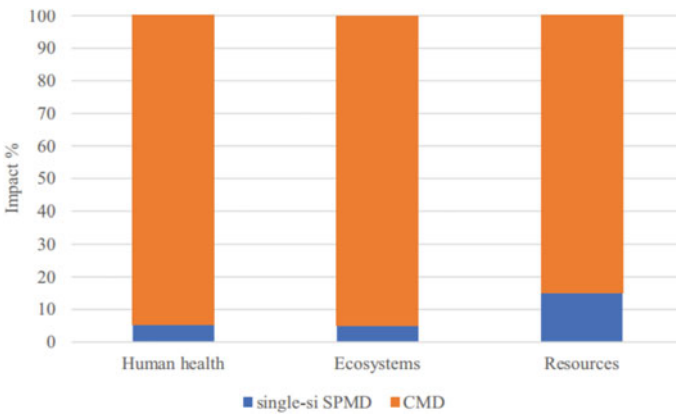


**Fig. 5** Affectability examination LCA discoveries for both SPMD single-Si and CMD and relating human well-being, environments and asset exhaustion endpoint sway classes as recovered from the product

circulation distance where many links and posts should be fabricated. Besides, energy request has shown that it impacts the climate more than 90% in by far most of the classes; in this way, it is fundamental for remember that to lessen the natural effects, energy interest just as the energy source should be considered [13].

### 3 Case Study: Geothermal

Geothermal water as a source of energy needed for the desalination process. Kalina cycle is concerned, an analysis was carried out that concentrated on using geothermal waters which have a temperature range of 80–95 °C when uprooted. The mass inflow rate of geothermal water directed to the power factory was assumed to be in the range from 10 to 150 kg/s. The mineral content of the geothermal water used in the model was 3 g/L. The density, mass flow rates of hot water directed towards evaporation and working fluid is calculated. The condensation temperature is espoused to be 25 °C. For ORC analysis dry & wet working fluids, such as R227ea, R600a etc. are selected, a superheating temperature of 3 °C is set and the calculations are done as per the assumptions and methodology. In case of Kalina cycle optimal range of ammonia contents are considered for different geothermal water temperatures. Turbine pressure range as 1500–3000 for optimal results [14].

#### 3.1 Case Study of Geothermal Energy in Poland

Poland has a significantly high potential of low-enthalpy geothermal waters and most of them are extracted in the central part of Poland (Polish Lowland) and the southern part of the country (Podhale Geothermal System). The research presented by [16], Tomaszewski [17] and Tomaszewska et al. [18] demonstrated that geothermal wastewater (cooled down in heat exchangers) could be purified using membrane. Processes and subsequently reused as potable water and after remineralization as water suitable for irrigation purposes. The best solution of treated water has been obtained for relatively low mineralized geothermal water exploited from the Podhale Geothermal Basin [19]. The geothermal waters with a temperature of 30 °C, contain total dissolved solids (TDS) as 2.6 g/L, boron as high as 9.0 mg/L, iron as 4.0 mg/L, arsenic as 0.03 mg/L, fluoride as 2.6 mg/L and silica as 43 mg/L. A schematic diagram of the desalination plant which has a capacity of 1 m<sup>3</sup>/h, is shown in Fig. 6. The preliminary treatment contained an iron removal system and two ultrafiltration (UF) membrane modules (UFC M5, X-Flow). Two steps of RO processes connected in series were equipped with spiral wound Dow FILMTEC BW30HR-440i polyamide thin-film composite membranes. The first step of RO had two filtration modules while the second step had one. The final treatment included remineralization and disinfection of the permeate (Fig. 6). During the pilot tests, no antipicants, biocides, or other chemicals were used. Before RO-1, the feed reaction was lowered to about 5.5 by dosing minuscule amounts of hydrochloric acid, which effectively prevented membrane scaling. The permeate pH at the exit of RO-1 was increased to 10–10.5 and directed to RO-2. The pressure of  $1.1 \pm 0.1$  MPa was used in both stages of RO.

The results of the pilot tests showed the electrical power consumption of the pumps in the UF pre-treatment process may be reduced to 5.9 kW due to the artesian pressure of the production wells [20]. The over pressure of the geothermal system during water

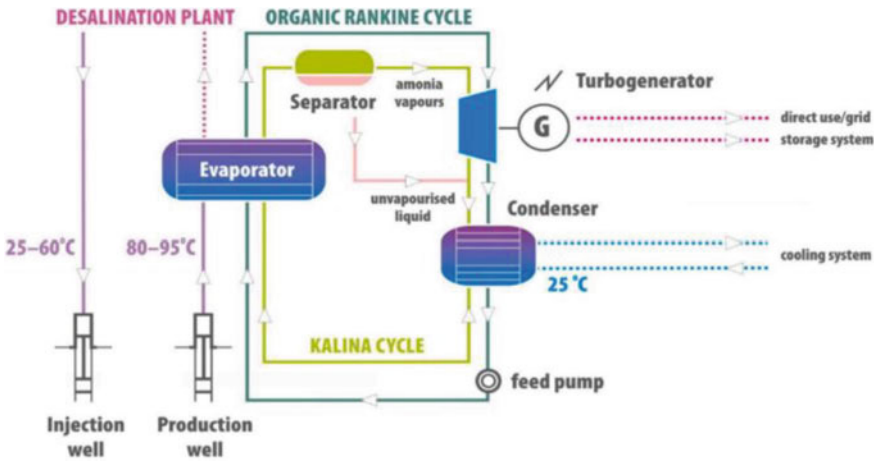
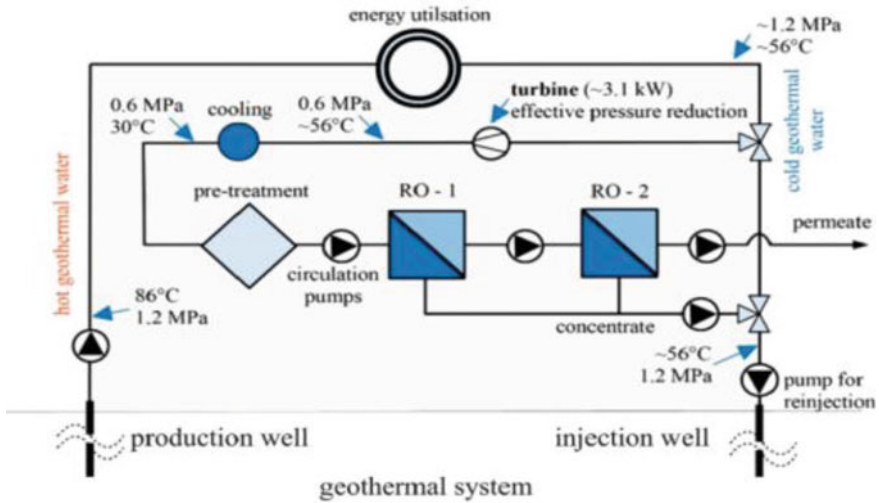


Fig. 6 Concept diagram of geothermal power plant integrated with desalination processes [15]

production from the boreholes was ca. 1.2 MPa and was additionally corrected by the use of a water turbine, located between the heat exchanger and the treatment station, which generated about 3 kW of energy (Fig. 7). The usage of reservoir artesian over pressure during the geothermal water desalination was the advantage of the system. Furthermore, low water mineralization and increased water temperature to 30 °C in the RO desalination led to a decrease in water viscosity. Generally, in the presented system, the net energy consumption of the water desalination per unit of freshwater produced was 1.40 kWh/m<sup>3</sup> [37]. An additional benefit can be achieved by using photovoltaic panels to supply the installation with electricity. Such activities are planned for the near future.

### 3.2 Difference Between Solar and Geothermal

(See Table 3).



**Fig. 7** The conception of geothermal water circulation and use (reproduced with permission from [36])

**Table 3** Difference between solar and geothermal [21]

	Solar	Geothermal
Availability	Ease availability of resources as of resources as sun is available all around the world [19]	Hard to find as it is limited to areas near tectonic flat boundaries [22]
Production	It is quite easy as you just need to install solar panels on the land or in your rooftop and given electricity [23]	It uses the Earth temperature that is near the surface or that can be used dry drilling miles into Earth [24]
Technology	In case of solar energy: (a) concentrated solar thermal (CST) [25] (b) Photovoltaics (PV) [26]	In case of geothermal energy: (a) Geothermal Power Plants [27] (b) Geothermal Heat Pumps [28, 29]
Cost	The cost range of solar energy depends on the type of panels and it is lesser compared to the cost of geothermal power plants [30]	Initial on for setting a geothermal power plant is more [31]
Environmental Impact	It is renewable and environmental friendly, some of the solar thermal system's not potentially dangerous fluids to transfer heat [32]	It is renewable and environmental friendly, it release hydrogen sulphide—a gas that smells like rotten eggs [33]
Efficiency	Less effective that geothermal power plants	More effective than solar power plants



## 4 Conclusion

Warm desalination advancements can assist with decreasing freshwater shortage, which influences two billion individuals around the world. In numerous nations in the Middle East locale, such innovations are the main wellspring of consumable water. Incorporating solar power with desalination plants might possibly decrease their energy-related impacts. Several suggestions can be made dependent on this review. We unequivocally suggest using LCA as a marker for ecological effects while picking between different sun-oriented desalination advancements, rather than taking a gander at explicit energy utilization, normal in desalination studies. Desalination utilizing an independent SPMD pilot plant with heat recuperation has been in activity since February 2006 in Aqaba, Jordan. The plant is taken care of with untreated regular seawater (without added substances) from the Red Sea and has a plan limit of 1000 l each day 1. The above framework can be improved on the off chance that various kinds of PV boards are utilized, as affirmed by the investigation of LCA. The CMD scored 100% in all effect classifications except for an unnatural weather change for multi-Si and single-Si PV types, while the SPMD scored 100% just in an Earth-wide temperature boost for the equivalent previously mentioned PV types. An affectability investigation was performed by changing the distance of the power dissemination network in the framework CMD from 1 to 5 km. According to the examination we realize that geothermal is more viable than sun oriented on the grounds that geothermal Energy gives clean energy supply to desalination plants and Geothermal Desalination addresses one of the arrangements of the Global Clean Water Desalination Alliance—"H<sub>2</sub>O short CO<sub>2</sub>". The benefit with geothermal source is that it can go about as a hotness source and a capacity vehicle for process energy use. Assuming these water sources have high broken-down solids, then, at that point, they can fill in as feed water for the desalination cycle. Since outside energy utilization is limited aside from the mechanical energy necessities, geothermal empowered desalination cycles could have less ecological effects when contrasted with other nonrenewable energy driven desalination processes. Co age plans for synchronous water and power creation are additionally conceivable with geothermal sources. Geothermal energy sources have a high limit factor which gives a steady and dependable hotness supply guaranteeing security of warm desalination and crossbreed desalination processes. Geothermal energy gives heat supply 24 h per day, 365 days per year, guaranteeing the dependability of the warm cycles of desalination. Average geothermal source temperatures are in the scope of 70–90 °C in many areas of the planet, which are great for low-temperature MED desalination. High-grade sources over 100 °C can be utilized for power age and other cycle heat applications. Geothermal desalination is savvy, and concurrent power and water creation is conceivable. Geothermal desalination is harmless to the ecosystem since it is the main environmentally friendly power utilized in the process without any outflows of air contamination and nursery gasses connected with petroleum derivatives. Involving the spent geothermal saline solution for rural exercises ought to be thought of. As an unexploited waste stream with high ionic substance, the spent geothermal brackish

water ought to be desalinated before use in the water system. High explicit energy utilization is the primary hindrance to the desalination cycle, however, if the legitimate innovation answer for being utilized (for example decreasing concentrate, applying a pyramidal plan of RO framework, blending RO pervade with well water at a specific proportion) may lessen the expense of sufficient water creation for water system. Further in the future, more geothermal warm sustainable power ought to be across the world and incorporate with better advances to stay away from the shortage of water.

## References

1. Organization, W.H.: Progress on Drinking Water, Sanitation and Hygiene: 2017 Update and SDG Baselines (2017)
2. Wada, Y., et al.: Human water consumption intensifies hydrological drought worldwide. *Environ. Res. Lett.* **8**(3), 034036 (2013)
3. Florke, M., Schneider, C., McDonald, R.I.: Water competition between cities and agriculture driven by climate change and urban growth. *Nat. Sustain.* **1**(1), 51–58 (2018)
4. Babel, M.S., Wahid, S.M.: Freshwater under threat South Asia: vulnerability assessment of freshwater resources to environmental change: Ganges Brahmaputra-Meghna River Basin, Helmand River Basin, Indus River Basin, UNEP (2009)
5. Haddeland, I., et al.: Global water resources affected by human interventions and climate change. *Proc. Natl. Acad. Sci.* **111**(9), 3251 (2014)
6. Padron, R.S., et al.: Observed changes in dry-season water availability attributed to human-induced climate change. *Nat. Geosci.* **13**(7), 477–481 (2020)
7. Yuan, X., et al.: Anthropogenic shift towards higher risk of flash drought over China. *Nat. Commun.* **10**(1), 4661 (2019)
8. <https://www.kent.co.in/blog/what-are-total-dissolved-solids-tds-how-to-reduce-them/>
9. <https://www.britannica.com/science/solar-energy>
10. <https://www.sciencedirect.com/topics/earth-and-planetary-sciences/geothermal-gradient>
11. Tomaszewska, B., Pająk, L., Bundschuh, J., Bujakowski, W.: Low-enthalpy geothermal energy as a source of energy and integrated freshwater production in inland areas
12. Banat, F., Jwaied, N., Rommel, M., Koschikowski, J., Wieghaus, M.: Performance evaluation of the ‘large SMADES’ autonomous desalination solar-driven membrane distillation plant in Aqaba, Jordan. *Desalination* **217**(1–3), 17–28 (2007)
13. Khayet, M., Matsuura, T.: *Membrane Distillation: Principles and Applications*. Elsevier, Amsterdam (2011)
14. Desalination via solar membrane distillation and conventional membrane distillation: Life cycle assessment case study in Jordan Abdelfattah Siefan, Eilin Rachid, Nadeen Elashwah, Faisal AlMarzooqi, Fawzi Banat, Riaan van der Merwe
15. Tarnacki, K., Meneses, M., Melin, T., van Medevoort, J., Jansen, A.: Environmental assessment of desalination processes: reverse osmosis and Memstill®. *Desalination* **296**, 69–80 (2012). <https://doi.org/10.1016/j.desal.2012.04.009>
16. Gorecki, W., Sowizd'zał, A., Hajto, M., Wachowicz-Pyzied, A.: Atlases of geothermal waters and energy resources in Poland. *Environ. Earth Sci.* **74**, 7487–7495 (2015)
17. Utilization of renewable energy sources in desalination of geothermal water for Barbara Tomaszewska, Gulden Gokcen Akkurt, Michał Kaczmarczyk, Wiesław
18. Tomaszewska, B.: New approach to the utilisation of concentrates obtained during geothermal water desalination. *Desalin. Water Treat.* **128**, 407–413 (2018)

19. Tomaszewska, B., Pająk, L., Bundschuh, J., Bujakowski, W.: Low-enthalpy geothermal energy as a source of energy and integrated freshwater production in inland areas: technological and economic feasibility. *Desalination* **435**, 35–44 (2018)
20. Bujakowski, W., Tomaszewska, B., Miecznik, M.: The Podhale geothermal reservoir simulation for long-term sustainable production. *Renew. Energy* **99**, 420–430 (2016)
21. Tomaszewska, B., Akkurt, G.G.A., Kaczmarczyk, M., Bujakowski, W., Keles, N., Jarma, Y.A., Baba, A., Bryjak, M., Kabay, N.: Utilization of renewable energy sources in desalination of geothermal water for agriculture. *Desalination* **513**, 115151 (2021)
22. Bujakowski, W., Tomaszewska, B.: Atlas wykorzystania wód termalnych do skojarzonej produkcji energii elektrycznej i cieplnej przy zastosowaniu układów binarnych w Polsce 2014, Instytut Gospodarki Surowcami Mineralnymi i Energią Polskiej Akademii Nauk, Krakow (2014)
23. Tomaszewska, B., Bodzek, M.: Desalination of geothermal waters using a hybrid UF-RO process. Part I. Boron removal in pilot-scale tests. *Desalination* **319**, 99–106 (2013)
24. <https://www.need.org/Files/curriculum/guides/EnergyfromtheSunStudentGuide.pdf>
25. <https://www.power-technology.com/features/what-is-geothermal-energy/>
26. <https://www.sciencedirect.com/science/article/abs/pii/S1364032110004533>
27. <https://www.thinkgeoenergy.com/thinkgeoenergys-top-10-geothermal-countries-2021-installed-power-generation-capacity-mwe/>
28. <https://www.sciencedirect.com/book/9780081005163/advances-in-concentrating-solar-thermal-research-and-technology>
29. <https://www.irena.org/publications/2019/Nov/Future-of-Solar-Photovoltaic>
30. <https://www.statista.com/statistics/525206/geothermal-complexes-worldwide-by-size/>
31. <https://www.geothermal-energy.org/pdf/IGAstandard/WGC/2020/01018.pdf>
32. [https://www.researchgate.net/publication/288938651\\_The\\_advance\\_of\\_geothermal\\_heat\\_pumps\\_world-wide](https://www.researchgate.net/publication/288938651_The_advance_of_geothermal_heat_pumps_world-wide)
33. [https://www.eai.in/ref/ae/sol/cs/sup/if/key\\_factors\\_to\\_consider\\_while\\_setting\\_up\\_a\\_solar\\_plant.html](https://www.eai.in/ref/ae/sol/cs/sup/if/key_factors_to_consider_while_setting_up_a_solar_plant.html)
34. <https://doi.org/10.1186/s40517-017-0074-z>
35. <https://kubyenergy.ca/blog/the-positive-and-negative-environmental-impacts-of-solar-panels>
36. <https://www.britannica.com/science/geothermal-energy/Environmental-effects-and-economic-costs>
37. <https://alternativeenergysourcesv.com/>

# The Impact of Market-Based Policies on Access to Electricity and Sustainable Development in Sub-Saharan Africa



Pitshou Ntambu Bokoro  and Kyandoghere Kyamakya 

**Abstract** The huge attention currently afforded to renewable energy-based decentralised energy systems, as means for accelerating rural electrification and hence development, has triggered massive consideration and interest given the cost involved in extending existing grids to rural communities of Sub-Saharan Africa (SSA). In most of these communities, access to electricity is essentially restricted to basic domestic utilisation or needs such as: lighting, cooking and storage purposes. Although, small-scale farming consists of the main occupation in rural communities of SSA, it remains less developed and does not take advantage of available renewable energy resources susceptible to promote its expansion and development. However, the potential in renewable energy resources (solar PV, wind, etc.) in SSA countries could be counted as important attribute for the enablement of access to electricity. As a direct consequence of this, sustainable agricultural development may be achieved in order to ensure food security and to prevent urban migration by promoting employment opportunities and poverty alleviation in rural communities of SSA countries as dictated by the United Nations (UN) sustainable development goals (SDGs). Despite the promotion of access to clean electricity being advocated in the literature as the stepping-stone for sustainable development and growth, the gap remains the choice of suitable policy option susceptible to balance access to electricity with sustainable development in rural communities of SSA. In this work, the six-step policy analysis is applied to probe the effectiveness of market-based policies in enhancing access to electricity and agricultural development in rural communities of selected SSA countries. Results show that despite the shortcomings in the implementation of

---

P. N. Bokoro (✉)

Department of Electrical Engineering Technology, University of Johannesburg, Doornfontein Campus, Johannesburg, South Africa

e-mail: [pitshoub@uj.ac.za](mailto:pitshoub@uj.ac.za)

URL: <http://www.uj.ac.za>

K. Kyamakya

Institute of Smart Systems Technologies, Alpen-Adria University Klagenfurt, Klagenfurt, Austria

e-mail: [kyandoghere.kyamakya@aau.at](mailto:kyandoghere.kyamakya@aau.at); [kyandoghere.kyamakya@gmail.com](mailto:kyandoghere.kyamakya@gmail.com)

URL: <http://www.uni-klu.ac.at>

Faculté Polytechnique, Université de Kinshasa, Kinshasa, République Démocratique du Congo

© The Author(s), under exclusive license to Springer Nature Switzerland AG 2024

343

K. Kyamakya and P. N. Bokoro (eds.), *Recent Advances in Energy Systems, Power*

*and Related Smart Technologies*, Studies in Systems, Decision and Control 472,

[https://doi.org/10.1007/978-3-031-29586-7\\_13](https://doi.org/10.1007/978-3-031-29586-7_13)

this policy in many SSA countries, this policy approach proves to be favorable to increased share of renewable energies, which translates into increased electrification of the agriculture sector.

**Keywords** Access to electricity · Rural communities · Policy options · Six-step policy analysis · Agricultural production · Renewable energy systems · Sustainable development goals

## 1 Introduction

The persistent threats of global warming and climate change have imposed on world governments the need for developing policy options, which aimed at reducing or curbing emissions of greenhouse gases (GHGs) [1, 2]. This has sparked the quest for new opportunities and ultimately ushered the world in energy transition. This implies partial or complete substitution of fossil fuel-based energy sources by clean or low-carbon energy systems in order to mitigate the devastating effects of global warming: flooding, rising sea levels, worsening droughts, melting glaciers, increasing tornados among others [3, 4]. Available sunlight, wind, biomass, water flow and others consist of important alternatives or renewable resources capable of providing clean energy to nations and to the human race [5]. Recent price reduction in the production of photovoltaic (PV) modules has favoured massive investments in the development of solar-based off-grid electricity systems in a bid to improve access to electricity in rural communities of SSA countries [6]. This approach is evaluated to be cost-effective given the cost implications related to extending electricity grids near such communities. Access to electricity in rural communities of SSA countries should be compensated by economic development and job creation in such areas, which should culminate into GDP growth and improved crop production index such as advocated by the UN SDGs. In most of the SSA countries, the achievement of UN SDGs requires development or formulation of innovative policy options in order to sustain investments in off-grid electricity systems, which are key to rural development. In most of these rural communities, small-scale farming consists of the main activity focussed on the subsistence of community dwellers [6, 7]. However, the currently formulated and implemented policies related to investments in clean electricity access in rural communities of many SSA countries are not necessarily favourable to the transformation of subsistence-based or small-scale farming into large-scale commercial farming entities or agricultural holdings, which could ensure mass production of agricultural crops for food industry sustainability. This is necessary for economic opportunities and rural development in SSA countries. In this work, the six-step policy analysis framework (problem definition, determination of evaluation criteria, identification of alternatives, evaluation of alternatives, comparison of alternatives and assessment of outcomes) is applied in order to probe the effectiveness of market-based policies (liberalisation, privatisation, unbundling, etc.) on the enhancement of access to electricity and development rural in the following regions of SSA: West-

ern, Eastern, Central and Southern. In this context, it should be noted that most SSA countries have experienced monopoly of state-owned electricity supply companies (vertically-integrated or nationalisation) prior to embracing market-based policies. Statistical data from selected countries of these regions are used for the purpose of this work. This work shows that market-based policies are consistent with increased share in renewables and electricity consumption in agriculture.

## 2 Current Status of Electricity Access in Sub-Saharan Africa

Sub-Saharan countries are reported to have the lowest rate of electricity access in the world. According to the International Energy Access (IEA) [7], about 600 million people living in SSA countries do not have access to electricity. The World Bank and the International Monetary Fund (IMF) [8, 9] report that thirteen of the Sub-Saharan countries have <25% access to electricity as compared to only one in Asian countries. Low-access to electricity in SSA countries, such as reported in 2018 by the International Monetary Funds (IMF), is estimated to be 2.8% as opposed to 7.1% in South Asian countries [10]. Despite available natural energy resources and reasonable economic potentials in this region, challenges resulting from poor electricity access are fundamentally responsible for a relatively slow pace of economic growth and lack of sustainable development. Furthermore, this is exacerbated by projections of rapid population growth expected in this region of the African continent. Therefore, according to the UN Department of Economic and Social Affairs (DESA) [11], the current one billion of people living in this African region is expected to double by year 2050, while under the current energy policies, the IEA outlook [12] reports that the total number of people, having no access to electricity, is expected to reach nearly 90% of the global population by 2030. The population growth estimates and access to electricity is indicated in Table 1. It is quite evident that the current installed electricity grid capacity is unable to cope with the continuously increased demand in both urban and rural areas. The investment cost implications, resulting from electricity demand

**Table 1** Electricity access in 2019, Population growth between 2019 and 2050 in Sub-Saharan African regions and GDP per region [12]

Region	Population growth	Total access	Urban	Rural	Total GDP per region
Central	119	31.5	44	6	306.221
Eastern	95.5	48.2	79	35	240.00
Southern	70.5	83.5	67	20	687.00
Western	102	44.6	87	28	724.983
–	%	%	%	%	Billion U.S dollar

projections versus grid capacity in the various sub-regions of SSA (Western, Eastern, Central and Southern Africa), is discussed in Sect. 2.1.

## 2.1 Demand Projections, Installed Grid Capacity and Investment Cost Implications per Sub-region

### 2.1.1 Western Africa

According to the International Renewable Energy Agency (IRENA) [13], the electricity demand projections in Western Africa is expected to rise from 50 TWh in 2010 to 250 TWh in 2030. Urban demand is expected to drop by 48% while an increase of 7% will be expected for rural communities. The electricity demand projections in this sub-region are shown in Fig. 1. However, an additional installed capacity of 60 GW will be required by 2030 in a bid to catch up with the rise in electricity demand in this sub-region. It is expected that Nigeria and Ghana, which both contribute 70% of the region's electricity, will continue to be the largest electricity producers in this region. Given the promotion of renewable sources, it is envisaged that solar PV would be one of the largest contributors of electricity supply by 2030. Data related to annual GDP and Population count for selected Western African states, whose GDPs constitute 83.71 % of the total GDP in this region, are used. This is given in Table 2.

The grid capacity per resource used, such as expected in the next decade, is depicted in Fig. 2.

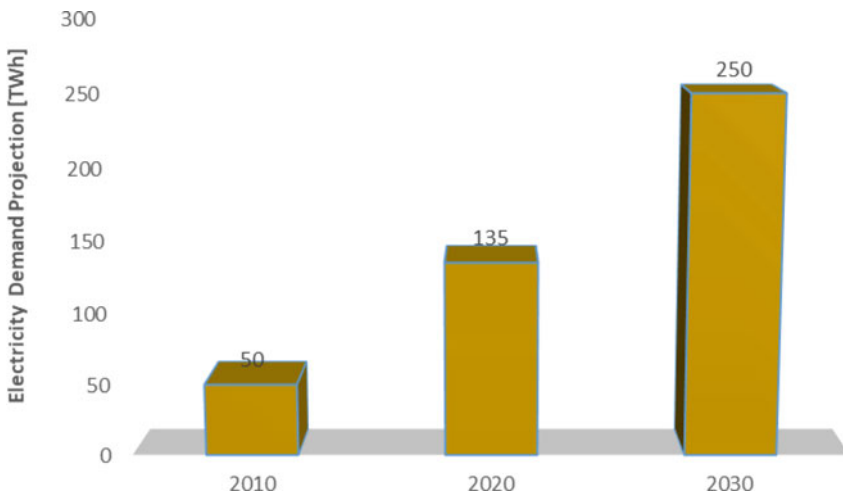
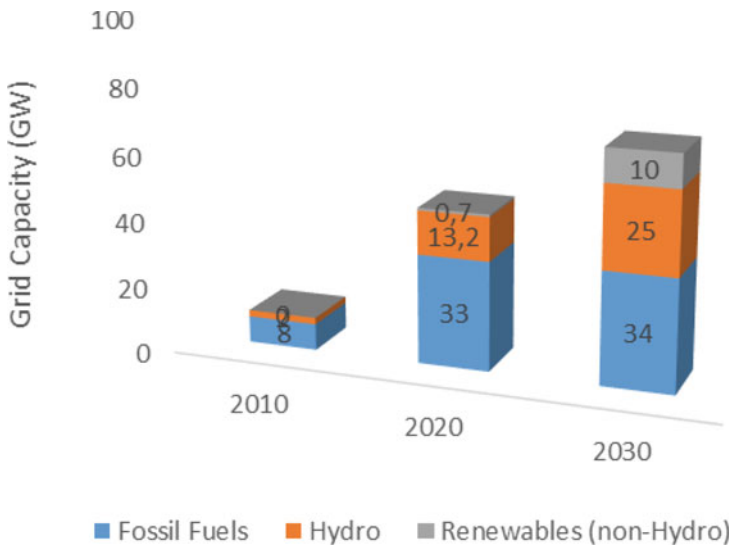


Fig. 1 Electricity demand projections in Western Africa [13]

**Table 2** Annual GDP and population count for selected Western African states

States	Annual GDP	Population count
Nigeria	448.120	200.963599
Ghana	66.984	30.417856
Cote d’Ivoire	61.35	26.38000
Senegal	23.579	16.296364
Sierra Leone	3.865	7.977000
Liberia	2.95	5.058000
–	Billion US dollar	Million



**Fig. 2** Grid capacity per resource used—Western Africa [13]

**2.1.2 Eastern Africa**

Electricity demand projections in the Eastern African region is expected to rise from 150 TWh in 2010 to 500 TWh in 2030 [13, 14]. Urban and rural demands in electricity will be expected to rise by 39 and 17% respectively. The projected electricity demand in this part of the Sub-Saharan Africa is indicated in Fig. 4. Data related to annual GDP and population count for selected Eastern African states, whose GDPs constitute 98.9 % of the total GDP in this region, are used. This is given in Table 3. The promotion of renewable sources, which is meant to boost grid capacity in this region, will require a total investment cost of 170 billion US dollar over the 2010–2030 period. The annualised system costs over the above-mentioned time-period is indicated in Fig. 3. According to studies conducted in [15], the Eastern African electricity grid requires additional capacity of 170 GW between 2010 and 2030 in order to meet



**Table 3** Annual GDP and population count for selected Eastern African states

States	Annual GDP	Population count
Kenya	98.607	53.771296
Ethiopia	91.166	114.963588
Uganda	30.666	45.741007
Rwanda	10.209	12.952218
Burundi	3.573	11.890784
Djibouti	3.166	988.000
–	Billion US dollar	Million

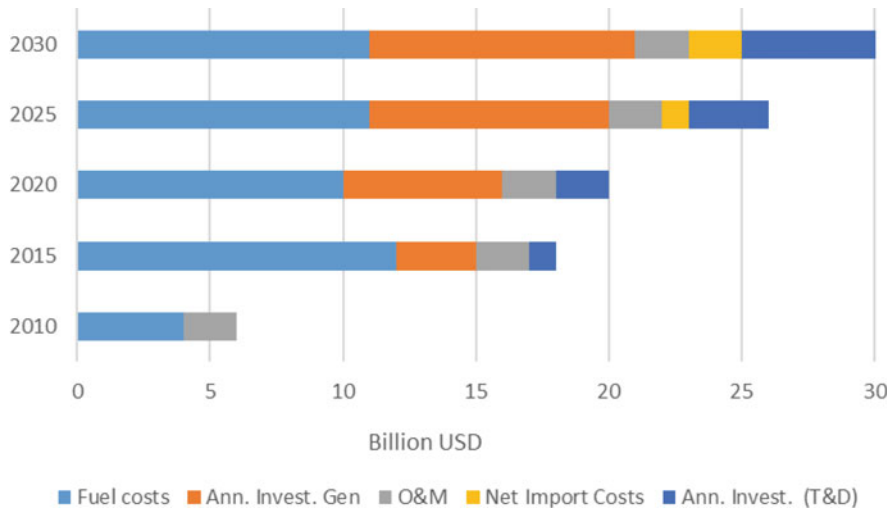


**Fig. 3** Annualised system costs of renewable sources—Western Africa [13]

increasing demand in this region. Given the highest PV potential per-square-metres basis, solar PV is expected to contribute 8 GW of expected installed capacity in 2030 [15, 16]. The grid capacity per resource used between 2010 and 2030 is given in Fig. 5. Despite Ethiopia being the major power house in this region, significant contribution from solar PV to the generation capacity is to be expected in Burundi, Djibouti and Rwanda. However, this will be dependent on the effectiveness of policies governing renewable energies in these countries. The cost of investment related to increased grid capacity in this region between 2010 and 2030 is estimated to 400 billion US dollar. The annualised system costs over the above-mentioned time-period is indicated in Fig. 6.

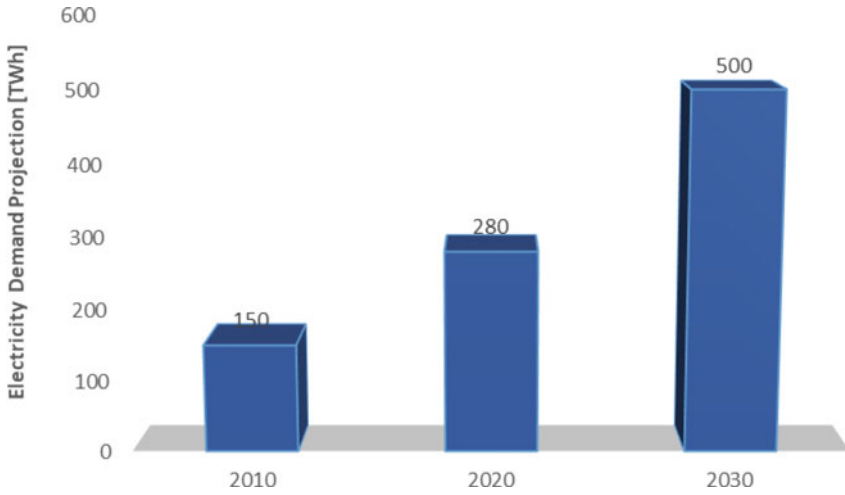


Fig. 4 Electricity demand projections in Eastern Africa [13, 14]

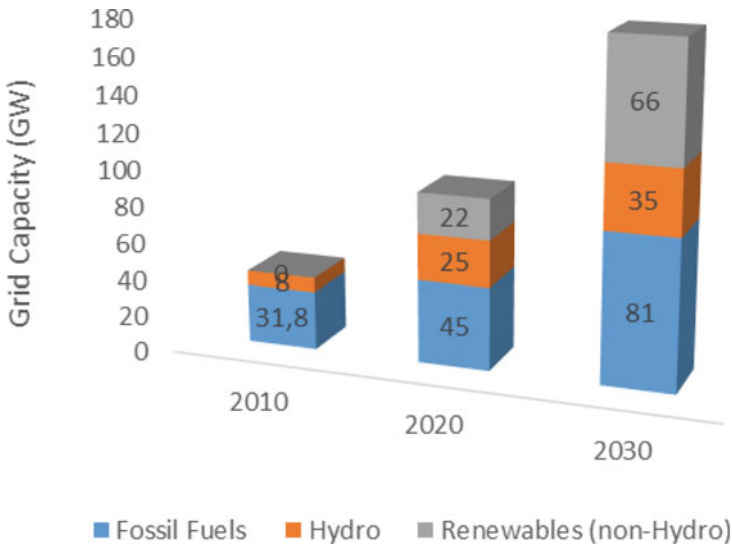


Fig. 5 Grid capacity per resource—Eastern Africa [15, 16]

### 2.1.3 Central Africa

Electricity projections in this region are expected to grow from 20 to 90 TWh in 2030 [13, 17, 18]. Urban consumers are expected to claim 57% share of electricity demand, while rural communities of Central Africa will require only 4% of electricity demand in 2030. The projections of electricity demand in this region such as expected

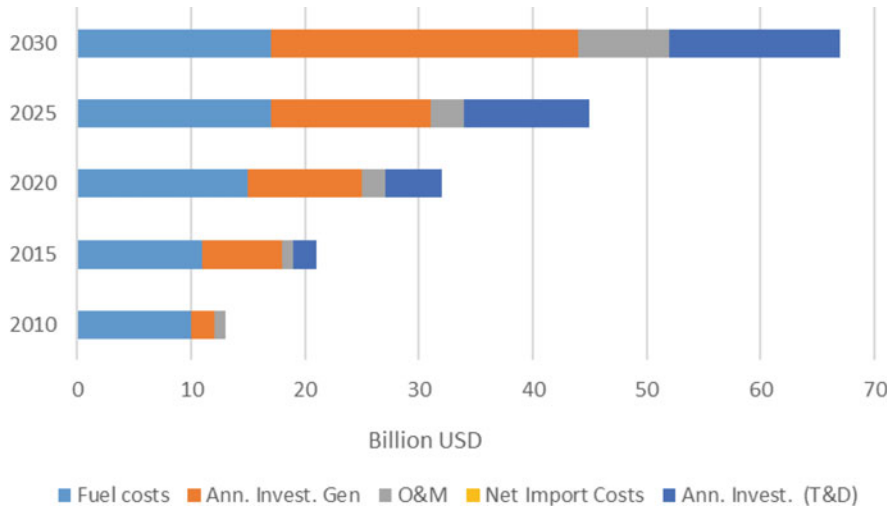


Fig. 6 Annualised system costs of renewable sources—Eastern Africa [13, 16]

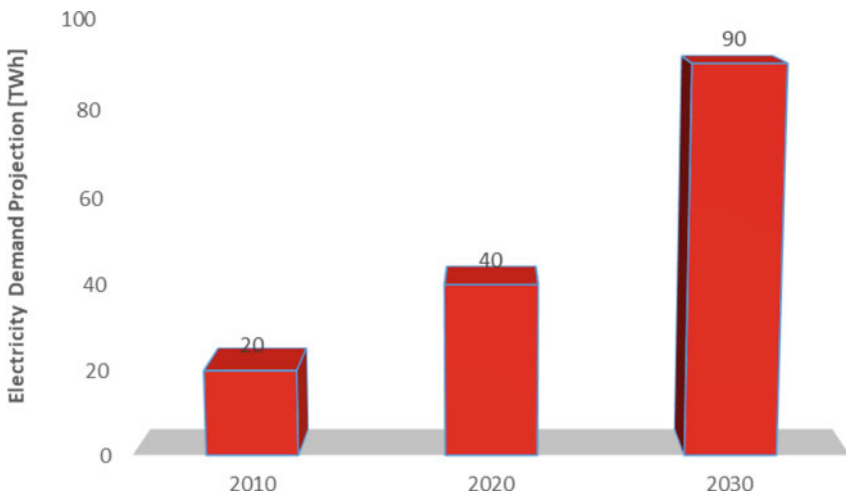
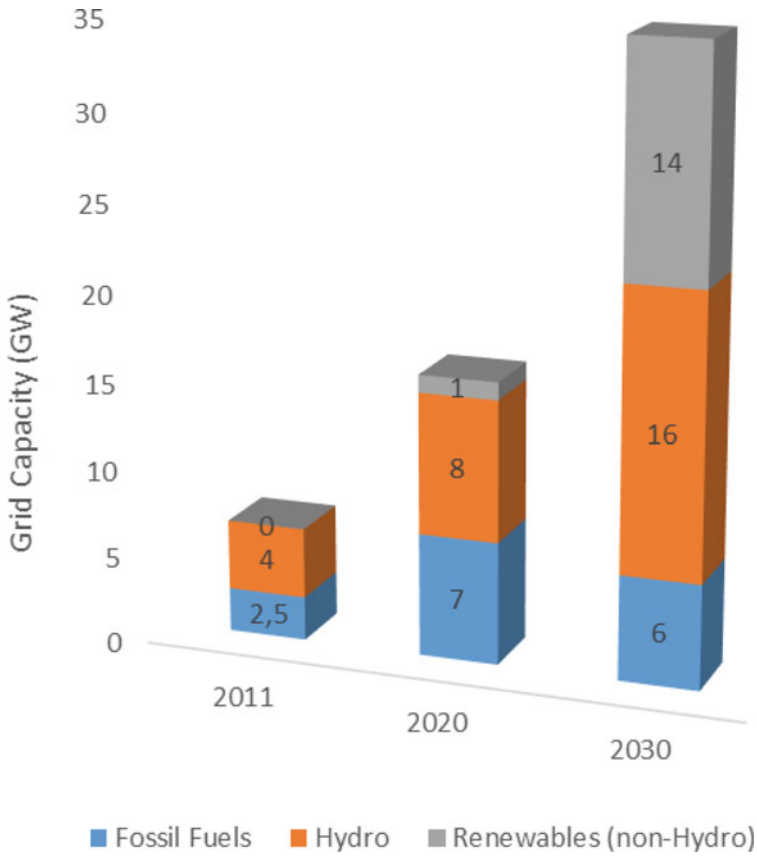


Fig. 7 Electricity demand projections in Central Africa [13, 17]

in 2030 are given in Fig. 7. This region of Sub-Saharan Africa is reported to have the lowest electrification rate [18, 19], with 75% of generation capacity being produced from incredible hydro-power resources in the region. The largest share of electricity production (about 80%) is obtained from the following power houses: Angola, DRC and Cameroon. In a bid to meet growing demand, additional grid capacity of 36 GW is expected in 2030. Although most of generated electricity is to be produced using hydropower, solar PV is estimated to contribute more than 8 GW of the generation mix between 2011 and 2030. The largest generation share of solar PV in this region



**Fig. 8** Grid capacity per resource—Central Africa [17, 18]

is expected to be in Angola. The expected growth in grid capacity per resource is shown in Fig. 8. Data related to annual GDP and population count for selected Central African states, whose GDPs constitute 63.00% of the total GDP of the region, are used. This is given in Table 4.

The total investment cost of increasing grid capacity in this part of the continent is estimated to be at least 60 billion US dollar. The annualised system cost is indicated in Fig. 9.

### 2.1.4 Southern Africa

Electricity demand in this region of the African continent is expected to double from 280 to 570 TWh in year 2030 [13, 20, 21]. The demand in urban and rural areas is expected to grow to 38 and 4% respectively. Despite coal and hydro-power being the

**Table 4** Annual GDP and population count for selected Central African states

States	Annual GDP	Population count
Angola	91.527	32.866272
DRC	48.994	89.561403
Cameroon	38.632	26.545863
Chad	11.026	16.425864
CAR	2.321	4.829767
Sao Tome & Principe	0.430	219.159
–	Billion US dollar	Million

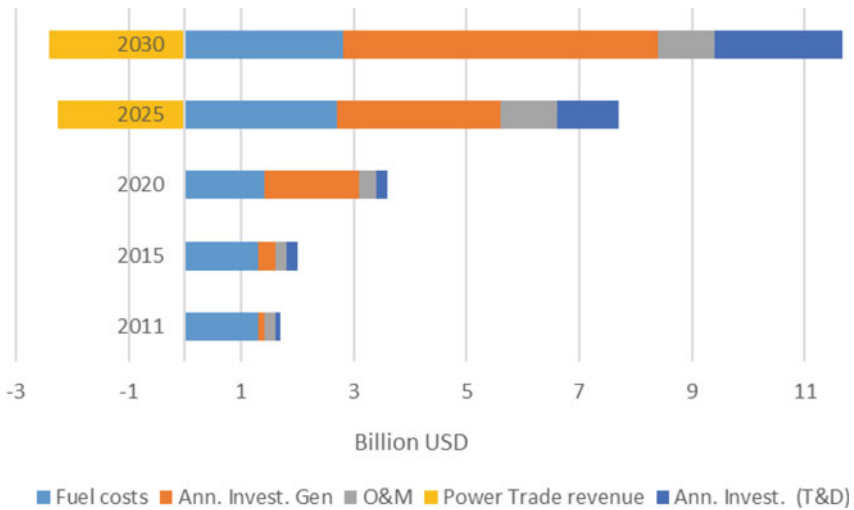


**Fig. 9** Annualised system costs of renewable sources—Central Africa [17, 18]

dominant resources for electricity generation, this region enjoys the best opportunities for solar PV as opposed to the rest of the continent [13]. Accordingly, the promotion of renewable energies, particularly solar PV, is such that its contribution to electricity generation is expected to rise from 12 to 46% in 2030. The projections in electricity demand in the southern African region is indicated in Fig. 10. For the purposes of coping with electricity demand in this region, additional grid capacity of about 110 GW will be required by 2030 [13, 21]. About 40 GW of PV solar options are estimated to feature in the required additional grid capacity by 2030. The forecasted grid capacity per resource exploited is given in Fig. 11. Data related to annual GDP and population count for selected Southern African, whose GDPs constitute 59.89 % of the total GDP of the region, are used. This is given in Table 5. The projected investment cost required for increasing grid capacity in the southern part of the continent is estimated to be at least 270 billion US dollar. The annualised system cost is indicated in Fig. 12. Therefore, the expected rise in electricity demand seems to

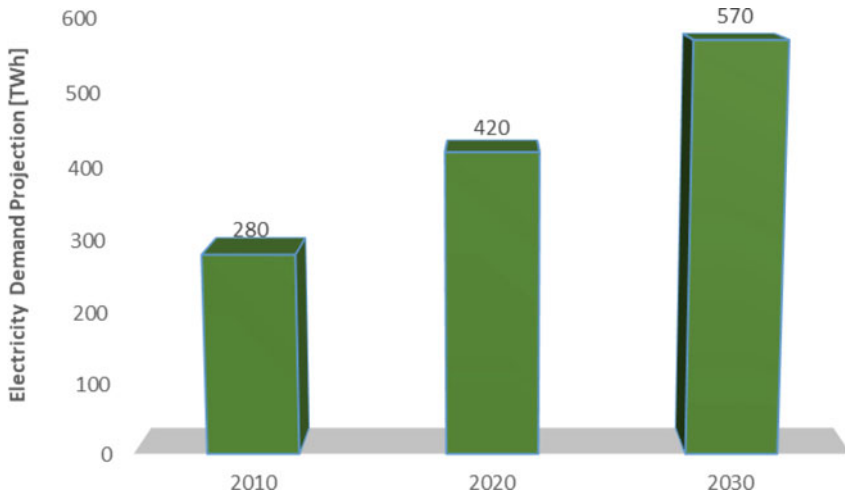


**Fig. 10** Electricity demand projections in Southern Africa [13, 20]

be inherent to population growth and the need for industrialisation. Owing to global warming and climate change, low-carbon decentralised energy systems consist of viable option for increasing supply capacity and thus improving electricity access for sustainable development. The selected countries used in this work represent 69.61% of the total population and 55.44% of the total GDP of SSA countries.

### 3 Agricultural Expansion: Food Security and Suppression of Undernourishment in SSA

SSA is reported to have high prevalence of poverty, hunger and undernourishment in the world [22, 23]. These concerning facts provide enough grounds for the deployment of policies and strategies that seek to promote food security in this part of the globe. Agricultural expansion has proven to be consistent with food security and economic growth in politically stable nations with appropriate governance systems [24]. According to the Comprehensive African Agricultural Development Programme (CAADP) report [25], the agricultural sector contributes 15% of the total GDP. In rural communities of the Sub-Saharan Africa, small-scale farms consist of approximately 80% of agricultural activity and provide employment to about 175 million people [26, 27]. Therefore, expanding the agricultural sector could actually ensure attainment of food security, employment opportunities and economic growth, which are consistent to the UN sustainable development goals.

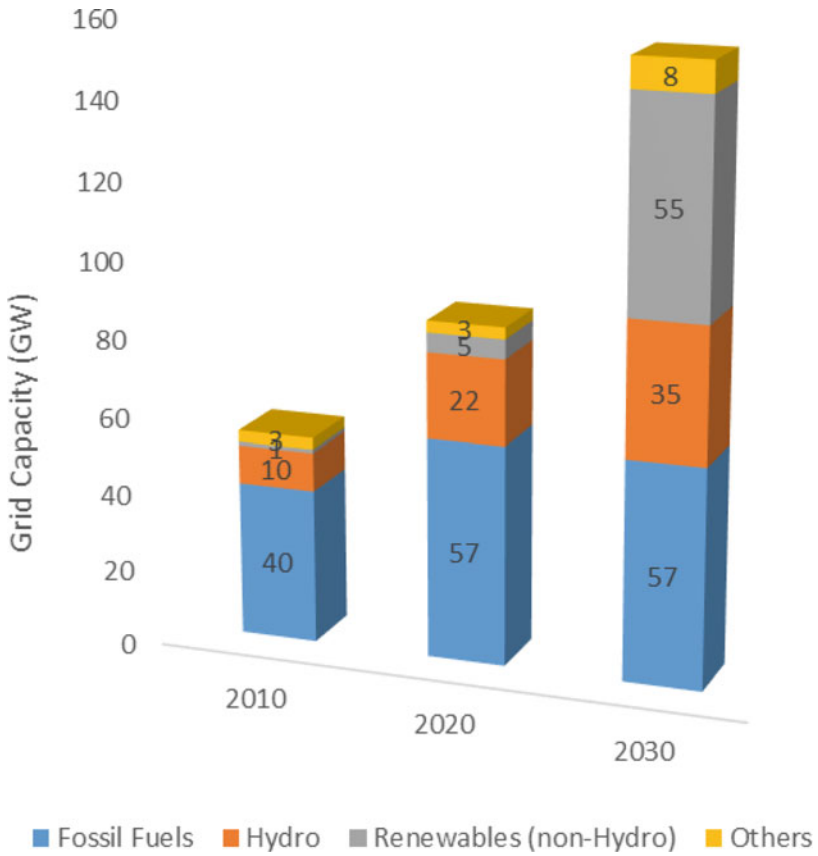


**Fig. 11** Grid capacity per resource—Southern Africa [20, 21]

**Table 5** Annual GDP and population count for selected Southern African states

States	Annual GDP	Population count
South Africa	351.4	59.308690
Zambia	23.31	18.383955
Botswana	18.36	2.351627
Namibia	12.57	1.160164
Eswatini	3.962	1.148000
Lesotho	1.845	2.142000
–	Billion US dollar	Million

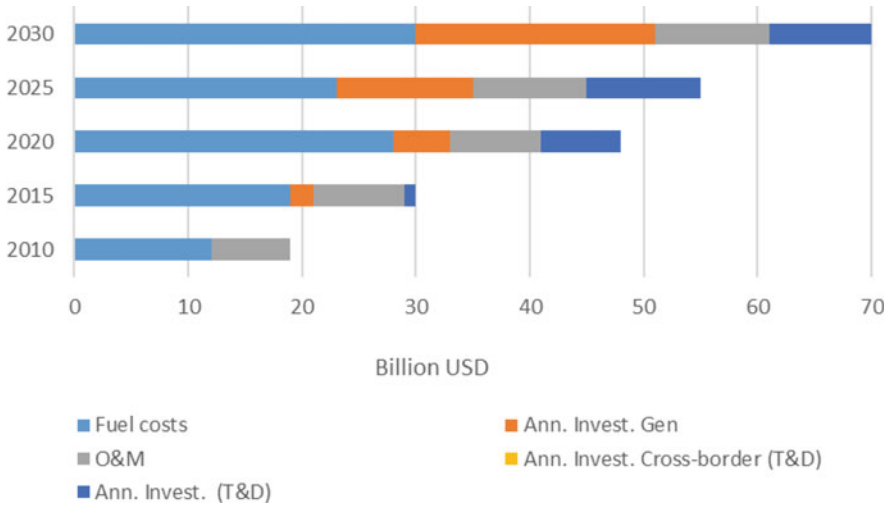


Fig. 12 Annualised system costs of renewable sources—Southern Africa [13, 21]

### 3.1 The United Nations’ Sustainable Development Goals

Building on the achievements of the Millennium Development Goals (MDGs), all UN member states—emerging from the 2012 Rio de Janeiro UN Conference on Sustainable Development—have committed to working together towards the end of poverty and hunger, to protect the planet against the threats of climate change, and to promote peace and security in the world. This initiative has culminated into the elaboration of seventeen integrated SDGs. Among these goals, an established synergy between goal number 7 and 2 could be an important factor for rural development in SSA. The targets to be achieved in 2030 as well as the global framework indicators for each of these two goals are as follows [28, 29].

**Goal 7:** Access to affordable and clean energy

For the purpose of this work, the following targets have been assigned to this goal:

1. Ensure universal access to clean energy;
2. Increase the share of renewable energy in the global energy mix.

The global framework indicators for this goal, such as applicable in this work, are as follows:

1. Proportion of population with access to electricity;
2. Renewable energy share in the total final energy consumption.

**Goal 2:** End hunger, achieve food security and promote sustainable agriculture

In this work, the following targets have been assigned to this goal:



1. Ensure access by all people to safe, nutritious and sufficient food all year long;
2. End all kinds of malnutrition, and address the nutritional needs of adolescent girls, pregnant and lactating women and older persons;

The global framework indicators for this goal, such as reviewed in this work, are as follows:

1. Prevalence of moderate or severe food insecurity in the population, based on the Food Insecurity Experience Scale (FIES).

### ***3.2 Electricity Poverty: Major Barriers to Agricultural Production and Rural Development***

The continued underperformance of agricultural production in SSA countries has been reported to be one of the major causes of food insecurity and prevalence of undernourishment in this region of the world [30, 31]. Various challenges have been identified as significant contributing factors to low agricultural production: electricity poverty, inadequate infrastructure, policy options, political instability as well as inability to attract funding or the necessary capital investments from international financial institutions [34]. The unavailability of an electricity grid in rural areas denies agricultural sector of an opportunity to employ motive power for water pumps, fodder choppers, threshers, grinders and dryers. In addition, no possibility to extend cultivable land through irrigation systems can be envisaged without access to electricity. Blimpo and Cosgrove-Davies [35] provided an evidence-based account on electricity demand for the enhancement of rural economics in predominantly agricultural villages of Senegal in Western Africa. This study shows that financial synergy is required for grid extension investment cost to enable access to electricity. The latter is essential for driving water-pumps, which permit irrigation during dry or off-seasons, and therefore ensuring continued production and revenue to be generated. Winklmaier et al. [36] proposed the concept of decentralised energy-water-food system as a solution for the development of rural communities of SSA. Therefore, the benefits of renewable resources could be used for electricity access, which in turn, could ensure access to clean water and irrigation all year-round, and thus increasing farming productivity and employment opportunities. According to Chaurey et al. [37], rural poverty strongly correlates with access to electricity given the impact of electricity on production. Kyriakarakos et al. [38] conducted a case-study in Rwanda on the financing of rural electrification. This investigation proposes that the high cost of rural electrification could be achieved through increased values of locally produced crops. In accordance with the targets assigned to SDG 7, fossil fuel energy should be abandoned or done away with in order to embrace clean technologies and energy-efficiency systems. Therefore, the need for sustainable agricultural production and rural economic development can be addressed by promoting access to affordable low-carbon and renewable energy technologies (grid-connected and/or off-grid solutions). However, the promotion of access to affordable

and clean electricity in rural communities of SSA cannot be achieved unless national governments and/or regional bodies embark into the development of effective policies capable of: mobilising necessary fundings or capital investments from either within or international funding organisations; ensuring adequate allocation of financial resources by prioritising eradication of electricity poverty for enhancement of economical development in rural communities; providing incentives to investment cost related to infrastructure planning and development of low-carbon or renewable energy projects; promoting interstate electricity exchanges (import and export) and development of regulatory frameworks to support regional electricity markets.

## **4 Policy Options for Improving Access to Electricity**

### ***4.1 Review of Regional Strategies***

For the last few decades, the development of policy options, related to electricity access in SSA nations, have fundamentally focussed on improving supply capacity (sustainable generation capacity) in a bid to meet the rising electricity demand, and thereby aligning key national or regional development objectives to the UN SDGs [39, 40]. In this respect, policy options, such as implemented in various countries of SSA, have been interrogated.

Karaki [41] conducted an assessment of energy policy of the Economic Community of West African States (ECOWAS) from the inception of this regional body back in 1975 until 2012. This author argued that the ideal of regional energy autonomy, which featured among the fundamental objectives of ECOWAS member states since the founding treaty, has led to the establishment of: the West African Power Pool (WAPP)—a regulatory authority—and the ECOWAS Energy Protocol in 2003 as well as the ECOWAS Centre for Renewable Energy and Energy Efficiency (ECREEE) in 2010. Following the adoption of the master plan for the generation and transmission of electrical energy, and the launch of the ECOWAS renewable energy facility (EREF) in 2011, the adoption of both the ECOWAS renewable energy policy (EREP) and energy efficiency policy (EEEP) came to effect in 2012. According to the ECREEE [42], the EREP proposed a comprehensive action plan aimed at enabling increased share of the ECOWAS member states' electricity supply and services from timely, reliable, sufficient, cost-effective uses of renewable energy sources (decentralised mini-grid systems, grid-connected renewable energy, etc..). The implementation strategies of the EREP include among others: the elaboration of the guiding principles, a legal and institutional framework, development of national renewable energy policy (NREP) with an associated implementation strategy and a five year rolling action plan, the making of renewable energy power production an attractive business for private investors/entrepreneurs, capacity development, financial intermediation, awareness and knowledge management, timeframe for policy implementation and progress monitoring. On the other end, the EEEP is meant to

complement the various other ECOWAS policies by promoting efficient use of the West African region's energy resources. Reiss [43] proposed the development of renewable energy sectors and technologies in West African countries arising from a dilemma in policy formulation due to the increasingly urgent need to mitigate GHG emissions while promoting regionally appropriate measures aimed at achieving sustainable development objectives. Peterson and Sampa [44] evaluated the impact of the African Continental Free Trade Area agreement (AfCFTA) on the intra-African energy investments and projects. The authors concluded that while the AfCFTA may lead to cheaper cost of energy and potentially change the continent, its continental success should overcome the risk of investing without in-built investor protections. Lam [45] examined the problematic issue of private investment in power transmission infrastructure in West African countries, and proposed investment models in the context of cross-borders electricity exchanges. This study argued that owing to state ownership being the traditional source of finances for interconnection projects, fiscal constraints in most regional governments consist of the major implementation barrier to these infrastructure projects. Therefore, private or merchant capital investment (privatisation), yet to be formally adopted as policy in SSA, could be of great benefit to these projects. Bungane [46] reported on recent financial support from the World Bank International Development Association (IDA) to the West Africa Regional Energy Trade Development Policy Financing Programme (West Africa Energy DPF). This financial support is intended to remove barriers to cross-country electricity trade, which is expected to lower cost of electricity for consumers, to enable competitiveness and to improve resilience and reliability of supply. Hafner et al. [47] developed a detailed account of each of the East African nations' renewable energy policy frameworks, which are aimed at: establishing institutional and legal framework to expand and develop renewable technologies; promoting public-private partnership (PPP); achieving universal access to energy in the respective countries. Kammen et al. [48] reviewed the energy planning such as elaborated by the East African Power Pool (EAPP)—created in 2005 and institutionalised as a specialised electric power body of the Common Market for Eastern and Southern Africa (COMESA) in 2006—in line with the green-growth model. This study argued that the EAPP Master Plan fall short of providing detailed plans for energy poverty alleviation in rural communities of East African countries (EAC). The approval of the regional policy initiative, which promotes cross-border electrification programme, was aimed at scaling up or improving access to energy in this region. Viiding and Tostensen [49] conducted a review of implementation strategy of this regional policy and related its failure to the following reasons: the EAC mandate does not prescribe any effective authority to influence the implementation of the regional policy, and the regional policy consists of ambitious objectives that are beyond the resource capacity of the partner states. Therefore, it is recommended that necessary steps be taken by the EAPP to ensure a balance between the push for more on-grid power and the need for increasing energy using techniques such as: pay-as-you-go solar, community mini-grids, etc. Ngalame [50] reported on the efforts of the governments of Central African nations to tackle power shortages, which consist of major barrier to economic growth in this region. In this light, the Central African Power Pool (CAPP),

created in 2003, has been tasked to develop the Regional Power Policy of the Economic Community of Central African States (ECCAS) in response to regional energy shortages and development objectives. Therefore, the following implementation plan has been endorsed: interstate electricity exchanges, investments in generation capacity and energy infrastructure; access to hydro-electricity while participating in a global transition to clean or low-carbon energy systems. The terms of reference of the CAPP regional power policy document [51] highlighted that the sharing strategy of abundant, yet unequally distributed energy resources among ECCAS member states, is based on a master plan and seeks to promote a limited number of priority projects, both in terms of energy projects and institutional capacity building efforts. The Infrastructure Consortium for Africa (ICA) [52] reported on the funding strategies for CAPP major projects. They consist of: organising ad hoc meetings attended by national and regional stakeholders (utilities, funding agencies, specialised institutions, ministries); convening specific donors' meetings for a particular regional project; the dependence on utilities' contributions, which are not always paid in due time, constrain the work progress of CAPP. In a bid to promote regional energy trade among the Southern African states, the Southern African Power Pool (SAPP) was created in 1995 and adopted the Southern African Development Community (SADC) Protocol on Energy, and of the SADC Energy Cooperation Policy and Strategy in 1996 [52]. Following this policy adoption, Kambanda [53] reported the introduction by the SAPP of the Short-Term-Energy Markets (STEM), in April 2001, which operates on daily and hourly contracts. This initiative facilitated the development of a Day-Ahead Market (DAM). These policy implementation strategies led to the establishment of a platform enabling effective cooperation among energy regulators in the SADC region [52, 54, 55]. This platform is referred to as the regional electricity regulatory association (RERA), which seeks to harmonise regulatory policies, legislation, standards and practices. Tchereni [56] argued that policy vacuum features among major barriers for low pace exploitation of renewable energy technologies in the SADC countries. According to the European Union Energy Initiatives (EUEI) [57], the SADC regional energy access strategy presented an account of electricity policy reforms in most of the SADC countries. The Electricity Act of 2000 which proposed the unbundling of Nampower and introduced independent power producers (IPPs) in order to increase domestic generation capacity and the establishment of five regional electricity distribution companies to supply electricity at the retail end of the industry. In South Africa, the Integrated National Electrification Programme (INEP) [58] increased electricity access from 36% in 1995 to 80% in 2007. The free basic electricity, introduced in 2003, enabled poor people to access 50 kWh for basic domestic needs [59]. This is paid in form of subsidy to electricity distribution companies by the government of South Africa. According to the South African Department of Minerals and Energy (SADME) [60], the Renewable Energy Policy was initiated in a bid to source 10 000 GWh of electricity from renewable resources by 2013. Subsequent to this, the Renewable Energy Target Monitoring Framework

was launched to ensure progress towards the 2013 target was effectively monitored [61]. In Zimbabwe, the Rural Electrification Agency (REA) [62] is meant to focus on rural centres where local government infrastructure (agricultural extension, health services, schools, etc..) are situated.

## ***4.2 From State Monopoly to Market-Based Policies***

In an effort to provide universal access, various countries in SSA have initiated policy reforms that sought to liberalise electricity markets. Therefore, Hall et al. [63] reviewed the trends of liberalisation and privatisation in developing countries. The authors noted that liberalisation mainly consisted of unbundling of electricity systems (Kenya, Nigeria, Namibia, Uganda, South Africa, etc..), which in many cases, paved the way for the development of IPPs through PPP framework or partial privatisation. In this model, long-term contractual agreement over power purchase, known as power purchase agreement (PPA), is entered between IPPs and state utilities. However, despite considerable support of this model of privatisation by international financial institutions [64], it is perceived to be more favourable to the private sector and detrimental to public utilities. This perception is one of the reasons for reversal of PPPs and continued vertically-integrated electricity utilities in some developing countries. Gabriele [65] conducted a survey on policy alternatives in a bid to reform energy utilities in developing countries, and concluded that full scale privatisation of power sector in developing countries attracts significant risks, and a flexibility is required in a policy initiative rather than firm commitment to extensive liberalisation. Victor et al. [66] proposed a critical review of common models of privatisation (PPP, outsourcing and granting of franchise to the private investors) and the different implementation strategies in selected Asian and African nations (Nigeria, Cameroon and South Africa). The authors argued that in the case of Nigeria and Cameroon, failure of privatisation policy came as a result of inadequate electricity supply, limited government funding to curb the incurred debt, and power sector expansion. The relative success in South Africa came as a result of the need to meet electricity demand and economic growth. According to these authors, privatisation policy is neither good nor bad as it depends on adopted environmental conditions, political will, government's tenacity to achieve its development goals and the implementation strategies. Bensch [67] conducted a systematic review on the effect of market-based reforms (liberalisation, privatisation, private sector involvement and regulation) on technical efficiency and on electricity access. Using mixed methods (quantitative and qualitative), the author noted that there is no sufficient evidence to suggest that market-based reforms can enhance electricity access in developing countries. Quantitatively, weak indications showed that privatisation plays less of a role than other market-based policies, and regulation showed mixed results which are dependant on implementation strategies. Qualitatively, this review showed that four parameters are essential to the likelihood of success or failure of market-based policy: commercial approach, competitive arrangements, cost-reflective pricing, as well as independent,

empowered and efficient regulation. Phalatsé [68] provided a historical context of the challenges faced by the South African power utility prior to analysing the unbundling strategy—such as adopted by the South African government for full implementation in 2022—based on the experiences of SSA countries (Kenya and Uganda) that have previously applied this policy. This study showed that despite increase in access rate (mostly in urban areas of Uganda), unbundling of vertically-integrated power utilities has led to rise in tariffs (in both Kenya and Uganda) to 50 %, growth in supply deficit (Uganda), and to 20 % increase in profit margin for private investors (Uganda). According to the International Trade Administration [69], privatisation entered the electricity sector of Nigeria in 2013. Consequently, eleven electricity distribution and six generation companies were privatised. However, it should be noted that 100% retention of the electricity transmission company was observed in this process. According to Ahmed and Landi [70]: the deficit in electricity infrastructure in the Nigerian power sector is the dominant cause of unreliable power supply. These authors also argued that the Nigerian government policy of meeting electricity demand could only be achieved through private investments. To date, the cost of investment in electricity infrastructure has reached close to 1 billion US dollar [69]. Providing an account of the Nigerian rural electrification agency (NREA), Olanrele [71] observed that among other objectives assigned to the NREA, this programme was also meant to facilitate the promotion of private sector participation in rural electrification through on or off-grid systems. Following a cohort of problems emanating from lack of generation capacity, ageing and/or poor infrastructure, and distribution system losses and inefficiencies, the government of Ghana opted for the privatisation of the electricity distribution, following the approval of the candidacy agreement with the US agency Millennium Challenge Corporation (MCC) in 2014 [72]. In terms of this agreement, the Government of Ghana received 500 million US dollar as a development grant from MCC. According to Sakyi [73], the joint venture or public private partnership thus created between Electricity Distribution of Ghana (EDG) and Manila Electric Company (MEC) — a private equity entity — afforded 49 % equity shares to the private entity while the Ghanaian Government retained 51%. Owing to the inability of the Ghanaian National Electrification Scheme to achieve successful outcome in terms of rural access to electricity through grid extension and following agreement with the World bank in 2007, the Ghana Energy Development and Access Project (GEDAP) was tasked in 2007 to carry out electrification development projects, which include off-grid solar PV systems, through the Global Environment Facility (GEF) funds. This strategy served as a catalyst to the development of solar merchants and rural banks [74]. Mawhood and Gross [75] reported that the Senegalese state monopoly on the generation, transmission and distribution of electricity first came to an end in 1999 with a shift to semi-privatisation subsequent to frequently encountered and prolonged outages and/or blackouts. However, this move did not last long as the electricity sector moved back to state monopoly a year later. Gokgur and Jones [76] suggested that a second attempt to privatise the Senegalese electricity took place in 2001 and failed. However, regulation and rural electrification responsibilities were taken away from the state-owned electricity company. This led to the establishment of the Senegalese Rural Electricity Agency (SREA). This

agency initiated the Senegalese Rural Electrification Action Plan (SREAP) whose role consisted of mobilising investment in renewable energies from the private sector through financial and technical support from the World Bank. Gualberti et al. [77] reported that the Mali electricity utility was partially privatised in 2000 to a consortium constituted of Saur, with 47% equity shares, and Industrial Promotion Services, with 13% shares. Accordingly, the Government of Mali's National Energy Policy (NEP), such as adopted in 2005, is based on decentralization, liberalisation, participatory approach, competitiveness and on the implementation of PPPs [78]. The Mali renewable energy fund (REF), such as initiated in 2000, is purposed to create a conducive environment that could enable private capital (national and international) to be channelled to rural energy projects. Manneh [79] indicated that the Gambian electricity act of 2004 partially liberalised the electricity market by introducing IPPs into the generation domain of electricity. The transmission and distribution remained the monopoly of the state entity. In a bid to improve access to electricity in rural areas, the Gambian Energy Roadmap, which includes the Organisation pour la Mise en Valeur du fleuve Gambia (OMVG) hydroelectric power plant and regional interconnection projects, has secured over 400 million US dollar in funding, to which the World Bank financed 175 million US dollar [80]. In Guinea-Bissau, the state is mainly responsible for the generation, transmission and distribution of electricity. However, inefficiencies related to generation capacity have led to small IPPs to contribute 10% of the total electricity generation [81]. In 2010, major reforms—aimed at mobilising public and private financial resources for grid extension as well as for the development of renewable energy sources—were adopted by the Government of Guinea Bissau. According to Karekezi and Mutiso [82], the adoption of the Electric Power Act of 1997 and the National Energy Policy of 2004, which paved the way for the establishment of the rural electrification authority, rationalisation and unbundling of the state-owned electricity company in Kenya. Following the implementation of the Energy Policy in 2010, KenGen was partially privatised, thus offering 30% of its equity to private entities. It is worth noting that the Kenyan model allows participation of private (both national and international) partnership at any sphere of the electricity business, and has proven to have attracted the highest number of IPPs in the continent. Girma [83] argued that despite the unbundling of the vertically integrated state-owned electricity company into two state entities in 2013, Ethiopia has not been able to attract any private participation (IPPs). This indicates that no actual privatisation has taken place. Despite the setting up of independent rural electrification secretariat and allocating rural electrification fund—supposedly accessible to private electricity producers to fund viable projects—rural electrification has remained under the generation and transmission of the state entity. Godinho and Eberhard [84] suggested that the electricity act of 1999 paved the way for a jurisdiction shift of the Ugandan Electricity Board (UEB) and of the establishment of the Electricity Regulatory Authority (ERA). However, this process fell short of completely removing political control from UEB making restructuring quite difficult to implement. According to these authors, unbundling finally came to be in 2001 which enabled privatisation to take place in form of concession agreements in generation, transmission and distribution. Accordingly, Eskom Uganda signed a

20 year concession agreement to operate a hydro plant. In the same vein, UMEME—a joint venture formed between Eskom Uganda (44%) and Globeleg (56%)—signed a 20 year concession agreement to operate the Ugandan distribution network. In terms of rural electrification, the Rural Electrification Agency (REA), established in 2003, is commissioned to source funds from the Rural Electricity Fund (REF) in order to extend the grid to rural areas. Such extended grids are leased to private operators in terms of concession agreement. According to AfDB group [85], the unbundling of national monopoly state-owned Electrogaz of Rwanda into separate electricity and water entities or parastatals resulted from the electricity law of 2008. In terms of this, bulk transmission and distribution or retailing are placed under the Rwanda Electricity Cooperation (RECO), while generation is to be assumed by private entities (IPPs) under PPAs. According to Mininfra [86], the adopted programmes of the rural electrification strategy are to be implemented using PPP. Nsabimana [87] suggested that despite the 2000 electricity reform in Burundi, which proposed unbundling of the vertically-integrated electricity company into generation, transmission and distribution layers, these measures could not be implemented. This lack of implementation led to the promulgation of the second act in 2015, which in turn created legal framework enabling private participation in the electricity sector. Therefore, the generation sector was opened to IPPs while the possibility of concession contracts was made available in transmission, distribution and retail. In addition, a regulatory and control body as well as a rural electrification agency were also created. According to Oxford Business Group [88], electricity independence and increase in access to electricity (in both urban and rural areas) through renewable energy resources (solar PV, wind, geothermal, etc..) consist of one of the key objectives of the Government of Djibouti. Accordingly, the liberalisation of the electricity sector was embraced in 2015. It is aimed at increasing private participation. Lukamba-Muhiya [89] reviewed the state of the DRC electricity supply industry from 1970 to 2006. This author argued that the vertically-integrated nature of this system has negative impact on the economy, given the numerous power outages. The lack of implementation of the master plan on urban and rural electrification despite the approval of the electrification programme. This author suggests structural reforms of the electricity utility and recommends PPP as an alternative model to be considered by the government of the DRC. According to the World Bank [90], the adoption of legislation related to the liberalisation of the electricity sector in 2014, was not supported by an effective and capable regulatory framework. In addition, this report also argued weak governance, lack of public financial capacity, unfavourable policies among others as challenges to the scaling up of decentralised renewable energy solutions. According to the Electricity Sector Regulatory Agency [91] provides a detailed account of the reforms of the Cameroonian electricity sector. This body reports that the vertically-integrated national power utility was unbundled in 1998 to pave the way for participation of the private sector in the development of the electricity sector. Mus'ud et al. [92] indicated that despite the many reference made to renewables in several energy laws enacted by the Government of Cameroon, hydropower is mostly used and fiscal limitations consist of major challenge to renewable implementation. For the purpose of improving electricity access, the rural electrification board has been established to provide allocation of





**Fig. 13** Comparative evaluation process of applied policy options in SSA

licences to power producers in remote areas. In addition, the Cameroon Renewable Energy Fund (CREF) and the National Investment Fund (NIF) have been created to provide expertise and funding to renewable energy projects [93]. As far as the electricity sector is concerned in Angola, the legal framework was built up on the general law of 1996, which reserved electricity generation, transmission and distribution to the state [94]. Therefore, under this framework, private sector required state concession to participate in the electricity business. Privatisation in the electricity sector came through Act No. 5/02 of 2002. The Angolan Government enacted the National Energy Security Policy and Strategy in 2011 [95]. This act promotes the diversification of national energy, and forms part of the national strategy together with the Integrated Rural Development and Poverty Combat programme. This strategy intends to improve access to electricity in rural areas using renewable energies as well as to promote public and private investment in the electricity sector. In terms of the adopted strategies, rural electrification board has been established and mandated to allocate licences to power producers in remote locations.

In the context of global warming and climate change, the impact of both market-based policies and state monopoly on the enablement of SDG 7, and consequently of SDG 2, should be comparatively evaluated. This could be illustrated in Fig. 13.

## 5 Six-Step Policy Analysis Framework

Although there is no single agreed-upon way to analyse policies [96, 97], basic process of policy analysis usually consists of six fundamental steps: problem definition, evaluation criteria, identification of alternatives, evaluation of alternatives, comparison of alternatives, and assessment of outcomes. The fundamental steps of a decision making model are given in Fig. 14. According to Jansson [98], policy analysis could be approached in terms of the six steps analysis framework whereby the first step

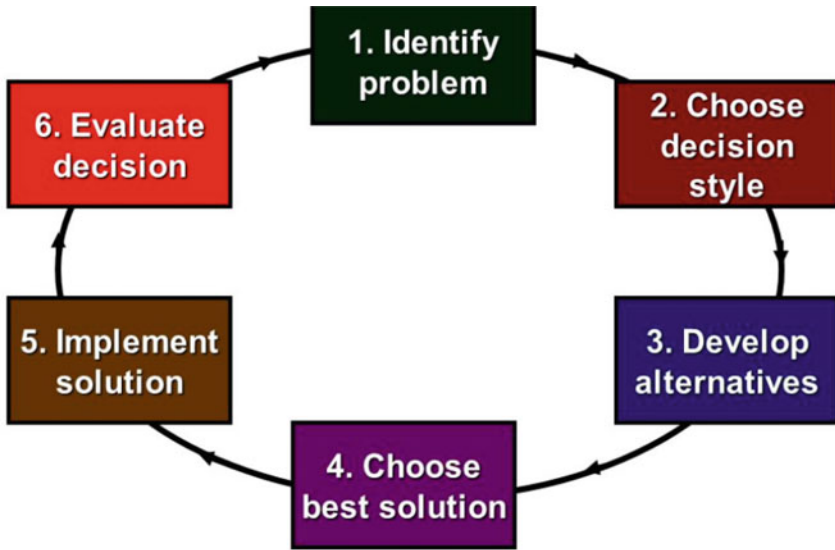


Fig. 14 Steps of decision making model [99]

should be to familiarise with a social problem or an issue and not a goal. Stone [99] argued that the point of departure in policy formulation should be the search for a cause of a problem or its root cause in order to solve such a problem.

### 5.1 Problem Definition

Owing to climate change and global warming, sustainable growth in agricultural production, which is essential to food security, requires access to affordable, reliable and low-carbon electricity. Therefore, an analysis of market-based policies and state monopoly approach—as catalysts or key enablers of SDG 7 and the causality between SDG 7 and 2 consists of the fundamental step. Therefore, the following problem is central to this work:

Will market-based policies (unbundling or common variants of privatisation) be more favourable than state monopoly approach in the enablement of SDG 7, hence SDG 2, in SSA countries?

### 5.2 Evaluation Criteria

The following indicators or criteria are used as basis of evaluation of the effectiveness of market-based policies two decades after its implementation:

1. Growth in access to electricity in both urban and rural areas—SDG 7.1
2. Increase share of renewable energies in final energy consumption—SDG 7.2
3. Electricity consumption in agriculture
4. Low prevalence of moderate or severe food insecurity in the population based on the Food Insecurity Experience Scale (FIES)—SDG 2.2.

### 5.3 Identification of Alternatives

The historic alternative to market-based policies in SSA consists essentially of state monopoly approach, which has been practised since colonial era. This approach rapidly became aligned to political ideology in many of post-colonial SSA countries and survived in many ways the assaults of the free-market world. In some instances, it has not completely paved the way to free-market policies. However, the many challenges faced by this approach (infrastructure investment cost, grid expansion restriction due to lack of investment, etc..) as well as the promotion of sustainable development have accelerated the need for new approach.

### 5.4 Evaluation of Alternatives

In this section, the performance of both policy options are evaluated on the basis of the criteria discussed in Sect. 5.2.

#### 5.4.1 Market-Based Policy Option

Data obtained after a decade (2010–2020) of implementation of market-based policies in selected SSA countries are given in Tables 6, 7, 8 and 9 [100, 101].

**Table 6** Selected countries of the Western region of SSA

Countries	Rural access	Urban access	Renew. share	Elec. Cons. Agric.	Food Ins.
Nigeria	23.5–24.6	79.8–83.9	7.5–5.5	–	36.5–57.7
Ghana	55.4–74.0	72.8–94.7	15.6–11.2	0.0–54.0	49.3–50.2
Senegal	35.2–47.4	83.9–95.2	1.1–4.6	270.0–164.0	39.3–40.9
Cote d'Ivoire	31.7–43.1	87.9–94.5	9.0– 9.7	360.0–818.0	–
Sierra Leone	0.9–4.8	34.3–54.7	–	–	78.4–83.9
Liberia	1.0–8.4	9.7–45.2	–	–	–80.6
–	%	%	%	TJ	%

**Table 7** Selected countries of the Eastern region of SSA

Countries	Rural access	Urban access	Renew. share	Elec. Cons. Agric.	Food Ins.
Kenya	7.2–62.7	58.2–94.0	2.9–3.8	–	53.0–68.5
Ethiopia	12.8–39.4	85.6–93.2	1.8–3.0	–	56.2–56.3
Uganda	3.5–32.8	48.0–69.9	18.5–22.0	–	58.0–69.2
Rwanda	2.6–38.2	44.5–86.4	7.7–8.0	–	–
Burundi	0.9–3.5	49.0–63.7	–	–	–
Djibouti	30.1–24.8	64.0–72.2	–	–	–
–	%	%	%	TJ	%

**Table 8** Selected countries of the Central region of SSA

Countries	Rural access	Urban access	Renew. share	Elec. Cons. Agric.	Food Ins.
Angola	0.8–7.3	73.7–73.7	4.3–8.8	–	–73.5
DRC	0.0–1.0	37.7–40.6	23.3–6.5	–	–69.2
Cameroon	15.9–25.0	87.4–94.0	12.3–19.4	216.0–223.0	–55.8
Chad	3.0–2.0	18.3–40.6	1.2–1.2	–	–
CAR	0.6–2.3	21.6–33.6	–	–	–61.8
Sao Tome & Principe	45.9–71.1	69.7–78.4	–	–	–
–	%	%	%	TJ	%

**Table 9** Selected countries of the Southern region of SSA

Countries	Rural access	Urban access	Renew. share	Elec. Cons. Agric.	Food Ins.
South Africa	75.9–75.3	87.1–88.8	4.3–5.6	21618.0–25135.0	42.9–44.9
Zambia	4.0–14.0	49.8–82.4	22.8–22.8	698.0–1125.0	48.8–51.4
Botswana	25.3–26.4	68.1–90.7	0.0–0.1	659.0–677.0	45.9–50.8
Namibia	24.4–36.3	73.0–74.7	18.5–20.2	–	53.2–57.6
Eswatini	39.8–75.8	65.4–92.2	–	–	62.6–64.1
Lesotho	4.4–34.9	55.2–77.7	–	–	–49.7
–	%	%	%	TJ	%

**Table 10** Selected countries of the Western region of SSA

Countries	Rural access	Urban access	Renew. share	Elec. Cons. Agric.	Food Ins.
Nigeria	4.0–21.3	82.4–84.0	4.4–4.6	–	52.0–23.0
Ghana	2.9–14.9	74.6–80.5	15.8–24.0	–	35.0–12.0
Senegal	4.9–12.8	58.6–74.6	0.3–0.2	130.0–101.0	20–22
Cote d'Ivoire	23.7–43.1	81.5–94.5	10.1–9.7	194.0–360.0	–
Sierra Leone	–0.6	–23.4	–	–	45–50
Liberia	1.0–8.4	6.9–45.2	–	–	32–40
–	%	%	%	TJ	%

**Table 11** Selected countries of the Eastern region of SSA

Countries	Rural access	Urban access	Renew. share	Elec. Cons. Agric.	Food Ins.
Kenya	1.1–6.5	42.5–49.8	3.2–1.7	158.0–133.0	42–36
Ethiopia	–1.7	–76.2	1.2–1.3	–	–
Uganda	2.0–1.5	33.6–41.0	0.6–19.5	–	–
Rwanda	–0.5	31.1–38.9	1.4–0.9	–	–
Burundi	–0.9	60.6–50.6	–	–	–
Djibouti	89.3–56.1	53.6–56.5	–	–	–
–	%	%	%	TJ	%

**Table 12** Selected countries of the Central region of SSA

Countries	Rural access	Urban access	Renew. share	Elec. Cons. Agric.	Food Ins.
Angola	–3.5	–44.8	2.7–2.9	–	60.0–49.0
DRC	–	–20.0	20.8–23.2	54.0–58.0	30.0–75.0
Cameroon	6.1–9.2	63.0–79.0	18.0–17.5	–	–
Chad	1.0–1.3	9.4–10.0	1.5–1.5	–	–
CAR	–0.8	8.0–15.6	–	–	50.0–42.0
Sao Tome & Principe	–40.1	–64.1	–	–	–
–	%	%	%	TJ	%

#### 5.4.2 State Monopoly Policy Option

Data obtained as a result of state monopoly implementation over a decade (1990–2000) have been given in Tables 10, 11, 12 and 13 [100–102].

**Table 13** Selected countries of the Southern region of SSA

Countries	Rural access	Urban access	Renew. share	Elec. Cons. Agric.	Food Ins.
South Africa	23.8–54.6	85.3–85.7	16.6–16.3	14249.0–14234.0	–
Zambia	2.8–2.1	34.7–44.1	22.6–22.3	644.0–500.0	45.0–48.0
Botswana	4.0–12.0	17.5–39.1	0.6–0.0	–202.0	17.0–22.0
Namibia	10.7–18.9	66.0–73.2	20.4– 16.2	–	–
Eswatini	–10.2	–54.3	–	–	–
Lesotho	–2.0	–13.6	–	–	–
–	%	%	%	TJ	%

## 5.5 Comparison of Alternatives

1. Growth in access to electricity in both urban and rural areas—SDG 7.1: the observed data indicate that the growth rate observed in both rural and urban access during 10 years is irrespective of policy options. Therefore, this suggests that both policy options are capable to favour or induce growth in access to electricity. Furthermore, access to electricity in rural areas seems to be generally below the 50 % threshold irrespective of which policy option has been practiced. In the few reported cases where access to electricity in rural areas is higher than 50 %, significant electricity consumption in the agricultural sector is also reported. This suggests that agricultural activity consists of a key driver or the main activity that could be used to increase electricity demand and thereby promoting rural development.
2. Increase share of renewable energies in final energy consumption—SDG 7.2: data observed reveal that such increase is marginally consistent with market-based policy option. This is noted in Cote d’Ivoire, all selected Eastern region countries, Angola, Cameroon, South Africa, Botswana and Namibia. However, when state monopoly policy was applied. However, a decrease trend seems to be dominant with state monopoly except in a few cases observed in Nigeria, Ghana, Angola as well as in the DRC. It should also be noted that the average share of renewable energies in the final energy consumption is below the 50% mark irrespective of any of the policies used. This suggests that additional capital investments could be possibly sourced under market-based policies. This could play a key role in overcoming financial restrictions, which are common under state monopoly. However, slow pace and/or inadequate regulatory framework could be attributed to insignificant impact of additional funds to the increase of electricity access during the 10 year implementation of market-based policies in the selected countries.
3. Electricity consumption in agriculture: the trends observed in the selected countries show consistency between growth in electricity consumption, such as

observed in agricultural sector, with the implementation of market-based policies. Since the industrialisation of the agricultural sector forms the basis of continuous increased electricity demand. This paved the way to distributed generation whereby electricity is produced and distributed to nearby consumers, which may include farmers [103]. Distributed generation concept is consistent with market-based policies [68, 104, 105].

4. Low prevalence of moderate or severe food insecurity in the population based on the Food Insecurity Experience Scale (FIES)—SDG 2.2: data trends observed indicate general rise in the prevalence of food insecurity irrespective of policy option. Despite the correlation between this factor and access to electricity, many other factors could play a significant role in the achievement of low prevalence of food insecurity. This is strongly argued in [32, 106–108].

## 5.6 *Assessment of Outcomes*

Both market-based and state monopoly policy options are catalysts of access to electricity. However, to achieve this developmental goal in rural areas with the use of off-grid low-carbon energy systems (community microgrids, etc.), significant capital investments should be systematically mobilised. Therefore, the observed pattern, which correlates the increased share in renewables as well as that of electricity consumption in agriculture with market-based policies, consists of reasonable advantage and the most probable factor that may influence the choice of this policy to fuel access to low-carbon and affordable electricity in rural areas of SSA countries. However, low prevalence of food insecurity consists of multi-dimensional phenomenon, which cannot be simply addressed by increasing access to electricity.

## 6 Conclusion

Access to affordable and clean electricity in rural communities of SSA has been reported to be low despite considerable renewable resources available to these nations. This reality poses massive challenges to the ever-growing population of this region of the world in terms of hunger, undernourishment and poverty as a result of government's the inability to promote modern agricultural production and food industry for sustainable development. Decentralised systems (off-grid solar PV systems, wind farms, etc.), grid extension and regional integration of electricity grids have been proposed as technical alternatives to accelerate access to electricity in rural areas of SSA nations. The effectiveness of market-based policies in enabling access to low-carbon and affordable electricity is probed using the six-step policy analysis method. This work suggests the following:

1. State monopoly policy: based on its performance in selected SSA countries over a decade, this model shows capability of enabling access to electricity. The main challenge remains fiscal constraints and inefficient and/or poor management of SSA state-owned utilities, which lead to supply shortages as a result of aged and delapidated infrastructure. The probability of such states to invest in adequate electricity infrastructure is often close to none. Therefore, investment in decarbonated and decentralised energy systems may experience prolonged delays—just as it is proven to be the case with most of the rural electrification programmes (REPs). This negatively impacts on the promotion and development of modern agriculture and sustainable food industry in rural communities.
2. Market-based policies: according to Hall et al. [63], this actually refers to unbundling or partial privatisation of state-owned utilities through public-private-partnership (PPP) or Equity Partnership. Based on the observed performance in selected SSA countries over a decade, this policy is capable to enable access to electricity as well as private capital. This provides an alternative funding, which may be used to invest in low-carbon decentralised energy systems. As a result of increased use of renewable energy systems, the agricultural sector will inevitably become beneficiary of electricity produced. Despite this attribute, this model is being confronted to inadequate or ineffective contractual agreement between state utilities and private business entities. Such agreements tend to guarantee profits to the private sector to the detriment of governments. This led to consumers having to pay higher tariffs for basic service. In addition, lack of electricity markets in rural communities constitute a major stumbling block to the viability.

In the light of the above, the attainment of SDG 7 does require catalysts: policy formulation and adequate implementation. However, access to low-carbon and affordable electricity consists of one factor among many others whose combination is consistent with low prevalence of moderate or severe food insecurity (SDG 2). Therefore, the need for robust and dynamic model capable of predicting a sustainable business case (whereby a decentralised low-carbon energy system providing electricity supply to a community whose dwellers are financially empowered through modernised agricultural activity, and therefore are able to pay electricity bills) is required.

## References

1. OECD Environment Directorate and International Energy Agency (IEA): Policies to reduce greenhouse gas emissions in industry—successful approaches and lessons learned (2003). <https://www.oecd.org/environment>. Accessed January 2021
2. Friends of the Earth: A pathway to net zero greenhouse gas emissions (2018). <https://www.friendsoftheearth.uk>. Accessed January 2021
3. Wade, K., Jennings, M.: The Impact of Climate Change on the Global Economy. Schroders (2016). <https://www.schroders.com>. Accessed January 2021
4. Lukyanets, A.S., Ryazantse, S.V.: Economic and socio-demographic effects of global climate change. *Int. J. Econ. Financ. Iss.* **6**(8), 268–273 (2016)



5. Pimentel, D., Herz, M., Glickstein, M., Zimmerman, M., Allen, M., Becker, K., Evans, K., Hussain, B., Sarsfeld, R., Grosfeld, A., Seidel, T.: Renewable energy: current and potential issues. *Bioscience* **52**(12), 1111–1119 (2002)
6. Quansah, D.A., Adaramola, M.S., Mensah, L.D.: Solar photovoltaics in sub-Saharan Africa: addressing barriers, unlocking potentials. *Energy Procedia (Elsevier)* **106**, 97–110 (2016)
7. International Energy Agency (IEA) World Energy Outlook 2015: Methodology for energy access analysis (2015). [https://www.worldenergyoutlook.org/media/weowebsite/2015/EnergyAccess\\_Methodology\\_2015](https://www.worldenergyoutlook.org/media/weowebsite/2015/EnergyAccess_Methodology_2015). Accessed January 2021
8. The World Bank News Report: Access to energy is at the heart of development (2018). <https://www.worldbank.org/en/news>. Accessed January 2021
9. International Monetary Fund (IMF) Survey: Africa's power supply crisis: unraveling the paradoxes, Africa's energy shortage (2008). <https://www.imf.org/en/News/Articles>. Accessed January 2021
10. Corfee-Morlot, J., Parks, P., Ogunleye, J., Ayeni, F.: Achieving clean energy access in sub-Saharan Africa: a case study for the OECD. UN Environment, World Bank project (2018). <https://www.oecd.org/environment/cc/climate-futures>. Accessed December 2020
11. UN Department of Economic and Social Affairs (DESA): Global policy dialogue series (2020). <https://www.un.org/en/desa/policy-dialogue>. Accessed December 2020
12. International Energy Agency (IEA): World Energy Outlook (2020). <https://www.iea.org/reports/world-energy-outlook-2020>
13. International Renewable Energy Agency (IRENA): Africa Power Sector: Planning and prospects for renewable energy synthesis (2015). <https://www.irena.org>
14. UN Economic Commission for Africa: Energy access and security in Eastern Africa: status and enhancement pathways. ECA Documents Publishing and Distribution Unit (2014)
15. Shabaneh, R., Corbeau, A.S., Nhamumbo, F.T.: Identifying the roadblocks for energy access: a case study for eastern Africa's gas. King Abdullah Petroleum Studies and Research Center (KAPSARC) (2018). <http://www.kapsarc.org>
16. Sridharan, V., Broad, O., Shivakumar, A., Howells, M., Boehlert, B., Groves, D.G., Rogner, H.H., Taliotis, C., Neumann, J.E., Strzepek, K.M., Lempert, R., Joyce, B., Huber-Lee, A., Cervigni, R.: Resilience of the eastern African electricity sector to climate driven changes in hydropower generation. *Nat. Commun.* **10**, 294–302 (2019)
17. Ouedraogo, N.S.: Africa energy future: alternative scenarios and their implications for sustainable development strategies. *Energy Policy* **106**, 457–471 (2017)
18. The United Nations Environment Programme (UNEP): Atlas of Africa energy resources (2017). <http://www.unep.org>. Accessed December 2020
19. UNDP Regional Bureau for Africa (RBA): Transforming lives through renewable energy access in Africa: UNDP's Contributions. UNDP Africa Policy Brief **1**(1), 1–32 (2018)
20. Infrastructure Consortium for Africa (ICA): Updated regional power status in Africa power pools report (2016). <https://www.icafrica.org>. Accessed December 2020
21. U.S. Energy Information Administration: Off-Grid electricity development in Africa: uncertainties and potential implications for electric power markets (2020). <https://www.eia.gov>. Accessed December 2020
22. OECD-FAO: Agriculture in sub-Saharan Africa: Prospects and Challenges for the Next Decade: in OECD-FAO Agricultural Outlook 2016–2025. OECD Publishing, Paris (2016)
23. Bjornlund, V., Bjornlund, H., Van Rooyen, A.F.: Why agricultural production in sub-Saharan Africa remains low compared to the rest of the world—a historical perspective. *Int. J. Water Resour. Dev.* **36**(1), 20–53 (2020)
24. Population Action International and the African Institute for Development Policy: Population, climate change, and sustainable development in Africa. Policy and issue brief (2012). <http://www.afidep.org>. Accessed December 2020
25. Office of the special adviser on Africa (OSAA): Comprehensive Africa Agriculture Development Programme (CAADP) (2015). <https://www.un.org/en/africa/osaa/peace/caadp.shtml>
26. Otsuka, K., Muraoka, R.: A green revolution for sub-Saharan Africa: past failures and future prospects. *J. Afric. Econ.* **26**(1), 73–98 (2017)

27. Moner-Girona, M., Solano-Peralta, M., Lazopoulou, M., Ackom, E.K., Valive, X., Szabo, S.: Electrification of sub-Saharan Africa through PV/hybrid Mini-grids: reducing the gap between current business models and on-site experience. *Renew. Sustain. Energy Rev.* **91**, 1148–1161 (2018)
28. UN Economic Commission for Africa (UNECA): Policy Brief 18: achieving SDG 7 in Africa (2018). <https://sustainabledevelopment.un.org/content/documents/17565PB18.pdf>. Accessed December 2020
29. The Global Indicator Framework: Global indicator framework for the sustainable development goals and targets of the 2030 agenda for sustainable development (2020). <https://unstats.un.org/sdgs/indicators>. Accessed December 2020
30. Munisi, S.E.: Food shortages in sub-Saharan Africa and population growth. *DEF* **6**, 6–10 (1982)
31. Clover, J.: Food security in sub-Saharan Africa. *Afric. Sec. Rev.* **12**(1), 5–15 (2003)
32. Fawole, W.O., Ilbasimis, E., Ozkan, B.: Food insecurity in Africa in terms of causes, effects and solutions: a case study of Nigeria. In: 2nd International Conference on Sustainable Agriculture and Environment, Konya, Turkey (2015)
33. Drammeh, W., Hamid, N.A., Rohana, A.J.: Determinants of household food insecurity and its association with child malnutrition in sub-Saharan Africa: a review of the literature. *Curr. Res. Nutr. Food Sci* **7**(3), 610–623 (2019)
34. Khapayi, M., Celliers, P.R.: Factors limiting and preventing emerging farmers to progress to commercial agricultural farming in the King William’s Town area of the Eastern Cape region, South Africa. *S. Afr. J. Agric. Ext.* **44**(1), 25–41 (2016)
35. Blimpo, M.P., Cosgrove-Davies, M.: Electricity access in sub-Saharan Africa uptake, reliability, and complementary factors for economic impact (2019). <https://openknowledge.worldbank.org/>. Accessed December 2020
36. Winklmaier, J., Santos, S.A.B., Trenkle, T.: Economic development of rural communities in sub-Saharan Africa through decentralized energy-water-food systems. In: *Regional Development in Africa* (2020). <https://www.intechopen.com/books>. Accessed February 2021
37. Chaurey, A., Ranganathan, M., Mohanty, P.: Electricity access for geographically disadvantaged rural communities—technology and policy insights. *Energy Policy* **32**(15), 1693–1705 (2004)
38. Kyriakarakos, G., Balafoutis, A.T., Bochtis, D.: Proposing a paradigm shift in rural electrification investments in sub-Saharan Africa through agriculture. *Sustainability* (2020). <http://www.mdpi.com/journal/sustainability>. Accessed February 2021
39. UN Development Programme (UNDP): Sustainable development goals (2015). <https://www.undp.org/content/undp/en/home/sustainable-development-goals/background.html>
40. UN Educational Scientific and Cultural Organisation (UNESCO): Sustainable development goals—resources for educators (2019). <https://en.unesco.org/themes/education/sdgs/material>. Accessed December 2020
41. Karaki, K.: Understanding ECOWAS energy policy: from national interests to regional markets and wider energy access? European Centre for Development Policy Management (2017). <http://www.ecdpm.org>. Accessed December 2020
42. ECOWAS Centre for Renewable Energy and Energy Efficiency (ECREEE): ECOWAS Renewable Energy Policy (EREP) (2015). <http://www.ecreee.org>. Accessed December 2020
43. Reiss, K.: Developing renewable energy sectors and technologies in West Africa (2020). <https://www.un.org/en/chronicle/article/developing-renewable-energy-sectors-and-technologies-west-africa>. Accessed December 2020
44. Peterson, R., Sampa, I.: Can AfCFTA solve Africa’s energy challenge? *Africa Connected Issue* (3) (2019). <http://www.dlapiper.com/Africa>. Accessed December 2020
45. Lam, J.: Leveraging private investment in power transmission infrastructure in West Africa. *Africa Connected Issue* (3) (2019). <http://www.dlapiper.com/Africa>. Accessed December 2020
46. Bungane, B.: World Bank programme to enable electricity trade in West Africa (2020). <https://www.esi-africa.com/industry-sectors/transmission-and-distribution>. Accessed December 2020

47. Hafner, M., Tagliapietra, S., Falchetta, G., Occhiali, G.: Renewables for Energy Access and Sustainable Development in East Africa. Springer Briefs in Energy (2019). <https://doi.org/10.1007/978-3-030-11735-1>
48. Kammen, D.M., Jacome, V., Avila, N.: A Clean energy vision for East Africa: planning for sustainability, reducing climate risks and increasing energy access. University of California, Berkeley, USA (2015). <http://rael.berkeley.edu>
49. Viiding, M., Tostensen, A.: Forward Looking Review of the Regional Strategy on Scaling Up Access to Modern Energy Services in the East African Community. Norplan (2013). <http://www.cmi.no/publications/file/4866-forward-looking-review-of-the-regional-strategy-on.pdf>. Accessed December 2020
50. Ngalame, E.N.: How Central Africa is tackling power shortages and poverty. World Economic Forum (2015). <https://www.weforum.org/agenda/2015/02/how-central-africa-is-tackling-power-shortages-and-poverty>. Accessed December 2020
51. Central African Power Pool (CAPP)—Regulatory Sub-committee: terms of reference development of the regional power policy (2011). <https://www.icafrica.org/fileadmin/documents>. Accessed January 2021
52. The Infrastructure Consortium for Africa (ICA): Regional Power Status in African Power Pools Report (2011). <http://www.icafrica.org>. Accessed January 2021
53. Kambanda, C.: International Trade in Sustainable Electricity: Regulatory Challenges in International Economic Law. The African Experience (Ed., Cottier, I. Espa), pp. 156–168. Cambridge University Press (2017). <https://doi.org/10.1017/9781316681275.010>
54. Rose, A., Stoner, R., Pérez-Arriaga, I.: Integrating market and bilateral power trading in the Southern African Power Pool. United Nations University World Institute for Development Economics Research (UNU-WIDER) (2016). <https://doi.org/10.35188/UNU-WIDER/2016/176-5>
55. Pappis, I., Howells, M., Sridharan, V., Usher, W., Shivakumar, A., Gardumi, F., Ramos, E.: JRC Technical Report: Energy projections for African countries. EU Science Hub (2019). <https://ec.europa.eu/jrc>. Accessed December 2020
56. Tchereni, B.H.M.: Greening economic growth in SADC: the role of trade policy (2015). [http://2015.essa.org.za/fullpaper/essa\\_2899.pdf](http://2015.essa.org.za/fullpaper/essa_2899.pdf). Accessed January 2021
57. European Union Energy Initiatives (EUEI): SADC regional energy access strategy and action plan (2010). <https://www.sadc.int/documents-publications/show/SADC>
58. Tinto, E.M., Banda, K.G.: The integrated national electrification programme and political democracy. *J. Energy Southern Africa* **16**(4), 26–33 (2005)
59. Eskom: Free Basic Electricity Policy (2003). <https://www.eskom.co.za/news>. Accessed December 2020
60. South African Department of Minerals and Energy (SA DME): White Paper on the Renewable Energy Policy (2004). [https://www.gov.za/sites/default/files/gcis\\_document](https://www.gov.za/sites/default/files/gcis_document)
61. Edkins, M., Marquard, A., Winkler, H.: South Africa’s renewable energy policy roadmaps. Energy Research Centre, University of Cape Town South Africa (2010). <http://www.erc.uct.ac.za/>
62. Zimbabwe Rural Energy Master Plan: Status review and assessment of barriers to rural energy supply (2015). <https://rise.esmap.org/data/files/library/zimbabwe/Energy>
63. Hall, D., Van Niekerk, S., Nguyen, J., Thomas, S.: Energy liberalisation, privatisation and public ownership (2013). [http://www.world-psi.org/sites/default/files/en\\_psi\\_ru\\_ppp\\_final](http://www.world-psi.org/sites/default/files/en_psi_ru_ppp_final)
64. World Bank/AFD: Africa’s Infrastructure (2010). <http://www.infrastructureafrica.org/>
65. Gabriele, A.: Policy alternatives in reforming energy utilities in developing countries. *Energy Policy* **32**(11), 1319–1337 (2004)
66. Victor, O.E. Aziz, N.A., Jaffar, A.R.: Privatization of electricity service delivery in developing nations: issues and challenges. *Int. J. Built Env. Sust.* **2**(3), 202–210 (2015)
67. Bensch, G.: The effects of market-based reforms on access to electricity in developing countries: a systematic review. *J. Dev. Effect.* **11**(2), 165–188 (2019)
68. Phalatshe, S.: Eskom: Historical background to its current crises. Institute for Economic Justice Working Paper Series, no. 4 (2020)

69. <https://www.trade.gov/country-commercial-guides/nigeria-electricity-and-power-systems>
70. Ahmed, A., Landi, J.H.: Assessment of private sector financing of electricity infrastructure in Nigeria. *J. Econ. Financ.* **1**(5), 13–24 (2013)
71. Olanrele, I.A.: Assessing the effects rural electrification on household welfare in Nigeria. *J. Infrastruct. Dev.* **12**(1), 7–24 (2020)
72. Power privatisation: Ghana case study (2016). <https://www.howwemadeitinafrica.com>
73. Sakyi, K.A.: Public corporation monopolies-case study of sale of electricity company of Ghana. *Adv. Soc. Sci. Res. J.* **6**(4), 148–167 (2019)
74. Global Partnership on Output-based Aid (GPOBA): Expanding electrification to low-income households in rural Ghana with microfinance (2018). <http://documents1.worldbank.org/>
75. Mawhood, R., Gross, R.: Institutional barriers to a perfect policy: a case study of the Senegalese rural electrification action plan. Imperial College Centre for Energy Policy and Technology, pp. 1–27 (2014). <https://www.imperial.ac.uk/media/imperial-college/research-centres-and-groups/icept/Senegal>
76. Gokgur, R., Jones, R.: Privatisation of Senegal electricity: assessing the impact of privatisation in Africa. Imperial College Centre for Energy Policy and Technology, pp. 1–27 (2006)
77. Gualberti, G., Alves, L., Micangeli, A., Graca Carvalho, M.: Electricity privatisations in Sahel: a U-turn? *Energy Policy* **37**(11), 4189–4207 (2009)
78. African Development Bank Group (ADB): Renewable energy in Africa: Mali Country Profile (2015). <https://www.afdb.org>
79. Manneh, M.: Challenges and possible solutions to electricity generation, transmission and distribution in the Gambia. *Am. Int. J. Bus. Manag.* **3**(10), 87–93 (2020)
80. International Trade Administration (ITA): Gambia, the Country Commercial Guide (2020). <https://www.trade.gov/country-commercial-guides/gambia-energy>
81. REEEP Admin: Guinea Bissau (2012). <https://www.reeep.org/guinea-bissau>
82. Karekezi, S., Mutiso, D.: Power Sector Reform: A Kenyan Case Study. Power Sector Reform in sub-Saharan Africa, pp. 83–120. Palgrave Macmillan (2000)
83. Girma, Z.: Success, gaps and challenges of power sector reform in Ethiopia. *Am. J. Mod. Energy* **6**(1), 33–42 (2020)
84. Godinho, C., Eberhard, A.: Learning from power sector reform: the case of Uganda. World Bank Energy and Extractives Global Practice (2019). <http://documents1.worldbank.org>
85. African Development Bank (AfDB) Group: Rwanda Energy Sector Review and Action Plan (2013). <http://www.afdb.org>
86. Ministry of Infrastructure (Mininfra): Rural Electrification Strategy (2016). <https://www.mininfra.gov.rw>
87. Nsabimana, R.: Electricity sector organisation and performance in Burundi. *Proceedings* **58**(26), 1–12 (2020)
88. Oxford Business Group: Djibouti looks to renewable energy to boost self-sufficiency and competitiveness (2016). <https://www.oxfordbusinessgroup.com/>
89. Lukamba-Muhiya, J.M.: The electricity supply industry in the democratic Republic of Congo. *J. Energy Southern Africa* **17**(3), 21–28 (2006)
90. World Bank: Increasing Access to Electricity in the Democratic Republic of Congo: Opportunities and Challenges. World Bank, Washington, DC. <https://openknowledge.worldbank.org/handle/10986/33593>
91. Electricity Sector: Legal and Institutional Framework: Reforms of the Cameroonian Electricity Sector (2021)
92. Mus’ud, A.A. Wirba, A.V. Firdaus, M.-S., Mas’ud, I.A. Munir, A.B., Yunus, N.M.: An assessment of renewable energy readiness in Africa: case study of Nigeria and Cameroon. *Renew. Sustain. Energy* **15**, 775–84 (2015)
93. Ngnikam, E., Hofer, A., Kraft, D.: Renewable energy in West Africa: country chapter, Cameroon. *Fed Minist Econ Coop Dev.* **49**, 38–51 (2009). [https://www.agcc.co.uk/uploaded\\_files/RenewableReports---BMZ.pdf](https://www.agcc.co.uk/uploaded_files/RenewableReports---BMZ.pdf)
94. REEEP Admin. Angola (2012). <https://www.reeep.org/angola-2012>

95. Renewable Energy Law and Regulation in Angola. <https://cms.law/en/int/expert-guides/cms-expert-guide-to-renewable-energy/angola>
96. Patton, C.V., Sawicki, D.S., Clark, J.J.: *Basic Methods of Policy Analysis and Planning*, 3rd ed., p. 480. Routledge (2015). <https://doi.org/10.4324/9781315664736>
97. Fischer, F., Miller, G.J., Sidney, M.S.: *Handbook of Public Policy Analysis: Theory, Politics, and Methods*. CRC Press Taylor & Francis Group (2007). <https://www.routledge.com/>
98. Jansson, B.: *Becoming an Effective Policy Advocate: From Policy Practice to Social Justice*, 8th edn. Cengage Learning, Boston, MA (2017)
99. Stone, D.: *Policy Paradox: The Art of Political Decision-Making*, 3rd edn. W.W.Norton & Company, New York, NY (2012)
100. International Energy Agency (IEA) (2020): *World Energy Outlook 2020*. IEA, Paris. <https://www.iea.org/reports/world-energy-outlook-2020>
101. World Bank Sustainable Energy for All (SE4ALL) (2018). <https://data.worldbank.org/indicator>
102. Food and Agriculture Organization of the United Nations: *The State of Food Insecurity in the World—monitoring progress towards the World Food Summit and Millennium Development Goals* (2003). <https://www.fao.org/3/j0083e/j0083e00.pdf>
103. Dempsey, P.: Load-shedding fallout for South African agriculture. *Farmer's Weekly Magazine* (2019). <https://www.farmersweekly.co.za/agri-news/>
104. Aminu, I., Peterside, Z.B.: The impact of privatization of power sector in Nigeria: a political economy approach. *Mediterranean J. Soc. Sci.* **5**(26), 111–118 (2014)
105. Chisari, O., Estache, A., Romero, C.: *Winners and losers from utility privatization in Argentina: lessons from a General Equilibrium Model*. Policy Research Working Paper Series 1824. The World Bank (1997). <https://ideas.repec.org/p/wbk/wbrwps>
106. Aggrey-Fynn, E., Banini, G., Croppenstedt, A., Owusu-Agyapong, Y., Oduru, G.: *Explaining success in reducing under-nourishment numbers in Ghana*. ESA Working Paper No. 03-10, Agriculture and Economic Development Analysis Division, The Food and Agriculture Organization of the United Nations (2003)
107. Benzekri, N.A., Sambou, J., Diaw, B., Sall, H.I., Ba, S., Guèye, N.F.N., Diallo, M.B., Hawes, S.E., Seydi, M., Gottlieb, G.S.: High prevalence of severe food insecurity and malnutrition among HIV-infected adults in Senegal, West Africa. *PLoS One* **10**(11), e0141819 (2015). <https://doi.org/10.1371/journal.pone.0141819>. PMID: 26529509; PMCID: PMC4631507
108. Tom, S.: Load-shedding very bad news for farmers who irrigate, export (2020). <https://www.foodformzansi.co.za/>
109. Rondolat, E., Holmås, H., Locke, C., Bickersteth, S.: *Scaling up energy access through cross-sector partnerships*. World Economic Forum (2013). <https://www.weforum.org>
110. Electricity Regulatory Authority, *Distribution tariffs* (2018). <https://www.era.go.ug/index.php/distribution-tariffs-link>

# Development of OTP Based Switch System for Power System Infrastructure Security and Personnel Safety



D. Prasad, M. Gopila, G. Suresh, and M. Porkodi

**Abstract** Electricity board in most of the countries is partially automated and the challenges faced due to cyber and infrastructure security must be dealt with to transform the system into fully automated. This work focuses in identifying a comprehensive set of cyber security challenges and need for security at multiple levels of the cyber physical power system mainly infrastructure security and personnel safety. The main challenge faced by electricity board is considered and solved using ICT. The research efforts are taken to ensure the substation and personnel safety using OTPs as they are not vulnerable to cyber-attacks since it will no longer be valid. This OTP concept is being used for electric lineman safety system and infrastructure security. In the conventional system there is a single password which is common and if any misuse leads to electrical accidents to the line man when they are in the maintenance and control of electric line repair. This is due to lack of communication and coordination between the maintenance staff and the electric substation staff. A onetime password based switch is implemented for the opening and closing of relay using Arduino and Proteus for software and hardware control. During natural calamities like flood, rains, and lightning the power system network will be damaged if the line is live. Hence the power system infrastructure security will be enhanced using this OTP method.

**Keywords** Infrastructure security · ICT · OTP · Power system · Arduino · Proteus

---

D. Prasad · M. Gopila (✉) · G. Suresh · M. Porkodi  
Department of Electrical and Electronics Engineering, Sona College of Technology, Salem,  
Tamilnadu, India  
e-mail: [gopilam@sonatech.ac.in](mailto:gopilam@sonatech.ac.in)

D. Prasad  
e-mail: [prasadd@sonatech.ac.in](mailto:prasadd@sonatech.ac.in)

G. Suresh  
e-mail: [sureshg@sonatech.ac.in](mailto:sureshg@sonatech.ac.in)

M. Porkodi  
e-mail: [porkodimp@sonatech.ac.in](mailto:porkodimp@sonatech.ac.in)

## 1 Introduction

India is steadily venturing into renewable energy resources like wind and solar. With such unpredictable energy sources feeding the grid, it is necessary to have a grid that is highly adaptive (in terms of supply and demand) [1]. A good electric supply is one of the key infrastructure requirements to support overall development; hence, the opportunities for building smart grids in India are immense [1]. Electric grids may be the targets for terrorist activity as they are controlled by the computers. Over the last decade, there have been so many schemes for protecting the power system infrastructure including password based circuit breaker by incorporating various technologies. Current state of the art solutions use Arduino based software and hardware for enhancing the security of infrastructure and personnel safety. Electric accident to the personnel is increasing day by day while repairing the line and during the maintenance time. These accidents are caused by the lack of contact between substation authorities with personnel. Eventually, these types of accidents will lead to the loss of personnel's life. The accident may also occur when some substation authority mistakenly turn on the line without noticing whether personnel came down from the line or not. The probability of occurrence is more in the rural areas where the maintenance area is far away from the substation. Hence to reduce this type of accident and to save the life of line man, we go for OTP based switching system.

In the year 2017, Lineman electrocuted while working on pole. A 20-year-old lineman working on a new electricity pole was killed after he was electrocuted on Saturday. On Saturday, one of his instruments got stuck to a live wire when he was working on the installation around 2.30 pm. Nasheeb was instantly electrocuted and got stuck to the line. An eyewitness said he was stuck for around half an hour. Other workers finally managed to switch off the line, and he was taken down. Nasheeb was rushed to the General Hospital in Civil Lines, where doctors declared him brought dead. Two of his colleagues, who were with Nasheeb at the time of the incident, are being questioned by police.

The proposed system gives a way to the mentioned problem to guarantee line man safety. The controlling of the electrical lines of the proposed system lies with line man. The maintenance personnel have to enter the password to open or close the electrical line which is decided by line man during maintenance. In case, any fault is ascertained in electrical line then line man has to open the power supply to the line. This is done by sending OTP to substation. Then he can safely repair the electrical line, and after performing maintenance work, line may be opened through OTP. This type of system is highly authenticated and hence system will be made to operate between on and off the line only when the personnel involved presses the OTP switch at the maintenance area. This type of system will save the life of line man and reduce the faulty accident occur during the maintenance time.

The proposed password operated circuit breaker uses only specified password by authorized person to control the circuit breaker. In the above case there may be a chance of changing the password [2, 3]. In [4], the safety of line man is enhanced with OTP based circuit breaker but is fully operated with microcontroller.

## 2 Existing and Proposed Model

User defined password is used to control the electrical line. The password is used to switching the line as ON or OFF. The main disadvantage of this system is everyone in station knows the password and also any time it could be operated without permission of the line man. In the conventional system the basic concept of generating password in the initial stage of operation is used. The pre-set password may be changed as per the convenience [4].

Figure 1 illustrates the existing model of password operated circuit breaker. In this, the electrical line may be controlled using Android platform. Application is developed with system requirements and using that the person (line man) has to open or close the line as per his convenience. But in this paper, securing the application is challengeable one.

One time password method is frequently used by banking sectors for securing their client transaction and information [5]. The same system is applied here and to make the transmission switching system more secured. By applying this system, it enables to save time during maintenance situation. OTP is send through GSM (Global System for Mobile communication) which confirms security of the line. Receiving end user either uses his mobile phone or GSM, or mostly prefers GSM based receiver.

The proposed system (see Fig. 2) gives a way to the mentioned problem to guarantee line man safety. The controlling of the electrical lines of the proposed system lies with line man. The maintenance staff has to enter the password to open or close the electrical line which is decided by line man during maintenance. In case, any fault

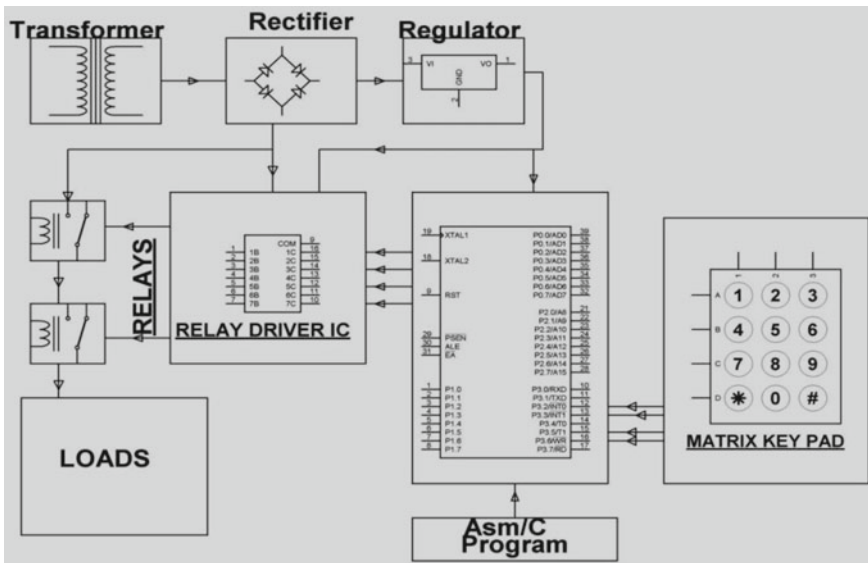
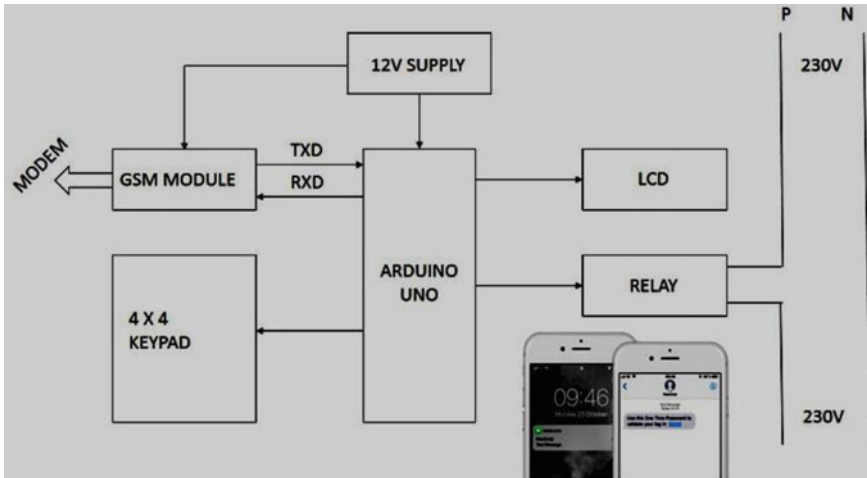


Fig. 1 Existing model of the proposed system





**Fig. 2** Proposed model

is ascertained in electrical line then line man has to switch OFF the power supply to the line [6]. This is done by sending OTP to substation. Then he can safely repair the electrical line, and after performing maintenance work, line may be switched ON through OTP. This system is fully controlled by an advanced Arduino UNO R3 model. Since OTP is to be entered a keypad is linked to the controller. The comparison of OTPs entered and stored is performed in the ROM of the controller. The opening and closing of line is based on the comparison. Once the indicator lamp glows it shows the activation of the switch and vice-versa. The one time password operated switching can also be implemented in other applications like automatic door locking system for improving security and to control electronic appliances to conserve energy [7].

### 3 Tools

Any embedded system requires hardware and software for performing a particular task.

#### 3.1 Hardware Requirements

- Arduino UNO R3
- LCD 16 X 2
- GSM module SIM800C

- Keypad 4 X 4
- Relay module
- 12 V adapter

### 3.2 Software Requirements

The software required for this proposed system are Arduino IDE (for programming Arduino controller) and Proteus (for simulation the system).

## 4 Operation of OTP Switch

For operation of One Time Password based switch, arduino program is written to operate the whole network. For that Arduino IDE is used and is open source which is easily available [8].

The required power supply of the system is 12 V. A 12 V AC—DC adapter is used for supplying the system. The supply is connected in parallel to GSM and Arduino. Using IC7805 relay module is supplied. Power supply for LCD is 5 V and it is supplied by Arduino Power port.

Arduino UNO takes 12 V DC for operation and similarly LCD takes 5 V to display current position of switch. 4 X 4 matrix keypad is used for entering password. The Nomenclature of keypad is as follows,

C stands for OTP for line open,

D stands for OTP for closing line,

A stands for password check for OTP line open,

B stands for password check for OTP closing line,

Similarly, \* stands for resetting the key.

As per setting in keypad based on written program, the line man wants to open the line to work, he should press “C” key on keypad. The controller generates 6 digits different code. The generated code is now sent to substation using GSM. The process of sending message by GSM is controlled by “AT” command in Arduino program.

Above code is used for the system. Instead of xxxx... we can replace it by 10 digit mobile number. The receiver after receiving the OTP, he will be entering the password using keypad and it is displayed by LCD [9]. After entering OTP, he will be pressing “A” key in keypad. The controller checks the password and send command to relay for opening the line. Actually relay consumes 5 V which is supplied by adapter and using IC7805, regulate the voltage into 5 V.

Initially the relay state is Normally Closed position, after receiving command from controller, now relay change the states to Normally Opened position [10]. So line will be open. Now the line man work as he wish and finishes his work, press “D” key in keypad. Now the controller generates OTP for closing the line. Similarly the generated OTP send to receiver side which means substation.

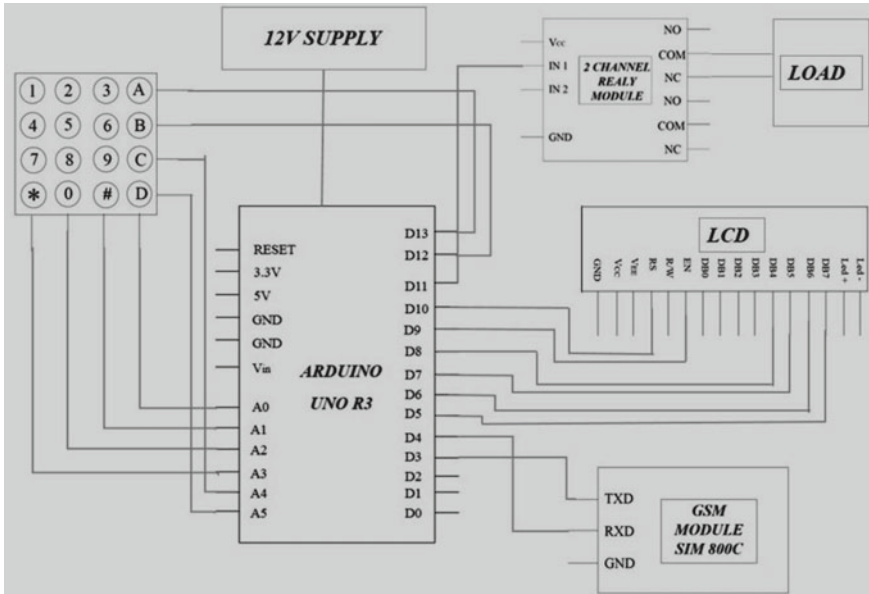


Fig. 3 OTP switch circuit diagram

## 5 Software Results and Discussion

### 5.1 Software Results

Figures 4, 5 is the simulation result of line in normal and open position. In Fig. 4, 230 V supply is connected across the relay. In normal condition, relay is in normally closed (NC) position. Hence the lamp is glowing (for indication). In real time, Single phase line or three phase line is connected across the relay. The flow of current in the line is indicated by LCD and is connected to any of the output pins of Arduino [11].

After entering OTP for opening the line, now the relay will change the position to normally closed (NO). It is indicated by the lamp (lamp isn't glowing) which is connected in the above Fig. 5.

## 6 Hardware Results and Discussion

Figures 3, 4, 5, 6, 7 explains the different hardware result of the proposed system.

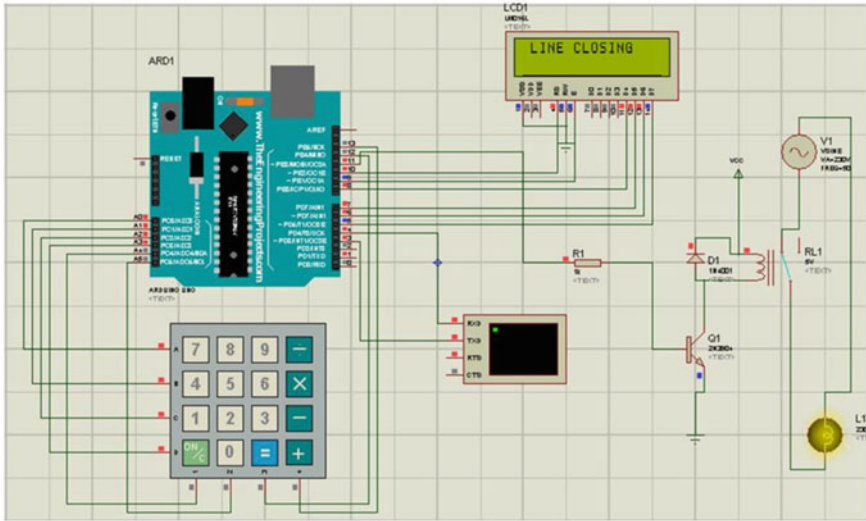


Fig. 4 Line in normal position (software)

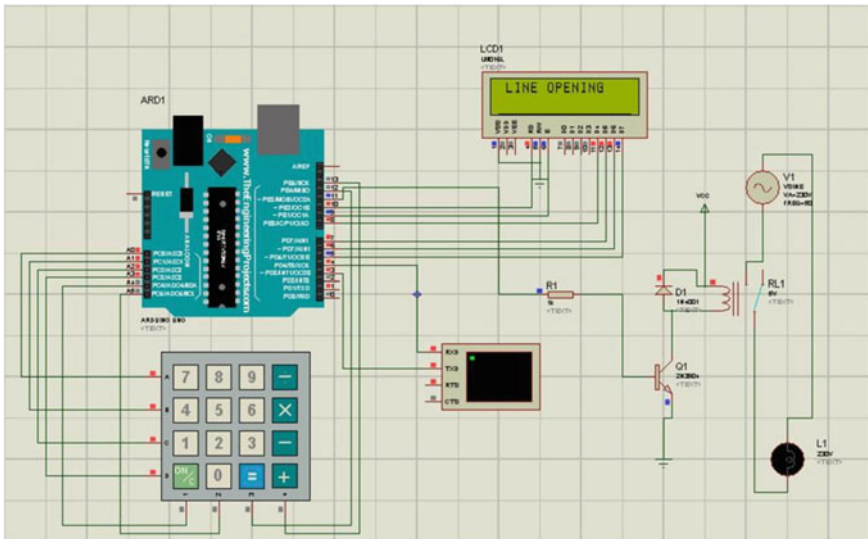
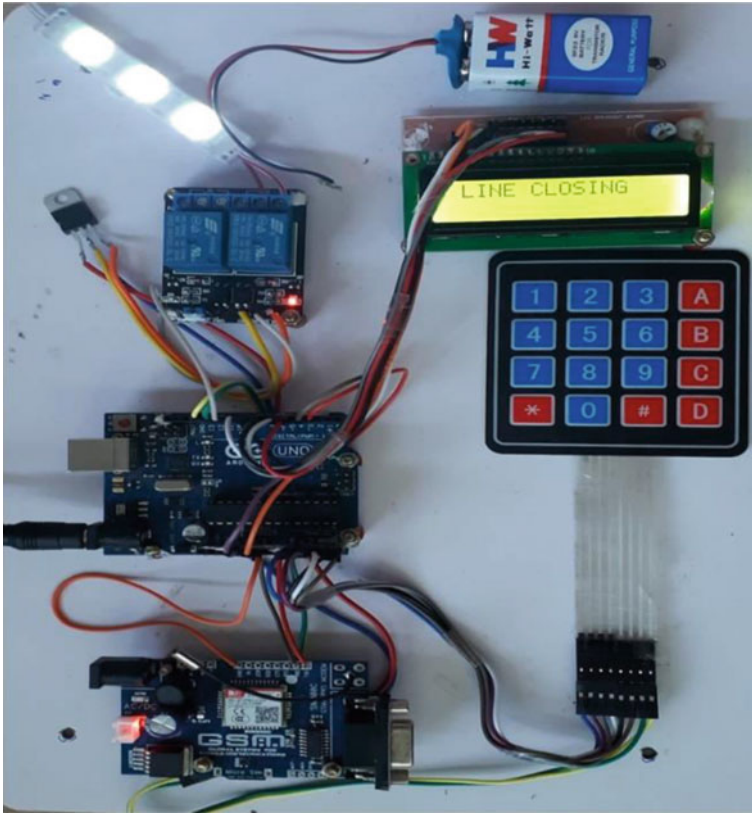


Fig. 5 Line in normal open (software)



**Fig. 6** Line in normal position (Hardware)

### ***6.1 Line in Normal Position***

Initial stage of system is in normal state, which means in closed circuit. Now the lineman wants to work on the line. So, he will send the OTP message to substation to open the line [12].

### ***6.2 Line in Open Condition***

During the maintenance time, lineman will press the OTP switch and the OTP will be generated. The generated OTP will be sent from the fault area to the substation through GSM module [13]. After receiving the OTP sent by the lineman, power station authority member will enter the received OTP in the keypad and check for matching conditions [14]. If condition satisfies, relay will trip the circuit (Fig. 8).



Fig. 7 Line in normal position (Hardware) showing OTP message

### 6.3 OTP Message for Closing the Line

After completing his work, lineman have to switch ON the line. For that he will send the OTP message to substation [15]. After receiving the OTP, now the line will be closed as normal (Fig. 9).

Figure 10 shows that the line has come back to its normal position (closed circuit). This OTP based switching system works on when line needs to be opened or closed.

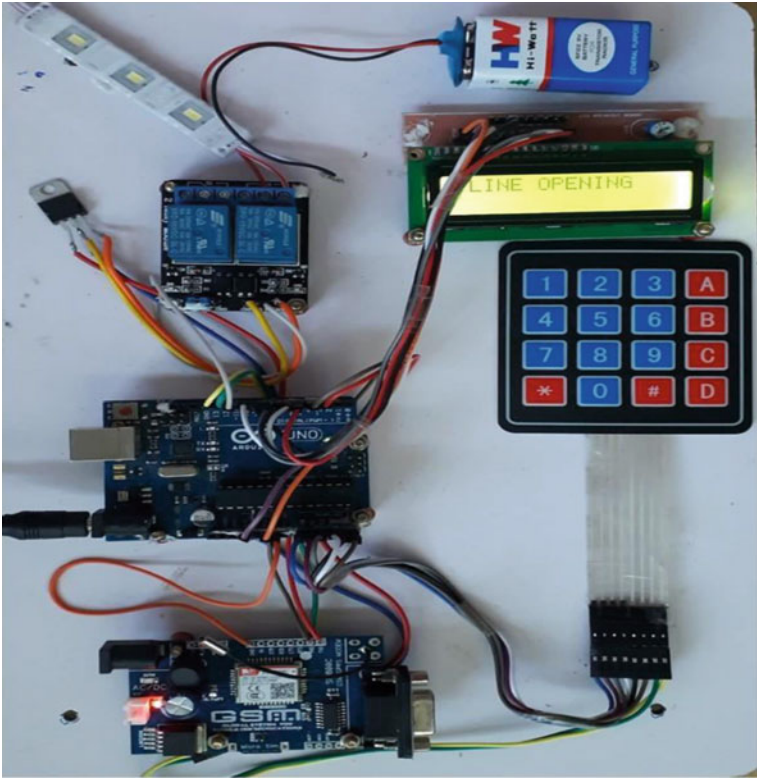
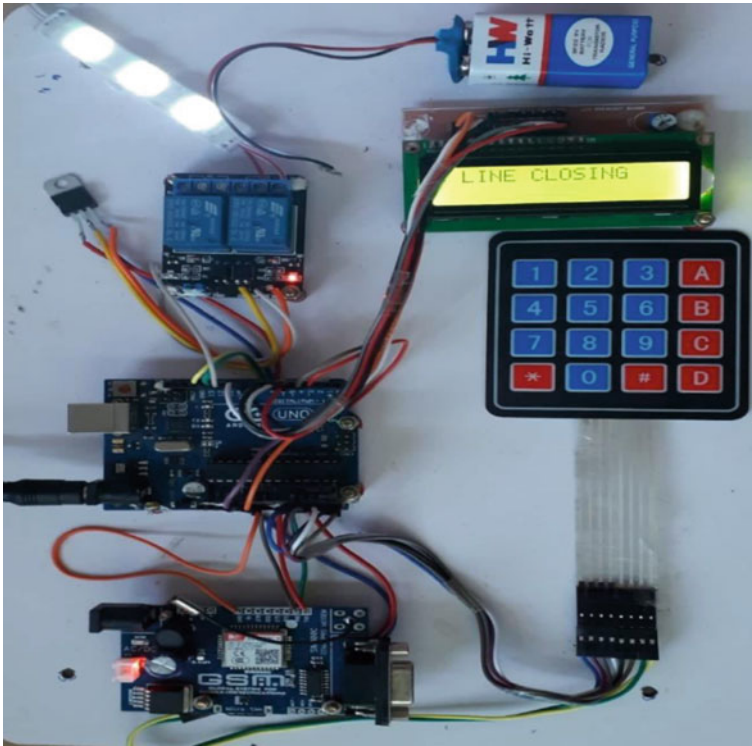


Fig. 8 Line in open (Hardware)



Fig. 9 Line in open (Hardware) with OTP message





**Fig. 10** Line reset to normal closed position

## 7 Conclusion

The OTP based switching system is designed to control the power system electric grid with help of a password only. The infrastructure utility and components threat can be secured by sending a onetime password as it elapses within short duration thus avoiding the stealing of passwords. Generating OTP and verifying it are the key features of this system. This technology improves the security of the system and minimizes the accidents and destructions of both the lineman due to electric shock and line during the maintenance. The main challenge of password misuse is rectified in this system as it is mainly based on one time password. The power system infrastructure is secured from any natural calamities especially during heavy rain and wind. If the line is live there may be chances of short-circuit or damage to power system devices and it leads to blackout if it's not isolated. Hence the power system will be secured by sending OTP to substation staff for opening the line during natural calamities.

## 8 Challenges and Opportunities

The main challenges to be faced are social attacks which are increasing due to the technological advancements such as artificial intelligence and deep learning. Modeling interdependencies is another challenge for the infrastructure security as they are prone to digital vulnerabilities. The opportunities are the latest technology like Arduino along with Proteus software which made the challenges to be overcome especially for Industrial control system type of infrastructure as in our electrical grid.

## References

1. Navneet, G., Apurva, J.: Smart Grids in India. A newsletter of ministry of new and renewable energy. <https://mnre.gov.in> (2011)
2. Mane Kirti, M., Attar Arifa, U., Dandile Aishwarya, A., Ghogale Pragati, S., Prof. Jagtap Sujit, P.: Password based circuit breaker. *Int. J. Res. Appl. Sci. & Eng. Technol. (IJRASET)*. 6(4): pp. 2229–2233 (2018)
3. Murari, P.M., Kinnerkar, M.V., Koppa, P.S., Kamble, V.S., Mendan, R.R.: Electric line man safety with password based circuit breaker and intimation of wire sag using GSM. *Int. J. Sci. Dev. Res.* 2(7), 111–116 (2017)
4. Athira P Nair, Josephin J, Anjana A S, Athira C P and Sebin J Olickal Electric line man safety system with OTP based circuit breaker. *Int. J. Res. Eng. Technology*. 4 (3): pp. 23 -26 (2015)
5. Leo, L.: Working principle of arduino and using it as a tool for study and research. *Int. J. Control., Autom., Commun. Systems*. 1(2), 21–29 (2016)
6. Ma May Zin Oo, Dr.Nay Win Zaw, Daw Khin San Win, SMS Alarm System for Weather Station using Arduino and GSM. *Int. J. Trend Sci. Res. Development*. 2(5): pp. 1903–1907 (2018)
7. Siddharth.: Interface 4x4 Matrix keypad with Microcontroller. *Embed Journal*. <https://embedjournal.com>. (2013)
8. Genis Marfa Martinez. 2- Channel Relay module. Summerfuel Robotics. <https://sites.google.com>
9. Gopila, M., Prasad, D.: Machine learning classifier model for attendance management system, In: 2020 Fourth International Conference on I-SMAC (2020)
10. Suresh, G., Prasad, D., Gopila, M.: An efficient approach based power flow management in smart grid system with hybrid renewable energy sources, renewable energy focus, 2021, ISSN 1755–0084, <https://doi.org/10.1016/j.ref.2021.07.009> (2021)
11. Gopila, M, Gnanambal, I.: Detection of inrush and internal fault in power transformers based on bacterial foraging optimization, *J. Sci. Ind. Res.*, Jan-2017, pp. -32–37, <http://nopr.niscair.res.in/handle/123456789/39297> (2017)
12. Shivakumar, R., Yamuna, K.: A novel Nature-Inspired improved grasshopper Optimization-Tuned Dual-Input controller for enhancing stability of interconnected systems, *J. Circuits, Syst. Comput.* 30(8), pp. 1–18, 2021. ISSN: 1793 6454, <https://doi.org/10.1142/S0218126621501346>, *SCI Journal—Impact Factor: 1.333* (2021)
13. Santhakumar, C., Shivakumar, R., Bharatraja, C.: A Pulse width modulation for PV connected Diode assisted Z source NPC- MLI to obtain High voltage Gain, *J. Electr. Eng.*, 17, Edition 4, pp. 290–297, 2017. <http://jee.ro/articles/WV1484300103W58789f47cbc90.pdf> (2017)

14. Shivakumar, R.: Implementation of an innovative cuckoo search optimizer in multimachine power system stability analysis, *J. Control. Eng. Appl. Inform.*, **16**(1), pp. 98–105, 2014. SCI Impact Factor: 0.338 (2014)
15. Shivakumar, R., Panneerselvam, M.: Stability analysis of multimachine thermal power systems using nature inspired modified cuckoo search (2014)

# **Concepts and Innovative Applications of Intelligent Systems and Technologies**

# Artificial Neural Net Based Performance Index for Voltage Security Assessment



Shubhranshu Kumar Tiwary, Jagadish Pal, and Chandan Kumar Chanda

**Abstract** A novel, uncomplicated and cursory process of transmission line outage analysis and evaluation for voltage security assessment is developed for real-time power system monitoring applications. The implied approach uses the bus voltage magnitudes to develop artificial-neural-network models to monitor the bus voltages in the power network and provide outputs in binary form signifying the power network state. These models of developed neural networks can then monitor the bus voltage magnitudes in real-time, to minimize the time taken in decision making process for the power system control operations. The binary outputs of the monitoring neural net are utilized to calculate an index to determine the state of the voltage security of the power network-grid, proposed in this papers work. The proposed approach was applied to a test bus system and a government-owned utility. The results are compared with the traditional method of voltage security assessment and ranking. The results testify that the proposed method will furnish good precision and interpretability with faster response and are apt for on-line voltage security assessment. The utilization of advanced computers with good memory reduces time consumption and provides results within 9 min. Also, the critical contingencies can be detected in a matter of seconds.

**Keywords** Artificial Neural Networks · Performance indexing · Static security · Voltage security · Voltage stability

## 1 Introduction

With the power-grids all over the world, transitioning from the under-developed category to developing category and developing category to developed category, the electricity demand in these countries is also skyrocketing. The utility networks in such

---

S. K. Tiwary (✉) · J. Pal · C. K. Chanda

Department of Electrical Engineering, Indian Institute of Engineering Science and Technology  
Shibpur, PO Box 711103, Howrah, West Bengal, India

e-mail: [mailshubh2005@gmail.com](mailto:mailshubh2005@gmail.com); [mail\\_shubh.rs2014@ee.iiests.ac.in](mailto:mail_shubh.rs2014@ee.iiests.ac.in)

countries are compelled to operate with smaller security margins [1]. The generation, transmission and distribution systems are constrained to operate much closer to their design limits which puts the power system at risk. Developing system specific rules and regulations to keep the power network in check is becoming progressively difficult [2].

Machine learning can serve as a better alternative to perform computationally demanding recursive functions and operations. Machine learning has been used in the field of power system and its associated fields of security and control [3, 14]. A large number of training samples collected from recorded data and simulation results of off-line studies can be used to train artificial neural networks (ANN's) to perfection, with minimum error [28]. On-line Phasor Measurement Unit (PMU) analysis has been used in conjunction with machine learning methods for security analysis of a power network [12]. Machine learning can provide superior computational adeptness and depiction [29]. To train and develop ANN's, good quality and appropriate quantity of learning samples with minimum noise is essential. Essential feature extraction methods are the basis of machine learning applications like decision trees [32], optimized training [29, 31] and k-nearest neighbour methods [32].

Since the 1980's machine learning has been applied to the various fields of power network control. It has been shown by Konatantelos et al. in [28], how the stability limit of transmission corridors at the Hydro-Québec power system has been improved using ANN's. There are many other similar research available that validate the real-time applicability of the neural networks to the power network security analysis procedures [8–10]. The traditional method of security assessment is to perform contingency studies in an EMS (energy management system) to find the consequences of (unscheduled) equipment outage [19–21] and this process is allotted up to 15 min in a real-time power network [4].

The contingency analysis and ranking process of a power network is the most time-consuming routines of the security assessment procedure. In this paper, a novel method to perform real-time contingency analysis and ranking method is proposed. The proposed method can reduce the time-consumption by 40%. The suggested method can provide quick response to severe contingencies in a real-time power network [16]. For accumulating training data for the proposed method, voltage magnitude data on buses are considered, historical records of voltage magnitude deviation from standard values and data based on scheduling and load-forecast are also taken in to account [11, 13, 15], index [35]. These data are then used for development of the ANN's to monitor the voltage at buses and provide outputs in binary form signifying the state of the network. These binary outputs are used here to develop a new indexing method, recommended in this work.

This paper has 5 sections. Section 1 introduces the work. Section 2 reviews traditional voltage security assessment method. In Sect. 3, the ANN based voltage security assessment method is proposed and elaborated. In Sect. 4, two case studies are provided with comparison to the traditional methods. Section 5 ends the paper with some insight into the work, followed by acknowledgments, appendices and references.

## 2 Networks Studied and MDNN Development

Traditional power system voltage-security-assessment includes contingency-analysis, ranking, selection, and evaluation as shown in Fig. 1.

The dilemma of voltage security has been a crucial factor affecting security and restricting transmission capacities of power network [5]. There are many examples of severe blackouts which researchers have attributed to voltage security and voltage collapse. Voltage collapse customarily transpire on power networks that are dangerously loaded, depleted by transmission interruptions, or exposed to reactive power deficit [33]. To identify the status of the power network after a disturbance, we usually perform voltage security studies. Newton–Raphson Load Flow program was used in this work to perform voltages security studies.

### 2.1 Voltage Security

Following the upset which leads to voltage issues, die down and the steady operational state is attained, the voltage profile analysis of the power network is performed. Power flow studies are the means to appraise the voltage-security of power network. Voltage magnitude for each contingency at all the buses can be computed by power flow studies. Voltage severity a power line is calculated using Voltage Performance Index (PIv). Larger the value of PIv, higher the voltage severity. The descending order of the voltage ranked list gives decreasing order of voltage severity of the line. Appropriate control and response are needed to be performed for most detrimental cases to restore the regular voltage profile of the network. The operator in control centres can then interpret proper control action based on the voltage-ranked-list.

### 2.2 Voltage Performance Index

Voltage security based on the severity of line outages is calculated using performance index for voltage magnitude, PIv, [21] as given in (1) below.

Fig. 1 Components of voltage security assessment



$$PI_V = \sum_{i=1}^{NB} \frac{W_{Vi}}{2n} \left( \frac{|V_i| - |V_i^{sp}|}{\Delta V_i^{lim}} \right)^{2n} \quad (1)$$

where,

$|V_i|$  = voltage-magnitude (calculated) at bus  $i$ .

$|V_i^{sp}|$  = standard voltage-magnitude at bus  $i$ .

$\Delta V_i^{lim}$  = voltage discrepancy limit.

$NB$  = number of (load) buses in a network.

$n$  = total number of lines out of service.

$W_{Vi}$  = Weighting-coefficient of bus  $i$ .

The index generated using (1), is used to compare the results of the ANN based indexing.

### 3 Sample Size Generated and Training Methodology

The traditional voltage security assessment has some drawbacks, that have been pointed out and lamented upon by researchers in the field of electrical engineering. Usually, the impact of a line outage is measured in terms of variation in bus voltage magnitude at buses. The whole method is a mathematical process which is robust, but very calculation intensive and time-consuming (as explained in preceding section) for real-time purposes. In this research work, a much simpler ANN-based calculative approach is recommended, which can reduce the time consumption for contingency-analysis and contingency-ranking by up to 40 percent.

In this new proposed approach, all the buses in the power network are monitored using dedicated supervised learning ANN's for each bus. The ANN's are trained to provide simple, binary output of 0 (specifying secure operational state of the power network) and 1 (specifying insecure operational state of the power network). Using these binary outputs, a new indexing method is developed which is elaborated in the following subsection.

In the proposed method, a knowledge base concerning maximum and minimum voltage fluctuation on a particular day in a particular season in previous years are considered [18]. Depending upon the specific operational standards of the grid under consideration, stable operational ranges of the voltage magnitude are ascertained [17]. Taking the upper and lower limits of the above-mentioned range as the secure state of voltage magnitude and the voltage magnitude outside the aforementioned range as insecure, the supervised learning ANN's are developed for monitoring each bus individually.



### 3.1 ANN Based Voltage Security

In the separate ANN monitoring mode, separate, single, dedicated ANN's are used to monitor all the buses individually [22]. The ANN's are simple, with one input node, three hidden node and one output node, in each of the ANN's. Here, the training data spans all critical scenarios and normal scenario, as well. The total numbers of the ANN's will be same as the number of buses to be monitored [23]. The separate ANN monitoring mode is represented as in Fig. 2.

As can be seen from Fig. 2. above, each bus is monitored using a dedicated ANN. Also, as described earlier, each ANN provides a binary output, i.e., 0 (meaning secure state) and 1 (meaning insecure state). These binary outputs can be used to develop an index, that can provide the severity of a line outage and its effect on a particular bus's voltage magnitude [36, 37]. The equation shown in diagram is as proposed below in (2).

$$NI_V = \frac{1}{NB} \sum_{i=1}^{NB} (W_i ANN_i + e_i) \tag{2}$$

where,

$NI_V$  = Neural Net Voltage Index.

$ANN_i$  = output of ANN monitoring bus  $i$ .

$NB$  = Total number of buses to monitored.

$i$  = Counter.

$W_i$  = Weightage given to bus  $i$  defining its criticality.

$e_i$  = Term for Erroneous Classification during  $N_i$  training.

Since, the ANN is trained to provide binary classifications of the states of the network, as explained previously, an error term is added to the results to compensate for the erroneous classification, if the accuracy during training is not 100%. This error term is usually significant when the error percentage during ANN training is large. The 'e<sub>i</sub>' term represents the cross-entropy-loss for binary classifications and is determined using the equation provided below.

$$e_i = -(g \log q + (1 - g) \log(1 - q)) \tag{3}$$

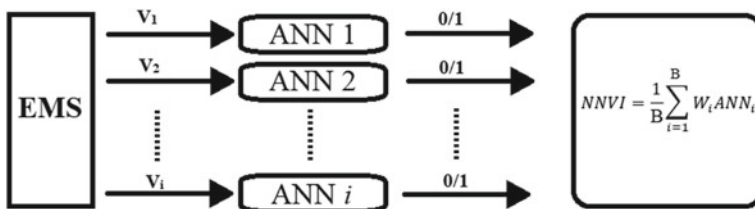


Fig. 2 ANN's monitoring voltage magnitude at buses

where  $g$  = binary indicator (either '0' or '1') if class marker 'x' is the correct classification for observation 'y';  $q$  = predicted probability that observation 'y' is of class 'x';  $\log$  = natural logarithm.

In this method, the output of all the ANN's, monitoring each line is summed up and divided by the total number of transmission lines, during the event of any contingency. The weighting coefficient signifies priority of any line and its corresponding value may be changed depending on the preferences of the power system operator at the dispatch centre. The whole process of the ANN-based security assessment method can be explained with the help of Fig. 2.

Using the above equation, the effect of each contingency on the voltage security and stability of the system can be quantified much faster than the traditional method [7, 38, 39]. The application of the above method has been tested and verified on the IEEE-14 bus standard system and the Damodar Valley Corporation's, DVC-46 bus utility system, as elaborated in the following sections.

## 4 Case Studies and Application

The above elaborated traditional and proposed methods of system security was performed on two power networks. The first test was on an IEEE 14-Bus standard system and the second test was on a real-time power network of Damodar Valley Corporation's DVC-46 bus system. In both cases the traditional load-flow method-based voltage security was performed first, followed by the proposed ANN based method. Thereafter, the time taken for the ANN based indexing method is provided [25].

### 4.1 IEEE 14 Bus Standard Network

The IEEE-14-bus test network is as represented in Fig. 3, below.

#### Traditional Voltage Ranking

The contingency-analysis for the IEEE-14-bus academic network is performed as elaborated through Sect. 2. The performance index and ranking are calculated based on (1) and is given in as Table 1.

The ranking is used as a reference to compute the error in the proposed method.

#### Proposed ANN-Based Voltage Ranking

Then, the ANN based contingency analysis method is performed. In this case, as mentioned previously, all bus voltage magnitudes are monitored by dedicated and specifically trained ANN [24]. These ANN's provide binary outputs, where 0 means secure state of power flow and 1 means insecure state of power flow [26, 27]. When the bus voltage magnitude is within the secure range of operational standards, the

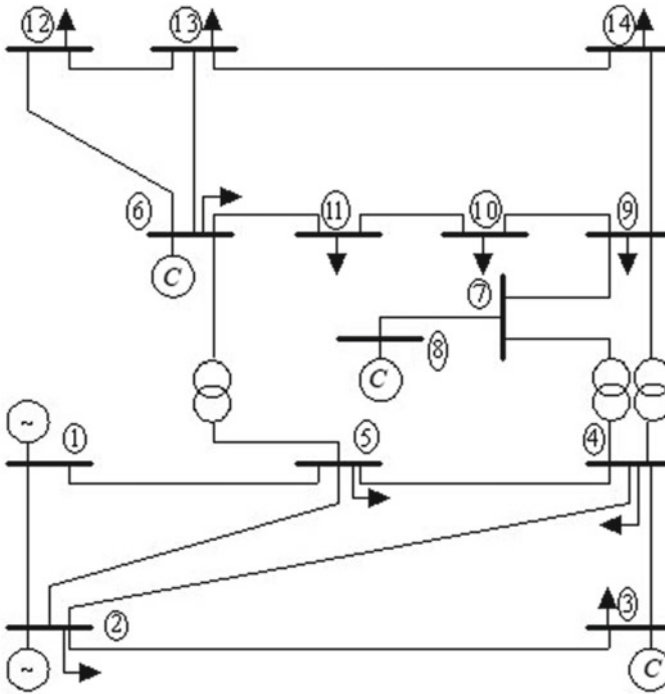


**Fig. 3** Line diagram of IEEE-14 Bus Network

**Table 1** Traditional ranking of IEEE-14 bus academic system

Rank	Line no	PI <sub>V</sub>	Rank	Line No	PI <sub>V</sub>
1	17	11.075	11	5	0.1803
2	3	5.7032	12	19	0.1511
3	16	3.8314	13	4	0.0892
4	15	2.3932	14	8	0.0632
5	20	1.8421	15	13	0.0601
6	14	0.5432	16	6	0.0353
7	12	0.3181	17	7	0.0283
8	9	0.2397	18	2	0.0161
9	1	0.2385	19	11	0.0142
10	18	0.1881	20	10	0.00

ANN classifies it as 0, otherwise 1. If in the event of contingency of any line, the bus voltage magnitude fluctuates in to the insecure range, its corresponding ANN acknowledges the state immediately. These ANN outputs can then be used to comprehend mathematically the state of the voltage stability and security of the power network immediately by using (2) as elaborated in Sect. 3. The outcome of the ANN based bus voltage security (contingency) analysis for the network of IEEE-14-bus network has been shown below in as Table 2.

As shown above, the ANN based ranking of the lines is arranged in decreasing order. Here, the closer the value of  $NI_V$  to 1 the more critical is the line to voltages security and the closer the value of  $NI_V$  to 0 the more non-critical is the line. The ANN based ranking is also almost exactly same as the traditional voltage ranking and takes much less time to generate the results. The time taken to attain the outcome is shown in as Table 3.

From Table 3, it can be deduced that the whole process of ANN-based contingency analysis and voltage ranking can be completed in a little under 7 min for the IEEE-14 bus network. And from the outcome of the voltage ranking of the power network, it can also be seen that the ANN-based ranking correctly specifies 90% of all contingency cases including critical ones. It may be noted here that the actual time taken for identifying line outages and detecting critical cases which is the main aim of the traditional security assessment procedure is completed within 13 s.

**Table 2** ANN based ranking of IEEE-14 bus academic system

Rank	Line no	$NI_V$	Rank	Line no	$NI_V$
1	17	11.075	11	5	0.29
2	3	5.7032	12	19	0.21
3	16	3.8314	13	4	0.14
4	15	2.3932	14	8	0.07
5	20	1.8421	15	13	0.07
6	14	0.5432	16	6	0.0
7	12	0.3181	17	7	0.0
8	9	0.2397	18	2	0.0
9	1	0.2385	19	11	0.0
10	18	0.1881	20	10	0.0

**Table 3** Time taken to obtain results by ANN based ranking

	Knowledge base development	Generating training data (all lines)	Training and ANN development	Identification of and calculate
Step				
Time	142 s	122 s	110 s	13 s

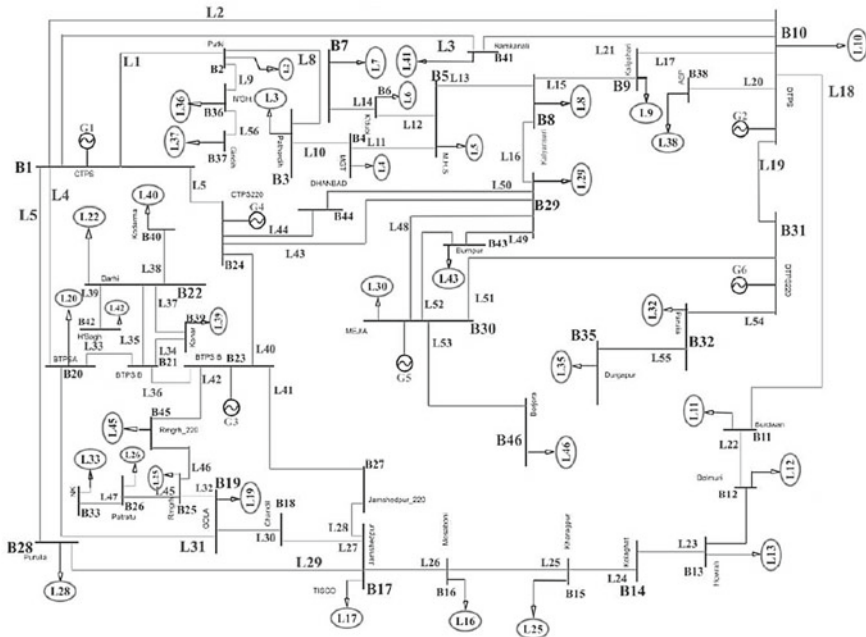


Fig. 4 Line diagram of DVC-46 bus network

### 4.2 Damodar Valley Corporation’s 46 Bus Network

The DVC 46 bus real world utility network of the Damodar Valley Corporation of India is as represented in Fig. 4.

#### Traditional Voltage Ranking

The contingency analysis for the Damodar Valley Corporation’s, DVC-46 bus 56-line utility network is performed as elaborated through Sect. 2. The performance index and ranking are calculated based on (1) and the list is given in as Table 4.

Here as well, the time taken for calculating the  $PI_V$  value for each contingency is recorded for comparison with the ANN based indexing method.

#### Proposed ANN Based Voltage Ranking

Next, the ANN based contingency analysis is performed for DVC-46 bus grid system. In this case also, all bus voltage magnitudes are monitored by dedicated and specifically trained ANN. These ANN’s provide binary outputs, as explained previously. When the bus voltage magnitude is within the secure range of operational standards, the ANN classifies it as 0, otherwise 1. The outcome of the ANN based bus voltage security (contingency) analysis for the network grid of DVC-46-bus-system has been shown below in as Table 5.

**Table 4** Traditional ranking of DVC-46 bus system

Rank	Line no	$PI_V$	Rank	Line no	$PI_V$
1	12	24.84	29	6	12.72
2	45	23.02	30	54	12.31
3	18	21.88	31	24	12.23
4	3	19.84	32	43	7.36
5	32	19.51	33	33	7.32
6	41	18.92	34	17	7.12
7	27	18.64	35	46	7.11
8	8	18.21	36	10	7.09
9	50	17.94	37	49	6.89
10	16	17.81	38	1	6.84
11	53	17.42	39	11	5.12
12	30	17.41	40	36	4.83
13	29	17.33	41	2	4.75
14	42	17.30	42	34	3.82
15	48	17.28	43	52	3.37
16	9	17.25	44	26	2.91
17	44	17.21	45	37	2.55
18	28	17.16	46	7	0.45
19	31	17.14	47	47	0.37
20	40	17.12	48	23	0.34
21	19	17.10	49	20	0.28
22	51	16.94	50	14	0.15
23	15	16.81	51	38	0.1
24	4	15.76	52	39	0.02
25	21	15.52	53	22	0.0
26	25	15.11	54	54	0.0
27	13	12.84	55	55	0.0
28	5	12.81	56	56	0.0

As shown above, the ANN-based ranking of the lines is organized in decreasing order. Here as well, the closer the value of  $NI_V$  to 1 the more critical the line to voltages security, and the closer the value of  $NI_V$  to 0 the more non-critical is the line. The ANN-based ranking is also almost the same as the traditional voltage ranking and takes much less time to generate the results. The comparisons between the time taken to attain the outcome are shown in Table 6.

From Table 6, it has been observed that even in the case of a utility grid of DVC-46 bus system, the whole process of ANN based contingency analysis and ranking can be completed in less than 9 min. And from the results of the ranking of the power

**Table 5** ANN based ranking of DVC-46 bus system

Rank	Line no	NI <sub>V</sub>	Rank	Line no	NI <sub>V</sub>
1	12	1.00	29	6	0.47
2	45	0.98	30	35	0.45
3	18	0.96	31	24	0.43
4	3	0.93	32	43	0.41
5	32	0.91	33	33	0.39
6	41	0.89	34	17	0.37
7	27	0.87	35	46	0.35
8	8	0.85	36	10	0.33
9	50	0.83	37	49	0.32
10	16	0.80	38	1	0.30
11	53	0.78	39	11	0.28
12	30	0.76	40	36	0.26
13	29	0.74	41	2	0.24
14	42	0.72	42	34	0.22
15	48	0.71	43	52	0.19
16	9	0.71	44	26	0.17
17	44	0.69	45	37	0.15
18	28	0.67	46	47	0.13
19	31	0.65	47	7	0.11
20	40	0.63	48	20	0.10
21	19	0.61	49	23	0.08
22	51	0.59	50	14	0.06
23	15	0.58	51	38	0.04
24	4	0.56	52	39	0.02
25	21	0.54	53	22	0.0
26	25	0.52	54	54	0.0
27	13	0.5	55	55	0.0
28	5	0.48	56	56	0.0

**Table 6** Time taken to obtain results by ANN based ranking

	Knowledge base development	Generating training data (All lines)	Training and ANN development	Identification of and calculate
Step				
Time	160 s	163.4 s	168.8 s	13 s

LO, Line Overloads; CC, Critical Contingencies

network, it can also be seen that the ANN based ranking correctly specifies 97% of all contingencies (including critical/severe contingencies) and correctly ranks them. It may be noted here, that the actual time taken for identifying line outages and detecting critical cases, which is the main aim of traditional security assessment procedure, is completed within 13 s using the novel proposed method. The results achieved in such short time prove the effectiveness of the proposed method for real-time/on-line applications to power system studies [34].

### 5 Comparisons Between the Methods

The comparison between the traditional and the ANN based rankings, for the IEEE-14-Bus network is shown in as Table 7.

Here, the ranking of the lines based on the two methods have been compared. As can be seen from the table above that 90% of all contingencies have been correctly ranked using the ANN ranking method. There are only two misclassifications, but they can also be properly ordered by using the binary-cross-entropy loss-function as described in (3).

Similarly, the ranking comparison for the DVC-46 bus system is shown in as Table 8.

Here as well, the ranking of the lines based on the two methods have been compared. As can be seen from the table above that 93% of all contingencies have been correctly ranked, using the ANN ranking method. There are only 4 misclassifications, but they can also be properly ordered by giving proper bias to the ANN’s monitoring those lines or alternatively by adding the binary-cross-entropy loss-function as elaborated in (3).

**Table 7** ANN based ranking of IEEE-14 bus academic system

Rank	Pl <sub>v</sub> line no	Nl <sub>v</sub> line no	Mismatch	Rank	Pl <sub>v</sub> line no	Nl <sub>v</sub> line no	Mismatch
1	17	17	CR	11	5	5	CR
2	3	3	CR	12	19	19	CR
3	16	16	CR	13	4	4	CR
4	15	15	CR	14	8	8	CR
5	20	20	CR	15	13	13	CR
6	14	14	CR	16	6	6	CR
7	12	12	CR	17	7	7	CR
8	9	9	CR	18	2	2	U1
9	1	1	CR	19	11	11	D1
10	18	18	CR	20	10	10	CR

Here, CR = Corrected Ranking; U1 = Upward shift by 1 position; D1 = downward shift by 1 position



**Table 8** ANN based ranking of DVC-46 bus system

Rank	Pl <sub>v</sub> line no	Nl <sub>v</sub> line no	Mismatch	Rank	Pl <sub>v</sub> line no	Nl <sub>v</sub> line no	Mismatch
1	12	12	CR	29	6	6	CR
2	45	45	CR	30	35	35	CR
3	18	18	CR	31	24	24	CR
4	3	3	CR	32	43	43	CR
5	32	32	CR	33	33	33	CR
6	41	41	CR	34	17	17	CR
7	27	27	CR	35	46	46	CR
8	8	8	CR	36	46	46	CR
9	50	50	CR	37	49	49	CR
10	16	16	CR	38	1	1	CR
11	53	53	CR	39	11	11	CR
12	30	30	CR	40	36	36	CR
13	29	29	CR	41	2	2	CR
14	42	42	CR	42	34	34	CR
15	48	48	CR	43	52	52	CR
16	9	9	CR	44	26	26	CR
17	44	44	CR	45	37	37	CR
18	28	28	CR	46	7	7	CR
19	31	31	CR	47	47	47	CR
20	40	40	CR	48	23	23	CR
21	19	51	CR	49	20	20	CR
22	51	51	CR	50	14	14	CR
23	15	15	CR	51	38	38	CR
24	4	4	CR	52	39	39	CR
25	21	21	CR	53	22	22	CR
26	25	25	CR	54	54	54	CR
27	13	13	CR	55	55	55	CR
28	5	5	CR	56	56	56	CR

## 6 Conclusions

The new concept of ANN based indexing to be used in place of the traditional voltage security assessment method was introduced and an inclusive scheme for its development and application has been proposed in this paper. The application and its results were corroborated in two case-studies. The primary case analysis was using an academic-test-bus power network, that can be easily replicated and the second situation analysis was using a real-time utility network grid of DVC-46-bus-system (operated as Public Sector Enterprise under the Government of India). The results

testify the feasibility that the proposed method will provide results in less than 9 min for real-world applications. Also, the results suggest that the method provides reasonably accurate results for practical on-line/real-time security assessment in power network security control.

The important objective as well as methodologies of the assorted modules and methods proposed in this paper are as mentioned below.

- Development criteria of the ANN’s based on recorded and load forecast data, hence the margin for error is low;
- Feasibility for the real-time application and development of ANN’s (as is evident from Tables 3 and 6);
- The whole process of evaluation and selection of critical contingencies is completed in less than 10 min, which again proves the real-time applicability.
- The total time taken for computation of critical contingencies is reduced by 40% compared to the traditional method, as is evident from Tables 3 and 6;
- The output provided by the ANN’s binary in nature, hence the calculation required for finding the critical cases can also be quickly verified manually by the power system operators;
- An error term is also included in the proposed indexing to compensate for the erroneous classifications of the ANN’s if they do occur in practice.

The process mentioned above may be applied to large scale power system using much advanced computers with better processing features and trite parallelization pathways to provide better results.

**Box 1 Data for the Damodar Valley corporation’s 46-bus 56-line system**  
 Line Data for Damodar Valley Corporation 46-Bus 56-Line System

Line No	From bus	To bus	Rp. u	Xp. u	B/2	Off-nominal ratio
1	1	2	0.0053	0.0134	0.048	1.0
2	1	10	0.1279	0.339	0.614	1.0
3	1	41	0.0667	0.159	0.0314	1.0
4	1	20	0.0142	0.0375	0.0296	1.0
5	1	24	0.0	0.0361	0.0	1.0
6	1	28	0.0257	0.0677	0.0534	1.0
7	1	34	0.0003	0.0009	0.0534	1.0
8	2	3	0.0031	0.0078	0.028	1.0
9	2	36	0.0165	0.0473	0.038	1.0
10	3	4	0.0165	0.0473	0.038	1.0
11	4	5	0.0005	0.0012	0.001	1.0
12	5	6	0.0053	0.0141	0.0026	1.0
13	5	8	0.0005	0.0012	0.001	1.0
14	6	7	0.0078	0.02	0.004	1.0

(continued)

(continued)

Line No	From bus	To bus	Rp. u	Xp. u	B/2	Off-nominal ratio
15	8	9	0.012	0.0306	0.0242	1.0
16	8	29	0.0	0.0481	0.0	1.0
17	9	10	0.0194	0.0439	0.0392	1.0
18	10	11	0.341	0.087	0.0702	1.0
19	10	31	0.0	0.0379	0.0	1.0
20	10	38	0.0031	0.0078	0.028	1.0
21	10	41	0.0667	0.159	0.0314	1.0
22	11	12	0.0237	0.0606	0.048	1.0
23	13	14	0.0264	0.0694	0.0536	1.0
24	14	15	0.0319	0.0814	0.0646	1.0
25	15	16	0.0319	0.0814	0.034	1.0
26	16	17	0.0138	0.0474	0.034	1.0
27	17	18	0.0206	0.0535	0.0106	1.0
28	17	27	0.0	0.0474	0.0	1.0
29	17	28	0.0353	0.0929	0.076	1.0
30	18	19	0.0373	0.097	0.019	1.0
31	19	20	0.0161	0.0423	0.032	1.0
32	19	25	0.0119	0.0315	0.024	1.0
33	20	21	0.0006	0.0016	0.0004	1.0
34	21	39	0.0224	0.0055	0.0116	1.0
35	21	22	0.0757	0.1884	0.042	1.0
36	21	23	0.0	0.0481	0.0	1.0
37	22	39	0.0553	0.137	0.0294	1.0
38	22	40	0.0371	0.0979	0.076	1.0
39	22	42	0.0371	0.0979	0.076	1.0
40	23	24	0.0027	0.1388	0.082	1.0
41	23	27	0.0118	0.0627	0.3842	1.0
42	23	45	0.0425	0.0227	0.1562	1.0
43	24	29	0.0072	0.0364	0.3176	1.0
44	24	44	0.0082	0.0424	0.3576	1.0
45	25	26	0.0138	0.0348	0.026	1.0
46	25	45	0.0	0.048	0.0	1.0
47	26	33	0.0	0.032	0.008	1.0
48	29	30	0.0047	0.0251	0.1536	1.0
49	29	43	0.0017	0.009	0.0576	1.0
50	29	44	0.0008	0.0084	0.0256	1.0
51	30	31	0.0037	0.0187	0.1134	1.0

(continued)

(continued)

Line No	From bus	To bus	Rp. u	Xp. u	B/2	Off-nominal ratio
52	30	43	0.0042	0.0221	0.1436	1.0
53	30	46	0.0012	0.0066	0.0416	1.0
54	31	32	0.0019	0.0094	0.1126	1.0
55	32	35	0.0012	0.0134	0.022	1.0
56	36	37	0.0165	0.0473	0.038	1.0

Bus Data for Damodar Valley Corporation’s 46-Bus 56-Line System

Bus No	BVM	BVA	Gen (MW)	Gen (MVAR)	Load (MW)	Load (MVAR)
1	1.06	0	150.00	100.00	0	0
2	1.00	0	0.0	0.0	116.4	56.4
3	1.00	0	0.0	0.0	162.24	78.0
4	1.00	0	0.0	0.0	0.6	0.36
5	1.00	0	0.0	0.0	44.4	13.8
6	1.00	0	0.0	0.0	80.4	38.4
7	1.00	0	0.0	0.0	52.8	24.0
8	1.00	0	0.0	0.0	65.76	32.4
9	1.00	0	0.0	0.0	141.60	67.2
10	1.00	0	90.0	42.0	30.96	14.4
11	1.00	0	0.0	0.0	94.8	16.8
12	1.00	0	0.0	0.0	36.0	4.8
13	1.04	0	0.0	0.0	9.6	0.0
14	1.00	0	0.0	0.0	0.0	0.6
15	1.00	0	0.0	0.0	1.2	9.6
16	1.00	0	0.0	0.0	22.8	60.0
17	1.00	0	0.0	0.0	126.0	0.0
18	1.00	0	0.0	0.0	0.0	0.6
19	1.00	0	0.0	0.0	21.6	8.4
20	1.00	0	0.0	0.0	54.0	26.4
21	1.00	0	0.0	0.0	0.0	0.0
22	1.00	0	0.0	0.0	40.8	19.2
23	1.00	0	550.0	270.0	0.0	0.0
24	1.00	0	500.0	288.64	0.0	0.0
25	1.00	0	0.0	0.0	126.0	60.0
26	1.00	0	0.0	0.0	1.2	0.24
27	1.00	0	0.0	130.0	0.0	0.0
28	1.00	0	0.0	0.0	7.2	3.6

(continued)

(continued)

Bus No	BVM	BVA	Gen (MW)	Gen (MVAR)	Load (MW)	Load (MVAR)
29	1.00	0	0.0	0.0	63.6	30.0
30	1.00	0	1200.0	576.0	82.8	39.6
31	1.00	0	200.0	98.6	0.0	0.0
32	1.00	0	0.0	0.0	136.8	66.0
33	1.00	0	0.0	0.0	37.2	16.8
34	1.00	0	0.0	0.0	247.2	119.28
35	1.00	0	0.0	0.0	115.2	55.2
36	1.06	0	0.0	0.0	25.2	12.0
37	1.00	0	0.0	0.0	127.2	60.0
38	1.00	0	0.0	0.0	44.4	20.4
39	1.00	0	0.0	0.0	18.0	7.2
40	1.00	0	0.0	0.0	72.0	33.6
41	1.00	0	0.0	0.0	10.8	4.8
42	1.00	0	0.0	0.0	27.6	12.0
43	1.00	0	0.0	0.0	180.0	84.0
44	1.00	0	0.0	0.0	0.0	0.0
45	1.00	0	0.0	0.0	12.0	4.8
46	1.00	0	0.0	0.0	64.8	30.0

r = resistance; x = reactance; p.u. = per unit; b/2 = half-line charging admittance; gen = Generation; BVA = Bus Voltage Angles; BVM = Bus Voltage Magnitude

## References

1. Anatoliy, P., Yuri, F., Vagiz, D., Yana, V., Aleksandr, V.: Aggregation process for implementation of application security management based on risk assessment. In: 2018 IEEE Conference of Russian Young Researchers in Electrical and Electronic Engineering (EIcon Rus), Russia, pp. 98–101 (2018)
2. Sekhar, P., Mohanty, S.: An online power system static security assessment module using multi-layer perceptron and radial basis function network. *Int. J. Electr. Power Energy Syst.* **76**, 165–173 (2016)
3. Liu, R., Verbiç, G., Ma, J.: A new dynamic security assessment framework based on semi-supervised learning and data editing. *Electr. Power Syst. Res.* **172**, 221–229 (2019)
4. Baghaee, H.R., Mirsalim, M., Gharehpetian, G.B., Talebi, H.A.: Unbalanced harmonic power sharing and voltage compensation of microgrids using radial basis function neural network-based harmonic power-flow calculations for distributed and decentralised control structures. *IET Generation, Transmission & Distribution* (2017)
5. Tiwary, S.K., Pal, J., Chanda, C.K.: Multi-dimensional ANN application for active power flow state classification on a utility system. In: 2020 IEEE Calcutta Conference (CALCON-2020), Kolkata, India, pp. 64–68 (2020)
6. MATLAB R2013a (8.1.0.604), The Mathworks Inc.

7. Khazaei, J., Piyasnghe, L., Miao, Z., Fan, L.: Real-time digital simulation modeling of single-phase PV in RT-LAB. In: 2014 IEEE PES General Meeting | Conference & Exposition, pp. 1–5 (2014)
8. Wang, J., Tang, X., Yin, Z.: Research on medium voltage battery energy storage system based on RT-LAB. In: 2014 IEEE Conference and Expo Transportation Electrification Asia-Pacific (ITEC Asia-Pacific), pp. 1–5 (2014)
9. Fei, Z., Lin, Z.X., Junjun, Z., Jingsheng, H.: Hardware-in-the-loop simulation, modeling and close-loop testing for three-level photovoltaic grid-connected inverter based on RT-LAB. In: 2014 International Conference on Power System Technology, pp. 2794–2799 (2014)
10. Mariut, L., Helerea, E.: Electromagnetic analysis Application to lightning surge phenomena on power lines. In: 2014 International Symposium on Fundamentals of Electrical Engineering (ISFEE), pp. 1–6 (2014)
11. Ding, N., Benoit, C., Foggia, G., Besanger, Y., Wurtz, F.: Neural network-based model design for short-term load forecast in distribution systems. *IEEE Trans. Power Syst.* **31**(1), 72–81 (2016)
12. Bulac, C., Tristiu, I., Mandis, A., Toma, L.: On-line power systems voltage stability monitoring using artificial neural networks. In: 2015 9th International Symposium on Advanced Topics in Electrical Engineering (ATEE), pp.622–625 (2015)
13. Sulaiman, S.M., Jeyanthi, P.A., Devaraj, D.: Artificial neural network based day ahead load forecasting using Smart Meter data. In: 2016 Biennial International Conference on Power and Energy Systems: Towards Sustainable Energy (PESTSE), pp. 1–5 (2016)
14. Yu, Q., Yan, R., Tang, H., Tan, K.C., Li, H.: A spiking neural network system for robust sequence recognition. *IEEE Trans. Neural Netw. Learn. Syst.* **27**(3), 621–635 (2016)
15. Basnet, S.M.S., Aburub, H., Jewell, W.: An artificial neural network-based peak demand and system loss forecasting system and its effect on demand response programs. In: 2016 Clemson University Power Systems Conference (PSC), pp. 1–5 (2016)
16. Bulo, S.R., Biggio, B., Pillai, I., Pelillo, M., Roli, F.: Randomized prediction games for adversarial machine learning. *IEEE Trans. Neural Netw. Learn. Syst.* **28**(11), 2466–2478 (2017)
17. Chen, S., Hong, X., Khalaf, E.F., Alsaadi, F.E., Harris, C.J.: Comparative performance of complex-valued B-spline and polynomial models applied to iterative frequency-domain decision feedback equalization of Hammerstein channels. *IEEE Trans. Neural Netw. Learn. Syst.* **28**(12), 2872–2884 (2017)
18. Yalcin, T., Ozdemir, M.: Pattern recognition method for identifying smart grid power quality disturbance. In: 2016 17th International Conference on Harmonics and Quality of Power (ICHQP), pp. 903–907 (2016)
19. Kamel, M., Karrar, A.A., Eltom, A.H.: Development and application of a new voltage stability index for on-line monitoring and shedding. *IEEE Trans. Power Syst.* **33**(2), 1231–1241 (2018)
20. Tiwary, S.K., Pal, J.: ANN application for MW security assessment of a large test bus system. In: 2017 3rd International Conference on Advances in Computing, Communication & Automation (ICACCA) (Fall), pp. 1–4 (2017)
21. Tiwary, S.K., Pal, J.: ANN application for voltage security assessment of a large test bus system: A case study on IEEE 57 bus system. In: 2017 6th International Conference on Computer Applications in Electrical Engineering-Recent Advances (CERA), pp. 332–334 (2017)
22. Tiwary, S.K., Pal, J., Chanda, C.K.: Mimicking on-line monitoring and security estimation of power system using ANN on RT lab. In: 2017 IEEE Calcutta Conference (CALCON), pp. 100–104 (2017)
23. Jiang, Y., Jiang, Z.-P.: Robust adaptive dynamic programming for large-scale systems with an application to multimachine power systems. *IEEE Trans. Circ. Syst. II Express Briefs* **59**(10), 693–697 (2012)
24. He, M., Zhang, J., Vittal, V.: Robust online dynamic security assessment using adaptive ensemble decision-tree learning. *IEEE Trans. Power Syst.* **28**(4), 4089–4098 (2013)
25. Zheng, C., Malbasa, V., Kezunovic, M.: Regression tree for stability margin prediction using synchrophasor measurements. *IEEE Trans. Power Syst.* **28**(2), 1978–1987 (2013)

26. Liu, C., Sun, K., Rather, Z.H., Chen, Z., Bak, C.L., Thogerson, P., Lund, P.: A systematic approach for dynamic security assessment and the corresponding preventive control scheme based on decision trees. In: 2014 IEEE PES General Meeting | Conference & Exposition, pp. 1–1 (2014)
27. Tiwary, S.K., Pal, J., Chanda, C.K.: Application of common ANN for similar datatypes in on-line monitoring and security estimation of power system. *Adv. Intell. Syst. Comput.* **755**(1), 3–11 (2019)
28. Konstantelos, I., Jamgotchian, G., Tindemans, S.H., Duchesne, P., Cole, S., Merckx, C., Strbac, G., Panciatici, P.: Implementation of a massively parallel dynamic security assessment platform for large-scale grids. *IEEE Trans. Smart Grid* **28**(2), 1978–1987 (2013)
29. Shu, Y., Tang, Y.: Analysis and recommendations for the adaptability of China's power system security and stability relevant standards. *CSEE J. Power Energy Syst.* **3**(4), 334–339 (2017)
30. Chappa, H., Thakur, T.: Identification of weak nodes in power system using conditional number of power flow Jacobian matrix. In: 2018 International Conference and Utility Exhibition on Green Energy for Sustainable Development (ICUE), pp. 1–6 (2018)
31. Kabir, H., Khosravi, A., Hosen, M., Nahavandi, S.: Partial adversarial training for prediction interval. In: 2018 International Joint Conference on Neural Networks (IJCNN), pp. 1–6 (2018)
32. Jiang, Z., Konstantinou, G., Zhong, Z., Acuna, P.: Real-time digital simulation based laboratory test-bench development for research and education on solar pv systems. In: 2017 Australasian Universities Power Engineering Conference (AUPEC), pp. 1–6 (2017)
33. Kundur, P.: Power system stability and control. In: Balu, N.J., Lauby, M.G. (eds.) 7th edn, pp. 199–269. McGraw-Hill, New York (1994)
34. Sun, H., Zhong, F., Wang, H., Wang, K., Jiang, W., Guo, Q., Zhang, B., Wehenkel, L.: Automatic learning of fine operating rules for online power system security control. *IEEE Trans. Neural Netw. Learn. Syst.* **27**(8), 1708–1719 (2016)
35. Tiwary, S.K.: Peak load management with wheeling in a gas turbine station under availability based tariff. In: 2021 International Conference on Sustainable Energy and Future Electric Transportation (SEFET), pp. 1–5 (2021). <https://doi.org/10.1109/SeFet48154.2021.9375649>
36. Tiwary, S.K., Pal, J., Chanda, C.K.: ANN-Based Faster Indexing with Training-Error Compensation for MW Security Assessment of Power System. *Lecture Notes in Electrical Engineering*, vol. 664. Springer, Singapore, (2020), pp. 35–46. [https://doi.org/10.1007/978-981-15-5089-8\\_4](https://doi.org/10.1007/978-981-15-5089-8_4)
37. Tiwary, S.K., Pal, J., Chanda, C.K.: Evaluation of the applicability and advantages of application of artificial neural network based scanning system for grid networks. In: *Advances in Intelligent Systems and Computing*, vol. 1198, pp. 231–243. Springer, Singapore (2020). [https://doi.org/10.1007/978-981-15-6584-7\\_23](https://doi.org/10.1007/978-981-15-6584-7_23)
38. Tiwary, S.K., Pal, J., Chanda, C.K.: Monitoring static security assessment in its full scope using common artificial neural network. In: *Intelligent Electrical Systems: A Step towards Smarter Earth*, vol. 1. CRC Press, Boca Raton, USA (2021), pp 100–104
39. Tiwary, S.K., Pal, J., Chanda, C.K.: Multiple-classification of power system states using multi-dimensional neural network. *J. Inst. Eng. India Ser. B* **104**, 893–900 (2023). <https://doi.org/10.1007/s40031-023-00892-1>

# Multi-Class Classification of Power Network States Using Multi-Dimensional Neural Network



Shubhranshu Kumar Tiwary, Jagadish Pal, and Chandan Kumar Chanda

**Abstract** During power system operation, for the optimized operation and control of power networks, its operation is usually segregated into several different operational states. This works in both real-time and offline monitoring scenarios. These operational states are based on the variation of the levels of parameters like voltage magnitude, angles, system operational frequency, switching states, active and reactive power flow on the transmission lines. Initially, Tomas Liacco proposed the categorization of power system operation into 3 functional categories, which was later, further sustained by Lester Fink and Kjell Carlsen into 5 different functional categories. These categories classify the power system operation into 5 different states subject to the severity of line outages and overloading capacities. This categorization of power network states using original mathematical approaches can be very cumbersome and time-consuming. In this work, a simplified method for the segregation of power network states has been suggested based on the application of a multi-dimensional artificial neural network, that has been employed for the prompt multi-class classification of power network states based on Fink and Carlsen's approach. The whole setup for this study, including the power network and the artificial neural network models, was developed on the Simulink environment of MATLAB (R2021a). The system was simulated on the RT Lab OP-5600 simulator in real-time. The results of this study prove that the application of the multi-dimensional neural networks will provide results in under 1s, which is faster than the operating time of many types of circuit breakers and relays, hence proving the practicality of the method.

**Keywords** Artificial neural networks · Power system control · Power system security · Power system simulation · Power system state estimation · Real-Time monitoring

---

S. K. Tiwary (✉) · J. Pal · C. K. Chanda

Department of Electrical Engineering, Indian Institute of Engineering Science and Technology, PO Box 711103, Shibpur, Howrah, West Bengal, India

e-mail: [mailshubh2005@gmail.com](mailto:mailshubh2005@gmail.com); [mail\\_shubh.rs2014@ee.iiests.ac.in](mailto:mail_shubh.rs2014@ee.iiests.ac.in)



## 1 Introduction

With an expeditiously surging populace, virtually touching 8 billion, the electricity use is also concurrently rising. Likewise, the strides in the technological field have also improved, resulting in the rapid increase in power consumption, ergo the rise in the power demand worldwide. Although the power demand has been on the rise exponentially, the expansion of the generating capacities and the existing grid and utilities have been traditionally very slow. As a result, the existing power grids and grid utilities are compelled to operate at their designed capacity limits or very close to it [5]. The sustained operation of a large power network is very sophisticated and burdensome both for man and machine [13]. So, to minimize the stress for the equipment involved as well the operators, in this work a multi-dimensional multi-classification artificial neural network (MDNN) has been applied for the identification of state transition of the power system from one state to the other [13, 20].

In 1967 Liacco proposed in his paper [8], that for the simplification and understanding of the power grid's working and control, its activity may be divided into three groups, specifically, "preventive, emergency and restorative". The method elaborated in this work assumes that a power grid may only exist in one of these three states at any given time [7]. It is shown in Fig. 1 below.

The work of Liacco was further simplified and extended by Lester [6]. In this work, the authors elaborated the grid-states in 5 different groups which are "normal, alert, emergency, extreme emergency, and lastly restorative", which were based "on three sets of generic equations, where one was differential and two were algebraic". The state progression from one to the other may be simplified by Fig. 2.

This work was performed assuming Fink et al.'s point of view. The study was performed using a licensed MATLAB R2021a software [10]. The network was developed on Simulink [1]. And it was simulated in real-time with a Hardware-In-Loop device of RT Lab from OPAL-RT [11, 18]. The network developed and simulated was an IEEE 57 bus network with 80 transmission lines [4].

This work is categorized into 5 categories. Section 1 introduces the work, Sect. 2 elaborates on the network studied and the MDNN development strategy, Sect. 3 explains the sample size generated for each line and bus and its training methodology in off-line mode, and Sect. 4 presents a detailed real-time application methodology

**Fig. 1** Grid state classification by [8]

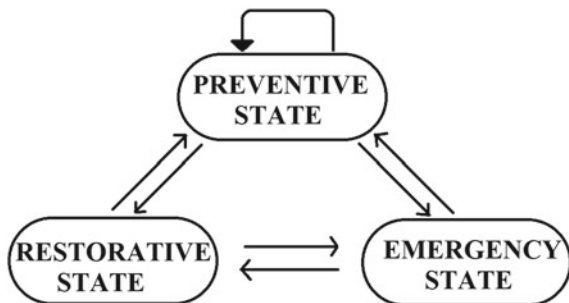
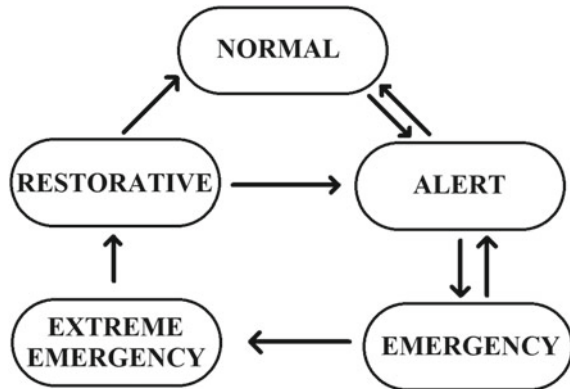


**Fig. 2** Grid state classification by [6]



of the study with some insights using confusion matrix, Sect. 5 concludes the paper citing the major contributions of the work followed by references, acknowledgments, and author biography.

## 2 Network Studied and MDNN Development

The power network used for performing this work was an IEEE 57 bus system that has 80 transmission lines, with a pair of parallel transmission lines [17, 18]. And minimize complexities in model design the parallel lines are represented with a single transmission line with equivalent capacitance, inductance, and resistance. Hence, the total number of transmission lines in the network will be 78. The line diagram is given in the following figure. The network diagram is shown in Fig. 3.

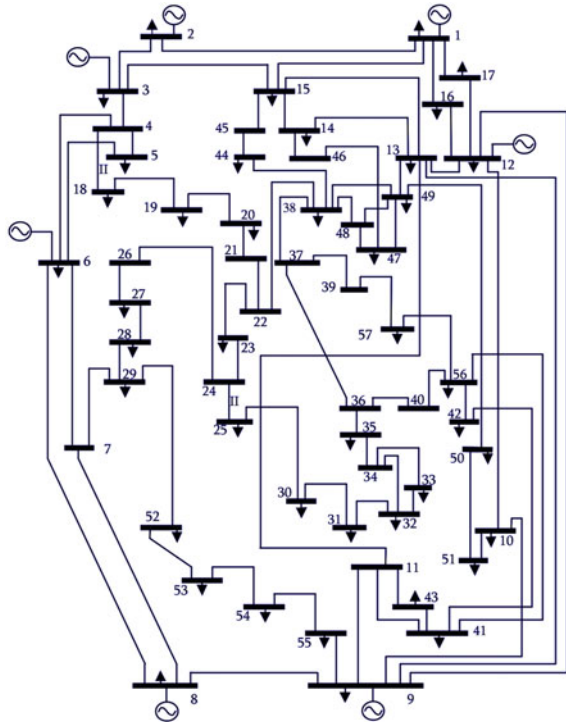
This network is developed on the Simulink environment of MATLAB version R2021a. The Simulink model of the network is developed as in the following figure [13] (Fig. 4).

Once developed, it is simulated in the off-line mode for training sample accumulation.

### 2.1 MDNN Development Strategy

To have a variation in the range of training data, all the crucial and critical contingencies were simulated, and its consequence on the other monitoring parameters of other lines, buses, and other equipment was recorded [23, 24]. A total of 9800 samples were generated for the system for each voltage angle at 57 buses, voltage magnitude at 57 buses, active power, and reactive power flowing on all 78 lines. All these data need to be tabulated into a data file. Here, each data array refers to a different state

**Fig. 3** IEEE 57 bus network line diagram



of the power network under investigation based on the Fink approach as explained previously [6]. Then for this training data, the target classification is set up. The target classification is assigned in the form of a binary set in a separate data file. The output classification is categorized binary dataset as in Fig. 5 below in different colors.

Here, each dataset is categorized into 5 states. Hence, the classification of the MDNN output defines the 5 categories based on the binary method using Fink’s approach [22]. So, the 9800 datasets are divided equally since the data generation was controlled. Each state has an array of 1960 datasets. Next, the MDNN is trained as elaborated in the following subsection.

### 3 Sample Size Generated and Training Methodology

As discussed in the previous section, the total number of training samples generated was 9800 datasets. Out of these, each state had a total of 1960 samples. In these training sample datasets, all of the critical outages, dangerous contingencies, crucial equipment breakdown, etc., were also incorporated, so that all possibilities of complications (or situations very similar) in a grid are encumbered at least twice [21]. These kinds of variation in training datasets allow for a proper convergence in the training

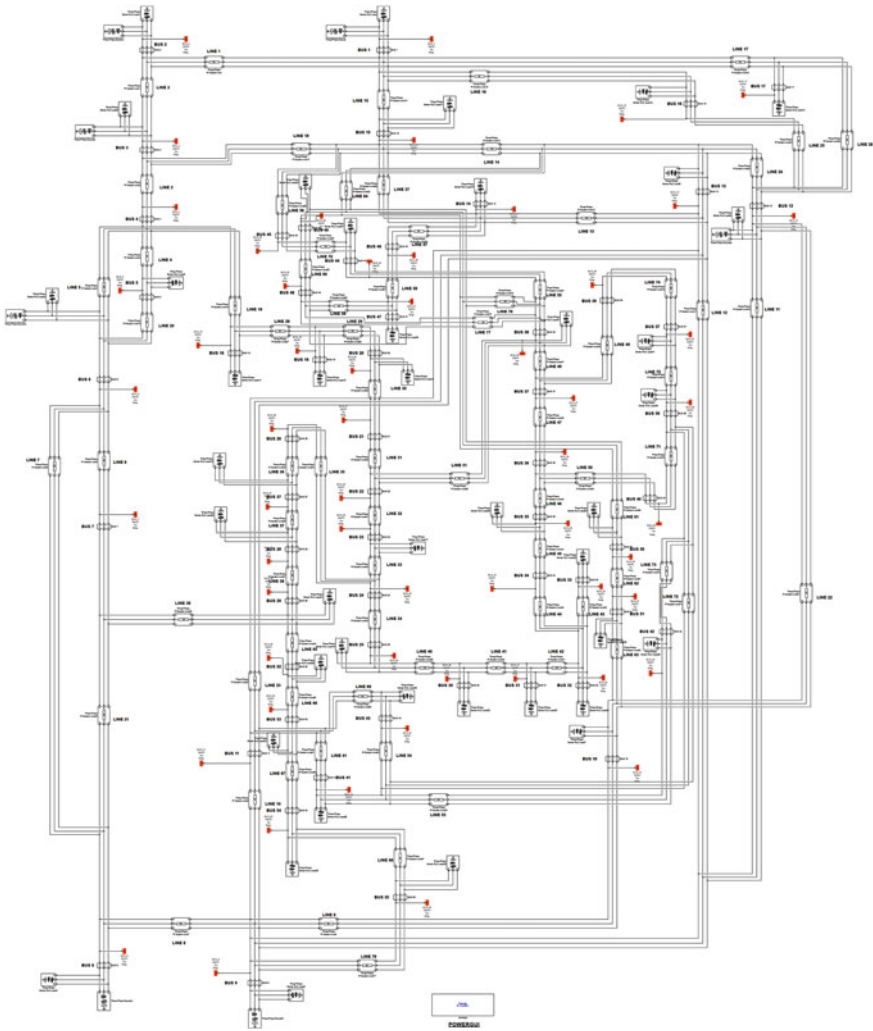
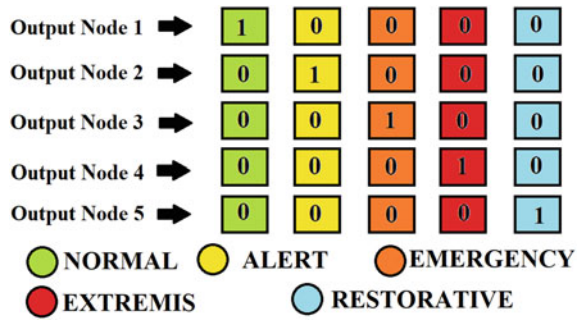


**Fig. 4** IEEE 57 bus network simulink model

of the ANN. Since we are monitoring four parameters of the power network, namely, voltage angle, voltage magnitude, active and reactive power [9]. So, there are a total of 4 training datasets and their corresponding 4 target output categorization. There is voltage angle training data file and its target classification datafile, voltage magnitude training data file and its target classification datafile, active power training data file and its target classification data file, and lastly reactive power training data file and its target classification data file.

**Fig. 5** MDNN output node data classification



### 3.1 MDNN Training Methodology

There are multiple types of machine learning methodology to choose for pattern recognition method that has been used for a variety of applications. The main two categories are the “Unsupervised” methodology of machine learning and the “Supervised” methodology of machine learning. Since the capital investments in a power system are vary huge and can affect the economy of a nation, using an unsupervised methodology of learning is inadvisable. And because there is some control of sorts in the supervised methodology of machine learning, it is very prudent to use it in some crucial systems.

As is evident from the preceding sections, the type of MDNN used here is the supervised learning type. The methodology was the feedforward neural net with error back-propagation. The optimization algorithm utilized was the Scaled Conjugate Gradient method which is intermediate to the Gradient Descent method as well as the Newton method but is better than both. During the training method, the data in the data file is divided into three categories of training, validation, and testing datasets, which are then used to train the MDNN [12]. When this initialization of the MDNN is complete the MDNN is then trained with the data in the training data file against the target data file, as has been elaborated in the preceding sections.

## 4 MDNN Development for Voltage Angle

The configuration of the MDNN structure used for training of Voltage angle monitoring MDNN is 57 input nodes for 57 buses in the network, 13 nodes in the hidden layer, and 5 nodes in the output layer. The structure of Voltage angle monitoring MDNN is as shown in Fig. 6 below.

The accuracy of the Voltage angle MDNN training using the confusion matrix is as shown below in Fig. 7.

The performance plot of the voltage angle MDNN training is shown in Fig. 8 below.

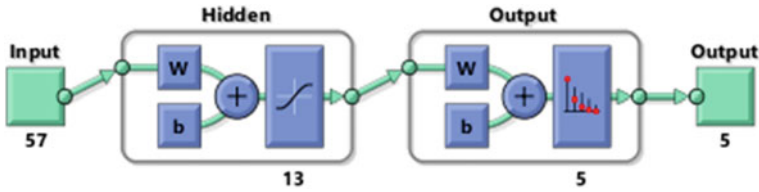


Fig. 6 Voltage angle MDNN structure

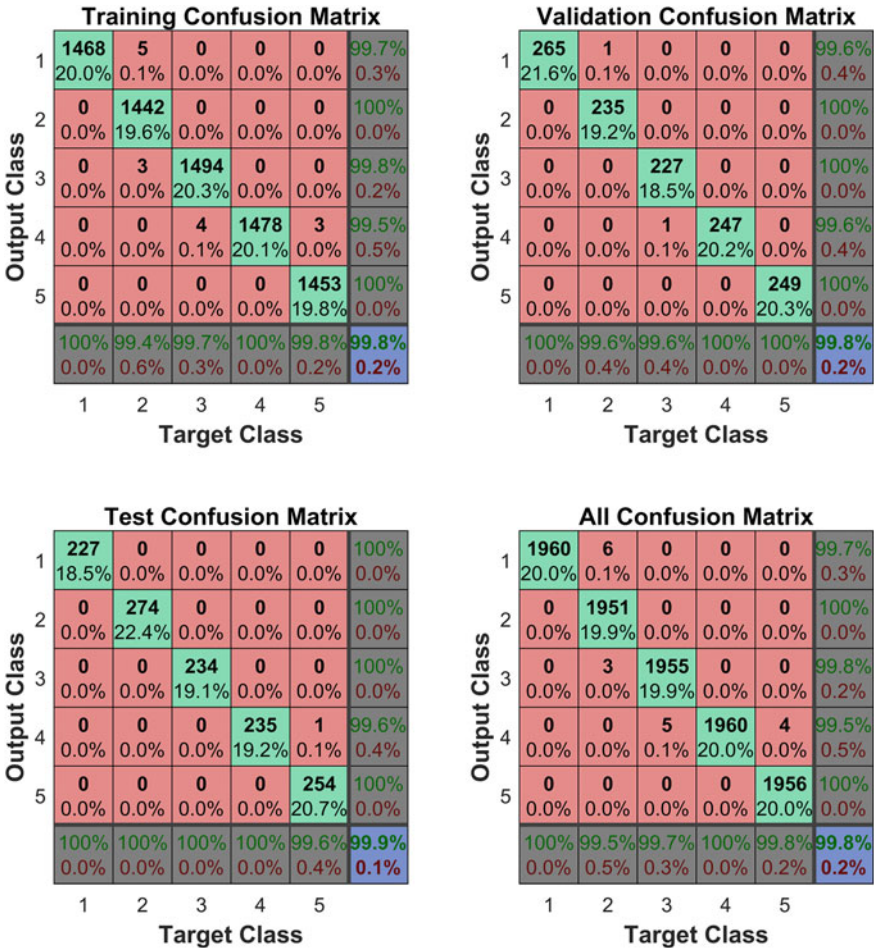
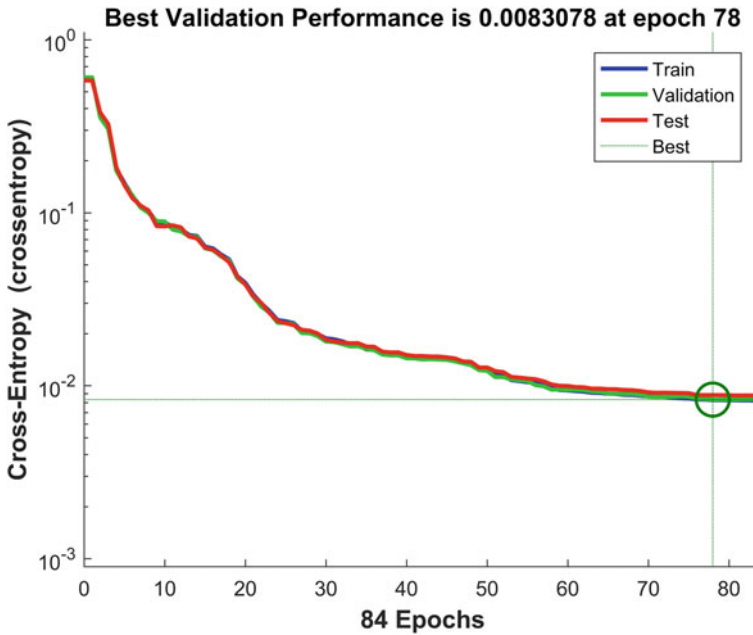


Fig. 7 Voltage angle MDNN's confusion matrix showing accuracy of training



**Fig. 8** Voltage angle MDNN's performance plot

The error histogram of the voltage angle MDNN training is shown in Fig. 9 below.

The training state of the voltage angle MDNN training is shown in Fig. 10 below.

As the Voltage angle, MDNN training converged properly and showed an accuracy of 99.8%, the network is saved for testing as well as real-time application.

## 5 MDNN Development for Voltage Magnitude

The configuration of the MDNN structure used for training of Voltage magnitude monitoring MDNN is 57 input nodes for 57 buses in the network., 14 nodes in the hidden layer, and 5 nodes in the output layer. The structure of Voltage magnitude monitoring MDNN is as shown in Fig. 11 below.

The accuracy of the voltage magnitude MDNN training using the confusion matrix is as shown in Fig. 12

The performance plot of the voltage magnitude MDNN training is shown in Fig. 13 below.

The error histogram of the voltage magnitude MDNN training is shown in Fig. 14 below.

The training state plot of the Voltage magnitude MDNN training is as shown in Fig. 15 below.

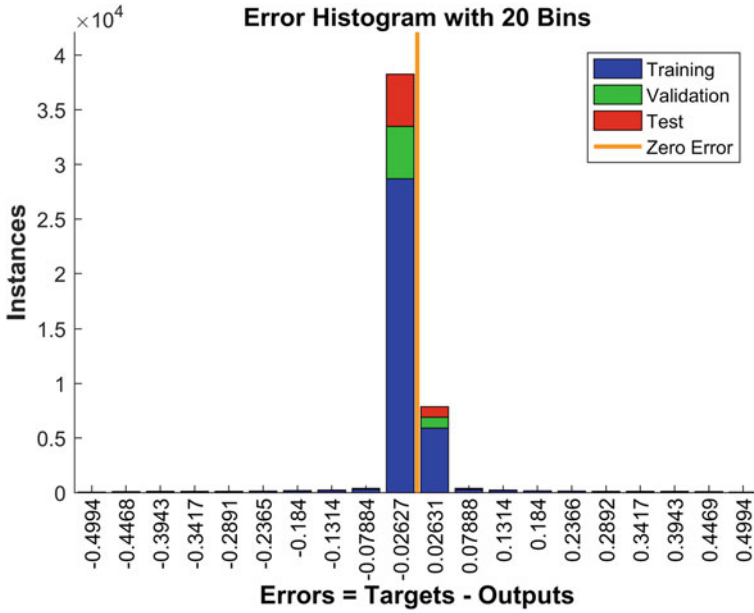


Fig. 9 Voltage angle MDNN's error histogram

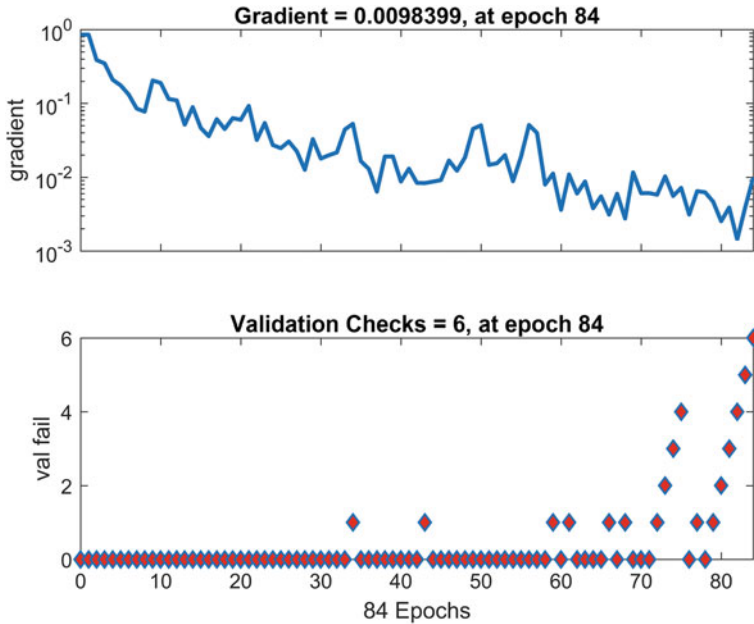


Fig. 10 Voltage angle MDNN's training state



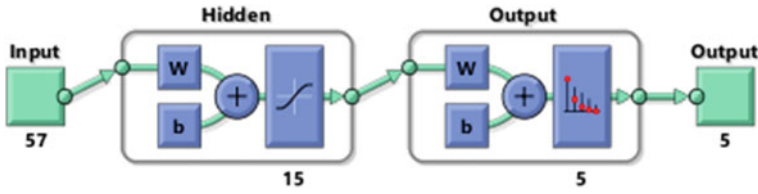


Fig. 11 Voltage magnitude MDNN's structure

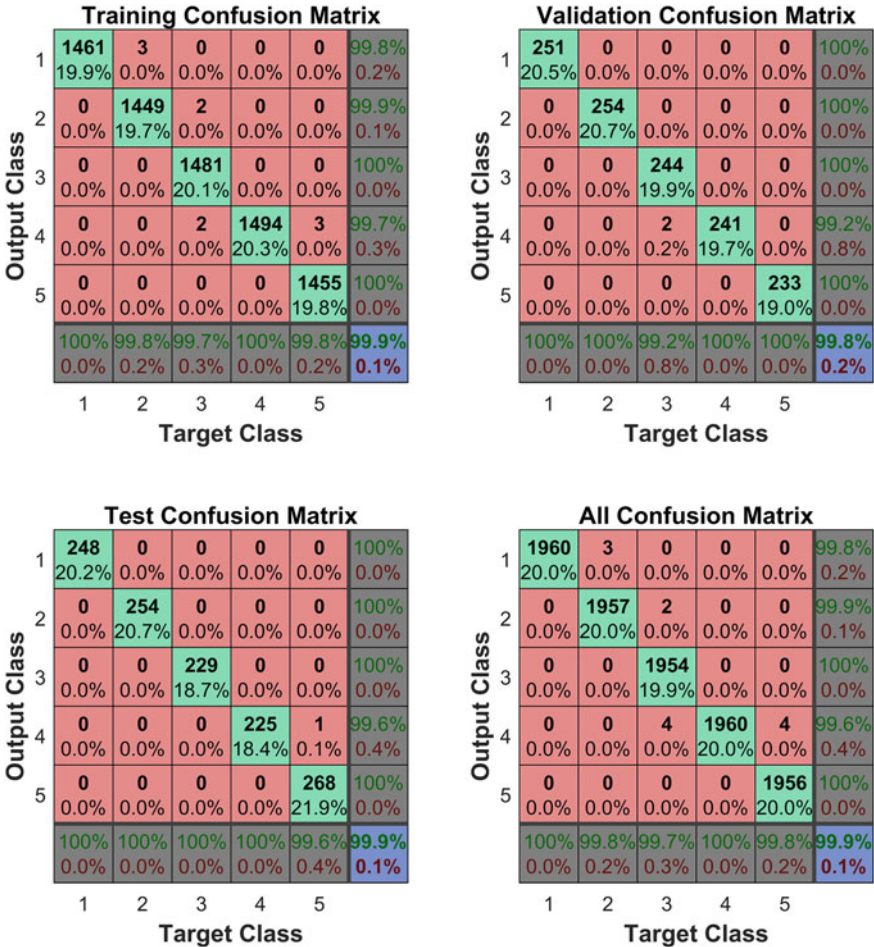


Fig. 12 Voltage magnitude MDNN's confusion matrix showing accuracy of training

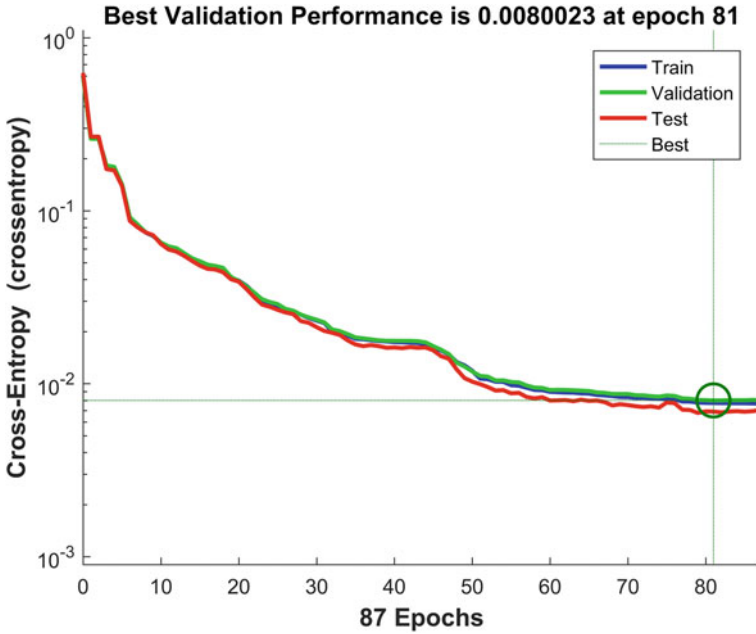


Fig. 13 Voltage magnitude MDNN's performance plot

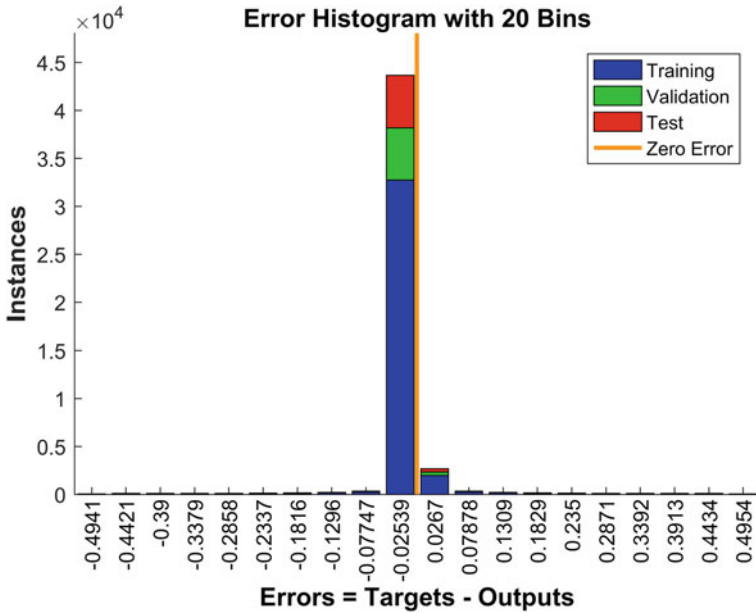


Fig. 14 Voltage magnitude MDNN's error histogram

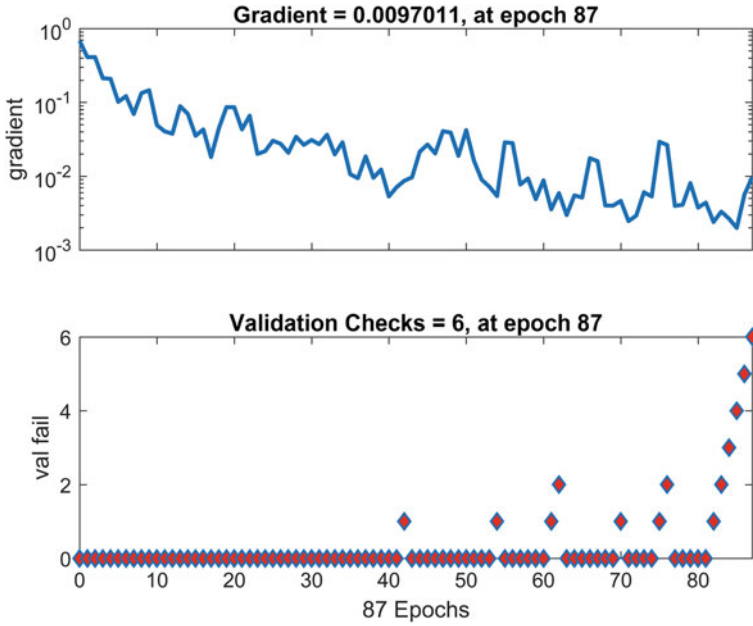


Fig. 15 Voltage magnitude MDNN’s training state plot

As the Voltage magnitude MDNN training converged properly and showed an accuracy of over 99.9%, the network is saved for testing as well as real-time application.

### 6 MDNN Development for MW Power/Active Power

The configuration of the MDNN structure used for training of MW power monitoring MDNN is 78 input nodes for 78 lines in the network, 17 nodes in the hidden layer, and 5 nodes in the output layer. The structure of the active power monitoring MDNN is as shown in Fig. 16.

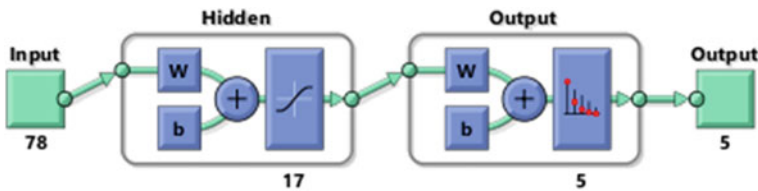


Fig. 16 MW power MDNN’s structure

The accuracy of the MW power MDNN training using the confusion matrix is as shown below in Fig. 17.

The performance plot of the MW power MDNN training is shown in Fig. 18 below.

The error histogram of the MW power MDNN training is shown in Fig. 19 below.

The training state plot of the MW power MDNN training is as shown in Fig. 20 below.

As the MW power, MDNN training converged properly and showed an accuracy of over 100%, the network is saved for testing as well as real-time application.



Fig. 17 MW power MDNN’s confusion matrix showing accuracy of training

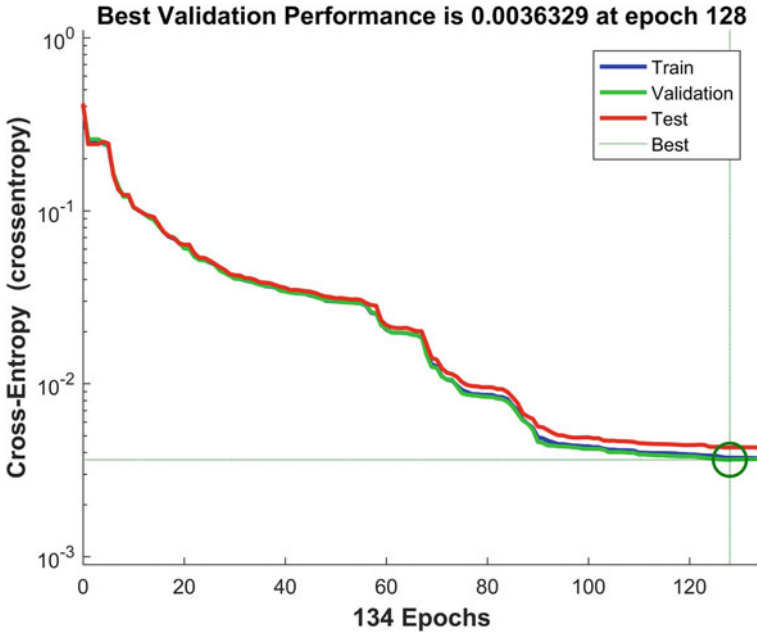


Fig. 18 MW power MDNN’s performance plot

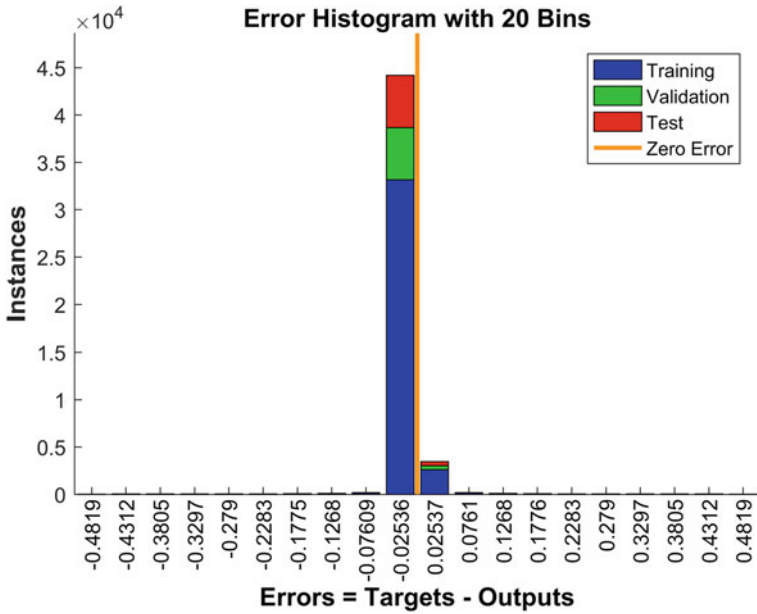


Fig. 19 MW power MDNN’s error histogram

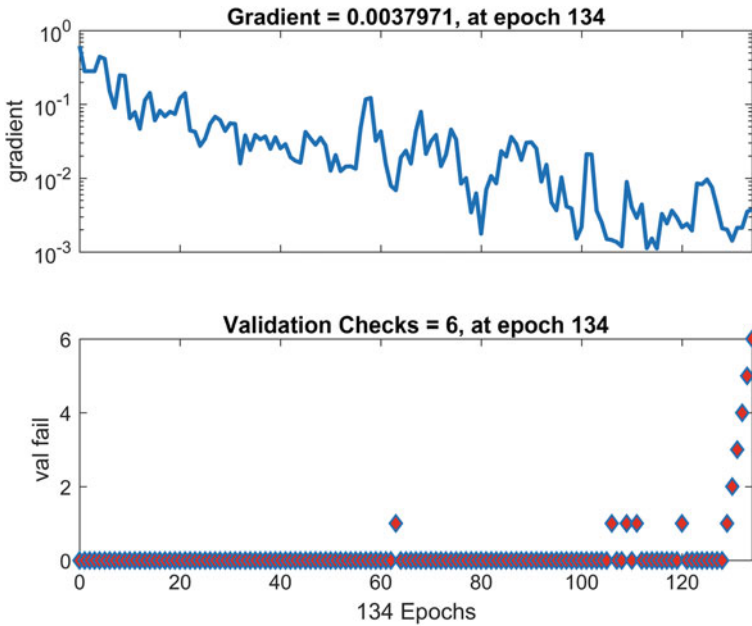


Fig. 20 MW power MDNN’s training state plot

### 7 MDNN Development for MVAR Power/ Reactive Power

The configuration of the MDNN structure used for training of MVAR power monitoring MDNN is 78 input nodes for 78 lines in the network 19 nodes in the hidden layer and 5 nodes in the output layer. The structure of the ANN is as shown below (Fig. 21).

The accuracy of the MVAR power MDNN training using the confusion matrix is as shown below in Fig. 22.

The performance plot of the MVAR power MDNN training is shown in Fig. 23 below.

The error histogram of the MVAR power MDNN training is shown in Fig. 24 below.

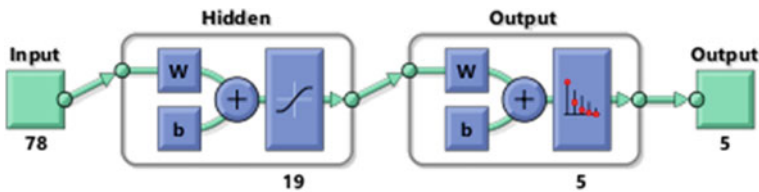


Fig. 21 MVAR power MDNN’s structure



Fig. 22 MVAR power MDNN’s confusion matrix showing accuracy of training

The training state plot of the MVAR power MDNN training is as shown in Fig. 25 below.

As the MVAR power MDNN training converged properly and showed an accuracy of over 99.8%, the network is saved for testing as well as real-time application.

From the above Figs. 6 through 25% the MDNN structure, the confusion matrix representing the MDNN training accuracy, performance plot represents “error against the training, validation, and test epoch performances of the training record TR returned by the function train” [2], error histogram helps “visualize errors between target values and predicted values after training a feedforward neural network” [3], and training state diagram “plots the training state from a training record tr returned by train”[3].

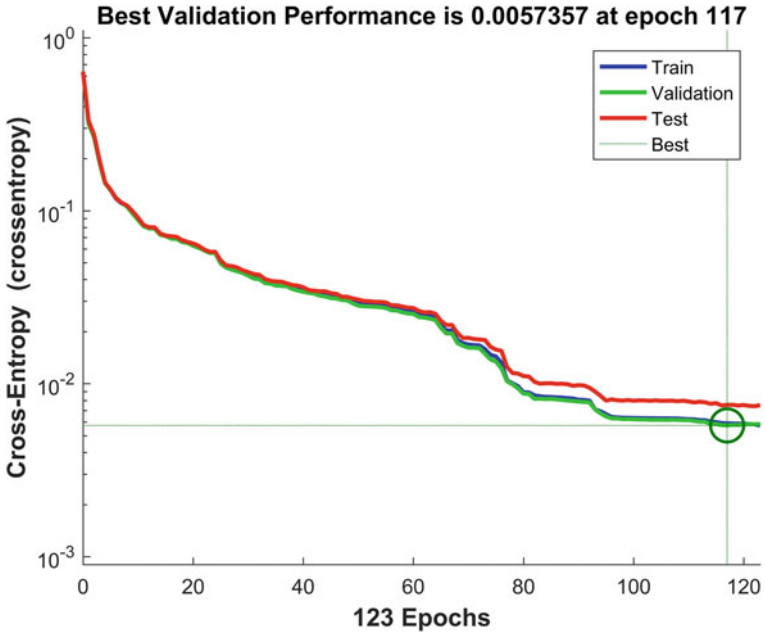


Fig. 23 MVAR power MDNN's performance plot

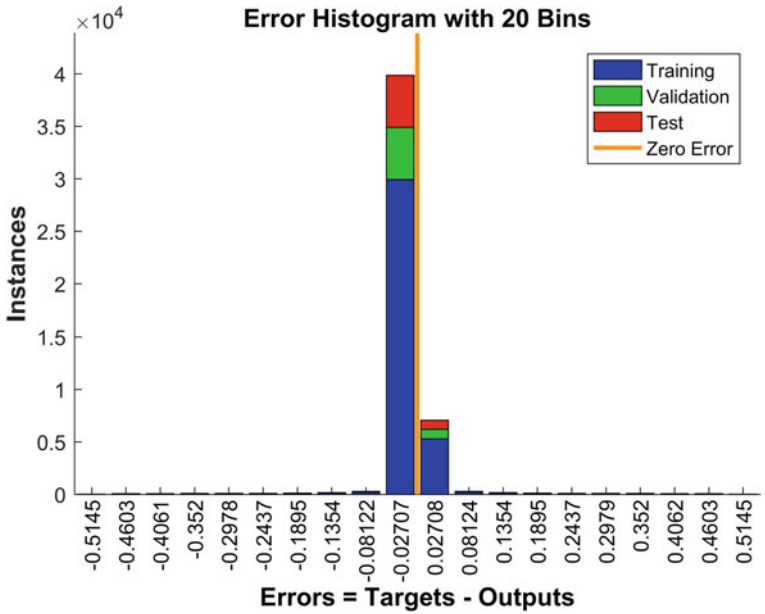


Fig. 24 MVAR power MDNN's error histogram



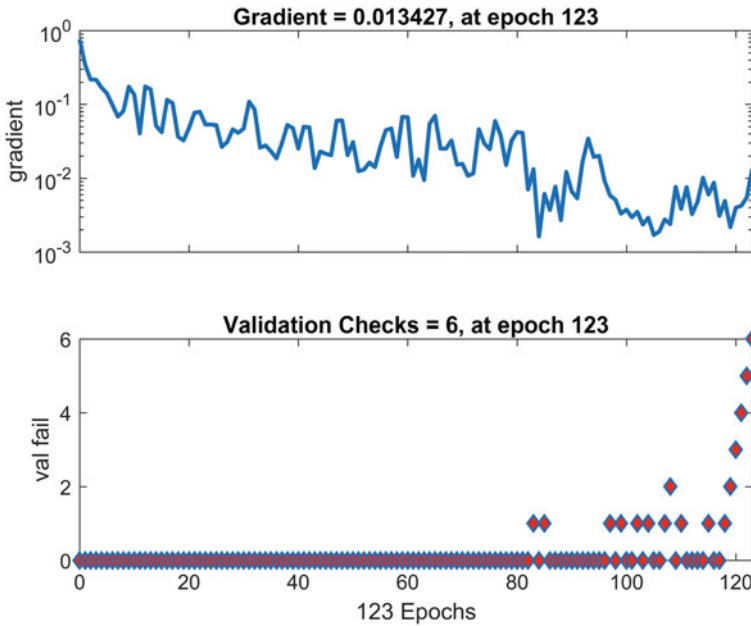


Fig. 25 MVAR power MDNN’s training state plot

The output of these 4 MDNN’s is recorded and then fed to train a fifth MDNN model to classify the overall power network operational state. This fifth MDNN will have 20 input nodes, 7 hidden nodes, and 5 output nodes to classify the state of the whole power network based on the above-mentioned 4 crucial parameters. The corresponding MDNN structure, confusion matrix, and other plots are shown in the following figures (Fig. 26).

The confusion matrix of the common MDNN representing the training accuracy is as shown below in Fig. 27.

The performance plot of the common MDNN training is shown in Fig. 28 below.

The error histogram of the common MDNN training is shown in Fig. 29 below.

The training state plot of the common MDNN training is as shown in Fig. 30 below.

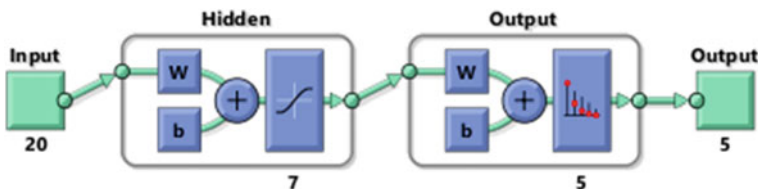


Fig. 26 Common MDNN’s structure



Fig. 27 Common MDNN’s confusion matrix

The whole setup of the MDNN network for the state transition monitoring of the power network is as shown in the Figure below (Fig. 31).

As it can be seen that some errors are inevitable while training an MDNN. To mitigate these errors, a function can be added with the results as compensation to calibrate the MDNN for better results [12]. The compensation function or the cross-entropy loss function for binary classification is as shown below.

$$E = - \sum_{c=1}^N y_{o,c} \log(p_{o,c}) \tag{1}$$

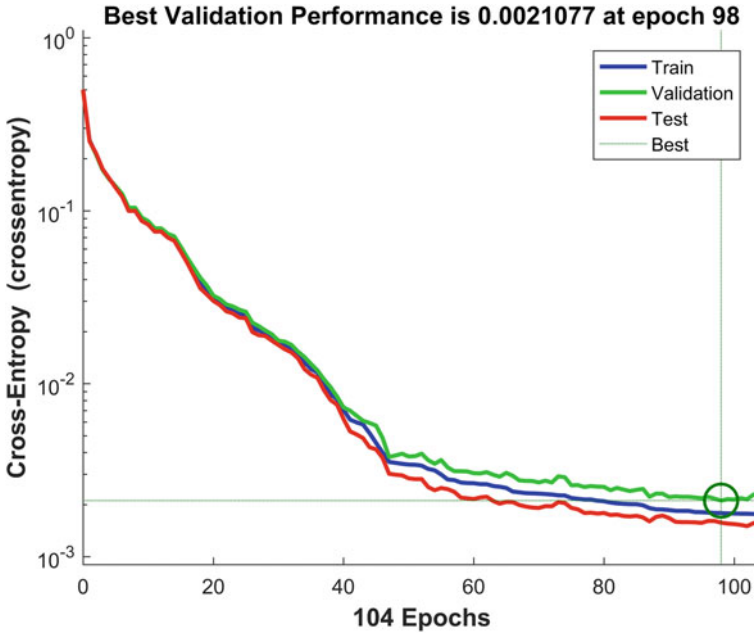


Fig. 28 Common MDNN’s performance plot

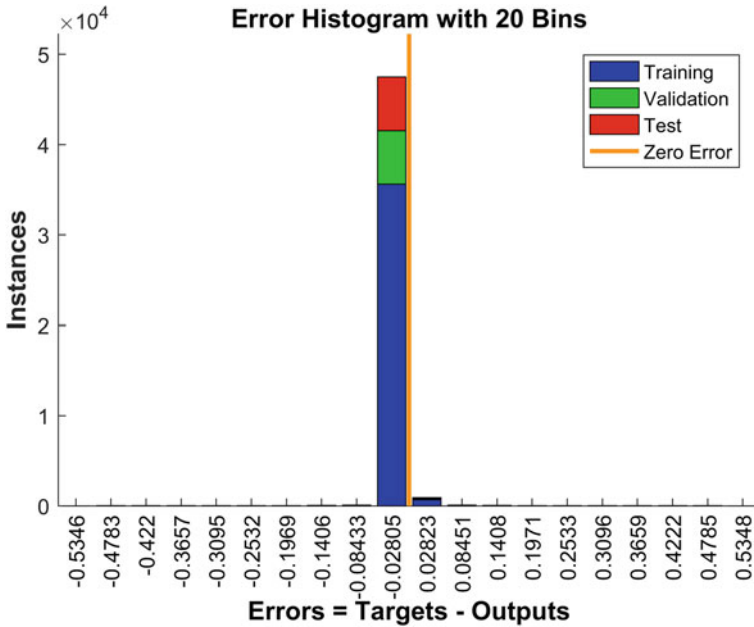


Fig. 29 Common MDNN’s error histogram

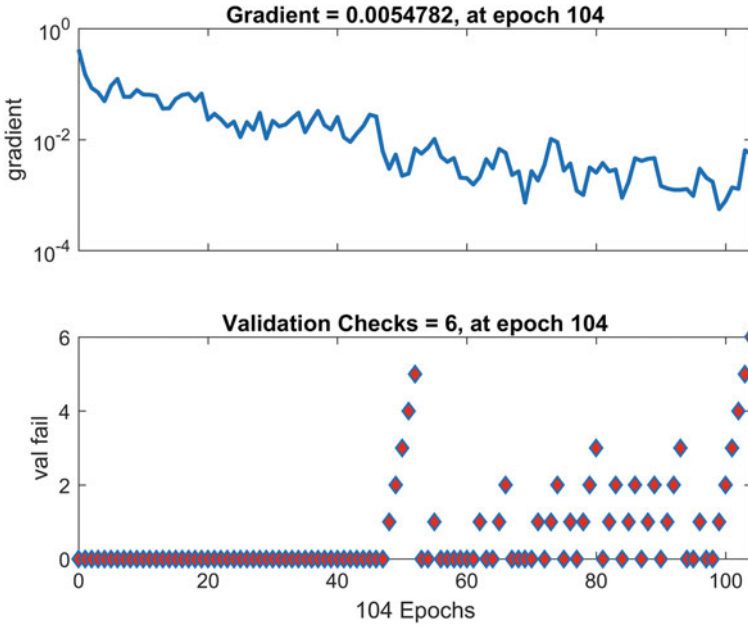


Fig. 30 Common MDNN’s training state plot

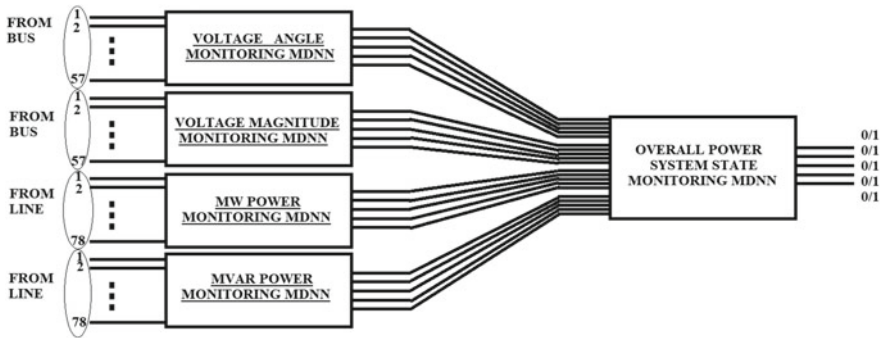


Fig. 31 Structure of the common MDNN state monitor

where, N- nnumber of classes; log- the natural log; y- binary indicator (0 or 1) for class identification of label c for the correct result of observation o; p - predicted probability observation o is of class c.

From the above-elaborated plots and training confusion matrix, it can be seen that the ANN training has properly converged and is ready for testing various contingencies and identifying their respective states. Also, to compensate for the error the above function, in (1), can be added to the results. The state identification using output nodes can be classified as below in Table 1.

**Table 1** MDNN outputs and its respective state classification

ANN output	Power system state
1-0-0-0-0	Normal-State
0-1-0-0-0	Alert-state
0-0-1-0-0	Emergency-state
0-0-0-1-0	In-extremis-state
0-0-0-0-1	Restorative -state

## 8 Real-Time Application Methodology

In the model in Fig. 32, everything except the scope block is selected and converted into a sub-system labeled Master Sub-system (SM\_in) and the scope is selected and converted into another sub-system labeled Console Sub-system (SC\_out). The error function is added to the output of the MDNN in the console sub-system as shown in Figure below.

In place of a “SCOPE” block, it is advisable to use a “MATFILE” block to record the results which put less stress on the real-time computation process in the RT Lab HIL device and the concerned computer. From the “MATFILE” the recorded results can be plotted. The whole RT Lab compatible model is shown in Fig. 34 below.

Now, for the real-time application and testing of the MDNN the 4200 various testing scenarios are programmed to be applied and tested in real-time on the RT Lab OP-5600 simulator which is discussed and presented in the following sections.

The results of the testing datasets in real-time are represented by the confusion matrices in the following figures.

From the above 4 figures (Figs. 35, 36, 37, 38) it can be seen that the accuracy of the MDNN monitoring the voltage angle, voltage magnitude, active power, and

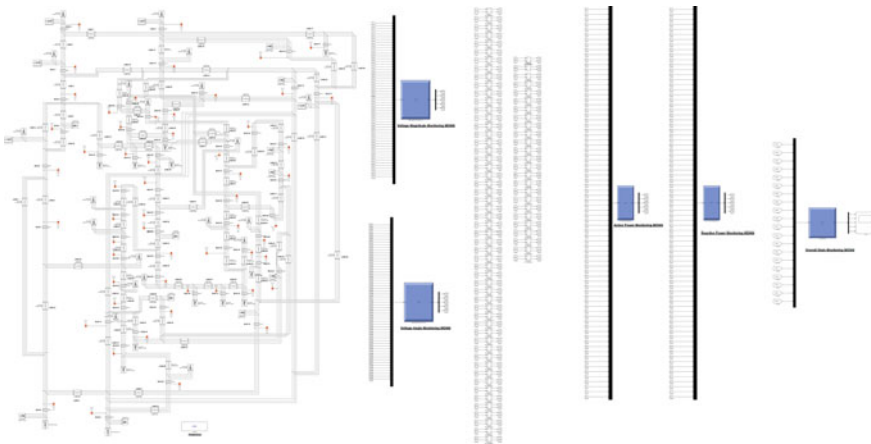


**Fig. 32** The complete model of the power system with the MDNN monitors

reactive power is 100 percent. There are minute errors or misclassifications which can be corrected using the error function as explained in previous sections and also as shown in the RT Lab compatible Simulink model diagram in Fig. 33 describing the console sub-system of the model. The accuracy of the common MDNN monitoring the output of all the other MDNN's is as shown in Fig. 39 below.

From the above Fig. 38, the accuracy of the MDNN monitoring all other MDNN's is 100 percent with zero errors. The performance plot of the testing results of the

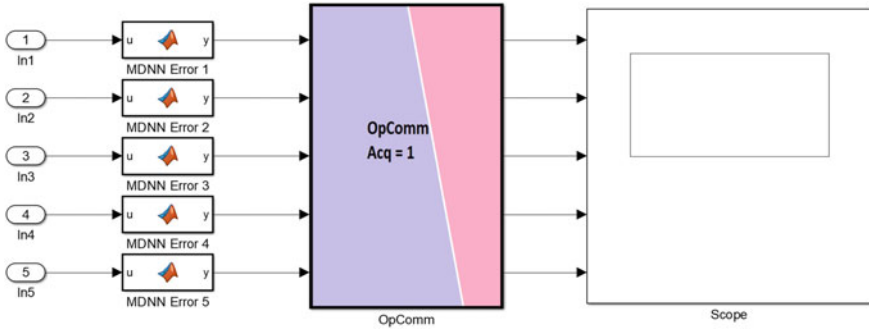


Fig. 33 The console Sub-system

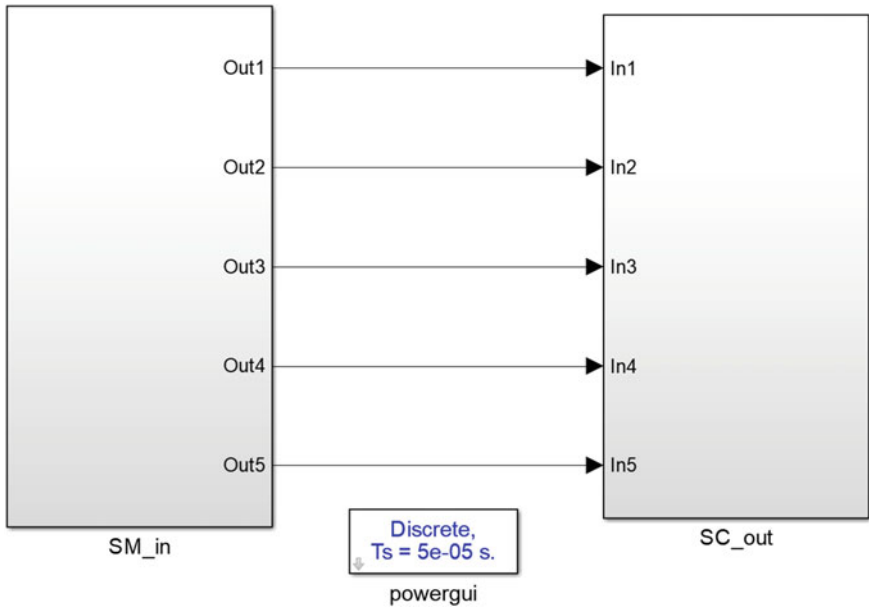


Fig. 34 The RT lab compatible model

**Fig. 35** Voltage angle MDNN testing results

**Confusion Matrix**

Output Class	1	839 20.0%	1 0.0%	0 0.0%	0 0.0%	0 0.0%	99.9% 0.1%
	2	0 0.0%	840 20.0%	0 0.0%	0 0.0%	0 0.0%	100% 0.0%
	3	0 0.0%	0 0.0%	840 20.0%	0 0.0%	0 0.0%	100% 0.0%
	4	0 0.0%	0 0.0%	0 0.0%	840 20.0%	0 0.0%	100% 0.0%
	5	0 0.0%	0 0.0%	0 0.0%	0 0.0%	840 20.0%	100% 0.0%
			100% 0.0%	99.9% 0.1%	100% 0.0%	100% 0.0%	100% 0.0%
		1	2	3	4	5	
		<b>Target Class</b>					

**Fig. 36** Voltage magnitude MDNN testing results

**Confusion Matrix**

Output Class	1	840 20.0%	0 0.0%	0 0.0%	0 0.0%	0 0.0%	100% 0.0%
	2	0 0.0%	839 20.0%	1 0.0%	0 0.0%	0 0.0%	99.9% 0.1%
	3	0 0.0%	0 0.0%	840 20.0%	0 0.0%	0 0.0%	100% 0.0%
	4	0 0.0%	0 0.0%	0 0.0%	840 20.0%	0 0.0%	100% 0.0%
	5	0 0.0%	0 0.0%	0 0.0%	0 0.0%	840 20.0%	100% 0.0%
			100% 0.0%	100% 0.0%	99.9% 0.1%	100% 0.0%	100% 0.0%
		1	2	3	4	5	
		<b>Target Class</b>					

common MDNN, monitoring the whole network is as shown in Fig. 40 below. It can be seen that the performance flatlines and arrives at a steady result.

From the performance plot, the best conduct was recorded at epoch 139 with a value of 0.0022778. The error histogram of the common MDNN testing results with 20 bins is as shown in Fig. 41 below.

The gradient plot of the testing results of common MDNN monitoring the whole power grid state is as shown in Fig. 42.

**Fig. 37** MW power MDNN testing results

	1	2	3	4	5	
1	840 20.0%	0 0.0%	0 0.0%	0 0.0%	0 0.0%	100% 0.0%
2	0 0.0%	840 20.0%	0 0.0%	0 0.0%	0 0.0%	100% 0.0%
3	0 0.0%	0 0.0%	839 20.0%	1 0.0%	0 0.0%	99.9% 0.1%
4	0 0.0%	0 0.0%	0 0.0%	840 20.0%	0 0.0%	100% 0.0%
5	0 0.0%	0 0.0%	0 0.0%	0 0.0%	840 20.0%	100% 0.0%
	100% 0.0%	100% 0.0%	100% 0.0%	99.9% 0.1%	100% 0.0%	100.0% 0.0%
	1	2	3	4	5	

**Fig. 38** MVAR power MDNN testing results

	1	2	3	4	5	
1	840 20.0%	0 0.0%	0 0.0%	0 0.0%	0 0.0%	100% 0.0%
2	0 0.0%	840 20.0%	0 0.0%	0 0.0%	0 0.0%	100% 0.0%
3	0 0.0%	0 0.0%	840 20.0%	0 0.0%	0 0.0%	100% 0.0%
4	0 0.0%	0 0.0%	0 0.0%	839 20.0%	1 0.0%	99.9% 0.1%
5	0 0.0%	0 0.0%	0 0.0%	0 0.0%	840 20.0%	100% 0.0%
	100% 0.0%	100% 0.0%	100% 0.0%	100% 0.0%	99.9% 0.1%	100.0% 0.0%
	1	2	3	4	5	

### 8.1 Time Consumption

From the confusion matrix shown in the preceding sections, it can be seen that there was very low miss-classification of data out of its respective state class. But with the help of the error function these errors can also be compensated for, as well as each dataset can be truncated to its correct respective class. The time taken for the correct classification of states in the testing dataset was 0.949 s, 0.952 s, 0.845 s, and 0.843 s for MW power, MVAR power, voltage magnitude, and angles, respectively. And the time taken by the fifth ANN to provide the state classification of the above power network parameters, based on monitoring the outputs of the four ANN's, is 0.398 s.



**Confusion Matrix**

<b>Output Class</b>	1	840 20.0%	0 0.0%	0 0.0%	0 0.0%	0 0.0%	100% 0.0%
	2	0 0.0%	840 20.0%	0 0.0%	0 0.0%	0 0.0%	100% 0.0%
	3	0 0.0%	0 0.0%	840 20.0%	0 0.0%	0 0.0%	100% 0.0%
	4	0 0.0%	0 0.0%	0 0.0%	840 20.0%	0 0.0%	100% 0.0%
	5	0 0.0%	0 0.0%	0 0.0%	0 0.0%	840 20.0%	100% 0.0%
		100% 0.0%	100% 0.0%	100% 0.0%	100% 0.0%	100% 0.0%	100% 0.0%
	1	2	3	4	5		
	<b>Target Class</b>						

**Fig. 39** Testing results of the common MDNN monitoring other MDNN's

The total time taken to obtain state identification and monitoring results in real-time can be found out by the equation mentioned below in (2).

$$T_M = \left( \frac{t_{MW} + t_{MVAR} + t_V + t_\delta}{4} \right) + t_c \tag{2}$$

where,  $T_M$  = total time taken for obtaining state identification results using the method proposed

- $t_{MW}$  = time taken for identifying MW power flow state on the lines.
- $t_{MVAR}$  = time taken for identifying MVAR power flow state on the lines.
- $t_V$  = time taken for identifying voltage magnitude state on the buses.
- $t_\delta$  = time taken for identifying voltage angle state on the buses.
- $t_c$  = time taken by fifth common ANN to identify the state of the previous 4 parameters.

Using the above-mentioned equation, the total time taken for the state identification of the power grid, in this case, can be found.

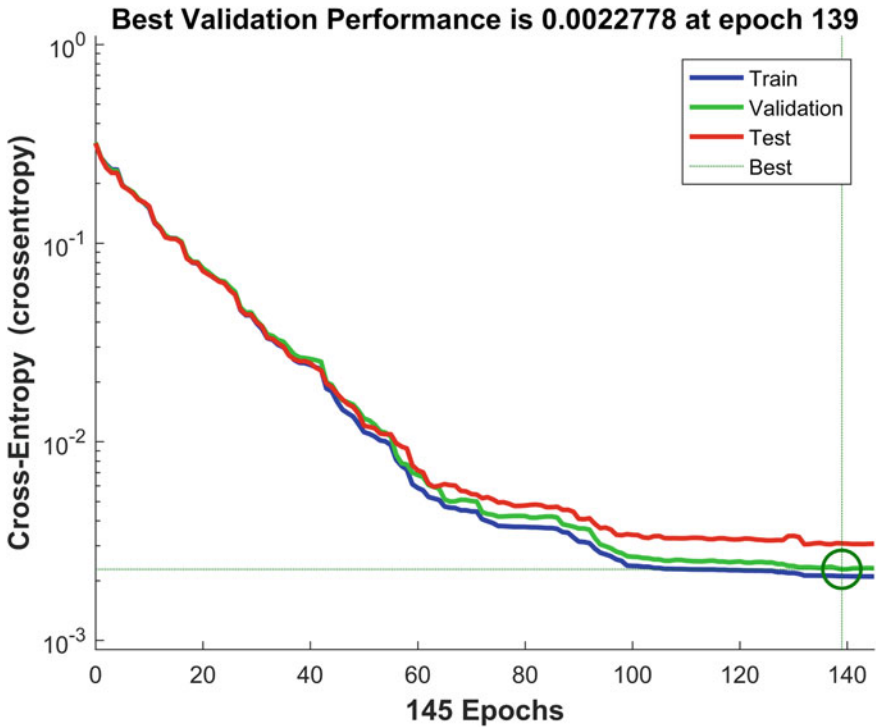


Fig. 40 Performance plot of the common MDNN monitor

$$T_M = \left( \frac{t_{MW} + t_{MVAR} + t_V + t_\delta}{4} \right) + t_c$$

$$T_M = \left( \frac{0.949s + 0.952s + 0.845s + 0.843s}{4} \right) + 0.398s$$

$$T_M = 0.89725s + 0.398s = 1.29525s \tag{3}$$

Hence, from (3), it can be seen that the total time taken to monitor the state of the power network under observation is 1.29525 s, which can be helpful for power system control operations in real-time. Using high-end computers with parallel processing features, the performance of the ANN's can be improved and the response time can be brought down further.

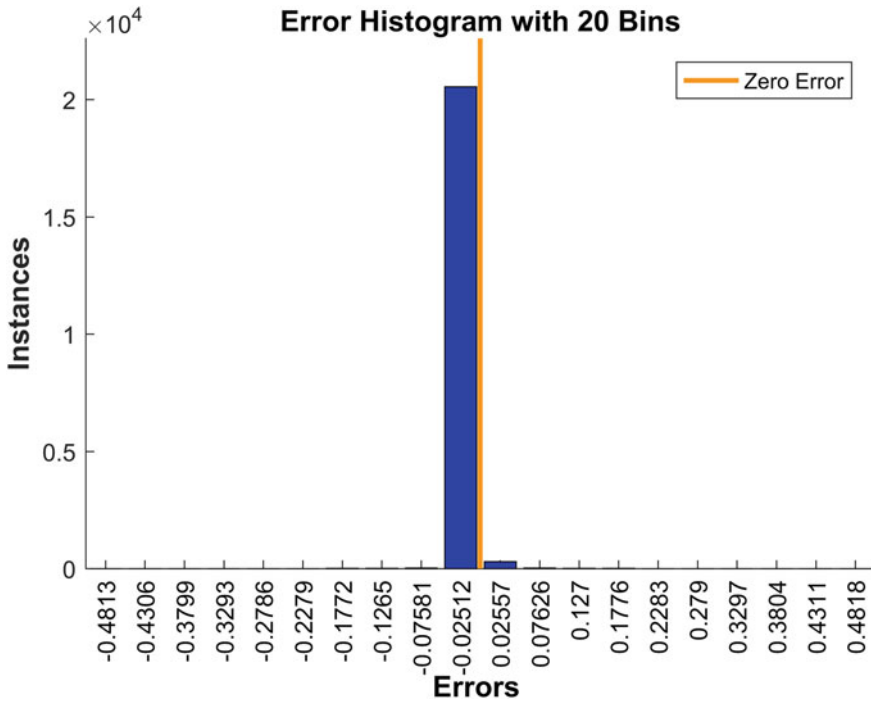


Fig. 41 Error histogram of the common MDNN monitoring results

## 9 Conclusions

From the above study, it can be seen that a multi-dimensional neural network (MDNN) was successfully developed and tested for multi-class classification of power network states in the IEEE 57-Bus test grid network. A total of 9800 different network operating states and their respective samples were used for the development and training of the MDNN. The trained and converged MDNN was then successfully tested with 4200 different network datasets, i.e., MW, MVAR, voltage magnitude, and angle. The highlights of the results are tabulated below.

The training was accomplished in 3.870 s, 3.879 s, 3.178 s, and 3.168 s, for MW power monitoring, MVAR power monitoring, Voltage magnitude monitoring, and bus voltage angle monitoring, respectively. The results of the application and testing of the MDNN were accomplished in 0.949 s, 0.952 s, 0.845 s, and 0.843 s for MW power, MVAR power, voltage magnitude, and angles.

The training and testing of the common MDNN monitoring these four MDNN were accomplished in 2.367 s and 0.398 s, respectively.

From the testing confusion matrix, it is obvious that there was minimal misclassification of states because the noise in the training data was minimum.

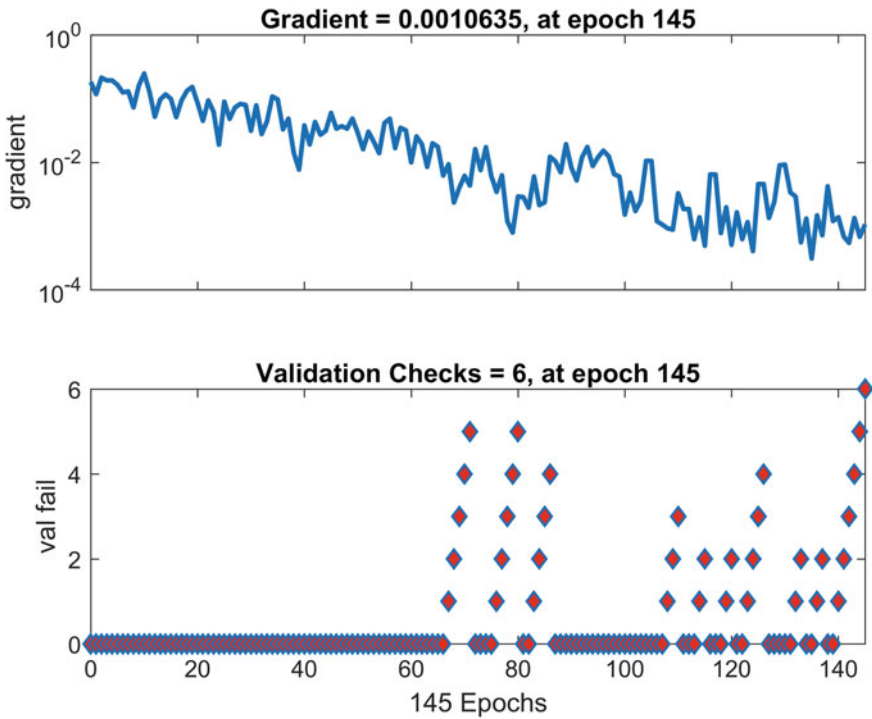


Fig. 42 Gradient plot of the common MDNN monitoring results

From the testing results, it is apparent that the developed multi-classifier, MDNN can successfully classify the input data into multiple different classifications, depending upon the requirements.

It is also evident that the response time for state identification of the network, using the proposed method is 1.29525 s, which can prove to be very helpful in the operation and control of a power grid in real-time.

For future endeavors, more simplified monitoring of the power network state transition can be accomplished, by utilizing a collection of such MDNN's, to collectively monitor the different parameters like circuit breakers states, switching states, load-tracking, etc., as mentioned previously. And, since the performance of the MDNN depends upon the quality and speed of the processor, a high-end computer can provide faster, better, and optimized results.

**Box 1. Technological opportunities** The training was accomplished relatively fast. The results of the application and testing of the MDNN are also comparable to the real-time devices currently utilized in the field

As shown in (3), the time taken for state identification of the grid is comparable to real-time protective devices, hence, there is a scope for real-time field application utilizing microcontrollers or signal processing devices

Since an error function is added to the output of the MDNN, the scope of optimization of the monitoring results is also available in the critical contingency scenario

There is also scope for further optimizing the results of the MDNN by utilizing better computers and accessories

## References

1. Anon., 2021a. Simulink. s.l.: Mathworks. Anon., n.d. Plot Error Histogram for a Neural Network. Available at: <https://www.mathworks.com/help/thingspeak/plot-error-histogram.html>, accessed May 2021
2. Anon., n.d.: Plot network performance—MATLAB Plot perform. Available at: <https://www.mathworks.com/help/deeplearning/ref/plotperform.html?jsessionid=7f1afef470cbb36195785bfb38d>, accessed May 2021.
3. Anon., n.d.: Plot training state values. Available at: <https://www.mathworks.com/help/deeplearning/ref/plottrainstate.html>, accessed May 2021
4. Christie, R., Dabbagchi, I.: IEEE 57 Bus test case. University of Washington, Washington, USA (1993)
5. Datta, S., Vittal, V.: Operational risk metric for dynamic security assessment of renewable generation. *IEEE Trans. Power Syst.*, **32**(2), pp. 1389–1399 (2017)
6. Fink, L.H., Carlsen, K.: Operating under stress and strain [electrical power systems control under emergency conditions]. *IEEE Spectr.* **15**(3), pp. 48–53 (1978)
7. Gholami, M., et al.: Static security assessment of power systems: A review. *Int. Trans. Electr. Energy Syst.* **30**(9), 1–23 (2020)
8. Liacco, T.E.D.: The Adaptive Reliability Control System. *IEEE Trans. Power Appar.Us Syst.* PAS-86(5), pp. 517–531 (1967)
9. Liu, T. et al.: A bayesian learning based scheme for online dynamic security assessment and preventive control. *IEEE Trans. Power Syst.* **35**(5), pp. 4088 - 4099 (2020)
10. Moler, C.: MATLAB R2021a. s.l.:MathWorks (2021)
11. OPAL-RT.: RT Lab. s.l.:OPAL RT Technologies (2013)
12. Tiwary, S.K., Pal, J., Chanda, C.K.: ANN-Based faster indexing with Training-Error compensation for MW security assessment of power system. *Lect. Notes Electr. Eng.* **664**(1), 35–46 (2020)
13. Tiwary, S.K., Pal, J., Chanda, C.K.: Monitoring static security assessment in its full scope using common artificial neural network. *Intell. Electr. Syst.: Step Smarter Earth* **1**(1), 107–115 (2021)
14. Tiwary, S. K., 2021. 5 Bus power network. Available at: <https://www.mathworks.com/matlabcentral/fileexchange/91610-5-bus-power-network>, accessed 27 May 2021
15. Tiwary, S.K.: Peak load management with wheeling in a gas turbine station under availability based tariff. Hyderabad, India, IEEE, pp. 1–5 (2021)
16. Tiwary, S.K.: Standard 6 bus system Look-alike model. Available at: [https://www.mathworks.com/matlabcentral/fileexchange/91730-standard-6-bus-system-look-alike-model?s\\_tid=prof\\_contriblnk](https://www.mathworks.com/matlabcentral/fileexchange/91730-standard-6-bus-system-look-alike-model?s_tid=prof_contriblnk), accessed 27 May 2021

17. Tiwary, S.K., Pal, J.: ANN application for MW security assessment of a large test bus system. Dehradun, India, IEEE, pp. 1–4 (2017)
18. Tiwary, S.K., Pal, J.: ANN application for voltage security assessment of a large test bus system: A case study on IEEE 57 bus system. Roorkee, India, s.n., pp. 332–334 (2017)
19. Tiwary, S.K., Pal, J., Chanda, C.K.: Mimicking on-line monitoring and security estimation of power system using ANN on RT lab. Kolkata, IEEE, pp. 100–104 (2017)
20. Tiwary, S.K., Pal, J., Chanda, C.K.: Application of common ANN for similar datatypes in On-line monitoring and security estimation of power system. *Adv. Intell. Syst. Comput.*, December, **755**(1), pp. 3–11 (2018)
21. Tiwary, S.K., Pal, J., Chanda CK.: Evaluation of the applicability and advantages of application of artificial neural network based scanning system for grid networks. *Adv. Intell. Syst. Comput.*, 30 October, **1198**(1), pp. 231–243 (2019)
22. Tiwary, S.K., Pal, J., Chanda CK.: Multi-dimensional ANN application for active power flow state classification on a utility system. Kolkata, IEEE, pp. 64–68 (2020)
23. Tiwary, S.K., Pal, J., Chanda, C.K.: Multiple-classification of power system states using multi-dimensional neural network. *J. Inst. Eng. India Ser. B* **104**, 893–900 (2023). <https://doi.org/10.1007/s40031-023-00892-1>
24. Zhang, Y. et al.: Intelligent early warning of power system dynamic insecurity risk: Toward optimal Accuracy-Earliness tradeoff. *IEEE Trans. Ind. Inform.* **13**(5), pp. 2544–2554

# Data Farming in a Smart Low Voltage Distribution System



Noah Sindile Fakude and Kingsley A. Ogudo

**Abstract** The energy utility industry's evolution instigated a technological shift where the global community is moving into digital technology and where modification and changes of systems are automated and computerized. While some philosophers are convinced that we are at the exodus of the 4IR into the 5th Industrial revolution, a big question is whether the 4IR was a success or not. It is unclear to determine the successes and failures since the energy industry is divided according to the first to the third world countries and their technologies. Due to technological limitations, many studies have proven that even the 3IR has not kicked in their power grid infrastructures. Developing countries like South Africa, India, Brasil, Argentina, and more have the 4IR concept in place but are not fully functional in most areas where their power grid extends. Since the power infrastructure already exists, the main limitation is ICT infrastructure. Most parts of the power grid do not have any real-time communication infrastructure and protocols, making it difficult for utilities to procure smart devices and grid monitors if there's no means to transmit and receive real-time information. These predicaments point to the 4IR enabler, that is, big data. There is no big data significance to harvest fundamental data. This book chapter addresses methods and ways to farm data, meaning putting entire systems in place to collect data. When data is available, it can be harvested to perform real-time tasks. Real data yields accurate information is vital for planning, simulation purposes, maintenance, and power outages computerized troubleshooting.

**Keywords** Big data · IoT · 4IR · Smart sensors · Smart devices · Power grid · Smart grid · Data analysis

---

N. S. Fakude (✉) · K. A. Ogudo  
Department of Electrical and Electronic Engineering Technology, University of Johannesburg,  
Johannesburg 2001, South Africa  
e-mail: [Noahfkd2@gmail.com](mailto:Noahfkd2@gmail.com)

K. A. Ogudo  
e-mail: [kingsleyo@uj.ac.za](mailto:kingsleyo@uj.ac.za)

© The Author(s), under exclusive license to Springer Nature Switzerland AG 2024  
K. Kyamakya and P. N. Bokoro (eds.), *Recent Advances in Energy Systems, Power and Related Smart Technologies*, Studies in Systems, Decision and Control 472,  
[https://doi.org/10.1007/978-3-031-29586-7\\_17](https://doi.org/10.1007/978-3-031-29586-7_17)

445

# 1 Background

The data concept appears in many different contexts, such as data capture, data analysis, data science, and database. Recently, we heard of data mobile or data bundle. The big question becomes

- What is data?
- How is data formulated?

There is no straightforward answer to describe it, but it is understood through applications; at the end of this chapter, you will be able to understand data, its importance, and its applications. Let us get to this analogy to put data in an application briefly.

A medical doctor sees two overweighing gentlemen, Tom and Jerry, and advises them to lose 5 kg each for 15 days with weekend rests. The doctor orders them to lose at least 1000 cal daily to achieve weight loss. Tom and Jerry both resolve to do daily exercises for 15 days. Tom buys a monitor watch to track his workouts and a diet guide to measure his calorie intake. Jerry goes the same session as Tom without diet and workout tracking. Table 1 shows the record of Tom's data table.

The record helps Tom to track his progress throughout the recommended program and informs him to adjust where necessary. During the program, Tom will know whether he is getting closer or away from the goal. On the other hand, Jerry will be hoping for a great outcome after the program, and there are more chances that he could be disappointed with the overall results.

This analogy shows the importance of data records and that standards and targets are measured through data. From day 1 in the first week, Tom realized that despite the workouts, it was not enough to burn calories in a day and adjust the intensity of the workouts, and he progressed throughout the week. In the second week, he adjusted his diet and lost hundreds of calories daily. However, one could argue that this is not raw data but a set of processed information, so it is just archived. The

**Table 1** Tom's calories record

Day no.	Cal intake/day	Cal workout/day	Net Cal/day
<i>Week 1</i>			
1	700	500	200
2	750	750	0
.	700	1050	-350
5	600	800	-200
<i>Week 2</i>			
1	350	500	-150
2	250	950	-700
.	250	1000	-750
5	300	1100	-800



argument could be challenged that though calorie is also processed information, it remains raw data when looking at them in terms of the magnitude of the calories lost or gained over time.

Data is captured through observation of a sequence of events, recorded from sensors, and tabulated for analysis and development of helpful information; it can also be visualized through plots or graphs.

## 2 Introduction

The electricity industry has become the leading essential in society. Now food is being processed, water is being purified and conveyed to the different parts of society, and it all takes Energy and electricity to deliver. So, preserving Energy is like preserving food and water. The utility industry is the primary driver of energy supply; business and economic models have been set for this industry to manage and supply electricity. Energy management is about decision-making, such as planning, organizing, leading, and controlling (POLC). POLC is achievable through information.

Information is gathered through facts, numbers, and figures, known as data. Data and information are two different things because information comes after data arrangements. Different information may be formulated from the same data source due to the structures of the algorithms for data sorting and analysis coming from the same data source. To achieve the accurate needed information, there must be a vast of facts or data, and those facts must be as raw as possible, meaning that data must be unadulterated before being processed.

Well-processed information provides sound guidance to electrical engineers working to improve the energy system at all costs. Energy management is a demanding task to pull through because of the system's irregularities and progression. Updated information is critical for continuous planning and decision-making. Data is facts and facts that inform a decision, and more data means more points, whereas more moments bring a pool of alternatives that can guarantee a city does not go blackout due to poor planning.

This chapter focuses on creating more data from the network so that planning, extensions, alterations, and maintenance of an electrical network system can be realized without a hustle. Data farming is a concept of reproducing data, breaking it down into its initial form level, and making it available for analysts and machines to decide. Let us take an example to narrow this phenomenon down to the electrical concept level. Equation (1) is the energy equation in kWh units in the energy business. This equation has been derived through power and time, whereas power is also a product of current  $I$ , voltage  $V$  and the phase angle between the current and the voltage, which is the power-factor  $\cos\theta$ . These three variables and time produces Energy. The time  $T$  is a period in hours, and that is within the period of the day. It can only indicate how much power was produced in that period. In energy planning, engineers may want to know how much current  $I$  or voltage  $V$  occurred at a specific hour of the day and how much phase displacement was between the current and the

voltage. In this case, (1) only provides the register in which power was consumed in the period, but not the finer details. To get data out of this equation, (1) must be broken down, and T must be broken down further into minutes, seconds, and even instantaneously. The breakdown of this measurement is the concept of this chapter, data farming

$$W = \int_0^T P.t \quad (1)$$

Data is not information, but a set of characters, numbers, symbols, and quantities that are recorded and computed for referencing and analysis. These numbers have no meaning to any random person but can be meaningful to data analyzers and computers. Information is processed data that are intuitive and intended for a reader. This means that information is extracted from data, not the other way around.

Data definition justifies that different information may be derived from the same data source depending on the interpreter. When data is interpreted, some characters are omitted to suit the view or submission of the author or analyst, which may be essential characters and focus points to the different analysts. So, it is necessary to keep all possible registers intact to view the system in all possible dimensions fully.

In an electrical network, data is recorded and formulated in terms of current 'I,' Voltage 'V,' frequency 'F,' power-factor 'cos  $\theta$ , ' and period in hours, minutes, or seconds 't.' These registers are vital in electricity records because, through these elements, the information such as the system's impedance 'Z' of the power delivered 'P,' the reactive power 'Q,' and the energy 'E' consumed over a period may be derived. For example, when you look at the power flow for planning and maintenance purposes, only P in Watts may be needed to determine the system capacity regardless of E, that is, the consumption in kWh. On the other hand, when looking at electricity from a business perspective for reports to stakeholders and possible investors, E in kWh is the focus because it speaks directly to the revenue collection, and that is money, the key driver of the business. Looking at the energy business from all sides, power and energy work together with the element of time because there is no energy without power, and there is no revenue without Energy.

### Energy Business

When we look at the history of the energy business, it started in the late eighteenth century when Thomas Edison designed the first commercial distribution system for his incandescent lamp clients. A copper strip was placed and weighed over a period, and the weight difference determined the amount of electricity passed through the weighed copper strip. The copper strip was one of the first methods to record the usage. As years passed, the measuring method evolved into different technologies where the Energy was measured and billed for a certain period.

The difference between the previous decades and today is energy consumption and demand. Decades earlier, the electric load in the houses was almost fixed and

minimal. The first distribution system was meant to illuminate incandescent lamps, but today nearly everything in the household is electricity enabled. For this reason, power flow must be considered in real-time to avoid unplanned power outages due to the system's strain caused by overconsumption or overload. The record needed to be taken into account is more than the Energy in kWh as it used to be. When conducting power flow analysis and planning using Energy, it is easy to mislead or conclude the processes based on incorrect assumptions. For example see below.

## 2.1 Data Recordings

In electrical systems, data may be recorded in terms of voltage, current, and phase angle. The voltage and current detected in the system are continuous at any instant. For accurate and real-time measurement, these values must be dictated instantaneously, as in expressions (2) and (3)

$$v(t) = V_{\max} \cos(\omega t + \delta) \quad (2)$$

$$i(t) = I_{\max} \cos(\omega t + \delta) \quad (3)$$

Power in watts can be derived from Eqs. (2) and (3), and Energy in kilo-watt-hour can be derived from power with an additional variable that is time (t). The flow of alternating current is sinusoidal and instantaneous values appear at any location of the cartesian plane. The maximum values shown in (2) and (3) are the peak values of the sinewave, and that is not necessarily the practical value, also called root-mean-square (RMS), as shown in Fig. 1. The RMS value is the average value slightly below the peak value.

Average measuring apparatus primarily consider the working voltage and current, and they do not measure the instantaneous values, which also show the peak current and voltage level. The peak voltage and current are practical in actual operation but only for split seconds. This is why they are ignored for the power flow analysis and application but could be helpful when performing power quality analysis.

The other important factor in data is time. To track the power flow in the system is the magnitude against time. In this context, time is explained in two folds: the clock and time in succession relating to the position of a 24-h day.

The graph in Fig. 2 shows the time, energy, and power graph. The power is tracked against the time of the day, and the energy is determined by the integral of the period as in (4)

$$\text{kWhr} = \int_0^T \text{kWt} \quad (4)$$

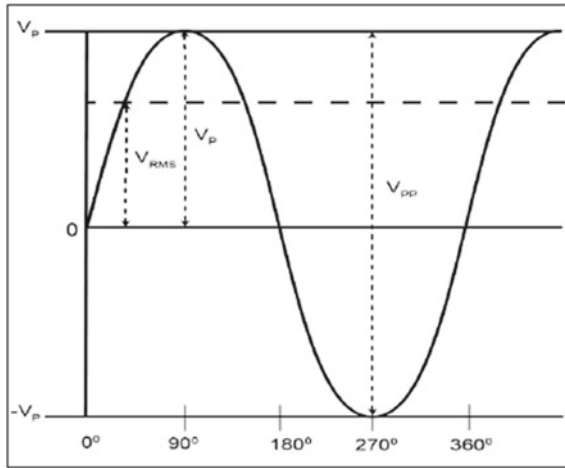


Fig. 1 Peak-to-peak sinusoidal graph [1]

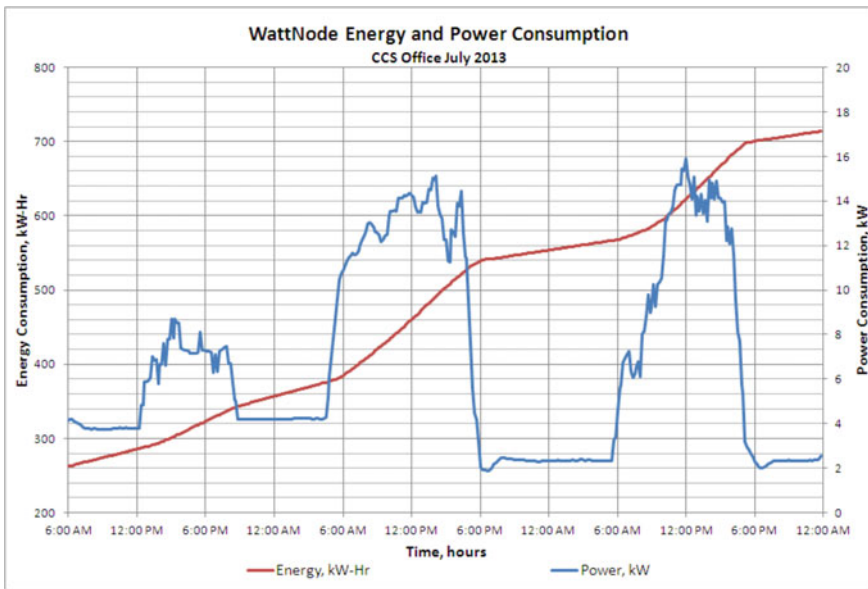


Fig. 2 Load curve in power (P) and energy (E) [2]

where kW-Hr is the total energy at period T  
kW—the real power consumed  
t—is the time in hours

When the data concerning the graph in Fig. 2 is captured, it is essential to keep the real-time hour of the day and not only the period the consumption occurs. Since

time never stops, the data may be recorded in intervals. In the 24 h period, these intervals may be sectionalized into an hour, minutes, seconds, or even split seconds. The length of the intervals determines the size of the data table and, subsequently, the data storage size.

## 2.2 *Data Tools*

It has already been mentioned that data are meaningless sets of variables used to formulate information. These variables are not garbage of random numbers and characters that are meaningless, but they are extracted from existing systems. Data tools are the devices or sensors used to extract that information. We use the term ‘Sensor’ because electricity is not grasped like water or any matter, but it can be measured as it flows, and the way to measure it is to sense the rate of its flow. Since electricity is expressed in voltage and current, these sensors must be able to measure both against time. To understand the sensing properties of voltage, current, and power, let us take a little detour to explain sensors and their evolutions. Then we will resume back to the topic of sensors concerning electric energy.

What is a sensor?

A sensor is a device that detects changes in physical properties and generates an electrical output in response to that change, which is a standard sensor definition. However, a sensor can also be defined as collecting other components to form a system. This device can only sense the change in the definition, but other elements, such as a convention, may be needed to interpret these changes. A sensor may also be required to perform data conversion and digital processing and be able to communicate with external devices. Therefore, sensors may be named per their capabilities based on their operational functions, such as standard, intelligent, and smart sensors. Standard sensors perform essential functions such as measuring and converting the measurements into useful information. An example of a primary sensor is a digital multimeter, as shown in Fig. 3. The digital multimeter does all necessary monitoring under the supervision of the user; they cannot be fixed in a unit to take continuous readings. These multimeters read instantaneous values and sample them through the analog and digital converters (AD), then calculate the average mean voltage or RMS; they cannot read the actual waves of the sinusoidal currents and voltages. Therefore, through a digital multimeter, we can say that you get simulated results of the current in the system when you place the testing leads on the terminals under test.

An oscilloscope can be the better option to get the complete picture of the analog wave of the current or voltage wave since it captures the analog waves of the currents and voltages. The oscilloscope graph the electrical signal as it fluctuates around time to track every instant. A scope will give you more accurate readings for instantaneous values than a standard electric meter. In data relation, we can say an oscilloscope measurement is much raw than a traditional energy meter since the energy meter is over-processed to get a picture of the measurements over time, while the oscilloscope

**Fig. 3** Digital multimeter [3]



gives the readings at each instant, though not 100% because it is also getting processed through AD converters and microprocessors. An oscilloscope can also measure the quality of a wave signal to detect any distortions caused by external discharges that do not form part of that electrical circuitry which helps to analyze and eliminate foreign electrical effects. Figure 4 shows the oscilloscope, though the range is far broader in terms of technology advancements.

Since the oscilloscope can measure different types and situations, it tells that it can need endless data registers or enormous data storage if it can record data instantly. The data size is determined by the sampling size, which is usually a typically datasheet, and logs that are typically columns in a data sheet. The other thing about the oscilloscope is that it can only measure the voltage directly in a circuit. You may need other interfacing circuits to measure the current, which may also increase possibilities or errors in measurement unless you employ sophisticated error signal correction measures within the scope. The reason for these additional corrections is due to the nature of the interfacing units that comes with their libraries to read and interpret current through the hall effects if current sensors are used so; therefore,

**Fig. 4** Oscilloscope [4]

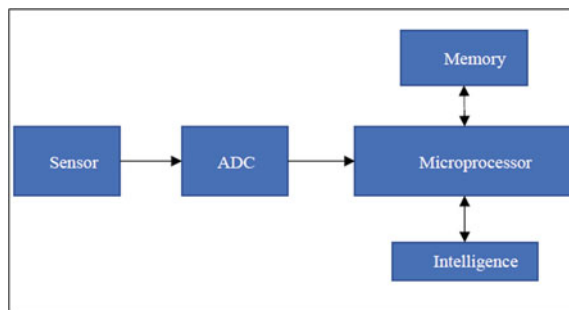


cascaded libraries will apply and that causes the incoming signal to lose its original or rawness shape since it goes through several conversions and interpretations. So, the main question will be, ‘Can an oscilloscope be used for current and voltage measurements?’ The answer will be that more work is needed before it may be applied.

The next generation of sensors is integrated and intelligent sensors. Integrated sensors can perform algorithms and do some functions, such as switching or displaying the results. The integrated sensors can measure, store, and process algorithms. Adding communication to the intelligence makes them smart sensors that can store or transmits information to external systems (Fig. 5).

The breakdown of the sensors takes us back to the theme of using sensors as data tools. Since the different sensor evolutions have been explained, it is clear that the standard sensor can do the preliminary work but cannot store data. I, it can only display the data during that time of measurement. Some of these multimeters have very little memory that can only last seconds before they can reset. The next phase was the intelligent meter that could store the data, depending on the device’s storage capacity. The capacity of any digital device is measured in bytes. A byte consists of 8 adjacent binary digits or characters called bits; this phenomenon means that the number of registers will determine the storage space. For example, if you need to keep track of the current in Amps only over a period, you will become a certain length at a specific storage interval. If you shorten the time intervals, you will store more characters and numbers, and the space will be limited. Another storage factor is the registers; from the example above, if we add a voltage and power measurement, the space will reduce even further. This concludes that the intelligent sensors are enabled to produce or mine the data, but the hatchery has fixed storage limitations. The latest generation of sensing devices is the smart device. The smart device is very close to the intelligent device, but its plus is external communication. External communication enables the sensor to generate data and export it to external systems such as the cloud. Clouds have almost infinite storage where data can be mined locally and sent to the big cloud storage. This ample data storage enables massive data mining from the sensors and as many registers as possible for analysis and applications. Figure 6 shows an example of a data table. This table consists of six columns or records. Under the clock register, the time interval is 15 min, meaning that the data table consists of

Fig. 5 Intelligent sensors



**Average, maximum & minimum figures: 1 Dec 2007 - 31 Jan 2008;  
Tuesdays, Wednesdays & Thursdays only (excluding 25, 26, 27 Dec  
2008; 1, 2 Jan 2008)**

Time	Average	Maximum		Minimum	
	kW	kW	Date	kW	Date
00:00	4,036.1	4,481.6	Wed, 30 Jan 2008	3,616.8	Wed, 19 Dec 2007
00:15	4,028.6	4,460.0	Wed, 30 Jan 2008	3,624.8	Wed, 19 Dec 2007
00:30	4,020.1	4,430.8	Wed, 5 Dec 2007	3,614.8	Thu, 24 Jan 2008
00:45	4,032.2	4,370.0	Wed, 30 Jan 2008	3,651.2	Thu, 24 Jan 2008
01:00	4,052.0	4,345.2	Thu, 10 Jan 2008	3,731.2	Thu, 24 Jan 2008
01:15	4,044.1	4,329.2	Thu, 11 Jan 2007	3,731.6	Thu, 24 Jan 2008
01:30	4,034.8	4,351.6	Wed, 30 Jan 2008	3,738.0	Tue, 18 Dec 2007
01:45	4,036.2	4,384.4	Wed, 30 Jan 2008	3,765.6	Thu, 24 Jan 2008
02:00	4,039.1	4,389.2	Wed, 30 Jan 2008	3,676.4	Thu, 24 Jan 2008
02:15	4,039.6	4,332.0	Wed, 30 Jan 2008	3,642.4	Thu, 24 Jan 2008
02:30	4,026.0	4,327.6	Wed, 30 Jan 2008	3,610.4	Thu, 24 Jan 2008
02:45	4,045.9	4,349.6	Wed, 30 Jan 2008	3,737.2	Thu, 24 Jan 2008

**Fig. 6** Data table with 15 min time interval [5]

97 rows, including the headings. If the interval time is doubled, the number of rows will be halved and the other way around.

Depending on the storage size, the registers can be added to infinity and reduced to a minimum.

From the intelligent sensors, storage will always be a problem. The bigger the storage will also affect the sizes of the devices, so external ad virtual storage is needed, giving birth to smart sensors.

Smart sensors are the latest generation that wins because of their communication abilities. Smart sensors are famous for their ICT interface ability. In this generation, the shared infinity storage is cloud storage.

In every smart-concepts, these sensors are used to read the local environment and communicate it to external units, and they can also im-port a set of instructions, codes, or algorithms in real-time.

Having discussed the sensors and their differences, let us revert to the topic of energy data systems. In this chapter, we are only going to focus on the sensing devices for

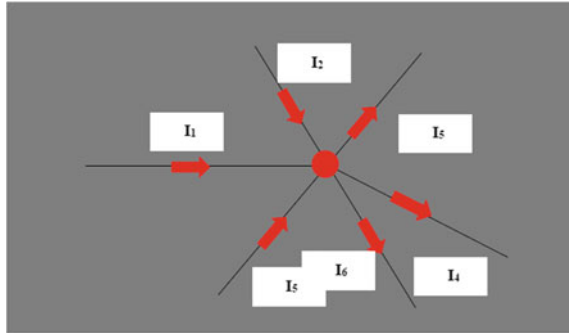
- Current (I) in amperes (A)
- Voltage (V) in volts (V)
- Power (P) in watts (W/kW)
- Time (t) in hours (h)
- Energy (E) in joules/watthour (J/Wh)

**Current data**

According to Kirchoff’s first law or Current law, the total current entering a junction or a node equals the current leaving that node. The first law means that the current



**Fig. 7** Kirchoff's current law



flowing in the branches must be measured in the branches. The current data can be measured in each branch, and the sum of the current in the branches can either be calculated or measured at the node. The illustration in Fig. 7 shows the current entering and leaving the node, and the summation is zero according to the Kirchoff first law.

The measurement of current in the system is essential to quantify the power flow so that the network is not overwhelmed and overloaded. The measurements must be carried out in each branch because the current flow does not change in a serial system until it reaches a branch. Data means any instantaneous value, as stated in (3). The recorded data is needed for sizing the network and planning for future expansions. They show the current burden of the network to see opportunities for connecting more consumers or upgrading the network if the demand exceeds the available capacity. The current sensors that are common and known in electricity are the current transformers. They come in various sizes depending on the network and circuit. They measure the current passing through feeding conductors and produce the corresponding value to the primary current. Since the current flowing out of the transformer is the reduced corresponding value, interfacing electronics circuits are needed to interpret this current. These interfacing units must be thoroughly calibrated to avoid error readings. The transformer windings ratio must also be intact to produce accurate corresponding output about the primary current. Due diligence processes are needed when the current flowing in the system is measured upstream. An electricity distribution system downstream is the network's LV side. At this level, current can be measured directly through electronic systems such as the Hall Effect sensors that no contact detection of current using a magnetic conversion element known as the Hall Effect.

The current transformer and Hall Effect sensor explained only apply to the current measurement.

#### Voltage sensors

The voltage law is also discussed in Kirchoff's second law, also known as the voltage law. The KVL states that the sum of voltages across the components which supply the electrical energy must be equal to the sum of all voltages across the other

components in the same loop. An electrical network is a string of conductors and elements; these components constitute a resistance that contributes to a voltage drop in the system. There are other factors that contribute to the resistance in the same as (5) suggests below:

$$R = \rho \times \frac{l}{A} \quad (5)$$

where R is the resistance

$\rho$  is the resistivity of the material

A is cross-sectional area

With the formula (5) in account, the voltage in the system will not remain the same throughout the system. In radial networks, any node or point adjacent to the supply will have a high voltage level, and the furthest point will have fewer voltage levels than the upstream of the system.

In electrical systems, voltmeters or voltage transformers are used as voltage sensors. These voltage sensors measure the RMS voltage of the system at any instant point. The output they generate can also be viewed at any point in time.

#### Power and energy sensors

The power and energy sensors depend on the values that are produced by the current and voltage sensors. In terms of power quality in AC systems, the angle between the current and the voltage is also considered to determine the power triangle that constitutes active, reactive, and apparent power. Therefore, we can conclude that power and energy are algorithms or arithmetically processed.

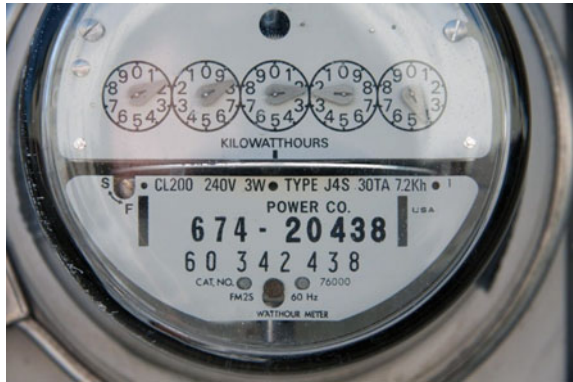
#### Data storage

Sensors' voltage, current, power, and energy variables do not offer data processing or storage. Still, they depend on electronic components such as registers, latches, or memories.

We have learned in the previous sections that data is the collection of basic information; this chapter defines it as the collection of measured electrical records. Devices and sensors are just used for measurements and monitoring; storage and processing are another business. In the energy business, measurement methods have evolved with technology from time to time. In the past decades, electromechanical rotary meters have been used to measure energy consumption. The electromechanical meter used the electromagnetic induction principle to turn a non-magnetic electrically conductive disc. The measurement of this meter comes from the count of the disc revolution. The speed of the turning disc is proportional to the power consumed. The meter is shown in Fig. 8.

The revolutions are recorded in the clock above the disc, as in Fig. 8. The clock is working as a register and storage of the record, but it cannot be reset, and it will only self-reset when it reaches 9999, then reset to zero. The periodic consumption data is only calculated by working out the difference in these readings within a period,

**Fig. 8** Electromechanical meter [6]



meaning that the history of the record must be known to determine the current usage. The data of this kind of meter is information that has been worked through the calculations on records, meaning that an error in the record will compromise the accurate data.

These meters evolved into digital meters with a minimum storage memory to keep the readings for a specific period. Some of these meters are counting continuously like the counterpart analog meters, whereas others can reset within the period. The readings are captured by utilities for billing and archiving purposes. The latest of these energy meters are the smart meters that we're able to communicate the consumption data remotely, and the data is stored in the server for further processing and billing.

The inclusion of data servers in the energy business means a severe business of information and communication technology (ICT). The data servers are called data concentrators in the smart-grid language because they connect different data channels with a common destination. From the data destination, this data is processed using different models of data management systems.

### Metering

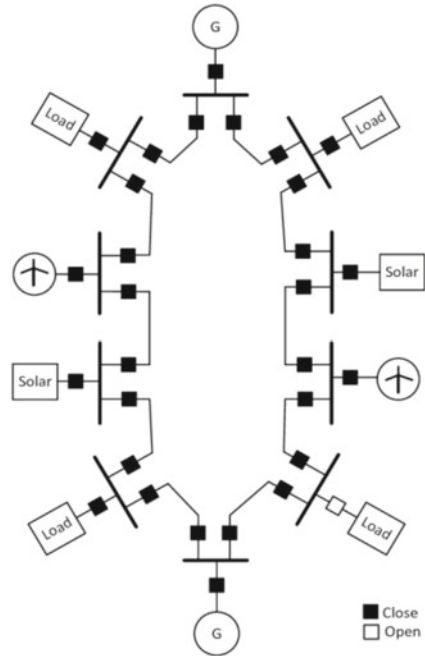
Two methods are used in distribution networks; these methods are

- Radial-network system
- Ring-network system

These two systems can be used interchangeably or separately. The ring diagram is shown in Fig. 9, the network is connected throughout the points, and the tail point is linked to the first point. Every node represents each node; in this case, some of these nodes inject electricity back into the system, whereas some are just consuming.

The voltage level will not remain the same throughout the connected points in the network. In the radial network, the voltage difference is even more severe if the network is stretched, as indicated in Fig. 10, as it can be seen that there are three different branches. These branches include 1-33, 1-18, and 1-22. The most extended branch is 1-18, and branch-18 will have the most minor voltage level, whereas branch-1 will have the most significant level since it is close to the transformer.

**Fig. 9** Ring electrical network [7]



In a distribution network, there will be thousands of these points, which must be accounted for. The more data collection points, the greater the energy analysis and management accuracy. That means data points will be millions if each device is installed for each register, such as voltmeter, ammeter, wattour meter, wattmeter, etc.

**Voltage levels**

As discussed, voltage levels are different at all the points because of the voltage drop. Voltage drop is the only issue resulting in the difference, and it also depends on some factors, as shown in (6):

$$V_{drop} = IR\cos\theta + IX\sin\theta \tag{6}$$

where

*V<sub>drop</sub>* is the voltage drop

*IRcosθ* is the active component, and

*IXsinθ* is the reactive component

*X* is the reactive resistance of the network

*R* is the resistance of the system

*R* and *X* are other elements that depend on other factors, as indicated in (5) and (7), respectively

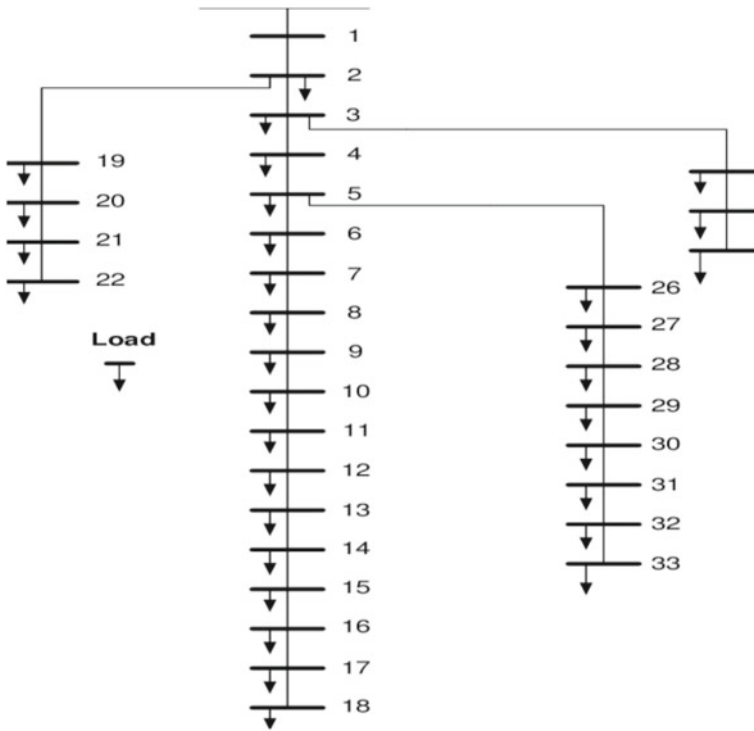


Fig. 10 Radial electrical network [7]

$$X_L = 2\pi fL \tag{7}$$

where

F is the system frequency

L is the line inductance

In Eq. (6), I is the common factor between the active and reactive components, but R and X contribute to the line impedance as in (8)

$$Z = R + jX_L \tag{8}$$

where

Z is the impedance

The impedance in (8) is needed to analyze the power flow, and since it is not known, the data devices can work out an algorithm to sample the measurements in each node to estimate the system’s impedance. Data Table 2 shows that the smart meters’ registers must provide the data analyses. The actual measurements that a standard energy meter performs are the voltage, current, phase angle, and frequency. The rest of the registers in the list are worked out by the arithmetic algorithms of the

**Table 2** Data table

Time (h)	Power (kW)	Energy (kWh)	Voltage (V)	Current (I)	Impedance (Z)
–	–	–	–	–	–

microchip. Network impedance is challenging to measure, especially when the load runs; algorithms are used to calculate network impedances.

The registers may all be found in a single device called an energy meter. Energy meters are installed closest to each premise where an electrical point is needed. As discussed in the previous section, these meters have been there for decades and evolved as technology changed. The latest generation of these energy meters is the smart meter that can create a communication channel to external controllers and concentrators.

The current implementation of these smart meters has a greater focus on energy consumption. The design of these meters has been more focused on the accuracy of the power consumed at each point than the actual quality of the supply. The possible method of using the smart meter for energy data plowing, high-quality voltage, and current filters must be embedded in these meters; by that, it means real-time currents and voltages are recorded and transmitted to the data concentrators.

### ***2.3 Data Capturing in Smart Distribution Network Simulation Model***

This is a brief simulation model that emulates data-capturing devices. The model consists of a 230 V AC source, twelve loads labeled as houses, twelve current sensors, twelve voltage sensors, and twelve power logic circuits. Each load consists of several resistors connected in parallel through step switches that randomly switch on different loads at different times. Figure 11 shows one of the internal configurations of the loads. The resistors are labeled to indicate what they represent and their load capacity. The run time of the model is 24 s which emulates 24 h of the day. Each step switch is connected to each load, and random switching times are set to be within the running time.

The complete model is shown in Fig. 12, where all the voltage and current sensors are demonstrated. These sensors are then connected to the MATLAB library's Goto transmission block. The Goto block copies the data from the sensors and delivers it to the relative block 'From,' and these blocks are meant to avoid crossing lines and to make the schematic more aesthetic.

The data is then transmitted to the power block as instantaneous current and voltage measured from each house. The current and voltage values are then converted into RMS values, and the phase angle between the current and voltage is calculated to determine the power factor of the load. The angle is essential to decide on the active and reactive power. Three more registers are formulated from this power block:

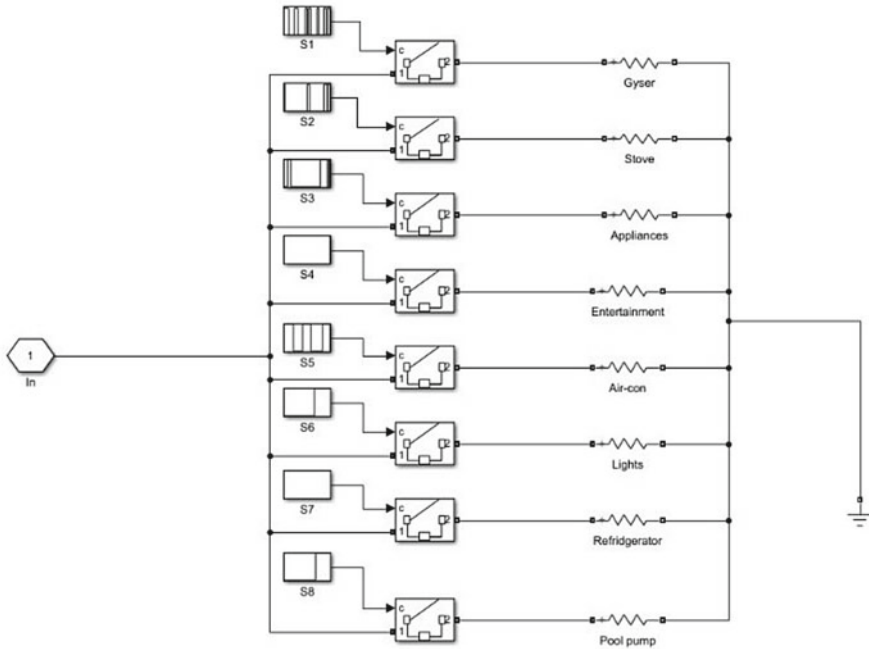


Fig. 11 Simulink model house loads

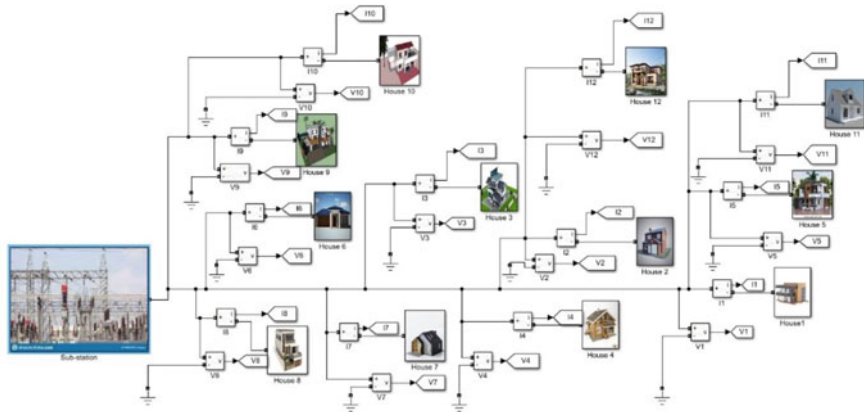
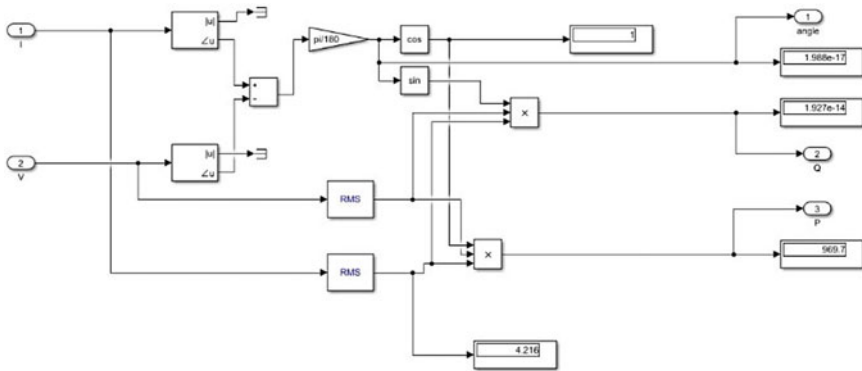


Fig. 12 Complete Simulink model energy distribution network

the active power  $P$ , reactive power  $Q$ , and phase angle. Figure 13 shows the power manipulation block.

The values that are manipulated in this box in Fig. 13 are then sent to the workspace through the logic box, as shown in Fig. 14. There is a multiplexer box or Mux box in



**Fig. 13** The power manipulation block

the Simulink library that combines all the data channels into one conveying channel and be decoded in the destination of the channels. For the sake of simulation, we have chosen data output for house 7 with four export data channels. These channels export the data for the two raw incoming currents and voltage feed, and the two manipulated channels that are the active and reactive power, P & Q, and exported to the works space. However, the data exports are not just limited to the workspace; the data could also be exported in excel C.S.V. files outside MATLAB for further data processing and arrangements. The ‘xlswrite’ tool makes it easy to work with the data outside of the program, and you can also read files from the outside workspace into the MATLAB program.

In Simulink, there are various options to log signals and send them to the workspace, as they can also be sent via the scope block in Simulink, where you can select if you want the structure, structure with time, or the entire array. The scope section also helps you choose the formats you wish to receive or sort the data before it gets into the workspace. After the data is reflected in the workspace, you

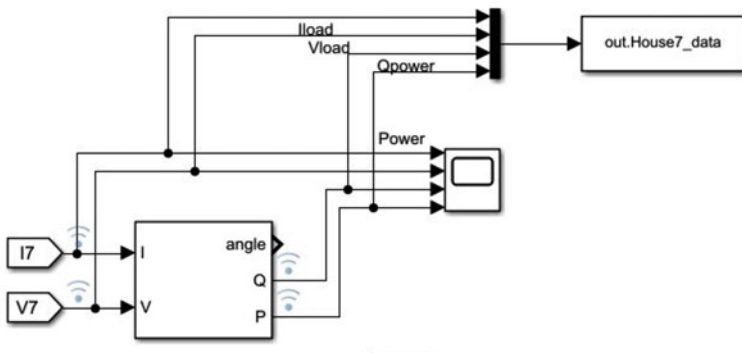
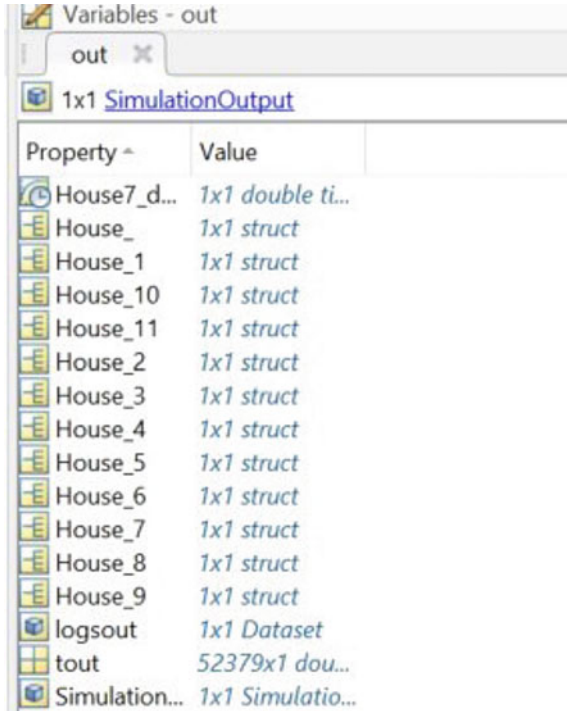


**Fig. 14** Simulink workspace data send



Fig. 15 Matlab workspace



can also sort it the way you want to see it and may also create plots that show the visual presentation of the data.

The workspace page, as shown in Fig. 15, records all the twelve houses collected data, and in Fig. 16 is the specific data from simulated house 7.

### 3 Results Discussion

The simulation model shows the endless possibilities of capturing data in a network without excessive technology sensors, but only through energy metering. The energy metering that currently exists in every point of electricity consumption can play a vital role over and above the energy usage it is now meant for. The infrastructure for this energy metering currently exists; only the devices themselves can be modified to address the smart-metering program. These energy meters are to be modified in terms of registers to record the vital elements such as the voltage, current, and phase angle. The rest of the logs will be manipulated from these three elements. The modification will include communication so that the sensors may communicate with the motherboard and the utilities. These devices will continually transmit the readings in real time to data concentrators managed by energy distributors and energy data

**Fig. 16** House 7 data

Time	Data:1	Data:2	Data:3	Data:4
1.5000	-1.519...	-8.286...	-1.125...	969.88...
1.7500	-2.747...	-1.498...	3.1174...	969.88...
2	2.3430...	1.2779...	1.9814...	969.88...
2.2500	2.2789...	1.2429...	6.8499...	969.88...
2.5000	1.9879...	1.0842...	-2.090...	969.88...
2.7500	5.2533...	2.8652...	1.0986...	969.88...
3	-3.038...	-1.657...	-8.670...	969.88...
3.2500	-1.228...	-6.699...	-6.407...	969.88...
3.5000	5.4950...	2.9970...	6.4787...	969.88...
3.7500	3.7981...	2.0716...	3.4511...	969.47...
4	4.6860...	2.5558...	9.6468...	969.92...
4.2500	-4.735...	-2.582...	-2.251...	969.88...
4.5000	-4.557...	-2.485...	-1.040...	969.88...
4.7500	2.9103...	1.5873...	1.4135...	969.88...
5	3.9757...	2.1684...	9.4845...	969.88...
5.2500	5.3174...	2.9002...	-3.960...	969.88...
5.5000	-1.050...	-5.730...	2.4766...	969.88...

management sites. In this simulation, the Simulation models the devices that generate data and the workspace models the data centres, cities, or distributors provide. In the following chapters, we will dive deep into these data management centres, as this chapter is only the introduction to data creation or data farming.

Smart Energy metering is the future energy management solution because it is usually placed at the tails of the electrical network. Each industrial, commercial or residential premise typically has a unique meter number to track energy consumption. Smart energy is just an energy meter that can be remotely controlled through its data-sending and receiving capability.

Storage needs to be considered to use a smart energy meter for electricity data logging. More data require more data storage systems since the registers and the sampling time carries ample information for hours, days, months, or even years.

**Real-time data and Historical data**

The sections above have alluded to and shown the reader about all elements of data and what data is. In the discussions, we learned that data is vital for electrical planning and design purposes. This section investigates the difference between these three types of data. The real-time data is mainly what has been discussed thus far; the data is recorded as the event is taking place and be used or analyzed at that instant. When the real-time data is kept in archives for future use, it becomes historical data rather than a real-time event.

The historical data differs slightly from data extracted from archives but is taken from real-time events. The difference is that this historical data previously recorded

real-time events being recorded after the event has taken place—for example, when a building burns down. Forensics and investigators find errors that might have led to the fire and archive the finding in a report, that is, the historical data because it was never recorded pre-event and when Thevenin was taking place.

The forecasting data is usually derived from the pre-sequence of events for predicted measurements and foreplaning. We will look at two case studies to put this difference in context.

#### Case 1 electric reliability council of Texas

Case one is taken from a study of a report [8] of a power crisis in Texas on 14 February 20 on 21, when a historic cold front hit Texas. Hit the Southern side of the US clocked 15 °C below the normal average temperatures n every city within the region. The duration of this front took over seven successive days without a breather, which was also unusual. The cold front started a week before when ergot communicated on 08 February 2021 for high electric demand anticipation. Due to the cold weather, a quarter of the total state capacity was already out on the 14th of February. It is 50% of the wind generation and 50% of the generators plants. On the other hand, Texas exceeded its the average 66 GW peak demand by an additional 4 GW to make it 70 GW peak demand at night when people cranked up their electric heaters to maximum due to the extreme cold weather. Units started tripping and further reducing the capacity because solar panels were covered by snow, wind turbines froze due to icing out cold, and gas pipes were no longer efficient. Gas delivery companies became inefficient due to weather; nuclear plants shut down due to frozen water supply and efficient pumping systems. The interconnected grids to Texas were facing the same problem leading them to be unable to help the state because they were also running at no reserves. On February 15, the state had half its capacity from the previous quarter 24 h prior. The condition resolved to load shedding to keep the balance of supply and demand, but this solution was almost late as the system frequency drastically dropped below the threshold for a few minutes. During this time, the whole of Texas was running at the grace of 9 min tolerance once the frequency dropped below 59.4 Hz for 9 min. Between 1:50 am and 1:55 am, the frequency below 59.4 Hz for five good minutes, only four minutes away before the system falls out of sequence and results in an entire state shutdown, which could take weeks and months before the plans are all brought back to normal.

Case study 1 summarises the event that took place in Texas from 14 to 18 February with an ongoing crisis. The question will be, “What kind of data was used for the decision-making?”. The question of the sequence of events brings us to the understanding that technical real-time and historical data was used. When the system showed signs of deteriorating when the voltages were dropping and the current rising, it shows where this whole scene is hoping that they might get other units up since they don’t want to resolve the load shedding yet, leaving people to die of cold. But as soon as the frequency began to drop, the officials realized that the state was now going for a total shut down which might cost a catastrophic failure to the entire grid system. The historical data is the plant capacity and the number of units in service, which also help to alert you that if you have two units and one unit goes,

then you only have one left. Another historical data they have is the percentages in all the different sets of generation technologies, as shown in Fig. 17, where it shows that gas has over 50% contribution to the grid. If they have gas supply issues, they will lose a substantial portion of the generation. The second highest contributor is wind generation, also sitting above the 3rd of the state generation. This kind of data helps you to make rational decisions. The historical data is archived chiefly because most data is found on blueprints of the entire design. This case study also shows that environmental factors play a part in data analysis since they directly affect the system.

### Case 2

On 14 August 2003, it was a typical hot day in the United States and Canada, and the ambient temperatures were high. The highest clocked in the day was almost 39 °C in Toronto and Cleveland, according to a report [9]. The average temperatures in these cities are 26 and 27 °C in August. During this time, an appointed electric reliability coordinator, Midwest Independent System Operator (MISO), was responsible for and predicted that the system could be operated safely. Though the grid was monitored in real-time, the transmission lines outside the region assumed MISO did not have complete monitoring control. MISO has a lot of sensors in the network that provide

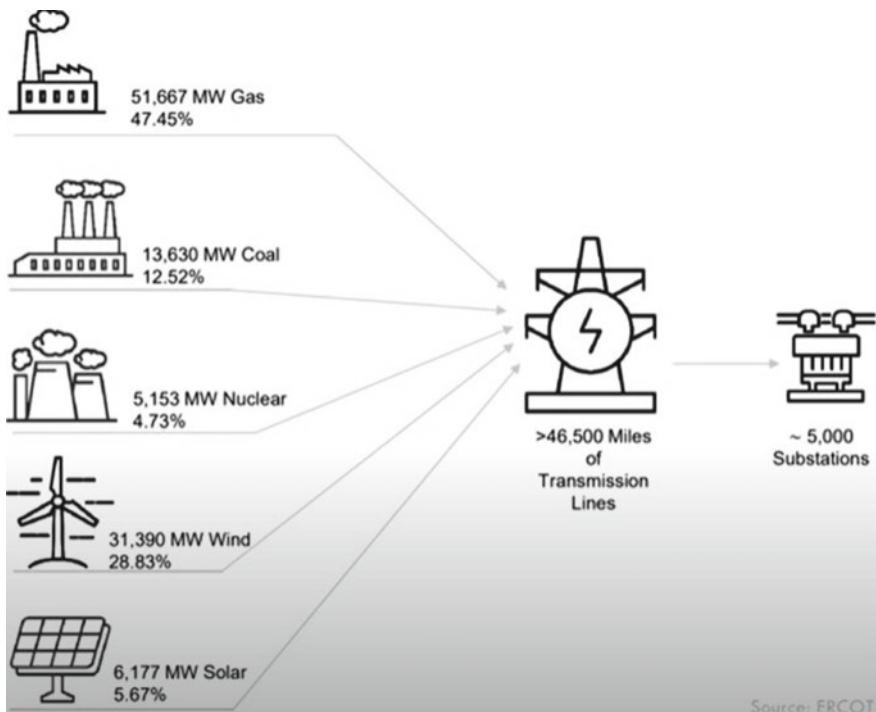


Fig. 17 Texas state generation in 2021 [8]

data in real-time such as system frequency, voltage, phase-angle, and current, as discussed in the previous sections. Due to electronic errors, the coordinators use a State Estimator (SE) system. The SE receives the real-time data and converts it into the possible estimated state, the assumption being the neural network algorithm, where the system is trained with data for less error accuracy predictions. On 14 August, this SE ran through some errors because it couldn't converge to possible matches after being fed by the data. This was apparently due to some transmission lines outside MISO control tripping twice daily, and the SE did not know that information. In due course, the state estimate was totally offline. The SE feeds into another system called Real-time Contingency Analysis (RTCA) which takes the information and does some algorithms to check all possible failures and predicted outages. The RTCA was also offline by its feeder being offline. This contingency analysis is vital to stay ahead of your system because you can run simulations of the scenario through it. On this day, the network was also vulnerable due to the unbearable heat; people had their air conditioners running at total capacity, which made the problems twice as accurate. The first problem, the monitoring system is offline. Secondly, the system is heavily loaded, especially with inductive loads that may lead to voltage drop in critical interconnections. In normal running conditions, MISO gives signals and warnings to their area-controlled operators.

First Energy (FE) is one of the control operators in Cleveland, Akron, Toronto, and Detroit. Due to the system's problems, MISO suffered. FE could also not get any warning and failed to match fluctuations in their connection point caused by the heavy induction loads in Cleveland. The transmission lines started to heat up, and conductors expanded, causing enough slack to short-circuit the trees. When each transmission line falls off, more strain is added to the system, and cascaded trips are inevitable. That happened in Cleveland, where they experienced a city blackout, as the events are well explained in the report.

Case study 2 differs from case 1, although the effects are not far distant. In this case, the real-time data is the centre pole of the entire event. The problems began when the monitor contingency analyser went offline. Historical data could be used at a very minimum, especially when reactive power was most needed and the bank of capacitors was off for the day. In engineering plants, preventative maintenance is meant for getting every system element in working conditions though not actively in use in emergencies like on 14 August 2003.

These case studies show the problems caused by a lack of data or caused by data errors. They also indicate that when working in electrical systems, data outside the scope of interest is as essential as data within the area. In the case of study 1, the severity of weather conditions must always be considered when designing and planning the system. Case study 2 shows that the transmission lines that were not part of the automated system control were the main contributors for the smart, automated systems to go offline, and the track of the grid status was lost, resulting in cascaded trips, which eventually brought Cleveland to a halt.

## 4 Conclusion

Data could come in any format. We do not only need sophisticated equipment to gather data, but technology can help us to grow data. To gather data, you must be intentional first, use what you have, and start with archiving. Records, when they are arranged intentionally, create a room to receive more data—for example, when a utility official or technician goes out for a call-up, he can have a report or template to do the 101 electric measurements such as voltage levels, current if possible, the system's frequency, the time, date, and the exact location. He can carry on with the work that they were dispatched for. This information can be archived and used to analyze patterns of load-flow, peak, and off-peak of that particular area and for extension needs analysis. The manual-archiving method can be used to get the necessary data, meaning that the network technicians can write down the findings on a job card, and the information is captured in the system. When budget allows, utilities can introduce apps or tablets for data capturing, and these data automatically load to the database as captured when preparing for future data sensors. These methods can also predict outages through data or information that is readily available.

This chapter reveals the importance of data management in the energy business. When you compare all the industrial revolutions from the first to the fourth industrial revolution 4IR, you realize computer programs ran the previous industrial revolutions. Still, data will run systems from the (4IR) going forward. The availability of data has become a new gold. Investors and government planners need data to plan their electrifying projects and to employ these green energy technologies, which require high capital. So the data can be used to scale up the programs and phase them in without surprises.

Utility industries must prioritize the existing data farming systems and those coming innovations and concepts to grow data in their design and manage them accordingly since data availability is also an enabler to energy students and researchers. In contrast, the lack of data discourages researchers from undertaking further studies due to a lack of resources, and that is data.

Through the data collection, utilities will be able to know their customers base, customers' behaviors, load profile, peak and standard peak times, the voltage levels at the extreme ends, and the nearest points to the supply so that they can adjust the current limits to keep voltage under safe use.

## References

1. Peak to Peak Voltage Calculator (VP-P)—Electrical Engineering & Electronics Tools. <https://www.allaboutcircuits.com/tools/peak-to-peak-voltage-calculator/>. Accessed 24 Feb 2022
2. Energy (kWh) vs. Power (kW)—Continental Control Systems, LLC. [https://ctlsys.com/support/energy\\_kwh\\_vs-\\_power\\_kw/](https://ctlsys.com/support/energy_kwh_vs-_power_kw/). Accessed 24 Feb 2022
3. Maya Digital Multimeter. <https://www.turbosquid.com/3d-models/maya-digital-multimeter/593168>. Accessed 24 Feb 2022

4. Choosing an Oscilloscope | Nuts & Volts Magazine. [https://www.nutsvolts.com/magazine/article/October2016\\_Choosing-Oscilloscopes](https://www.nutsvolts.com/magazine/article/October2016_Choosing-Oscilloscopes). Accessed 24 Feb 2022
5. Energy Consumption Charts from Energy Monitoring Software. <https://www.energylens.com/outputs>. Accessed 24 Feb 2022
6. How to Read Your Electric Meter: An Energy Use Guide—Chariot Energy. <https://chariotenergy.com/chariot-university/read-your-electric-meter-energy-consumption-guide/>. Accessed 24 Feb 2022
7. Islam, F.R., Prakash, K., Mamun, K.A., Lallu, A., Pota, H.R.: Aromatic network: a novel structure for the power distribution system. *IEEE Access* **5**(October), 25236–25257 (2017). <https://doi.org/10.1109/ACCESS.2017.2767037>
8. Lin, N.: The Timeline and Events of the February 2021 Texas Electric Grid Blackouts (2021)
9. Liscouski, B., Elliot, W.: U.S.-Canada Power System Outage Task Force (2004) [Online]. <https://reports.energy.gov/BlackoutFinal-Web.pdf>.

# Decision-Making Approach Using Fuzzy Logic and Rough Set Theory for Power Quality Monitoring Index of Microgrid



Sahil Mehta, Jitender Kaushal, and Prasenjit Basak

**Abstract** The determination process of the Power Quality Monitoring Index (PQMI) for the microgrid is a complex calculation that considers numerous power quality-related factors like voltage and frequency deviations, power factor, total harmonic distortion (THD), etc. Hence, the ideology of designing an efficient decision-making approach based on a complex set of data and its analysis is a critical issue. Besides, a resourceful decision-making approach has a beneficial effect on the smooth and stable operation of the microgrid system. Thus, in this chapter focusing on the complexity of data handling, data processing, and its dependent decision making, the well-renowned and efficient fuzzy logic and Rough Set Theory (RST) based methodology have been discussed in detail. These methodologies work to display the value of PQMI, and the decision-making approach based on the available data. These methods are verified by analyzing the data set of power quality assessment in a grid-connected/islanded microgrid. From the observations, the fuzzy logic- approach provides the PQMI status in the given range (poor to best). At the same time, the RST method provides a simplified decision based on the indiscernibility of the developed combinations.

**Keywords** Microgrid · Data analysis · PQMI · Fuzzy-logic · RST · Decision-making

---

S. Mehta (✉) · P. Basak

Electrical and Instrumentation Engineering Department, Thapar Institute of Engineering and Technology, Patiala, India  
e-mail: [sahilmehta.chd@gmail.com](mailto:sahilmehta.chd@gmail.com)

P. Basak

e-mail: [prasenjit@thapar.edu](mailto:prasenjit@thapar.edu)

J. Kaushal

Apex Institute of Technology, Chandigarh University, Mohali, Punjab, India  
e-mail: [jitender.e14621@cumail.in](mailto:jitender.e14621@cumail.in)



## 1 Introduction

In microgrid (MG), good power quality (PQ) is an essential aspect of stability as it ensures its healthy operation, consumer satisfaction, reliable power, smooth power exchange between the grid and MG, etc. Thus, it is significant to monitor and analyze the PQ of the system depending upon the various parameters at all instants of the MG operation. It is noteworthy that PQ monitoring plays an essential role in enhancing MG stability as it leads to quick decision-making, taking necessary actions, and balancing system configuration under uncertain conditions [1]. As in literature, the power quality of a system can be well-defined as the electromagnetic phenomena of variation in the voltage and current values at a given time corresponding to the specific location (geographical longitude and latitude) in a power system [2]. These disturbances occurring in the power system due to voltage deviation, frequency mismatch, etc., can be classified as power system harmonics, voltage fluctuations, voltage sags and swell, interruptions and imbalance, power–frequency variations, induced low-frequency voltages, etc. Thus, power quality is the priority of the operators and is dependent upon various parameters that need to be monitored and analyzed at each location (generation to load) and every instant of time [3] and [4]. Thus, monitoring is also essential to assess the data for various parameters and control such power quality issues. Therefore, it becomes necessary to add some intelligent power system controllers and utilize the full potential of these resources [5] and [6]. In such conditions, the data collected with proper assessment leads to better operation and control of MG. But, during the complex process of power quality assessment (PQA), the various tasks involved include monitoring various parameters, colossal data collection, and, based on the analysis, quick decision making.

Initially, this massive set of data for various parameters, like voltage deviation, frequency deviation, power factor, total harmonic distortion, etc., creates a challenging condition at a particular instant of time for the complete system. It further leads to data analysis, preparation for future prediction problems, and a quick decision-making process, a complex and challenging task. Thus, the Rough Set Theory (RST) was proposed in [7] to overcome such uncertain data handling and decision-making problems. RST can be explained as the new mathematical tool to solve problems with a vague, incomplete, and uncertain set of conditions, making the system less complex to implement and understand its performance [8]. The critical thought behind RST in decision-making is that the total amount of information and knowledge available in the given information system is related to any available object present in the universe of discourse. Thus, producing valuable data for all the given and available information that may or may not be similar in characteristics and therefore reducing the size of data is known as decision-making. The most critical and vital components of RST are the information system, condition/objects, attributes, decisions, approximations, reduct, and core [9].

Comparing the advantage of RST over the other statistical method or any simulation-based system, the theory works with a given set of data, enough for decision-making while eliminating similar types of data/conditions. Thus, making the

data handling, analysis, and decision-making process less complex to understand and implement [10, 11]. With such an advantage in data analysis and decision-making, several applications of RST are in computational intelligence like machine learning, clustering, knowledge discovery, intelligent systems, etc. [12–14]. In the real world, the surrounding area of applications includes medical sciences, risk management, system protection, engineering fields, etc., i.e., wherever the decision-making must be done based on complex data handling. Particularly in electrical engineering, RST finds a lot of applications like fault diagnosis, parameter selection, forecasting, data handling, operation management, etc. [15–18].

In addition to RST, the fuzzy logic approach/ fuzzy inference system (FIS) has also been well-considered for decision-making because of a vague and complex set of available data. As per the literature, a fuzzy approach can be employed for the operation and control of MG, considering various parameters and their wide range of values. The different aspects of data analysis and further decision-making, issues related to energy management of MG, manufacturing systems, networking and communication, smart grids, traffic management, etc. have been discussed in [19–25]. The other applications of rough set theory and fuzzy logic approach based on advanced data analysis and its impact on conditional responsiveness include the analysis of water quality [26], sustainable supplier selection under a vague environment [27], decision-making for the multi-agent-based system, etc. Besides, considering the ability of quick decision-making, the fuzzy logic approach has also been employed in advance load shedding, forecasting, and tariff calculation in smart/microgrids. demand-side management in smart/microgrids, PQ improvement using FACTS devices, etc. [28–31].

Thus, in this chapter, motivated by the trending concept of MG and its issues related to a wide range of data, advanced analysis, etc., one such problem related to the power quality of the grid-connected MG system has been considered. Out of the various data-driven approaches related to the power system and MG, like strategy, design, marketing, communication, management, decision-making, reasoning, policymaking, etc., this chapter has employed the decision-making approach. Such an approach focuses on efficiently using the raw data from the primary source for some significant action. Therefore, considering the above, the system design depends on four parameters: voltage and frequency deviation, THD, and power factor. In contrast, both the RST and fuzzy logic approaches have been applied. The chapter presents the wide range and impact of these parameters on the power quality monitoring index (PQMI), its advanced assessment based on the presented methodologies, and dependent decision-making. Hence, based on the comprehensive literature survey and other necessary details, RST and FIS are stated as most favorable for the problems related to massive data analysis followed by quick and crisp decision-making. Although in addition, the multi-criteria decision-making approach (MCDM) has also been identified in the literature. But the comparative analysis from [1] shows the fuzzy approach significantly better.

Considering MG and its issue related to PQ, the application of RST and FIS in related decision-making has not been very well explored. The purpose of dealing with a huge set of data considering multiple MG parameters using RST/FIS needs

to be well investigated. Therefore, this chapter considering a low voltage MG model contributes in the way of discussing both the above-mentioned approaches for quick decision-making aiming at stable microgrid operation.

The chapter has been organized as follows. Section 1 presents the introduction of the chapter. Section 2 presents the designed system description followed by the proposed methodology in Sect. 3. Section 4 presents the results and discussion of the chapter. Section 5 presents the comparative study and case analysis followed by conclusions in Sect. 6.

## 2 System Description and Proposed Methodology

An MG model has been considered for data analysis and validation of the presented approaches. This section discusses the brief system description of the MG model through a block diagram and proposed methodology. It must be notable that detailed system modeling has been done in [1]. In contrast, the focus of this chapter lies in the data analysis and decision-making using RST and the fuzzy logic approach.

### 2.1 System Description

The assessment of PQMI based on the wide range of values for different parameters using fuzzy logic in a typical MG has been proposed in [1]. As per this reference, a 10-kW single-phase MG in the Indian scenario with a 50 Hz frequency has been considered as shown in Fig. 1. The system includes two distributed energy resources (DERs) in the form of photovoltaic (PV) along with the other as a wind energy source which relates to the primary utility grid located at a distance of 500 m from the point of common coupling (PCC). The distance between the DERs and PCC is less than 100 m. A load of a fixed magnitude of 10 kW is connected at 300 m from the PCC.

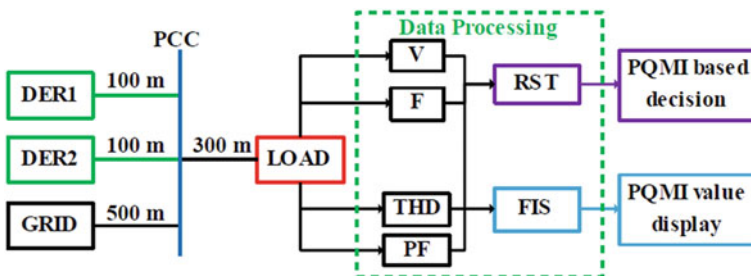


Fig. 1 Layout of the proposed model

From Fig. 1, the various parameters at the load side have been observed for data monitoring and collection, advanced data analysis, and related decision-making for enhanced and better operation of the system. These include system voltage, system frequency, power factor, and total harmonic distortion. The data collected at the load side of MG is processed and analyzed using the data analysis technique of both FIS and RST. Data processing includes setting up various ranges (minimum to maximum) for all parameters, system condition monitoring, etc. In addition to the above, the PQMI is calculated based on the data processing using FIS against the reference set of values, i.e., system voltage at 230 V, system frequency at 50 Hz, system power factor as unity, and minimum THD. It is important to note that the PQ must be maintained to stabilize the MG operation with enhanced performance and better consumer satisfaction. Thus, considering the most critical parameters affecting PQ, monitoring them and their dependent decision-making plays a crucial role. The figure represents the system layout with data processing of an MG model via RST and FIS for stable MG operation. Thus, the simultaneous application of fuzzy logic and rough set theory approach for data analysis and decision-making has been proposed in the present research, as shown in Fig. 1. The advantage of employing RST in the decision-making process is robust data analysis and dynamic response.

In contrast, FIS analyzes a wide range of values for each parameter and its dependent decision-making. In addition, the RST and FIS-based approaches are responsible for the smooth operation of MG related to the issues of power quality considering a high level of situational awareness via developed system information and data analysis. Therefore, with such benefits, the simultaneous use of both approaches avails the display of PQMI for grid-connected MG and quick decision-making for its smooth operation.

### 3 Proposed Methodology

#### 3.1 Fuzzy Logic Approach

Focusing on uncertain system conditions and the vague problem of decision-making, the fuzzy logic-based approach can be well utilized considering the huge and complex set of data. Such an approach allows designing a given problem by substituting the possible range of values available from the analysis of a huge set of data in the form of membership function and respected linguistic variables. Based on the various variables and functions, fuzzy rules can be developed, initiating the decision-making process for the specific value of the parameters [32]. Figure 2 shows the various components of the fuzzy logic approach. The advantage of using a fuzzy logic approach is its ability to handle complex and vague problems with a high number of inputs or output parameters.

For the problem of decision-making based on PQMI, which depends on four electrical parameters (voltage regulation, frequency deviation, total harmonic distortion,

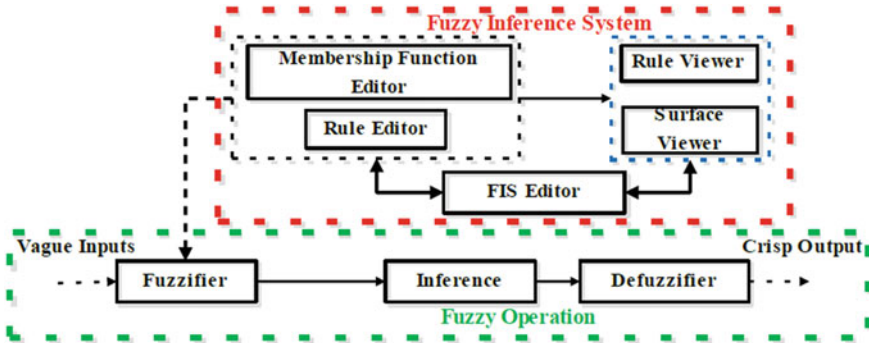
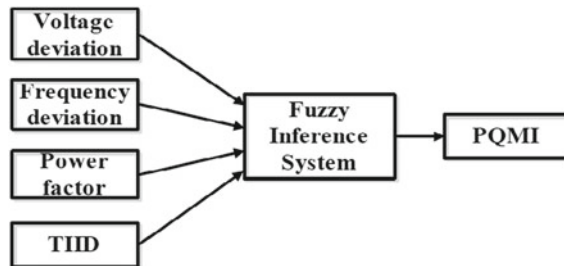


Fig. 2 Components of fuzzy inference system (FIS)

Fig. 3 Components of fuzzy inference system (FIS)



and power factor), a similar fuzzy-based system has been developed. Figure 3 shows the layout of a proposed system for PQMI decision-making.

To develop the FIS considering the layout as mentioned above, Table 1 shows the detail of input and output membership functions [1]. Considering the different parameters, the triangular membership function has been used in this work. As per the standard IEEE Std. 1250–2011, the voltage deviation (VD) – allowable to  $\pm 10\%$  of nominal value has been distributed between (- 10, 0, 10). As per the standard IEC 61,000–3-2, the most favorable or accepted range of frequency deviation has been set between 49.5 Hz and 50.5 Hz, with a maximum limit exceeding 47 Hz to 52 Hz. For the input parameter of power factor (PF), as per standard IEC 60,831–1/2, the acceptable range (Best) value is set as 0.9–1.0, considering it is favorable for the electric load. With the presence of non-linear loads in MG, as per standard (IEEE Std. 519–2014), the value of THD should be equal to or lower than 5% for the LV power system, and thus, in this case, the acceptable range of THD (Best) has been set between 0–5.8%. Considering the previous work related to PQ, the THD rises significantly in the presence of uncertain and non-linear loads in the islanded mode of MG operation. Thus, in this work, the maximum value of THD has been taken as 115%.

**Table 1** Range(s) of membership functions for designed FIS

MFs	Range			
<b>VD</b> - 10 to 25%	Best - 10, 0, 10	Good 8, 10, 14	Poor 13, 15, 20	V. Poor 18, 20, 25
<b>F</b> 47 to 52 Hz	More Poor 47, 48, 48.5	N. Poor 48, 48.7, 49.6	Best 49.5, 50, 50.5	P. Poor 50.4, 51, 52
<b>PF</b> 0.4 to 1.0	Poor 0.4, 0.55, 0.7	Good 0.65, 0.75, 0.85	V. Good 0.8, 0.85, 0.92	Best 0.9, 0.95, 1.0
<b>THD</b> 0 to 115%	Best 0, 2.5, 5.8	Average 5, 7.5, 10	Poor 9, 25, 35	V. Poor 30, 75, 115
<b>PQMI</b> 0 to 8	Best 0, 1, 2.5	Good 2, 3, 4.5	Average 4, 5, 6.5	Poor 6, 7, 8

In addition to the input parameters, the corresponding output variable is the PQMI depending on the status of all four input parameters and developed rules. The membership functions for different input and output parameters are given in Figs. 4, 5, 6, 7 and 8.

Thus, considering all the above information related to the design of membership functions, the 256 rules have been developed based on all the possible combinations available. Below, the sample set of rules is presented in Table 2.

Rule no. 20 can be defined as if voltage deviation is best; frequency deviation is average; power factor is poor, and THD is also very poor, then the PQMI will be poor.

**Fig. 4** Membership function for voltage deviation

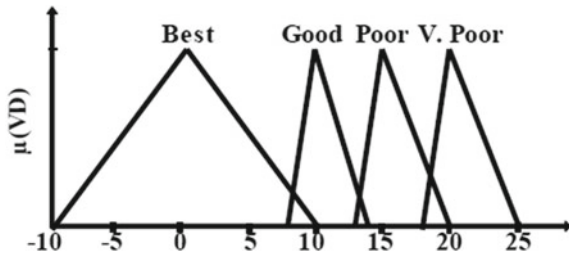


**Fig. 5** Membership function for power factor

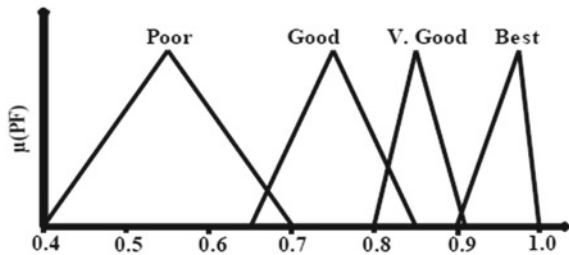


**Fig. 6** Membership function for frequency

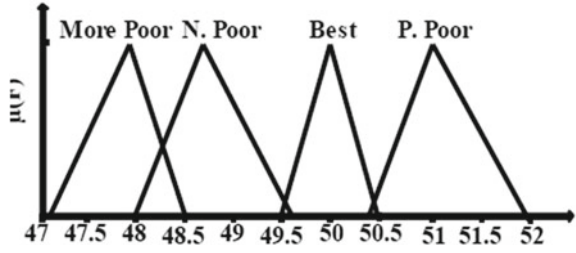


**Fig. 7** Membership function for THD

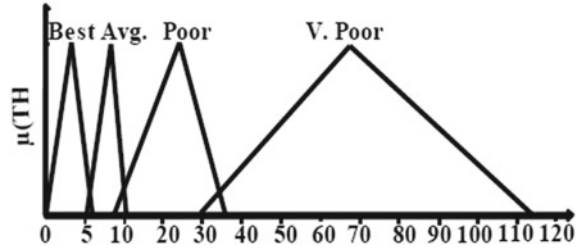


**Fig. 8** Membership function for PQMI

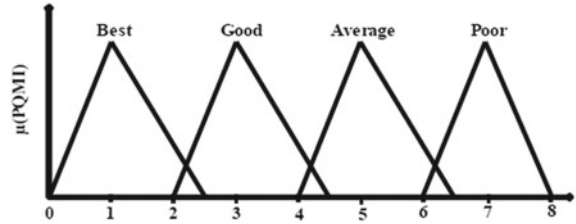


**Table 2** A sample set of rules for FIS/information system

Rule No.	V.D	F	P.F	THD	PQMI
4	Best	Poor	Poor	V. Poor	Poor
20	Best	Avg	Poor	V. Poor	Poor
30	Best	Avg	Best	Avg	Avg
38	Best	Best	Good	Avg	Avg
61	Best	Good	Best	Best	Avg
75	Good	Poor	V. Good	Poor	Poor
96	Good	Avg	Best	V. Poor	Poor
101	Good	Best	Good	Best	Good
140	Poor	Poor	V. Good	V. Poor	Poor
175	Poor	Best	Best	Poor	Poor
189	Poor	Good	Best	Best	Avg
206	V. Poor	Poor	Best	Avg	Poor
221	V. Poor	Avg	Best	Best	Poor
250	V. Poor	Good	V. Good	Avg	Poor

Rule no. 221 can be defined as if the voltage deviation is very poor; the frequency deviation is average; the power factor is best, and THD is best, then the PQMI will also be poor.

It is to be noted that the ideal condition or the most favorable condition will appear when all the value of each parameter lies in the “best range” characteristics.

### 3.2 *Rough Set Theory and Its Components*

The rough set theory (RST) uses the information-based system associated with the objects of the universe [16]. According to RST, every object/condition/case, etc., that exists in the universe of discourse has some similar characteristics. The amount or type of information shared by the two or more can be deduced as one piece of information. This condition in terms of RST is known as indiscernibility. In other words, indiscernibility can be defined as a set of information like another set of information; both are available in the same universe of discourse. The advantage of using the RST over the other decision-making theory is that it utilizes a set of information rather than a crisp set of values making it more robust and reliable. This condition in RST theory is termed the lower and upper approximation range. These ranges specify the level of significance within the range of values. The values or conditions that mainly and indeed belong to the system combined form the lower approximations.

In contrast, the values possibly in favor combine and form the upper approximation values. The other key terms in RST theory are the decision table or the information system, which constitutes all the possible amounts of data or information based on which decisions must be made. It includes the input or independent attributes and the output parameter or decision attributes. The input attributes make the set of a condition like “if  $x_1$  and  $y_1$ ” or “if  $x_5$  and  $y_3$ ” and likewise such that all the possible conditions between  $x$  and  $y$  dependent upon the amount of data are included. In the decision attribute, the dependent decision based on the developed condition is stated like the complete developed condition is “if  $x_5$  and  $y_3$  then  $z_7$ ” where  $z_7$  is the action or the decision taken on behalf of  $x_5$  and  $y_3$ .

In RST, these conditions and the information set are further discriminated against based on either the information attributes or the decision attributes. The decision-making can be improved and simplified. In the case of discrimination based on the decision attribute, the benefits to the system operator are more. In the case of system/data analysis, discrimination can be done on the information attributes. Here, in this chapter, the indiscernibility is developed on the decision based on the power quality monitoring index.

Along with the indiscernibility and lower/upper approximations, the other essential components of RST are the reduct and the core. Reduce term can be explained as the reduction in the size of the complete information system while keeping in mind the conditions of indiscernibility, i.e., out of all the objects present in the universe of discourse which is similar in characteristics can be eliminated, leading towards the



reduced information system with an equal quantity of knowledge. In contrast, the term core can be defined as the most important attribute of the information system without which the system shall be considered incomplete and thus not suitable for making decisions. Below the mathematical expression for all the above key terms are given:

**Decision table/ Information system.** Let  $T = (U, A)$ ,  $\{A = B \cup C\}$  be the components of the Information system, where  $U$  is a non-empty and finite set of objects called the universe and  $A$  is a set of input/output attributes with  $B$  and  $C$  as the condition attribute and decision attribute respectively. The elements of  $U$  include objects, cases, conditions, observations, etc. whereas the attributes can be interpreted as features or characteristics such that:

$a: U \rightarrow \forall a \in A, \forall a$  is called the value set of  $a$ .

Let  $a \in A, P \subseteq A$ , the indiscernibility relation  $IND(P)$ , is defined as:

$$IND(P) = \{(x, y) \in U \times U: \text{for all } a \in P, a(x) = a(y)\}.$$

In other words, the two or more objects are indiscernible in nature if the discrimination between them based on certain given terms cannot be done, i.e., all the objects possess similar characteristics.

**Lower and Upper approximations.** Let  $B \subseteq C$  and  $X \subseteq U$ , i.e., the set with all its elements present in  $U$  that certain, be termed the set of lower approximations, as shown by Eq. 1.

$$B(X) = \{x \in U : B(x) \subseteq X\} \tag{1}$$

whereas the values present in the universe ( $U$ ) of discourse that is known to possibly belong to any set are termed as the upper approximation values of set  $X$ .

$$B(X) = \{x \in U : B(x) \cap X \neq \emptyset\} \tag{2}$$

Equations (1) and (2) represent the lower and upper sets of approximations.

**Boundary region of a system:** The boundary region can be defined as the set of values that cannot be classified into either a favorable or unfavorable set of values. The equation shows the boundary region to be the in-between values of the upper and lower approximations.

$$BNB(X) = B(X) - B(X) \tag{3}$$

**Rough set and crisp set:** Dependent upon the values of the lower and the upper approximations, a rough set can be defined as the non-empty set with all the values present in the lower and upper approximations being unequal in nature as shown below,

$$B(X) \neq \underline{B}(X) \quad (4)$$

whereas the subset with no difference between the values of lower and upper approximations is termed the crisp set as shown below,

$$B(X) = \underline{B}(X) \quad (5)$$

**Positive and negative region:** The positive region can be defined as the set of all the values present in the universe of discourse that can be classified as per the class of U/D employing attributes from C.

$$POSC(D) = \cup C(X) \quad (6)$$

where  $C(X)$  represents the lower values of approximations with respect to C, whereas the negative region of a system consists of those elementary sets that have no predictive power for a subset X given a concept R. They consist of all classes that have no overlap with the concept. That is,

$$NEGR(X) = U - R(X) \quad (7)$$

**Reduct and core:** A system with let  $T = (U, A, C, D)$  can be termed as independent or non-dependent in nature if all values of c in the set C are necessary and therefore mandatorily present. Then, a set of values or the information  $R \subseteq C$  can be termed as the reduct of C if  $T' = (U, A, R, D)$  is independent and  $POSR(D) = POSC(D)$ . Furthermore, there is no  $T \subset R$  such that –

$$POST(D) = POSC(D) \quad (8)$$

In other words, the reduct is the minimal set of elements or the values that con-serve the indiscernibility relation of the complete information system. There is a minimum loss of information and maximizing indiscernibility is conserved. Thus, eliminating the repeating or non-required information from the information table to make it less complex is called reduct in RST. Whereas the most important component of the

reduct is the core value or attribute of the system, i.e., the attribute without which the information system and the knowledge of the system are incomplete in any condition. The core can be well explained by Eq. (9) as given below,

$$\text{CORE}(C) = \cap \text{RED}(C) \quad (9)$$

where  $\text{RED}(C)$  is the set of all the values present in the values present in the reduct values of set  $C$  whereas the values which intersect with the values present in the reduct of the complete information system.

**Accuracy of approximation:** The accuracy of the approximations can be defined as the ratio of the lower and upper values of the approximations. If the ratio given by  $\alpha$  is equal to 1 that implies the nonexistence of the boundary region between the upper and the lower approximations. The mathematical expression for the same is given below for a sample set  $X$ .

$$\alpha(X) = \text{Lower approx.}(X) / \text{Upper approx.}(X) \quad (10)$$

Thus, the values present in set  $X$  with an accuracy level equal to 1 are termed the crisp set. Otherwise,  $X$  is known as a rough set i.e.,  $0 \leq \alpha \leq 1$ .

Hence, considering the parameters mentioned above related to rough set theory, their correlation with the present problem can be stated as  $U = \{C1, C2, C3, \dots, C256\}$ , i.e., the total number of combinations available in the universe, the condition attribute is given by:  $B = \{Vd, Fd, THD, PF\}$  and  $C = \{PQMI\}$ , where  $B$  and  $C$  may vary from very poor to best. In addition to the information system, the indiscernibility (given in Table 3) explained as the unique relation of the input and the output w.r.t each other is given as  $\text{IND}(\text{BEST}) = \{C45\}$ ,  $\text{IND}(\text{POOR}) = \{C1, C7, \dots\}$ . Following the general procedure of calculating the reduct and the core for the PQMI calculation, each parameter in the given sequence must be eliminated. The indiscernibility must be analyzed, whereas the condition attribute that shows the features is termed the core. The combination of the same with the other attribute is the reduct. In the present problem, the only reduct possible is the combination of all the condition attributes such that all parameters are core of the decision i.e., all the four input parameters (Vd, Fd, THD, PF). Thus, based on the above descriptions of the terms related to RST, the key advantages in decision-making can be given as, small and less complex data analysis, quick action, accurate approximations, and clear decisions with comparatively low results and less vagueness. The results for the designed fuzzy logic and RST-based system and their advantages are presented in Sect. 3.

**Table 3** Indiscernibility for decision attribute

IND (BEST)	{C45}
IND (GOOD)	{C26, C29, C37, C41, C46, C101, C105, C109, C165, C169, C173}
IND (AVERAGE)	{C5, C6, C9, C10, C13, C14, C21, C22, C30, C33, C34, C38, C39, C40, C42, C43, C44, C47, C48, C53, C54, C57, C61, C69, C73, C77, C85, C89, C93, C97, C102, C106, C107, C110, C111, C117, C121, C125, C137, C141, C149, C153, C157, C161, C166, C170, C174, C189, C229, C233, C237}
IND (POOR)	{C1, C2, C3, C4, C7, C8, C11, C12, C15, C16, C17, C18, C19, C20, C23, C24, C25, C27, C28, C31, C32, C35, C36, C49, C50, C51, C52, C55, C56, C58, C59, C60, C62, C63, C64, C65, C66, C67, C68, C70, C71, C72, C74, C75, C76, C78, C79, C80, C81, C82, C83, C84, C86, C87, C88, C90, C91, C92, C94, C95, C96, C98, C99, C100, C103, C104, C108, C112, C113, C114, C115, C116, C118, C119, C120, C122, C123, C124, C126, C127, C128, C129, C130, C131, C132, C133, C134, C135, C136, C138, C139, C140, C142, C143, C144, C145, C146, C147, C148, C150, C151, C152, C154, C155, C156, C158, C159, C160, C162, C163, C164, C167, C168, C171, C172, C175, C176, C177, C178, C179, C180, C181, C182, C183, C184, C185, C186, C187, C188, C190, C191, C192, C193, C194, C195, C196, C197, C198, C199, C200, C201, C202, C203, C204, C205, C206, C207, C208, C209, C210, C211, C212, C213, C214, C215, C216, C217, C218, C219, C220, C221, C222, C223, C224, C225, C226, C227, C228, C229, C230, C231, C232, C234, C235, C236, C238, C239, C240, C241, C242, C243, C244, C245, C246, C247, C248, C249, C250, C251, C252, C253, C254, C255, C256}

## 4 Results and Discussion

In this section, the results based on the fuzzy and RST have been presented and discussed. As per the designed system, corresponding to the problem of large data handling and its analysis related to PQMI of a grid-connected MG, the 256 possible rules for the fuzzy and similar number of conditions for RST have been considered. It is significant to note that the designed FIS and RST cover all the possible ranges of values for different parameters based on the data collection and analysis. Thus, the methodologies have been significantly employed for decision-making based on advanced data analysis leading to enhanced MG operation.

Figure 9 shows the rule viewer of the designed fuzzy logic-based system. As per the Figure, the voltage deviation is in the acceptable range, i.e., the deviation is 13.5 V, the frequency is 49.6 Hz, the power factor is 0.95, and the THD is 3.4%, i.e., all the parameters are in the acceptable range, and therefore the PQMI which must be ideally near to 0 is recorded as 1.52 on the scale of 0 - 10. Thus, for the purpose of decision-making, it is necessary to develop a fuzzy-based system and proceed further in a very complex manner. In the case of determining the crisp value of the PQMI, the fuzzy logic approach is best suitable. It must be noted that the rule viewer window allows the operator to make quick decisions based on the value of the PQMI displayed. In addition to this, dependent upon any parameter's value within the permissible range, the value of PQMI shall be displayed, benefiting the power system operator in future situations.

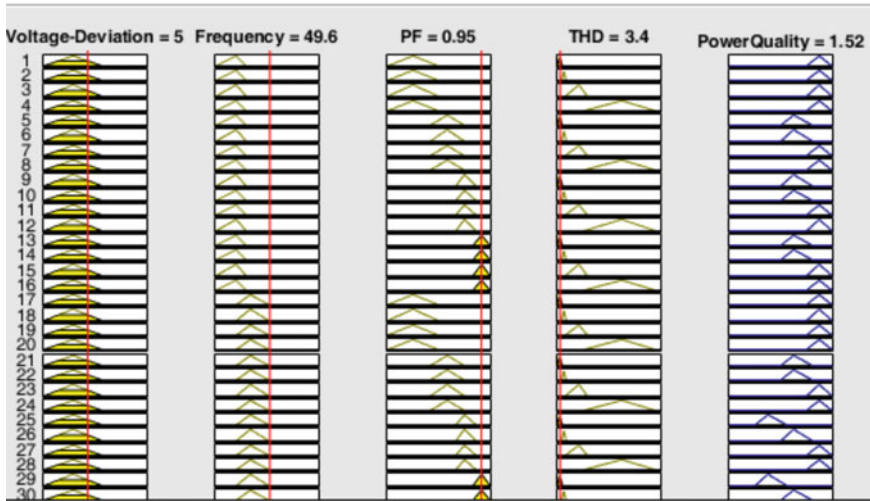


Fig. 9 Fuzzy rule viewer

On the other hand, in RST, decision-making based on the given set of information is comparatively less complex as any system development is not necessary. Like the fuzzy logic approach, the crisp value for the given condition may not be available. In the given problem of PQMI monitoring and decision-making, the in-discernibility based on the decision attribute has been initially done. It is such that with all the possible combinations and dependent decisions, discrimination based on the decision can be done. Thus, based on the information table with 256 conditions, the IND (decision attribute) has been shown. It must be noted that based on a similar set of uncertain data, the combinations have been made, considering all all-possible conditions of MG operation. Table 3 shows all the possible conditions ranging from C1 to C256 divided among poor, average, good, and the best PQMI.

It is such that further decision-making is comparatively more straightforward based on the decision attribute. The other parameter, i.e., the reduct and the core, along with their basic calculations for the given information table, is given below.

**Core:** To find the reduct of an information system, the first steps are to eliminate each condition attribute one by one. In this case, remove the voltage deviation and check the case of indiscernibility concerning the conditions being the same, but the decision is different. Repeat this step for each attribute. Even if a single case of indiscernibility is present in the system, the eliminated attribute will be termed the system’s core attribute. Following this step, each of the given input values based on the 256 possible conditions is the core of the table. Without any of these attributes, confidence in the decision-making process may decrease significantly.

**Reduct:** In the case of finding the reduct values, the critical step is to check the indiscernibility between the conditions and the decision based on certainty. In case the conditions tend to be similar in nature. Still, the decision is different, i.e., the case is not completely similar in nature and thus eliminated. In contrast, the conditions

that are not like any other condition are termed a single support rule, with 1 similar case it is known as two support or double support rule, and so on. With high support and a high number of rules, the optimal combination of the re-duct attributes can be considered. But in the present problem, with all the four at-tributes being the core of the system, the reduct cannot be determined. In the case of incomplete data set, the reduct can be calculated and is significant in nature.

Lower and upper approximations: In favor of the best value of PQMI, the condition with a particular decision is only C45 which is the lower approximation of the system, whereas all the other conditions are in the upper approximation, if the decision with the indeed poor decision is considered then the lower approximation include all the conditions that are IND (poor) as in Table 3 and rest are the values of upper approximation. Accuracy of approximation: As discussed in the previous section, the accuracy of approximation for the set of decisions that are poor can be calculated as:

$$\alpha(\text{poor}) = \text{Lower}(\text{poor})/\text{Upper}(\text{poor}) \text{ i.e., } 66/190 = 0.3473.$$

whereas, for the decision to be the best:

$$\alpha(\text{best}) = \text{Lower}(\text{best})/\text{Upper}(\text{best}) \text{ i.e., } 1/255 = 0.003921.$$

Hence, based on the value of  $\alpha$  (ranging from 0 to 1), the system is rough in nature with  $\alpha$  0.34 and 0.003 respectively, i.e., roughness increases with  $\alpha$  nearer to 0 and is crisp in nature if equal to 1.

Therefore, based on the observations, it can be briefly stated that both the above-mentioned approach can be well employed to handle a huge set of uncertain data along with its analysis. In addition to this, it can also be noticed that it is essential to develop a FIS system including membership functions for each variable and thus the rule base in case of fuzzy logic approach. This approach gets complex if and only if many input/output parameters are considered, leading to a higher number of rules. Whereas RST-based decision-making is complex as based on the analysis of a huge set of uncertain data, all the possible conditions must be developed. Further, these conditions can be subdivided based on their characteristics such that if the condition is not indeed in favor or certainly in favor of a possible condition, the decision can be made quickly without any time delay. Thus, the combination of the two can be advantageous for various objectives of the power system model, like huge data handling, advanced data analysis, decision making, and smooth operation of MG.

## 5 Comparative Study and Case Analysis

This section presents the comparative study between the two decision-making methodologies in various aspects. Besides, a case study has been performed to realize the application of these methodologies in the designed MG system. The 2 subsections are discussed below:

**Table 4** Comparative study between fuzzy logic and rough set theory

Parameter/Aspects	Fuzzy logic approach	Rough set theory approach
Understanding level	High	Medium
Implementation level	Low difficult	Medium difficult
Processing time	Medium	Medium
Applicability in real life	High	Low
Decision making and processing	Medium difficult	High difficult
Decision-making speed	Medium	High
Design difficulty	Medium	Low
Output accuracy	High	Medium
Working range of parameters	Limited and low	Limited and medium
Power system applications	High	Medium
Aspects of extension/hybridization	High	Medium

### 5.1 Comparative Analysis

Focusing on the real-time applications and usage of the discussed methodologies, the tabulated comparison is presented in Table 4 [33].

From the tabulated comparison, it is evident that the fuzzy logic approach proves to be highly advantageous compared to the rough set theory. Although the design of the approach needs serious attention, knowledge, and experience, it still is termed as the better one. Thus, taking this into account, a case study on processing the crisp output value of the fuzzy logic approach for corrective action aiming better PQMI and thus stable MG operation has been done. The details and results of the same are given in the next subsection.

### 5.2 Case Analysis

The case analysis performed in this subsection presents the ideology of using the fuzzy logic-based PQMI decision-making data for control and operation in a developed MG system. The purpose of this investigation is to stabilize the system under uncertain conditions. For this purpose, Fig. 10 presents the developed system, whereas the corresponding results are presented in Figs. 11 and 12. The considered inputs include the status of PV Power, wind energy source power output, and battery power output. In return for this, the output has been given to the connected electrical

load, where the non-critical load shedding has been considered for stabilizing the system if required.

Considering this system, the results have been compiled as – a system with poor PQMI leads to an unstable system, and a system with the best PQMI where system stability is maximum. Below, Fig. 11 shows the unstable system performance where the influence of poor PQMI is observed on system voltage, DC-Link voltage as well as the frequency of the system.

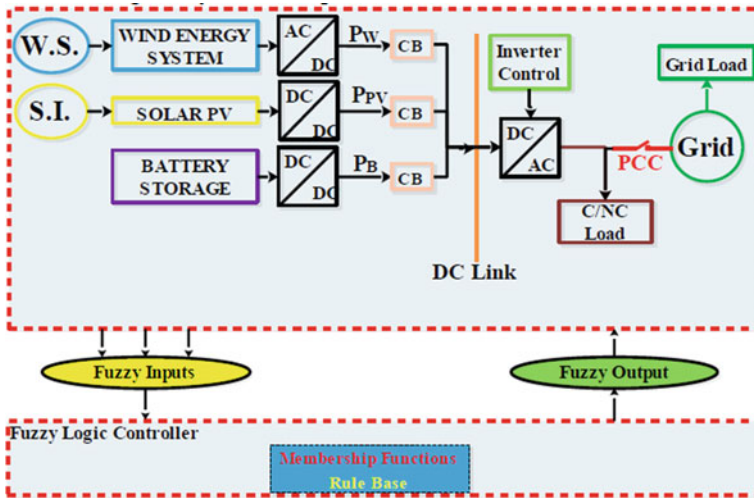
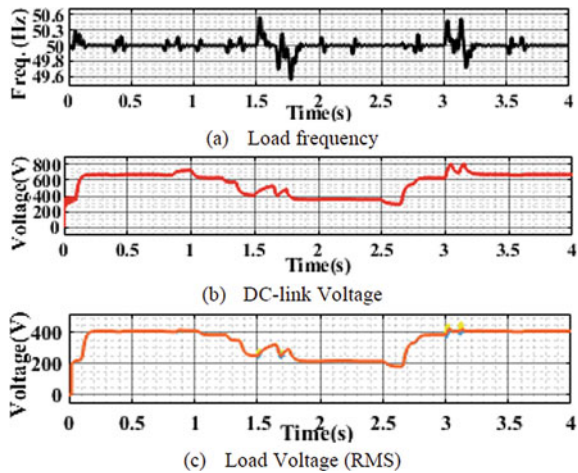


Fig. 10 Microgrid model under investigation

Fig. 11 Result for unstable MG system under poor PQMI





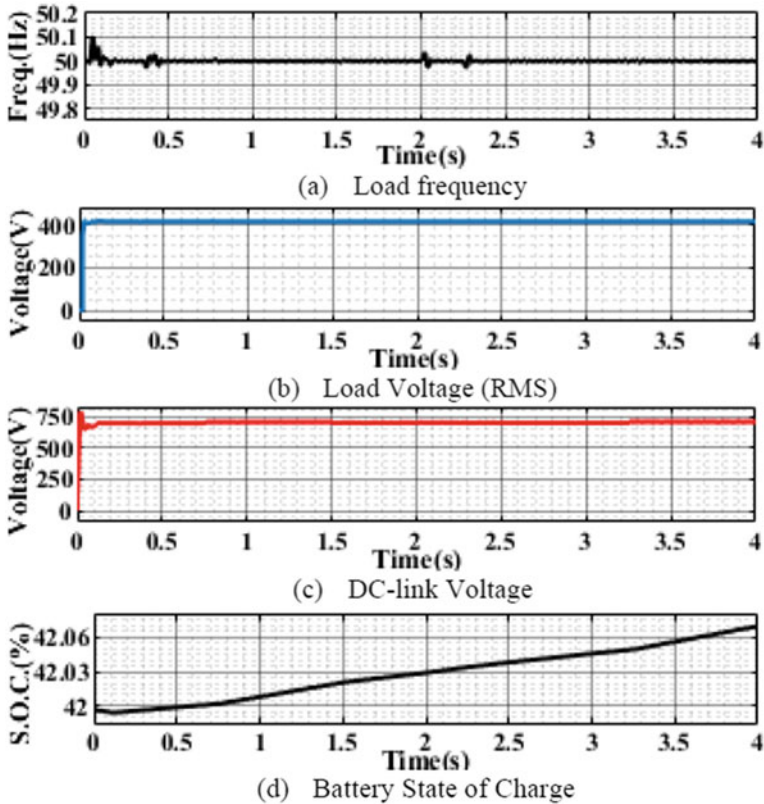


Fig. 12 Results for stable MG system under best PQMI

Following this, with the best PQMI value, a similar system has been investigated and the results are presented below. The result shows the best PQMI on all the related parameters such that the MG system can be termed a stable system.

Thus, it is conclusive that the fuzzy logic approach can be well implemented and have the flexibility to perform well under given conditions. Besides, it is notable that the rough set approach delivers the decision quickly compared to fuzzy logic but cannot be further employed for any corrective action.

## 6 Conclusions

Based on the observations and the recent research trends, continuous power quality monitoring must be done to characterize the system's performance. This may include the data analysis of specific electrical parameters like power factor, voltage, frequency, level of harmonics, etc. Specifically, the data acquisition and processing of

power quality parameters will ensure enhanced power quality service for a microgrid at all times of operation. Such an analysis helps to characterize and acknowledge the specific system problems that can be cured in a short period under the maintenance section. This complete process will support and enhance the reliability and security of the microgrid system.

Thus, in this chapter, the application of two renowned decision-making approaches based on fuzzy logic and RST to analyze the power quality has been presented for the stable operation of the microgrid system. Remarkably, the chapter focuses on a detailed discussion of both the known methodologies and the quick decision-making approach. Hence, a case study has been presented to showcase its application, highlighting its impact on system stability and power quality at all operating times. From the analysis, it can be concluded that both the decision-making approaches prove to be advantageous in handling the complex set of data during microgrid operation. The fuzzy logic-based approach provides the decision-making capability considering crisp value, whereas the RST provides the tabulated decision based on the combination of input/output attributes. Hence, both decision-making approaches generate satisfactory results for solving the issues related to complex data handling and its analysis in a microgrid system.

This work can be extended with the help of multiple attribute decision-making (MADM) and multiple criteria decision-making (MCDM) approaches soon. Also, it can be validated through real-time and practical implementation with an individual or combination of the techniques. In addition to this, a study can be performed to analyze the optimal location for installing the power quality monitoring components. These locations primarily depend upon the objective of monitoring and thus need proper analysis. Following this, devices like digital fault recorders, smart relays, LEDs, voltage/current recorders, power quality monitoring devices (specially designed digital boards), etc. can be used in islanded microgrid prototypes for power quality monitoring and stable operation.

**Declarations Authors' Contributions** – All the authors have worked hard for finalizing this chapter. The authors collectively discussed the design of the work, whereas Sahil Mehta and Dr. Jitender Kaushal were responsible for both data collection and analysis. With the guidance and in supervision of Dr. Prasenjit Basak, the drafting of the article has been done. All the authors have checked and corrected the minor errors in the chapter with the major corrections done by Sahil Mehta. The final approval of the version to be published was given by Dr. Jitender Kaushal and Dr. Prasenjit Basak. The authors tend to clearly state that the acquisition of funding, collection of data, or general supervision of the research team, does not justify authorship in the present work.

**Ethics approval** – The work is not submitted to any other journal, and it is not published in any previous work.

**Competing interests** – The authors declare no competing interests.

**Funding** – The authors wish to submit that no funding has been taken for carrying out the present work.

## References

1. Kaushal, J., Basak, P.: A novel approach for determination of power quality monitoring index of an AC Microgrid using fuzzy inference system. *Iran J. Sci. Technol. Trans. Electr. Eng.* **42**, 429–450 (2018)
2. IEEE Recommended Practice for Monitoring Electric Power Quality, in IEEE Std 1159–2009 (Revision of IEEE Std 1159–1995), (2009)
3. Huang, Z., Zhu, T., Lu, H., Gao, W.: Accurate power quality monitoring in Microgrids. 15th ACM/IEEE Int Conf Inf Process Sens. Networks, IPSN – Proc., pp. 1–6 (2016)
4. Sontakke, S.: Novel method for estimation of PQ indices in Microgrids. *Int. Conf. Energy Effic. Technol. Sustain.*, pp. 1159–1163 (2013)
5. Srikanth, K.S., Mohan, T.K., Vishnuvardhan, P.: Improvement of power quality for microgrid using fuzzy based UPQC controller', International conference on electrical, electronics, signals, communication, and optimization (EESCO), pp. 1–6 (2015)
6. Nirmal., Kumar, P.: Effect of increasing rated torque of PMSG with variable wind speed on per phase output voltage for off-grid wind energy conversion system. *International Conference on Advances in Computing and Communication Engineering*, 2015, pp. 49–52. CONFERENCE 2016, LNCS, vol. 9999, pp. 1–13. Springer, Heidelberg (2016)
7. Pawlak, Z.: Rough sets. *J. Comput. Inform. Sci.* **11**, 341–345 (1982)
8. Pawlak, Z.: *Rough Relations. Reports*, Institute of Computer Science, Polish Academy of Sciences, Poland, 435 (1981)
9. Pawlak, Z.: Information systems-theoretical foundations. *Inf. Syst.* **6**, 205–218 (1981)
10. Pawlak, Z., Slowinski, R.: Decision analysis using rough sets. *Intern Trans. Operat. Res.* **1.1**, 107–114 (1994)
11. Pawlak, Z., Slowinski, R.: Rough set approach to multi-attribute decision analysis. *Eur. J. Oper. Res.* **72**, 443–449 (1994)
12. Sai, Y., Nie, P., Xu, R., Huang, J.: A rough set approach to mining concise rules from inconsistent data. *IEEE International Conference on Granular Computing*, pp. 333–336 (2006)
13. Nasiri, J.H., Mashinchi, M.: Rough set and data analysis in decision tables. *J. Uncertain Syst.* **3(3)**, 232–240 (2009)
14. Chen, D., Cui, D.W., Wang, C.X., Wang, Z.R.: A rough set-based hierarchical clustering algorithm for categorical data. *Int. J. Inf. Technol.* **12(3)**, 149–159 (2006)
15. Li, Y., Ren, X., Niu, J.: Application of rough sets theory in a forecast of power generation for grid-connected photovoltaic system. *Chinese Control and Decision Conference*, pp. 5064–5069 (2015)
16. Li, Q., Chi, Z., Shi, W.: Application of rough set theory and artificial neural network for load forecasting. *Proceedings of the First International Conference on Machine Learning and Cybernetics*, pp. 1148–1152 (2002)
17. Couto, Do., Gomes, L.F.A.M.: Application of rough set theory in decision-making with replicated and inconsistent data. *ALIO - INFORMS Joint International Meeting*, pp. 1–27 (2016)
18. Chaturvedi, P., Daniel, A.K., Khushboo, K.: Concept of rough set theory and its applications in decision making processes. *International Journal of Advanced Research in Computer and Communication Engineering (ICACTRP)*, pp. 43–46 (2017)
19. Srivastava, V.K., Goel, R.K., Bharti, P.K.: Application of fuzzy logic in decision making & grid technology. *Int. J. Eng. Res. Technol.* **2(8)**, 761–765 (2013)
20. Valášková, K., Klieščík, T., Mišánková, M.: the role of fuzzy logic in decision making process. *2nd International Conference on Management Innovation and Business Innovation – ICMIBI*, 44, pp. 1–6 (2014)
21. Pirmez, L., Delicato, F.C., Pires, P.F., Mostardinha, A.L., de Rezende, N.S.: Applying fuzzy logic for decision-making on Wireless Sensor Networks. *IEEE International Fuzzy Systems Conference*, pp. 1–6 (2007)

22. Menon, B.R., Menon, S.B., Srinivasan, D., Jain, L.: Fuzzy Logic decision-making in multi-agent systems for smart grids. *IEEE Computational Intelligence Applications in Smart Grid (CIASG)*, pp. 44–50 (2013)
23. Coroiu, A.M.: Fuzzy methods in the decision-making process - A particular approach in manufacturing systems. *Mater. Sci. Eng.*, pp. 1–6 (2015)
24. Sahraei, Y., Rajaei, A., Jamshidi, M., Kelley, B.T.: Intelligent decision making for energy management in microgrids with air pollution reduction policy. *International Conference on System of Systems Engineering (SoSE)*, pp. 13–18 (2012)
25. Yuan, H., Li, G.: A survey of traffic prediction: from spatio-temporal data to intelligent transportation. *Data Sci. Eng.* **6**, 63–85 (2021)
26. Zavareh, M., Maggioni, V.: Application of rough set theory to water quality analysis: a case study. *Data-MDPI* **3**(4), 1–15 (2018)
27. Lu, H., Jiang, S., Song, W., Ming, X.: A rough multi-criteria decision-making approach for sustainable supplier selection under vague environment. *Sustain. MDPI* **10**(8), 1–20 (2018). LNCS Homepage, <http://www.springer.com/lncs>, last accessed 2016/11/21
28. De Nadai, N.B., De Souza, A.C.Z., Da Silva Neto, J.A., De Carvalho Costa, J.G., Porcelina, F.M., Marujo, D.: 'An OffLine Fuzzy-Based Decision-Making to Load Shedding in Microgrids' 2019 IEEE PES Conf. Innov. Smart Grid Technol. ISGT Lat. Am., 1–6 (2019)
29. Mehta, S., Kaushal, J., Basak, P.: Tariff calculation using hybrid smart energy meter and fuzzy inference system. *IEEMA Engineer Infinite Conference (eTechNxT)*, pp. 1–6 (2018)
30. Hossam-Eldin, A., Mansour, A., Elgamal, M., Youssef, K.: 'Power quality improvement of smart microgrids using EMS-based fuzzy controlled UPQC' Turkish. *J. Electr. Eng. Comput. Sci.* **27**(2), 1181–1197 (2019)
31. Zarković, M., Dobrić, G.: 'Fuzzy expert system for management of smart hybrid energy microgrid' *J. Renew. Sustain. Energy* **11**(034101), 1–11 (2019)
32. Mehta, S., Basak, P.: Solar irradiance forecasting using fuzzy logic and multilinear regression approach: A case study of Punjab, India. *Int. J. Adv. Appl. Sci.* **8**(2), 125–135 (2019)
33. Mehta, S., Basak, P.: A comprehensive review on control techniques for stability improvement in microgrids. *Int. Trans. Electr. Energy Syst.* **31**, 1–28 (2021). <https://doi.org/10.1002/2050-7038.12822>

# Enabling Technologies in IoT: Energy, Sensors, Cloud Computing, Communication, Integration, Standards



S. N. Sangeethaa, P. Parthasarathi, and S. Jothimani

**Abstract** The Internet of Things is a developing technology that extends deep into the internet and provides a fabulous smart environment. This chapter highlights several technologies of IoT which includes energy sectors, sensors, cloud computing, communication, IoT integration, and IoT protocol and standards. The energy sector is a crucial industry that enables the production of power, the movement of products, and numerous other essential human activities. This section provides a wide-ranging of applications in the field of energy supply, transmission and distribution, and demand. In the IoT ecosystem, the two main things are the Internet and physical devices like sensors and actuators. Sensors enable the Internet of Things (IoT) by collecting data from the environment. These sensors are connected directly or indirectly to IoT networks for smarter decisions. This section describes a brief about the types of sensors since all the sensors are not the same, but different IoT applications may require different types of sensors. Next, cloud computing permits users to carry out tasks using services provided over the Internet. Cloud computing and the Internet of Things are interconnected. Large amounts of data may need to be stored, processed, and accessed due to the quick development of technology. Cloud computing can be used to process this data. This chapter also covers the integration of robust data stream processing with monitoring and sensory services. IoT Communication deals with the infrastructure, technologies, and protocols that are used to connect IoT devices to gateways and cloud platforms. IoT devices are embedded with electronics, software, network, and sensors that help in communication. Communication between smart devices is processed by gathering and exchanging data which contributes to the success of that IoT product/project. The second technology is IoT integration, which binds new IoT devices, IoT data, IoT platforms, IoT applications integrated with business apps, and mobiles to cooperate when developing end-to-end IoT business solutions. This chapter also gives a study about how IoT integration enables IoT implementers to successfully integrate end-to-end IoT business solutions. It also

---

S. N. Sangeethaa (✉) · P. Parthasarathi · S. Jothimani  
Bannari Amman Institute of Technology, Sathyamangalam, India  
e-mail: [dr.snsangeethaa@gmail.com](mailto:dr.snsangeethaa@gmail.com)

S. Jothimani  
e-mail: [jothimanis@bitsathy.ac.in](mailto:jothimanis@bitsathy.ac.in)

provides an overview of popular protocols and standards helping power IoT devices, apps, and applications.

**Keywords** Internet of things · Cloud computing · Sensor · Communication

## 1 Introduction

The term “Internet of Things” (IoT) refers to the interaction of networks with physical things that have electronics built into their architecture to communicate and detect interactions between one another [1–4]. All the electronic devices will be connected to each other in a local area, forming a system [2, 3]. These systems are interconnected with each other and form the building blocks of IoT. The devices or nodes are a vital part of the IoT which act as active sensing devices and actuators which are used to collect the data and perform ground-level processing [5]. In the upcoming years, IoT-based technology will offer a range of services and essentially transform how people live their daily lives. Gene therapies, smart cities, smart homes, agribusiness, and the medical field all advocate the use of IoT devices.

There are four main components used in IoT:

1. **Low-power embedded systems:** Two important factors that play a vital role in the design of electronic systems such as less battery consumption and high performance.
2. **Cloud computing:** In IoT devices, data collection is a very huge process, and it can be stored on a reliable storage server. Here, cloud computing plays a role. The data is processed and learned and the faults/errors occur within the system.
3. **Availability of big data:** In real-time, IoT depends heavily on sensors. Electronic devices are spread throughout every field and the usage of the data is going to trigger a massive flux of big data.
4. **Networking connection:** For communication, internet connectivity is a must thing in which the physical object is represented by an IP address. However, it has a restricted number of addresses depending on the IP naming.

### 1.1 Building IoT

#### IoT Enablers

- **RFIDs:** uses radio waves to track the tags electronically attached to each physical object.
- **Sensors:** used to detect changes in a domain
- **Nanotechnology:** Uses extremely small devices with dimensions usually less than a hundred nanometres.

- **Smart networks:** It is a network with intelligence that builds the network identification and transformation through protocols that automatically identify what things are deep learning technology, validate, and confirm.

## 1.2 Characteristics of IoT

- Scalable
- Efficient
- Dynamic and self-adapting
- Self- Configuring
- Interoperable communication protocols
- Unique Identity
- Integrated into information network
- Intermittent connectivity

## 1.3 Features of IoT

- **Connectivity:** Connectivity refers to establishing a proper connection between all the things of IoT. Once it gets connected, it needs high-speed messaging between the devices and the cloud to enable dependable, secure, and bi-directional communication.
- **Analysing:** Once the connection gets over, it comes to real-time analyzing the data collected. It is basically used to build effective business intelligence.
- **Integrating:** It is used to improve the user experience.
- **Artificial Intelligence:** IoT makes things smarter and enhances life using data.
- **Sensing:** Without sensors, there could not hold an effective or true IoT environment. The sensor devices used in IoT technologies detect and measure the changes in the environment and report on their status.
- **Active Engagement:** IoT makes the connected technology, product, or services active engagement between each other.

## 2 Energy Sectors in IoT

IoT devices can build intelligent networks in the energy sector through the collection, transport, and utilization of vast amounts of data [4].

The obtained data from the new Internet-connected gadgets can be utilized to develop new services, boost productivity and efficiency, enhance real-time decision-making, solve pressing issues, and design novel experiences.

## ***2.1 IoT in the Energy Production Chain***

IoT technologies make information more accessible along the entire value chain and provide better tools for making decisions, including artificial intelligence or autonomous learning [5, 6]. It enables automated execution of these judgments and remote control of them.

These technologies do the following four tasks:

1. A physical process, such as the production, transmission, or use of electricity
2. Process of measurement: The sensors take measurements of the outputs and statuses of the physical process.
3. Independent and decentralized decision-making or coordination with other components.
4. The actuators that are set up on the network get the decisions and carry them out.

Given the interconnectedness of this control loop's components, interoperable IoT designs, and standards are necessary for its implementation.

## ***2.2 IoT Applications in the Energy Sector***

Here are the important advantages for the energy sector.

1. **Automated control of the network:** The transition from a reactive perspective to a proactive one permits the automation of efficient processes to focus on the strategic part of the systems. Also, the decentralization of the energy systems must be in line with digitalization [7].
2. **Higher stability and reliability of the network:** Using IoT technologies to connect, add and control the industrial and residential loads permits regulation of frequencies and balancing of the network operation.
3. **Reduction of maintenance and operating costs:** IoT data is predictive maintenance. Testing and repair reduce the time that the machines are inactive, as well as the maintenance costs.
4. **Boost the generation of renewable energy:** The IoT products and solutions supply construction blocks for fundamental systems that facilitate integration, reduce development costs, and accelerate the commercialization time for new and innovative technologies.

## ***2.3 Advantages of Transforming the Energy Sector with IoT Technology***

IoT is representing a new reality, covering the energy sector with its real-time applications and state-of-the-art innovations. It uses sensor devices and gateway connectivity



to derive actionable insights and use them to develop new and advanced services for enhanced productivity [8, 9]. It further improves real-time decision-making, complex operability, and overall experiences.

- Process Monitoring and Resource Optimization
- Advanced Analytics
- Intelligent Grid
- Cost-savings and Data Management
- Sustainability
- Reliability
- Energy system management
- Automated process
- Disaster prevention
- Increased efficiency
- Smart Energy Meters
- Zero Net Energy Buildings
- Smart Decision Making

## ***2.4 IoT Application in the Energy Industry***

Here are some examples of IoT applications in the energy market.

1. **Optimization of Energy Resources:** By placing smart monitors that automatically control the room temperature of a factory, hall, or even a room, energy consumers can optimize and potentially reduce the amount of energy that they consume.
2. **Empowering Microgrids:** In the energy sector, smart grids refer to a network of electric circuits that support a two-way energy flow and have a self-healing capacity for maintenance issues.
3. **Predictive Protocols for Disasters:** By using past data to develop predictive patterns and forecast manmade or natural disasters, the energy sector can place smart sensors that can regulate energy consumption, distribution, and management.
4. **Smart Meter Technology:** Referring to the measurement and analysis of energy consumption by a particular household, building, or organization, the smart meter installation technology can help to analyze the areas where the energy is spent the most and the places where energy can be conserved substantially.
5. **Proactive Repair Mechanism:** IoT in the energy sector is a way to install a proactive repair mechanism that sends off alarms and warning signs, in case a circuit is broken, or equipment requires maintenance. This application has been proven to save substantial maintenance costs in the sector and is a rapid system of addressing problems.

### 3 Sensors in IoT

Sensors play an important role in creating solutions using IoT. Sensors are commonly utilized in the architecture design of IoT devices. Sensors are used to detect objects and devices, among other things. In response to a specified measurement, a device produces a usable output. Sensors are devices that detect external information, replacing it with a signal that humans and machines can distinguish.

With the use of sensors, data collection may be done effectively. Devices called sensors react to inputs from the outside world and use that information to display, transmit for further processing, or work with artificial intelligence to make judgments or change operational conditions [10].

#### 3.1 Characteristics of the Sensor

**Static characteristics:** How a sensor's output responds to an input change after reaching steady state.

- **Accuracy:** Accuracy is the capacity of measuring devices to produce results that are reasonably close to the actual value of the quantity being measured. It measures errors. It is measured by absolute and relative errors. Express the correctness of the output compared to a higher prior system. Absolute error = Measured value – True value, Relative error = Measured value/True value.
- **Range:** Indicates the physical quantity's greatest and lowest values that the sensor is capable of sensing. There is no sense or form of reaction outside of these values. For instance, the temperature measuring range of an RTD is between -200 °C and 800 °C.
- **Resolution:** Resolution is a crucial requirement for choosing sensors. The precision improves with increased resolution. The threshold is the point at which the accretion is zero. Give the smallest input changes that a sensor can detect.
- **Precision:** Precision is the ability of a measuring device to consistently produce the same reading measuring the same quantity under the same prescribed conditions.

It implies an agreement between successive readings, NOT closeness to the true value.

It is related to the variance of a set of measurements.

It is a necessary but not sufficient condition for accuracy.

- **Sensitivity:** Sensitivity describes the relationship between the incremental change in the system's response and the incremental change in the input parameters. It can be found from the slope of the output characteristics curve of a sensor. It is the smallest amount of difference in quantity that will change the instrument's reading.

- **Linearity:** The sensor value curve's departure from a particularly straight line. The calibration curve determines the linearity. The static calibration curve plots the output amplitude versus the input amplitude under static conditions. A curve's slope resemblance to a straight line describes linearity.
- **Drift:** This is the variation in a sensor's measurement from a certain reading when it is maintained at that value for an extended length of time.
- **Repeatability:** This is the variation in measurements made consecutively under the same circumstances. The measuring time needs to be brief enough to prevent severe long-term drift.

**Characteristics of dynamics:** Some of the systems' attributes are displayed.

- **Zero-order system:** The output reacts instantly to the input signal. Energy-storing components are not present. Example: measuring linear and rotary displacements with a potentiometer.
- **First-order system:** When the output steadily approaches its ultimate value. Consists of an element for energy storage and dissipation.
- **Second-order system:** intricate output reaction Before reaching a steady state, the sensor's output response oscillates.

### 3.2 *Classification of Sensors*

1. **Passive Sensor:** Is unable to sense input on its own. Examples include sensors for temperature, water level, soil moisture, and acceleration.
2. **Active Sensor:** Sense the input on their own. Examples include altimeters, sounders, and radar sensors.
3. **Analog Sensor:** The sensor's reaction or output is a continuous function of one or more of its input parameters. Examples include a temperature sensor, an LDR, an analog pressure sensor, and an analog hall effect.
4. **Digital sensor:** Binary response from a digital sensor. Designing to avoid the drawbacks of analog sensors Additionally, it includes additional circuitry for bit conversion in addition to the analog sensor. example: a digital temperature sensor plus a passive infrared sensor
5. **Scalar sensor:** Only determines the input parameter's magnitude. The sensor's response depends on the size of some input parameter. not impacted by how the input parameters are oriented. For instance, a sensor for smoke, gas, strain, or temperature.
6. **Vector sensor:** The sensor's response is influenced by the direction and orientation of the input parameter and its magnitude. For instance, sensors with an accelerometer, gyroscope, magnetic field, and motion detector.

### 3.3 *Types of IoT Sensors*

Sensors are made to react to a certain range of physical situations [11]. They then produce a signal (often electrical) that might reflect the severity of the condition being measured [12]. Light, heat, sound, distance, pressure, or another particular circumstance, such as the presence or absence of a gas or liquid, may be among those conditions. The usual IoT sensors that will be used are as follows:

- Gyroscopic sensors
- Pressure sensors
- Optical sensors
- Acceleration sensors
- Image sensors
- Motion sensors
- Proximity sensors
- Smoke sensors
- Water quality sensors
- Temperature sensors
- Level sensors
- Chemical sensors
- Gas sensors
- Infrared (IR) sensors
- Humidity sensors

Below is a description of each of these sensors.

**Temperature sensors:** Convert the temperature of the air or a physical item into an electrical signal that may be precisely calibrated to reflect the temperature being monitored.

**Pressure sensors:** measure the force or pressure per unit area that is delivered to the sensor and can detect things like ambient pressure, the pressure of a gas or liquid that has been kept in a sealed system like a tank or pressure vessel, or the weight of an object.

**Motion sensors:** Use any of a number of technologies, such as passive infrared, microwave detection, or ultrasonic, which uses sound to identify objects, to detect the movement of a physical object.

**Level sensors:** converts a liquid's level in relation to a reference normal value into a signal.

**Image sensors:** capture the pictures so they may be saved digitally and processed. Examples include facial recognition technology and license plate readers.

**Proximity sensors:** a variety of various technological designs, including inductive, capacitive, photoelectric, and ultrasonic technologies, can be used to detect the presence or absence of things that approach the sensor.

**Water quality sensors:** They may be required to sense and measure parameters related to water quality in numerous production processes. Chemical presence, oxygen levels, electrical conductivity, pH levels, and turbidity levels are a few examples of what is felt and measured.

**Chemical sensors:** detect the presence of specific chemical chemicals that may have unintentionally escaped from their containers into areas where people are present and are helpful in regulating the conditions of industrial processes.

**Gas sensors:** determine whether there are any poisonous, flammable, or combustible gases nearby the sensor.

**Smoke sensors:** commonly uses optical sensors (photoelectric detection) or ionization sensors to detect smoke conditions that could be a sign of a fire.

**Infrared (IR) sensors:** detect the infrared radiation that things release.

**Acceleration sensors:** determine an object's rate of velocity change. One of the numerous technologies used in acceleration sensors is:

- Hall-effect sensors are devices that rely on magnetic field variations to measure changes.
- Capacitive sensors: rely on two surfaces to measure voltage changes.
- Piezoelectric sensors: provide a voltage that fluctuates in response to pressure through sensor distortion.

**Gyroscopic sensors:** Using a 3-axis system, one may measure an object's rotation and calculate its angular velocity, or rate of movement. The orientation of the object can be determined using these sensors without needing to physically view it.

**Humidity sensors:** find out the gas's relative humidity, which is a measurement of the quantity of water vapor it contains.

**Optical sensors:** These sensors detect the interruption or reflection of a light beam brought on by the presence of an object. Among the several optical sensor types are:

- Retro-reflective sensors.
- Diffuse reflection sensors.

## 4 Cloud Computing in IoT

Cloud computing is one factor that contributes to the IoT's enormous success [13]. Users can complete computing activities using services made available through the Internet thanks to cloud computing, a fantastic breakthrough that addresses the issue of storing, processing, and accessing enormous volumes of data in conjunction with the Internet of Things and cloud technologies. Combining advanced processing of sensory data streams with new monitoring services will be possible.

## 4.1 IoT Cloud Functions and Benefits

The benefits of integrating these services are numerous.

1. It offers a variety of connectivity choices, indicating extensive network access. Mobile gadgets, tablets, and laptops are the best examples. Users will find this convenient, but it raises the issue of a requirement for network access points.
2. It can be accessed as a web service without any assistance or special authorization. Access to the Internet is the sole prerequisite.
3. Users have the option to scale the service to meet their demands [14].
4. Resource pooling is implied by cloud computing. It encourages more cooperation and forges strong bonds amongst users.
5. IoT cloud computing is practical since you receive exactly what you paid for from the provider.

## 4.2 Relation Between IoT and Cloud Computing

The IoT and Cloud Computing are complementary to one another, frequently used as a collective noun when referring to technical services and collaborating to deliver an all-around superior IoT solution [15]. IoT cloud computing is used to store IoT data and functions as a team effort. A centralized server with computer resources that can be accessed whenever needed is called the Cloud. IoT-generated big data packages can easily flow via the Internet using cloud computing. Big Data can be useful in this process as well. IoT and cloud computing work together to make it possible to automate systems in an economical fashion that provides real-time control and data monitoring. The Internet of Things has extended several possibilities with the development of wireless connection methods [16].

**Data Storage:** Remove part of the system's components and place them on the cloud, which can be accessed via the internet, to better comprehend the function of cloud computing in IoT. Now, the system still functions as intended, but it offers an alternative method for storing and processing data in an IoT and cloud computing system. For instance, you might set up Alexa to alert you each morning to the most recent news, weather, and traffic information. A cloud-based Internet of Things (IoT) called Alexa makes requests to cloud services like Google Maps and others to retrieve information and deliver it to you (Fig. 1).

**Fig. 1** Data storage in IoT



**Data Security:** IoT and cloud computing integration that is secure aids in preventing data breaches and assaults. It is generally not a good idea to save the data on a local device. The security of industrial applications can be improved by encrypting sensitive data before sending it to the cloud [17]. A significant volume of data might also be expensive and time-consuming to store locally. The processing capacity of local devices is similarly constrained, therefore the cloud appears to be a viable alternative for complicated procedures and applications.

### ***4.3 IoT's Use of Cloud Computing***

With wiser innovations, the power of technology is giving our lives new directions every day. We have benefited greatly from the separate fields of IoT and cloud computing [18]. Assume IoT is the key to integrating smart home solutions into corporate tools and opening the door for cutting-edge solutions in healthcare, logistics, transportation, energy, and many other industries.

### ***4.4 Advantages of Cloud Computing in IoT***

Storage solutions for both commercial and personal use have seen a significant change because of cloud computing. Additionally, cloud solutions' scalability and data dynamics make data accessible from a distance.

**Speed and scale:** The networking and mobility of the Internet of Things make these two primary cloud computing characteristics an unbeatable combination. IoT and cloud computing work best together, so their combined power maximizes their potential. Unquestionably, some factors show that the cloud is necessary for the success of IoT. Some advice is provided here:

1. Cloud acts as remote processing power.
2. Cloud enhances the security and privacy of IoT data.
3. No need for on-premises hosting
4. Better inter-device communication
5. Reduced cost of ownership
6. Business continuity programs
7. Low Entry Barrier
8. Inter-device Communication

## ***4.5 Challenges That Cloud and the IoT Bring Together***

- Handling Large Amounts of Data
- Network and Communication Protocol
- Sensor Networks

## ***4.6 IoT and Cloud Complement Each Other***

Cloud computing and the IoT are dedicated to improving the efficiency of daily tasks, and there is a complementary relationship between the two. Here are some key reasons why the cloud is essential to the success of the IoT [19].

- Remote Computing Capability
- Security and Privacy
- Data Integration
- Low Threshold
- Business Continuity
- Communication
- Edge Computing

## **5 Communication in IoT**

There are hundreds and different types of protocols for the communication of the internet of things. There is no other way to select the best protocol for any specific application to route the messages of IoT devices. The selection of protocol is totally dependent on the need of the application. The protocol selection also depends on the cost of the device's power, limitations, and physical size, limitations of geographic regions, security, and time.

### ***5.1 Components for IoT Device Communication***

The architecture of IoT systems is in a different format, there are few standard components that are common,

**Communication:** Local communication is a method which is used to communicate with the neighbourhood devices.

**Application Protocol:** When the information is transformed the protocol defines how it should be transported.



**Gateways:** When the local networks are connected to the devices the gateways are used to re transmitting the information by translating.

**Network servers:** The data that are in the cloud-based data centres, the acceptance and the transmission of those data managed by the network servers.

**Cloud applications:** The IoT data must be processed to present to the user. This is done by the cloud applications.

**User Interface:** The people need to issue the commands to the IoT devices, by handling and manipulating the information, the user interfaces are used.

**IoT Devices:** The IoT devices connect to the networks wirelessly to transmit the data. The IoT devices can communicate over the internet and can interact with each other. These IoT devices can be monitored remotely and controlled over the internet.

The IoT devices can be in any of the following groups: Enterprise, Industries and Consumer. The consumer IoT devices are smart gadgets like Smart Watch, smart TVs, Smart Speakers and smart Applications.

**Connecting Wireless Devices:** Although most of the devices do not come with internet capabilities, these devices can be modified with market solutions. Anyhow these devices are designed with internet capabilities nowadays to reduce the cost and to increase the functionality. Although the IoT device's structure and components depend on the need, some basic components are common that must be incorporated into all devices.

- A sensor that is necessary to detect any kind of physical occurrences like motion
- An actuator to create any physical change like closing the door, switching on the light
- A microprocessor that connected with these sensors and actuators to run the IoT functionality
- A communication component like radio or Ethernet

These components are placed in an enclosure, which is a smaller one. This enclosure may be sealed or vented to balance the heat.

## ***5.2 Local Communications Methods and Protocols***

The way of communicating with IoT devices is different. Some devices only send information or data. Some devices do both send and receive. Some IoT devices communicate with peer devices while others communicate remotely. Remote communication needs a gateway for information to reach its destination. The above model represents Wireless Communication and the role of each node in the communication. The above network is a star network, where the coordinator node communicates with each of the router nodes and extends the communication to end devices (Fig. 2).

**Fig. 2** Wireless communication

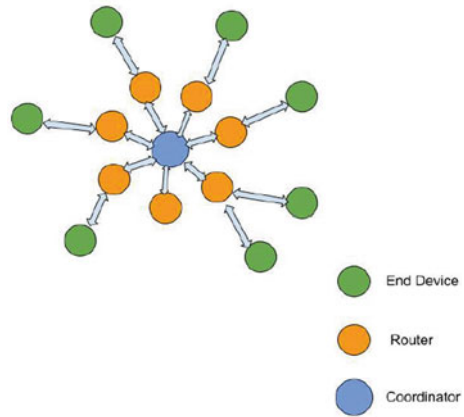
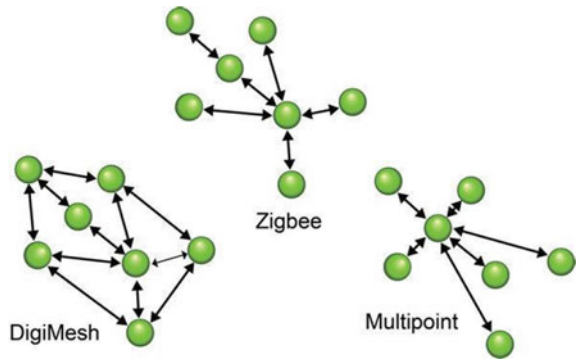


**Fig. 3** Different types of network protocols



The above-mentioned scenario is different for a variety of combinations of wireless devices and different protocols. The protocol depends on the distance between the communication nodes (Fig. 3).

## 6 Integration in IoT

### 6.1 Cloud computing and IoT Integration

In the recent era, the combination of IoT and Cloud Computing is more profitable in different fields. The heterogeneous devices can be connected in IoT, which allows the cloud also able to connect with different physical objects. The limitations of IoT like storage, processing, and energy can be managed through cloud computing with its resources and capabilities.

The cloud and the IoT are two different environments (Table 1).

**Table 1** Complementary aspects of Cloud and IoT

Terminologies	Cloud computing	IoT
Reachability	Ubiquitous	Limited
Storage capacity	Unlimited	Limited storage
Big data	Mens to manage	Source
Computational capabilities	Unlimited	None/limited

### 6.2 Cloud-based Internet of Things

Cloud computing and the Internet of Things are the most prominent and booming services with their own characteristics. The internet of Things enables Ubiquitous Cloud computing since the IoT is the smart device that communicates with these devices through global networks and infrastructures that are dynamic. Although the Internet of things devices are limited to capacity and storage, it is a widely distributed devices among global networks. Because of these limitations' performance, privacy and reliability are the main issues that have been faced commonly among all kinds of IoT devices. Since this is the greatest challenge for IoT devices, hence supporting computing technologies like cloud computing gives the greatest result.

Cloud computing, which has massive storage capacity with unlimited capabilities and computation power, offers a flexible and robust environment for dynamic data integration with a variety of resource factors. The future internetworking services completely relied on the most challenging technologies which are IoT and Cloud Computing. The users get effective computing infrastructure and information in a reasonably cost-effective way with the cloud-based Internet of Things. The features of Cloud Computing and the internet of things are almost complementary.

### 6.3 Cloud-based IoT Architecture

The Cloud base IoT architect has three layers.

1. Application Layer
2. Perception Layer
3. Network Layer

The network Layer is the Cloud Environment, and the Perception layer is used to sense the input through the components like sensors, camera, and RFID tags etc. (Fig. 4).

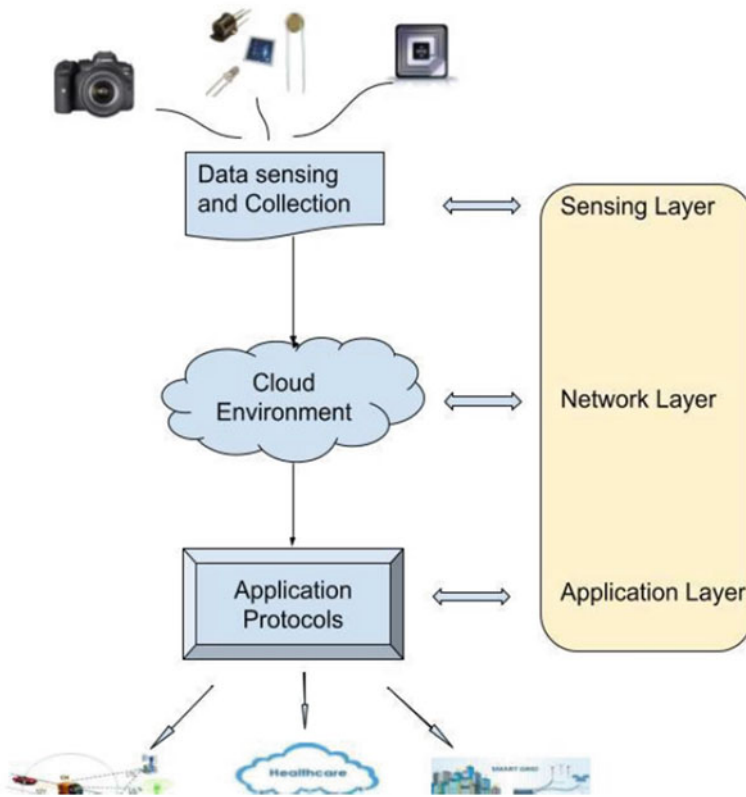


**Fig. 4** The cloud-based IoT architecture

For the integration of cloud and IoT, there are some Main Cloud-based IoT drivers called Cloud IoT that are in need. These drivers are mainly in three categories.

1. Communication
2. Storage
3. Computation

With these Cloud IoT, there are some main applications that can be most effectively served for wellness. These Applications include healthcare, Automation, Smart City communication, smart mobility, smart energy, smart grid, smart logistics, environment monitoring, and so on.

## 6.4 Integration Challenges

The number of factors affecting the integration of IoT devices that includes, environmental setup, mobility, network access, power supply, etc.

**Environmental setup/Device Placement:** In an environmental layer, the basic networking facility provided including setting up of the devices in the physical environment is the most challenging one. The placing of devices in the physical environment is easy and very complex work. The environment is chosen based on the requirement of the device that is going to be fitted. The best example of this is the temperature sensor. The temperature sensor behaves differently when it is placed in a different environment with heating control like the sun.

**Mobility:** Since most of the protocols and the devices are static, smart devices like mobile phones, smartwatches, and smart wearable devices are the most challenging. Even Though the dynamic protocols are designed for supporting these kinds of devices, the devices need to be robust and should be precise under mobility.

**Network Access:** For the integrated environment, broad network availability requires the necessary bandwidth and internet connectivity. And environmental factors such as the manufacturing hall also limitations for network access.

**Power Supply:** The energy consumption of IoT devices varies based on the requirement and the task they involve. For stationary devices, the power supply is not a big issue, but mobility-oriented devices and wearable devices require a lot of power supply which results in the shutdown of the devices.

## 7 Standards in IoT

### 7.1 IEEE 802.15.4

The most used common IoT standards are IEEE 802.15.1 and IEEE 802.15.4. This standard defines the way it communicates with IoT devices, and the Frame format, source, destination address, and headers. Some of the traditional old frame formats are not suitable for IoT because of their overhead. The extension of IEEE802.15.4 is IEEE802.15.4e which was created in 2008 for the support of devices with low-power communication. It enables high reliability by utilizing the synchronization of time and channel hopping. It is also low cost and the requirement of IoT communications is also satisfied.

## 7.2 IEEE 802.11 AH

The light version of IEEE 802.11 is IEEE 802.11AH. The IoT requirement is satisfied with this lite version since it has less overhead. The most used standard for Wifi is IEEE 802.11. This is the commonly used standard widely. This standard is suitable for most digital devices like mobile phones, smart devices such as TV, tablets, and smart wearable devices. The original IEEE standard is not available for some IoT applications because of a lot of power consumption and frame overhead. Hence the 802.11ah is developed to support low overhead and less power consumption. The communication protocol is also very much suitable for all kinds of sensors and motors of IoT devices.

## 8 Conclusion

The enabling technologies appropriate for IoT applications are covered in this chapter. It will be important to support the widespread deployment of various IoT systems in various regions soon due to the growing demand from various industrial, business, and social organizations. Since embedded wireless technologies are based on global standards, they will be scalable and simple to upgrade. Energy sectors, sensors, cloud computing, communication, IoT integration, and IoT protocol and standards are just a few of the IoT technologies. Cost-effective network architecture, support for extensive coverage and reliability, spectrum requirements, energy requirements, and numerous other associated problems are some of the major hurdles.

## References

1. Sigov, A., Ratkin, L., Ivanov, L.A. et al.: Emerging enabling technologies for industry 4.0 and beyond. *Inf. Syst. Front* (2022). <https://doi.org/10.1007/s10796-021-10213-w>
2. Zaman, Umar, Imran, Faisal Mehmood, Naeem Iqbal, Jungsuk Kim, Muhammad Ibrahim: Towards secure and intelligent internet of health things: a survey of enabling technologies and applications. *Electronics* **11**(12), 1893 (2022)
3. Praveen Kumar Reddy Maddikunta, Quoc-Viet Pham, Prabadevi, B., Deepa, N., Kapal Dev, Thippa Reddy Gadekallu, Rukhsana Ruby, Madhusanka Liyanage: Industry 5.0: A survey on enabling technologies and potential applications. *J. Ind. Inf. Integ.* **26**, 100257, ISSN 2452–414X (2022) <https://doi.org/10.1016/j.jii.2021.100257>
4. Md. Shahjalal, Woojun Kim, Waqas Khalid, Seokjae Moon, Murad Khan, ShuZhi Liu, Suhyeon Lim, Eunjin Kim, Deok-Won Yun, Joohyun Lee, Won-Cheol Lee, Seung-Hoon Hwang, Dongkyun Kim, Jang-Won Lee, Heejung Yu, Youngchul Sung, Yeong Min Jang: Enabling technologies for AI empowered 6G massive radio access networks, *ICT Express* (2022), ISSN 2405–9595, <https://doi.org/10.1016/j.ict.2022.07.002>
5. Ramachandran, Veerachamy, Ramar Ramalakshmi, Balasubramanian Prabhu Kavin, Irshad Hussain, Abdulrazak H. Almaliki, Abdulrhman A. Almaliki, Ashraf Y. Elnaggar, and Enas E. Hussein: Exploiting IoT and its enabled technologies for irrigation needs in agriculture. *Water* **14**(5), 719 (2022). <https://doi.org/10.3390/w14050719>

6. Fawad Zaman, Hing Cheung So, Daehan Kwak, Farman Ullah, Sungchang Lee: Smart antennas and intelligent sensors based systems: enabling technologies and applications. *Wireless Commun Mob Comput* **2022**(9820571), 3 (2022). <https://doi.org/10.1155/2022/9820571>
7. Kothari, M., Mistry, Z., Kamat, A., Ragavendran, U.: Multi-antenna-enabled technologies for IoT-driven smart cities. In: Nath Sur, S., Balas, V.E., Bhoi, A.K., Nayyar, A. (eds) *IoT and IoE Driven Smart Cities*. EAI/Springer Innovations in Communication and Computing. Springer, Cham. [https://doi.org/10.1007/978-3-030-82715-1\\_3](https://doi.org/10.1007/978-3-030-82715-1_3)
8. Zarlish Ashfaq, Abdur Rafay, Rafia Mumtaz, Syed Mohammad Hassan Zaidi, Hadia Saleem, Syed Ali Raza Zaidi, Sadaf Mumtaz, Ayesha Haque: A review of enabling technologies for Internet of Medical Things (IoMT) Ecosystem. *Ain Shams Eng. J.* **13**(4), 101660 (2022), ISSN 2090–4479, <https://doi.org/10.1016/j.asej.2021.101660>
9. Menniti, Daniele, Anna Pinnarelli, Nicola Sorrentino, Pasquale Vizza, Giuseppe Barone, Giovanni Brusco, Stefano Mendicino, Luca Mendicino, Gaetano Polizzi: Enabling technologies for energy communities: some experimental use cases. *Energies* **15**(17), 6374. <https://doi.org/10.3390/en15176374>
10. Liu, A., Wang, Y., Wang, X.: Enabling technologies of data-driven engineering design. In: *Data-Driven Engineering Design*. Springer, Cham (2022). [https://doi.org/10.1007/978-3-030-88181-8\\_9](https://doi.org/10.1007/978-3-030-88181-8_9)
11. Moraru, Sorin-Aurel, Adrian Alexandru Moşoi, Dominic Mircea Kristaly, Ionuţ Moraru, Vlad Ştefan Petre, Delia Elisabeta Ungureanu, Liviu Marian Perniu, Dan Rosenberg, Maria Elena Cocuz.: Using IoT assistive technologies for older people non-invasive monitoring and living support in their homes. *Intern. J. Environ. Res. Public Health* **19**(10), 5890 (2022). <https://doi.org/10.3390/ijerph19105890>
12. Peter Brida, Ondrej Krejcar, Stavros Kotsopoulos: Enabling technologies for smart mobile services 2020. *Mobile Inf. Syst.* **2022**(9870706), 3 (2022). <https://doi.org/10.1155/2022/9870706>
13. Syreen Banabilah, Moayad Aloqaily, Eitaa Alsayed, Nida Malik, Yaser Jararweh: Federated learning review: Fundamentals, enabling technologies, and future applications. *Inf. Proc. Manag.* **59**(6), 103061 (2022), ISSN 0306–4573, <https://doi.org/10.1016/j.ipm.2022.103061>
14. Schaffers, H., Komninos, N., Pallot, M., Trousse, B., Nilsson, M., Oliveira, A.: Smart cities and the future internet: Towards cooperation frameworks for open innovation. in *The Future Internet Assembly*, Springer, pp. 431–446 (2011)
15. Hernández-Muñoz, J.M., Vercher, J.B., Muñoz, L., Galache, J.A., Presser, M., Gómez, L.A.H., Pettersson, J.: Smart cities at the forefront of the future internet. in *The Future Internet Assembly*, Springer, pp. 447–462 (2011)
16. Droste, H., Zimmermann, G., Stamatelatos, M., Lindqvist, N., Bulacki, O., Eichinger, J., Venkatasubramanian, V., Dotsch, U., Tullberg, H.: The METIS 5G architecture: A summary of METIS work on 5G architectures. in *2015 IEEE 81st Vehicular Technology Conference (VTC Spring)*, pp. 1–5 (2015)
17. Gallala, Abir, Atal Anil Kumar, Bassem Hichri, Peter Plapper: Digital twin for human–robot interactions by means of industry 4.0 enabling technologies. *Sensors* **22**(13), 4950 (2022). <https://doi.org/10.3390/s22134950>
18. Al Kalaa, M.O., Balid, W., Bitar, N., Refai, H.H.: Evaluating bluetooth low energy in realistic wireless environments. *Proc. IEEE Wireless Communications and Networking Conference*, pp. 1–6 (2016)
19. Farhan, L., Alissa, A.E., Shukur, S.T., Alrweg, M., Raza, U., Kharel, R.: A survey on the challenges and opportunities of the Internet of Things (IoT). *Proc. IEEE 11th International Conference on Sensing Technology* (2017)
20. Louis Coetzee, Dawid Oosthuizen, Buhle Mkhize: An analysis of CoAP as transport in an internet of things environment. *IST-Africa Week Conference (IST-Africa)*, IEEE, Gaborone, Botswana (2018)

# Secure Group Communication Among IoT Components in Smart Cities



P. Parthasarathi, S. N. Sangeethaa, and S. Nivedha

**Abstract** The rapid growth in the information technology leads a path way on smart computing in engineering application. The Internet of Thing (IoT) supports smart computing in numerous real time application in the user environment. IoT technologies applied in manufacturing industries, service sectors and home applications. Most of the situation, the IoT technologies handle the users raw data in their service and businesses. There are countless IoT components are interconnected through the internet mediums. To provide better service to the user, all the IoT components are sensing inputs in the environment, handling operations, computing certain values, predating the action in the process, and so on. The modern smart cities are developed with lot of IoT applications. The cost for constructing smart cities are mainly focusing on cost of the IoT applications. In the working environment, data are the priceless entity. Ensuring the security services like authentication, confidentiality and integrity on the data, the communication channel in the IoT application and message sharing protocol are monitored and secured with defined security mechanism. The IoT components are frequently communicated with each other. All the components are integrated as defined Clusters and the communications among all the components are called Group Communication. During the group communication, forward secrecy and backward secrecy are the important security service which can be ensured with key management scheme among the encryption and decryption in the communication. Dealing with key management schemes, the communication cost and computational cost are primary factors to be considered. This article discussed about the dynamic key management scheme for secure group communication among IoT components for constructing smart cities.

**Keywords** Internet of things · Smart city · Secure group communication

---

P. Parthasarathi (✉) · S. N. Sangeethaa  
Bannari Amman Institute of Technology, Sathyamangalam, India  
e-mail: [sarathi.pp@gmail.com](mailto:sarathi.pp@gmail.com)

S. Nivedha  
Hindusthan College of Engineering and Technology, Coimbatore, India



# 1 Introduction

## 1.1 *Internet of Things*

The Internet of Things (IoT) [1, 2] is also called Internet of Every things which tells that electronic devices and electromechanical hardware components are connected together to provide certain services to the end user. In general, they are connected over the internet for the purpose of sending environmental data to each other. All the communications are performed as internet data communication even the components are mechanical components. The agenda for the usage of IoT is to build our environment as a workspace as a smart work station by means of doing the merge of physical location with virtual location. This is possible only through the methods of connecting each component over the internet. And all are sending and receiving internet data to share or interact with each other in the collaborative environment. The high end sensor with latest technology and Integrated Circuits (ICs) with advanced micro programs are used to create such components to work better and produce improved service to the end user. Sample Heading (Third Level). Only two levels of headings should be numbered. Lower level headings remain unnumbered; they are formatted as run-in headings.

In the IoT environment, multiple entities work for the applications, they are simply classified into two groups. This classification are hardware modules and software modules. The hardware modules include sensors, transmitting devices, internet connectivity devices, transmitting medium and extra based on the application. Similarly, the software modules include User Interface platforms, Graphical User Interface, Application Programs data storage, cloud storage and extra based on the application.

Nowadays, a number of IoT applications are developed to produce noteworthy results in the business and also applied in all streams of engineering and technology. IoT applications are simplifying the user interaction, detecting environment input, reducing computational processes and creating immediate response in industries. IoT applications play an important role in creating smart cities, smart healthcare, smart transportation, and smart tools for engineering applications and so on. It leads to making smart decisions, reducing manufacturing cost, reducing manufacturing time and reducing manpower in the workplace. IoT is also used to identify the problems even before they occur because of its analyzing and predicting pattern. Slowly IoT becomes occupying the industry and user day by day lifestyle with comparatively lower costs.

## ***1.2 Working of IoT***

The IoT is a group of techniques, systems and architecture ideas related to the recent wave of IT services and internet connected components that are based on the environment. The IoT working modules include hardware and software components [1, 2]. The sensor components are used to collect the environmental input related to the user applications. The collected information is transmitted to the cloud storage. The set of user applications process the stored information in the cloud storage. Based on the stored data, the appropriate instructions and events are performed with the help of User Interface platforms, Graphical User Interface, Application Programs. In IoT applications, the sensors, microcontroller and some components are connected to Information and Communication Technology (ICT) through both wired and wireless network technology.

## ***1.3 IoT Architecture***

In IOT, sensors play a vital role in data collection and processing of data. Initially sensors will sense the environment and collect the data about the particular environment and forward it to the concerned server or base station to do various facilities to the people in the various societies. Nowadays the cloud is used for storing large volumes of data i.e. big data either using private or public cloud.

The data sensed by the sensor will be stored in the cloud server using various facilities like Wi-Fi, satellite communication etc. After data is stored in the cloud, it is processed using different software to make it beneficial for the particular user. IOT plays its major role almost in all the fields to make the users work very modestly by saving their time and money. Sometimes it also acts like the decision maker by detecting common problems when it senses the data about the particular environs before it is sent for processing and analyzing, such applications are health care, agri, traffic management etc. IOT also made all benefits to the user with less cost (Fig. 1).

## ***1.4 Technology for IoT to Build Smart City***

The IoT is one of the important technology supports to construct smart cities. Nowadays, the population in the metropolitan area is a challenging problem [3]. The employability, education, hospital and new lifestyle forced the people to walk into the nearby cities. So, the population in the city is slowly increasing day by day. It creates too many problems such as pollution, waste management, heavy traffic, and unavailability of basic utilities. To overcome these problems, developing countries like India, China and Singapore are starting to construct smart cities. Making automatic service provide specialties is one of the major components to build smart

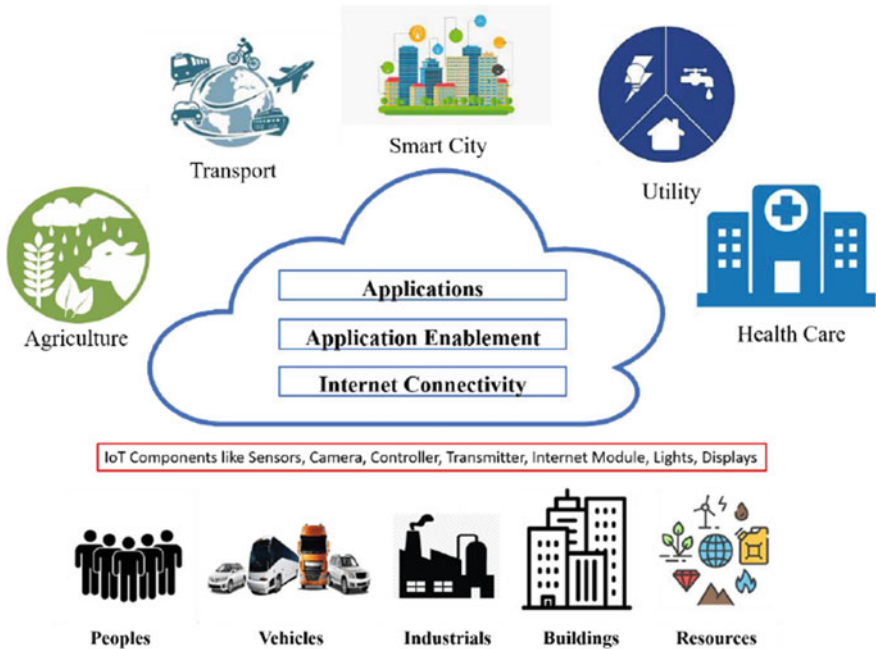
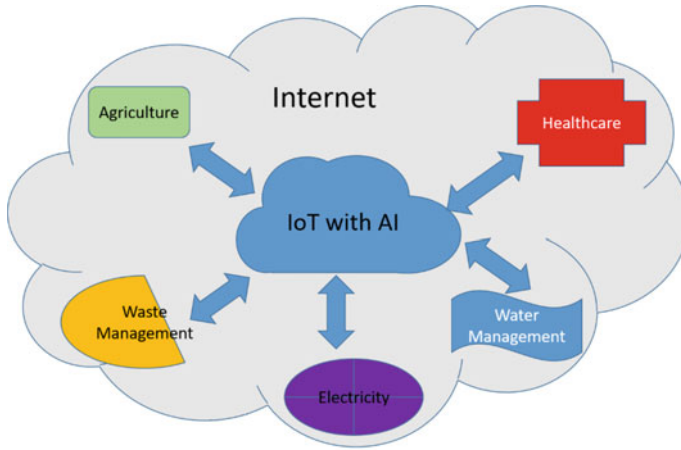


Fig. 1 Architecture of IoT

cities. In this area, IoT technologies are slowly starting to be used in the day by day activities such as milk vending machines, automatic ticket counters in bus stands, smart surveillance security systems and so on.

During the smart city constructions, two primary problems are addressed. They are hardware ventures and software used for database management systems. The first problem is about identifying the hardware for specific applications, purchases of hardware at economy cost, arrangement and maintenance, etc. The second problem is handling data in smart environments. The IoT components such as sensors, cameras continuously generate the data in the work floors. All the data are stored in the cloud storage as the definition of the IoT architecture. This data is handled by the set of application programs and user interfaces. The data are the primary component for all the information technology services. Based on the data, the IoT service is provided to the end user at the lowest cost and minimized time duration.

Apart from the hardware and software problem, the third problem is about the rule making in the smart cities. The policy frame and implementation are considered during the construction of the smart city. Because of the IoT component arrangement, the proper usage to be carried out. For example, during the smart traffic management system, everyone needs to follow the traffic light signals and code. Similarly, with automatic vending machines, the people should give the proper input and money to get the services (Fig. 2).



**Fig. 2** IoT with AI for building smart city

### 1.4.1 Digital Twins (DT)

During the constructions of the smart cities, installation of the digital element in the environment is a major process. Identifying the digital element and proper positions to get the signals and configuring the digital element are key features of the construction of smart cities. The physical components and services virtually increased its availability into double the time. The DT with IoT are required to improve the efficient and consistent data management. And also consider the safety of the data and service over the internet [3]. The DT also provides an advancement in engineering. Suppose the computer is improved to wisdom or analyses the physical environment in the defined area and answer consequently. The DT is also a significant feature for the digital transformation of the smart city. The DT is exhibited as the growing urban, Self-Learning, professional interdependence, and public contribution in smart city.

### 1.4.2 Internet of Everything (IoE)

The Internet of Everything is defined as IoT based applications used to collect the environmental data and comprehensive function to process them. In IoE [6], the recent technologies and methodologies such as artificial intelligence with smart computing, trained applications, real time computing, mixture analysis are used to get and analyses environmental data.

### 1.4.3 Big Data Analysis (BDA)

Big Data Analysis (BDA) is a data analysis system which is used to analyse the existing data and predict the upcoming event or data from the data set. During the IoT implementation in the smart city [3–6], there are too many data entries for each service and responsibility. In such a situation BDA is applied. For example, there is a public bus service that operates from one point to another. The service provider wants to identify the peak hours in the bus service route to operate multiple buses in the same route. It can be done with the help of BDA.

### 1.4.4 Sentimental Analysis (SA)

The Sentimental Analysis is the recommendation system which is used to provide the desired service to the end user. Based on the existing information about the given task, it refers to certain upcoming tasks with respect to the prediction and environmental input. Near the festival days, the market and shopping areas are fully crowded. During that time, the basic utilities like drinking water pipelines, toilets, health centers, security outposts, electricity and broadcasting (public address system) and etc. During the day, people do shopping, watch movies, and spend time sightseeing. But between 12.00 noon to 2.00 pm, all are visiting nearby hotels for their lunch. In smart cities, the sentimental analysis recommendation system will predict how many people will visit the hotel for the lunch? This system mentions the count almost similar to the exact one in advance based on the IoT support in the smart city. This happens only because of collecting the information from the shops, theatres, and fun event centers. The IoT and AI supports us to collect physical data [5]. The SA recommendation system does some analysis over the data collected in the shops. For example, the people in the tea shop or soft drinks shop are identified and grouped as people who will take their lunch in later. And also used to identify the people who will not take their lunch based on their travel history, it will identify their house locations. If it is near the shopping area, the recommendation system will conclude that the set of people will go home for their lunch. Similar to this, the SA systems used to provide the better services for healthcare, traffic systems in the smart cities.

### 1.4.5 Artificial Intelligence (AI)

The Information and Communication Technology delivers the basis to develop the application which will work autonomously with given knowledge on a certain process or event is simply called as Artificial Intelligent (AI) [5]. In IoT, there are too many electrical and electronic components employed to provide the efficient and cheapest service to the end user. AI consists of a set of predefined programs with a well-trained data set for an action. AI plays an important role in the industry to reduce the human role event decision making, large range of computation, etc. The IoT sensors and other input components collect the environmental inputs, the AI system

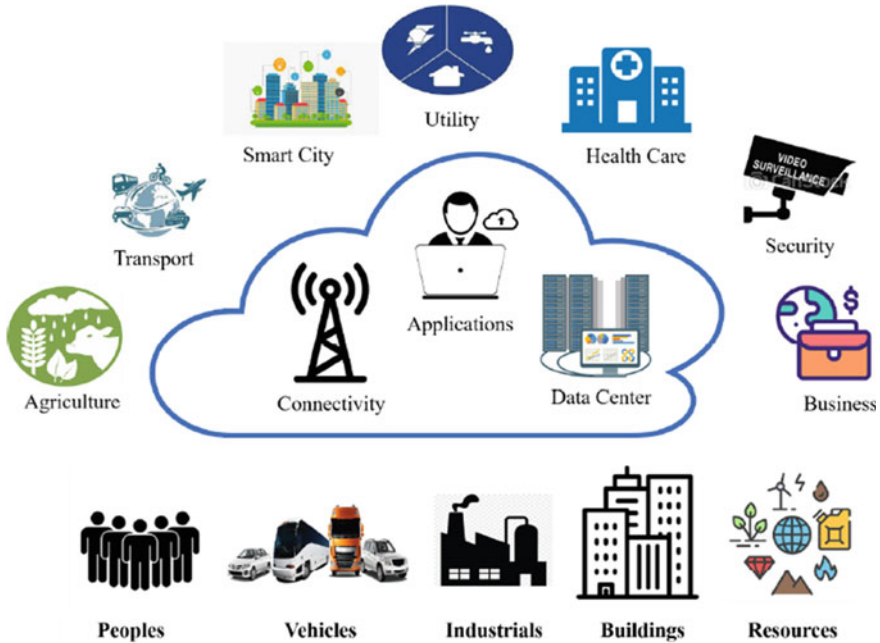


Fig. 3 IoT with AI for building smart city

programs in the microprocessor will react based on the inputs. The IoT systems with AI occupies the industries in all the streams of engineering and technology, even the civil engineering uses the IoT with AI to measure the load and support of the building blocks in large scale. Sound engineering, wind engineering, structural engineering, water engineering and management, earthquake engineering are sub streams of civil engineering where the IoT with AI technology plays a vital role to offer the endless services in the civil engineering. Similarly, the IoT with AI is used among all the engineering fields such as mechanical, electrical, instrumentation, transportation and so on during the construction of smart cities (Fig. 3).

### 1.4.6 Machine Learning (ML)

Engineering in ICT develops the next level of AI technology with modern tools and algorithm usage is called Machine Learning [7]. The ML is the sub-stream of AI based on where the machine learns from the data set, it identifies the structure and makes conclusions with less human interface. The pattern recognition, graph theory and computational statistics are the origin of the ML. ML system learns without system programs about what to do and perform given work. Also it takes decisions over the action being executed the event with input. The IoT with AI provides the

platform for the IoT with ML. The system with environmental input learns from the data and decides the action to be performed. Actually, they learn from the expressions of other computations to give repeated decision, reliable results. The Google Car, Online Shopping recommendation system are some of the examples for ML. ML is used to suggest the alternate path, identify the peak hour of the traffic, suggest the bus flow of the route and so on in the smart transport. Similarly, to suggest the nearby hospital or the medical centre in the city.

#### **1.4.7 Deep Learning (DL)**

In addition to the IoT support in the smart city project, the data analyse systems are used to improve the services. Even though there are too many analyse systems like BDA, SA and ML are used, the smart city required more than the existing one. In order to overcome the user requirement and provide desired services, the Deep Learning (DL) is used with IoT applications. DL is the next generation technique of ML, which trains the machine to achieve the action that comes naturally to humans. Some of the examples of DL are driverless cars, voice controlled remote control for home appliances such as Televisions, Air Conditioners, Sound Systems, and etc. In general, the DL is used to classify multimedia objects like text, image and sound. DL is used to increase the computing capability of the IoT application. Comparing DL with AI approach, the DL accepts multi-level data features from the given data problems. DL approaches also reduce human interaction, so the man power cost, material resource cost and time costs are reduced. Information technology leads the opportunity to develop the business in all aspects because of the power of the algorithms. DL supplies the multi-features of environmental data. This digital era prediction increases the accuracy in all the fields of smart city.

#### **1.4.8 Fog Computing in IoT**

The advanced computing architecture gives the decentralized computing model namely Fog Computing (FC) [6, 8], where data sets, computability code, storage and applications are maintained in different locations and interconnected over the Internet and Cloud services. FC is the new generation of distributed computing model, used to compute certain tasks in cheapest cost and minimal time consumptions. FC used to make smarter to become smarter. So, the construction of smart cities uses IoT applications with FC. The main advantage of FC is on demand computing for the user services.

## ***1.5 Application of Electronic Technology of IoT in Smart City***

### **1.5.1 Network Sensing Technology**

For the construction of intelligent smart city, the network sensing plays important role which is utilised frequently on the internet of things [6]. This network sensing will do the following operations like data collection using IOT devices in the particular environment, processing of data and change into useful information for the client. In data processing, this network technology will do data classification which will help to maintain large volume of data in the proper order for future use i. e. while building smart cities. Also it affords the supportive resource for planning and building smart cities.

### **1.5.2 Radio Frequency Technology**

During remote information sharing, radio frequency technology is mainly used to provide good communication support. This is mainly used in wireless communication technology. It will not use any contact means, but it will obtain better communication support. In smart city building process, the radio frequency technology plays the major role by reducing the effort of human beings and material resources and also it provide the improved efficacy of electronic technology in the IoT applications. This radio frequency helps to collect data from the environment very fast at the same time data processing time also gets reduced so as to improve the efficiency of info refinement. Therefore the radio frequency will give better feasibility and also it operates on stable state which is the good quality for the even creation of smart city.

### **1.5.3 Cloud Computing Technology**

In smart city construction, cloud computing plays the significant role in handling data. There are lot of difference among the network sensing and radio frequency technology [8]. The combination of various brainy technology will helps the cloud to manage the large volume of data. This cloud computing will have the great effort to do data analysis process and provides the valued decisions to the smart city constructors. It also involved in providing better support in three aspects like intellectual health care, brainy logistics and smart transportation.



## ***1.6 Application of Electronic Technology for Internet of Things in Smart City***

- With the great support of electronic technology in IoT, the modification of urban management in smart city construction will provide the esteemed data to improve the stages of the urban management services [9]. The main modification in urban management is to do some basic changes like the way the people living and their style, people sense of identity and their fulfilment while living in the city. The participation of residents in urban area for doing some modifications and changes in urban management also gives the major support and uphold the urban area to the intellectual smart city both resourcefully as well as systematically.
- The E commerce technology is now stimulated to the greater extent with the electronic technology in smart city development. It is also endorsed for the development of intellectual logistics in building smart cities. Now a days, the online shopping become very famous and handy among the people to purchase their requirements. The china become more popular in online shopping i.e. e commerce. It will show their power and their development in e- technology of the IOT and smart city. This e-technology also provides services to locate the consumer groups to stimulate the wealth of e-commerce in market field. It also uphold the growth in the creation of smart city with greater maturity of its related industry arena.
- Modern IoT technology also involved in the development of agriculture field. Since it is the backbone of our country, this field should be improved to the greater extent. The new improvement is done by using e-technology in IoT for planting techniques which would provide the greater changes in the agri field. The standard agriculture field will do planting based on the weather and seasonal condition and they grow only seasonal crops, fruits and veggies. If the person wants to eat good crops, fruits and vegetables with the less cost, they need to buy only the seasonal items. If not, non-seasonal items become very costly and they need to afford high cost for it. With the improvement in agriculture field using IoT and greenhouse technology, the planting mode is changed and we can plant all varieties of crops in any season and it will gradually increases the throughput of the crops. The e-technology of the IoT will also do some analysis for planting crops which makes the former to cultivate the crops quickly as well as the status of planting method also gets improved efficiently to obtain more harvests and profits.
- In smart city construction, the main demand is electric power. Since it is a smart city, everywhere we need is electricity. So automatically the demand is raised in the transmission of electric power to make the maturity in technology for the development of our country. This demand is modified in different stages. Some areas still there is a mandate in supply of even power supply so it should be solved immediately for initiating the good power transmission. The integration in the improvement of e-technology in IOT will afford the multiplicity of electricity supply in different modes for the people based on their requirements. The steadiness and the security of the electricity provision is progressively developed by

merging the e-technology in the IoT and the smart city construction. Safety is one of the major point that should be ensured while doing electricity transmission in smart city and also for harmless process for all IoT devices.

## ***1.7 IoT Applications***

### **1.7.1 Home Appliance**

With the help of smart devices like PC and Mobile, all the home appliances are interconnected each other's. Now a days, the smart phones are used to be a home becomes smart homes. Once they are switched on, then they are became smart home utility component. Peoples control the operations of the home appliance in from remote location. Some of the examples are remotely controlled washing machine, room temperature monitor, lights, and finally the security systems.

### **1.7.2 Smart Grid**

The applications of IoT in the electricity is more benefitted to optimize the use of electrical components. The ICT is applied to understand and analyse the usage of the electricity of each and every consumers where IoT plays an important role to measure the usage, send the usage information to the cloud storage and analyse these data for the purpose of knowing the time of the usage, amount of usage and etc. This process is to be done to improve the efficiency of the system.

### **1.7.3 Industrial Internet of Things**

The IOT is now enhanced in the industry field to provide benefits to manufacture goods, transportation of materials, mining and also involved in various sections in industry field for its development. The improved IOT technology in industry field, it afford upright worth of materials with upgraded security. The IOT application involves the exchange of accounts among the consumers. Also it provide the better services like tracking goods, delivery of goods etc. IOT also gives worthy possibility for supportable and improved Value of Services.

### **1.7.4 Smart Retail**

IOT is very much improved in field of retail business. It plays a major role in 'retail industry involves maintenance of good relationship among customers and intellectual logistics. The IOT provides the good customer review in the field of digital signing,

smart mirrors etc. IOT also provides the frictionless services like sensing of data, analysing and processing of data.

### **1.7.5 Smart Healthcare**

Now a days, IOT is greatly improved in the field of healthcare system. Initially it helps the patients to maintain their health by using smart devices like smart watch, smart bp and sugar maintenance kit etc. Also it maintain the reports of the patients by storing them in the cloud. IOT also afford the greater lifesaving service for the rural area people when the doctors are not physically appeared for treatment. It is well supportive for the people who are not able to move because of their health issue. This IOT smart device frequently monitor those people and forward the concerned report to the doctors for their evaluation and preserve the good health. IOT devices also provide good quality of services to all the patients to provide endless services to the patients.

### **1.7.6 Smart Cities**

The population exist in cities is ever increasing with express urban development rinsing the already existing infrastructure. To tackle the growing demand of service and infrastructure, new demand of cities urban IoT is rapidly growing area of research. The IoT technology is used to reduce and monitor the traffic in the field of city traffic management. IoT is applied to find the nearby hospital and medical centre as soon as quick and provide the pathway to reach out the same. Similarly, the waste management, water management, electricity management and food chain of the individual.

## **2 Smart Cities**

Governments around the world have decided to develop their nations into smart cities or smart countries, in terms of public transport, railway, airways, cleanliness, waste disposal, supplying of water and many more [9]. For example, Singapore is the best example for collecting the information of the people who are smoking in the restricted area. India has also started the work progress for making the nation smarter and also assigned a fund which is pretty much close to 30 billion dollars for making the smart city mission.

There is no general definition for smart city. It has different meanings related to different locations because area to area, the needs of becoming a smart city may differ [17]. Developing smart cities may depend on different factors such as development level, resources of the city residents etc. If the city is going to change over to the smart city mission, it needs to attain certain boundaries. Most of the citizens in

India, know their own look to make the city smarter, in terms of infrastructure and services. To satisfy the needs of the residents, promoters targeted building up the whole environment to focus on social, physical and economic structure. It can be considered as a long term goal, working towards the city as a smart city, by adding the multilayer of smartness in the field of social and economic development. In the smart city mission, the main aim is to highlight the infrastructure and provide a quality life such as clean and sustainable applications and environment to the citizens.

## ***2.1 Needs of Smart City Construction***

Developing the new cities is a highly energetic and high—powered process. Constructing a smart city is the process of intelligent module to traditional module, based on the order of upgrading the environmental quality [10]. Currently, the development of China into a smart city is the vibration, many cities introduced and followed their own measures and actions for developing their city as a smart city. In China, in the year of 2018, 95% of the cities were above the rural level and 83% of the cities were under the government of a prefect and around 500 cities are framed for developing the smart cities. The construction made in China mainly depends on four factors such as the requirements based on the urban citizens, the advancement based on local and national policies, the urging role inside the government and the idea based on the type of peoples' needs. The smart city of China has been constructed promptly in the past five years based on the internal factors such as digitalized infrastructure, social physical and economic development and innovated technology. However, the Smart city construction in China is still in the developing stage compared to countries like Europe and America. The construction of smart city in China is based fully on government oriented, different applications, effective use of technological devices and various models.

The several characteristics of smart City in China are:

1. To meet the requirements of industry, information technology, modernized agriculture, good urbanization.
2. The planning and management is controlled by the China Government.
3. Fund may sponsored from different countries.
4. Public service level.
5. Use of big data to enhance the smart devices based on the intelligent systems.

A smart city always follows the development of a new city and innovation model which relates to the long term development of the city. It not only improves the resource allocation, effect and vibrancy of the city but also encourages the growth of the industries related to small and medium sized cities.

## ***2.2 Design of the Smart City with IoT Applications***

The construction and architecture of the smart city infrastructure depends on various sensor technologies, functionalities of the ecosystem, which interacts with each management, control and automation [11]. The connectivity is fully dependent on all smart devices by intelligent based remote communication. These devices are fully dependent on the network, data analytics and actuation. The centralized functional features work well with schools, public hospitals, offices etc. With the invention of the network, more hardware and software technologies are introduced in the market for the purpose of communication with IOT technology. The Internet of Things is a drastic change in recent years and it has a high immense potential on every human lives.

Opportunistic networks called as OppNets, subclass of networks, intermittent connectivity is in between the sender node and the goal node. In the smart infrastructure model, the OppNets allows the connection between the service provider and requester. OppNets is used to solve the intermittent connectivity issue that arises between the edge server and the mobile IoT nodes. Mobile Computing service also solves the connectivity issue which occurred during the transformation of the direct and indirect message.

## ***2.3 Concepts of IoT in Smart City***

A meaningful association among networks and objects is termed as Internet of Things (IoT). Different kinds of devices can be operated remotely with the help of IoT. Currently, IoT has inevitable role in various arenas such as intelligent transportation, environmental protection, government work, public security, safe homes, intelligent fire control, industrial monitoring, ecological monitoring, elderly care, personal health, flower farming, aquatic system monitoring, food traceability, enemy investigation and intelligence collection. Also, it is important to note that IoT is based on the Internet, and it requires higher technical support. It prerequisites not only network links and extension of the Internet but also the support of satellite remote detecting and additional positioning systems. By this way, IoT could precisely pinpoint any object and comprehend remote execution. It has robust feasibility in domains like power grid construction and maintenance, bridge design, highway maintenance and other people's livelihood projects. In simple words, it is claimed that IoT can simplify day to day activity of people and also enhances the range of intelligent home-based life style. Particularly, IoT has major contribution in the initial construction of smart cities. Smart cities are considered to be composition of four layers, i.e., the layered arrangement of the network, that take account of the application layer, support platform, network layer and perception layer.

The fundamental policy of an intelligency city is more essential for the further development of the city. It is mostly exemplified in marketable operations, logistics

and transportation, medical & tourism management and additional features of the city. In order to advance the intelligent level of the city, it is compulsory to relate the IoT technology as a prominent factor. The comprehension of intelligent cities will have a notable role towards the development of science and technology and the intellectualization of cities. It is tremendously beneficial to the expansion of the city. Furthermore, in the long run, the realization of intelligent cities will bring more improvement chances in the city's business, tourism, industry and other areas.

A smart city has an orderly arrangement, its point of intelligence is comparatively more, and it has a delicate perception, which is also one of the elementary aspects of information transmission. Moreover, the intelligent city has a comprehensive structure, consistent information communication, and high intelligence, which can rapidly process a huge quantity of information. The perception of smart city project lies in fewer requirements for management and more dependence on the operation of the system. To a great extent, this can diminish the existence of manual blunders and increase the competence and quality of intelligent management.

IoT has an optimistic implication in stimulating the growth of urban industry, encompassing the industry nearby the city and commercial progress in the dominant area of the city as well as other industries. Awareness about IoT is much important which aims at the reformation of the industrial arrangement of a city, which represents the features of the centralized consumption of resources and the optimization of the structure in a smart city. Awareness about IoT is much important which aims at the reformation of the industrial arrangement of a city, which represents the features of the centralized consumption of resources and the optimization of the structure in a smart city. The direct outcome of the execution of the IoT is to minimize the cost of urban information management. For the reason that the IoT is centred on the network, it processes and quickly stores and transfers a huge quantity of information.

## ***2.4 Smart City Applications***

The applications are characterized based on the smart features and technology that can be implemented in the city. There may be enormous ways to implement smart city systems in the day to day jobs. It gives innovative ideas to make things smarter. The various applications while constructing the smart city includes are.

- Controlling Air Pollution
- Waste Management
- Smart Transportation
- Disaster Management

Let see discuss in detail about all the major applications in smart city.

### **2.4.1 Controlling Air Pollution**

Air pollution is the major issue mainly seen in the bigger cities of India, due to heavy traffic, more vehicles, it can be solved by introducing smart systems to keep the air pollution under control. China has solved this issue with smart solutions by introducing the experimental tower of 300 feet in height which acts as a Air Purifier. This air purifier tower acts as improving the air quality.

### **2.4.2 Smart Transportation**

Smart transportation is the approach of building modern technology into the transportation systems. Modern technology includes cloud computing, wireless communication, intelligent models, computer vision etc., Smart transportation makes our environment clean and efficient. It results in reduced traffic congestion and energy consumption. It highly results in environmental benefits.

### **2.4.3 Disaster Management**

Smart technology in disaster includes effectively preparing and responding to disasters. This results in lesser cause when disaster occurs. It involves managing the prevention of disaster, preparedness from disaster, response, and recovery from disaster. In many of the cities likely to be Mumbai or Delhi, can mainly cause natural calamity, due to the smartness under disaster can help to minimize loss of human life.

### **2.4.4 Waste Management**

The waste management begins with the waste made by the individuals or group. The disposing of waste materials through garbage cans. The garbage cans are contracted with trucks at the present time and automatically moved to the allotted assortment centres and trash for recycling purposes. It results in preventing an unhygienic environment and most of the time people are not separating the normal waste and the recycling waste. All these issues are solved by developing the smartness in the waste management system.

### 3 Secure Group Communication

#### 3.1 Cluster Communication

Secure Group Communication (SGC) is the communication among the clusters of people or the components who are working together to perform a certain task [12]. In this communication model, framing the cluster is the primary process where we need to identify the people or the component who wants to communicate with each other. The communications may be related with sharing the information about the certain process, sending the control commands to perform certain tasks, giving input for the particular programming model, granting the permission to access the memory locations, providing access rights to use any resource like hardware or software models.

In these communication models, there are two basic problems that are identified over the experience. They are the reliability of the communication channel or the connection between the communication entities. The second problem is about the security of communication information. To address the first problem, the network management protocols are to be strictly followed. The network management systems provide the end to end reliability on the physical connection and logical connection protocols. And these kinds of problems are identified and rectified with the help of recent technology and advancement in Electronics and Communication Engineering. The security problems are rectified through network security mechanisms. The Cryptography Techniques are used to identify the security attacks such as active attack and passive attack, also used to ensure the security services such as authentication, information confidentiality, resource access restrictions, information integrity and resource, data availability through the defined security mechanism such as specific security mechanism and pervasive security mechanism.

#### 3.2 Dynamic Cluster

In Cluster Communication (CC), the cluster dynamic is the important services rather than security services [13]. Dynamic cluster means any person may join as a new member into the cluster. Similarly, any existing person may leave the cluster as of his/her will. The cluster communication will support a person to join and leave at any time during the communication, before the communication or at the end of the communication. These communication models will not fix the size of the cluster. The total strength of the cluster is always a dynamic number. Based on the applications, cluster strength is maintained dynamically. These dynamic conditions only cause security issues. To address and prevent these security issues, security mechanisms are applied in the cluster communications.

When the security mechanisms are applied in the cluster communication then that cluster communication will become Secure Cluster Communication (SCC) also



known as SGC [14, 15]. Even though there are too many security services listed, authentication and confidentiality are primary security services that are addressed in the SCC. To achieve these two services, the basic mechanisms like forward secrecy and backward secrecy is maintained in the cluster communication. During the forward secrecy, the leaving person will not take participants in any upcoming communications and should not access existing cluster communication. Similarly during the backward secrecy, the newly joined person should not know the details about previous communications which happen before the joining of the particular person in the cluster communications.

### ***3.3 Key Information***

In SCC, the public key cryptography method is applied to ensure the authentication and confidentiality [16–19]. Two keys are used to encrypt and decrypt the communication messages. They are namely cluster key and individual key. All the people in the cluster are owning their own personal key which is called an individual key. It is acting as the private key in the public key cryptography. Similarly, all the people in the cluster are commonly sharing one key information which is called cluster key. It is acting as the public key in the public key cryptography. During the group dynamic conditions, both the cluster key and individual's keys are frequently changed whenever there is a change in the people strength in the cluster. That is, all the people join and leave operation, the individual key and cluster key information also changed to ensure both forward secrecy and backward secrecy.

### ***3.4 Cluster Communication Among IoT***

In the Smart City project, there are too many IoT components that play an important role to provide uninterrupted services in terms of utility services. These IoT components frequently interact with each other to share signals, processed data and other information. For examples, the traffic management system in the smart city includes sensors to identify the vehicle in the road, collect the vehicle count in the route and other information about road transport [20–23]. All the collected data are send to the cloud storage. Programs with BDA, ML, SA, DL and FC algorithms are used to extract the knowledge about the road [24, 25]. While collecting the data, there are some security issues and privacy problems. So that, proper security mechanism has to be implemented in IoT component communications. Similarly, to ensure the data collected about VIPs, government decisions are also need to be keep secure. The cryptography techniques are generally choose for implementing forward secrecy and backward secrecy. Providing a conditions, to maintain the reliability of the service, the IoT component strength is kept dynamic numbers [26–28].

## 4 Conclusion

This chapter deals with the various hardware and sensor component used in the IoT environment and also consider the basic organisation of component to construct the IoT based smart city. Even though the advancement IoT and its benefits are important to reduce the computational cost and communication cost, the security system of the organization is very important. Embedded wireless technologies will be scalable and easily upgradable as they are based on international standards. several technologies of IoT which includes energy sectors, sensors, cloud computing, communication, IOT integration and IOT protocol and standards. So, here discussed about the need of IoT, construction of smart city and Security of the communications of components. To provide the better service to the end user, the IoT based smart cities are proposed.

## References

1. Patel, K.K., Patel, S.M.: Internet of things-IoT: definition, characteristics, architecture, enabling technologies, application & future challenges. *Int. J. Eng. Sci. Comput.* **6**(5):6122–6131 (2016)
2. Mishra, N., Singhal, P., Kundu, S.: Application of IoT products in smart cities of India. In: 9th IEEE International Conference on System Modelling & Advancement in Research Trends (2020)
3. Li, X., Liu, H., Wang, W., Zheng, Y., Lv, H., Lc, Z.: Big data analysis of the internet of things in the digital twins of smart city based on deep learning. *Futur. Gener. Comput. Syst.* **128**, 167–177 (2022)
4. Zhang, C.: Design and application of fog computing and internet of things service platform for smart city. *Futur. Gener. Comput. Syst.* **112**, 630–640 (2020)
5. Bhardwaj, K.K., Banyal, S., Sharma, D.K., Al-Numay, W.: Internet of things based smart city design using fog computing and fuzzy logic. *Sustain. Cities Soc.* **79** (2022)
6. He, H.: Research on the application of electronic technology of internet of things in smart city. In: 2020 International Conference on Intelligent Transportation, Big Data & Smart City (2020)
7. Kour, K., Kour, J., Singh, P.: Smart applications of internet of things. In: 2018 First International Conference on Secure Cyber Computing and Communication (ICSCCC) (2018)
8. Cyril Jose, A., Malekian, R., Ye, N.: Improving home automation security; integrating device fingerprinting into smart home. *IEEE Access* (2016)
9. Raghuvanshi, A., Singh, U.K.: Internet of things for smart cities- security issues and challenges. *Mater. Today: Proc.* (2020)
10. Pradhan, M.: Interoperability for disaster relief operations in smart city environments. In: 2019 IEEE 5th World Forum on Internet of Things, pp 711–714 (2019)
11. Ponnusamy, M., Alagarsamy, A., Traffic monitoring in smart cities using internet of things assisted robotics. *Mater. Today: Proc.* (2019)
12. Peng, S., Han, B., Wu, C., Wang, B.: A secure communication system in self-organizing networks via lightweight group key generation. *IEEE Open J. Comput. Soc.* **1**(2), 182–192 (2020)
13. Parthasarathi, P., Shankar, S.: Decision tree based key management for secure group communication. *Comput. Syst. Sci. Eng.* **42**(2), 561–575 (2022)
14. Parthasarathi, P., Shankar, S.: Weighted ternary tree application for secure group communication among mobile applications. *Wirel. Pers. Commun., Springer*, **117**(4), 2809–2829 (2021)

15. Viji, C., Beschi Raja, J., Parthasarathi, P., Ponmagal, R.S.: Efficient fuzzy based k-nearest neighbor technique for web services classification. *Microprocess. Microsyst., Elsevier Publication* **76**(103097), 1274–1278. ISSN No: 0141-9331
16. Parthasarathi, P., Shankar, S., Nivedha, S.: A survey on dynamic key management system in secure group communication. In: *IEEE Explore under 6th IEEE International Conference on Advanced Computing and Communication Systems (ICACCS)*, pp. 1440–1443 (2020)
17. Nivedha, S., Parthasarathi, P.: Energy-efficient and coverage based data collection in sparse wireless sensor and actor networks. *Int. J. Comput. Eng. Appl.* **12**, Special Issue, 48–58. ISSN No: 2321-3469 (2018)
18. Venkatesh, V., Parthasarathi, P.: Trusted third party auditing to improve the cloud storage security. *CiiT Int. J. Wirel. Commun.* **5**(4), 183–187. ISSN 0974-9640. WC042013008 (2013)
19. Luo, X., Yin, L., Li, C., Wang, C., Fang, F., Zhu, C., Tian, Z.: A lightweight privacy-preserving communication protocol for heterogeneous IoT environment, special section on communication and fog/edge computing towards intelligent connected vehicles (2020)
20. Xue, K., Meng, W., Li, S., Wei, D.S.L., Zhou, H., Yu, N.: A secure and efficient access and handover authentication protocol for internet of things in space information networks. *IEEE Internet Things J.* **6**(3) (2019)
21. Yao, C., Liu, Y., Wei, X., Wang, G., Gao, F.: Backscatter technologies and the future of internet of things: challenges and opportunities. *Intell. Conver. Netw.* **1**(2), 170–180 (2020)
22. Dammak, M., Senouci S.M., Messous, M.A., Elhdhili, M.H., Gransart, C.: Decentralized lightweight group key management for dynamic access control in IoT environments. *IEEE Trans. Netw. Serv. Manag.* (2020)
23. Esposito, C., Ficco, M., Castiglione, A., Palmieri, F., De Santis, A.: Distributed group key management for event notification confidentiality among sensors. *IEEE Trans. Secur. Dependable Comput.* (2018)
24. Porombage, P., Braeken, A., Schmitt, C., Gurtov, A., Ylianttila, M., Stiller, B.: Group key establishment for enabling secure multicast communication in wireless sensor networks deployed for IoT applications. *IEEE Access* (2015)
25. Chien, H.-Y.: Group-oriented range-bound key agreement for internet-of-things scenarios. *IEEE Internet Things J.* (2018)
26. Mughal, M.A., Shi, P., Ullah, A., Mahmood, K., Abid, M., Luo, X.: Logical tree based secure rekeying management for smart devices groups in IoT enabled WSN. *IEEE Access* **7**(1), 76699–76711 (2019)
27. Dhanujalakshmi, R., Kartheeban, K.: Smart and secure group communication in Iot using exponential based self-healing group key distribution protocol. *IEEE Access* (2019)
28. Park, J., Jung, M., Rathgeb, E.P.: Survey for secure IoT group communication. In: *SPT-IoT'19—The Third Workshop on Security, Privacy and Trust in the Internet of Things, IEEE Explore* (2019)

# SCPS: An IoT Based Smart Car Parking System



Harikesh Singh, Animesh Pokhriyal, Anmol Sachan, and Meghna Saxena

**Abstract** With increasing population and increase in purchasing capacity, the need for personal transportation has seen a tremendous increase over the years hence the increase for parking spaces at public places such as malls, supermarkets, and big housing societies has also increased to provide adequate parking space for the people. With huge parking spaces comes the responsibility to manage it efficiently and conveniently so as to provide fast and easy parking solutions for the users. Currently, the parking facilities hiring assisting staff to help customers who are driving in the facility with finding parking slots. To automate this task and minimize human intervention while users park their car, the proposed system, SCPS (Smart Car Parking System) maps the parking slots into a dynamic real-time virtual map that updates the parking slot availability as the user parks their car, by sensing the existence of a vehicle in a parking area using IR sensors (Infrared sensors). The SCPS system updates that particular slot as occupied and then updates the display. In this paper, we have developed a Smart Car Parking System (SCPS) using IOT, Arduino, NodeMCU esp8266 with a wi-fi module and an android application for booking the parking slots by the user that can be monitored from anywhere around the world. As a result, we minimize the unnecessary human interference that was required for the parking facility. This helps to utilize the human skills for other tasks and creates a smooth parking facility without multiple assistances.

**Keywords** IoT · IR sensors · Arduino · Parking lot · NodeMCU ESP8226

---

H. Singh (✉) · A. Pokhriyal · A. Sachan · M. Saxena  
Department of Information Technology, ABES Engineering College, Ghaziabad, Uttar Pradesh,  
India

e-mail: [harikesh.singh@abes.ac.in](mailto:harikesh.singh@abes.ac.in)

A. Pokhriyal

e-mail: [animesh.17bit1139@abes.ac.in](mailto:animesh.17bit1139@abes.ac.in)

A. Sachan

e-mail: [anmol.17bit1058@abes.ac.in](mailto:anmol.17bit1058@abes.ac.in)

M. Saxena

e-mail: [meghna.17bit1147@abes.ac.in](mailto:meghna.17bit1147@abes.ac.in)

## 1 Introduction

The technology of the Internet of Things (IoT) allows the transfer of information and data through the network of connected devices without physical connection of the network. This technology helps the user to transmit the information without the wired connections. Also with IoT a user can save and access its data on the cloud. With IoT there is transparency within data exchange which happens through IoT. The basic idea of IoT was to connect different devices together. Then those connected devices need to be monitored. They are monitored with the help of computers using the internet. IoT stands for Internet of Things which are basically the two words, “Internet” and “Things”, here internet can be defined as a global and vast connection of computer networks or connection of different servers with different devices on a vast network. The Internet helps to exchange information within a network. If we see parking is a problem in a populated country like India, it also leads to pollution and traffic jams.

Due to increased traffic, finding a parking spot is getting difficult day by day. A survey recently stated that there is going to be a breakneck increment in the total number of vehicles used and it might go up to 1.6 billion by 2035 [1, 2]. To fuel all these vehicles millions of barrels of oil are needed and thus burnt every day. This situation thus demands a better parking system. This will reduce the wastage of fuels. A smart car parking system is the need of the hour to reduce the overconsumption of fuel and it minimizes the user’s time and efforts to search for a parking lot [3, 4]. So, the proposed model of a smart car parking system will help to find the parking spot without wasting fuel and wandering in the lot or requiring human resources to guide the users. Also, there will be an application for user convenience to check free slots in the parking lot. The app will update the status of the parking lot in real-time and the user can check the location on his phone instead of finding it manually.

## 2 Related Work

Building up a Smart Car Parking System with various difficulties. Among them was identifying and following vehicles that were entering the parking garage. Our shrewd smart car parking framework was created to give permission for the recognition of a vehicle when placed in the parking area and communicate the required to the user with the end goal. There have been various tasks chipping away at the same frameworks. Among them was Guangdong AKE Innovation Company Limited, of China.

The Guangdong AKE Innovation Company Limited, China is a futuristic venture which manages information procurement and data operation as its center innovation and development. This association has created indoor, outdoors and city urban smart vehicle parking frameworks and parking management frameworks. This indoor leaving framework utilizes a module which is ultrasonic and there is a camera as

sensor to peruse the item, and car to convey the framework through the RS485 communication cable. The framework measures the data, which is accumulated securely from the sensors and showcases the conclusion through RED markers and GREEN markers to the framework clients. A similar thought is implemented in the open air parking framework; the solitary distinction of this model is that it extensively uses a sensor which is geomagnetic and distinguishes the difference in magnetic field in that particular allotted territory and conveys the equivalent remotely to the worker giving the current status of parking lot to the client. This smart parking framework utilizes referential sorts of recognition sensors as outside frameworks for checking the accessibility of user parking slots in the whole parking area.

The solitary contrast is that the status of the parking area is imparted through the LED lights or transmitted over the internet and its status can be seen through the mobile application or a web server by the clients provided for the user. A comparable task had been finished by Elakya R., Juhi Seth, Pola Ashritha and R. Namith (Smart Car Parking System utilizing IoT) [2]. In this model, they gathered information from the sensor and got the yield by examining and preparing the information. Then Arduino transmits the signal from itself to the servo motor and GSM module which is connected to it which then helps in giving instructions and sending notifications to the user. Every vehicle must have a RFID card so when a vehicle enters the parking lot the RFID card of that particular vehicle will be scanned by the reader module which will help in maintaining the authenticity of the user details. Also, this will help in giving the information about the available parking slots to the user along with the details of the lot which the user would have registered through an SMS on the registered mobile number of the user.

This model can be divided into three parts. The first part consists of the Arduino devices and IR sensors. Interaction of users and parking lots will happen via these devices. The second section comprises cloud web services that will interconnect the user and vehicle parking area. All the updates in parking availability happen on the cloud side by side. There is an admin to administer the cloud, but the user can check the availability of the slots too. The third section of the model architecture is dedicated to the end users. The availability of the user parking spots and the details of the registered slots is sent to the user via SMS. This is done through the GSM module. The user uses the mobile application to interact and find the parking area which is updated at real time because it is connected to the cloud. The user receives notification about the availability of parking lots. This helps in saving time and fuel.

### 3 System Objective

The technology of the Internet of Things (IoT) allows the transfer of information and data through the network of connected devices without physical connection of the network [5, 6]. This technology helps the user to transmit the information without the wired connections. Also, with IoT a user can save and access its data on the cloud. With IoT there is transparency within data exchange which happens through IoT [7].

The basic idea of IoT was to connect different devices together. Then those connected devices need to be monitored. They are monitored with the help of computers using the internet. IoT stands for Internet of Things, which are basically the two words, “Internet” and “Things”, here internet can be defined as a global and vast connection of computer networks or connection of different servers with different devices on a vast network.

The Internet helps to exchange information within a network. If we see parking is a problem in a populated country like India, it also leads to pollution and traffic jams [8]. Due to increased traffic, finding a parking slot is getting difficult day by day [9]. A survey recently stated that there is going to be a breakneck increment in the total number of vehicles used and it might go up to 1.6 billion by 2035 [10]. To fuel all these vehicles, millions of barrels of oil is needed and thus burnt every day. This situation thus demands for a better parking system. This will reduce the wastage of fuels. Smart car parking system is the need of the hour to reduce the overconsumption of fuel and also it minimizes the user’s time and efforts to search for a parking lot. So, the proposed model of a smart car parking system will help to find the parking spot without wasting fuel and wandering in the lot or requiring human resources to guide the users. Also, there will be an application for user convenience to check free slots in the parking lot. The app will update the status of the parking lot in real time and the user can check the location on his phone instead of finding it manually.

## 4 System Requirements

The parking area is segregated into 2 parking lots: Parking A and Parking B. Every vehicle leaves three spaces and each opening has an infrared sensor integrated in it. For each parking lot we have 1 IR sensor (infrared sensor), therefore there will be a total of 6 IR sensors. Each IR sensor is utilized to identify the presence of a vehicle which comes at that particular parking spot. These IR sensors are connected to Arduino. When a vehicle enters the parking slot, Arduino sends signals to the connected NodeMCU esp8266 wifi module, at that point NodeMCU sends signal to the mobile app through the cloud.

### 4.1 *Arduino*

We will be using an Arduino board to convert the input to output. Arduino is a developed reliable opensource platform for electronic development which is very developer friendly in terms of both hardware and software [11, 12]. Then these Arduino boards take the inputs from the sensor which is activated whenever a light falls on it or when a finger is put to the button or a specific type of message notification and it turns it into desired output which could be turning a device motor on, switching on an LED [13]. The board can be programmed such that it does a particular task

on a particular set of instructions which are sent to the 4 microcontroller which is attached to the system. To do the programming on Arduino an IDE is used which facilitates the same [14]. Arduino board is cost effective in terms of what they have to offer and are easy to get hands on.

**Cross-Platform:** Arduino softwares run on most of the popular Operating Systems like windows, linux, Macintosh OSX. **Developer friendly programming environment:** Arduino programming environment is easy to get started on and has less or less learning curve thus becoming beginners friendly yet it also advanced enough for experienced developers to take full advantage of the system [15]. **Open Source:** Arduino software is open source published software also available for custom extensions made by experienced developers, language can be developed and expanded through C++ libraries.

## 4.2 IR Sensor

An IR sensor is used to detect the vehicle in this particular model. These sensors detect and capture the infrared emitted radiation. These radiations have wavelength greater than  $0.7 \mu\text{m}$  There are three male headers in IR sensors named, VCC, GND and OUT (from left to right respectively). We connect the Arduino to the VCC pin of the IR sensor. Ground of the IR sensor is connected to the ground of the Arduino. And finally the OUT pin of the IR sensor is connected to IO pins of the Arduino.

The IR sensors are the turnaround one-sided diode made up of appropriate band gap material, when infrared radiation falls on the finder electron gap sets are produced within the consumption locale which is cleared by the large electrical field accessible within the consumption locale. In this way a current gets set up. Since infrared radiation has less vitality compared to obvious light (since it has more frequency compared to obvious light and the vitality of occurrence photon =  $h\nu$ , where  $\nu$  is the frequency,  $h$  is Planck steady) so fabric with appropriate band hole ought to be chosen. Silicon, which is widely used in electronics, is not a choice because it has a band gap of 1.2 eV, and the incident infrared radiation does not have this much energy. So for infrared detectors the material of suitable bandwidth is Mercury Cadmium Telluride (MCT).

## 4.3 NodeMCU ESP8266

NodeMCU ESP8266 is a budget friendly, Wi-Fi module which is used to connect models of IOT or similar domains, to the internet. The electrical and mechanical equipment which we use today don't have an inbuilt feature to connect to the internet on their own. One can integrate this equipment with NodeMCU ESP8226 to perform many operations like controlling, monitoring etc. which require internet connectivity. NodeMCU ESP8266 can be considered as a System on Chip or SoC. A System on



Chip is basically a circuit which integrates and includes every component of the computer or any other electronic device to be used.

## 5 System Design

The primary stage is to distinguish the left vehicle. For that one IR sensor will be introduced in each parking lot. The sensor will be introduced before the vehicle, at a height of hundred centimeters from the beginning. The principal stage will be effective when the sensor will recognize the vehicle inside its vicinity. When Arduino transmits the signal to an IR sensor and those signals are received by IR sensors then sonic waves are emitted by it. These waves then travel and reach the vehicle standing in the parking lot and are reflected by it. After reflection of these waves, they are sensed by IR sensors. Which then tells us if the lot is empty or not. The time elapsed between this process of reflection and sensing highly depends on the distance at which the object (in this case our vehicle) is present with respect to the IR sensor. Sensor then sends signal to the Arduino. The signal sent is in the form of a timing pulse. The timing of this pulse depends on two factors, distance and program which is uploaded in the module. If after processing the information the distance between the sensor and a vehicle comes out to be greater than 150 cm, it will consider the slot to be empty and the red led in the user application is turned green. And if the distance comes out to be less than 150 cm then similarly green led turns red in the application (Figs. 1, 2 and 3).

## 6 Results and Discussion

As a result of the Smart Car Parking system, we aim to increase the convenience to the users and save the need to hire helping staff by the parking facility. We further plan on adding some more convenience and advanced features like an Automated payment gateway through the cars RFID tag, Nearest parking slot navigation assistance, integrating nearby parking facilities to work in tandem, parking slot booking in advance, etc.

In a simulation, we successfully implemented the Smart Car Parking system which uses RFID. Any car without RFID will not be permitted inside the parking lot. The status of the parking slots will be displayed on the LCD screen in real-time. We further plan on adding some more convenience and advanced features like an Automated payment gateway through the cars RFID tag, Nearest parking slot navigation assistance, Integrating nearby parking facilities to work in tandem, and parking slot booking in advance, etc. as shown in Fig. 4.

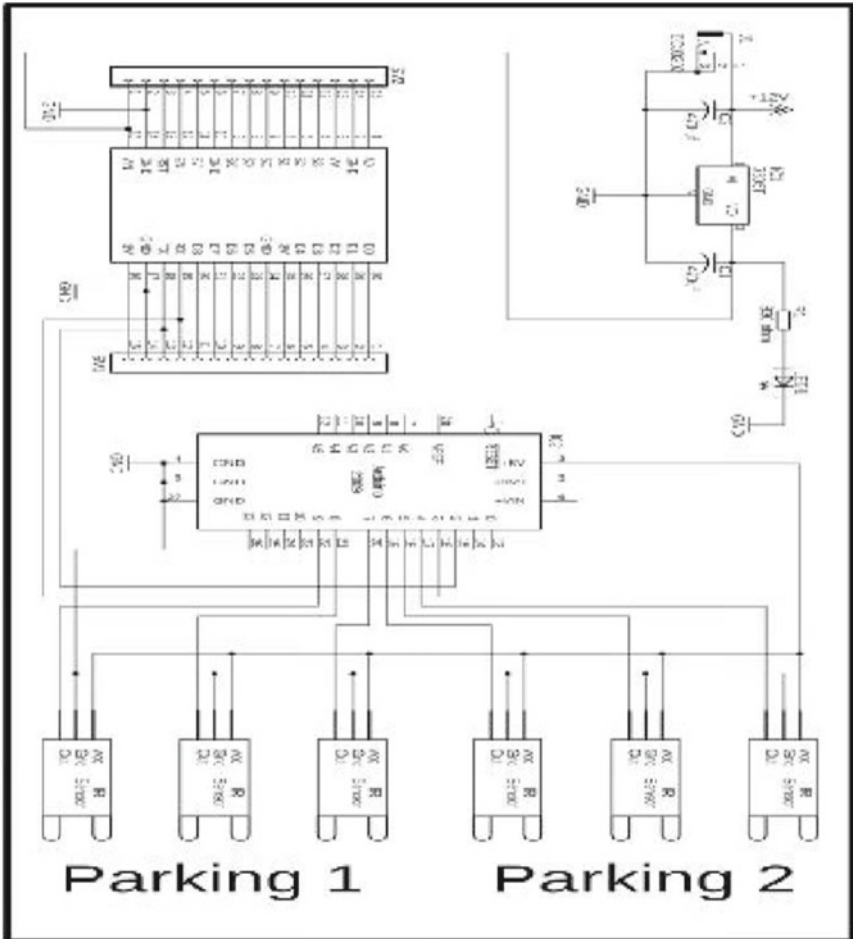


Fig. 1 Circuit diagram

## 7 Conclusion and Future Work

A smart car parking system will successfully help in parking without the help of human assistance and thus increase the efficiency of the parking facility through automation. In future scope, we can further like to add the following features:

- Automated payment gateway through the cars RFID tag
- Nearest parking slot navigation assistance
- Integrating nearby parking facilities to work in tandem.



Fig. 2 Use case diagram

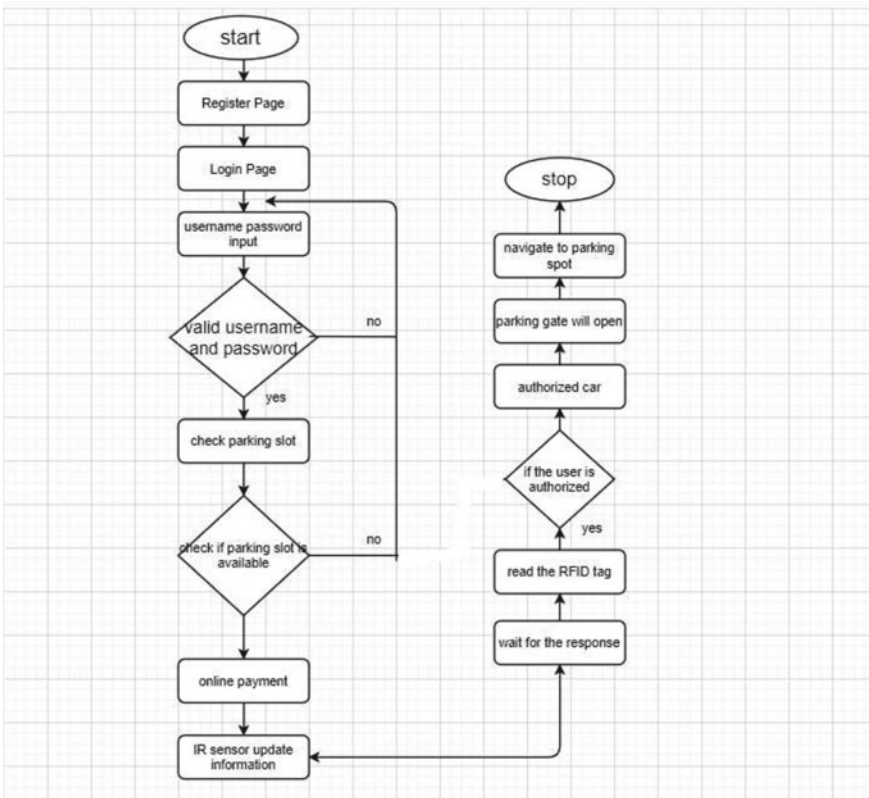


Fig. 3 Flow diagram

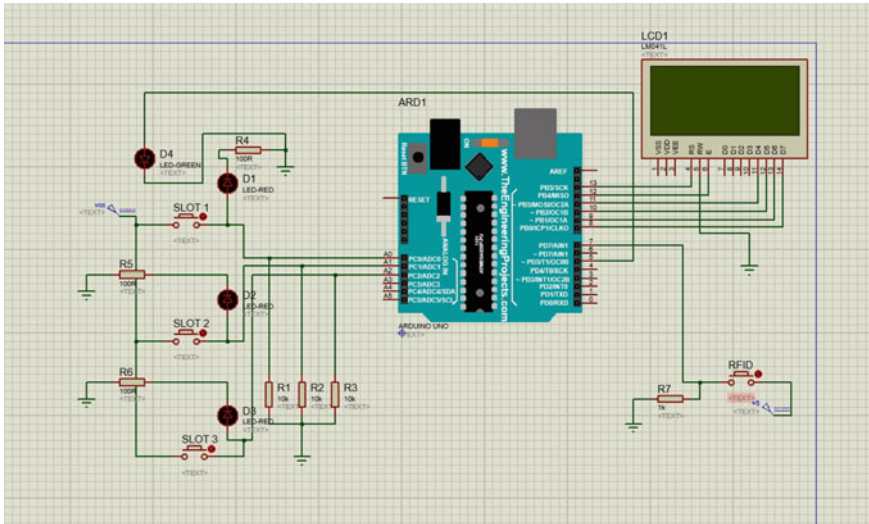


Fig. 4 Smart car parking system

## References

1. Biyik, C., Allam, Z., Pieri, G., Moroni, D., O’Fraifer, M., O’Connell, E., Olariu, S., Khalid, M.: Smart parking systems: reviewing the literature, architecture and ways forward. *Smart Cities* **4**, 623–642 (2021)
2. Kalašová, A., Čulík, K., Poliak, M., Otahálová, Z.: Smart parking applications and its efficiency. *Sustainability* **13**, 6031–6048 (2021)
3. Atiqur, R.: Smart car parking system for urban areas. *Comput. Sci. Inf. Technol.* **2**(2), 95–102 (2021)
4. Abrar, F., Mehedi, H., Muhtasim, A.C.: Smart parking systems: comprehensive review based on various aspects **7**(5) (2021)
5. Aswatha, R., Deepalakshmi, N., Dinesh, A., Arun, K.R., Gokulram, R.: Cost efficient automatic car parking facility towards smart city. *J. Phys. Conf. Ser.* **1916**, 1–6 (2021)
6. Amira, A.E., Mahmoud, S.: The smart parking management system. *Int. J. Comput. Sci. Inf. Technol. (IJCSIT)* **12**(4), 55–63 (2020)
7. Tanti, H., Kasodariya, P., Patel, S., Rangrej, D.H.: Smart parking system based on IoT. *Int. J. Eng. Res. Technol.* **9**(5), 73–77 (2020)
8. Vennila, G., Arivazhagan, D., Jayavadeivel, R.: An analysis of smart car parking management system. *Int. J. Sci. Technol. Res.* **9**(1), 1892–1895 (2020)
9. Joshi, A., Hariram, A.T., Somaiya, K.M.V., Hussain, M.: Smart car parking system. *Int. J. Eng. Res. Technol.* **9**(9), 484–487 (2020)
10. Azshwanth, D., Koshy, M.T., Balachander, T.: Automated car parking system. *J. Phys. Conf. Ser.* **1362**, 1–9 (2019)
11. Gawande, S., Kamle, S.: Smart car parking system. *Int. J. Comput. Sci. Eng.* **7**(12), 43–45 (2019)
12. Elakya, R., Seth, J., Ashritha, P., Namith, R.: Smart parking system using IoT. *Int. J. Eng. Adv. Technol.* **9**(1), 6091–6095 (2019)
13. Nandyal, S., Sultana, S., Anjum, S.: Smart car parking system using Arduino UNO. *Int. J. Comput. Appl.* **169**(1), 13–18 (2017)

14. Arduino Uno R3 Development Board-Control Voltage Obstacle Avoidance Reflection Photo-electric Sensor Infrared Alarm Module. [www.alexnlid.com](http://www.alexnlid.com)
15. NodeMCU ESP8266 V3 Lua CH340 WiFi Dev Board In India, Robu IOT based Car Parking System using Arduino and NodeMCU esp8266. [www.electronicclinic.com](http://www.electronicclinic.com)

# **Conclusions and Outlook**

# A Comprehensive Summary of the Contributions and the Quintessence of This Book



Kyandoghère Kyamakya and Pitshou Ntambu Bokoro

## 1 Concluding Remarks

The chapters presented in this book originate from several years of intensive research work conducted by mostly experienced teams of international authors from various affiliations worldwide. The main criteria, which were relied upon in order to constitute the different parts of this book, were based on the thematic convergence of the topics proposed. Furthermore, novel concepts of technologies and innovative applications presented in this book ought to be essential to the advancement of energy systems, in the context of the fourth industrial revolution and energy transition. The potential influence of smart technologies on economic decisions, which are critical to sustainable development, consisted of the major attribute of the expected contributions of the book chapters. Therefore, concepts and principles of smart technologies have been the discussion focus of the first four parts of this book, whereas innovative applications have been the preferential topics in Part V. The scientific contributions, which emerge out of the conceptual and application parts of this book, could be summarised as follows:

- **Part I:** the knowledge produced in this part ranges from the novel design concept of an energy storage system to the formulation of a realistic mathematical model for GEP deployment.

---

K. Kyamakya

Smart Systems Technologies, University of Klagenfurt, Klagenfurt, Austria

Université de Kinshasa, Kinshasa, République Démocratique du Congo

K. Kyamakya

e-mail: [kyandoghère.kyamakya@aau.at](mailto:kyandoghère.kyamakya@aau.at); [kyandoghère.kyamakya@gmail.com](mailto:kyandoghère.kyamakya@gmail.com)

P. N. Bokoro (✉)

Electrical Engineering Technology, University of Johannesburg, Johannesburg, South Africa

e-mail: [pitshoub@uj.ac.za](mailto:pitshoub@uj.ac.za)

- **Part II:** proposes, amongst others, an ontological smart grid, which addresses the interoperability and technological integration between the IEC CIM and the IEC 61850 models, a design approach for a cost-effective smart microgrid as well as a reliable and environmentally friendly hybrid microgrid.
- **Part III:** introduces the DPC-SVM concept for improvement of converter control during unsymmetrical faults. A realistic replication of a microgrid model using a small size PV-assisted microgrid model with the effect of line impedance is also proposed in this part prior to model evaluation of converters' control strategies for distributed power flow and reduced harmonics components. In addition, this part demonstrates the alleviation of nuisance tripping in distribution substations because of hybrid technologies of circuit breakers.
- **Part IV:** proposes a few accounts of environmentally friendly-based designs of a domestic dwelling system as well as desalination plants using solar and geothermal energies. Furthermore, this part proposes policy evaluation for the attainment of SDG 7 and 2 in SSA prior to advocating for security at multiple levels of the cyber-physical power system infrastructure security and personnel safety.
- **Part V:** proposes innovative applications of intelligent technologies, which range from the use of ANN, multi-dimensional ANN, fuzzy logic, and Rough Set Theory to IoT techniques for real-time power system monitoring, classification of power network states, data farming, for decision-making approach based on the complex set of data applications or for a smart car parking system.

Generally, the major contribution of the topics discussed in this book could be crystallized in terms of the following:

- Smart or intelligent concepts have proven to be important and relevant enablers to both current and newly developed or embraced technologies. This enablement is essential in the sense that it introduces cognitive capabilities to these technologies, thus advancing and empowering them to be able to source and process complex data necessary for making important decisions related to energy systems.
- The concept of a technology-enabled economy for the attainment of sustainable development goals is indeed consistent with the advancement of energy systems. This book presents an account of contextually based innovative applications of technologies, which are favorable to the promotion of a green economy. This implies that technological advancement mindful of the environment yet capable of driving developmental needs.

## 2 Outlook

The attainment of sustainable development goals is related to the advancement of energy systems. In the current context of an increase in greenhouse gases, global warming, and climate change, the transition from fossil-based energy to renewables



has slowly been embraced by the global community despite concerns about production losses and economic slowdown due to the perceived intermittent availability of most renewable resources. Owing to these concerns, a need for perpetual improvement adaptation of existing technologies and/or for developing new concepts, which could enable the emergence of new technologies, consisting of logical steps to maintain if not to accelerate the developmental progress. In this respect, this first issue of this book could be regarded as one of its first kind aimed at serving as a platform for the dissemination of the latest technological advances.

The future of energy and power systems will significantly be shaped by a more intense involvement of artificial intelligence (AI), respectively, machine learning (ML) technologies. Artificial Intelligence (AI/ML) has knowingly the capability of self-learning from data, and thereby with a relatively low dependence on mathematical models of physical systems, which provides an effective solution to breaking through a series of tough technical challenges. Indeed, AI/ML techniques have and shall become more popular than today for solving different problems in power and energy systems like control, planning, scheduling, forecast, and diverse forms of data analytics (i.e. descriptive data analytics, diagnostic data analytics, predictive data analytics, and prescriptive data analytics), etc. These AI/ML techniques can deal with a series of difficult and sensitive tasks/endeavors faced by applications in modern large power systems with even more interconnections installed to meet the increasing and still very dynamics (in time and space) load demands.